SAND--97-0579

1996

Laboratory Directed Research and Development Annual Report

Compiled by
C. E. Meyers, C. L. Harvey,
L. M. Lopez-Andreas, D. L. Chavez and
C. P. Whiddon

DISCLAIMER

Engineered Processes and Materials

Computational & Information Sciences

Microelectronics and Photonics

Engineering Sciences

Pulsed Power

Advanced Manufacturing Technologies

Biomedical Engineering

Energy and Environmental Science and Technology

Advanced Information Technologies

Counterproliferation

Advanced Transportation

National Security Technology

Electronics Technologies

Idea Exploration and Exploitation

Production

Science at the Interfaces: Engineering with Atoms

"...exceptional service in the national interest."

Science and technology are at the heart of United States industrial competitiveness, national security, energy resources, environmental quality, and leadership in fundamental and applied science.

At Sandia, the Laboratory Directed Research and Development Program provides the knowledge that drives our future. We initiate research and development that spawn the knowledge that revolutionizes technology. Areas of emphasis center on our core technical competencies and the major strategic thrusts of Sandia's Institutional Plan. Leading-edge experiments that validate our work are constructed and operated on schedule, within budget, and in a safe and environmentally responsible manner.

Our work continues to produce many scientific and technological breakthroughs that lead to new technologies, markets, and businesses for the nation.

To all those who have contributed so generously of their time and talent, thanks and congratulations for a job well done.

Laboratory Directed Research and Development Program Overview

C. E. Meyers

The Laboratory Directed Research and Development (LDRD) Program at Sandia National Laboratories is an essential element of the Laboratories' strategic intent to provide "exceptional service in the national interest." These activities assist in building the core competencies of the Laboratories through investigator-originated research and development. LDRD also supports the shared strategic vision of the U.S. Department of Energy (DOE) and Sandia. LDRD funds basic and applied research and development projects, focusing on exploration and exploitation of innovative concepts, selected by a technical and programmatic peer review process. The LDRD Program represents a primary link between immediate and emerging needs and the nation's future.

For fiscal year (FY) 1996, the Sandia LDRD Program was divided into three principal elements: Research Foundations, Technology Initiatives, and Novel Projects. Principal elements were further subdivided into areas as follows: **Research Foundations** (Engineered Processes and Materials, Computational and Information Sciences, Microelectronics & Photonics, Engineering Sciences, and Engineering with Atoms); **Technology Initiatives** (Pulsed Power, Advanced Manufacturing Technologies, Advanced Information Technologies, Electronics Technologies, Energy & Environmental Science and Technology, National Security Technology, Production, Counterproliferation, Transportation, and Biomedical Engineering); and **Novel Projects.** Each area funded projects that strengthened Sandia's core science and technology base and focused on future DOE and national needs. The projects permitted Sandia staff to explore innovative scientific and technological opportunities that hold high potential for payoff in future applications. Many of these projects have led to tangible new tasks and programs.

FY 1996 Funding Levels (MIL $)

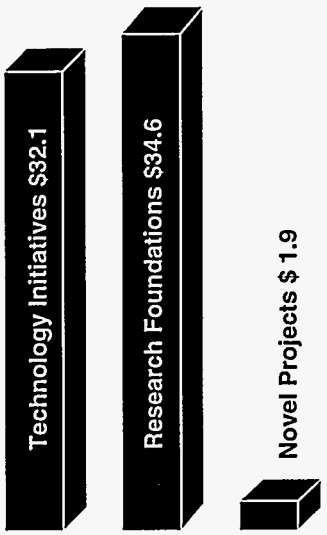

FY 1996 Selected Statistics

Full-time staff	262
Smallest project	$ 10K
Average project	$ 265K
Average project (FTE)	1.01
Largest project	$ 727K
1ST-year projects	132
2ND-year projects	99
3RD-year projects	28

FY 1996 Performance

Refereed publications	265
Other publications	243
Patent disclosures	30
Patent applications	20
Patents	1
Copyrights	10

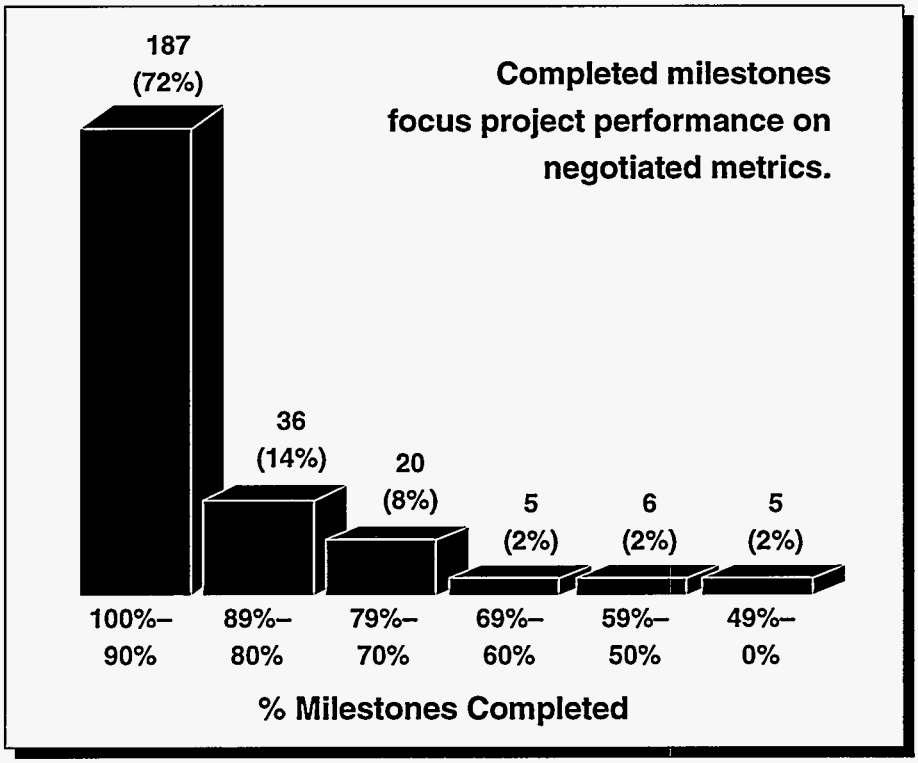

A majority of projects have dual-use applications.

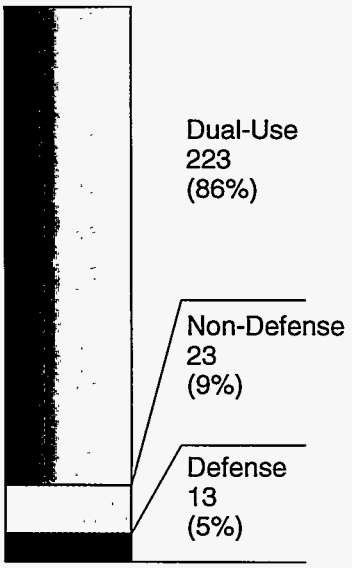

Core Competencies are an integration of technical skills, enabling strategic technologies that represent a significant differentiation, transcend many laboratory activities, and are difficult to imitate or replicate. Strategic Initiatives implement the major strategic thrusts contained in Sandia's Institutional Plan. Novel Projects extend the boundaries of the Laboratories' research foundations into fertile new areas.

Selection of LDRD projects is a formal process." Projects proposed for extension beyond one year must submit a request for continuation of funding, showing progress achieved to date toward the objectives and describing the tasks to be performed in the next year.

Proposals are subjected to two independent evaluations. An independent technical review evaluates the technical content of the proposed work, the technical approach proposed, and the technical potential of the project. Proposals are technically scored, ranked, and subjected to a programmatic evaluation by one of several review boards. In this evaluation, a proposal is reviewed with regard to its growth potential, its impact on future laboratory activities, and how the work supports Sandia's strategic intent. Selected projects are submitted to DOE headquarters for final approval.

In FY 1996, LDRD provided $68.6 million to fund 259 projects (selected from 1087 submitted).

The LDRD Program plays a major role in allowing Sandia to remain at the leading edge of research and technology. As a result, work performed in LDRD projects has earned many of the nationally and internationally recognized awards for excellence in research. Over the last four years, technology developed through the LDRD program received 14 of the 19 R&D 100 awards received by Sandia. All six Sandia awards for 1996 were supported by LDRD. Internationally recognized prizes included the Gottardi Prize for Glass Technology, the American Physics Society Welch Prize, and the Office of Energy Research Young Scientist Award.

The majority of FY 1996 projects had both defense and industrial (dual-use) applications and, at the same time, supported all nineteen DOE critical technologies. Clearly, the LDRD Program plays a key role in allowing Sandia to provide "exceptional service in the national interest" and is truly the link from today to tomorrow.

This report summarizes the progress achieved by all ongoing and completed projects. Reports are grouped in the three principal areas. Project abstracts are shown in italic text. FY 1996 accomplishments are shown in plain text. Refereed publications and other publications and presentations for each project are provided at the end of the project. Appendix A contains an author index. A project number/title cross-index may be found in Appendix B. Awards and other recognition are listed in Appendix C. Goal and milestone metrics are contained in Appendix D. LDRD projects are mapped to DOE critical technologies in Appendix E. Appendix F lists the major national programs supported, and Appendix G provides the dual benefits and national critical technologies categories.

Additional information on the 1996 Sandia LDRD Program is contained in the following report, which is available directly from Sandia: FY 1996 Annual Report to DOE/Defense Programs in Support of the Annual Report to the Congress on the Laboratory Directed Research and Development Program, Sandia National Laboratories, February 1997.

Goals and hypothesis status reveal the dynamics of research as each project unfolds.

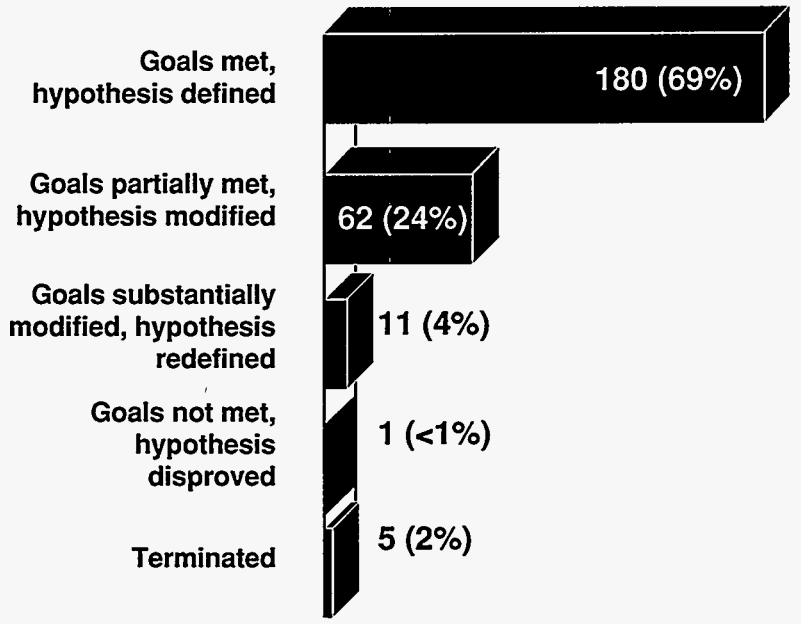

Engineered Processes and Materials

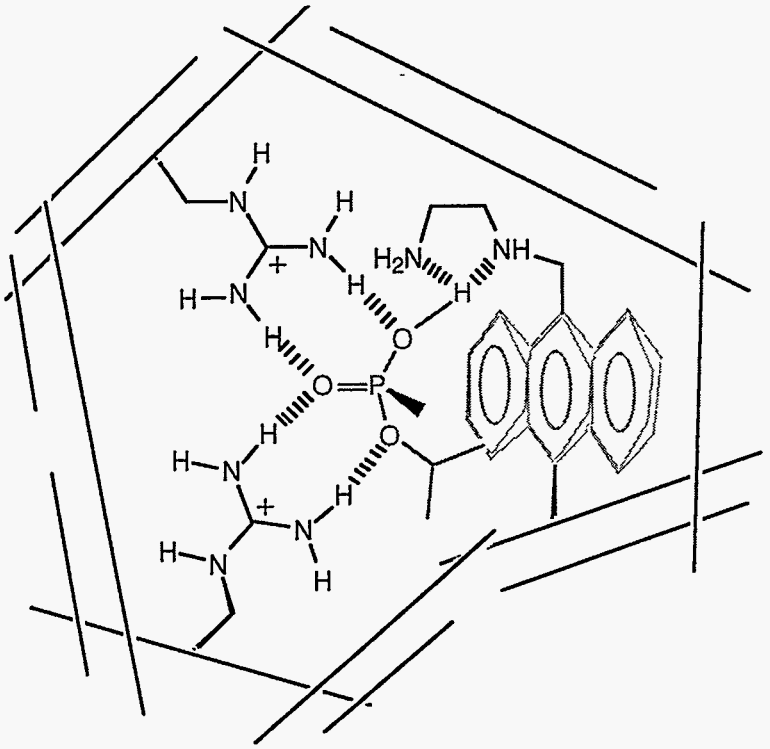

Molecular-recognition sites are being prepared in silicate materials with fluorescence response to the binding event.

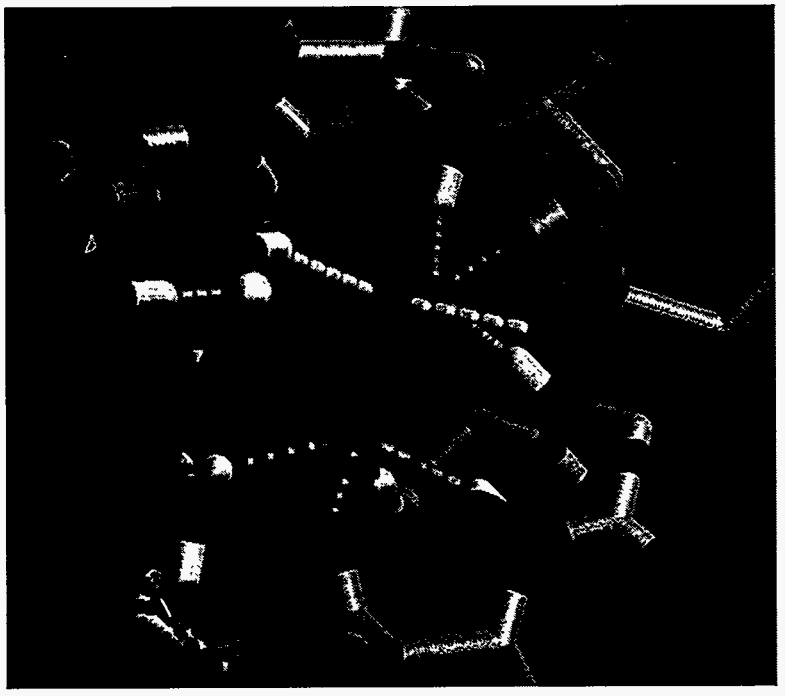

Computer modeling is used to evaluate and design recognition sites for phosphate compounds.

Adaptive Scanning Probe Microscopies

B. S. Swartzentruber, J. W. Bartholomew, G. C. Osbourn, A. M. Bouchard

Sandia used the recently developed atom-tracking scanning-tunneling microscope (STM) to quantitatively measure single-lattice–site kinetic processes on the Si(001) crystal surface. The atom tracker locks onto and tracks individual atoms and clusters in real time as they diffuse across a crystal surface. Using atom-tracking mode, the time response with which individual atomic-scale events can be resolved increases by more than a factor of 1000 over conventional STM imaging techniques. We measured the rotation kinetics of adsorbed Si dimers as a function of applied electric field and the binding free energy of adsorbed Si dimers at islands and steps.

In the short time that STM has been on the scene, it has demonstrated great potential to contribute to fundamental materials science problems, process science studies, and new approaches to production-quality control. However, current data-acquisition and analysis procedures severely restrict our ability to extract quantitative information regarding, for example, atomic-scale rate processes or local chemical compositions. In this project we combine innovative pattern-recognition (PR) techniques with state-of-the-art STM to develop a new paradigm for operating STM whereby the microscope adapts its data acquisition to focus on the most important features of the structure under examination. We designed and implemented novel STM electronics and control software (so-called "atom tracking") that enables the microscope to lock onto and track individual atoms in real time as they diffuse across a crystal surface. With this adaptive scanning approach, we located, tracked, and imaged features of interest without the overhead of acquiring data over the entire sample region. This decreases the time required to collect information by more than three orders of magnitude, which enables the study of kinetic processes with unprecedented microscopic, real-space resolution. We used this technique to study the rotation of Si dimers adsorbed on the Si(001) crystal surface at temperatures between 25° C and 65° C. By quantitatively measuring the change in the rotation rate as a function of temperature, we extracted an activation barrier for rotation of 0.75 eV. Measuring the change in the rotation rate as a function of applied electric field yields electronic structure information that can be compared with theoretical calculations. Because of the individual-lattice–site sensitivity provided by atom tracking, we were able to quantitatively measure the dimer-substrate binding free energy as a function of distance from substrate lattice steps. We found that dimers bind at steps with ~ 50 meV, and the binding energy falls off over the range of two lattice sites. Quantitative measurements of atomic-scale kinetic processes enable not only the validation but also the information necessary to develop and refine theoretical predictive models.

Publications

Refereed

Swartzentruber, B. S. 1996. 1996. "Direct Measurement of Surface Diffusion Using Atom-Tracking Scanning-Tunneling Microscopy." *Phys. Rev. Lett.* **76** (15 January): 459–462. New York, NY: American Physical Society.

Swartzentruber, B. S. 1996. "Si Ad-dimer Interactions with Steps and Islands on Si(001)." *Surface Science*, in press. Amsterdam, Netherlands: Elsevier.

Swartzentruber, B. S., A. P. Smith, and H. Jonsson. 1996. "Experimental and Theoretical Study of the Rotation of Si Ad-dimers on the Si(001) Surface." *Phys. Rev. Lett.* **77** (16 September): 2518–2521. New York, NY: American Physical Society.

Other

Swartzentruber, B. S. 1996. "Atom-Tracking STM Measurements of Si Adsorbate Diffusion and Interactions on Si(001)." Paper presented to the 2nd Asian STM Conference, Seoul, South Korea, 14–18 August.

Swartzentruber, B. S. 1996. "Direct Measurements of the Kinetics of Si Ad-dimers on Si(001) Using Atom-Tracking Scanning-Tunneling Microscopy." Paper presented to the TMS Annual Meeting, Anaheim, CA, 4–8 February.

Swartzentruber, B. S. 1995. "Direct Measurements of the Kinetics of Si Ad-dimers on Si(001) Using Atom-Tracking STM." Paper presented to the Fall Meeting of the Materials Research Society, Boston, MA, 27 November–1 December.

Swartzentruber, B. S. 1996. "Measurements of Si Ad-dimer Kinetics on Si(001) Using Atom-Tracking STM." Paper presented to the International Workshop on Nanoscale Science on Surfaces and Interfaces, Sendai, Japan, 29–30 January.

Swartzentruber, B. S. 1996. "STM Measurements of Adsorbed Si Dimer Kinetics on Si(001)." Paper presented to the Meeting of the Northern California Chapter of the American Vacuum Society, Stanford, CA, 17 September.

Engineered Monodisperse Porous Materials

R. S. Saunders, P. P. Newcomer, R. R. Lagasse, G. M. Jamison

This project involves the use of block copolymers to construct monodisperse mesoporous materials. We constructed block copolymers by ring-opening metathesis polymerization (ROMP) that phase-separates into extremely well-ordered mesophases. We designed one phase to be thermally labile and the other to be thermally stable. Thus the mesopores are created by thermally treating the samples at a predetermined temperature to selectively remove one of the phases. Small-angle x-ray scattering confirms phase separation of these systems, and high-resolution scanning-electron microscopy (SEM) and porosimetry measurements confirm the presence of mesopores.

We designed three block copolymer systems in FY96. The first contained one phase with chlorosilane groups that could be treated with water to form chemical crosslinks, and the other phase was thermally labile at 450° C. Treatment of a film of this cross-linked block copolymer system at 450° C appeared to cause the pores to collapse. The second system contained triethoxysilane groups in the thermally stable phase and a different thermally labile phase. We took a different approach with this system—making it into an aerogel through sol-gel processing. The sample did not gel under base hydrolysis, but did gel under acid hydrolysis. The gel was then pyrolyzed and analyzed by porosimetry. The pre-pyrolyzed sample had a surface area of 150 m^2/g, with a broad pore-size distribution, and the post-pyrolyzed sample showed a surface area of 650 m^2/g with a rather narrow pore-size distribution in the mesoporous range. Thus, pyrolysis of the sol-gel cross-linked polymer system showed the creation of well-defined mesopores. We designed the third block copolymer system so that one phase could be chemically crosslinked through triethoxysilane groups to make it thermally stable, and the other phase would lose more than 90% of its weight on thermal treatment at 130° C. We made this system into both aerogels and thick films. The aerogels did not show anything unusual by SEM. However, the thick films, on crosslinking with an aqueous hydrochloric acid solution and then heating at 130° C for 45 minutes, showed a practically monodisperse porous morphology by SEM. We were therefore able to make the desired monodisperse porous materials through the third and final block copolymer system.

The modeling of phase separation of block copolymers using density functional theory was also successful. We completed the modeling using a generic block copolymer system, then showed it to predict accurately the phase behavior of some existing literature systems.

We were successful at creating mesoporous materials that have fairly narrow pore-size distribution by using block copolymers that form gels through sol-gel processing. We were also successful at creating nearly monodisperse mesoporous materials through a new block copolymer that requires only very mild thermal treatment. Also, we developed modeling that accurately predicts the phase behavior of block copolymer systems.

Publications

Refereed

Nath, S. K., J. D. McCoy, and J. G. Curro. 1995. "Modified Self-Consistent Field Theory: Applications to a Homopolymer Melt Near a Hard Wall." *J. Chem. Physics* **103**: 1635–1636.

Nath, S. K., J. D. McCoy, J. G. Curro, and R. S. Saunders. 1995. "Density Functional Theory of Polymer-Polymer Phase Separation Behavior." *J. Poly. Sci. Part B: Poly. Phys. Ed.* **33**: 2307–2317. New York, NY: John Wiley & Sons, Inc.

Nath, S. K., J. D. McCoy, J. G. Curro, and R. S. Saunders. 1997. "The Behavior of Diblock Copolymers: Comparison of Self-Consistent Field and Density Functional Approaches." *Macromolecules* (February). Washington, DC: American Chemical Society.

Saunders, R. S. 1995. "New Polymers from Ring-Opening Metathesis Polymerization of Quadricyclane Adducts." *Macromolecules* **28** (June): 4347–4349. Washington, DC: American Chemical Society.

Demonstration of Molecular-Based Transistors

J. S. Jacobs, R. G. Kepler, R. A. Anderson, M. B. Sinclair

Recent discoveries in the field of conjugated polymers in environmental stability, regiochemical regularity, and electrical conductivity, particularly of polythiophene and polyaniline, have intensified interest in device applications. Present or anticipated applications include micropatterning of circuits, perhaps down to nanometer scale, as well as conducting and semiconducting materials for a variety of applications, including thin-film transistors and batteries. Sandia investigated a series of compounds comprising conjugated segments coupled to photochromic elements. The photochromic reaction in these compounds reversibly alters the conjugation length and provides a mechanism for switching both the electrical and optical properties of these materials. We are currently investigating the nature and scope of this switching mechanism and preparing extended materials that take advantage of this novel form of switching behavior. We describe here preparation and photochromic behavior of several of these materials.

We made considerable progress toward the synthesis and characterization of a number of new compounds. In particular we synthesized 3′-fulgide-2:2′-5′:2″-terthiophene (1), a thiophene trimer coupled to a dimethylenesuccinic anhydride (fulgide), a well-known element of many organic photochromes. Upon irradiation with UV light, solutions of (1) rapidly change from yellow to deep red, indicating photochromic behavior. Under irradiation by 500-nm light, the solution color reverts back to yellow, indicating a reversible photochromic response of this compound. We also observed photochromic switching of (1) in thin films. To understand the electronic structure of (1), we performed quantum chemical computations. These studies revealed that the electronic states responsible for the photochromic response were largely decoupled from the delocalized pi orbitals of the thiophene trimer.

We synthesized several polymers, including homopolymers of (1) and co-

polymers of (1) with 3-alkylthiophene. We investigated the photoconductive response of polymers of (1) prepared electrochemically. We observed no conductivity changes when they were illuminated in either the undoped or doped states. We did not perform chemical characterization.

Publications

Other

Jacobs, S. J., M. B. Sinclair, R. A. Anderson, and R. G. Kepler. 1995. "Photochromic Building Blocks for Conjugated Polymers." Paper presented to the 39th National Organic Symposium of the American Chemical Society, Williamsburg, VA, 11–15 June.

Jacobs, S. J., T. P. Pollagi, R. A. Anderson, R. G. Kepler, and M. B. Sinclair. 1995. "Photochromism as a Switching Mechanism for Electronically Active Organic Materials." Paper presented to the Materials Research Society Fall Meeting, Boston, MA, 27 November–1 December.

Chemical Functionalization of Oligosilanes: Economically Attractive Routes to New Photoresponsive Materials

G. M. Jamison, D. J. Hobbs, R. G. Kepler, J. G. Curro, J. V. Beach, D. A. Loy

The purpose of this project is to fabricate novel photoactive polysilane materials for potential applications as sensors, novel preceramic materials, or photoconducting/photorefractive chromophores through an economically attractive synthetic strategy. Sandia's approach is to take advantage of the s-*bond metathesis oligomerization of primary silanes, $RSiH_3$, as a safe and inexpensive alternative to reductive (Würtz) coupling of dichlorosilanes. This strategy also is inherently attractive in that it allows for chemical modification of the resulting oligophenylsilane to suit a variety of applications. Sandia extended high-accuracy,* ab initio, *electronic structure calculations to determine energetic barriers for polysilane backbone rotations. These are necessary for molecular mechanics modeling and estimation of polarizabilities for future statistical mechanics models. We accessed new hybrid polysilane-polysiloxane materials through free-radical hydrosilation of terminal alkenyl(alkoxy)-silanes and verified retention of polysilane* s-*conjugation in these materials.*

We conducted computer modeling studies by semiempirical and *ab initio* calculations of a number of oligophenylsilanes. More detailed *ab initio* calculations (3-21G*) established equilibrium geometries associated with various linear conformations to better approximate rotational barriers and to parameterize these systems for molecular mechanics modeling. We concluded that a standard set of geometrical parameters should be acceptable for studies of longer oligomers and high polymers. Furthermore, we calculated oligomer polarizabilities that were taken on for statistical mechanical calculations; 3-21G*–level calculations are acceptably accurate. Polarizability determination for helical conformations should be investigated.

We conducted Monte Carlo statistical mechanics for polysilane solutions from the detailed *ab initio* calculations. Others have demonstrated that this transition occurs in polysilane solutions as the temperature is lowered below a critical value. This prediction is consistent with ultraviolet (UV) spectroscopic studies; however, others question this prediction. We included polymer-polymer contributions to investigate electron delocalization effects in polysilanes, employing rotational isomeric-state chain models for $[(Ph)(H)Si]_n$ for n = 50, assuming that the polarizability scales quadratically with the number of consecutive trans-states. We followed the average chain size as a function of temperature. Results indicate that the delocalization length within the polysilane chains increases in a manner consistent with the experimentally observed thermochromism in the UV solution spectra of numerous polysilanes, and supports the electron delocalization model. Interestingly, rather than undergoing a coil/rod reansition as proposed by Schweizer, we see that the polysilane chains are predicted to collapse on themselves in solution, having long trans-segments along their backbone; gauche defects allow the chains to fold back on themselves.

Amorphous polysilane-polysiloxane hybrid nanocomposites can be prepared by the mild, acid-catalyzed sol-gel hydrolysis-condensation of polysilane-based precursors at the pendant alkoxysilane residues. Absorption and multinuclear-nuclear magnetic resonance (NMR) spectroscopies establish the retention of the polysilane chromophore and attached organic residues; NMR also reflects the degree of condensation at the siloxane-silicon nuclei. The bulk morphology of the resulting dried gels can be influenced by the choice of solvent removal from the wet gel. Aqueous extraction of solvent results in nonporous xerogels, while solvent removal by supercritical carbon dioxide yields mesoporous aerogels with retention of the wet gel surface area. In these hybrid materials the polysilane chromophore is homogeneously dispersed in, and covalently bound to, a highly cross-linked siloxane matrix.

Publications

Other

Jamison, G. M., D. A. Loy, K. A. Opperman, and J. V. Beach. 1996. "Oligosilane-Siloxane Nanocomposites." Paper presented to the Materials Research Society 1996 Spring Meeting, San Francisco, CA, 8–12 April.

Jamison, G. M., D. A. Loy, K. A. Opperman, J. V. Beach, and R. M. Waymouth. 1996. "New Hybrid Polysilane/Polysiloxane Nanocomposites." *Polymer Preprints* **37** (2): 297.

Jamison, G. M., D. A. Loy, K. A. Opperman, J. V. Beach, and R. M. Waymouth. 1996. "New Hybrid Polysilane/Polysiloxane Nanocomposites." Paper presented to the 212th American Chemical Society National Meeting, Orlando, FL, 25 August.

PbO-Free Composites for Low-Temperature Packaging

R. K. Brow, L. Kovacic, K. G. Ewsuk

Sandia prepared inorganic sealing materials that have the requisite thermal and chemical properties to replace PbO-based solder glasses currently used in a variety of low-temperature packaging applications. We evaluated the structures and properties of candidate zinc-phosphate–based systems. We fabricated hermetic seals to float glass substrates at temperatures below 500°C using both furnace and laser technologies. We prepared composite materials based on mixtures of low-temperature zinc-phosphate glasses and low-expansion ceramic fillers and evaluated their sealing properties.

PbO-based sealing glasses are used for a variety of electronic and optoelectronic packaging applications. These glasses can be sealed at relatively low temperatures (< 500° C), they have thermal-expansion matches to a variety of important substrate materials, and they generally have good chemical, electrical, and mechanical stabilities. However, the toxicity of PbO has raised concerns about potential applications of these materials and led Sandia to examine alternate glass-forming systems.

Zinc-phosphate glasses have an unusual combination of good chemical durability, low glass-transition temperature, and low thermal-expansion coefficient, making them replacement candidates for some of the low-temperature PbO glass-sealing applications. We completed a study of glass formation, properties, and the short-range structures of binary Zn-polyphosphate glasses and ternary Zn-Sn–phosphates and found that the desirable properties are related to the open molecular structures.

By modifying the basic composition through the addition of mixed alkali oxides and several other oxides, we developed glasses with transition temperatures under 400° C, expansion coefficients < 100×10^{-7}/° C, and aqueous durabilities similar to PbO-solder glasses. We made seals to float glass substrates in ovens at temperatures as low as 500° C and by local heating with a CO_2 laser.

We also made composite materials using a zinc-phosphate–based glass with a variety of ceramic fillers. The composite approach yields a lower-expansion sealing material (to match, for example, alumina substrates) without sacrificing the lower sealing temperature of the glassy matrix. We conducted sintering experiments to determine the effects of filler loading on the composite behavior.

Publications

Refereed

Brow, R. K. 1996. "An XPS Study of Oxygen Bonding in Zinc Phosphate and Zinc Borophosphate Glasses." *J. Non-Cryst. Solids* **194** (January): 267–273.

Other

Brow, R. K. 1996. "Spectroscopic Studies of Phosphate Glasses." Paper presented at the International Symposium on Glass Problems, Istanbul, Turkey, 4–6 September.

Brow, R. K., and D. R. Tallant. 1995. "Oxygen Bonding and Polyhedral Arrangements in Transition-Metal Oxide/Phosphate Glasses." Paper presented at the 97th Annual Meeting of the American Ceramic Society, Cincinnati, OH, 30 April–4 May.

Brow, R. K., D. N. Bencoe, and L. Kovacic. 1995. "PbO-Free Glasses for Low-Temperature Hermetic Packages." Paper presented at the 7th Annual Joint Meeting of the New Mexico Sections of the American Ceramic Society and the Materials Research Society, Albuquerque, NM, 30 October.

Brow, R. K., D. R. Tallant, J. J. Hudgens, and T. M. Alam. 1996. "Rings and Things in Phosphate Glass." Paper presented at the Fall Meeting of the American Ceramic Society, San Antonio, TX, 30 October–2 November.

Atomic-Scale Measurement of Liquid-Metal Wetting and Flow

N. D. Shinn, T. M. Mayer, E. H. Chason, A. J. Ricco, F. G. Yost, S. J. Martin

The wetting and flow of liquid metals plays an important role in materials synthesis and joining technologies. Despite the pervasive presence of liquid-metal interfaces in materials problems, solutions are almost always the result of trial and error rather than scientific understanding. Just as microscopic flow processes determine the stability of thin grain-boundary films, macroscopic liquid flow is controlled by atomic motions at the droplet edge. Current continuum spreading models do not address atomic-scale mechanisms and fail to predict correctly wetting, flow, and stability of interfacial liquid metals. We developed a new acoustic-wave damping (AWD) experimental technique and are using it to make the first viscoelastic measurements of ultra-thin liquid-metal layers on solid substrates. Molecular dynamics (MD) simulations performed in parallel with the experiments provide mechanistic insights into the atomistic motions responsible for the measured nanometer-scale viscoelasticity. This project impacts scientific issues common to a wide variety of materials problems by providing new atomic-level understanding that can be used to develop improved predictive engineering models for liquid flow and spreading phenomena.

We developed an AWD technique with sufficient sensitivity to measure the viscoelastic properties of nanometer-thick molecular films. Using AWD, we showed that the mechanical properties of a macroscopic film area can be related to molecular-scale structure. We initiated MD simulations to gain atomistic insights into the dynamics of these films undergoing shear deformation. We devised and implemented a method for AWD measurements at elevated temperatures, enabling the first-ever studies of ultra-thin metal-film melting

and undercooled liquid-metal viscoelasticity. Alkane thiol molecules, $HS(CH_2)_nCH_3$, self-assemble on gold substrates to form an ordered array of inclined molecules. Using a multifrequency AWD method, we found that the complex shear modulus of these monolayer films is dependent upon the hydrocarbon chain length. Films consisting of n=18 molecules exhibit a storage modulus three orders of magnitude greater than films consisting of n=12 alkane thiols. A 50% increase in the molecular length alone cannot account for this large effect; however, films consisting of longer molecules are known to be better ordered due to steric packing constraints. MD simulations of a perfectly ordered, n=16 alkane thiol infinite monolayer predict a purely elastic response with an even greater storage modulus. The constituent molecule apparently determines the intermolecular ordering and hence the film elasticity. Measurements of the loss modulus exhibited no systematic correlation with alkane chain length. Interestingly, the purely elastic response of the perfectly ordered "model film" suggests that energy dissipation in real molecular films originates at domain boundaries and packing defects. AWD measurements at elevated temperatures are complicated by the thermal expansion of the piezoelectric transducer itself and accompanying interfacial stresses. We successfully used the multifrequency response approach to study the melting of 30–100-nm-thick indium films under clean, ultra–high-vacuum conditions. Furthermore, we are able to carefully undercool the liquid indium and are now devising an analytical method to extract the temperature-dependent viscosity of the metastable liquid phase. We are developing a simplified single-frequency AWD detector to acquire viscoelastic data for ultra-thin liquid-metal and amorphous ceramic layers undergoing interfacial flow.

Synthesis and Processing of High-Strength SiC Foams: A Radically New Approach to Ceramic-Ceramic Composite Materials

L. L. Whinnery, G. M. Jamison, D. A. Loy, M. C. Nichols

Sandia used thermally induced phase separation (TIPS) to engineer the macrostructure of polysilane foams. Liquid-liquid phase separation during unidirectional solidification resulted in 10–60-mm-wide channels. We also observed mesoporosity within the channel walls. Decreasing the polymer concentration resulted in incomplete formation of the channel walls. We investigated several solvents yielding a variety of macrostructures. Faster cooling rates gave more narrow (10 mm), less continuous channels.

Due to the low melting point of the polysilanes, we performed a stabilization step to prevent the foam from melting prior to decomposition during pyrolysis. Pyrolysis of these stabilized polysilane foams yields a porous ceramic that contains the pore network originally induced into the polymer by the TIPS process.

We investigated the effect of the extent of exposure to the oxygen plasma. We showed that longer exposure times produce more silicon dioxide in the SiC foam. We suspended SiC powder within the polysilane foams to provide a source of nucleation. However, this nucleation did not increase the crystallinity of the SiC foam, but did increase the order of the carbon present as an impurity. We substantially increased the crystallinity of the SiC foam upon heating the sample to 2000° C. Another benefit of heating the SiC foams above 1300° C is that the SiO_2 and carbon present as impurities react with each other to form SiC, increasing the overall purity of the foam.

We attempted several alternative (to oxygen plasma) stabilization methods that would not incorporate oxygen to raise the glass-transition (Tg) temperature of the polymer foam above the decomposition temperature, preventing melting during pyrolysis, thus preserving the engineered macrostructure. We incorporated several highly functional chemical cross-linking agents along with appropriate catalysts (when necessary) into the polysilane foams. Unfortunately, none of the chemical crosslinks were successful enough to drive the Tg of the polymer high enough. We were also unsuccessful in our efforts to use gamma irradiation (CO_{60}) to crosslink the polysilane.

Publications

Refereed

Whinnery, L. L., W. R. Even, J. V. Beach, and D. A. Loy. 1996. "Engineering the Macrostructure of Thermally Induced Phase-Separated Polysilane Foams." *J. Polymer Science: Polymer Chemistry* 34 (June 15): 1623–1627. New York, NY: John Wiley & Sons, Inc.

Other

Whinnery, L. L., D. J. Coutts, W. R. Even, J. V. Beach, and D. A. Loy. 1996. "Engineering Macrostructure in Ceramics." Paper presented at the 211th ACS National Meeting, New Orleans, LA, 28 March.

Whinnery, L. L., D. J. Coutts, W. R. Even, J. V. Beach, and D. A. Loy. 1996. "Engineering Porosity in Ceramics." Paper presented at the Spring Meeting of the MRS, San Francisco, CA, 12 April.

Carbon Nanotube Composites

P. A. Cahill, A. G. Baca

Sandia investigated both the mechanical and electrical properties of composites of carbon nanotubes in various matrices. Carbon nanotubes are a graphitic form of carbon in which one or more graphite layers are rolled into a seamless, hollow tube, and may have from one up to about 50 layers. Nanotubes are prepared either by a metal-catalyzed electric arc process that yields single-walled, 1-nm-diameter "buckytubes," by an uncatalyzed electric arc process that produces multiwalled tubes, or by a catalyzed vapor phase-deposition process that can produce tubes or fibers up to 100-nm diameter with aspect ratios as high as 1000. Computational studies indicated that chemical modification of the surface of single-walled tubes was thermodynamically favorable, and suggested that strong bonds between the tubes and the matrix could be formed that might provide improved mechanical properties. Experimentally, however, separations of single-walled tubes from soots and catalyst particles yielded only partially purified samples, in low yield, and at great cost on a per-pound basis. Therefore, we focused the majority of the experimental work on vapor-phase–grown carbon nanotubes and the unique combination of mechanical and electrical properties available of composites with these fillers.

We found nanotube composites to have a usefully high electrical conductivity at sub-1% carbon loadings. This property is apparently unique to high-aspect-ratio fillers such as the nanotubes. Mechanical properties of polymers are not significantly degraded by the filler at these low loadings. Dispersion of the nanotubes into the mixture required significant process development, but we showed that uniform composites (uniform under optical microscopy to 500x), can be obtained through a two-stage mixing process. The details of the electrical properties and processing parameters are currently considered commercially sensitive.

The theoretical studies in FY96 were limited to extensions of previous computations as the project focused on experimental work this year.

Publications

Refereed

Cahill, P. A. 1996. "*Ab Initio* Computational Study of Selected $C_{60}H_6$ Isomers." *Chemical Physics Letters* **254** (24 May): 257–262. Amsterdam, Netherlands: Elsevier.

Cahill, P. A., and C. M. Rohlfing. 1996. "Theoretical Studies of Derivatized Buckyballs and Buckytubes." *Tetrahedron* **52** (1 April): 5247–5256. Oxford, UK: Elsevier.

Other

Cahill, P. A. 1995. "Addition to Fullerenes and Nanotubes." Paper presented to Pacifichem, Honolulu, HI, 18 December.

Cahill, P. A. 1995. "Relative Energies of Multiply Addended Fullerenes: $C_{60}H_6$." Paper presented to the Materials Research Society Spring Meeting, San Francisco, CA, 19 April.

Cahill, P. A. 1995. "Semiempirical Study of Hydrogen Addition to Single-Walled Carbon Nanotubes." *Proc. 187th Electrochem. Soc. Mtg.* **95-10** (Reno, NV, 25 May): 1271–1275.

Cahill, P. A., and S. J. Jacobs. 1995. "Addition Chemistry of Carbon Nanotubes." Paper presented to the Materials Research Society Spring Meeting, San Francisco, CA, 19 April.

Cahill, P. A., C. M. Rohlfing, C. C. Henderson, R. A. Assink, K. T. Gillen, and S. J. Jacobs. 1996. "Hydrogenated Fullerenes: Quantitative Comparison of Theory and Experiment." Paper presented to the American Chemical Society National Meeting, Orlando, FL, 25 August.

Nanocomposite Materials Based on Hydrocarbon-Bridged Siloxanes

T. A. Ulibarri, J. A. Emerson, J. G. Curro, G. M. Jamison, D. A. Loy

Silicones (polydimethylsiloxane [PDMS] polymers) are environmentally safe, nonflammable, weather-resistant, thermally stable, low glass-transition temperature (Tg) materials, which are attractive for general elastomer applications because of their safety and performance over a wide temperature range. However, PDMS is inherently weak due to its low Tg and lack of stress crystallization. The major goal of this project was to create a family of reinforced elastomers based on silsesquioxane/PDMS networks. We synthesized and purified a series of known silsesquioxane monomers, including the ethylene-, propylene-, hexylene-, octylene-, decylene-, phenylene-, and biphenylene-bridged trialkoxysilane systems. In addition, we synthesized blocked site monomers and branched silsesquioxanes. To understand the reactivity of the silsesquioxane monomers relative to the PDMS, we studied their hydrolysis and condensation, as well as their miscibility with the PDMS polymers. We synthesized and tested all proposed PDMS/silsesquioxane materials relative to their mechanical and adhesive properties.

We completed reactivity studies with the tin(II) catalyst, tin octoate, to establish the effectiveness of tin catalysis for silsesquioxane condensation. We determined that tin catalysis is more effective for alkylene-bridged species than for arylene-bridged monomers. Studies on the miscibility between the silsesquioxane monomers and the PDMS polymers demonstrated that the arylene systems had greatly enhanced miscibility. Physical gels could be formed with the alkylene species. Utilizing stoichiometric water addition and solvent addition to improve miscibility, we synthesized and tested all proposed PDMS/silsesquioxane materials with respect to their mechanical and adhesive properties. Contrary to what

would be expected based on miscibility, the strongest materials were generated either from arylene-based monomers or alkylene monomers that were partially hydrolyzed. Close examination of the monomeric alkylene systems showed that they are capable of undergoing nonproductive cyclization reactions, which may explain their lower properties, regardless of higher reactivity. The optimal materials had adhesive strengths approximately five times greater than commercially used silicone adhesives.

Publications

Other

Loy, D. A., S. E. Bates, T. A. Ulibarri, R. A. Assink, S. T. Myers, G. M. Jamison, and K. J. Shea. 1995. "Synthesis and Characterization of Bridged Polysilsesquioxane-Polydimethylsiloxane Nanocomposites." Paper presented to the Intersociety Polymer Conference, American Chemical Society, Baltimore, MD, 7–10 October.

Scharfer, D. W., G. Beaucage, D. A. Loy, T. A. Ulibarri, E. P. Black, K. J. Shea, and R. J. Buss. 1996. "Origin of Porosity in Aryl-Bridged Silsesquioxanes." *Proc. 1996 Spring Mtg. Mater. Res. Soc.* **435** (San Francisco, CA, 8–12 April): 301–306.

Ulibarri, T. A., D. A. Loy, S. E. Bates, E. P. Black, G. M. Jamison, S. T. Myers, R. A. Assink, and K. J. Shea. 1996. "Synthesis and Characterization of Bridged Polysilsesquioxane-Polydimethylsiloxane Nanocomposites." Paper presented to the 1996 Spring Meeting, Materials Research Society, San Francisco, CA, 8–12 April.

Ulibarri, T. A., R. A. Assink, G. M. Jamison, D. A. Loy, S. E. Bates, E. P. Black, S. T. Myers, and K. J. Shea. 1996. "Bridged Polysilsesquioxane-Polydimethylsiloxane Nanocomposites: A Reactivity Study." Paper presented to the 211th American Chemical Society National Meeting, New Orleans, LA, 24–29 March.

New Adhesive Systems Based on Functionalized Block Copolymers

M. S. Kent, J. A. Emerson, R. S. Saunders

Sandia is exploring the use of functionalized block copolymers to promote adhesion at thermoset/metal interfaces. We synthesize the copolymers to contain two blocks of monomers with different functionalities by living ring-opening metathesis polymerization (ROMP). We designed one block to bind to the metal surface, while the second block was designed to bond to the thermoset polymer. The structure of the adsorbed copolymer layer is critical to the performance of the copolymers as coupling agents. We used neutron reflectivity and time-of-flight (TOF) secondary ion mass spectroscopy (IMS) to characterize the conformation of the block copolymers after adsorption from solution onto polished metal mirrors. We examined the effects of block molecular weights, solvent quality, and concentration on the adsorbed conformation. We evaluated adhesion promotion testing using lap-shear and peel geometries.

Sandia accomplished the following in FY96:

(1) Discovered that adhesion and durability are greatly enhanced if the block copolymer is applied directly to a bare copper surface rather than to the native oxide. We studied growth of the oxide and determined that after etching away the native copper oxide, roughly 20 minutes in air is required before a newly grown oxide is detectable. Therefore, the block copolymer can be applied directly to copper by submerging the copper coupons into the block copolymer solution immediately after etching.

(2) Discovered that the adsorbed amount of block copolymer is a strong function of its concentration in the treating solution. The structure of the adsorbed monolayer is thus also strongly affected. The peel testing done up to this point likely involved concentrations of block copolymer that were too low, resulting in very little coverage of the surface. The strong dependence of the adsorbed amount and monolayer structure on concentration appears to be at odds with the typical behavior observed for adsorption of nonfunctionalized homopolymers and block copolymers.

(3) Synthesized a block copolymer functionalized with a benzotriazole pendant functional group. This functional group is known to bind strongly to copper but may be more thermally stable than the imidazole rings used up to this point to bond to copper.

(4) Measurements of contact angles of water on copper (with and without oxide) and silicon (with and without oxide), where these surfaces are coated with films of the block copolymer and the respective homopolymers, showed that surface energies can be manipulated by this method to some degree. However, the range of variability is limited by the dominant contribution of the norbornene backbone, which is the same in all blocks synthesized by this method.

Publications

Refereed

Kent, M. S., R. S. Saunders, J. Emerson, and M. Hurst. 1995. "New Functionalized Block Copolymers for Bonding Copper to Epoxy." *Proc. 27th Internat. SAMPE Tech. Conf.* **27** (Albuquerque, NM, 9–12 October): 1019–1025.

Other

Kent, M. S., R. S. Saunders, G. C. Nelson, and A. P. Y. Wong. 1996. "The Conformation of Functionalized Diblock Copolymers Adsorbed from Solution onto Metal Substrates." Paper presented to the Meeting of the American Physical Society, St. Louis, MO, 18–22 March.

Saunders, R. S., and M. S. Kent. 1995. "Novel Adhesives Based on Functionalized Block Copolymers." Paper presented to the Fall Meeting of the Materials Research Society, Boston, MA, 1–5 December.

Small, J. H., R. S. Saunders, and M. S. Kent. 1996. "Amine-Containing Block Copolymers: Long-Term Adhesion Promoters and Corrosion-Resistant Coatings." Paper presented to the Fall Meeting of the American Chemical Society, Orlando, FL, 25–29 August.

Modeling Electrodeposition for Metal Microdevice Fabrication

S. K. Griffiths, W. D. Bonivert, R. H. Nilson

LIGA, an acronym from the German words for lithography, electroforming, and molding, is a promising new process for producing metal microdevices having micron-to-millimeter features. Currently under world-wide development, this process offers a means to manufacture high-resolution, high-aspect-ratio devices, including microscale valves, motors, solenoid actuators, and gear trains. Most research in LIGA has focused on the lithography process used to produce LIGA molds. Filling these molds by electrodeposition has received much less attention, despite several serious problems. Device-scale voids in the deposited metal occur frequently and often without apparent cause. These problems are likely due to the depletion of metal ions and the accumulation of hydrogen in the stagnant layer between the top and bottom of the mold. The presence of this diffusion layer distinguishes LIGA electrodeposition from traditional electroplating and electroforming processes.

To help understand and optimize the electroforming portion of the LIGA process, Sandia is developing a one-dimensional (1-D) numerical model describing the electrodeposition of metal into high-aspect-ratio molds having lateral dimensions on the micron scale. To guide model development, and later to validate this model, we are also conducting a series of 1-D/1-D laboratory experiments.

We developed a preliminary 1-D model describing the quasi-steady electric field and multispecies ion transport within the LIGA mold. This model includes the eight ion species important to the deposition of nickel or iron alone, and to the co-deposition of nickel-iron alloys. We obtained electric potentials by solving an elliptic field equation, taking into account variations in electrolyte conductivity with ion concentration. The kinetics of the electrode reactions are incorporated through Butler-Volmer equations relating current density to electrode polarization. We computed metal-ion and hydrogen concentrations by solving a multicomponent system of implicitly coupled, quasi-steady conservation equations describing simultaneous transport and reaction of ions diffusing from the bath to the deposition surface.

We also designed and built a laboratory apparatus for simulating LIGA electrodeposition in deep molds having high-aspect ratios. We conducted several preliminary experiments to explore nickel deposition in cylindrical molds using a nickel sulfamate bath. Experiments performed over a range of total currents showed a strong influence of the current on the morphology of deposited metals.

Catalytic Membrane Sensors

T. J. Boyle, A. G. Sault, T. J. Gardner, G. C. Frye, J. C. Brinker

The goal of this project is to develop a fundamentally new catalytic membrane-based sensor (CMS) with enhanced sensitivity and specificity through modification of a Sandia-developed Pd/Ni-based hydrogen sensor. Sandia will accomplish this through overlays of a size-selective gas-separation membrane and ion-exchangeable titanate catalyst. Furthermore, our goal is to process these CMS elements into an array that utilizes different catalysts and membranes. This will enable us to significantly improve both the selectivity and specificity via pattern-recognition (PR) methodologies. The first milestones toward the synthesis and processing of these CMSs were (1) synthesis and characterization of double alkoxides, (2) membrane-modified sensor (H_2 sensor), (3) catalytically active HTO or HTO-like layer on a membrane, (4) catalytic adjustability by ion exchange, and (5) catalyst layer on the sensor. Although we experienced technical difficulties related to several mechanical failures required to fabricate the hydrogen sensor platform, we substantially met all the milestones.

We successfully produced the individual components of the CMS prototype and demonstrated that these components can be integrated easily. We synthesized the desired double alkoxides ($NanTi(OCHMe_2)_{4+n}$) and initiated characterization. We demonstrated that these double alkoxides can be catalytically activated by ion exchange of the Na for Rh. We achieved modification of the H_2 sensor with a sol-gel membrane after the appropriate cleaning of the Pd/Ni surface and identified shorting due to the high processing temperatures as a serious problem. Changes in the processing of the membrane by *in situ* measurements show the highest allowable processing temperatures that are acceptable for catalytic exchange to be at 400°C. We realized integration of these individual components and started production of a complete CMS-altered hydrogen sensor. We investigated the unusual reactivity of the H_2/O_2 mixtures as they are passed over the membrane surface.

Surface-Micromachined Flexural Plate Wave Device Integrated on Silicon

B. A. Tuttle, J. A. Ruffner, D. D. Chu, D. B. Dimos, J. H. Smith, G. C. Frye

Small, reliable chemical sensors are needed for a wide range of applications, such as weapon state-of-health monitoring, nonproliferation activities, and manufacturing emission monitoring. Significant improvements in state-of-the-art acoustic chemical sensors could be achieved by developing a flexural plate wave (FPW) architecture in which acoustic waves are excited in a thin sensor membrane. Development of the FPW devices requires integration of sensor technology, Si surface micromachining, and piezoelectric (PZT)

thin films. Miniaturized, rugged, highly reliable sensors with improved sensitivity and frequency operation compatible with standard digitial microelectronics will result from this integration.

Sandia accomplished the following in FY96:

(1) Fabricated AlN and ZnO films on Si and determined the amount of oxygen incorporated into the AlN film using Rutherford backscattering. Low-oxygen–content AlN films are required for reasonable PZT response.

(2) Determined diffusion barrier for PZT films on Si and SiN. The use of titania is essential for good PZT films on AlN.

(3) Developed methods for characterizing PZT properties; methods include a macro cantilever beam technique to measure PZT constant and the coupling coefficient. We developed a design for direct measurement of PZT effect.

(4) Fabricated Si micromachined membrane devices using polysilicon membrane structures. Devices using SiN membranes will be through lot fabrication soon.

(5) Fabricated lead titanate films with Sm, La, and Mn.

(6) Fabricated surface acoustic-wave (SAW) structures that did not electrically short using PZT and AlN films; a new design is required to measure SAW properties.

(7) Designed a mask set for new SAW devices. We deposited PZT films on both lanthanum strontium cobalt oxide and platinum electrodes. The films had exceptionally good ferroelectric properties and were demonstrated to have reasonable PZT response.

(8) Fabricated highly oriented AlN films.

Model Determination and Validation for Reactive Wetting Processes

J. L. Roberts, P. A. Sackinger, K. S. Chen, T. J. Bartel, F. G. Yost

Dissolutive wetting occurs when a liquid wets and spreads over a solid surface with simultaneous dissolution of the solid into the liquid. We show that this process initially yields a metastable equilibrium, and we describe a compact model for the kinetics of approach to this metastable state. The technique for constructing these kinetics stems from the early work of Onsager and begins with a relationship for the entropy production. From this, we can write directly a coupled set of nonlinear, ordinary differential equations. We solved the equations numerically for the wetted area and compared it with experimental data. The model captures many of the subtle complexities of dissolutive wetting such as multiple equilibria. The main weaknesses of the model are the assumptions of fully stirred liquid and a spherical solid/liquid interface, which we made to keep the analysis simple.

We subscribed thermodynamic equilibrium conditions for a spreading droplet that is simultaneously dissolving a solid substrate. We showed the conditions for contact-angle equilibrium to be incompatible with those obtained from the equilibrium-phase diagram and reasonable shape assumptions. We employed a technique for restoring compatibility and derived an expression for the entropy production. From this, we established the kinetic equations for wetting in the manner of Onsager. We solved the rate equations numerically and compared them with experimental data. We found that good agreement can be obtained with use of this technique for describing wetting kinetics in the Sn-Bi on Bi system. We found time-varying quantities, such as atom fraction Bi dissolved in the liquid, to converge to the values expected from the metastable equilibrium analysis. To obtain a compact model of these kinetics, the model explicitly neglects diffusion and any form of convection in the liquid. The model assumes that spherical caps are sufficient geometric descriptions of the interfaces and that the liquid is an ideal solution. To relax these assumptions, more detailed models employing the same Onsager methodology could be constructed. Additional difficulties are possible if preferred dissolution occurs at grain boundaries in the substrate, if the substrate is inherently anisotropic, and if the flux efficacy is strongly time-dependent. The technique clearly shows the importance of secondary thermodynamic effects in the wetting process.

Publications

Refereed

Yost, F. G., P. A. Sackinger, and E. J. O'Toole. 1996. "Energetics and Kinetics of Dissolutive Wetting Processes." Paper presented to the 3rd International Workshop on Interfaces, Santiago, Spain, 16–20 September.

Integrated Thin-Film Structures for IR Imaging

J. A. Ruffner

Uncooled pyroelectric infrared (IR) imaging systems, such as night-vision goggles, offer important strategic advantages in battlefield scenarios and reconnaissance surveys. Unfortunately, the current technology for fabricating these devices is limited by low throughput and high cost, which ultimately limits the availability of these sensor devices.

Sandia is developing an alternative design for pyroelectric IR imaging sensors that utilizes a multilayer thin-film deposition scheme to create a fully integrated thin-film element on an active silicon substrate for the first time. Our approach combines a thin-film pyroelectric imaging element with a thermally insulating SiO_2 aerogel thin film to produce a new type of uncooled IR sensor that offers significantly higher thermal, spatial, and temporal resolutions at a substantially lower cost per unit.

The development of our proposed uncooled pyroelectric imaging system is well under way. Based on thermal modeling studies, non-opacified aerogels with ~ 80% porosity should have thermal conductivities comparable to air (25 mW/m-K). We successfully deposited aerogel thin films using dip and spin-coating techniques with appropriate porosities (70–80%) onto oxidized Si substrates. We characterized the surface morphology of the aerogels using a new atomic force microscopy (AFM) technique and found the roughness to be much lower (< 30 nm) than originally anticipated. We used a number of techniques in an attempt to "planarize" the aerogel thin-film surface for subsequent thin-film sputter deposition. We determined the easiest and best technique to be sputter-coating a sufficiently thick overlayer of SiO_2 or TiO_2 on the aerogel. AFM analysis indicates that a 120-nm coating of TiO_2 reactively sputtered onto an aerogel thin film has a root-means-square (RMS) surface roughness of only ~ 8–9 nm and can serve as both the planarization and the etch-stop layers. Presently, we are investigating the benefits of depositing a Ti thin film and oxidizing it to increase adhesion at the aerogel/TiO_2 interface. We established sputter-deposition parameters for the overlying adhesion (Ti), electrode (Pt and LSCO), and blacking agent (LSCO) layers.

We identified two candidates for the solution-deposited pyroelectric imaging elements. These two candidates, $PbZr_{.30}Ti_{.70}O_3$ (PZT 30/70) and $Pb_{.95}La_{.05}Zr_{.30}Ti_{.70}O_3$ (PLZT 5/30/70), offer much higher pyroelectric responses than single-crystal $(Ba,Sr)TiO_3$ (BST), which is the imaging element used in state-of-the-art night-vision goggle systems. The noise-equivalent temperature difference calculated from the measured pyroelectric properties of PLZT 5/30/70 is 2.5 times better than the pyroelectric film composition BST, which, combined with the excellent thermal insulating properties of the aerogel thin film, will result in superior performance of these integrated thin-film structures for IR imaging. We also investigated the possibility of enhancing dielectric behavior by doping the material with either a donor (Nb) or an acceptor (Fe, Mn, Co, Ni). In addition, we are presently developing sputter-deposition parameters for another promising pyroelectric material, $PbSc_{.5}Ta_{.5}O_3$.

We developed a computer-controlled data-acquisition system that allows accurate measurement of pyroelectric coefficients of thin films. We chose this measurement technique in place of deep-level transient spectroscopy as we originally proposed in order to increase the accuracy of the pyroelectric measurements.

Publications

Other

Tuttle, B. A., H. N. Al-Shareef, J. A. Ruffner, C. J. Brinker, T. J. Garino, and D. Dimos. 1996. "Pb(Zr,Ti)O_3 Thin Films for Integrated Sensor Applications." Paper presented to the American Ceramic Society Fall Meeting, San Antonio, TX, 2 November.

Tuttle, B. A., H. N. Al-Shareef, T. J. Garino, J. A. Ruffner, C. J. Brinker, D. Dimos, W. L. Warren, T. J. Headley, and M. O. Eatough. 1996. "Structure-Property Relationships for Pb (Zr,Ti) O_3 Thin-Film Microsensors." (Invited) Paper presented to the 10th International Symposium on Applications of Ferroelectrics, New Brunswick, NJ, 18–21 August.

Tuttle, B. A., J. A. Voight, H. N. Al-Shareef, and D. Dimos. 1996. "An Overview of Ferroelectric Thin-Film Technology." (Invited) Paper presented to the Meeting of the American Chemical Society, New Orleans, LA, 28 August.

Molecular Imprinting in Aerogels for Remote Sensing of Chemical Weapons and Pesticides

D. Y. Sasaki, J. S. Schoeniger, P. I. Pohl, A. J. Ricco, M. A. Butler, J. C. Brinker

Recent events in the world underline the need for reliable, inexpensive sensors for chemical warfare (CW) agents. Nerve agents belong to a general class of phosphate and phosphonate esters that have a broad range of activities, including materials for nuclear weapons production, pesticides, and biological cellular signals. Current methods to detect these agents are limited to laboratory analysis. An in-field, real-time, sensor-based approach with remote-sensing capability is highly desired.

Sandia proposed to design and develop highly sensitive, specific optical sensors for phosphate and phosphonate esters using molecular-recognition sites in high-surface-area aerogels. We will design molecular-recognition sites using computer-aided molecular design (CAMD) and engineer it via a "template-imprinting" technique into aerogels. We will design the material with active fluorophores at the receptor site reporting on target molecule recognition via fluorescence through complexation with the phosphonate guest. We will develop these materials as visual detectors that monitor color changes or use fluorescence lifetimes for extremely low-level sensing applications. We will develop granular bulk aerogels for our "smart pebbles" concept, providing a remote-sensing system for covert CW agent production facilities, battlefield alert for CW release, and agricultural pesticide application and runoff.

We performed molecular modeling studies to aid in the design of biomimetic molecular-recognition materials that bind phosphate and phosphonate ligands. There are two design goals: (1) to examine phosphonate and phosphate binding in known biological systems and identify the key molecular-recognition features, and (2) to build 3-D molecular models of a proposed receptor site in a synthetic material to evaluate possible interactions based on these key features. We studied phosphonate binding in natural and engineered materials in three steps. First, we culled the protein data bank for suitable phosphate-binding structures. Next, we evaluated the binding energy of these using a combined molecular mechanics/Monte Carlo technique. Finally, we suggested the positions of the engineered binding pocket atoms based on the previous results and ran molecular dynamics (MD) simulations of phosphate ion and a phosphonate molecule in a model aerogel.

Some of the striking features found in the initial characterization of these proteins were the large number of hydrogen bonds (as many as three per phosphate oxygen) and their unusual tightness. Key functionality at the receptor site includes guanidinium from arginine, amine from lysine, imidazole from histidine, amide hydrogens from the protein backbone, and hydroxyls from serine and water. We modeled the synthetic receptor in the silicate matrix using MD. We used the functional group guanidinium, which we placed randomly in a porous silica model grown by cluster-cluster aggregation. We placed a phosphate or phosphonate substrate near the matrix surface and allowed the system to energy minimize. The extraordinary result is that the guanidine functionality collapsed around the phosphate, or phosphonate, ion as indicated by the pair correlation functions between nitrogen atoms and phosphate atoms. This suggests that a siloxane matrix functionalized with guanidinium groups would have good probability in forming receptor sites with high molecular recognition for phosphate or phosphonate ion.

Following guidelines set forth by the modeling studies, we prepared several monomers with amine and guanidine functionality for olefinic polymers and aerogel materials. We are studying both functionalized organic polymers and aerogels as candidate matrices to provide a range of materials characteristics for future facile materials coupling to the sensor platform. Currently we are testing these materials for binding affinity to phosphate substrates in chromatography experiments. We also prepared fluorescent-probe monomers, trinsyl and dansyl propyltrimethoxysilane, via multistep synthesis and are currently incorporating them into aerogel materials.

Synthesis and Modeling of Field-Structured Anisotropic Composites

J. E. Martin, D. B. Adolf, R. A. Anderson

Sandia proposed to develop the modeling, synthesis, and processing capability to create novel anisotropic polymer/ceramic and polymer/metal composite materials by applying external electric or magnetic fields to systems consisting of a polymerizable continuous phase into which particles having an electric permittivity or magnetic permeability mismatch are suspended. A linear field will create one-dimensional (1-D) particle chains, a well-known effect. But we recently discovered that rotating fields create 2-D particle sheets in the plane of the field. We will capture these unique structures by polymerizing the continuous phase during a field anneal. A key aspect of this project will be modeling and controlling the evolution of structure in these materials.

Sandia developed computer-modeling algorithms and codes for 1-D/2-D nanocomposites. These codes simulated structural evolution in a system of spherical particles to which dipole moments were induced via the application of a uniaxial or rotating electric or magnetic field. We analyzed the kinetic and structural data from these simulations, including computation of the dielectric constant. We synthesized electric-field–quenched, 1-D, polymer/ceramic nanocomposites for several ceramic particles over a broad range of particle loadings. We synthesized magnetic-field–quenched, 1-D, polymer/metal oxide nanocomposites for several iron oxides over a broad range of particle loadings.

We characterized the sample anisotropy by electron microscopy, complex permittivity, and magnetic susceptibility measurements. We made 2-D, time-resolved, light-scattering measurements of structural evolution in the 1-D systems. These measurements indicate that we can control the sample anisotropy most effectively by controlling the quench time and the particle concentration. The dielectric anisotropy computed from the simulation data agrees very well with the measured anisotropy, and this anisotropy can be inverted, relative to the uniaxial field, by applying a rotating field.

Engineered Stationary Phases for Chemical Separations

T. J. Shepodd, D. S. Anex

Sandia developed capillary separation technologies, coupled with laser detection techniques, to quantify neutral environmental samples with attomole sensitivity, a million theoretical plates/meter efficiency, using nanoliter volumes, in a few minutes. The resolving power of our capillary electrochromatography (CEC) columns exceeds that of commercial high-performance liquid chromatography (HPLC) instruments by more than an order of magnitude. In this project, we address one specific technical need that may facilitate achievement of further advances in chemical-analysis technologies.

CEC combines the strengths of capillary electrophoresis (CE) and HPLC. Rather than using pressure to drive the flow through the column, we utilized electroosmotic flow. We achieved polycyclic aromatic hydrocarbon (PAH) separations utilizing porous 3-micron particles in the stationary phase in ~ 1 hour. Upon switching to nonporous 1.5-micron particles, we reduced analysis time to ~ 1 minute with no loss in separation efficiency.

To make further advances toward extremely fast, efficient chemical separations, we propose to derivatize and test selectively engineered, minute-particle, stationary phases for use in capillary separations. Chemical analysis using nanoparticle stationary phases will be the exclusive domain of electro-osmotically driven CEC technologies. The proposed work is crucial to maintaining our lead in advanced chemical-analysis technologies, as well as future progress toward "chemical-analysis-on-a-chip."

We accomplished the following in FY96:

(1) Successfully synthesized and isolated 1.5 and 0.5 C_{18} derivatized silica.

(2) Established methodologies for successfully packing these media into capillary columns.

(3) Successfully demonstrated that the aforementioned media will support electroosmotic flow.

(4) Demonstrated that these packed columns could separate mixtures of organic compounds while operating as the stationary medium for capillary electrochromatography.

The successes of these experiments show that materials having particle sizes too small for conventional HPLC separations because of prohibitive back-flow pressures can be used as chromatography media when separation is driven by electroosmotic flow. The manifestation of these microseparations could be new, ultra-miniature devices for the separation and detection of chemical species. The successes of this work support new projects and chem-lab-on-a-chip–type devices. These experiments demonstrated only one type of derivatization on one type of substrate. Innumerable types of both substrates and derivatizing agents are available to capitalize on the concepts proven here. Specific surfaces can be designed on this scale that are efficiently tailored to a specific separation. Surfaces can be customized to attract or repel species of interest.

System Studies in Materials

M. J. Carr

This is a classified project. The work consisted of a review of relevant literature, model development, production of prototypes, and experimental verification.

Computational & Information Sciences

Calculated electrostatic component of the free energy of solution for the carbonate ion CO_3^{-2}.

The Charged Heterogeneous Electrostatic-Boundary Element Method (CHE-BEM) enables modeling of atomistic electrons that self-consistently interact with a heterogeneous dielectric continuum resulting, for example, from a molecule interacting with a catalyst or protein. This technique allows realistic systems modeling in areas from microelectronics and synthesis and processing of new materials to biotechnology, energy conversion, and environmental cleanup.

Coordinating Robotic Motion, Sensing, and Control in Plans and Execution

P. G. Xavier

The fundamental purpose of this project is to develop a framework for robotic planning and execution that provides a continuum of adaptability with respect to model incompleteness, model error, and sensing error.

After working on a problem in the area of flexible object manipulation last year, this year we returned to robot motion. Specifically, we addressed problems in modeling changing environments, on-line motion planning, and robust collision detection in dynamically changing modeled environments.

Sandia accomplished the following in FY96:

(1) Updated the Configuration Space Toolkit (C-Space Toolkit) to enable it to model changing environments and to efficiently answer queries for such environments. The new techniques improved both the capabilities and the performance of the C-Space Toolkit.

(2) Collaborated to integrate the SANDROS motion planner and the C-Space Toolkit. We tuned both components. The resulting system is roughly 2000 times as fast as the previous version of the SANDROS motion planner for problems that are realistically geometrically complex. We integrated it with the Telegrip robotic programming-and-simulation graphical user interface (GUI); the resulting system is the subject of a paper submitted to the 1997 International Conference on Robotics and Automation.

(3) Developed and implemented a new technique for fast-swept volume-distance computation and clash detection (interference detection). This technique is a building block for fast, robust collision detection and support queries that arise in run-time collision avoidance, assembly planning, simulation, motion planning, and other robotic problems.

Publications

Refereed

Watterberg, P. A., and P. G. Xavier. 1997. "Path Planning for Everyday Robotics with SANDROS." Paper to be presented to the IEEE International Conference on Robotics and Automation, Albuquerque, NM, 20–25 April.

Xavier, P. G. 1997. "Fast-Swept Distance for Robust Collision Detection." Paper to be presented to the IEEE International Conference on Robotics and Automation, Albuquerque, NM, 20–25 April.

Self-Repairing Control for Damaged Manipulators

G. R. Eisler, D. W. Lobitz

Remote operation of a robotic system is a requirement for operation in hazardous workplaces and in contaminated clean-up sites. Robust methods of control are needed that can deal with unexpected changes or damage to the system. The goal of this project is to develop software to enable damaged robotic manipulators to reconfigure their control systems autonomously, approximating their original tasks in a hazardous and constrained workspace. This effort seeks to develop off-line techniques for redundant sensor/actuator placement and on-line algorithms that account for various combinations of surviving assets. We will employ a nonlinear estimation-based fault-detection and -isolation scheme. We will implement this software on an experimental manipulator that will be able to simulate failed joints and sensors, as well as deformable flexible links.

Our accomplishments in FY96 include the following:

(1) Made the horizontal test-bed operational, and tested the fault-tolerant robot joint design. We added redundant angle encoders and strain gauges to the test-bed. Flexible and rigid links could be used interchangeably.

(2) Developed and tested an extended Kalman filter-based fault-detection and -isolation strategy. We built filters to test for a specific fault and operated them in parallel, each receiving the current sensor readings, either good or damaged, simultaneously.

(3) Developed a nonlinear control strategy that naturally utilizes available sensor information after fault isolation is accomplished. The scheme entailed using a computed torque algorithm, accounting for the known and unknown parts of the robotic model due to damaged sensors. We embedded proportional-derivative feedback from the sensors in the algorithm to "control" the "reduced" systems.

(4) Developed an analysis code for assessing the computational requirements for real-time, parallel computing applications.

(5) Developed and tested a nonlinear, minimum-time optimization code. The code embraced a new optimization method for computing minimum-time, rest-to-rest maneuvers of redundant link robotic configurations slewing in the horizontal plane. We then graphically animated these open-loop control solutions.

Publications

Other

Parker, G. G. 1996. "Operator-in-the-Loop Control of Rotary Cranes." Paper presented to the SPIE Smart Structures and Materials Conference, San Diego, CA, 27–29 February

Wilson, D. G. 1997. "Modeling and Robust Control of a Flexible Manipulator." Paper presented to the AIAA Symposium on Nonlinear Dynamical Systems, Reno, NV, 6–9 January.

Parallel Optimization Methods for Agile Manufacturing

J. C. Meza, S. A. Hutchinson, G. M. Reese, B. A. Hendrickson

The rapid and optimal design of new goods is essential for meeting national objectives in advanced manufacturing. Currently almost all manufacturing procedures involve the determination of some optimal design parameters. This process is iterative in nature and, because it is usually done manually, it can be expensive and time-consuming. The goal of this project is to develop optimization algorithms and software tools that will enable automated design, thereby allowing for agile manufacturing. Although the design processes vary across industries, many of the mathematical characteristics of the problems are the same, including large-scale, noisy, and nondifferentiable functions with nonlinear constraints. The goal of this research is to develop a common set of optimization tools using object-oriented programming techniques that will be applicable to these types of problems. We concentrated on several applications that are representative of design problems. Because the function evaluations are computationally expensive, we will emphasize algorithms that are adaptable to massively parallel (MP) computation.

We made the following accomplishments in FY96:

(1) We implemented a new class hierarchy for bound constrained objects. This allows for the general solution of optimization problems with simple upper and lower bounds.

(2) We implemented an active set Quasi-Newton method that handles bound constrained problems. We successfully used this method to solve an application controlling the deposition rate of a chemical vapor deposition (CVD) furnace.

(3) A bound constrained parallel direct search (PDS) method was delivered. This method can be used on any parallel machine that uses MPI (Message Passing Interface).

(4) We presented two talks at the Society for Industrial and Applied Mathematics (SIAM) Optimization Meeting in Vancouver, Canada.

(5) We copyrighted OPT++ and gave out four licenses.

(6) We developed a new interface to the nonlinear optimization package NPSOL.

Publications

Refereed

Meza, J. C., R. S. Judson, T. R. Faulkner, and A. M. Treasurywala. 1996. "A Comparison of a Direct Search Method and a Genetic Algorithm for Conformational Searching." *J. Computational Chem.* **17** (July): 1142–1151

Moen, C. D., P. A. Spence, J. C. Meza, and T. D. Plantenga. 1996. "Automatic Differentiation for Gradient-Based Optimization of Radiatively Heated Microelectronics Manufacturing Equipment." *Proc. 6th AIAA/NASA/ISSMO Symp. on Multidisciplinary Analysis and Optimization* **2** (Bellevue, WA, 4–6 September): 1167–1175

Other

Diebolt, J., and E. H. S. Ip. 1995. "A Stochastic EM Algorithm for Approximating the Maximum Likelihood Estimate." SAND95-8201, March.

Ip, E. H. S. 1995. "A Stochastic EM Estimator in the Presence of Missing Data—Theory and Applications." SAND95-8103, April

Ip, E. H. S. 1995. "Estimation in Second-Order Dependency Model for Multivariate Binary Data." SAND95-8100, April.

Ip, E. H. S., and J. Diebolt. 1995. "A Stochastic Difference Equation Approach to Inference with Missing Data: Some New Results." SAND95-8101, April.

Meza, J. C., and T. D. Plantenga. 1995. "Optimal Control of a CVD Reactor for Prescribed Temperature Behavior." SAND95-8224, April.

Moen, C. D., P. A. Spence, and J. C. Meza. 1995. "Optimal Heat Transfer Design of Chemical Vapor Deposition Reactors." SAND95-8223, April.

Physical Simulation of Nonisothermal Multiphase Flow in Porous Media

M. J. Martinez, C. K. Ho, R. J. Glass, J. N. Shadid, R. R. Eaton, P. L. Hopkins

The objective of this project is to develop a fundamental understanding of, and parallel computational tools for, simulation of nonisothermal, multiphase, multicomponent flow in heterogeneous porous media. This capability is critical to Sandia's business development in environmental remediation, nuclear waste management, reservoir engineering, fuel-spill fires for weapon safety, and manufacture (curing) of sol-gel coatings.

The successful completion of this project raised simulation capabilities for multiphase flow in porous media to a new level; large-scale, 3-D multiphase simulations with high resolution of heterogeneities are feasible and can be performed routinely. The simulator not only runs on Sandia's massively parallel (MP) computers (Intel Paragon), but can also be run on networked systems using the message passing interface (MPI) software. To date, mostly 2-D simulations had been possible, due to limitations in simulator capabilities, thereby severely compromising the ability to perform realistic simulations. Simulations performed with our MP code demonstrated that full 3-D, high-resolution simulations of highly heterogeneous geologic media are possible. As a result, we negotiated and performed a series of high-resolution, pre-emplacement groundwater simulations for the Yucca Mountain Project (YMP). Such capability enables realistic simulations of subsurface transport in highly heterogeneous media.

We achieved successful development of a general-purpose, unstructured grid, nonisothermal, multiphase simulator for subsurface transport in heterogeneous geologic media. We implemented a nonisothermal, two-phase (liquid and gas), two-component (water and air) mathematical model for use on MP computers via message-passing and domain decomposition techniques that

can also be used on scalar computers. We used the MPSalsa code as the platform for this development effort. This project development effort leveraged Sandia expertise in domain decomposition, linear solver technology for parallel computers, finite-element (FE) technology applied to flow problems, and expertise in modeling multiphase flow problems.

We verified the code by applying it to a series of model problems for which (numerical) solutions are available. We verified the simulator for isothermal unsaturated flows and, more importantly, for two-phase, heat-driven flows in homogeneous and heterogeneous domains, thus verifying the multiphase implementation. We also verified the parallel implementation by comparing simulations performed on a single-processor computer with those performed on parallel computers. These problems also demonstrated scalability of the MP algorithms. A common misconception is that the parallel capabilities are accessible only on MP computers, but in fact, parallel simulations have been performed on a network of workstations, which are fairly common to the scientific community

Because of its unique capabilities, we applied the code to a high-resolution, fractured-flow simulation in cross-sections of Yucca Mountain. The numerical grid for this cross-section contains over 73,000 grid points, with some grid spacings as small as one meter. This is the first flow simulation of Yucca Mountain to include such fine geologic detail. The study demonstrated that the moisture flow in the vicinity of the proposed repository horizon can be highly dependent on the stratigraphic units included in the model. To further demonstrate the benefits of MP processing, we applied the code to model hydrothermal flow in a large-scale, 3-D model of the Yucca Mountain region. We obtained pressure, temperature, and moisture distributions for simulations on a mesh consisting of 358,000+ grid points in which over 1 million equations are solved at each time-step in simulations requiring many hundreds of time-steps to simulate flow over many thousands of years. This is a unique capability.

Based on preliminary experiments, we completed the fabrication of the experimental system for conducting multiphase flow experiments. We designed the experiments to measure temperature, saturation, and velocity fields within a forced convective field driven by heating of opposing boundaries. We performed several side-heated experiments. Unfortunately, the data indicate insufficient control of heat-losses through the test cell faces, rendering the data unusable as a 2-D convection cell, the original intent of the experiment. Because of the heavy heat losses, the convection is 3-D. However, the heat loss distribution is unknown, so the data are not sufficiently characterized for validation, but are useful for understanding two-phase flow phenomenology.

To enable statistical analysis of the impact of spatially correlated heterogeneity and uncertainty analysis, the ability to couple the code with geostatistical property simulators should be implemented. The code's applicability to nonaqueous phase liquid (NAPL) remediations could be greatly enhanced by implementing a three-phase, multicomponent capability, which would entail a significant development effort.

Publications

Refereed

Ho, C. K. 1995. "Multicomponent Three-Phase Equilibria." SAND95-1063, June.

Ho, C. K. 1995. "Numerical Simulations of Multicomponent Evaporation and Gas-Phase Transport Experiments Using M^{2}NOTS." *Proc. 1995 ASME/AIChE National Heat Transfer Conference* (Portland, OR, 5–9 August).

Martinez, M. J. 1994. "Formulation and Numerical Analysis of Nonisothermal Multiphase Flow in Porous Media." SAND94-0379, June.

Martinez, M. J. 1995. "Mathematical and Numerical Formulation of Nonisothermal Multicomponent Three-Phase Flow in Porous Media." SAND95-1247, September.

Martinez, M. J., and R. H. Nilson. 1996. "Estimates of Barometric Pumping of Moisture Through Unsaturated Fractured Rock." *J. Water Resources Research,* submitted.

Martinez, M. J., P. L. Hopkins, and J. N Shadid. 1994. "A Nonisothermal Multiphase Subsurface Transport Simulator for Unstructured Grids on Parallel Computers Using Domain Decomposition and Message-Passing Techniques." Paper presented to the 4th SIAM Conference on Mathematical and Computational Issues in the Geoloscience, Albuquerque, NM, 16–18 June.

Martinez, M. J., P. L. Hopkins, and J. N. Shadid. 1996. "Physical Simulation of Nonisothermal Multiphase Multicomponent Flow in Porous Media." SAND report, in preparation.

Martinez, M. J., P. L. Hopkins, and M. W. Glass. 1995. "Modeling Flow in Porous Media on Parallel Computers." First Biennial Tri-Laboratory Engineering Conference, Pleasanton, CA, 31 October–2 November.

Other

Hopkins, P. L., M. J. Martinez, and M. W. Glass. 1995. "Benchmarking the Implementation of Unsaturated Flow Capabilities in SALSA." Memo to distribution, June 30.

Monte Carlo Simulation of Radiation Heat Transfer in Reacting Flows by Massively Parallel Computing

J. F. Grcar, A. Ting, J. N. Shadid, W. G. Houf

Since radiant transport is a significant means of energy transfer in many applications, its determination is of considerable practical importance. For example, clean, easily controlled radiant heating is the preferred source of energy in advanced manufacturing. Monte Carlo (MC) methods represent the only practical approach capable of easily incorporating almost any desired radiative feature. This project therefore investigates simulating radiative thermal transport by MC methods on massively parallel (MP) computers. We prepared the MC simulations for coupling with simulations of thermal conduction. The combined simulations will provide a capability to simulate the reactive and radiative environments found in many manufacturing and energy-conversion processes.

We rewrote the radiation transport simulation code completed during the previous year to make use of message-passing interface (MPI) software. This communication protocol is evolving into the standard for portable parallel computing. In contrast to the NX message-passing software developed for Intel Paragon machines, MPI imposes explicit data types on receive operations. This subtly complicates the manager/worker structure of the simulation software, where it is desirable to receive arbitrary mixtures of command and data messages distinguished by a data type determined after receipt. Nevertheless, we successfully converted the simulation code to the MPI interface and ran it on an SGI (Silicon Graphics, Inc.) shared-memory parallel computer different from Sandia's distributed-memory Paragon machines.

We wrote a preprocessor for the radiation code to enable it to read problem geometries maintained in Sandia's Exodus data base format. The preprocessor previously prepared for the code enables it to read problem definitions from the data bases maintained by the Patran commercial meshing software. The radiation code can accept input prepared from a variety of internal and external sources.

We examined the electromagnetic formulation of thermal radiation for feasibility of refining the geometric laws of transmission. It is known that both the angle and the fraction of transmission vary not only with the angle of incidence but also with the phase of the incident wave. The effect on absorption is pronounced but the effect on angle is marginal; both are usually ignored in radiative heat transfer calculations. However, in special cases, such as transmission through many thin, partially absorbing films, these effects may be significant. The customary laws of transmission are obtained by assuming nonabsorbing media, and usually additionally, that all angles of polarization are equally likely, i.e., unpolarized radiation. Verification of these laws in terms of electromagnetic theory rests on analyses performed at the turn of the century. Modern tools for the manipulation of mathematical formulas, such as Mathematica, might permit the derivation of more refined laws that would enable the MC simulation to capture subtle effects of absorption and polarization. We obtained some formulas by this method, but despite much effort we were unable to find a workable simplification of the formulas, and we decided to forgo including these effects in the simulation.

MP System Software Libraries: Making High Performance Practical

K. S. McCurley, D. S. Greenberg

Sandia augmented the system software for distributed-memory/message-passing programs and tested it with actual applications. In particular, we implemented the MPI-1 (Message Passing Initiative) standard on both the Intel Paragon and the prototype hardware for the DOE/ASCI (Department of Energy/Accelerated Strategic Computing Initiative) teraflop machine. We implemented a version of the yet-to-be-ratified MPI-2 one-sided communication protocols and tested it for acceptability. Production codes at Sandia are using these libraries, and all three weapons labs have reported good success using the libraries on the prototype hardware.

We defined a one-sided communication syntax that conforms to the draft MPI-2 standard. One-sided communication allows a programmer to set up a "window" into a processing elements address space from which other processing elements can put and get data. We implemented this protocol on the teraflops prototype hardware. Users at all three weapons labs have used the implementations. Of particular note is that the Los Alamos National Laboratory (LANL) users felt that for many codes our implementation was competitive with the Cray T3D's hardware implementation.

We implemented several optimized routines for collective communication.

We worked with applications coders at Sandia and LANL to convert their codes to use the MPI interfaces. We used new concepts such as communicators that isolate independent portions of the code, and collective communications that allow optimized routines to be used for common operations such as broadcast.

Publications

Other

Brightwell, R., and A. Skjellum. 1996. "MPICH on the T3D: A Case Study of High-Performance Message Passing." Paper presented to the MPI Developers Conference, Notre Dame, IN, 2 July.

Brightwell, R., and L. Shuler. 1996. "Design and Implementation of MPI on Puma Portals." Paper presented to the MPI Developers Conference, Notre Dame, IN, 1 July.

A Massively Parallel 2-D Hybrid Continuum-to-Noncontinuum Fluid Code

T. J. Bartel, R. J. Cochran, M. L. Hudson

Many fluid-flow problems in manufacturing, weapons nonproliferation, and weapons design require the solution of gas flows that combine continuum and noncontinuum flow regions within a single domain. Examples of such flowfields include those within plasma etch or deposition reactors, which are used to manufacture semiconductor wafers and flowfields around space vehicles. Currently, these mixed flowfield problems are entirely computed with either a continuum or a noncontinuum model. Continuum models do not accurately simulate the molecular transport processes within the noncontinuum regions of the flowfield. Applying a noncontinuum model, such as the particle-based Direct Simulation Monte Carlo (DSMC) technique, to mixed noncontinuum/continuum problems will provide accurate results; however, the computational resources needed in both memory and compute time are enormous and not even possible for engineering design problems. We identified hybrid strategies to be used for two different flow regimes: (1) incompressible, subsonic, and (2) compressible, supersonic. We propose to develop 2-D hybrid codes that can use the appropriate formulation of the continuum/noncontinuum transport equations in regions where they are valid. We will develop these hybrid codes for the massively parallel (MP) computing environment to take advantage of the tremendous speedups for particle-based algorithms. We will investigate two methods for solving the continuum flowfield: a partial differential-based hybrid and an all particle-based method. The first is the direct solution of the Navier-Stokes (N-S) equations; the second is particle-based methods that simulate the N-S equation. We will validate the three hybrid codes with existing flowfield data from various manufacturing applications. This new capability will be directly applicable to new programs with our current customers as well as provide access to new customers.

We developed and investigated the coupling of a hybrid technique for solving the chemically reacting plasma system for a microelectronics etch chamber. We used a continuum code for the electrons/ions and a particle code for the ions and neutrals. After the necessary mechanics of developing the required interface codes as an interpolation between grids, we investigated the convergence of hybrid methods for low-pressure systems versus consistent continuum solvers. We concluded that hybrid techniques will never really converge since the physics being modeled is interpreted differently in the two methods. Particle methods are inherently different from continuum methods. For example, a gas-phase chemical reaction in a continuum code is simply modeled by the appropriate rate equation. However, in a kinetic code, the collisional cross-section must be determined so that the reactants can collide, and a steric factor used to determine if they will react. There can be no reaction if they do not collide, which is a big problem for low-pressure systems. Based on this work, we are currently moving away from the hybrid strategy and developing a self-consistent particle plasma code for these problems.

We tried to extend the DSMC technique to very high-pressure applications. Flow through a microelectromechanical system (MEMS) was the test problem. The pressure range was from 1–2 atm, and the flow was very subsonic. We used the collision limiter work, which greatly decreased the runtime for the traditional DSMC technique. However, the average flow velocity was so low (< 1 m/s) that the average thermal speed of the particles (350 m/s) dominated the statistical uncertainty. We tried to develop strategies where the particles were transported at the mean velocity rather than the thermal velocity, but we are currently unsuccessful at achieving this. This part of the project represented the highest risk or level of uncertainty.

Publications

Other

Bartel, T. J., J. E. Johannes, and D. J. Economou. 1996. "Continuum Versus Kinetic (DSMC) Plasma Reactor Scale Model." Paper presented to the American Vacuum Society Meeting, Philadelphia, PA, 14–18 October.

Hudson, M. L., and T. J. Bartel. 1996. "DSMC Simulations of Reactor Feature Scale Flows." *J. Vac. Sci. & Technol. B*, in press.

Johannes, J. E., T. J. Bartel, D. M., Sears, and J. L. Payne. 1996. "Gemini: A Hybrid Plasma Modeling Capability for Low-Pressure Systems." SAND96-0590, October.

Wong, C. C., M. L. Hudson, T. J. Bartel, and J. L. Payne. 1996. "Simulation of Rarefied Flows in MEMS Devices." *J. Vac. Sci. & Technol. B*, in press.

General Techniques for Constrained Motion Planning

P. A. Watterberg

The objective of this project was to build a hierarchy of motion planners based on a novel search strategy called SANDROS. *The motion planners are hierarchical in that the motion planner for a particular-dimensional task decomposes a task into a series of lower-dimensional tasks and invokes the motion planner for those tasks. Sandia also developed a method to select the optimal robot-base position and orientation that result in the shortest path for the robot manipulator. The project also makes a significant contribution to the field by the development of a systematic classification of robotic tasks and the development of motion planners according to this classification.*

To accomplish the desired task, almost all robots must move their joints in a coordinated, deliberate manner. This turns out to be a problem since the movement has to respect the manipulator kinematic constraints and task-related constraints on the toolpaths, and to avoid collisions with objects in the work space. To manually teach a robot such a path can take weeks. Some applications are completely unfeasible. We made great strides in making this process computationally feasible. Problems that took hours or days on the computer are now done in seconds.

In the last year, we completed work on motion planners to do zero-dimensional (0-D) tasks (such as welding spots or drilling holes) and 1-D tasks (such as cutting sheet metal or finishing an edge). We sketched out extending the planners to higher dimensions (such as painting, 2-D, or building volumes, 3-D). The implementation of these algorithms confirmed the SANDROS strategy as an extremely fast one. We implemented versions of these algorithms in real projects to test them in real environments. Results of these tests show that the planners are fast enough to use everyday.

We also developed an algorithm to help with robot placement for achieving minimum cycle time. Thus the robot can do each task faster.

Publications

Refereed

Hwang, Y. K. 1996. "Completeness vs. Efficiency for Real Applications of Motion Planning." Paper presented to the IEEE International Conference on Robotics and Automation, Minneapolis, MN, 22–28 April.

Hwang, Y. K., and P. A. Watterberg. 1996. "Optimizing Robot Placement for Visit-Point Tasks." Paper presented to the AAAI Workshop on Artificial Intelligence and Manufacturing, Albuquerque, NM, 24–26 June.

Hwang, Y. K., P. C. Chen, and P. A Watterberg. 1996. "Interactive Task Planning Through Natural Language." Paper presented to the IEEE International Conference on Robotics and Automation, Minneapolis, MN, 22–28 April.

Automated Meshing: A Critical Link in Realizing Large Massively Parallel Adaptive Finite-Element Analysis

R. R. Lober, S. W. Attaway, S. J. Plimpton, C. T. Vaughan, T. J. Tautges

The finite-element (FE) method is an established, widely used modeling technique in the engineering analysis community. Although massively parallel (MP) machines have proven useful for these calculations, adaptive FE analysis on these machines has largely been unexplored. The paving mesh-generation algorithm provides adaptive meshes that match typical error function distributions with appropriately sized quadrilateral elements. However, the algorithm is completely serial in nature, and in its present form would not provide the meshing capabilities needed for parallel adaptive analysis. Sandia investigated the feasibility of providing a framework for parallel mesh generation (paving) in support of parallel adaptive FE analysis (h-remap method full-remeshing). The work focused on the parallel redesign of the paving- meshing algorithm and how that parallel design compares to the serial version of the algorithm.

Parallel computing is required to achieve large-scale adaptive analysis, a compute-intensive operation. Some of the difficulties in performing this analysis in a parallel environment include generating a large mesh model and distributing the model over the compute nodes, then regenerating and redistributing each time the analysis "adapts." The parallel methods to accomplish this must compare favorably with their serial counterparts for performance and quality. This research addresses these issues by prototyping a parallel version of the paving-meshing algorithm.

We determined that the paving itself could be used serially to generate a coarse background mesh that provided a topology to be decomposed into subdomains. We then created the final dense mesh in parallel by paving each subdomain independently once the subdomain boundary discretizations were negotiated between adjacent subdomains. Both the initial coarse background mesh and the final dense mesh can be generated adaptively if desired, where the local element size is determined by querying a field function (typically an error function from a previous run), yielding an appropriately sized mesh that captures error gradients for finer resolution and increased solution accuracy.

The generation of a paved mesh in parallel is feasible from both a performance and a mesh-quality standpoint. Performance data on an IBM SP2 parallel machine yielded super-linear speedups over a variety of problem sizes (1040 to 21286 FE nodes) with parallel runs of

two, four, and eight compute nodes. Efficiencies from these runs (speedup/number of processors) ranged from 83 to 122 percent, becoming more efficient as more parallel compute nodes are employed. Mesh quality between the serially paved mesh and the 8-node parallel equivalent was acceptable: element aspect ratio and skew degraded by 9 and 23 percent, respectively, while element taper improved slightly by 9 percent. Conclusions regarding the performance of the dynamic load balancer cannot be stated yet, as time limitations precluded the testing of this capability sufficiently. When the mesher begins to generate adaptively, the parallel subdomains will go out of balance rapidly, necessitating a capable parallel load balancer.

Publications

Refereed

Lober, R. R., T. J. Tautges, and R. A. Cairncross. 1995. "The Parallelization of an Advancing-Front, All-Quadrilateral Meshing Algorithm for Adaptive Analysis." *Proc. 4th Internat. Meshing Roundtable* (Sandia National Laboratories, Albuquerque, NM, 16–17 October): 59–70.

Other

Tautges, T. J., R. R. Lober, C. T. Vaughan, and J. Jung. 1995. "The Design of a Parallel Adaptive-Paving All-Quadrilateral Meshing Algorithm." *Proc. 6th Internat. Symp. on Computational Fluid Dynamics III* (Lake Tahoe, NV, 4–8 September): 1255–1260. Japan Society of CFD.

Parallel Quantum Chemistry for Material Aging and Synthesis

C. F. Melius, M. E. Colvin

Massively parallel (MP) computers will be used to predict the aging of materials and optimize the synthesis of new materials. Sandia is developing a new hybrid quantum chemistry procedure for accurately calculating the thermochemical properties of these materials. The procedure will incorporate a combination of density functional theory (DFT) methods and Hartree-Fock (HF) methods along with Möller-Plesset perturbation theory methods, using various basis sets for each calculation step. We will implement the methods to run on MP machines as well as on distributed shared-memory machines.

We determined the thermochemical accuracy of various quantum chemistry methods, involving hybrid Hartree Fock-Density Functional Theory (HF-DFT) and Möller-Plesset second-order perturbation theory (MP2), using a variety of different basis sets. We found that while the absolute errors in the heats of formation for the various methods can be quite large, the errors are, for the most part, systematic, and that the bond additivity approach (BAC) should work for both the hybrid HF/DFT and the MP2 methods. We also implemented object-oriented code to treat open shell molecules (i.e., radicals) on the MP quantum chemistry code MPQC. We developed algorithms to calculate vibrational frequencies for both the HF and MP2 perturbation theory methods. We also developed algorithms for incorporating generalized gradient corrected density functionals into the MP version of the DFT code QUEST.

Publications

Refereed

Melius, C. F., M. E. Colvin, N. M. Marinov, W. J. Pitz, and S. M. Senkan. 1996. "Reaction Mechanisms in Aromatic Hydrocarbon Formation Involving the C_5H_5 Cyclopentadienyl Moiety." *Proc. 26th Internat. Symp. on Combustion* (Pittsburgh, PA, 28 July–3 August).

User-Interface Test-Bed for Technology Packaging

H. W. Allen, T. L. Edwards

This project addresses the design and development of a generic graphical user-interface (GUI) test-bed for technology packaging. This test-bed will facilitate the design and development of effective GUIs for existing and future applications. Designers and developers can use this test-bed to compare, evaluate, and select GUI features. The test-bed will provide a means to qualitatively and quantitatively assess GUI complexity, adherence to human factors principles and guidelines, and adherence to development standards (e.g., OSF/Motif). In addition, it will provide (1) tools to teach the developer human factors engineering (HFE) and how to apply it to their designs, (2) an automated HFE testing capability, (3) an on-line HFE reference document, (4) a capability to observe and statistically analyze users interacting with the applications, (5) an environment to teach users to interact with GUI elements in general, and application-specific elements in particular, and (6) a demonstration platform to educate application developers.

Evaluating a user-interface design is a time-consuming but necessary part of the software engineering process. To evaluate a design, the engineer must find a way to record a user's interactions to the user interface and then analyze the interactions. With this information an interface designer will know how the user interface was used in a particular session. Typically this work is completed with a VCR and exhaustive analyzing of the recorded or edited tapes. We need software methods to automate some of the analyzing process.

This project created prototype applications that will record the interactions of a GUI and display the interactions in a visual method to the HFE. We created these applications to run on the Unix and Windows95 platforms.

We created the prototype to help interface designers and HFEs visualize their link analysis of GUIs. Link analysis is a method to evaluate an interface by recording the interactions between buttons and menus of an interface.

We encountered many problems in gathering information about the GUI in order to duplicate it. Instead we captured an image of the GUI and stored it to disk. The hardware graphics system presented a problem with gathering information about GUIs. There are numerous graphics systems available today, and being able to grab an image off the GUI differs per graphics hardware system. We created a user-interface laboratory to test user-interface designs.

Self-Consistent Coupling of Atomistic and Continuum Electrostatics Using Boundary Element Methods

C. F. Melius, E. Mori, W. D. Wilson

The Charged Heterogeneous Electrostatic-Boundary Element Method (CHE-BEM) is providing realistic environments for molecular interactions. Sandia developed the capability to couple electronic structure, atomistic, and continuum calculations in a self-consistent framework satisfying the fundamental laws of electrostatics. This is enabling high-performance computers to accurately simulate material properties at the molecular level. CHE-BEM enables the atomistic, quantum mechanically treated electrons to self-consistently interact with a heterogeneous dielectric continuum. The CHE-BEM technique is applicable to areas ranging from aging of the nuclear stockpile and synthesis and processing of new materials to biotechnology, energy conversion, and environmental cleanup.

We developed the CHE-BEM to incorporate solvent effects, including ionic strength, into the *ab initio* electronic structure methods. The method couples the Schrodinger equation with the Green's function involving the linearized Poisson-Boltzmann equations, and includes both the single- and double-layer surface-charge distributions induced at the molecular-solvent interface. We generalized the method to include an arbitrary number of boundaries with the single and double layers. This enables the molecule to interact with different dielectric environments and with different ionic concentrations at different parts of the molecule. We investigated various gridding schemes for discretizing the boundary between the molecule and the dielectric continuum and applied the method to a variety of systems. In one example, we investigated both the solvation of both neutral and charged molecular species in an ionic solvent containing differing pH strengths and the various counter ion concentrations. In another example, we investigated the interaction of molecules with the surfaces of solids. The environment conditions above the surface included both the vacuum and a dielectric solvent, and we investigated various ionic concentrations in the solvent above the surface.

Computation of Chemical Kinetics for Combustion

M. L. Koszykowski, R. C. Armstrong

This project addresses the implementation of Quantum Monte Carlo (QMC) techniques to the direct evaluation of fully quantum mechanical rate constants. As part of this project we implemented a QMC code on a variety of platforms, including the Paragon. The code demonstrated a scaling efficiency of > 95% on the Paragon, demonstrating the applicability of parallel methods to solving this class of computational problems. We confronted the task of understanding in greater detail the convergence of the path integrals used in this work.

This project sought to perform fully exact quantum mechanical rate calculations using the QMC method. Quantum mechanical rate calculations correctly treat tunneling and recrossing, effects that are either approximated or ignored in conventional rate-constant calculations. Tunneling is the process by which an atom (typically H-atom) travels through a classically forbidden barrier to reaction. In this way, reaction can occur without the reactants having enough energy to surmount the reaction barrier. Reactions involving tunneling are expected to be important in materials aging processes. Since extrapolation of higher-temperature data to lower temperatures underestimates rates of reactions mediated by tunneling, often by orders of magnitude, accurate modeling of these reactions will be a necessary adjunct to accelerated aging studies. We successfully constructed a code to carry out the required calculations, used Parallel Object-Oriented Environment and Toolkit (POET) to parallelize it, then ported it to the Paragon. We tested the code on the H + H_2 reaction and found that it yields accurate, precise answers. In benchmarks on the Paragon we observed scaling efficiencies > 95%, validating our use of POET for the code parallelization.

We assembled enough information to recognize that convergence was going to be a greater problem than was noted before. We therefore modified our plans and devoted considerable effort to the characterization of the convergence behavior and the patterns in path cancellation, which would help us accelerate convergence. This work uncovered a number of properties of the path integrals used that had not been found by previous workers in the field. These properties allowed us to extend our calculations to longer times than had been previously possible.

Publications

Refereed

Gentile, A. C., D. A. Evensky, J. L. Durant, N. J. Brown, and M. Koszykowski. 1996. "Convergence and Path Cancellation in Quantum Monte Carlo Real-Time Path Integration." *J. Chem. Phys.* **105** (1 November): 7613–7616. New York, NY: AIP.

Parallel, Object-Oriented Toolkit for Simulation Software

M. E. Colvin, D. E. Womble, M. L. Koszykowski

Advances in computational simulation methodology and computer technology have made it possible to accurately model

many physical processes. However, the development of simulation algorithms that utilize high-performance computer architectures is a difficult and time-consuming task. This is due to the fundamental complexity of the processes being simulated and the practical need to efficiently utilize a variety of computing environments, including single processors, shared-memory multiprocessors, distributed workstations, and massively parallel (MP) processors. To simplify this task, we will develop a simulation toolkit in the C++ language. This toolkit will consist of a flexible set of classes that can be used to rapidly implement specialized applications optimized for available computer hardware. Additionally, we will design this toolkit to be readily extendible to new computational simulation methods.

The goal of this project was to develop and apply to real applications a sophisticated C++ class library supporting parallel matrix operations. We successfully completed this library, SCMAT (Scientific Computing MATrix library), and integrated it into several scientific applications.

We designed the SCMAT around a set of matrix abstractions that permit very general matrix implementations. This flexibility is needed to support diverse computing environments. This library supports a wide range of architectures: uniprocessors, loosely coupled clusters of processors (each with enough memory to store all matrices), tightly coupled clusters of processors with a fast interconnect network (such as the Intel Paragon), and clusters of machines that do not have enough memory to hold entire matrices.

The design of SCMAT differs from other object-oriented matrix packages in an important way. The matrix classes are abstract base classes. No storage layout is defined, and virtual function calls must be used to access individual matrix elements. The interface to the matrix classes is rich enough to avoid individual matrix element access for any computationally significant task.

The primary abstract classes are SCMATrix, SymmSCMATrix, DiagSCMATrix, and SCVector. These represent matrices, symmetric matrices, diagonal matrices, and vectors, respectively. These abstract classes are specialized into groups of classes based on the parallel distribution scheme of the matrix. If a needed matrix operation is missing, mechanisms exist to add more general operations. Operations that depend only on individual elements of matrices can be provided by specializations of the SCElementOp class.

Other features of SCMAT include run-time–type facilities and persistence. Castdown operations (type conversions from less to more derived objects) and other run-time–type information are provided by the DescribedClass base class. Persistence is not provided by inheriting from SavableState base class as is the case with many other classes in the SC utility class hierarchies because it is necessary to save objects in an implementation-independent manner.

Publications

Refereed

Colvin, M. E., C. L. Janssen, and E. T. Seidl. 1995. "Object-Oriented Quantum Chemistry Programs for Parallel Computers." Paper presented to the American Chemical Society Symposium on Application of Parallel Computing to Computational Chemistry, Anaheim, CA, 2 April.

Other

Janssen, C. L., E. T. Seidl, I. M. B. Nielsen, and M. E. Colvin. 1996. "The Scientific Computing (SC) Matrix Library." Sandia Technical Report, SAND97-8200, October.

Optical Communication for Future High-Performance Computers

Y. Frankel, P. D. MacKenzie

This report analyzes Sandia's research on routing algorithms applicable to optical networks for high-performance parallel computers. Sandia designed a new dynamic routing protocol in which the expected time any message spends in the system is constant, independent of the number of processors connected to the network. We then studied when rates are high enough (but strictly less than the capacity of the network), and the expected time a message spends in the system for all dynamic routing protocols.

We developed a protocol in which messages are transmitted in constant expected time over the network, i.e., independent of the number of processors connected to the network. Outside researchers developed a previous protocol with average message waiting time that grows only logarithmically in the number of processors. Assuming that processors can reach agreement on a global clock, they developed a protocol with constant average message waiting time. Our protocol does not need global agreement on a clock, which is difficult to achieve, but it still can achieve constant average message waiting time.

Another accomplishment was proof that in any protocol, messages will be delayed for linear time, on average, if the rate is sufficiently high (but still below the capacity of the network). Previously, this was known for only certain classes of protocols. This type of proof helps us to understand dynamic routing in optical networks, shows limits to what we are able to accomplish in designing routing protocols, and guides us toward realistic goals.

Publications

Refereed

Goldberg, L. A., and P. D. MacKenzie. 1996. "Analysis of Practical Backoff Protocols for Contention Resolution with Multiple Servers." Paper presented to the ACM-SIAM Symposium on Discrete Algorithms, Atlanta, GA, 28 January.

Computer-Designed Molecular Memory and Switching Elements

J. A. Shelnutt

Sandia is developing the computational methods necessary to engineer photophysical properties of molecules for optical-switching and memory applications, with the primary purpose of engineering the basic physical and chemical processes. We are extending massively parallel (MP) quantum and classical molecular modeling methods and using them to tailor the magnetic, optical, and/or structural properties of materials for molecular-scale memory devices. By using conformational trapping mechanisms and modifying the structure of the organic part of the molecules, the photophysical properties (e.g., state lifetimes, magnetic and optical properties) of a class of organometallic compounds are being controlled to an unprecedented degree. We are synthesizing some of the designed molecules and characterizing their optical and magnetic properties for validation of the theoretical predictions.

We identified nanoscale bioelectronic devices as having the highest value and probability of success for both near-term and future commercial and defense needs. These materials offer significant advantages in access and switching speeds, radiation hardness, and weight relative to metallic systems for emerging ultra–high-density memory technologies. Possible applications are for monolithic optoelectronic integration, sensors, bio-optics, displays, optical-switching windows, optical communications, and computing. High-information–density devices are of preeminent commercial interest and offer opportunities for quantum improvements in information storage.

We completed benchmark electronic structure calculations of Ni porphine (NiP) with Hartree-Fock (HF) *ab initio* methods and with density functional theory (DFT) at various levels of approximation. We compared the results of these calculations with the structure of NiP obtained by x-ray crystallography. At the HF level of theory, we used four different basis sets to compute the electronic and geometric structures of NiP. Because of the shallow nature of metalloporphyrin potential energy surfaces, we used very tight convergence thresholds to ensure that we achieved true stationary points (such as minima or saddle points). Comparison with the experimental x-ray structure of NiP showed good agreement. Sensitivity of the geometrical parameters to basis set size is apparent only in the Ni-N bond distance and not in the organic framework. We obtained similar results using DFT for different basis sets and levels of approximation. We also completed single-point calculations of energies of NiTtBuP conformers using both HF and DFT methods, and we compared the energies to those given by classical molecular mechanics. We completed single-point energies of the three conformers of NiTtBuP (ruffled, domed, and waved) given by Model 1 at the HF/STO-3G and HF/3-21G levels and the LDA/STO-3G level. The ruffled conformer is lowest in energy with all computational approaches; the dome and waveforms are at higher energy. These results are in agreement with the experimental detection of only the ruffled conformer by Raman spectroscopy.

We initiated geometry optimizations of the NiTtBuP conformers with *ab initio* methods. We obtained experimental results for comparison with theory and to deduce structure-function relationships. Specifically, we obtained new time-resolved absorption data for the tetra-adamantyl porphyrin, which gave further supporting evidence of an "induced-fit" mechanism for independently controlling barrier heights and conformer energies of the molecular memory materials. We completed continuous wave (CW) resonance Raman and absorption measurements on a series of 12 tetra-substituted Ni porphyrins to determine the effect of axial ligation on the energies of the "off" and "on" states and the effect of macrocycle distortions on axial ligand affinity.

Publications

Refereed

Jentzen, W., I. Turswska-Tyrk, W. R. Scheidt, and J. A. Shelnutt. 1996. "Solid-State and Solution Structures of (Porphinato)nickel(II) Are Planar by X-Ray Diffraction and Resonance Raman Spectroscopy." *Inorg. Chem.* **35** (May): 3559–3567. Washington, DC: American Chemical Society.

Jentzen, W., X. Z. Song, and J. A. Shelnutt. 1996. "Conformation of the Porphyrin Macrocycle Is Conserved in Hemoproteins of the Same Functional Class." *J. Am. Chem. Soc.*, in press. Washington, DC: American Chemical Society.

Song, X. Z., W. Jentzen, S. L. Jia, J. G. Ma, L. Jaquinod, D. J. Nurco, C. J. Medforth, K. M. Smith, and J. A. Shelnutt. 1996. "Metal-Dependence of the Relative Contributions of Low-Frequency Normal Coordinates to the Sterically-Induced Distortions of meso-di-Substituted Porphyrins." *J. Am. Chem. Soc.*, to be submitted. Washington, DC: American Chemical Society.

Song, X. Z., W. Jentzen, S. L. Jia, L. Jaquinod, D. J. Nurco, C. J. Medforth, K. M. Smith, and J. A. Shelnutt. 1996. "Representation of Nonplanar Conformers of Nickel(II) 5,15-Di-Substituted Porphyrins in Terms of Displacements Along Low-Frequency Normal Coordinates of the Macrocycle." *J. Am. Chem. Soc.* **118**: 12975–12988. Washington, DC: American Chemical Society.

Other

Gao, F., H. Qin, M. C. Simpson, J. A. Shelnutt, D. B. Knaff, and M. R. Ondrias. 1996. "Resonance Raman Characterization of Cytochrome bc1 Complexes." *Proc. Internat. Conf. on Raman Spectroscopy* **1** (Chichester, UK, 11–16 August): 466–467. New York, NY: John Wiley & Sons, Inc.

Jentzen, W., X. Z. Song, and J. A. Shelnutt. 1996. "Quantitative Description of Out-of-Plane Distortion of the Macrocycle of Synthetic and Protein-Bound Porphyrins." Paper presented to the Annual Meeting of the Biophysical Society, Baltimore, MD, 17–21 February.

Jentzen, W., X. Z. Song, and J. A. Shelnutt. 1996. "Structural Characterization of the Macrocycle of Protein-Bound and Synthetic Metalloporphyrins in Terms of the Lowest-Frequency Out-of-Plane Normal Coordinates." Paper presented to the Freie Universität, Berlin, Germany, 15 May.

Jentzen, W., X. Z. Song, J. G. Ma, and J. A. Shelnutt. 1996. "Decomposition of the Structures of Hemes of Proteins into Equivalent Displacement Along the Lowest-Frequency Out-of-Plane Normal Coordinates of the Porphyrin Macrocycle." *Proc. Gordon Res. Conf. on Chemistry & Biology of Tetrapyrroles* **1** (Henniker, NH, 14–18 July): 37.

Jentzen, W., X. Z. Song, S. L. Jia, J. G. Ma, L. Jaquinod, D. J. Nurco, C. J. Medforth, K. M. Smith, and J. A. Shelnutt. 1996. "Resonance Raman Studies of the Nonplanar Distortions of Nickel(II) 5,15-Di-Substituted Porphyrins: A Combination of Displacements Along Two of the Lowest-Frequency Normal Coordinates." *Proc. Internat. Conf. on Raman Spectroscopy* **1** (Chichester, UK, August 11–16): 528–529. New York, NY: John Wiley & Sons, Inc.

Jia, S. L., X. Z. Song, W. Jentzen, J. G. Ma, T. Ema, N. Y. Nelson, C. J. Medforth, K. M. Smith, M. Veyrat, M. Mazzanti, R. Ramasseul, J. C. Marchon, and J. A. Shelnutt. 1996. "Resonance Raman Studies on the Axial Ligation of Nickel(II) meso-Tetra-Substituted Porphyrins." *Proc. Internat. Conf. on Raman Spectroscopy* **1** (Chichester, UK, 11–16 August): 530–531. New York, NY: John Wiley & Sons, Inc.

Lemke, C., J. A. Shelnutt, J. M. E. Quirke, R. Schweitzer-Stenner, and W. Dreybrodt. 1996. "Symmetry Lowering of Nickel(II) Octaethyl-5,15-Di-meso-nitro-porphyrin in CS_2 Detected by Resonance Raman Spectroscopy." *Proc. Internat. Conf. on Raman Spectroscopy* **1** (Chichester, UK, 11–16 August): 270–271. New York, NY: John Wiley & Sons, Inc.

Ma, J. G., W. Jentzen, M. Laberge, J. Vanderkooi, X. Z. Song, S. L. Jia, J. D. Hobbs, and J. A. Shelnutt. 1996. "Conformational Analysis of Nickel-Reconstituted Cytochrome c by Resonance Raman Spectroscopy." *Proc. Internat. Conf. on Raman Spectroscopy* **1** (Chichester, UK, 11–16 August): 458–459. New York, NY: John Wiley & Sons, Inc.

Schweitzer-Stenner, R., A. Sticternath, W. Dreybrodt, X. Z. Song. J. A. Shelnutt, C. J. Medforth, and K. M. Smith. 1996. "Out-of-Plane and In-Plane Distortions of Ni(II) Octaethyltetraphenylporphyrin Probed by Resonance Raman Dispersion Spectroscopy." *Proc. Internat. Conf. on Raman Spectroscopy* **1** (Chichester, UK, 11–16 August): 98–99. New York, NY: John Wiley & Sons, Inc.

Song, X. Z., W. Jentzen, S. L. Jia, J. G. Ma, L. Jaquinod, D. J. Nurco, C. J. Medforth, K. M. Smith, and J. A. Shelnutt. 1996. "Resonance Raman Studies of Nonplanar Distortions of Metal 5,15-Di-Substituted Porphyrins." *Proc. of the Internat. Conf. on Raman Spectroscopy* **1** (Chichester, UK, 11–16 August): 532–533. New York, NY: John Wiley & Sons, Inc.

Song, X. Z., W. Jentzen, S. L. Jia, L. A. Jaquinod, D. J. Nurco, C. J. Medforth, K. M. Smith, and J. A. Shelnutt. 1996. "Nonplanar Distortions of Nickel(II) Dialkylporphyrins Along Combinations of the Lowest-Frequency Out-of-Plane Normal Coordinates." Paper presented to the Annual Meeting of the Biophysical Society, Baltimore, MD, 17–24 February.

Gradient-Driven Diffusion of Multi-Atom Molecules Through Macromolecules and Membranes

G. S. Heffelfinger, D. J. Hobbs, J. A. Shelnutt

The goals of this work are to (1) develop a new molecular simulation method able to model diffusion of multi-atom molecules through macromolecules under conditions of a chemical potential gradient, (2) develop a companion parallel algorithm to breach the computational challenges of the most important applications of the new method, and (3) apply the new method to three such problems. Currently, no such method exists; thus, the many important industrial and technological materials problems where gradient-driven diffusion of multi-atom molecules is the predominant phenomenon are beyond the reach of today's molecular simulation. The study includes (1) diffusion in polymers, the fundamental problem underlying polymer degradation in aging weapons, (2) how to design chiral polymer membranes in order to separate ceramic mixtures into chirally pure compounds, and (3) the permeation of drug analogs through lipid bilayers to enable molecular engineering of drug delivery systems. In addition, this work will impact related problems in areas of security and the environment (e.g., devices that sniff for compounds present in explosives and toxic gases, and separation membranes to treat hazardous waste streams).

Our novel extension of the DCV-GCMD (Dual-Control Volume–Grand Canonical Molecular Dynamics) method specifically designed for the study of gradient-driven diffusion of large molecules (those too large to be inserted/deleted in the GCMD-like control volumes) was implemented in the LADERA code and tested for a simple atomic mixture. For this test, we simply used the standard DCV-GCMD method to set up two regions of different composition for a binary gas mixture (A and B); then we implemented two changes. First, we replaced the periodic boundary conditions in the direction of diffusion by two pistons. We applied the same force per unit area to each. Second, we switched off the insertions and deletions of species B. We located the initial position of each piston well outside the control volumes. The latter must remain fixed in space during the course of the simulation. As the simulation progresses, species B diffuses from the high- to the low-mole fraction side. To satisfy the simultaneous constraint of the set pressure and chemical potential of species A, the diffusion of B is accompanied by a reduction of volume on the side with the higher mole fraction of B, and a volume increase on the side with low mole fraction of B. The volume change is not conserved due to the differences in volume changes of mixing for the two different compositions in the system.

Publications

Other

Van Swol, F. B., and G. S. Heffelfinger. 1995. "Gradient-Driven Diffusion Using Dual-Control Volume–Grand Canonical Molecular Dynamics (DCV-GCMD)." Paper presented to the Materials Research Society Fall Meeting, Boston, MA, 27 November–1 December.

Modeling Complex Turbulent Chemically Reacting Flows on Massively Parallel Supercomputers

J. N. Shadid, A. R. Kerstein, R. C. Schmidt, R. J. Cochran, K. D. Devine

This project is to develop a massively parallel (MP), adaptive, unstructured finite-element (FE) code for simulating 3-D high-Reynolds-number and turbulent chemically reacting flows in complex geometries. Important applications of such flows include the safety calculations for nuclear weapons transport and storage; jet-mixed chemical reactor design; internal-combustion engine analysis; high-performance compact heat exchanger design for aircraft, automobiles, and chemical process plants; and high-temperature combustion process modeling for the destruction of hazardous waste. Currently, these large, multiple, length- and time-scale problems can be solved only in 2-D for a limited number of species due to the required computational resources. These difficult problems strongly couple turbulent momentum, thermal energy, and mass transfer with chemical reaction kinetics, making current 2-D models unsuitable.

With the scheduled code development, MPSalsa will be capable of solving very large, strongly coupled multiphysics turbulence problems with multiple time and length scales. This tool will be immediately useful for Sandia's weapons program responsibilities (Accelerated Strategic Computing Initiatives [ASCI]) as well as many advanced engineering technology problems.

We completed the following: (1) selected and implemented a convection stabilization scheme—streamline upwind Petrov-Galerkin (SUPG), (2) partially validated the implementation of a low-Reynolds-number, two-equation, (k-) model against a standard turbulence benchmark problem, (3) began the procedural implementation of the higher-order hydrodynamic turbulence models, (4) completed the selection of the species-mixing and reaction kinetics models, (5) completed the complexity and scalability analysis of the participating media radiation model, (6) began initial implementation of a participating media radiation model using discrete ordinance methods, and (7) produced an adaptive mesh refinement and dynamic load-balancing strategy.

Quantitative Predictability of Computer Simulations of Complex Systems

T. G. Trucano

A major objective of this project is to develop methods for quantifying the predictability of physical simulation models applied in studying complex, large-scale systems. We focused on the application of methods of statistical inference to achieve this objective. Statistical technology, or something like it, is required to quantitatively deal with uncertainty in complex calculations. Statistics also has the advantage that it produces a language that is more relevant to stockpile quality and manufacturing issues. Our applications focus was on shock-wave physics simulation. However, the methods studied have broader application.

The paradigm shift from test-centered to simulation-centered, science-based stockpile stewardship (SBSS) is the major driver for this research. For this paradigm shift to be successful, unprecedented predictive power for complicated physics and engineering simulations will be required. The purpose of this project was to identify and develop statistical methods for quantifying the predictability of these simulation models. The key issues addressed are (1) to characterize the relevance of existing statistical methods, (2) to identify potential "show stoppers" for this approach to simulation prediction, and (3) to perform illustrative application of selected statistical methods to shock-wave physics. The primary conclusion of the project is that there currently exists a sufficiently rich statistical framework to achieve quantitative characterization of the uncertainty in complicated scientific simulations. The resulting quantification is necessarily statistical, which requires the use of statistical tools in model verification, validation, and the assessment of prediction. The major work will be to systematically implement such a methodology in a way that it applies to our physics and engineering codes.

Density Functional Theory for Classical Fluids at Complex Interfaces

L. J. D. Frink, F. B. Van Swol

Sandia made progress in developing a novel materials modeling tool based on nonlocal density functional theory for classical fluids (C-DFT). Accomplishments centered on (1) optimizing a C-DFT for fluids confined by planar surfaces, (2) applying the planar surface code to a variety of problems, including the superposition of solvation and electrostatic forces, stress isotherms in sol-gel films, and adhesive forces measured with the surface forces apparatus, and (3) beginning development of a 3-D C-DFT for fluids near complex planar interfaces and spherical particles.

We developed a C-DFT code to treat a wide variety of fluids confined by planar interfaces. The code can treat hard sphere fluids, Lennard-Jones fluids, Yukawa fluids, and Coulombic fluids. The surfaces may be either neutral or charged. The fluids may be treated in either a local or nonlocal density approximation, and the fluid component sizes, interaction energies, and valencies can be varied arbitrarily. In the process of developing the current code, we developed strategies for automating preconditioning algorithms, handling discontinuities, enforcing constraints (e.g., charge neutrality), automating mixing schemes for enabling stable iterations to the solution, introducing non-uniform grids, and ultimately performing parallelization. We worked through all of these issues in various versions of code, thus providing a sound basis for proceeding to a massively parallel (MP) 3-D implementation.

In addition to code development, we undertook initial applications of the code. We modeled electrical double layers to understand the superposition of electrostatic and solvation forces. Both forces are present in many experimental systems. To deconvolute experimental data, it is often assumed that the electrostatic forces may be modeled by a restricted primitive model where the solvent is a featureless continuum. We showed that the superposition approximation is good only in the limit of low

surface charge. We also modeled the capillary forces in sol-gel films to provide a sound basis for the interpretation of some novel beam-bending experiments developed at Sandia. These experiments show monotonically increasing solvation forces as the relative pressure is varied from vacuum to saturation. With the C-DFT analysis we showed that the observed results stem from non-uniformity in the pores of the film due either to a pore-size distribution or to roughness on the molecular scale inside the pores. Finally, we modeled adhesion forces as measured with the surface forces apparatus. Adhesion is an important issue in the aging of polymeric materials, but is not well understood. We showed that the qualitative features of pull-off forces measured with the surface forces apparatus are dependent on the strength of the molecular interactions between the surfaces and the fluid as compared with the fluid-fluid interactions. Therefore, adhesion measurements may be used to estimate molecular interaction parameters and to differentiate between fluids that all spontaneously spread on a given surface. These applications demonstrate the wide range of uses possible with the C-DFT technology.

Publications

Refereed

Frink, L. J. D., and F. Van Swol. 1996. "A Molecular Theory for Surface Forces Adhesion Measurements." *J. Chem. Phys.*, submitted. New York, NY: American Institute of Physics.

Frink, L. J. D., and F. Van Swol. 1996. "Oscillatory Surface Forces: A Test of the Superposition Approximation." *J. Chem. Phys.* **105** (15 August): 2884–2890. New York, NY: American Institute of Physics.

Samuel, J. S., C. J. Brinker, L. J. D. Frink, and F. Van Swol. 1996. "Direct Measurement of Solvation Forces in Microporous Thin Films: A New Means of Microstructure Characterization." *Science*, submitted. New York, NY: American Institute of Physics.

A Massively Parallel Sparse Eigensolver for Structural Dynamics Finite Element

G. M. Reese, M. P. Sears, J. A. Schutt, R. S. Tuminaro, R. W. Leland

This effort focuses on development of a massively parallel (MP) eigensolver for structural dynamics analysis. We implemented a parallel sparse eigensolver, Parpack, on Sandia's Intel Paragon. The largest challenge is its integration with a robust, accurate linear solver. Multilevel solvers require especially tight integration of the numerical and finite-element (FE) analysis fields. We evaluated a parallel linear solver, sparse Cholesky for symmetric positive definite systems. We compared and evaluated iterative solvers using AZTEC (Sandia's parallel iterative solver package) and FETI (Finite Element Tearing and Interconnecting) for scalability and convergence within the Parpack framework. We evaluated hybrid subspace iteration/Lanczos eigensolvers to reduce risk of missing modes when using iterative solvers.

We implemented a parallel sparse eigensolver, Parpack, on Sandia's Intel Paragon. Parpack is a parallel Lanczos-based eigensolver for computing some extreme eigenvalues and eigenvectors of large sparse matrices. Parpack requires several linear systems to be solved. Since this is the principal computational kernel, we focused much of our effort on parallel solution methods for large linear systems. Although not viable for very large systems, direct solvers are the best solution procedure for intermediate range problems (e.g., 100,000 degrees of freedom). We ported a parallel linear solver to Sandia's Paragon. We factored and solved several modest-sized structural dynamics problems at 15 MF/processor (30% peak). We will use the direct solver to produce eigenvalues for modest problems and to test iterative methods results. We interfaced Parpack to AZTEC. AZTEC solves the linear systems, and Parpack solves the overall eigen problem, but convergence rates are slow and scalability is limited. For the most part, slow convergence of the linear solver remains the primary bottleneck to solving large problems. The FETI method uses domain decomposition and Lagrange multipliers to produce a Schur complement-like system augmented by a series of constraints. The new reduced system is solved via a projected conjugate gradient method, which requires that a coarse grid problem be solved at every iteration. They achieved good success on a number of complicated but still somewhat academic structural mechanics problems.

We developed a prototype code based on FETI. We tested it on some model structural mechanics problems and found that it shows promise for large structural mechanics applications. A key issue will be to evaluate the method on a wide variety of examples using different element types, elements with poor aspect ratios, and structures with nonhomogeneous components. The more accurately the FETI projection matches the coarse grid physics, the better it converges. We anticipate that the underlying algorithm will need to undergo important modification to address more difficult coarse grid physics. We examined issues related to the dependence of the eigen solution on the accuracy of the linear solver. Both Lanczos and subspace iteration methods show good promise using currently available iterative solvers.

Automated Geometric Model Builder Using Range Image Sensor Data

C. F. Diegert, J. T. Sackos

Sandia's goal is to develop algorithms that automatically construct realistic, three-dimensional (3-D) models of physical environments based on range and optical reflectance information collected with Sandia's Scannerless Range Imager (SRI). We will design algorithms to analyze and reduce the complexity of the data collected from multiple range images taken from different perspectives, recognize and eliminate redundancies in the images, and integrate them into a simplified geometric model. The resulting model will be compatible with virtual reality (VR) and computer-aided-design (CAD) software. The algorithms will be flexible enough to accommodate massively parallel (MP) processing for future applications involving large volumes of data.

The SRI is a special kind of camera system that provides distance and reflected light intensity to each pixel in a field of view (FOV). It has no moving parts and is built with off-the-shelf components.

The resulting capabilities could be used to rapidly survey unknown terrain or hazardous environments, monitor remote sites for security, plan clandestine activity, and enhance the ability of robotic systems to move about an environment.

We established a calibration methodology for the SRI instrument. To do this, we wrote a computer code (called rng²dmp) and completed calibration of Sandia's "Timmy" prototype instrument with a 24-mm, fixed-focus Nikon lens. We found that (1) a pinhole camera model, with square-aspect ratio, a 28.5-degree FOV, and zero roll angle, describes "Timmy's" imaging to within about 2 cm over lens-to-subject distances of four to seven meters, and that (2) at distances between 4 and 7 meters, "Timmy" measures ranges to small, flat targets with error less than 2 cm. There was no systematic error (bias) in these measurements.

In addition to the calibration work, we accomplished two analyses of SRI acquisitions on military assets, demonstrating that we can determine the location of a few objects in an SRI view using known, rigid models of these objects. In one analysis we used a crude model of a tank to recover the position of the SRI instrument relative to the tank. In the second experiment, we analyzed range images of underground rock formations and accurately established locations of cooperative targets we deliberately placed in the SRI instrument's FOV.

Finally, we recorded integrated information on the SRI instrument's compass bearing, tilt angle, and roll angle, together with the range and reflectance imaging.

Publications

Other

Sackos, J., B. Bradley, R. Nellums, and C. Diegert. 1996. "The Emerging Versatility of a Scannerless Range Imager." Paper presented to the Laser Radar Technology and Applications, SPIE Symposium on Aerospace/Defense Sensing and Controls, Orlando, FL, 10 April. New York, NY: IEEE.

Sensing and Compressing 3-D Models

J. C. Krumm

Sandia is developing a novel method of building 3-D models of the environment. Most methods for this task, including laser range-finding, fail under fairly common conditions. Our method uses stereo vision. We take images of the scene from two cameras spaced slightly apart. Instead of traditional stereo, we exploit the power of computer graphics to interpret the images. Our program searches through the space of possible 3-D scenes to find the one that best reproduces the stereo image pair. We represent the scene as a 3-D field of voxels (volume elements). Because computer graphics can deal with so many different, realistic phenomena, our stereo algorithm should work in situations where no other 3-D sensor has worked before.

We made the following accomplishments in FY96:

(1) *Calibrated stereo cameras to 1-mm accuracy in 3-D.* We calibrated our cameras to 0.23-mm accuracy using an array of 11 calibration targets in known 3-D positions.

(2) *Programmed a simple computer graphics rendering of 20 K voxels/second.* We achieved a rendering speed of approximately 320 voxels/second, exceeding this goal by 16 times. Much of this speed is due to an efficient search algorithm described next.

(3) *Experimented with search-and-choose algorithm.* We chose to begin with an exhaustive search algorithm. By carefully studying the search space, we made surprisingly dramatic reductions in its size. For a 15x15x15-voxel volume, our discoveries reduced the search space by about 23 orders of magnitude.

(4) *Achieved voxel compression of 10:1.* Using a modified runlength encoding algorithm, we achieved a compression ratio of better than 80:1.

(5) *Built stereo camera jig, version 1.* We designed and built a jig to hold a pair of stereo cameras in the proper relative orientation.

Scalability of Cryptographic Algorithms and Protocols

K. S. McCurley, Y. Frankel

The goal of this project is to explore scalability and other issues in cryptography, with the intent of developing new methods to address existing and future information-security requirements. A cryptographic system may be scaled in multiple dimensions, including security and the performance of the system. Scalability is very desirable for many applications, including those that require high speed, those that have export control requirements, and those that are designed to meet a wide range of security requirements. A primary example where performance is paramount is the encryption and authentication of information that traverses the Internet. In addition to the topic of scalability, there are a number of other topics in authentication being addressed by this project, including authentication techniques that are tolerant of small changes to the authenticated information.

This project focused on fast software encryption techniques, cryptoanalysis on existing proposals, and design of new techniques. We developed new high-speed software encryption and authentication algorithms. We developed a modified version of the RC5 block cipher encryption algorithm that has better cryptographic properties than the original proposal and is scalable in wordsize, security, and key length. Benchmarks show that it runs very fast in software, and the same round function can form the basis of a fast authentication method. We developed a fast method for batch verification of digital signatures. This is extremely useful in cases where multiple signatures from the same source need to be verified quickly, as in a web server. We developed a new method for authenticating documents subject to measurement errors. This method can be applied to the authentication of biometric identification templates such as those produced by current iris scanners. The technique reveals very little about the original scan while authenticating that the scan is associated with an individual.

Development of Time-Dependent Monte Carlo Techniques for Massively Parallel Computers

R. J. Pryor, T. Quint, N. Basu

Sandia investigated numerical techniques that can be applied to time-dependent Monte Carlo problems solved in a massively parallel (MP) computing environment. The use of Monte Carlo methodologies has become more widespread because today's computers have the increased capacity to treat physical details on a microscale level. The difficulty in using Monte Carlo is that passing the needed data from one processor of the computer to another is time-consuming and somewhat random when viewed over a finite period of problem time. This randomness greatly reduces the effectiveness of traditional optimization methods.

This project used Sandia's MP Paragon computer to develop strategies that reduce the overhead of this data-passing communication. The knowledge gained from this project will be important to all problems that we want to consider for Monte Carlo solutions on the Paragon.

With two economists on board, our work focused on developing a more robust economic model. This model focused on monetary policy, which seems to produce the least predictable outcomes. The model will include at least more industry classes and a banking system. We also worked on forming alliances with outside organizations to continue the project beyond the current funding.

We completed all work on time and under budget. Under other funding, we will develop an economic-energy model using the Aspen technology.

Publications

Other

Pryor, R. J., N. Basu, and T. Quint. 1996. "Development of Aspen: A Microanalytic Simulation Model of the U.S. Economy." Sandia Technical Report, SAND96-2459, February.

Microelectronics and Photonics

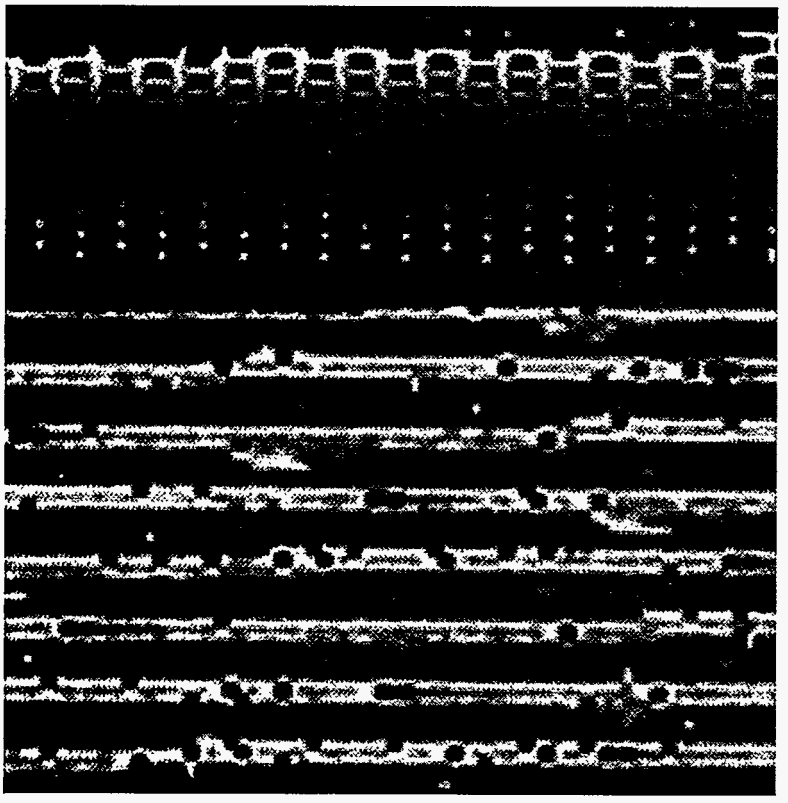

Catalyst-covered microfilaments are used for the detection of hazardous combustible-gas mixtures, requiring only a few mW of power and responding in milliseconds. This is a cross-sectional view of a high-surface-area platinum catalyst-coated micromachined polysilicon filament, produced using a high-energy focused ion beam. The roughness of the catalyst enhances sensitivity and longevity.

InP-Based Materials for Photonic and Microelectronic Devices

O. B. Spahn, R. L. Dawson, A. J. Howard, R. J. Shul, I. J. Fritz, M. L. Lovejoy, K. L. Lear, J. F. Klem

This work will explore the growth of heteroepitaxial materials on InP substrates, and their application to novel photonic and electronic devices, thereby giving Sandia a unique capability in important optical communications and microelectronics areas. For photonic devices, we will investigate the growth of InGaAsP/InP, InGaAs/InAlGaAs, and AlAsSb/GaAsSb materials and heterostructures and apply them to vertical-cavity technologies such as vertical-cavity surface-emitting lasers (VCSELs), resonant cavity LEDs (RCLEDs), and reflectance modulators operating at the critical 1.1–1.75-mm wavelength range. We will also study InGaAs/InP materials for heterojunction bipolar transistor (HBT) technology. The initial objective will be development of the materials growth and processing technologies, a task that will vary widely in difficulty, depending on the materials system. We will use metalorganic vapor phase epitaxy (MOVPE), molecular beam epitaxy (MBE), and gas source molecular beam epitaxy (GSMBE) to grow these materials. A key aspect of this work will be the eventual development of dual Sb/P growth capability on Sandia's new, state-of-the-art GSMBE system. Sandia will thus be in a unique position to contribute to critical next-generation compound semiconductor device research based on InP substrates.

We grew several AlAsSb/(Al)GaAsSb distributed Bragg reflector (DBR) structures by MBE on InP substrates. We obtained reflectivities in excess of 99% with 202 mirror pairs and fitted them by theoretical models. We investigated role transport in *p*-type AlAsSb/GaAsSb and found them promising for electrically injected devices such as RCLEDs and VCSELs. We fabricated and tested electrically injected RCLEDs. Also, we grew and tested optically pumped VCSEL structures. Preparation for integration of Sb- and P-bearing materials in our new GSMBE system is currently under way. We carried out initial studies of oxidation of AlAsSb for use in laterally oxidized DBRs and observed interesting new phenomena (Sb separation). We fabricated and tested InGaAsP/InP edge-emitting laser structures for 1.5-μm operation. We also investigated strain-balanced InAlGaAs/InAlAs active regions for 1.75-μm emission. We developed new wet- and dry-etch capabilities for Sb-bearing materials. We integrated InGaAs/InP high-performance bipolar transistor (HBT) amplifier structures with InGaAs p-i-n photoreceivers for optoelectronic applications. We characterized photoreceiver performance and met system requirements.

Tunneling Heterostructure Devices for Millimeter-Wave Applications

C. P. Tigges, J. F. Klem, J. A. Simmons, K. L. Lear, T. A. Plut, G. A. Vawter, J. R. Wendt, V. M. Hietala

Sandia is developing quantum-transport device structures for millimeter-wave (mm-wave) applications. These structures, such as resonant tunnel diodes (RTDs), have demonstrated potential for very high-speed operation. This research and development project focuses on the evaluation of novel heterostructure materials to construct these devices and explore their relative performance in the context of mm-wave applications. Based on the results of the initial device characterization, we proceeded to optimize the design and fabrication of tunneling heterostructure devices suitable for mm-wave applications. In addition, we developed a detailed process technology for one of the applications we are pursuing. This process enables a novel power combination technique by coupling a microstrip patch antenna structure to a resonant tunneling matrix structure to form a mm-wave power generator.

We solved several problems in fabricating the complex RTD-microstrip antenna (MSA) structure. As a result, we developed and demonstrated a process producing complete devices and can now test the electrical properties of the device to compare with the performance of the individual components.

The first attempt at RTD post formation utilized a reactive ion beam etch (RIBE) with a slightly reentrant profile 5 microns deep. We subsequently abandoned this process after modeling indicated an antenna efficiency of only 10% while the desired minimum efficiency of 70% requires a 20-micron electrode spacing. We tried an inherently isotropic hydrofluoric (HF)-based wet etch with the RTD post sidewalls metal-coated to help disperse high-current densities. This process failed because the profile turned slightly reentrant after only 15 microns of etching. We tried a special SiNOx etch mask, but it failed to solve this problem. Instead, we abandoned the deep etch in favor of a 20-micron build-up. The first attempt at this used a 20-micron-thick photoresist (PR) layer with a single patterned hole reflowed to accommodate a subsequent metal coating. Unfortunately the reflow failed, with the side-wall profile slightly obstructing the hole, preventing the next metal-deposition step.

The next attempt used a two-level process. We made the first layer thin enough to ensure that the reflow would not obstruct the hole. The second layer incorporated a much larger hole, allowing the top resist to be reflowed without creep into the lower hole. This process failed because the second-layer thickness needed to obtain the required electrode spacing resulted in bubble formation during subsequent processing. We resolved this issue by introducing a third PR layer.

The final process is composed of eight steps. Step 1 forms the RTD posts. Step 2 passivates the post sidewalls and insulates pads from top metal using SiN. Step 3 encapsulates the posts using the three-layer PR method. Step 4 deposits Ti/Au metal, connecting the diodes and acting as the seed for Ni plating. Step 5 patterns a plating mask, defining the antenna and access holes in the top metal for subsequent PR removal. Step 6 plates Ni, which is used for strength to stabilize large-area bridges after PR removal. Step 7 removes, by ion milling, the exposed seed metal defining the antenna and exposing the access holes. Step 8 uses a plasma etch to remove PR from under the top metal layer.

Microsensors for In-Process Control and Monitoring During Semiconductor Fabrication

R. C. Hughes, R. J. Bastasz

Advances in microelectronic fabrication technologies are essential for U.S. electronic firms to maintain and expand their position in an increasingly competitive international market. One area that requires new technology is the monitoring of residual gases in sputtering systems. The electronics industry uses sputtering systems extensively for deposition of thin films on microelectronic components, including metallization layers on integrated circuits (ICs), magnetic materials on computer disk platters, and various dielectric layers. Most modern sputtering systems have multiple chambers, each of which may exhibit spatial variations in residual gases, especially hydrogen.

In this project, Sandia is developing the knowledge necessary to build a microelectronic hydrogen sensor that will work in vacuums of 10^{-7} to 10^{-3} torr with response times in the 1–20-second range. While our current robust hydrogen sensor will not work in its present form, we believe that a small sputtering system integral to the sensor structure will permit a periodic cleaning of the catalytic metal on the robust sensor and allow it to perform the task. Inexpensive point sensors will make it possible to monitor spatial variations of hydrogen in real time in a large chamber.

We conducted an extensive study of the performance and behavior of the latest generation of integrated hydrogen microsensors (IHMs) in the high-vacuum (HV) and ultra–high-vacuum (UHV) environments. The main study areas were (1) mapping out the response isotherms over the pressure range from 10^{-9} to 10^{-4} torr and over the temperature range from 25° C to 160° C, (2) development of *in situ* cleaning techniques, including the design and use of a miniature sputter-cleaning attachment, (3) comparing the response characteristics of *in situ* cleaned sensors over the operating range of temperatures, (4) studying the effect of UHV contaminant gases, such as CO, on sensor performance, (5) studying the transient sensor response to H_2 gas pulses and developing a kinetic model to explain the observed sensor response, and (6) monitoring the long-term stability and response of IHMs in the UHV environment.

The main results obtained from these studies are the following:

(1) The experimentally determined isotherms were useful in developing a Langmuirian model that can predict the response of IHMs. In this model, hydrogen equilibrates among the external interface, the metal film, and the internal sensing junction.

(2) *In situ* sputter-cleaning of sensor surfaces improves response and recovery times, evidently by removing impurities that impede H_2 dissociation and recombination.

(3) At all temperatures between 25° C and 160° C, the sensor signal reaches an equilibrium value with a given partial pressure of H_2, but the rate of reaching that equilibrium is quite temperature-dependent. For temperatures of 100° C and above, the sensor is fast enough for most industrial applications.

(4) CO, the most abundant nonhydrogenic residual gas in UHV systems, has a negligible effect on the performance of IHMs, even at abnormally high partial pressures (10^{-4} torr). The small amounts of other residual gases present in UHV systems do not appreciably affect IHMs.

(5) The behavior of IHMs in UHV to short pulses (1–200 msec) of H_2 gas at pressures in the range of 10^{-7} to 10^{-5} torr as a function of surface condition and temperature can be reproduced by a kinetic model employing shallow trap sites at the sensing junction, diffusive transport through the catalytic gate film, and rapid adsorption and recombination at the sensor surface.

(6) IHMs can function reliably through hundreds of H_2 exposure and purge cycles without noticeable loss of performance.

Smart Packaging for Photonics

R. F. Carson, D. C. Craft, C. J. Helms, P. K. Seigal, C. T. Sullivan, J. H. Smith

This project is designed to extend the low-cost "drop-in" techniques for device mounting and data interconnection in optical fiber packages to single-mode optical waveguides and fibers by the use of adaptive optical alignment, built into a silicon submount. In this approach, waveguides and/or fibers are aligned to the active photonic devices and input waveguides by the use of electrostatically controlled micromechanical elements. Rough alignments would be achieved by the standard "drop-in" techniques of flip-chip solder bonding, and the fine alignments required for single-mode optics would be achieved by the micromechanics. Such techniques form an enabling technology for low-cost, single-mode, multichannel optical waveguide and fiber computer backplanes. These types of systems are currently the subject of intense interest in the computer industry. In addition, this work is being extended to include switching and alignment for high-power edge-emitting laser arrays with multimode optical fibers. We found the micromechanical waveguide switching function, in particular, to add a great deal of value to systems of interest to Sandia.

Horizontal micromachines appear to be much more useful than the basic *y*-deflection cantilever waveguide first proposed by this project. This was further verified by our activities during FY95, where we built and tested waveguides on cantilevers. In that work, we determined that the basic cantilever, in addition to being constrained in deflection travel, was also constrained to high actuation voltage. These factors all motivated us to concentrate our FY96 efforts on a horizontally actuated waveguide switch with an interdigitated comb drive. To this end, we completed a design and developed basic enabling techniques to allow integration of polymer waveguides with micromachined polysilicon comb drive structures. These structures included waveguide switch arrangements such as ganged 2 x 2 structures that could form n x n switches and a "perfect shuffle" switching arrangement. All of these switches could be used for signal routing between sets of waveguides, thus allowing reconfiguration of interconnects.

Publications

Other

Smith, J. H., R. F. Carson, C. T. Sullivan, and G. B. McClellan. 1996. "Monolithic Integration of Waveguide Structures with Surface-Micromachined Polysilicon Actuators." *Proc. Smart Structures and Mater. '96, Smart Electron. and MEMS Symp.* (SPIE) **2722** (San Diego, CA, 21–25 February): 75–81.

Microfabricated Combustible-Gas Detector

A. J. Ricco, P. J. McWhorter, D. J. Moreno, R. C. Hughes, J. H. Smith

A sizable commercial market exists for an inexpensive, low-power, reliable microsensor suitable for the detection of explosive (or near-explosive) gas mixtures. When any combustible species reacts with oxygen on the surface of a hot platinum (Pt) wire, the Pt changes its resistance, an effect that is measurable well below the explosive limit. By placing this technology on chip and integrating the control and measurement circuitry, many markets will be opened, including natural gas-using appliances in homes and industry, automobiles (especially those using methane, propane, or hydrogen), the petrochemical/energy industry, and numerous military applications.

We met all milestones, resulting in significant progress in key aspects of the program. We completed fabrication and testing of integrated control/measurement circuits on the same chip with combustible-gas detector filaments. We thoroughly characterized the sensors in terms of their thermal behavior and refined the design. We improved control electronics and the catalyst chemical vapor deposition (CVD) process as well. We investigated pulse deposition in detail and showed the ability to deliberately control catalyst morphonolgy through control of the temperature duty cycle during the CVD process. The sensor also showed good response to hydrogen in nitrous oxide environments (as found in the Hanford storage tanks). We also characterized filament response to other combustibles and interferents such as relative humidity. We also designed, built, and tested a range of pure Pt microfilaments to demonstrate feasibility for high-temperature applications where polycrystalline silicon may be unsuitable.

Publications

Other

Ricco, A. J., J. H. Smith, R. C. Hughes, D. J. Moreno, S. D. Senturia, and R. J. Huber. 1995. "Combustible-Gas Sensor Using Micromachined Si Filaments." Paper presented to the International Chemical Congress of Pacific Basin Societies, Honolulu, HI, 17–22 December.

In Situ Spectral Reflectance for Improved Molecular Beam Epitaxy Device Growth

W. G. Breiland, M. E. Sherwin, J. L. Reno, K. L. Lear, J. F. Klem, K. P. Killeen

A pregrowth control strategy using in situ *reflectance led to an unprecedented demonstration of process control on one of the most difficult device structures that can be grown with compound semiconductor materials. Sandia grew hundreds of vertical-cavity surface-emitting lasers (VCSELs) with only ±0.3% deviations in the Fabry-Perot cavity wavelength—a nearly tenfold improvement over current calibration methods.*

Although equipment limitations prevented us from achieving all of our stated second-year goals in this project, it is clear that *in situ* reflectance has made a major impact on thin-film processing control and almost assuredly will change the way that compound semiconductor devices are made in the future. We installed a single-wavelength reflectance probe on the EPI molecular beam epitaxy (MBE) machine. Growth rates extracted with the ADVISOR method agreed within statistical deviations with growth rates obtained using conventional Reflection High-Energy Electron Diffraction (RHEED) methods. We monitored test structures during MBE growth, demonstrating an ability to detect even very thin features such as 100-angstrom superlattice structures. Unfortunately, manufacturing defects in the machine prevented us from implementing tests of real-time control. However, we developed a pregrowth control strategy on the EMCORE MOCVD reactor. This strategy led to an unprecedented demonstration of process control on one of the most difficult device structures that can be grown with compound semiconductor materials. We grew hundreds of VCSELs with only ± 0.3% deviations in the Fabry-Perot cavity wavelength—a nearly tenfold improvement over current calibration methods.

The success of this work led to a great deal of interest from the commercial sector, including use of the ADVISOR method by Hewlett-Packard and Honeywell. We will submit an improved reflectance design for a patent. A small company, Pacific Lightwave, is incorporating the ADVISOR analysis method in its reflectometer product; EMCORE Corporation plans to use Pacific Lightwave reflectometers in its new MOCVD reactors.

Publications

Refereed

Breiland, W. G., and K. P. Killeen. 1995. "A Virtual Interface Method for Extracting Growth Rates and High-Temperature Optical Constants from Thin Semiconductor Films Using *In Situ* Normal Incidence Reflectance." *J. Appl. Phys.* **78** (1 December): 6726–6736. New York, NY: American Institute of Physics.

Breiland, W. G., H. Q. Hou, H. C. Chui, and B. E. Hammons. 1997. "*In Situ* Pregrowth Calibration Using Reflectance as a Control Strategy for MOCVD Fabrication of Device Structures." Paper to be presented to the 9th International Conference on Vapor Growth and Epitaxy, Amsterdam, Netherlands, 4–9 August.

Hou, H. Q., H. C. Chui, K. D. Choquette, B. E. Hammons, W. G. Breiland, and K. M. Geib. 1996. "Highly Uniform and Reproducible Vertical-Cavity Surface-Emitting Lasers Grown by Metalorganic Vapor Phase Epitaxy with *In Situ* Reflectometry." *IEEE Photon. Technol. Lett.* **8** (October): 1285–1287. New York, NY: IEEE.

Integration of Diffractive Optics and VCSEL Arrays for Optical Interconnects

M. E. Warren, I. A. Erteza, P. K. Seigal, J. R. Wendt, G. A. Vawter, R. G. Hadley, K. L. Lear

Sandia is fabricating and testing arrays of vertical-cavity surface-emitting lasers (VCSELs) with diffractive optical elements etched into their transparent substrates that act as holographic optical interconnects. The project includes fabrication of substrate-emitting VCSEL arrays, including both phase-locked and individually addressed incoherent arrays, and fabrication of diffractive optical structures on the substrates of the arrays that would provide fixed beam splitting, direction and focusing, or collimation functions. In addition, we are investigating diffractive optical structures on transparent substrates that can be bonded to VCSEL arrays for top-emitting devices and visible-wavelength VCSELs that do not have transparent substrates. The integration of diffractive optical elements with VCSEL arrays will allow fabrication of optical systems-on-a-chip that provide nearly arbitrary free-space optical interconnect functions for applications in advanced computer bus architectures and multichip module (MCM) interconnections.

The integration of diffractive optical elements with VCSEL arrays will allow fabrication of optical systems-on-a-chip that provide nearly arbitrary free-space optical interconnect functions in very compact miniaturized systems. We successfully fabricated arrays of VCSELs with diffractive lenses on their substrates for control of beam divergence and obtained improvements in device performance. The VCSELs are bottom-emitting lasers operating at 980 nm developed and fabricated at Sandia. The gallium arsenide (GaAs) substrate of the laser is transparent at that wavelength and is used as an optical medium in which to fabricate lenses and other diffractive optical elements.

We extended this work to top-emitting VCSEL designs that are bonded to transparent substrates for shorter-wavelength applications in which the VCSEL substrate is not transparent. We fabricated computer-generated diffractive lenses in fused silica substrates that have the necessary metal patterns aligned to the optical elements to precisely locate the VCSEL arrays relative to the lenses. The lenses include on-axis collimating lenses and off-axis collimating elements that allow the beam to propagate at a 10° angle to the substrate surface. The other lenses are anamorphic designs that distort the beam to produce an elliptical or line focus. We fabricated these lenses by direct-write electron-beam lithography to produce eight phase-level structures that exhibit high efficiencies. We fabricated arrays of visible-wavelength (670 nm) VCSELs with contact pad patterns to align with contacts on the silica substrates for flip-chip bonding. Equipment problems delayed final bonding of the devices together to form miniaturized optical systems, although we demonstrated preliminary assembly of test devices. We plan to complete the assembly soon. This technology is of increasing interest for future programs, including "chemlab-on-a-chip" concepts that are heavily dependent on miniaturized optical systems and for weapons applications requiring miniaturized optomechanical assemblies and sensors. Additional work in this project included modeling of beam propagation in VCSEL substrates for a novel optical interconnect design and improvements in our diffractive optical element design capability. We developed new processes for fabrication of submicron structures in silica that will be useful for future optical device work.

Publications

Other

Carson, R. F., M. L. Lovejoy, K. L. Lear, M. E. Warren, P. K. Seigal, G. A. Patrizi, S. P. Kilcoyne, and D. C. Craft. 1996. "Low-Power Modular Parallel Photonic Data Links." *Proc. IEEE Electron. Components and Technol. Conf.* (Orlando, FL, 28–31 May): 321–326.

Erteza, I. A., and M. E. Warren. 1996. "Waveguiding Properties of Vertical-Cavity Surface-Emitting Laser Structures." Paper presented to the Optical Society of America Annual Meeting, Rochester, NY, 20–24 October.

Warren, M. E., T. C. Du, J. R. Wendt, G. A. Vawter, K. L. Lear, S. P. Kilcoyne, R. F. Carson, P. K. Seigal, M. Hagerott-Crawford, H. Hou, and R. P. Schneider, Jr. 1996. "Integration of Diffractive Optical Elements with Vertical-Cavity Surface-Emitting Lasers." *Proc. Topical Mtg. on Diffractive Optics and Micro-Optics, Optical Soc. of Amer.* **5** (Boston, MA, 29 April–2 May): 67–70.

Wafer Fusion for Integration of Semiconductor Materials and Devices

K. D. Choquette, D. M. Follstaedt, M. H. Crawford, K. L. Lear, S. H. Kravitz, O. Blum

Sandia continued to develop wafer fusion for integrating semiconductor materials and heterostructures with widely disparate lattice parameters, electronic properties, and optical properties for novel devices not now possible on any one substrate. In addition to developing robust wafer fusion processes, we look to extend the scope of the technology to include such materials systems and devices as AlGaAs-based vertical-cavity surface-emitting lasers (VCSELs) on Si substrates and AlGaInP-based light emitters on transparent GaP substrates. With an emphasis on the materials processes responsible for the atomic-scale fusion, we believe that mixing and matching a broad spectrum of materials will be feasible, enabling novel devices to be pursued. As a baseline fabrication technology applicable to many semiconductor systems, wafer fusion will revolutionize the way we think about possible semiconductor devices.

We made the following accomplishments in FY96:

(1) Established a custom furnace system to perform wafer fusion experiments (constructed and calibrated furnace system, designed new sample holders).

(2) In cooperation with UC–Davis, completed preliminary experiments on fusion of GaAs to Si.

(3) Examined effects of hydrogen and oxygen plasma pretreatments on surfaces before fusion (found that

hydrogen plasma processing produces low-interface defect densities).

(4) Examined wafer fusion process that avoids hydrogen gas and pressure during heat treatment (determined that hydrogen gas may not be necessary, but applied pressure may be advantageous).

(5) Utilized two new methods to characterize bonded interfaces: infrared and ultrasonic imaging (found ultrasonic imaging to be more sensitive to defects at bonded interfaces; ultrasonic measurements showed that bonding temperature is critical to reduce defects at interface).

(6) Characterized GaAs bonded to Si substrate via transmission electron microscopy analysis; GaAs/InP and InP/Si are ongoing (achieved low-defect density, but with inferior bond strength).

Subwavelength Diffractive Optics

M. E. Warren, W. W. Chow, J. R. Wendt, G. A. Vawter, R. J. Shul, R. E. Smith, R. G. Hadley, O. Blum

Sandia investigated subwavelength surface-relief structures fabricated by direct-write e-beam technology as unique and very high-efficiency optical elements. A semiconductor layer with subwavelength-sized etched openings or features can be considered as a layer with an effective index of refraction determined by the fraction of the surface filled with semiconductor relative to the fraction filled with air or other material. Such a layer can be used to implement planar gradient-index lenses on a surface. Additionally, the nanometer-scale surface structures have diffractive properties that allow the direct manipulation of polarization and altering of the reflective properties of surfaces. With this technology a single direct-write mask and etch can be used to integrate a wide variety of optical functions into a device surface with high efficiencies, allowing, for example, direct integration of polarizing optics into the surfaces of devices, forming antireflection surfaces or fabricating high-efficiency, high-numerical-aperture lenses, including integration inside vertical semiconductor laser cavities.

We continued to design and fabricate subwavelength diffractive optical elements designed for operation at 975 nm. We fabricated the structures in gallium arsenide (GaAs). One device is a polarization-dependent optic that has high transmission for transverse electric (TE) polarized light and does not have significantly increased transmission for transverse magnetic (TM) polarization. For TE polarization at normal incidence, the subwavelength grating structure acts as an effective antireflection coating. This type of structure can be optimized for use as a polarizer, waveplate, or polarization beamsplitter. These structures exhibit very high performance and helped demonstrate that Sandia can be a major player in the emerging field of nanofabrication and artificially structured optical materials. We also fabricated the first microlenses based on subwavelength grating structures. The design of these structures is based on an optimization procedure using rigorous coupled-wave analysis. The etched grooves in a period are varied in size and position during the optimization process, constrained by the appropriate fabrication limitations. Fabrication of subwavelength diffractive structures in this wavelength range in GaAs required fine-scale electron-beam lithography and a deep, anisotropic, dry-etching process developed at Sandia.

We compared the performance of microlenses formed with subwavelength gratings with the performance of microlenses formed by more conventional techniques. We also performed some preliminary experiments on fabrication techniques for making these types of optical elements in fused silica for visible-wavelength applications. This requires deep anisotropic etching in fused silica, which is much less developed than for GaAs. The initial results are very encouraging, with submicron features fabricated with 6:1 height-to-width aspect ratios. We need to obtain ratios of better than 10:1 to fabricate high-performance devices in fused silica. Diffractive optical elements allow more functionality to be integrated into photonic components and reduce the weight, size, and complexity of photonic systems and subsystems. Subwavelength diffractive elements have the potential to simplify the fabrication of high-performance optical elements and of unique "optical surfaces."

Publications

Refereed

Smith, R. E., M. E. Warren, G. A. Vawter, and J. R. Wendt. 1996. "Polarization-Sensitive Subwavelength AR Surface on Semiconductors for 975 nm." *Optics Lett.* **21** (1 August): 1201–1203. Washington, DC: Optical Society of America.

Smith, R. E., M. E. Warren, J. R. Wendt, and G. A. Vawter. 1996. "Subwavelength Diffractive Elements Fabricated in Semiconductor for 975 nm." *Proc. Diffractive Optics and Micro-Optics Topical Mtg., Optical Soc. of America* **5** (Boston, MA, 29 April–3 May): 325–327.

Wendt, J. R., G. A. Vawter, R. E. Smith, and M. E. Warren. 1996. "Fabrication of Subwavelength, Binary, Antireflection Surface-Relief Structures in the Near Infrared." *J. Vac. Sci. and Technol. B* **14**: 4096–4099. New York, NY: American Vacuum Society.

Wendt, J. R., G. A. Vawter, R. E. Smith, and M. E. Warren. 1996. "Nanofabrication of Subwavelength, Binary, Antireflection Surface-Relief Structures in the Infrared." Paper presented to the 40th International Conference on Electron, Ion, and Photon Beam Technology and Nanofabrication, Atlanta, GA, 29–31 May.

Wendt, J. R., G. A. Vawter, R. E. Smith, and M. E. Warren. 1995. "Nanofabrication of Subwavelength, Binary, High-Efficiency Diffractive Optical Elements in GaAs." *Proc. 39th Internat. Conf. on Electron, Ion, and Photon Beam Technol. and Nanofabrication* **13** (Scottsdale, AZ, 30 May–2 June): 2705–2708. New York, NY: American Vacuum Society.

Photonic Integrated Circuits for Millimeter-Wave Generation

G. A. Vawter, V. M. Hietala, A. Mar

This project will explore techniques for millimeter-wave (mm-wave) generation using active photonic integrated circuits (PICs). These PICs are based on passively mode-locked ring diode lasers that generate a continuous train of short pulses (≈1 ps) at mm-wave frequencies (50 GHz). Through development of PIC technology, the ring-laser will be integrated with an optical amplifier and high-speed photodetector such that the mode-locked pulse train will be direct waveguide-coupled into the photodetector to generate a mm-wave electrical output at higher power levels and efficiency than presently available using semiconductor technology.

The technical problem to be addressed by this project is the development of a new technology for the generation of millimeter waves at frequencies ≥ 50 GHz. This new PIC-based technology is projected to provide up to an order-of-magnitude improvement in output power and efficiency over current mm-wave technology using Gunn or IMPATT diodes. It is also extendible to frequencies not accessible with conventional semiconductor approaches and will provide a substantial reduction in package size (including potential for direct integration with mm-wave ICs for use as a frequency reference).

During FY96 we completed the fabrication of second-generation fully integrated PICs. The revised PIC design incorporates oxygen implantation for electrical isolation between laser, amplifier, and detector as well as a simplified photodiode for improved manufacturability.

We tested a fully functional, completed PIC at all three design frequencies. All PICs used passive mode-locked rings at the specified diameter with integrated optical amplifiers for independent control of output power while the laser is in a mode-locked condition. We used various-length detectors with the result that the shorter lengths are required for the highest frequencies. This fact indicates that a traveling-wave photodiode would be a good choice for this application due to its ability to optimize both speed and quantum-efficiency. We achieved mode-locked operation without using special filtering to prevent spontaneous emission feedback to the ring laser. We measured limits on laser-injection current prior to loss of mode-locking. We identified a range of amplifier-injection current for good PIC operation. We measured total mm-wave output power and identified the main limiting factor as catastrophic damage of the photodiode.

Publications

Refereed

Vawter, G. A., A. Mar, V. M. Hietala, and J. Zolper. 1997. "A Complete Monolithically Integrated Circuit for All Optical Generation of Millimeter-Wave Frequencies." Paper presented to the Meeting of the Optical Society of America, Incline Village, NV, 17–19 March.

Other

Vawter, G. A., A. Mar, V. M. Hietala, and J. Zolper. 1997. "Millimeter-Wave Signal Generation Using an Integrated Mode-Locked Semiconductor Laser and Photodiode." Paper presented to the Meeting of the Optical Society of America, Baltimore, MD, 18–23 May.

Novel Low-Permittivity Dielectrics for Si-Based Microelectronics

J. P. Sullivan, D. R. Tallant, C. A. Apblett, T. M. Mayer, C. J. Barbour, T. A. Friedmann, M. P. Siegal

Sandia investigated novel dielectrics for application as low-permittivity interconnect materials in ultra–large-scale-integration Si-based microelectronics to enable faster, more reliable devices. We developed three classes of materials and explored their properties: novel ceramic dielectrics, fluoropolymer dielectrics, and SiO_2-derived dielectrics. The novel ceramic dielectrics included amorphous tetrahedrally coordinated diamond-like carbon (DLC), boron nitride, aluminum nitride, carbon-nitrogen alloys, carbon-boron-nitrogen alloys, and alloys of boron-nitrogen-oxygen, all deposited using pulsed-laser deposition. The fluoropolymer materials included plasma-polymerized as well as thermal chemical vapor-deposited films. The SiO_2-derived dielectrics included electron-cyclotron resonance (ECR)-deposited fluorinated SiO_2. We measured the dielectric properties of these materials using metal-insulator-metal and metal-insulator-semiconductor structures, and we assessed specific integration issues, such as film stress, gap-fill, and thermal stability. The guidelines for assessment were established by the requirements for integration into a submicron complementary metallic oxide semiconductor (CMOS) baseline process.

Several significant developments occurred during FY96 on the development of low-permittivity dielectrics for microelectronics. (1) We broadened the research to include two new classes of materials: fluoropolymers and fluorinated SiO_2. These material systems also attracted great interest outside of Sandia. We showed that (a) plasma-polymerized fluoropolymers—although promising for

their low dielectric constant and potential thermal and dimensional stability—exhibit unacceptable dielectric loss due to a high free-radical density that is inherent to the deposition process, yet there may be some processes to reduce this high free-radical density; (b) a potential new fluoropolymer that is deposited by a nonplasma technique, thermal chemical vapor deposition (CVD), has low free-radical density and may be an alternative; and (c) the popular new low-permittivity dielectric, fluorinated SiO_2 deposited by high-density plasma deposition, may actually not be as suitable as previously thought due to serious thermal stability problems in the presence of Al and moisture.

(2) We found a new technique to relieve the high compressive stress inherent in pulsed-laser–deposited amorphous tetrahedrally coordinated carbon. This material is promising for many applications in electronics as well as outside of electronics (tribological coatings, for example). However, the very high compressive stresses (typically > 5 GPa) limit its application. We developed an approach whereby simple thermal annealing cycles can relieve the stress (< 0.1 GPa) and still preserve the desirable film properties, thus enabling implementation of this material in electronics.

(3) We fabricated new alloys of boron-carbon-nitrogen and boron-nitrogen-oxygen and assessed them for their dielectric properties. We found that the addition of nitrogen to carbon-bearing alloys has very deleterious effects on the insulating properties of the films. The effect is due to the stabilization of threefold bonding in the amorphous network. Large bandgaps and low permittivities require a dominance of fourfold bonding. Elimination of carbon and moving toward a boron-nitrogen-oxygen alloy introduces degradation problems associated with moisture absorption. Although these problems were shown to be unacceptable for low-permittivity dielectric applications, there may be promise for applications in vacuum microelectronics or tribology.

In conclusion, we found the fluorinated SiO_2 to represent the best near-term low-permittivity dielectric, provided adequate diffusion barriers are employed to inhibit interfacial reaction.

Publications

Refereed

Sullivan, J. P., P. B. Mirkarimi, K. F. McCarty, T. A. Friedmann, N. Missert, L. J. Martinez-Miranda, M. P. Siegal, and M. L. Lovejoy. 1996. "Electrical Permittivities for Thin-Film Cubic BN and Amorphous Tetrahedrally-Bonded Diamond-Like Carbon." *Appl. Phys. Lett.*, in review.

Sullivan, J. P., T. A. Friedmann, D. R. Tallant, L. J. Martinez-Miranda, J. Mikkalson, D. J. Rieger, and A. G. Baca. 1996. "Stress Relief in Pulsed Laser-Deposited Amorphous Tetrahedrally-Bonded Carbon Films." *Appl. Phys. Lett.*, in review.

Sullivan, J. P., T. A. Friedmann, N. Missert, D. R. Tallant, J. C. Barbour, P. P. Newcomer, S. C. Fleming, S. R. Kurtz, and M. L. Lovejoy. 1996. "Structural and Electrical Properties of Pulsed Laser-Deposited Boron-Carbon-Nitrogen Thin Films." *J. Appl. Phys.*, in review.

Other

Friedmann, T. A., D. R. Tallant, J. C. Barbour, J. P. Sullivan, M. P. Siegal, K. F. McCarty, and P. Mirkarimi. 1995. "Growth of CNx Films Using Ion-Assisted Pulsed-Laser Deposition." Paper presented to the Fall Meeting of the Materials Research Society, Boston, MA, 27 November–1 December.

Friedmann, T. A., D. R. Tallant, J. C. Barbour, J. P. Sullivan, M. P. Siegal, R. L. Simpson, J. Mikkalson, and K. F. McCarty. 1995. "Characterization of Carbon Nitride Films Produced by Pulsed-Laser Deposition." Paper presented to the Spring Meeting of the Materials Research Society, San Francisco, CA, 17–21 April.

Sullivan, J. P. 1996. "Novel Dielectrics for Microelectronics." Paper presented to the 16th Annual Tennessee Valley AVS and East Tennessee MRS Meeting, Knoxville, TN, 21 May.

Sullivan, J. P., C. A. Apblett, T. A. Friedmann, M. P. Siegal, M. L. Lovejoy, P. B. Mirkarimi, and K. F. McCarty. 1995. "Comparison of the Dielectric Properties of h-BN and c-BN." Paper presented to the Spring Meeting of the Materials Research Society, San Francisco, CA, 17–21 April.

Sullivan, J. P., J. C. Barbour, P. P. Newcomer, C. A. Apblett, C. H. Seeger, and A. G. Baca. 1996. "Thermal Stability of Fluorinated SiO_2 Films: F-Induced Interfacial Reaction." Paper presented to the Fall Meeting of the Materials Research Society, Boston, MA, 2–6 December.

Sullivan, J. P., T. A. Friedmann, C. A. Apblett, M. P. Siegal, M. L. Lovejoy, N. Missert, P. B. Mirkarimi, and K. F. McCarty. 1995. "Evaluation of Amorphous Diamond-Like Carbon and Boron Nitride Films as Low-Permittivity Dielectrics." Paper presented to the Spring Meeting of the Materials Research Society, San Francisco, CA, 17–21 April.

Sullivan, J. P., T. A. Friedmann, M. L. Lovejoy, C. A. Apblett, N. Missert, M. P. Siegal, P. B. Mirkarimi, and K. F. McCarty. 1995. "Dielectric Properties of Diamond-Like Carbon and Boron Nitride: Potential Applications in Microelectronics." Paper presented to the 3rd International Conference on the Application of Diamond Films and Related Materials, Applied Diamond Conference, Gaithersburg, MD, 21–24 August.

Sullivan, J. P., T. A. Friedmann, M. P. Siegal, S. C. Fleming, M. L. Lovejoy, P. P. Newcomer, W. R. Bayless, J. C. Barbour, and S. R. Kurtz. 1995. "Electrical and Structural Characterization of AlxN, BxC, BxCyN Thin Films." Paper presented to the Fall Meeting of the Materials Research Society, Boston, MA, 27 November–1 December.

Double Electron Layer Tunneling Transistor

J. A. Simmons, J. F. Klem, H. C. Chui, S. K. Lyo, M. E. Sherwin

The goal of this project is to implement the recently discovered phenomenon of 2-D/2-D tunneling in GaAs double quantum wells (DQWs) as the operating principle for a new device proposed at Sandia, the double electron layer tunneling transistor (DELTT); 2-D/2-D tunneling offers vastly superior advantages for device possibilities over 3-D/2-D tunneling in traditional tunneling devices. These include (1) much sharper tunneling resonances, (2) the ability to modulate conductivity with a third terminal, and (3) the possibility of constructing low-power, high-speed, unipolar complementary logic. We seek to (1) build a prototype DELTT and (2) continue basic research on DQW physics with theoretical support. The report describes progress in addressing the fundamental issues of achieving (1) separate contacts to the emitter and collector QWs, (2) design for compatible input/output voltages (gain), and (3) design for high-temperature, high-speed operation. It also describes advances in fundamental basic research on the physics of tunneling in DQW structures.

We met almost all milestones in FY96, and the project plan remains unchanged. Our major accomplishments are:

(1) *Invention of novel Epoxy-Bond-and-Stop-Etch (EBASE) technique.* We invented a technique for backgating epitaxial layers to form contacts to the individual quantum wells (QWs). The procedure involves patterning the sample's frontside normally, epoxying the frontside down onto a new substrate, and etching away the original substrate. A smooth back surface, free for additional lithographic processing, is exposed only a few 1000 Å from the active layers.

(2) *Observation of transistor action in DELTT structures made by EBASE.* We observed clear transistor action. Depletion gates formed individual contacts to the QWs, and a third control gate changed the QW densities to modulate tunneling conductivity by a factor of 10. This negative transconductance, absent in conventional field-effect transistors (FETs), is a clear proof-of-concept for the DELTT.

(3) *Design, fabrication, and electrical testing of DQW far-infrared (FIR) detectors.* We designed, and fabricated by EBASE, FIR detectors using meander-line grating gates to enhance photon coupling. At 0.3 K, all gates were operating correctly.

(4) *Optical measurements of new DQW FIR detectors made by EBASE.* We performed photoresponse measurements at 4 K. Although all gates were operating correctly, we detected no photoresponse. We believe this is due to Sandia's IR light source having insufficient intensity. We are now collaborating with the University of Maryland, which has better-suited equipment. We sent EBASE FIR detectors to this institution.

(5) *Fabrication of novel 1-D/2-D tunneling structures using surface grating gates.* We fabricated several structures using electron-beam-written grating gates to form 1-D wires in the top QW. Measurements are under way.

(6) *Design of DELTT structures for high-gain, high-temperature, and high-speed operation.* We designed structures having high-density and hence high-T operation, and grew some high-gain structures. We produced an improved mask set.

(7) *Development of a linear response theory of DQW FIR detector photoresponse.* We developed a theory and performed numerical calculations for DQW detectors. We included effects of magnetic fields and temperature. Unlike conventional detectors, the response is narrowband and persists to high temperature.

(8) *Complete mapping of the Fermi surface of DQWs vs. in-plane magnetic field.* We mapped the magnetoresistance vs. both perpendicular and in-plane fields up to ~ 9 Tesla each. This constitutes a complete mapping of the Fermi surface vs. in-plane field, enabling us to quantify magnetic breakdown of the Fermi surface and compare with previously existing theory.

Publications

Refereed

Harff, N. E., J. A. Simmons, G. S. Boebinger, J. F. Klem, L. N. Pfeiffer, and K. W. West. 1996. "Magnetic Breakdown in Double Quantum Wells." *Proc. 23rd Internat. Conf. on the Phys. of Semiconductors* **3** (Berlin, Germany, 21–26 July): 2199–2202. Singapore: World Scientific Publishing.

Harff, N. E., J. A. Simmons, J. F. Klem, G. S. Boebinger, L. N. Pfeiffer, and K. W. West. 1996. "Observation of Magnetic Breakdown in Double Quantum Wells." *Superlattices and Microstructures, Proc. Nanostructures and Mesoscopic Syst. Conf.* **20** (Santa Fe, NM, 19–24 May): 595–600. New York, NY: Harcourt, Brace, Jovanovich, Ltd.

Lyo, S. K. 1996. "Magnetic Quenching of Backscattering in Coupled Double Quantum Wires: Giant Mobility Enhancement." *J. Phys. Condensed Mat.* **8**: L703–L706. London, UK: Institute of Physics Publishing.

Lyo, S. K. 1996. "Magnetotunneling Absorption in Double Quantum Wells." *Proc. Nanostructures and Mesoscopic Syst. Conf.* **20** (Santa Fe, NM, 19–24 May): 609–613. New York, NY: Harcourt, Brace, Jovanovich, Ltd.

Lyo, S. K., J. A. Simmons, N. E. Harff, and J. F. Klem. 1996. "Novel Magnetic Field-Induced Minigap Transport in Double Quantum Wells." *Condensed Mat. and Rel. Phys., Proc. Chancellor's Symp.* (University of California–Los Angeles, Riverside, CA, 18 March). Singapore: World Scientific Publishing.

Lyo, S. K., J. A. Simmons, N. E. Harff, T. M. Eiles, and J. F. Klem. 1995. "Magnetic Field-Induced Tunneling and Minigap Transport in Double Quantum Wells." *Proc. 22nd Internat. Symp. on Compound Semiconductors* **145** (Cheju Island, South Korea, 28 August–2 September): 845–850. London, UK: Institute of Physics Publishing.

Weckwerth, M. V., J. A. Simmons, N. E. Harff, M. E. Sherwin, M. A. Blount, W. E. Baca, and H. C. Chui. 1996. "Epoxy Bond and Stop-Etch (EBASE) Technique Enabling Backside Processing of (Al)GaAs Heterostructures." *Superlattices and Nanostructures, Proc. Nanostructures and Mesoscopic Syst. Conf.* **20** (Santa Fe, NM, 19–24 May): 561–567. New York, NY: Harcourt, Brace, Jovanovich, Ltd.

Other

Harff, N. E., J. A. Simmons, J. F. Klem, and M. V. Weckwerth. 1996. "Magnetic Breakdown in Double Quantum Wells." *Proc. March Mtg. Amer. Phys. Soc.* **41** (St. Louis, MO, 18–22 March): 77. New York, NY: American Institute of Physics.

Development of a Process Simulation Capability for the Formation of Titanium Nitride Diffusion Barriers

M. D. Allendorf, D. A. Outka, C. F. Melius, R. S. Larson, P. Ho

Sandia is making experimental and theoretical efforts to develop a verified model for predicting the chemical vapor deposition (CVD) of titanium nitride from the reactants $TiCl_4$ and NH_3. This report presents experimental measurements of TiN CVD rates in a stagnation-flow reactor. We measured deposition rates as a function of NH_3 and $TiCl_4$ concentration. The measured TiN deposition rates are in good agreement with the predictions of a deposition model based on elementary gas-surface reactions. We also describe results of experiments using ultra–high-vacuum surface techniques to probe the reaction of NH_3 with TiN surfaces. Finally, we discuss theoretical methods developed to predict thermodynamic parameters (such as heats of formation) for titanium-containing compounds.

The objective of this project is to develop a first-generation model for simulating titanium nitride (TiN) chemical vapor deposition (CVD) that predicts deposition rates as a function of reactor parameters (temperature, pressure, flow rates). TiN is a prime candidate to replace sputter-deposited titanium due to its superior properties as a diffusion barrier and lower electrical resistivity. It is also of interest for wear- and corrosion-resistant coatings and as a coating used to improve the energy efficiency of glass.

In FY96, we deposited TiN films on silicon substrates in a stagnation-flow reactor. We used the reactants $TiCl_4$ and NH_3; deposition occurred at 600° C and 6^{-10} torr. Auger electron spectroscopy (AES) and low-energy ion scattering indicate that the films are nearly stoichiometric. We detected no chlorine, although the near-surface region contained significant amounts of oxygen. Scanning-electron microscopy (SEM) and x-ray diffraction indicate that the films are amorphous.

We measured deposition rates as a function of input concentrations and found them to be independent of $TiCl_4$ concentration and linearly dependent on the concentration of NH_3. We compared these rates with predictions of a deposition model that predicts TiN deposition rates as a function of reactant concentration, deposition temperature, and total pressure. The experimental results are in good agreement with predictions, providing confidence that the model can be used to optimize reactor designs for TiN deposition processes.

The dependence of the deposition rate on NH_3 concentration suggests that the interaction of NH_3 with the surface may be the rate-limiting step. Consequently, we characterized the interaction of NH_3 with TiN surfaces using temperature-programmed desorption and AES. We measured a sticking coefficient of 0.06, which is similar to that determined in the modeling study.

Finally, we tested theoretical methods that predict electronic energies of titanium-containing compounds from which heats of formation can be derived. Such data are necessary for the further development of deposition models. We used two methods: fourth-order Möller-Plesset perturbation theory and density functional theory (DFT). Both methods accurately predict the heat of formation of $TiCl_4$ and can predict heats of formation for other $TiX_{4-n}Y_n$ species (X=NH_2, Cl, H; n=0-(4). However, neither method was successful in determining electronic energies for open-shell compounds (n = 1-3), indicating that further research is necessary before reliable predictions of thermodynamic data for these compounds can be obtained.

Publications

Refereed

Larson, R. S., and M. D. Allendorf. 1996. "A Reaction Mechanism for Titanium Nitride CVD from $TiCl_4$ and NH_3." *Proc. 13th Internat. Symp. on Chemical Vapor Deposition, The Electrochemical Society* **96-5** (Pennington, NJ, 5–10 May): 41–46.

Schulberg, M. T., M. D. Allendorf, and D. A. Outka. 1996. "Aspects of Nitrogen Surface Chemistry Relevant to TiN Chemical Vapor Deposition." *J. Vac. Sci. Technol. A* **14**: 3228. Woodbury, NY: American Vacuum Society.

Schulberg, M. T., M. D. Allendorf, and D. A. Outka. 1996. "The Reaction of NH_3 with TiN: Implications for CVD." *Proc. Covalent Ceramics III–Sci. and Technol. of Non-Oxides, Fall Mtg. Mater. Res. Soc.* **410** (Boston, MA, 27–30 November): 453–458.

Other

Larson, R. S., and M. D. Allendorf. 1995. "A Reaction Mechanism for Titanium Nitride CVD from TiC_{l4} and NH_3." Paper presented to the AIChE Annual Meeting, Miami, FL, 12–16 November.

A Passive, Self-Aligned, Micromachined Device for Alignment of Arrays of Single-Mode Fibers to Binary Optics for Manufacturable Photonic Packaging

S. H. Kravitz, M. E. Warren, P. K. Seigal, M. G. Armendariz, C. T. Sullivan

During the first year, CLASP (Capture and Locking Alignment Spring Positioner) succeeded in all of its goals. Sandia designed a fiber alignment and capture test mask. We evaluated several designs of capture devices with various spring forces and pocket shapes. We built the optimal design and released the moving part of the spring from the substrate. We built a coarse alignment holder for pre-alignment of the fiber array. We succeeded in capturing four optical fibers and measuring that the capture was within ±2 μm. Our goal for the second year was to improve the accuracy of capture to ±1 μm.

Alignment of single-mode optical fibers to photonic devices has proven to be the most expensive single item in the cost of packaged photonic devices. This work provides a method of passive mechanical alignment of an array of single-mode fibers. The technique uses a micromachined metal spring that captures a vertical, pre-positioned fiber, moves it into accurate alignment, and holds it for attachment. The spring is fabricated from electroplated nickel, using photodefined polyimide as a plating mask. We refer to this entire concept as CLASP.

During the first year, CLASP succeeded in all of its goals. We designed a fiber alignment and capture test mask. We evaluated several designs of capture devices with various spring forces and pocket shapes. We built the optimal design and released the moving part of the spring from the substrate. We built a coarse alignment holder for pre-alignment of the fiber array. We succeeded in capturing four optical fibers and measuring that the capture was within ± 2 μm. Our goal for the second year was to improve the accuracy of capture to ±1 μm. We assumed that the accuracy would improve if the plated springs had perfectly straight walls.

The approach for improvement was to change from polyimide as a masking material for electroplating (which did not give straight-wall profiles) to straight-wall positive photoresist. The original mask used for electroplating was photodefined polyimide. The profile that resulted from this material had both a protruding head and a protruding foot. AZ4903 positive photoresist became available, and we developed a process to yield straight-wall profiles. We succeeded in plating springs 50-μm tall with vertical walls. Measurements are not complete on the accuracy of alignment at this time.

A second, unexpected difficulty that we overcame was the low-release yield of the capture springs. That is, the moving portion of the spring did not totally release, or would release only if prodded by hand. Analysis then showed that the spring was actually "ripped" from the surface, rather than being chemically released. We increased the titanium release-layer thickness to 1 μm, which allowed for easy release. An accompanying hydrofluoric (HF) etch done in a rough vacuum helped remove the hydrogen bubbles generated during the release etch, thus speeding the etch from 8 hours to 1 hour.

Publications

Refereed

Kravitz, S. H., J. C. Word, T. M. Bauer, P. K. Seigal, and M. G. Armendariz. 1996. "A Passive Micromachined Device for Alignment of Arrays of Single-Mode Fibers for Hermetic Photonic Packaging—The CLASP Concept." *IEEE CPMT Transactions, Part B: Advanced Packaging* **19 (1)** (February): 883–892.

Other

Kravitz, S. H., J. C. Word, M. B. Snipes, M. G. Armendariz, P. K. Seigal, and C. T. Sullivan. 1994. "A Passive Micromachined Device for Alignment of Arrays of Single-Mode Fibers for Manufacturable Photonic Packaging." *Proc. LEOS '94* **1** (Boston, MA, 31 October): 226–227.

Kravitz, S. H., J. C. Word, P. K. Seigal, M. G. Armendariz, and T. M. Bauer. 1995. "CLASP—A Micromachined Device for Alignment of Arrays of Single-Mode Fibers." *Proc. Manufacturable Photon. Packaging Mtg., Optical Soc. of Amer. Conf.* **1** (Portland, OR, 11–15 September): 108.

Red-to-Blue-Wavelength Photonic Devices

M. H. Crawford, T. J. Drummond, W. W. Chow, R. J. Shul, E. J. Heller, K. D. Choquette, K. P. Killeen

Sandia plans to become a world leader in broad-spectrum visible photonic devices, covering the wavelength range from red to blue, using III–V materials. The initial phase of this project focuses on extending the wavelength of lasers and light-emitting diodes (LEDs) based on the AlGaInP alloys and heterostructures as short as possible, from short-wavelength red (620–640 nm, including 633 nm) through orange, yellow, and green (at ~ 565 nm). Sandia has extensive experience now in the growth of these materials, so we anticipate that the primary issues in the development of the devices will be associated with their design. We will place particular emphasis on the development of novel resonant-cavity photonic devices, including resonant-cavity LEDs (RCLEDs) and vertical-cavity surface-emitting lasers (VCSELs). In addition, we will develop a new metalorganic vapor phase epitaxy (MOVPE) growth capability as a parallel path to obtaining device-quality nitride materials. In the second phase of the work, the primary focus of the device effort will be on building blue light-emitting photonic devices from the nitrides. The main emphasis will be on fabrication of efficient blue LEDs and RCLEDs. At the completion of this work, Sandia will have demonstrated novel photonic devices, including surface-emitting lasers, RCLEDs, and conventional LEDs from red to blue wavelengths.

In the second year of this project, work progressed at such a rate that we completed all of the milestones. Here is a summary of those milestones and accomplishments:

(1) Demonstrated 1-mW output-power room-temperature 633-nm AlGaInP VCSELs: Efforts to extend the short-wavelength emission range of visible VCSELs focused on design and MOVPE growth of alternative VCSEL active regions. We found significant losses in optical efficiency when as little as 10% aluminum was introduced into the quantum wells to shorten the emission wavelength. This has been reported by many groups and is thought to be due to oxygen impurity-related nonradiative recombination. As an alternative approach, we optimized our growth system to enable thin quantum wells. Specific designs included 42-Å InGaP quantum wells or 50-Å quantum wells in place of the nominally 70-Å wells in standard designs. We implemented these short-wavelength active regions into VCSEL heterostructure designs for the first time. We fabricated ion-implanted VCSELs and demonstrated continuous-wave (CW) room-temperature lasing over the 648–675-nm range. Under pulsed operation (5% duty cycle) the 42-Å quantum-well structure achieved lasing at 636 nm, close to the 633-nm goal. We reported short-wavelength emission last year for selectively oxidized VCSELs, whereas these results are for ion-implanted VCSELs, which are currently less efficient but more manufacturable.

(2) Demonstrated RCLEDs covering the 565–620-nm range: Our efforts in this area focused on designing and growing active regions covering the yellow-to-red spectral regions and also developing alternative mirror designs for shorter wavelengths. We grew a series of AlGaInP alloys with Al mole fraction varying from 0 to 0.8, and we characterized band-edge emission intensity and wavelength by low-temperature photoluminescence.

(3) Developed a comprehensive model to evaluate short-wavelength VCSEL designs: We completed a comprehensive microscopic theory to determine the gain of short-wavelength VCSEL designs. The theory includes leakage currents, which are increasingly important in shorter-wavelength designs.

(4) Demonstrated dominant band-edge emission from MOVPE-grown materials: We made significant progress this year in the development of an MOVPE growth capability for the III–N materials. We constructed a Sandia-designed rotating disk reactor and designed, programmed, and installed new automated control and monitoring systems. We grew GaN bulk films on sapphire substrates.

(5) Grew and characterized AlGaN and InGaN ternary materials.

(6) Demonstrated low-background carrier concentration in GaN materials.

Publications

Refereed

Chow, W. W., M. H. Crawford, and R. P. Schneider, Jr. 1995. "Minimization of Threshold Current in Short-Wavelength AlGaInP Vertical-Cavity Surface-Emitting Lasers." *IEEE J. Selected Topics in Quantum Electron.* **1** (June): 649–653.

Other

Weckworth, M. V., K. P. Killeen, R. M. Biefeld, T. J. Drummond, M. H. Crawford, and J. C. Zolper. 1996. "The Effects of Helium vs. Hydrogen as a Carrier Gas for MOCVD Growth and Nucleation of (In)GaN on Sapphire." *Proc. 38th Electron. Mater. Conf.* (Santa Barbara, CA, 26–28 June).

High-Speed Modulation of Vertical-Cavity Surface-Emitting Lasers

K. L. Lear, M. G. Armendariz, V. M. Hietala, K. D. Choquette, H. C. Chui

Sandia will complete work on developing high-speed vertical-cavity surface-emitting lasers (VCSELs) for multi-gigabit-per-second (Gb/s) optical data communications applications. The project will result in devices that operate at up to 20 GHz. Replacing the insulating damage region in VCSELs with an insulating and low-index oxide increased the maximum VCSEL bandwidth from 12 GHz to a record 16 GHz. Work is proceeding on reducing parasitic capacitance and improving modal properties with the projected result being bandwidths in excess of 20 GHz. The oxide-confined devices also exhibit very low-threshold currents and rapid increases in bandwidth at small currents, making them attractive for direct digital modulation, which should simplify drive electronics for high-data-rate communications systems. We used the oxide-confined VCSELs in 1 Gb/s data-rate tests with encouraging results. We de-emphasized polarization switching work due to the successes in direct modulation of oxide-confined devices.

We accomplished the following in FY96:

(1) Designed and fabricated VCSELs with increased conventional modulation bandwidth based on oxide-confined structures.

(2) Measured the microwave-frequency response of oxide-confined VCSELs.

(3) Developed equivalent circuit models and extracted parameter values for oxide-confined VCSELs.

(4) Designed a high-speed VCSEL package to facilitate systems tests of oxide-confined VCSELs.

(5) Developed a new polyimide planarization process with adequate metal adhesion and low enough capacitance for high-frequency operation.

(6) Performed large signal (digital) modulation experiments.

(7) Developed high-speed 850-nm devices for compatibility with new short-haul data communication standards.

We will complete work on developing high-speed VCSELs for multi-Gb/s optical data communications applications, resulting in devices that operate up at to 20 GHz. Replacing the insulating damage region in VCSELs with an insulating, low-index oxide increased the maximum VCSEL bandwidth from 12 GHz to a record 16 GHz. Work is proceeding on reducing parasitic capacitance and improving modal properties with the projected result being bandwidths in excess of 20 GHz. The oxide-confined devices also exhibit very low-threshold currents and rapid increases in bandwidth at small currents, making them attractive for direct digital modulation, which should simplify drive electronics for high-data-rate communications systems. We used the oxide-confined VCSELs in 1-Gb/s data-rate tests with encouraging results. We de-emphasized polarization switching work due to the successes in direct modulation of oxide-confined devices.

As a result of the substantial successes in the conventional modulation of oxide-confined VCSELs, we de-emphasized investigations of polarization modulation. The oxide-confined VCSELs show stronger polarization properties, decreasing the ability to modulate the polarization direction in these structures. We are considering particular structures that could still allow polarization modulation of oxide-confined devices and will include any promising candidates in the next high-speed mask layout. One interesting feature of the orthogonal polarization of transverse modes is that the frequency response while operating in the transverse mode regime is polarization-sensitive.

Publications

Refereed

Lear, K. L., A. Mar, K. D. Choquette, S. P. Kilcoyne, R. P. Schneider, Jr., and K. M. Geib. 1996. "High-Frequency Modulation of Oxide-Confined Vertical-Cavity Surface-Emitting Lasers." *Electron. Lett.* **32** (29 February): 457–458. London, UK: IEEE.

Other

Lear, K. L., V. M. Hietala, A. Mar, K. D. Choquette, H. Q. Hou, and R. P. Schneider, Jr. 1996. "High-Frequency Modulation of Oxide-Confined Vertical-Cavity Surface-Emitting Lasers." Paper presented to the 2nd International Conference on High-Speed Optoelectronics Devices and Systems, Snowbird, UT, 11–15 August.

GaAs PIC Development for High-Performance Communications

C. T. Sullivan, R. J. Shul, R. G. Hadley, H. C. Chui, V. M. Hietala, J. R. Wendt, S. H. Kravitz, M. G. Armendariz, G. A. Vawter

Sandia is establishing a foundational technology in photonic integrated circuits (PICs) based on the (Al,Ga)As material system for optical communication, guidance and control, and network switching applications at the important 1.3-μm/1.55-μm wavelengths. We are investigating the optical and electrooptical performance characteristics of the fundamental building-block PIC elements designed to be as simple and process-tolerant as possible, with particular emphasis placed on reducing optical insertion loss. We are building relatively conventional device array and circuit designs using these PIC elements to establish a baseline performance standard; to assess the impact of epitaxial growth accuracy and uniformity, and of fabrication uniformity and yield; and to resolve the requisite optical and radio-frequency (RF) packaging issues. More novel and complex PIC designs and fabrication processes, viewed as higher payoff but higher risk, are explored in a parallel effort and will be meshed into our baseline higher-yield capability as they mature. The first application focus targeted the design and fabrication of packaged solitary modulators meeting the requirements of future 10-Gb/s digital links and 60-GHz analog links. We expect successfully prototyped devices to feed into more complex PICs, solving specific problems in high-performance communications such as optical beam-forming networks for phased-array antennas (PAAs).

On our baseline effort, we demonstrated record low-loss optical-waveguide routing and distribution components for (Al,Ga)As PICs, including (1) single-mode attenuations < 0.5 dB/cm (our best 0.4±0.1 dB/cm), (2) right-angle turning mirror insertion loss of 0.4±0.1 dB, a world-best record, and (3) excess loss of 0.4±0.2 dB for lateral mode interference (LMI) 1x2, 1x4, 1x8, and 1x32 splitters, all with typically ~ 95% on-chip yields. We developed an approach to velocity match (< 10% mismatch) low-loss transmission line electrodes to undoped (Al,Ga)As optical-waveguide modulators with ~ 95% on-chip yields, fabricated wideband electrooptic waveguide modulators, and developed fiber packaging for loss-limited small-signal bandwidth > 50 GHz and fiber-waveguide–fiber-insertion loss of < 6 dB. We invented a novel fiber-waveguide coupler and demonstrated it to have ~ 1.5-dB insertion loss with substantial misalignment tolerance, a dramatic improvement over the 8 ~ 10-dB range typically expected for very high electrooptic figure-of-merit (FOM) modulators. We demonstrated high-FOM modulators with 15.5-dB (V^1 =2.6V) and 14-dB extinction ratios using novel *XY* combiner and cutoff mesa waveguide designs, respectively, and recently measured them to have small-signal bandwidths > 40 GHz (instrument-limited) and on-chip losses of about 7 dB. We invented a novel 1x32 switch based on LMI splitters, phase-modulated arrayed waveguides, and electrooptic in-plane focusing effects to address optical control problems in phased-array radars.

Publications

Refereed

McClellan, G. B., R. J. Shul, and C. T. Sullivan. 1996. "Dry Etching of GaAs Using an Inductively Coupled Plasma." Paper presented to the 32nd Annual Symposium of the New Mexico Chapter of the American Vacuum Society, Albuquerque, NM, 2 April.

Shul, R. J., C. T. Sullivan, M. B. Snipes, G. B. McClellan, M. Hafich, and C. T. Fuller. 1995. "Attenuation Losses in Electron Cyclotron Resonance Plasma-Etched AlGaAs Waveguides." *Solid-State Electron.* **38** (October): 2047–2049. London, UK: Pergamon.

Smith, R. E., C. T. Sullivan, G. R. Hadley, G. A. Vawter, J. R. Wendt, M. B. Snipes, and J. F. Klem. 1995. "Reduced Coupling Loss Using a Tapered-Rib Adiabatic-Following Fiber Coupler." Paper presented to the 8th Annual Meeting of the IEEE Lasers and Electro-Optics Society, San Francisco, CA, 30 October–2 November.

Smith, R. E., G. A. Vawter, G. R. Hadley, C. T. Sullivan, J. R. Wendt, M. B. Snipes, and J. F. Klem. 1996. "Tapered-Rib Adiabatic-Following Fiber Coupler." Paper presented to the Integrated Photonics Research Meeting, Boston, MA, 29 April–2 May.

Smith, R. E., G. A. Vawter, G. R. Hadley, C. T. Sullivan, J. R. Wendt, M. B. Snipes, S. H. Kravitz, and J. F. Klem. 1996. "Reduced Coupling Loss Using a Tapered-Rib Adiabatic-Following Fiber Coupler." *Photon. Technol. Lett.* **8** (August): 1052–1054. New York, NY: IEEE.

Sullivan, C. T. 1996. "Guided-Wave Optics Developments at Sandia National Laboratories." Paper presented to the Workshop on Electro-Optics for the Next Century, La Jolla, CA, 24 February.

Vawter, G. A., V. M. Hietala, J. R. Wendt, B. A. Fuchs, M. Hafich, M. Housel, M. G. Armendariz, and C. T. Sullivan. 1996. "High-Speed Traveling-Wave Electrooptic Intensity Modulator with a Doped PIN Semiconductor Junction." Paper presented to the Integrated Photonics Research Meeting, Boston, MA, 30 April.

Achromatic Nonlinear Optics for Sensing and Process Control

R. P. Trebino, S. E. Bisson

Sandia is developing a robust, compact, inexpensive, and general technique called achromatic phase-matching *(APM) to achieve efficient nonlinear-optical conversion for tunable laser light at any wavelength. It is simple and involves no moving parts; it is entirely passive. It involves a simple few-prism arrangement, which automatically directs each wavelength into the nonlinear-optical crystal at its appropriate incidence angle, satisfying the numerous constraints required for high nonlinear-optical efficiency. While simple in appearance, APM is quite subtle in its underlying theory. For example, a prism by itself lacks sufficient dispersion for this application (gratings, which have sufficient dispersion, are too inefficient). However, a prism, followed by a spatial-beam compressor (also consisting of prisms), has its dispersion magnified by the spatial-compression factor. Thus, with this trick, sufficient dispersion can easily be achieved. In addition, a number of additional constraints exist, and using a newly developed 4x4 ray-pulse matrix technique as well as more precise programs that use the entire refractive-index curve for the nonlinear crystal, we showed theoretically that a simple class of APM designs satisfies these as well. Our goal is to find a practical arrangement that provides efficient harmonic generation over a wide range of wavelengths.*

We performed extensive, more detailed, precise modeling of several APM designs, and experimentally tested several designs, achieving a tuning range of 50 nm, about 500 times the range of a crystal without APM.

We significantly extended the accuracy of our model by including the precise refractive-index-vs.-wavelength curve of the nonlinear crystal beta barium borate (BBO) so that nonlinear dependencies of the phase-matching angle with wavelength are included. All previous models of APM included only the linear dispersive term. We now very accurately calculate the beam incidence angle at the crystal, the phase mismatch vs. wavelength, and the second-harmonic-generation (SHG) efficiency vs. wavelength. We optimized the overall efficiency with respect to all prism incidence angles. The nonlinear terms yielded complex behavior in the tuning curve; for crystal thicknesses of a few millimeters or more, slight deviations from perfect phase-matching can cause large dips in the efficiency. Some arrangements avoid these dips.

Three-, four-, and five-prism arrangements generally do not suffice because of insufficient dispersion, the need for large-incidence angles for which antireflective coatings are difficult to make, or no point where all wavelengths cross (thus requiring a large crystal). Six-prism designs generally work well, both in theory and in practice. The need for as many as six prisms is not problematic because prisms are inexpensive, compact, and easy to work with. The additional degrees of freedom (DOFs) help to compensate phase-matching nonlinearities, just as the use of several lens elements achieves more achromatic performance in a lens.

We experimentally demonstrated several arrangements, the best being a six-prism arrangement with an 8-mm-thick type-1 BBO crystal. We used an optical parametric oscillator (normally used in lidar [laser radar] experiments) between 600 and 700 nm as input to the APM apparatus. We achieved a tuning range of about 50 nm. The tuning curve for the crystal without an APM apparatus is only 1 nm. Unfortunately, the angular divergence of the beam was slightly larger than the angular acceptance of the crystal. We are correcting this by using designs with less compression and a larger beam.

The use of diffraction gratings, which have greater dispersion than prisms, may now be possible because of very rapid, recent progress at Lawrence Livermore National Labs (LLNL) in the production of highly efficient gratings. We are discussing this issue with the LLNL researchers and have used gratings in some of our design calculations and experiments.

Publications

Other

Trebino, R., B. A. Richman, S. E. Bisson, M. Mitchell, and K. W. DeLong. 1996. "A Compact, Robust, Instantaneously Tunable Harmonic Generator for Lidar Applications." *Proc. Internat. Laser Radar Conf.* (Berlin, Germany, 22–26 June): in press. Berlin, Germany: Springer-Verlag.

Integrated Separation and Optical Detection for Novel On-Chip Chemical Analysis

M. E. Warren, P. K. Seigal, P. L. Gourley, D. S. Anex

The future of advanced chemical detection and analysis is in miniature devices that are able to characterize increasingly complex samples, a "laboratory-on-a-chip." In this concept, chemical operations used to analyze complicated samples in a chemical laboratory—sample handling, species separation, chemical derivatization and detection—are incorporated into a miniature device. By using electrokinetic flow, this approach does not require pumps or valves because fluids in microfabricated channels can be driven by externally applied voltages. This is ideal for sample-handling in miniature devices. This project will develop truly miniature on-chip optical systems based on vertical-cavity surface-emitting lasers (VCSELs) and diffractive optics. We will build these into a complete system that also has on-chip electrokinetic fluid-handling and chemical separation in a microfabricated column. The primary goal is the design and fabrication of an on-chip separation column with fluorescence sources and detectors that, using electroki-

netic flow, can be used as the basis of an automated chemical analysis system. Secondary goals involve investigation of a dispersed fluorescence module that can be used to extend the versatility of the basic system and on-chip, intracavity laser absorption as a high-sensitivity detection technique.

The primary goal of the first-year effort was to develop the key components of the on-chip chemical analysis system. These components consist of the capillary flow channels fabricated in a fused silica substrate, the VCSELs for fluorescence excitation, and microoptics to be fabricated on the substrate for direction and control of the VCSEL output. Other important parts of a final system are the detector and the mounting of the components on the substrate. We are also fabricating special external-cavity VCSELs for intracavity absorption detection and integrating them with similar capillary flow channels. These are being evaluated and can be integrated into a system with the capillary electrophoresis separation system.

We fabricated flow channels in three-inch-diameter fused-silica substrates using photolithography and wet etching. These are configured with reservoirs and intersections to allow control of sample sizes and flow by applying voltages to induce electroosmotic flow. We fabricated cover plates from fused silica plates and bonded the parts together using UV-cured adhesives. We wired the sealed system with open microchannels and integrated buffer reservoirs with platinum electrodes and successfully tested them for flow and electrical continuity. We placed fluorescent dye in the channel and demonstrated voltage-driven electroosmotic flow as a first step toward electrokinetic separation in the channel. Under voltage control, we flowed solutions between reservoirs. Flow between reservoirs and sample introduction are the two operations required for chemical analysis in a planar format.

We fabricated and packaged VCSEL arrays of 780-nm wavelength in the CSRL for testing in the existing capillary electrophoresis test-bed. We used individual VCSELs on the array to excite infrared (IR)-fluorescent dyes that were separated within freestanding capillaries having inner diameters of 100 microns. The ability of the VCSELs to excite the fluorescent dyes within the small dimensions of the capillaries shows that the VCSELs will be an excellent excitation source for analytes separated within microchannels.

Integrated Heterojunction Bipolar Transistor Control Electronics and LED/VCSEL Drivers for High-Density Optical Data Links

K. D. Choquette, D. C. Craft, A. G. Baca, R. F. Carson, D. J. Rieger, R. J. Shul, M. H. Crawford, H. C. Chui

Sandia will continue efforts toward developing high-density, 2-D arrays of photonic interconnects for either multichip modules (MCMs) or board-to-board applications, which require integration of drivers and logic circuits near the optical sources. The drivers are needed because typical logic outputs cannot source the needed current, and standard line drivers do not exhibit sufficient current regulation. Moreover, on-chip logic is necessary for bidirectional channels, maximum interconnect density, and for low packaging costs. Since high-density optical interconnects demand low-power dissipation requiring low-current biasing, source drivers must supply high currents with subnanosecond risetimes in large signal operation. This project will demonstrate control electronics and drivers for light sources first within a hybrid technology, then develop the necessary materials growth and processing technologies for monolithic integration of transistors with light-emitting diodes (LEDs) or vertical-cavity surface-emitting lasers (VCSELs). In partnership with systems engineers, we will establish specifications for driver and logic circuits to ensure compatibility with current and future systems to enhance Sandia's world leadership in VCSEL technology. Ultimately, this high-density interconnect technology would enable the required real-time processing needed in intelligent weapons application such as target recognition.

We made the following accomplishments in FY96:

(1) Compared the attributes of field-effect transistors (FETs) and heterojunction bipolar transistors (HBT) for utilization in laser driver circuitry. We pursued HBTs in the first year because of their lower input impedance necessary for impedance matching to the laser, and the potential for higher-current density necessary for supply to the laser. In addition, HBTs with thin base regions (< 100-nm thick) exhibit high gain and excellent microwave characteristics.

(2) Designed mask layout for discrete HBTs.

(3) Completed process development for HBT fabrication, including technique for contacting 70-nm-thick base region.

(4) Grew epitaxial materials by metalorganic vapor phase epitaxy (MOVPE) (five wafers) and fabricated viable HBTs. The fabricated HBTs exhibited maximum current gains of 600 for Vbc=0 volts and 900 for Vbc=2 volts. Also, the breakdown voltage was Vbco > 4 volts.

(5) Accomplished hybrid integration of HBT with selectively oxidized VCSELs.

(6) Achieved a maximum gain of 581, which produced ≈ 40 mA of injection current to the VCSEL for 12-mW output light from the VCSEL with an HBT base current of only 68 μA. Furthermore, we achieved large signal modulation of the VCSEL (output changing from 0 to 15 mW) at frequencies up to 10 MHz. The maximum frequency was limited by the packaging of the circuit rather than the discrete devices.

Virtual Reactor for the Semiconductor Manufacturing Plant of the Future

R. E. Smith, J. F. Klem, M. E. Coltrin, I. J. Fritz

This project will develop a sophisticated system to enable model-based agile manufacturing in the critical metalorganic chemical vapor deposition (MOCVD) and molecular beam epitaxy (MBE) materials growth processes essential to high-speed microelectronics and optoelectronic components. This effort will be founded on a modular and configurable process automation system that will serve as a backbone allowing integration of process-specific models and sensors. We will develop and integrate both MOCVD- and MBE-specific models in this system and demonstrate the effectiveness of both model-based and sensor-based real-time feedback control in improving the accuracy and reproducibility of semiconductor heterostructure growth on MOCVD and MBE systems. In addition, within this framework we will construct "virtual reactor" models for both growth processes and show how these models can be used to greatly shorten the epitaxial growth process development cycle.

We made the following accomplishments in FY96:

(1) We performed MBE effusion-cell characterization on an EPI dual-filament gallium source. We developed a fourth-order auto-regression (ARMAX) discrete time model that accurately describes the dynamic performance of the cell, thus satisfying the effusion-cell milestones.

(2) We installed a multiple-pass optical flux monitor and tested it on the MBE system, satisfying a project milestone.

(3) We developed a generic automation backbone and tested it on the MBE system, thus satisfying automation-system milestones. Customizing and refining of the MBE automation system is ongoing.

(4) We completed the initial piping model and are testing and refining it. The interfacing to our ALE model and control system is under way.

(5) We constructed a virtual reactor prototype using the Lab View software. The virtual reactor can be driven by the Programmable Logic Controller (PLC) and responds to exactly the same set of electrical signals/commands that the PLC sends to the actual reactor to drive the hardware. The virtual reactor gives a graphical display showing the status of all relevant components of the system (valve positions, flow rates, etc.). The virtual reactor model will find immediate application in developing safety interlocks on our MOCVD systems.

Selective Oxidation Technology and Its Applications Toward Electronic and Optoelectronic Devices

O. Blum, H. C. Chui, J. P. Sullivan, C. I. H. Ashby, J. F. Klem, G. A. Vawter, K. D. Choquette, K. L. Lear

Selective oxidation of AlGaAs compounds has improved the performance of near-infrared (NIR) vertical-cavity surface-emitting lasers (VCSELs). Sandia proposes to (1) expand our understanding of this technology, (2) explore its applicability to other Al-bearing materials, (3) demonstrate a variety of new electronic and optoelectronic devices, and (4) establish the reliability and manufacturability of oxidized devices. Specifically, we will investigate conditions required to maximize control of the oxidation process as well as those required to facilitate/inhibit etching of the resultant oxide. Concurrently, we will perform preliminary studies to extend the technology to other Al-bearing compounds such as Al(Ga)AsSb, InAl(Ga)P, and Al(Ga)N. Selective oxidation of AlGaAs will facilitate an exciting new approach toward nanofabrication that requires only lithographic patterning on a micron scale. We will consider several new devices utilizing the selective oxidation technology. We will investigate layers of oxidized AlGaAs as a means of forming various optical elements, such as convex and concave lenses that could be embedded into an assortment of surface-normal, multilayer devices. We will also apply oxidized AlGaAs to fabrication of microdisk laser diodes. On a separate front, we will also explore the possibility of using oxidized AlGaAs to form GaAs/AlGaAs field-effect transistors (FETs). Finally, we will address reliability and manufacturability issues of the high-performance VCSELs fabricated using selective oxidation technology.

We obtained the oxidation rates of AlGaAs as a function of several parameters and for several oxidation conditions. These enabled us to design improved, more reliable device structures. We also determined oxidation rates of other Al-bearing materials, such as Al(Ga)AsSb, as a function of several parameters and for several oxidation conditions. This will enable us to design and fabricate devices on InP utilizing oxidation technology. We characterized oxidized AlAsSb layers using transmission-electron microscopy (TEM), Auger and Raman spectroscopy (AES), and scanning-electron microscopy (SEM). We also designed appropriate Al mole fraction profiles, which resulted in fabrication of buried optical microlenses for applications in a variety of surface-normal structures. We evaluated suitability of continuous vs. digital alloys of AlGaAs for buried lens formation and determined that digital alloy was the more appropriate choice. We designed

and fabricated a GaAs/AlGaAs microdisk laser using oxidation technology. We evaluated its performance and will incorporate improvements into the second-generation device. We obtained lifetime data for VCSELs fabricated by an existing oxidation process. To accelerate the failure process, we designed and fabricated a special, high-temperature fixture. We are currently testing devices at higher temperatures to obtain a sufficient number of failures to statistical analysis. Also, we progressed in etching the oxides. We found that C_{l2}-based reactive ion etches remove AlGaAs five times quicker than the oxide. We found wet-etching chemistries, such that selective removal of oxide is possible. Finally, we determined segregation of As upon oxidation to be the mechanism by which interfacial states were formed between the oxide and GaAs.

Publications

Refereed

Blum, O., K. L Lear, H. Q. Hou, and M. E. Warren. 1996. "Buried Refractive Microlenses Formed by Selective Oxidation of AlGaAs." *Electron. Lett.* **32** (18 July): 1406–1407. London, UK: The Institution of Electrical Engineers.

Blum, O., K. M. Geib, M. J. Hafich, J. F. Klem, and C. I. H. Ashby. 1996. "Wet Thermal Oxidation of AlAsSb Lattice Matched to InP for Optoelectronic Applications." *Appl. Phys. Lett.* **68** (27 May): 3129–3131. Woodbury, NY: American Institute of Physics.

Top-Surface Imaging Resists for Lithography with Strongly Attenuated Radiation

A. K. Ray-Chaudhuri

For extreme ultraviolet (EUV) lithography at 13 nm, strong-resist photoabsorption necessitates the use of top-surface imaging resists. An earlier team developed a bilayer silylation resist process that demonstrated < 0.13-μm-thick layer. In this project, we undertook additional chemistry and materials developments to support the eventual goal of a top-surface imaging resist for 0.1-μm critical dimension (CD). Specifically, we examined new imaging-layer polymer resins for improved silicon uptake contrast with reduced deleterious flow, and synthesized new silylation crosslinkers for more facile resist silylation and improved reagent stability.

To reduce deleterious flow of silylated resist, we showed in our earlier work that two-component silylating reagents that contain both a majority disilane silylating agent and a minority silylation crosslinker are effective. To avoid fractional distillation and thus improve the long-term compositional stability of these two-component reagents, we identified, synthesized, and tested new matched-volatility crosslinkers as part of this project. We synthesized the new crosslinker, bis(dimethylamino) methylethylsilane, having a boiling point of 146° C, for use with dimethylaminopentamethyl disilane (BP of 149° C). This new reagent mixture yielded more facile silylation of several resists; we found its composition to be far more stable than our original reagents. To identify improved silylation resist formulations, we performed experiments during this project on imaging layer resist resins developed by the Shipley and JSR companies. To obtain quantitative information on (1) the shape of the silylation mask, (2) unwanted parasitic silylation in cross-linked areas, and (3) unwanted flow of the silylated resist that occurs during the silylation process, we employed cross-sectional etch staining and scanning-electron microscopy (SEM). In our cross-sectional analysis work, the process parameters that we adjusted include the silylation time, delivered vapor pressure, process temperature, and percentage of crosslinker in the silylation reagent. The effect of these variables on the silylation process strongly depends on the glass transition temperature (Tg) of the formulated resist. A resist with a Tg higher than the silylation process temperature will have a significantly decreased amount of resist flow. A recent series of formulations have Tg ranging from 110°–140° C. The formulation with the highest concentration of photoacid generator (PAG) also exhibits the lowest Tg but is still higher than the silylation process temperature (95° C). This indicates the importance of selecting PAG materials with a high Tg. The origin of parasitic silylation is presently attributed to the volatility of the PAG at the surface of the resist. This creates a thin surface region across the surface where there is a reduction in cross-linked densification. This surface layer requires a nonselective breakthrough etch that reduces CD control. Initial experiments utilizing Shipley XP-9472 required a nonselective etch removal of approximately 45 nm to remove parasitic silylation. Cross-sectional SEM verified 40 nm of surface material. Recent work with Shipley XP-9691 shows significant improvement, yielding a thinner (10–15 nm) parasitic silylation layer. This result points the way to the development of silylation resist materials with the desired attributes of increased silicon contrast and reduced flow.

Publications

Other

Kubiak, G. D., A. Ray-Chaudhuri, and C. Henderson. 1996. "Basic Issues Associated with Four Potential EUV Resist Schemes." *Extreme Ultraviolet Lithography, Trends in Optics and Photonics* **4** (Boston, MA, 1–3 May).

Advanced Concepts for High-Power VCSELs and VCSEL Arrays

K. D. Choquette, H. C. Chui, E. J. Heller, K. L. Lear, W. W. Chow, M. E. Warren, R. G. Hadley

Sandia will continue to investigate and develop vertical-cavity surface-emitting lasers (VCSELs) for operation at high continuous-wave (CW), single-mode, output power and pulsed high-power operation. The high-power CW approach will center on "leaky-mode" concepts that utilize a higher index surrounding the laser cavity to provide index antiguiding and discrimination against the higher-order transverse modes. We adopted an alternate approach of using lateral modification of the cavity resonance to provide leaky-mode behavior. VCSEL heterostructure designs for high-power operation, particularly pulsed high power, are generally not appropriate for efficient CW operation. Thus, examining pulsed high-power VCSELs could open up an entirely new opportunity for VCSEL applications. In this area, we are pursuing both new cavity designs and heterostructure active regions optimized for high-power pulsed operation. We will also examine device structures incorporating high thermal-conductivity encapsulation for enhanced heat sinking. The overall project objective is to develop pulsed high-power sources appropriate for many applications and that have the many inherent advantages of VCSELs.

We made the following accomplishments in FY96:

(1) Developed mask set for and fabricated 850- and 980-nm broad-area, high-power, vertical-cavity surface-emitting lasers (VCSELs).

(2) Obtained 1.1-W output power under pulsed operation from broad-area 980-nm VCSEL (measurement power supply limited; work in progress for higher-current measurement setup).

(3) Completed analysis and design of leaky-mode VCSELs via cavity-resonance modification (predicted high modal discrimination for diameter of 7–10 μm and index steps of 0.02–0.08).

(4) Fabricated and tested oxide-confined VCSELs and exhibited single-mode operation to 2x threshold (further analysis shows effects of phase discontinuity on modal discrimination).

(5) Developed many-body dynamical carrier/photon model predicting new phenomena (model agrees with quasi-equilibrium results and predicts new damped relaxation effects).

(6) Demonstrated hydrogen plasma processing to remove native oxides from GaAs.

(7) Designed and grew "half VCSELs" for external cavity experiments.

(8) Developed metalorganic vapor-phase epitaxy (MOVPE) regrowth process for epitaxial deposition of distributed Bragg reflector (DBR) mirrors over etched GaAs (showed process to be robust over a wide-parameter space of etch depth and growth temperature).

Publications

Refereed

Choquette, K. D. 1996. "Oxide-Confined Vertical-Cavity Lasers." Paper presented to the 26th Winter Colloquium on Physics of Quantum Electronics, Snowbird, UT, 7–10 January.

Choquette, K. D., H. Q. Hou, W. W. Chow, G. R. Hadley, K. L. Lear, M. H. Crawford, and K. M. Geib. 1996. "Performance and Fabrication Issues of Oxide-Confined VCSELs." Paper presented to the Engineering Foundation High-Speed Optoelectronic Devices and Systems Meeting, Snowbird, UT, 11–15 August.

Choquette, K. D., K. L. Lear, R. P. Schneider, Jr., H. C. Chui, and K. M. Geib. 1995 "Selectively Oxidized Vertical-Cavity Lasers." Paper presented to the LEOS Annual Meeting, San Francisco, CA, 30 October–2 November.

Choquette, K. D., R. P. Schneider, Jr., K. L. Lear, M. H. Crawford, and K. M. Geib. 1996. "Advances in Oxide-Confined Vertical-Cavity Lasers." Paper presented to the Conference on Lasers and ElectroOptics (CLEO '96), Anaheim, CA, 2–7 June.

Choquette, K. D., R. P. Schneider, Jr., K. P. Killeen, M. H. Crawford, and K. L. Lear. 1995. "Epitaxial Design and Process Issues for Vertical-Cavity Surface-Emitting Lasers." Paper presented to the 42nd National Symposium of the American Vacuum Society, Minneapolis, MN, 16–20 October.

Choquette, K. D., W. W. Chow, G. R. Hadley, H. Q. Hou, and K. M. Geib. 1996. "Properties of Small-Aperture Selectively Oxidized VCSELs." Paper presented to the LEOS Annual Meeting, Boston, MA, 18–21 November.

Choquette, K. D., W. W. Chow, G. R. Hadley, H. Q. Hou, and K. M. Geib. 1996. "Scalability of Small-Aperture Selectively Oxidized Vertical-Cavity Lasers." *Appl. Phys. Lett.*, accepted.

Choquette, K. D., W. W. Chow, K. M. Geib, and R. P. Schneider, Jr. 1996. "Threshold Analysis of Oxide-Confined Vertical-Cavity Laser Diodes." *Appl. Phys. Lett.* **68** (24 June): 3689–3691.

Hadley, G. R., K. L. Lear, M. E. Warren, and K. D. Choquette. 1996. "Comprehensive Numerical Modeling of Vertical-Cavity Surface-Emitting Lasers." *IEEE J. Quant. Electron.* **32** (February): 607–617.

Lear, K. S., R. P. Schneider, Jr., K. D. Choquette, and S. P. Kilcoyne. 1996. "Index Guiding Dependent Effects in Implant and Oxide-Confined Vertical-Cavity Surface-Emitting Lasers." *IEEE Photon. Tech. Lett.* **8** (March): 740–742.

Li, J., J. F. Seurin, S. L. Chuang, K. D. Choquette, K. M. Geib, and H. Q. Hou. 1996. "Correlation of Electrical and Optical Characteristics of Selectively Oxidized Vertical-Cavity Laser Diodes." *Appl. Phys. Lett.*, accepted.

Other

Choquette, K. D. 1996. "Vertical-Cavity Surface-Emitting Lasers." *Compound Semiconductor* **2** (May/June): 46–48.

Midwave-Infrared (2–6 μm) Emitter-Based Chemical Sensor Systems

S. R. Kurtz, M. H. Crawford, R. L. Dawson, A. J. Howard, R. M. Biefeld, A. J. Ricco, G. A. Vawter

Long-wavelength (2–6 μm) diode emitters are desirable for many applications, including monitoring of chemical species in the environment and in manufacturing, long-wavelength fiber-optic communications, lidar, and infrared (IR)-detector countermeasures. No practical diode lasers are available for any of these applications because the band structure of bulk III–V, II–VI, and IV–VI semiconductor alloys results in large Auger recombination rates at these wavelengths. Experimental and theoretical work at Sandia resulted in new understanding of the electronic properties of narrow-bandgap III–V heterostructures, and we found methods of reducing the Auger rates in certain InAsSb superlattices and quantum wells. These devices enable us to begin chemical-sensing demonstrations of important species such as CO-CO_2 and numerous other compounds. This project will involve developing chemical-sensing systems and determining the sensitivity and limitations of these systems. Concurrently, we will improve upon IR emitters used in these systems.

Progress in the growth of metalorganic chemical vapor deposition (MOCVD) materials and devices exceeded expectations. We demonstrated the first injected, midwave-infrared (MWIR) lasers with InAsSb heterostructure active regions grown by MOCVD. These devices utilized InPSb cladding layers and displayed the highest characteristic temperature (T0=33 K) for a 3.5-μm laser. Later, we achieved the first growth of AlSb waveguide materials by MOCVD, and rapidly demonstrated new record-setting performances in injection lasers and light-emitting diodes (LEDs). Molecular beam epitaxial (MBE) growth of IR devices was delayed by machine start-up and repair problems. Presently, the MBE machine is functional and growing GaInAs materials. We expect to begin growing Sb-based materials for IR devices with MBE in the immediate future.

We demonstrated the first electrically injected laser grown by MOCVD employing AlAsSb for optical confinement. The laser also utilizes a GaAsSb/InAs semimetal heterojunction to provide electron injection into the InAsSb strained quantum-well active region. The semimetal may eliminate problems associated with electron injection into AlAsSb devices, and this novel device is compatible with MOCVD materials and background dopings. Under pulsed operation, the semimetal injection lasers exhibited characteristics superior to previously published results. We observed laser emission at 3.9 μm at 210 K with a characteristic temperature of approximately 40 K.

Publications

Refereed

Allerman, A. A., R. M. Biefeld, and S. R. Kurtz. 1996. "InAsSb-Based Mid-Infrared Lasers and Light-Emitting Diodes." *Appl. Phys. Lett.* **69** (22 July): 465–467. New York, NY: AIP.

Kurtz, S. R., R. M. Biefeld, and A. A. Allerman. 1996. "Pseudomorphic InAsSb Multiple Quantum-Well Injection Laser." *Appl. Phys. Lett.* **68** (4 March): 1332–1334. New York, NY: AIP.

Supersonic Cluster Jet Source for Debris-Free EUV Production

G. D. Kubiak

The objective of this project is to develop a new laser-produced plasma source of extreme ultraviolet (EUV) radiation based on van der Waals clusters produced in supersonic gas expansions. This source demonstrated a laser-to-EUV conversion efficiency equal to that of many conventional solid metal targets. Simultaneously, we demonstrated that such a source produced approximately 100,000 times less deleterious debris than conventional laser plasma sources. As a result of this work, the supersonic cluster source is now the leading commercial EUV source candidate for EUV lithography.

In FY96 we designed, constructed, and characterized a supersonic nozzle source of high-density gas clusters. The cluster stream is irradiated with a focused pulsed laser propagating transverse to the jet axis to produce a plasma source. We found that conical nozzles yield significantly more EUV power than sonic-free jets. Measurements of the 2π-integrated conversion efficiency (CE) from laser energy to in-band 13.5-nm radiation revealed that the cluster source now yields 58% of the EUV yield from solid gold targets. The corresponding absolute CE for the Xe jet is 0.0026 J/eV-J_L, very close to the values for solid Cu, Mo, and W targets. We completed the spectroscopic characterization of Xe as well as the new clustering gases O_2 and Kr, revealing that Xe is still the best target for 13.5-nm radiation, but that O_2 and Kr yield more radiation than Xe at other wavelengths.

To quantify the level of debris reduction achieved with the jet source, we exposed multilayer-coated condenser optics to the jet source operating at full power and measured their reflectance as a function of time during exposure. Initially, we placed the condenser optic 100 mm from the source, taken to be the canonical source-condenser separation. Condenser reflectance measurements showed that mirror reflectance was reduced by 15% after 5.0×10^7 full-power plasma pulses. We then identified and corrected mirror contamination sources. Subsequent experiments demonstrated an improved reflectance lifetime of 1.4×10^8 pulses, a factor of 200 times better than the best lifetimes exhibited by solid targets. We analyzed nozzle geometry and material modifications that are estimated to reduce the deposition of debris by another factor of 30.

To support the eventual use of a continuous rather than pulsed nozzle, we collaborated with Northrop-Grumman to design a high-throughput diffuser. The best design to date yields > 95% capture efficiency of the nozzle effluent with little obscuration of the EUV beam path being collected by the condenser.

Publications

Other

Kubiak, G. D., L. Bernardez, K. D. Krenz, D. O'Connell, R. Gutowski, and A. Todd. 1996. "Debris-Free EUVL Sources Based on Gas Jets." *Proc. OSA Topical Conf. on Extreme UV Lithography* **4** (Boston, MA, 1–3 May): 66–71.

EUVL Experiments for the 0.1-Micron Lithography Generation

D. A. Tichenor

Sandia used the 10x–II laboratory extreme ultraviolet lithography (EUVL) *tool as a test-bed for dose, vibration, and overlay development. An integrating EUV shutter achieves precise average dose to wafer. We measured spatial dose variation of 20% using a thinned step-junction (PN) diode installed in the wafer stage. We measured floor vibrations to be 105 micro-inches per second; however, an apparent mechanical resonance causes the base table to be less stable than the floor it sits on. Wafer stage stability remains at 5.5-nm root-means-square (RMS). We replaced the mask-to-wafer alignment mirror by a more robust design to improve overlay.*

Our activities focused in three work areas in FY96:

(1) *Dose control*: We implemented a vacuum photodiode on the 10x–II laboratory EUVL tool to measure the EUV dose per pulse. The detector uses the reflection losses in the 10x–II turning mirror to produce the signal, thereby measuring the EUV dose without incurring additional loss of EUV flux. We achieved efficient operation by applying a –120-volt bias to the turning mirror and using a capacitively coupled shielded line to acquire the per-pulse dose. We incorporated a control program to digitally integrate the pulse data, determine the accumulated dose, and shut down the laser plasma source when the desired dose is achieved.

To measure dose uniformity, we installed a thinned PN diode, sensitive to EUV radiation, on the wafer stage of the 10x–II. The sensitive area is 1 square cm. To achieve spatial resolution, we placed a 150-micron pinhole over the diode. For spectral purity we placed a 1-micron beryllium foil over the pinhole. We scanned this detector in two dimensions over the field of view of the 10x–II and observed a dose variation of 20%.

(2) *Vibration control*: We recorded measurements of floor and base-table vibrations. The floor has an RMS vibration level of 105 micro-in./s, which is less than half of the specification for commercial semiconductor fabrication facilities. However, the base table vibrates about 10 times that amount. We installed machinery jacks under the base table but observed no improvement in base-table vibration. Dampers tuned to a measured resonance at about 180 Hz may lower the vibration level.

We achieved stage vibrations of 5.5-nm RMS in two-axis radial displacement from the desired position by tuning the magnetically levitated (maglev) fine stage to notch out resonances. The vibration level increased to 13-nm RMS over time, apparently due to changes in the magnetic actuators. Retuning of the maglev stage restores the stability to about 5.5 nm.

(3) *Overlay*: We demonstrated using a visible-light moiré technique mask-to-wafer alignment sensitivity at the 15-nm three-sigma level. The absolute overlay is about 0.5 micron due to a variable offset in the visible-light illumination system. We replaced the alignment mirror assembly with an improved design to stabilize the offset. We also designed a stage alignment reference system to measure the offset and correct for it.

Engineering Sciences

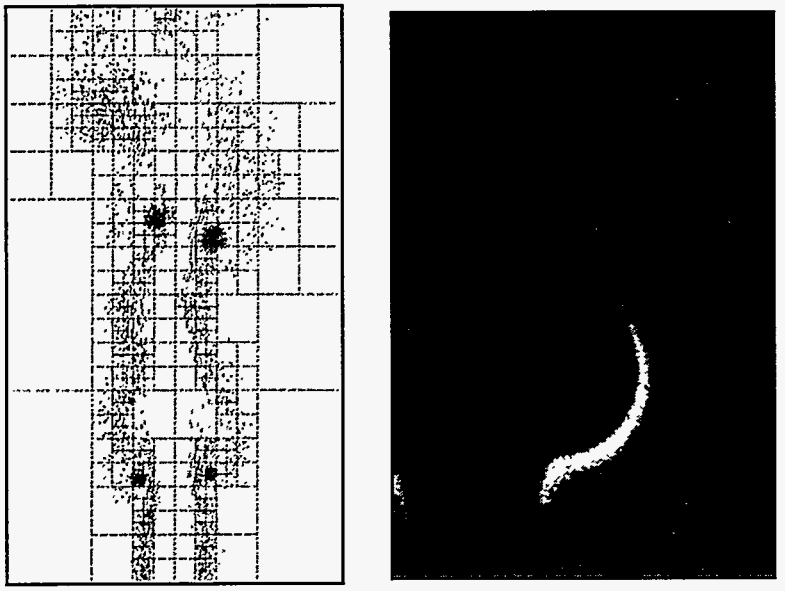

The modeling of pool fires is complicated by unsteady vortex-flame interaction in reacting jet flow. On the left is an experimental laser-induced fluorescence image of OH in an acoustically forced rectangular jet methane-air flame flow. The bulge indicates the presence of a large vortex structure. The numerical computation of this forced jet flow (without reaction) using the two-dimensional vortex method is shown at right.

Impact and Thermal-Shock Response of Metal-Cutting Tools for High-Strength, High-Speed Milling Operations

W. T. Hobson

Sandia has begun to apply advanced analytical and experimental capabilities to model machining processes in a manner not possible before. We extended several areas of research to milling situations: (1) an advanced plasticity/rupture constitutive model, (2) adaptive depth elements, (3) code-coupling methodologies linking conjugate-gradient and explicit-Lagrangian approaches, (4) materials characterizations at elevated temperatures (tungsten carbides), (5) advanced friction/slide-line interface capabilities, and (6) adaptive-mesh and mesh-regeneration techniques. We commenced experiments on a precisely instrumented lathe test-bed. We began to analyze, machine, and monitor actual parts under simulated milling conditions. We made initial comparisons between predicted and measured stresses in cutting tools.

Our ultimate aim is to better understand the thermal and impact loads that repeatedly shock milling tools, the mechanics of tool breakage, and the separation failure of coated cutting inserts. Such understanding will assist the fabrication of defense components by enabling industry to design high-performance metal-cutting tools, and further manufacturing productivity technologies in general (e.g., diamond-coated carbides).

Metal has been "cut" analytically. We generated newly cut surfaces using Sandia's ductile rupture material model, conjugate-gradient finite element (FE) codes, and adaptive "death" elements. The predicted stresses produced in the cutting tool exhibit good comparisons with experimentally measured stresses. We measured temperatures produced in tools with molten salts and thermal paint techniques. We conducted experiments using high-speed photometrics to identify tool failure modes. We designed carbide specimens and procured them for high-temperature materials characterization. We also carried out complementary analyses of the metal-cutting experiments using arbitrary Lagrangian-Eulerian (ALE) approaches.

Publications

Refereed

Kistler, B. L 1997. "Finite Element Analyses of Tool Stresses in Metal-Cutting Processes." Sandia Technical Report, SAND97-8224, January.

McDonald, A., A. Hazelton, and B. L. Kistler. 1997. "LDRD Final Report: Impact and Thermal Shock Response of Metal-Cutting Tools for High-Strength, High-Speed Milling Operations." Sandia report, in preparation.

Coherent Structures in Compressible Free-Shear-Layer Flows

D. P. Aeschliman, J. H. Chen, R. S. Baty

Sandia is studying the formation and evolution of large-scale coherent structures (LSSs) (eddies) in the compressible free-shear-layer between a high-speed, axisymmetric helium jet and a coflowing high-speed air freestream. Coherent structures dominate the turbulent mixing process in many shear layers in practical fluid-flow systems and are therefore critical to a variety of important defense and commercial technologies. The goal of the work is to develop a new analytical model to describe coherent structures that is robust and computationally efficient and is less dependent on empiricism than existing models. This work utilizes a synergistic blend of experiment, analysis, and direct numerical simulation (DNS).

Sandia is studying the formation and evolution of LSSs (eddies) in the compressible free-shear-layer between a high-speed, axisymmetric helium jet and a coflowing high-speed air freestream. Coherent structures dominate the turbulent mixing process in many shear layers in practical fluid-flow systems and are therefore critical to a variety of important defense and commercial technologies. The goal of the work, which utilizes a synergistic blend of experiment, analysis, and DNS, is the development of a new analytical model to describe coherent structures that is robust and computationally efficient and is less dependent on empiricism than existing models.

In the experimental portion of this work, we designed, developed, and demonstrated a capability to generate compressible, turbulent free-shear-mixing layers in which the mixing-layer Reynolds number can be reliably and repeatably varied over the range 0–500,000, a unique capability. We developed and demonstrated a traversing mass sampling probe to measure mean helium concentration as a function of radial and axial location in the flow. We determined global kinematic features of the coherent structures, such as the spatial and temporal frequencies, using time-resolved schlieren movies of the flow at up to 18,000 frames per second, a first for such flows. The mean concentration and kinematic data are input required for the analytical model development.

In the numerical simulation portion of the work, we solved for the flow variables in a hot, planar air jet issuing into air as a necessary first step toward solving the more complicated case of an axisymmetric helium jet into air. The results, particularly for the two-point velocity data, are required input to the analytical model and will be used to demonstrate the solution methodology for the analytical model.

In the analytical work, we developed the equations that describe the coherent structures using two mathematical approaches: instability wave modeling (linear analysis) and dynamical systems (nonlinear analysis). We developed the solution methodology for each of these approaches. In addition, we developed and demonstrated the numerical techniques required to manipulate and solve the very large matrices generated in solving the equations. We have not yet obtained experimental data at the detail required for the analytical model development.

Publications

Other

Aeschliman, D. P., R. S. Baty, and J. F. Henfling. 1996. "Initial Experiments on Large-Scale Structure Evolution in Coflowing Axisymmetric Jets." Paper presented to the 84th Supersonic Tunnel Association Meeting, Tokyo, Japan, 15–19 October.

Optimization of Computationally Challenging Problems in Engineering Sciences

M. S. Eldred, D. E. Outka

Computational simulation methods in the Engineering Science disciplines are important tools in understanding complex systems and reducing design cycle costs through the use of virtual prototypes. We propose to leverage these capabilities by integrating complex simulations with advanced optimization algorithms and strategies. The utility of computational methods will be greatly increased by providing a systematic means of design optimization.

The response of the simulations to variations of the parameters describing the physical configuration tends to be highly nonlinear, discontinuous, noisy, and multimodal. These traits and others made it difficult to apply conventional optimization techniques to such problems. The thrusts of this research are to extend capabilities in fundamental optimization algorithms, to develop hybrid methods having global optimal identification capabilities and rapid local convergence, and to develop effective function approximation strategies that minimize the number of full simulation runs. In addition, we are investigating the techniques of automatic differentiation, for obtaining analytic gradients from simulation codes, and parallel processing, by developing algorithms and strategies for massively parallel (MP) and distributed architectures.

We accomplished the following in FY96:

(1) In determining worst-case fire scenarios on the SP2, parallel coordinate pattern search (CPS) can perform three simulations simultaneously (limited by software licenses). We decreased wallclock time by a factor of 10 over previous studies, and reductions of 20 times are possible.

We used nonlinear programming (NLP) to optimize MPSalsa simulations of chemical vapor deposition (CVD) on Sandia's Intel Paragon. The design parameters determine the operation and shape of a CVD reactor, and the objective function incorporates estimates of operating costs and semiconductor value.

(2) We produced analytic gradient capabilities for the TWAFER and TACO codes using ADIFOR. Performance studies in CVD reactor design showed that analytic gradients improve convergence and accelerate solution time by up to a factor of five relative to numerical gradients.

(3) We investigated hybrid combinations of genetic algorithms (GAs), CPS, and NLP on the worst-case fire application. CPS/NLP hybrids found optimal solutions in half the time required by NLP alone, while finding more optimal results than achievable by CPS alone.

We conceptualized the design for sequential approximate optimization and developed neural network approximation capabilities under contract.

We developed parallel GAs, parallel CPS algorithms, and hybrid GA/CPS algorithms within SGOPT. We incorporated convex programming algorithms (ellipsoid and modified barrier methods) into OPT++.

We solved the transient TWAFER problem with 1000 parameters using a large-scale optimization capability to determine both the optimal ramp rate and the open-loop control law that achieves it. In coating die design, we are extending geometry parameterization, simulation interface generality, and analytical sensitivity capability. In vibration isolation, GAs has determined discrete isolator locations that decrease disturbance transmission by 32 to 70 times (verified on isolation hardware to result in 7 to 46 times reduction).

Publications

Refereed

Eldred, M. S., D. E. Outka, W. J. Bohnhoff, W. R. Witkowski, V. J. Romero, E. R. Ponslet, and K. S. Chen. 1996. "Optimization of Complex Mechanics Simulations with Object-Oriented Software Design." *Computer Modeling and Simulation in Engineering*, accepted.

Hart, W. E. 1996. "A Theoretical Comparison of Stochastic Optimization Algorithms: Simulated Annealing, Evolutionary Algorithms and Markovian Search Algorithms." *Evolutionary Computation*, accepted.

Other

Eldred, M. S., D. E. Outka, and W. J. Bohnhoff. 1995. "Optimization of Complex Engineering Simulations with the DAKOTA Toolkit." Paper presented to the First Biennial Tri-Laboratory Engineering Conference on Computational Modeling, Pleasanton, CA, 31 October–2 November.

Eldred, M. S., W. E. Hart, W. J. Bohnhoff, V. J. Romero, S. A. Hutchinson, and A. G. Salinger. 1996. "Utilizing Object-Oriented Design to Build Advanced Optimization Strategies with Generic Implementation." *Proc. 6th AIAA/USAF/NASA/ISSMO Symp. on Multidisciplinary Analysis and Optimization* **AIAA-96-4164-CP** (Bellevue, WA, 4–6 September): 1568–1582.

Harding, D. C., M. S. Eldred, and W. R. Witkowski. 1995. "Integration of Finite Element Analysis and Numerical Optimization Techniques for RAM Transport Package Design." Paper presented to the 11th International Conference on the Packaging and Transportation of Radioactive Materials (PATRAM '95), Las Vegas, NV, 3–8 December.

Hart, W. E. 1996. "A Stationary Point Convergence Theory for Evolutionary Algorithms." Paper presented to the Foundations of Genetic Algorithms 4 Meeting, San Diego, CA, 3–5 August.

Hart, W. E. 1996. "A Theoretical Comparison of Evolutionary Algorithms and Simulated Annealing." Paper presented to the 5th Annual Conference on Evolutionary Programming (EP '96), San Diego, CA, 29 February–2 March. SAND95-2079.

Hart, W. E. 1995. "Evolutionary Pattern Search Algorithms." SAND95-2293, October.

Hart, W. E., S. Baden, R. K. Belew, and S. Kohn. 1996. "Analysis of the Numerical Effects of Parallelism on a Parallel Genetic Algorithm." Paper presented to the 10th International Parallel Processing Symposium (IPPS '96), Honolulu, HI, 15–19 April.

Moen, C. D., P. A. Spence, J. C. Meza, and T. D. Plantenga. 1996. "Automatic Differentiation for Gradient-Based Optimization of Radiatively Heated Microelectronics Manufacturing Equipment." *Proc. 6th AIAA/USAF/NASA/ISSMO Symp. on Multidisciplinary Analysis and Optimization* **AIAA-96-4118-CP** (Bellevue, WA, 4–6 September): 1169–1175.

Ponslet, E. R., and M. S. Eldred. 1996. "Discrete Optimization of Isolator Locations for Vibration Isolation Systems: An Analytical and Experimental Investigation." Paper presented to the 6th AIAA/USAF/NASA/ISSMO Symposium on Multidisciplinary Analysis and Optimization, Bellevue, WA, 4–6 September. SAND96-1169.

Predicting Weld Solidification Cracking Using Continuum Damage Mechanics

D. J. Bammann, E. A. Fuchs, J. J. Dike, J. A. Brooks

Sandia is developing a finite-element model (FEM) to describe weld solidification cracking behavior. To accomplish this one must be able to predict thermal response, solidification behavior, mechanical response, and material failure. We are using the Sandia-developed FE codes JAQ3D and JAC3D. We perform the analyses in a loosely coupled fashion—doing the thermal analysis with JAQ3D—and we use the resulting temperature calculations as input for the mechanical analysis using JAC3D. We are using weld solidification models in conjunction with the thermal models to predict solidification temperature range and volume fraction of solid and liquid as a function of temperature and position. We developed a multiphase continuum model to describe the liquid and solid phases. The solid phase incorporates the effects of rate and temperature sensitivity as well as modeling the nucleation and growth of voids. We implemented the model into the JAC codes; simulation of actual weld processes is in progress. We are conducting an extensive experimental program to validate various aspects of the model. We will make comparisons of analytical predictions with solidification cracking experiments.

We developed and validated the tools and methodology that will allow us to predict and control weld solidification cracking, which is a very critical, costly, and common weld defect. In doing this we validated a solidification model for Al alloys and added the capability to easily include solidification behavior into thermal finite analysis. We also developed a two-phase (solid + liquid) material model using internal state variables and a modified rule of mixtures. We developed software to manipulate the solidification models to obtain rate of solidification and distribute the heat of fusion over the solidification temperature range. To predict the solidification crack initiation, we developed a model including directionality to the damage incorporated into the two-phase material model. We developed extensive experimental data and a new technique to obtain critical data. These included *in situ* strain measurements obtained during welding using high magnification video techniques and fiber-optic strain gages. We conducted welding experiments on uniquely designed weld-cracking specimens to validate weld-cracking model predictions.

Publications

Refereed

Brooks, J. A., J. J. Dike, and J. S. Krafcik. 1995. "On Modeling Weld Solidification Cracking in Al Alloys." *Proc. Internat. Conf. on Modeling Processes, AWS* (Orlando, FL, 12 December): 174.

Brooks, J. A., J. J. Dike, D. Bammann, and M. Li. 1996. "Predicting Weld Solidification Cracking Behavior Using FEM Techniques." Paper presented to the American Welding Society Conference, Chicago, IL, 24 April.

Dike, J. J., J. A. Brooks, and J. S. Krafcik. 1995. "Thermal-Mechanical Behavior in the Weld Pool Region." *Proc. 4th Internat. Conf. on Trends in Welding Res., ASM/AWS* (Gatlinburg, TN, 5–8 June): 159.

Dike, J. J., J. A. Brooks, D. Bammann, M. Li, and J. S. Krafcik. 1996. "Modeling Solidification Cracking Behavior in Al 6061 Alloy." *Welding J. Res. Suppl.*, accepted. Miami, FL: AWS.

Model Reduction Techniques for Nonlinear Systems and Control

M. W. Heinstein, D. J. Segalman, L. D. Harwell

Sandia increasingly is using modeling and computational simulation to develop insight into the physical behavior of engineering systems. These models can be used as virtual prototypes in a manufacturing cycle, as final qualification certification for systems that cannot simulate the full environment in ground tests, and as modules in multidisciplinary analyses, including control of flexible structures. However, often these models involve an intractable number of degrees of freedom (DOFs) and cannot be reduced to smaller models by conventional methods because of some inherent nonlinearity.

This work focuses on developing general model reduction techniques with application to metal-cutting. This is motivated by the enormous economic importance of machining processes and the desire to adjust processes to optimize product and throughput. The reduced model developed here is a neural net used to simulate the control of a typical machining process.

We used smooth particle dynamics (SPH) methods to simulate a virtual orthogonal cutting machine. We explored the various common configurations of rake angle, depth of cut, and tool sharpness with different levels of mesh discretization. This technique appears to capture the most important physics of the problem—reproducing the following phenomena observed in actual cutting processes:

(1) Cutting forces and moments vary nearly linearly with depth of cut.

(2) Cutting-to-plowing transition occurs at large negative rake angles.

(3) Stagnation point develops in front of a dull cutting tool.

(4) Dull tools require more energy for cutting.

Though the above phenomena were well-known, most were not predicted by a previous simulation technique.

Viewing the cutting process as an interface phenomenon that connects linear subsystems, one would like a simple model for the aggregate behavior of that interface in steady state. We performed that task by training a neural net to reproduce with very little computational cost the aggregate behavior predicted by the above detailed and expensive calculations. We then incorporated that neural net model into a low-order dynamics model of the machining process.

Another component of the nonlinear model reduction effort was to develop inverse dynamics methods to extract the nonlinear component of a dynamic system. Fourier methods that we had tried earlier in this project suffered from inherent problems of Fourier inversion of filtering. We developed and tested an alternate technique using dynamic programming to minimize a residual of a corresponding dynamic system this year. This new technique appears to have substantial advantages of robustness and efficiency.

Publications

Refereed

Segalman, D. J., and C. R. Dohrmann. 1996. "Identifying Damping of a System by Two Inverse-Dynamics Methods." *Proc. 1996 SPIE Symp. on Smart Structures and Mater., Passive Damping and Isolation* **2720** (San Diego, CA, 25–29 February). Published by Connor Johnson.

Numerical and Experimental Investigation of Vortical Flow-Flame Interaction

H. N. Najm, K. D. Devine, S. N. Kempka, R. W. Schefer

The goal of this project is to develop a coupled Lagrangian-Eulerian numerical scheme for modeling low-Mach-number reacting flow, and to validate this model with a concurrent experimental investigation of a reacting methane-air planar jet flow. The scheme uses the Lagrangian vortex method, for computing the momentum and continuity equations, and a Eulerian finite-difference approach, with adaptive mesh refinement (AMR), for solving the energy and species conservation equations. Sandia will use a fast n*-body solver to accelerate the vortex method, and we will develop the overall code and run it on available parallel machines. We will use a single global-reaction mechanism to describe the combustion of methane. We will use the numerical model to study flow-flame interaction in a two-dimensional (2-D) low-Mach-number reacting jet flow, and to compare with the concurrent planar jet experimental investigation. We force the experimental jet acoustically to enhance the organization of the large-scale flow structures. Measurement techniques include particle imaging velocimetry (PIV) for velocity field measurement, and multispecies spectroscopic laser-sheet imaging techniques to measure species concentrations, and provide information on flame dynamics and reaction rates. We will use experimental measurements to validate the numerical model and provide improved understanding of flow-flame interaction in unsteady vortical flow.*

We accomplished the following:

(1) Modified the initial AMR code and enhanced it to allow necessary data structures for finite-difference computations. We added the energy and species conservation equations along with

detailed chemical kinetics capability. The resulting code allows adaptive mesh-refinement computation of detailed flames with variable transport properties.

(2) Wrote and tested the vortex code for computing jet flow. This code includes detailed viscous transport of vorticity, allowing for spatially varying viscosity, and implements a potential panel method solution for domain boundaries. We wrote a fast parallel multipole n-body solver to allow efficient computation of the velocity field induced by vortex elements. A fast panel-method implementation is nearing completion.

(3) Devised a time-stepping strategy to couple the multilevel time integration on the adaptive mesh with the Lagrangian field integration in a second-order Runge-Kutta scheme.

(4) Developed the framework for injection of baroclinically generated vortex elements and began implementing the code.

(5) Designed and built a planar-slot burner, including acoustic forcing hardware. We tested and studied this setup over a wide range of forcing frequencies to achieve optimal forcing conditions.

(6) Constructed and successfully used a PIV setup to measure unsteady nonreacting forced jet dynamics. Data provided include flow visualization and numerical velocity and vorticity data in instantaneous time-evolving frame-sequences.

(7) Set up OH and CH imaging diagnostics hardware and used it to provide CH and OH imaging of the dynamics of the forced jet flame.

We compared the nonreacting forced jet dynamics computed and measured experimentally, using similar forcing environments, jet geometry, and flow conditions. Comparisons revealed general preliminary agreement in terms of vortex structure sizes, shapes, and dynamics.

Enhanced Vapor-Phase Diffusion in Porous Media

S. W. Webb, M. J. Martinez, C. K. Ho

Vapor-phase diffusion in porous media may be significant in the flow of subsurface fluids and the transport of contaminants. In many environmental remediation and isolation applications, such as removal of nonaqueous phase liquid (NAPL) contaminants from low-permeability layers in the subsurface, vapor-phase diffusion is the limiting transport mechanism. Vapor-phase diffusion may also be important in high-level nuclear-waste repositories, in porous catalysts, in the drying of textiles, and in agricultural processes. Enhancement of vapor-phase diffusion by up to several orders of magnitude was postulated, but not definitively confirmed, in the presence of its liquid through local condensation and evaporation at vapor-liquid interfaces.

The objectives of the work are to (1) resolve critical processes and questions associated with postulated enhanced vapor-phase diffusion mechanisms, and (2) develop a defensible model for incorporation into porous media multiphase simulators. The approach taken in the present research is to perform modeling and experimental investigations of enhanced vapor-phase diffusion at various-length scales, including the pore scale and the laboratory scale. Results to date indicate possible enhancement of vapor-phase diffusion at the pore-scale, which remains to be confirmed by experimental data.

We accomplished the following:

(1) *Evaluation of gas-phase diffusion models*: We compared the commonly used advective-dispersive model to the more mechanistic Dusty-Gas Model. We found significant differences in gas-diffusion results. Gas-phase diffusion should be analyzed by the Dusty-Gas Model instead of the advective-dispersive approach.

(2) *Critical review of enhanced vapor-phase diffusion*: Enhanced vapor-phase diffusion has been postulated and is often assumed in many porous media applications. The existence of enhanced vapor-phase diffusion, however, has yet to be conclusively demonstrated. Additional experiments focusing on the enhancement questions are needed to resolve this issue.

(3) *Pore-scale modeling of enhanced vapor-phase diffusion*: We performed initial pore-scale modeling, which indicates that enhanced vapor-phase diffusion may exist through increased local vapor-phase temperature gradients and by condensation/evaporation processes in liquid islands in pore throats.

(4) *Evaluation of possible importance of enhanced vapor-phase diffusion on NAPL removal*: As part of a numerical study of soil vapor extraction (SVE), including the effects of heating, we investigated the impact of enhanced vapor-phase diffusion on NAPL removal time. For SVE without heating, NAPL removal times can be significantly reduced if enhanced vapor-phase diffusion exists.

Publications

Other

Ho, C. K., and S. W. Webb. 1996. "A Review of Porous Media-Enhanced Vapor-Phase Diffusion Mechanisms, Models, and Data—Does Enhanced Vapor-Phase Diffusion Exist?" *Proc. Internat. Conf. on Porous Media and Its Applic. in Science, Engineering, and Industry* **1** (Kona, HI, 16–21 June): 173–198. Engineering Foundation.

Webb, S. W. 1996. "Gas-Phase Diffusion in Porous Media—Evaluation of an Advective-Dispersive Formulation and the Dusty-Gas Model." *Proc. Internat. Conf. on Porous Media and Its Applic. in Science, Engineering, and Industry* **1** (Kona, HI, 16–21 June): 559–599. Engineering Foundation.

Investigation of Nonequilibrium Microscopic Hydrodynamic Phenomena

C. C. Wong, N. D. Shinn, S. J. Plimpton, K. S. Chen

This research focuses on microscale hydrodynamics phenomena. Recent advances in microscience and technology have generated a group of unique fluid-flow problems that question the traditional continuum and equilibrium approaches used to analyze these transport phenomena. Such problems are fluid flows in microscopic geometries or under high stress. Our goal is to develop molecular dynamics (MD) simulation capability so that it will provide "hard-to-obtain" quantitative physical information, and to develop constitutive relationships and models to complement existing continuum methodologies. The ongoing activities include (1) analyzing the fluid-structure interaction of a physical domain of micron size, (2) defining the flow boundary conditions (BC) at the fluid-solid interface, (3) deriving macro-transport coefficients such as apparent viscosity, and (4) bridging MD simulations with Navier-Stokes (N-S) solvers for fluid-flow analyses.

We modified a high-performance MD computer program to simulate flow between solid walls. We developed pograms to create initial states. We validated the MD program on microscale Couette and Poiseuille flow problems. Simulation at the molecular level is crucial in determining the BC (e.g., stick or slip) at the fluid-solid interface. This BC is undetermined in continuum theory, but is an important input into continuum calculations. For the microscale Couette flow problems, MD results show that stick BC, i.e., fluid layers being locked with the solid wall, will occur if there is a strong wall-fluid interaction. If the wall-fluid interaction is weak, slip BC will occur at the interface. Shear direction with respect to the wall-lattice orientation is also important. Preliminary results also show that stick-and-slip phenomena may become less influential as the channel width increases. For the microscale Poiseuille flow problems with appropriate parameters, the MD simulations produce a parabolic velocity profile that agrees with analytical predictions by solving the NS equations with no-slip boundary conditions. As the fluid density decreases, our MD simulations indicate that a transition to slip flow will occur at the wall.

Publications

Other

Lopez, A. R., C. C. Wong, M. J. Stevens, and S. J. Plimpton. 1996. "Numerical Simulation of Microstructure Hydrodynamics." Paper presented to the American Vacuum Society 43rd National Symposium and Topical Conference on MEMS, Philadelphia, PA, 14–18 October.

Wong, C. C., A. R. Lopez, M. J. Stevens, and S. J. Plimpton. 1996. "Investigation of Microstructure Hydrodynamics with Molecular Dynamics Simulations." Paper presented to the US–Japan Joint Seminar on Molecular and Microscale Transport Phenomena, Santa Barbara, CA, 8–10 August.

Constitutive Models of Stress-Strain Behavior of Granular Materials

E. Askari, J. S. Glass, J. G. Arguello

The objective of this project is to understand and predict the behavior of granular assemblies. The mechanical behavior of granular materials is of utmost importance to many commercial products and weapons components, such as neutron tubes, electronic packages, and lightning arrestors. The work on this project had numerical, analytical, and experimental components to address the overall problem. The numerical effort focused on evaluating several discrete element codes (including 3-D SHEAR and TRUBAL) to determine their suitability for the granular particulate modeling problem. In addition, Sandia verified contact laws and examined their relevance to particle-to-particle interaction. The analytical work began with the process of developing the incremental constitutive relations that describe the particulate compaction process. The approach was to identify a set of internal state variables from micromechanical considerations and to formulate rules for their evolution.

The experimental effort had several components, including designing and building a test apparatus and using this apparatus for non-invasive magnetic resonance imaging (MRI) experiments. The MRI technique gave amazing detail for the particle arrangements. Moreover, the technique tracked particle locations and gave void volumes and contact locations.

Accomplishments began with a state-of-the-art review of all aspects of the problem. This included reviews of ceramic powder compaction experiments, non-invasive measurements by MRI, discrete element methods, and granular material constitutive modeling.

We developed an MRI technique to image particles during uniaxial compaction tests. We used several types of particles, including vitamin-filled pharmaceutical particles and glass spheres. We achieved amazing resolution. The associated data reduction software tracked particle locations and gave void densities and contact locations.

We also made progress in modeling the contact mechanics of spherical particles. We took the first step of numerically verifying (using 3-D finite-element models) that Hertz-Mindlin contact theory did indeed apply to the contact of elastic spheres. The next step would be to allow the particles to behave nonlinearly, probably plastically, and to examine how the contact forces distribute.

We established the framework for the continuum constitutive model development. This framework established regimes of low-, medium-, and high-stress ratio loading. We expect different mechanical behaviors in each of these regimes; thus, we were devising different mechanistic models for each type of behavior.

We conducted a number of granular particle experiments investigating the effect of initial packing density and particle size. We planned to use these data to help refine the mechanical response models.

Publications

Other

Jenkins, J. T. 1996. "Inelastic Behavior of Random Arrays of Identical Spheres." Paper presented to the Mechanics of Granular and Porous Materials Meeting, Cambridge, UK, 14–17 July.

Using Higher-Order Gradients to Modeling Localization Phenomena

D. J. Bammann, D. A. Mosher, N. R. Moody, D. A. Hughes

This research is directed toward bridging the micro- to macroscales in mechanics of materials to bring better descriptions of material response into numerical calculations. Sandia introduced a length scale into the continuum by introducing spatial gradients into the evolution of the state variables, which are identified with specific underlying micromechanisms. We wrote accurate balance laws to describe the evolution of the microstructure. We used this same approach to model two different effects. First, by introducing gradients in void evolution, both coalescence and ductile failure can be accurately modeled while eliminating mesh dependency. We plan experiments to help guide the choice of length scale and provide insight into boundary conditions (BCs) and an accurate identification with microstructural features. We also introduced gradients into the hardening evolution. This allows an improved description of shear bands and an understanding of when shear-band failure occurs. The experimental program to support this aspect of the work enables a correlation between predicted bands and those observed. This also brings a better understanding between the orientation of cells and bands to macroscopic anisotropy. Of particular importance is an attempt to develop a better friction model by accurately describing the gradients in hardness that occur near interfaces.

We developed two models, one with spatial gradients in the evolution of the isotropic hardening and one with a spatial gradient in the evolution of the porosity of the damage variable, and implemented them into the finite-element (FE) code HICKORY. The spatial gradient in the hardening is derived from a dislocation model utilizing a Taylor assumption between the internal stress and the density of dislocations. We coupled this gradient term to the temporal evolution equations of an existing plasticity model. The spatial gradient in the damage evolution is motivated from a model where voids were introduced as a center of dilatation, and has been coupled with a damage model.

We used these models in the solution of several problems and compared the results with literature solutions using standard empirical nonlocal theories. The first problem is the notched axisymmetric tensile specimen. We performed tests to compare the local theory with the spatial gradient theories. The presence of the gradient in the damage tends to diffuse the porosity in comparison to the local theory. This is one manner in which mesh sensitivity can be dealt with in damage localization problems. The introduction of the spatial gradient in the isotropic hardening variable, however, results in a "spreading" of the hardening, thereby further enhancing concentration of porosity and plastic flow. This effect may prove to be critical in the accurate description of localization phenomena. We also used both models in the solution of the "Tveergard-Needleman" problem, which is a name we attached to the problem of the compression of a plate containing a periodic distribution of holes. We compared both gradient models with local theory and empirical nonlocal theories with results similar to those obtained in the notched tensile specimen. We used the dislocation-based model (gradients in isotropic hardening) in the extension of a rod with non-uniform initial state. The solutions illustrated a pronounced effect of the spatial gradient term on the neck that formed in the rod.

We extended the model to consider two coupled scalar hardening parameters derived from the interaction of mobile and immobile dislocations. Implementation of this model into HICKORY will study the effect of these interacting variables on strain localization.

Characterization of Fluid Transport in Microscale Structures

P. H. Paul, J. H. Smith

This report summarizes progress in (1) the development of a optical diagnostic capable of in situ *measurements of liquid flows in microscale structures (a few to 100 microns scale), and (2) the application of these tools to provide a flow data base to support the development of accurate models of microscale fluid transport. The study includes both pressure and electrokinetically driven flows.*

The diagnostic tool is based on a "tag-and-read" technique that involves writing a known pattern into the flow (tag step), then recording the differential motion of this pattern in time (read step). The fluid velocity profile is then recovered by inversion of the conserved scalar advection-convection equation. We can obtain information concerning fluid transport properties by using tag species that have a range of molecular diffusivities.

Sandia's primary effort in the first year was to build a flow-imaging instrument, identify a suitable molecular tag species, and proof the data-processing algorithm.

We accomplished the following in FY96:

(1) We completed the design, construction, and testing of the flow-imaging instrument. Detailed analysis of the optical system, including the effects of beam deviation and chromatic/optical aberrations, suggests that a spatial resolution of 4 microns can be achieved for velocity measurements.

(2) We identified and proofed a suitable "tag-and-read" molecular system, specifically a caged fluorescence dextran dye added as a trace to a slightly basic fluid carrier. The dye is uncaged with 355-nm light from a tripled YAG laser and read out using 488-nm light from an Ar-ion laser. Signal levels are sufficiently high that single-pulse measurements can be made with a high-performance CCD video camera. The molecular weight of the dye can be selected from 440 (no dextran group) to 120,000 (multiple dextran groups).

(3) We demonstrated flow measurements in both pressure-driven and electrokinetically driven flows for a cylindrical geometry.

(4) We initiated fabrication of a channel geometry (high-aspect rectangular channel) with optical access. We are pursuing two configurations: a channel etched in Si with a thin SiN membrane window, and a channel etched in silica with a bonded silica window.

Scaling Laws for Strength and Toughness of Solid Materials

E. P. Chen

This report analyzes the premise of applying fractal theories to scale strength and toughness of solid materials. The approach is to cast fractal cracks in the thermodynamic laws and to formulate an expression for energy release rate associated with the crack. We then use the resulting energy release rate to study the scale effect in solids. Results indicate that fractality by the nature of a continuous crack surface is not the predominant factor for observed size effects. We also discuss here the effects of fractal cracks on scaling.

The goal of the project was to investigate the premise of applying fractal theories to scale strength and toughness of solid materials. The motivation was twofold: (1) crack surfaces are not smooth and may best be described by fractals, and (2) crack parameters involve fractional-length dimensions that may be the root cause of size effects and may be remedied by fractal theories. Based on existing studies, we can conclude that crack surface roughness can be described by fractals. The approach is to cast the fractal cracks in the thermodynamic laws and formulate an expression for energy release rate associated with a fractal crack. We then use the resulting energy release rate to study the size effect. We successfully formulated an energy release rate expression that satisfies all thermodynamic laws. In the size effect study, we paid special attention to the derivation of asymptotic expressions to compare with physical observations. Results indicate that fractality by the nature of a continuous crack surface is not the predominant factor for the observed size effects in solids.

Temporal and Spatial Resolution of Fluid Flows

S. R. Tieszen, L. D. Perea, R. W. Schefer, T. J. O'Hern

The purpose of this project is to develop an experimental technique for velocity field measurements in single-phase fluids with two orders of magnitude in temporal and spatial (two dimensions) resolution. A successful outcome will permit validation tests data to support the development of the next generation of computational fluid dynamics solvers. The experimental technique is based on particle image velocimetry (PIV). We will conduct diagnostic development experiments in nonreacting and reacting plumes of base diameter of 1 meter. Nonreacting flows will be helium/nitrogen mixtures, and reacting flows will be hydrogen and methane. The flow conditions are representative of those found in fires. We are making extensive use of prior investments in staff expertise and facilities.

The two primary objectives were (1) to complete the design and fabrication of the test apparatus and begin testing, and (2) to conduct laboratory-scale proof-of-concept tests. We estimate 90% completion against the first objectives. Final approval of the pressure data package is pending final assembly and leak checking. We completed the design of all subsystems and estimated hardware fabrication to be 80% complete. Non-completion was due to a significant design change mid-year as a result of a design review involving PIV experts and numerical tool developers.

In addition to hardware preparation, we conducted proof-of-concept tests at laboratory-scale to select seed particles and film type consistent with the laser wavelength chosen. We successfully conducted the tests and demonstrated the feasibility of the measurement concept with the laser, optics, seed particles, and film selected for the large-scale tests. We also successfully conducted subsystem checkout tests at large scale in which we recorded particle images in the large-scale test facility.

Stress Evaluation and Model Validation Using Laser Ultrasonics

W. Y. Lu, L. W. Peng, J. J. Dike

This report describes the development of a new method in stress evaluation—laser ultrasonics (LU). To qualify this innovative method as a viable stress measurement technique, the investigation includes (1) experimental evaluation of the acoustoelastic effect by using laser-generated Rayleigh waves, (2) model LU generation and wave propagation by finite-element (FE) methods, (3) design measurement techniques based on the guidance of FE analyses, (4) determination of the resolution of the LU technique to in-plane stresses, and (5) determination of the stress gradient through thickness. The work focused on the experimental setup of an optical-mechanical system, wave-velocity measurement methods, and FE models development.

The purpose of this project is to develop a noncontact stress measurement technique that is needed for experimental evaluation of stresses for validation of constitutive models and structural analyses. The technique is based on acoustoelasticity, $^{1}V/V_{o}=k_{R}{}^{1}\sigma$, and LU, a novel method for the optical generation and detection of ultrasound. The LU technique allows velocity measurements made over a pathlength of a few millimeters, an improvement in spatial resolution of at least an order of magnitude over conventional methods. This promising technique has not been investigated before; it faces many experimental challenges. FE modeling can provide insight of the LU generation and propagation and can guide the experimental endeavor, which is a necessary part of this project.

We accomplished the following:

(1) We completed the setup of acoustoelastic experiments. We devised a table-top mechanical loading system mounted on *xyθz* stages. We successfully integrated LU instruments with the mechanical loading system and high-speed data-acquisition units—Tektronix RTD710 (200 MHz) and RTD720 (1 GHz).

(2) We developed two-point detection techniques. One method is using a polished specimen; another is utilizing an elliptical mirror. The two-point detection scheme allows us to measure transit time with better precision.

(3) We began measuring the acoustoelastic effect of AA6061-T6. For the Rayleigh wave propagating parallel to the direction of loading, the acoustoelastic constant is estimated to be $k_R = 0.027/\text{GPa}$. The distance between two receiving points is about 15 mm. If the accuracy of transit time is ±1 ns, the corresponding stress resolution is about ±10 MPa. More experiments are needed to verify this result.

(4) We developed an FE model to analyze the transient thermal response from the heating of a laser pulse by using COYOTE code. We verified the model for the cases of both continuous wave (CW) laser and pulsed laser where the analytical solution and/or experimental data are available. The FE model prediction compares very well with the exact solution and data.

(5) We developed an FE model of wave propagation based on the temperature distribution obtained from the thermal analysis model. We mapped thermal histories to a mechanical mesh using MERLIN; we used PRONTO2D for mechanical analyses. We compared preliminary model predictions with the experimental waveforms. The model correctly predicts wave speed and frequency.

Ultra–High-Speed Studies of Shock Phenomena in a Miniaturized System

W. M. Trott, K. L. Erickson, A. M. Renlund, L. C. Chhabildas

This project focused on the development of a quantitative, laboratory-scale capability for the investigation of material response to short-duration shock compression. We assembled and tested an experimental system that is designed to probe shock compression states in thin-film energetic materials or high-density metal foils. This system utilizes two high-speed optical diagnostic tools (optically recording velocity interferometry and single-pulse Raman spectroscopy) to probe physical and chemical changes in samples subjected to planar shock loading generated by laser-driven flyers. We developed procedures for reproducible deposition of explosive thin films on the required substrates (e.g., the output end of optical fibers), and designed and implemented a strategy for detailed characterization of the thickness, density, and porosity of polycrystalline thin films.

We designed the experimental system around a common laser source for flyer generation (the shock driver) and excitation of Raman scattering (a frequency-doubled optical probe of the shock-loaded material). Using precisely variable optical delay legs, we demonstrated the requisite timing control (< 1 ns) between shock driver and optical probe. The Raman detection system includes a large spectrometer and a fast-gated optical multichannel analyzer. The use of optical fibers for both delivery of Raman excitation light and collection of Raman scattered light resulted in a system with adequate sensitivity for single-pulse experiments on thin films deposited on the ends of the fibers. We developed procedures for reproducible physical vapor deposition of nearly planar films of two explosive materials of interest (triaminotrinitrobenzene [TATB] and hexanitrostilbene [HNS]) in the thickness range needed for these studies (i.e., 1–5 mm). We developed a strategy for characterizing the density and porosity of the polycrystalline films. This involves deposition on low-mass substrates to permit accurate measurement of thin-film mass using a microbalance with 0.1-mg sensitivity. The flatness and uniformity of the thin films are determined using a noncontact profilometer; grain sizes and void distributions are determined using scanning-electron microscopy (SEM). We performed preliminary tests on both energetic material thin films and inert foil materials (using velocity interferometry to measure particle velocities upon shock loading). In one test, we shocked a 12.5-mm-thick sample of tantalum to 25 GPa; the free-standing foil exhibited the expected free surface velocity plus an apparent spall signature. We demonstrated many aspects of the proposed miniaturized shock compression research system (despite obvious funding and time limitations).

Pulsed Power

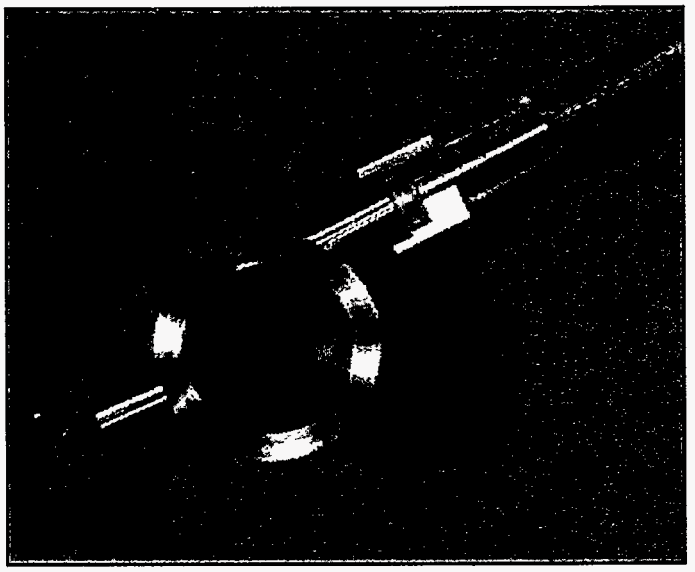

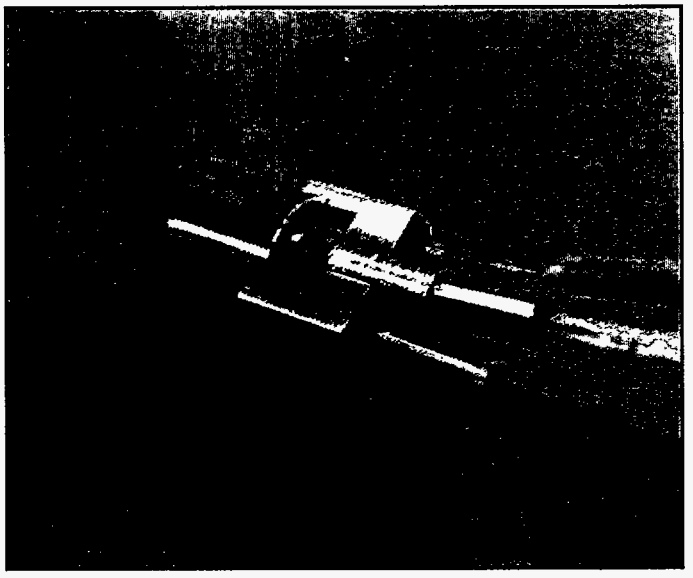

Obtaining the first precision measurements of pressure-volume states at Mbar pressure using pulsed-power accelerators is an important new capability for weapons physics, safety, and reliability. We developed advanced diagnostics and experimental techniques for using pulsed-radiation sources to perform shock physics experiments at multi-Mbar pressures.

Synchronization of Multiple Magnetically Switched Modules to Power Linear Induction Adder Accelerators

K. W. Reed, H. C. Harjes, L. X. Schneider

In applications where multiple magnetic modulators are used to drive a single linear induction voltage adder (LIVA) or linear accelerator (linac), it is essential that the outputs of the modulators be synchronized. Output risetimes are typically in the 10-ns-to-20-ns range, often making it necessary to synchronize to within less than 1 ns. We developed and demonstrated microprocessor and electronic feedback schemes that achieve the required level of synchronization; however, they are sophisticated and potentially complex. In a quest for simplicity, this work seeks to determine the achievable level of modulator-to-modulator timing jitter that can be obtained with simple design practices and passive techniques. We reviewed sources of output pulse-time jitter in magnetic modulators and discussed some basic modulator design principles that can be used to minimize the intrinsic time jitter between modulators. We also developed a novel technique for passive synchronization.

We accomplished the following:

(1) *Measured timing jitter and voltage jitter of dual modulator systems*: We built a pair of magnetic modulators that characterize timing jitter in magnetic modulators, identify sources of timing jitter, and develop simple passive techniques for controlling timing jitter. A study of the possible causes of jitter indicated that the main source of random time variations in the output of a magnetic modulator or between a pair of magnetic modulators is voltage variations in the input charge voltage. These voltage variations are caused by fluctuations in the output of the prime power supply and reflections from downstream switches and the load. We verified this theory by measuring the voltage variations at the input of the magnetic modulators and comparing the calculated timing variations that they would cause to the measured timing variations at the output of the modulators. The 1-second standard deviation of the calculated timing variation was 1.7 ns compared to the standard deviation of the measured timing variation of 2.1 ns, which is within the error limits of the measurement.

(2) *Measured B-H curves of magnetic switches*: We measured B-H curves for the magnetic switches. Volt-second products calculated from this data were within 5% of the design values.

(3) *Measured timing jitter in the modulator output pulses and developed jitter control techniques*: We made the timing jitter measurements for an individual modulator and between the two modulators for various conditions. We invented a magnetic coupling technique and demonstrated that it significantly reduces the jitter between a pair of magnetic modulators. We submitted this novel technique for patent.

(4) *Defined and designed parallel magnetic modulator*: We completed modulator definition and design.

Publications

Other

Reed, K. W., and P. D. Kiekel. 1996. "Synchronization of Multiple Magnetically Switched Modules to Power Linear Induction Adder Accelerators." *Proc. 22nd Internat. Power Modulator Symp., Inst. Electrical and Electronics Engineers* **96-CH35877** (Boca Raton, FL, 25–27 June): 205–208.

Electromagnetic Impulse Radar for Detection of Underground Structures

G. M. Loubriel, D. H. Cress

This project will develop and demonstrate a ground-penetrating radar (GPR) that is based on high peak power, high repetition rate, and low center-frequency impulses. Sandia will discharge a 10-ns-long transmission line at 100 kV with photoconductive semiconductor switches (PCSS) at a repetition rate of 1 kHz into a matched antenna. This type of radar has applications to remedial site reconnaissance for the detection of buried objects, for the detection of underground bunkers and tunnels, and as a sensor for a self-aware weapon or a height-of-burst sensor. We built a pulse-forming line producing a pulse with center frequency of 100 MHz, designed and constructed a suitable antenna, and designed a computer model to guide the effort.

We built a computer model of the complete radar system that allowed us to test the effects of varying the type of voltage pulse into the antenna (we studied monopulse or bipolar pulses), the antenna transfer function, the transmission at the air/soil interface, different types of soil with varying attenuation and dispersion characteristics, and different targets to be detected. This model guided the design of the pulser and validated our initial estimates of radar penetration. The second effort was the design of the pulser—the subsystem that sends a voltage pulse to the top of the antenna. The main problem here is a modulator that we designed and constructed (two were built). Finally, we built an antenna and measured its transfer function. The key conclusion/finding is that the model predicts that a system will have 10-m penetration for detection of large structures in dry sand and San Antonio clay loam with 5% water. This is a great accomplishment since most ground-penetrating radars cannot penetrate more than one foot in water-containing clays.

Publications

Refereed

Loubriel, G. M., M. T. Buttram, J. F. Aurand, and F. J. Zutavern. 1996. "Ground-Penetrating Radar Enabled by High-Gain GaAs Switches." Paper presented to the Ultra-Wideband Short-Pulse Electromagnetics 3 Meeting, Albuquerque, NM, 27–31 May. New York, NY: Plenum Press.

Other

Loubriel, G. M., F. J. Zutavern, W. D, Helgeson, D. J. Brown, and M. W. O'Malley. 1996. "High-Gain GaAs Switches for Ground-Penetrating Radar." Paper presented to the 22nd Power Modulator Symposium (IEEE), Boca Raton, FL, 24–27 June.

Life-Cycle Costing for Nuclear Weapons Security

M. K. Snell, R. G. Cox, M. M. Madsen

This project developed methods and tools for analyzing the life-cycle costs and security effectiveness of nuclear weapons security, to better identify technologies that lead to reduced life-cycle costs while maintaining appropriate levels of security. Sandia applied activity-based costing (ABC) techniques to a hypothetical Department of Energy (DOE) facility to cost out three possible changes to security, one being administrative, another involving reduced system testing through smarter use of security system information, and the final examining of the effect of using a newer, more capable weapon on the guard force. We then analyzed these options from a security performance perspective.

This project developed methods and tools for analyzing the life-cycle costs in nuclear weapons security to better identify technologies that lead to reduced life-cycle costs while maintaining appropriate levels of security. There were two basic problems: (1) the analysis of costs, which we approached using ABC methods and their association with security activities and infrastructure, and (2) the quantification of performance measures for nuclear security systems. On the ABC side, we developed a hypothetical facility with security requirements representative of a general DOE facility. We then applied ABC techniques to financial data representative of data commonly found at DOE facilities for the security and material control and accountability activities.

We made the following conclusions: (1) ABC can provide a good understanding of true costs, including overhead costs. Moreover, the thought process of identifying activities, when taught to operations staff, helps them to independently identify cost-cutting measures. For both reasons, ABC can help identify areas of inefficiency in nuclear weapon security systems and consequently reduce costs for the same level of protection. (2) An analysis of costs can be performed using ABC within 4–6 months based on typical, existing DOE costing data. This analysis will allow costs of security options at that time. A further effort would be required to change the accounting system of that organization so that up-to-date costing data could be provided. We used these cost data to support a DOE task on developing a cost-benefit analysis tool.

On the performance side, we investigated how to display the effectiveness of the security system and costed out the three options for the hypothetical facility. The first two options are "security neutral" if implemented properly; the last option, concerning the improved weapon, will create security trade-offs. While such an improved weapon could allow the security force to operate with fewer personnel than otherwise required, the smaller force is less robust to certain adversary attacks (e.g., an insider tampers with the better weapons so that they are no longer "improved"). It is also difficult to demonstrate that the smaller force with the better weapons is just as good as the larger force with the older weapons for "most" scenarios. Either very expensive force-on-force exercises must be performed, or less expensive man-in-the-loop simulations must be performed to demonstrate this. In either case, rarely can we perform more than 100–200 simulations to collect this comparison information. Extrapolation of this data is difficult.

High-Power Ion Beam (HPIB) Modification of One- and Two-Layer Metal Surfaces

T. J. Renk, R. G. Buchheit

Sandia demonstrated pulsed high-power ion beams (HPIB) to modify metal surfaces by a rapid melt and resolidification (RMR) cycle. We investigated here the potential for using surface modification to improve hardness and corrosion-resistance for both commercial and national security applications. After a literature search that identified candidate bilayer systems for HPIB treatment, we undertook treatment in conjunction with a modeling code that helped guide beam intensity. We obtained significant improvements in hardness, corrosion-resistance, and wear-resistance in a number of different cases. We also began to formulate a prescription for treatment (number of pulses, thickness of top layer, etc.).

We began by studying previous experiments with HPIB treatment to produce nonequilibrium metallic states. In addition, we conducted a comprehensive literature search to identify promising elements to combine with the substrates we planned to study: aluminum (Al), iron (Fe), and titanium (Ti). From this search, we planned the following bilayer mixing experiments: transition metals (Ti, Cr, Nb, others) to improve corrosion resistance of Al, and Si with Al to improve hardness; Cr and Ta with Fe; and noble metal additions (Pd, Pt) to Ti to improve corrosion-resistance. We prepared coatings of all the metals listed above, in addition to others, and treated them on the repetitive high-energy pulsed-power (RHEPP-1) facility. In addition to these bilayer metals, we identified some alloy surfaces for surface modification by the HPIB, including Al and Fe alloys (e.g., stainless steel). We then subjected exposed samples to various diagnostic tests to measure both changes in corrosion-resistance or hardness and microstructural changes caused by the rapid heating and resolidification produced by the HPIB.

Using a well-characterized ion beam plus a simple modeling code, we obtained significant improvements in both hardness, corrosion, and wear-resistance in the following cases: Si mixed into Al (hardness), RMR treatment of 440° C stainless steel (wear-resistance), Cr mixed into Al (corrosion-resistance), and Pt mixed into Ti (corrosion-resistance). The overcoated materials appear to have diffused through the entire melted substrate layer during the RMR cycle, implying that a convective process is driving the mixing. Multiple RMR cycles led to reduced surface microcratering and improved mixing homogeneity. Some samples exhibit a crystalline structure consistent with a simple solid solution of the overcoated material and the substrate. Others show a less desirable mixed state.

These survey experiments serve as a basis for downselecting the bilayer systems and alloy surfaces for a more comprehensive characterization. We also treated and evaluated several parts created by the LENS™ process. We completed initial experiments to characterize the Ni-Fe system for its ability to reduce hydrogen diffusion into Fe.

A Feasibility Study of Space-Charge-Neutralized Ion Induction Linacs

S. A. Slutz, T. R. Lockner, T. J. Renk

Sandia studied the feasibility of using magnetic insulation and space-charge neutralization as a means of increasing the ion current that can be accelerated by an induction linear accelerator (linac). We studied numerically the control of the focusing of the beam at each acceleration stage and the charge-neutralization of the beam between stages. We experimentally measured the degree of charge-neutralization obtained by an ion beam propagating under a variety of conditions.

Magnetic insulation can be most conveniently applied using a cusp field geometry, which eliminates the need for a central electrode. This geometry has the important advantage that no structure intercepts the beam, and thus the beam azimuthal symmetry is maintained. Previous attempts to magnetically insulate an induction linac, which used a radial applied field, showed beam disruption in the location of the central supports. However, the cusp geometry introduces the complication that the acceleration gap is a strong function of radius. Since the beam is not charge-neutralized during acceleration, ions are pushed outward by different amounts, depending on the radius. Furthermore, the accelerating field has a focusing effect on the anode side of each accelerating gap and a defocusing effect on the cathode side.

We performed a series of numerical simulations to determine how to balance these forces. Adjustment of the radial current density profile of the beam, the accelerating potential, the gap, and the angle of the feed (same concept as the Pierce electrode) allowed us to achieve a rough balance of these forces in simulations. We numerically designed an injector for a six-stage multicusp accelerator to drive potassium ions to 180 MeV. The difficult part of the design is shaping the anode correctly to compensate for the space-charge–driven expansion of the beam before it reaches the virtual cathode where it can be charge-neutralized. We then simulated the next five stages of this accelerator with encouraging results. Very little of the beam was lost, even at current densities as high as 50 A/cm^2. The final radial divergence was approximately 30 mrad, which could certainly be reduced by optimization. A fusion driver would require significantly lower divergence, but for other applications such as neutron generation, beam divergence is not so critical. In addition, higher beam current densities should be possible with lower M/q ions such as protons. The maximum beam current density that can be transported between acceleration stages depends on focusing strength and the degree of charge-neutralization. Electrons are drawn from the drift tube walls along the cusp magnetic field to neutralize the beam. However, the accelerating field causes the electron density to be larger near the virtual cathode, which leads to relatively poor neutralization of the beam in the drift region. We found numerically that electron injection did not significantly help the charge-neutralization process. However, analytical calculations and computer simulation indicate that a preformed plasma should be quite effective at charge-neutralizing an ion beam. The plasma could be injected before the arrival of the beam at the critical locations near the virtual-cathode. We used the ALIAS facility to test the effectiveness of a preformed plasma to charge-neutralize a proton beam in the presence of a magnetic field. An array of sparks at approximately 1-cm spacing generated a carbon plasma at a density of a few times ten to the thirteen. The results indicate that the space-charge of the beam was reduced significantly by the presence of the plasma. Plasma could also be used to neutralize a light ion beam between acceleration stages.

Publications

Refereed

Slutz, S., T. Lockner, and T. Renk. 1995. "Space-Charge-Neutralized Ion Induction Linacs with Cusp Insulation." Paper presented to the Tri-Lab Meeting, Lawrence Livermore Laboratory, Livermore, CA, 16–17 November.

Other

Renk, T. J., S. A. Slutz, T. R. Lockner, and P. Primm. 1995. "Study of Ion Beam Neutralization in a Vacuum Drift Channel." Paper presented to the 36th Annual Meeting, APS Division of Plasma Physics, Minneapolis, MN, 7–11 November.

Slutz, S. A. 1996. "Space-Charge-Neutralized Ion Induction Linacs." Paper presented to the International Workshop on the Physics of High-Energy Density in Matter, Hirschegg, Klein-Walsertal, Austria, 28–30 January.

Slutz, S. A., T. R. Lockner, and S. Humphries, Jr. 1995. "Space-Charge-Neutralized Ion Induction Linacs with Cusp Insulation." Paper presented to the International Symposium on Heavy Ion Fusion, Princeton, NJ, 6–9 September.

A 700-kV, Short-Pulse, Repetitive Accelerator for Industrial Applications

F. J. Zutavern, L. F. Rinehart

This project is presently developing and demonstrating the feasibility of a small, 700-kV accelerator that can produce 7-kA particle beams with pulse lengths of 10–30 ns at rates up to 50 Hz. Sandia is testing two switching technologies: (1) spark gaps, conventional high-power switches, and (2) photoconductive semiconductor switches (PCSS), a new solid-state switching technology. We characterized the spark gap system. We tested the field-enhanced diode and tested the linear induction accelerator (LIA) to design modifications for continuous operation at 50 Hz. We designed and tested the PCSS-based pulser as a module (1/8th) of the total system. We performed experiments to test optical triggering and improve device lifetime.

We accomplished the following:

(1) *Spark gap-driven accelerator*: We met radiation safety requirements. We mounted a field-enhanced, single-tip cathode for initial testing of the diode and checking the radiation safety calculations. Radiation dosimetry verified the safety calculations and obtained approval for full-power operation. We adjusted the impedance of the diode by adding multiple tips. Maximum voltage and current delivered to date are 480 kV and 5.5 kA at two-thirds of the charging voltage. We added cooling to the anode for repetitive operation. We estimated and measured heat dissipation in the cores. We designed a cooling retrofit. Activities included increasing operation to full power and full repetition rate (50 Hz) in short bursts.

(2) *PCSS pulser*: We completed a design for the PCSS pulser. We fabricated one module (1/8th) of the system to test the design and PCSS triggering at 250 kV. We ordered one-hundred 2" GaAs wafers for fabrication into switches for the initial testing and demonstration of the PCSS pulser. We withdrew the laser to trigger the complete system from storage and refurbished it to better-than-original specifications. To maximize switch lifetime, we designed a fiber-optic triggering system to produce 1600-current filaments and limit the current per filament to less than 50 A. We tested 200 fibers for homogeneity and assembled them into an alignment structure for the PCSS. We assembled a pulse-charging system and appropriate diagnostics for testing the module. We initiated trigger testing of the PCSS and charged the switches as high as 150 kV.

Publications

Other

Hjalmarson, H. P., F. J. Zutavern, and G. M. Loubriel. 1995. "A Collective Impact Ionization Model for Optically Triggered Switches." Paper presented to the Joint Fall Meeting of Texas APS and AAPT, Lubbock, TX, 26–28 October.

Hjalmarson, H. P., F. J. Zutavern, G. M. Loubriel, and D. R. Wake (University of Illinois). 1996. "A Current Transport Theory for Optically Triggered GaAs Switches." Paper presented to the American Physical Society March Meeting, St. Louis, MO, 18–22 March.

Kang, S., C. W. Myles (Texas Tech. U.), and H. P. Hjalmarson. 1995. "An Impact Ionization Model for Lock-on Current Filaments in GaAs." Paper presented to the Joint Fall Meeting of Texas APS and AAPT, Lubbock, TX, 17–20 October.

Kang, S., C. W. Myles (Texas Tech. U.), and H. P. Hjalmarson. 1996. "Lifetime Considerations in GaAs Photoconductive Semiconductor Switches." Paper presented to the American Physical Society March Meeting, St. Louis, MO, 18–22 March.

Loubriel, G. M., F. J. Zutavern, A. G. Baca, H. P. Hjalmarson, W. D. Helgeson, and M. W. O'Malley. 1995. "Optically Activated GaAs Switches for Firing Set and Laser Applications." High-Voltage Workshop, Salt Lake City, UT, 17–19 October.

Loubriel, G. M., F. J. Zutavern, H. P. Hjalmarson, A. G. Baca, M. W. O'Malley, and W. D. Helgeson. 1996. "Triggering Optically Activated GaAs Switches." Paper presented to the American Physical Society March Meeting, St. Louis, MO, 18–22 March.

Zutavern, F. J., G. M. Loubriel, H. P. Hjalmarson, A. G. Baca, M. W. O'Malley, and W. D. Helgeson. 1996. "Characteristics of Current Filamentation in High-Gain GaAs Switches." Paper presented to the American Physical Society March Meeting, St. Louis, MO, 18–22 March.

Zutavern, F. J., G. M. Loubriel, H. P. Hjalmarson, A. G. Baca, W. D. Helgeson, and M. W. O'Malley. 1995. "Experimental Properties of Optically Triggered High-Gain GaAs Switches." Paper presented to the Joint Fall Meeting of Texas APS and AAPT, Lubbock, TX, 26–28 October.

Zutavern, F. J., G. M. Loubriel, W. D. Helgeson, M. W. O'Malley, M. H. Ruebush, H. P. Hjalmarson, and A. G. Baca. 1996. "Optically Activated GaAs Switches for Compact Accelerators." *Proc. 22nd Power Modulator Symp.* (Boca Raton, FL, 24 June). New York, NY: IEEE.

Advanced 3-D Electromagnetic and Particle-in-Cell Modeling

D. B. Seidel, D. J. Riley

Recent advances led to the development of techniques to embed unstructured free meshes into standard three-dimensional (3-D), rectilinear, finite-difference grids. The resulting hybrid-grid modeling capability allows the higher resolution and fidelity of modeling afforded by free meshes to be combined with the power and efficiency of rectilinear techniques. Sandia proposes to extend current particle-in-cell (PIC) methods for operation on these hybrid unstructured/rectilinear meshes. Several technical innovations are required, including proper treatment of space-charge-limited emission, particle transport on unstructured meshes, charge-conserving particle current/charge allocation, and proper treatment of particles in transition between structured and unstructured grid regions. This project provides a broadened simulation capabil-

ity impacting the areas of nuclear weapons effects, weapon physics, and inertial confinement fusion (ICF). Critical technologies that benefit with the improved capability to simulate the details of complex, irregular structures include anode shaping for focusing of ion diodes for ICF and the design of post-hole convolutes and other high-current magnetically insulated power-flow components for the advanced pulsed-power accelerators.

We completed the following tasks: (1) critical issue identification and feasibility assessment, (2) necessary algorithms designed and implemented in test-bed codes, and (3) algorithm evaluation and final algorithm selection. Several technical innovations were required to meet these milestones. We wrote and successfully tested algorithms for particle location and particle-to-grid interpolation coefficient computation on unstructured grids. These algorithms also correctly determine when a particle leaves the unstructured grid (either through a conducting boundary or into the structured portion of the grid), as well as the precise location at which the boundary face is crossed. We tested the use of the "pseudo-current" technique (Marder) for minimizing errors in charge conservation in a test-bed code. We also demonstrated that a time-averaging field-advancement scheme (Riley) can successfully damp the high-frequency particle-induced noise that often plagues PIC computations. This is important because treatment of this noise problem will no longer require an iteratively implicit algorithm whose use presents significant difficulties for the proper connection of the structured and unstructured grid field solutions. We generalized the design and implementation of the data structure required to support the connection of structured and unstructured grid regions to treat the inclusion of particles into the algorithm. We successfully incorporated the unstructured grid field solver into the QUICKSILVER 3-D rectilinear-mesh PIC code. This will provide the platform upon which our newly developed algorithms will be implemented.

Development of Advanced Shock-Wave Diagnostics for Precision EOS Measurements on PBFA-Z/SATURN at Mbar Pressures

L. C. Chhabildas, C. A. Hall, K. J. Fleming, R. E. Setchell, C. H. Konrad

The purpose of this project was to integrate the core instrumentation techniques and diagnostics previously developed for equation-of-state (EOS) measurements on light-gas guns with the unique pressure-generating capabilities of the PBFA-Z and Saturn accelerators to provide the first precision measurements of pressure-volume states at Mbar pressures using pulsed-power accelerators. The integrated diagnostics include subnanosecond velocity interferometry and fast-streak photography for simultaneously measuring particle velocity and shock-wave speed. These techniques enable highly accurate EOS measurements with pulsed-radiation sources at pressures exceeding current laboratory capabilities. We also designed and fabricated a sample configuration that allows the study of the EOS of materials to multi-Mbar pressures.

Gun-launched techniques and the associated instrumentation diagnostics played a central role in understanding the dynamic response of matter at extreme pressures and temperatures. With these techniques it is possible to achieve pressure-volume accuracies of 1–2% at Mbar pressures. The key problem addressed in the present study was to modify gas-gun diagnostics so they could be used with pulsed-radiation sources to perform high-pressure EOS studies. These applications require about an order of magnitude improvement in time resolution.

To accomplish the goal of improved time resolution for EOS studies, we modified a velocity interferometer for use on the pulsed-power accelerator, PBFA-Z. We interfaced the modified interferometer with fast-streak photography to allow a time resolution of about 0.1 ns. This is sufficient to provide 1% accuracy for particle velocity measurements in shock-wave profiles. We also acquired a software analysis program and modified it to allow data acquisition during an experiment and reduction of the data immediately after the experiment to provide a record of particle velocity during time. We successfully demonstrated this system, which will allow easy use of the velocity interferometer in pulsed-radiation environments.

To allow use of the velocity interferometer on PBFA-Z, we designed and fabricated a target configuration. We designed the target holder for performing experiments on PBFA-Z to greatly simplify the use of EOS experiments in pulsed-radiation environments. It is a self-contained assembly that allows for precision preparation of specimens for study on PBFA-Z and easy installation of the assembly into the PBFA-Z environment. With this configuration, it will be possible to easily measure shock and particle velocity in shock waves for a variety of loading conditions and to pressures previously inaccessible in the laboratory.

Another development in this project involved creation of innovative techniques for bonding LiF laser windows to specimens. Present bonding methods use an epoxy glue to bond windows to specimens. However, this technique will result in time resolutions that exceed the desired goals of the project by about an order of magnitude. The new technique is a solid-phase bonding that results in migration of Li ions into aluminum under the application of strong electric fields, moderate pressure, and high temperature. The resulting bond is apparently very strong and has an effective thickness on the order of atomic dimensions since lattice distortions will result.

Advanced Manufacturing Technologies

Integrated piezoelectric actuators provide active vibration suppression in this boring bar, yielding increases in metal-removal rates and workpiece quality.

Intelligent Tools for On-Machine Acceptance of Precision-Machined Components

N. G. Christensen

On-machine acceptance (OMA) is an agile manufacturing concept being developed for machine tools at Sandia. The concept behind OMA is the integration of product design, fabrication, and qualification processes by using the machining tool as both the fabrication and the inspection tool. The benefits of OMA include decreased product-cycle time, decreased product cost, less scrapped product, agile response to design changes, real-time product disposition, reduced cost related to fixture and gage design, fabrication, maintenance, and a more reliable and consistent process output.

We made the following accomplishments:

(1) Machined third run of artifacts and characterized their geometry.

(2) Analyzed and summarized data from third run of artifacts.

(3) Demonstrated OMA technology.

(4) Began to transfer OMA technologies to Allied Signal.

(5) Completed characterization of machine tool error budgets and modeling of the LaBlond lathe.

VIEWS—Virtual Interactive Environment Work Space

A. Breckenridge

Virtual environments (VE) are a collection of technologies that offer the opportunity to integrate the human into a computing system. This work proposes to apply VE technologies to manufacturing process in parallel with a current physical design project.

In the past two years, Sandia has made steady improvements in the human computer interface for virtual environments. We concentrated on an enhanced surety system that exemplifies the application of virtual environments in several aspects of manufacturing.

We made the following accomplishments in FY96:

(1) We installed the VIEWS/MuSE OpenGL version in product development and computational mathematics.

(2) We demonstrated a working prototype called virtual collaborative environments (VCE) at Supercomputing Conference '95 (SC '95) by combining three collaborative tools: (a) virtual reality, (b) X-Application–sharing with extensions for "direct" support, and (c) video conferencing.

(3) We gave a medical demonstration at SC '95 on the Global Information Infrastructure (GII).

(4) We developed several models demonstrating computer-aided design, including the ship model that was featured in a *Cavalcade of Enchantment* documentary on Sandia's work.

(5) We gave an invited presentation for a DOE2000 workshop for tools to aid DOE in more efficient operation in the future collaborative, virtual laboratory environment.

(6) With the PHANToM haptic interface, we studied and developed several key issues involved with force feedback and texture generation. We developed an algorithm for force interaction that includes collision detection, force representation, and graphics deformation of arbitrary polygonal data sets.

Publications

Refereed

Bauer, K., and A. Breckenridge. 1995. "Virtual Collaborative Environments." Paper presented to Supercomputing '95, San Diego, CA, December 4–7.

Anderson, T., and F. Yeh. 1996. "A Haptic Universe." Paper presented to Supercomputing '96, Pittsburgh, PA, 17–22 November.

Monks, C., P. Crossno, G. S. Davidson, C. Pavlakos, A. Kupfer, C. Silva, and B. Wylie. 1996. "Three-Dimensional Visualization of Proteins in Cellular Interactions." Paper presented to Visualization '96, San Jose, CA, 29–30 October.

Active Control of a Grinding Machine Using Magnetic Bearings

J. J. Allen, E. D. Apodaca, P. G. Stromberg

The objective of this project is to demonstrate the use of magnetic bearings in a grinding machine to mitigate vibration response during the manufacturing process. We obtained a 12-in. surface grinder and modified the spindle to accept magnetic bearings. We completed the system-integration tasks of the project and are developing the spindle levitation control algorithms.

We performed grinding experiments using ceramics and alumina with the original mechanical spindle grinding machine. The purpose of these experiments was to obtain data on the grinding forces involved in grinding alumina. These experiments verified that the spindle being designed was within the capability of the magnetic-bearing spindle under design. The grinding forces were also lower than the steel-grinding experiments performed during the previous year.

We redesigned the existing mechanical spindle in the grinding machine to accept a magnetic-bearing spindle. The design effort faced constraints on the magnetic-bearing size that could fit in the existing grinding machine. The redesign was trying to maintain the natural frequencies of the spindle shaft at approximately the same frequency as the original mechanical spindle. This was a consideration to prevent mechanical flexibility from complicating the magnetic-bearing spindle control design problem.

We installed the modified magnetic-bearing spindle in the grinding machine and are designing levitation control algorithms. The objective of the spindle levitation algorithm is to maintain a stiff suspension of the shaft in the face of system uncertainty and destabilizing forces from the spindle motor. We were unable to develop control algorithms and grinding experiments due to the late delivery of the spindle.

Holding Things Fast: Automatic Design of Fixtures and Grasps

R. C. Brost, R. R. Peters

This project produced an implemented algorithm that automatically designs fixtures and assembly pallets to hold three-dimensional (3-D) parts. The fixtures and pallets designed by the algorithm rigidly constrain and locate the part and obey task constraints. They are robust to part shape variations, easy to load, and economical to produce. The algorithm is guaranteed to find the global optimum solution that satisfies these and other pragmatic conditions. We demonstrated the fixture design algorithm on several practical examples. This project also produced an automatic gripper design software with similar characteristics.

We improved the code's robustness, speed, and analytical capabilities. We obtained robustness improvements by implementing fixture robustness checks that verify the fixture's robustness to shape variations, verify that the fixture will load robustly without jamming due to friction or overcoming clamp actuation force limits, and by removing bugs from the code. We sped up the code by a factor of 100 on hard problems by improving the efficiency of the algorithm's search methods. Finally, we implemented advanced quality metrics that measure a fixture's ability to meet or exceed task requirements, considering the forces and position tolerance requirements associated with the given assembly or machining task.

In the domain of gripper design, we implemented code that performs a full-force quality analysis, including friction, gripper squeeze-force limits, and an arbitrary set of task-specific disturbance forces. We also implemented two multigripper design codes. The first code designs multiple grippers for a single part that are mutually compatible, allowing the part to be handed off from one gripper to another. We used this code to design grippers for an automated component cleaning workcell. The second code designs a single gripper that can handle multiple parts; this capability is quite useful in agile manufacturing scenarios where multiple products are being manufactured in small lots.

Publications

Refereed

Brost, R. C., and R. R. Peters. 1996. "Automatic Design of 3-D Fixtures and Assembly Pallets." *Proc. IEEE Internat. Conf. on Robotics and Automation* **1** (Minneapolis, MN, 22–28 April): 495–502.

Other

Brost, R. C., and R. R. Peters. 1995. "A CAD Tool that Automatically Designs Fixtures and Pallets." Paper presented to SME Autofact '95, Detroit, MI, 14 November.

Intelligent Tool and Process Development for Robotic Edge Finishing

M. A. Powell

This report describes a project to develop an agile, automated, high-precision, edge-finishing system. The project involved redesigning and adding additional capabilities to an existing finishing workcell. The resulting workcell may serve as a prototype for production systems to be integrated in highly flexible automated production lines. The system removes burrs formed in the machining process and produces precision chamfers. The system uses an expert system to predict the burr size from the machining history. Within the computer-aided design (CAD) system, tool paths are generated for burr removal and chamfer formation. Then, we automatically select the optimal grinding process from a data base of processes. We then download the tool trajectory and the selected process definition to a robotic control system to execute the operation. The robotic control system implements a hybrid fuzzy logic-classical control scheme to achieve the desired performance goals regardless of tolerance and fixturing errors.

We developed an automated robotic edge-finishing system that is fully integrated into the CAD-CAM system. Within the CAD system the component designer specifies the machining process to be used to fabricate the part. Similarly, the edge-finishing tool paths are also generated. Then we invoke an expert system to predict the size and shape of the burrs produced by the machining processes. We use a data base characterizing the material removal rate and tolerance capabilities of a variety of edge-finishing tools as a function of feedrates and applied forces to select the optimal edge-finishing tool and to specify the process parameters of feedrate and force along the finishing trajectory. We then export the manufacturing process information from the CAD system and fabricate the part. We perform the finishing operations in a robotic workcell. The real-time controller that we developed for this purpose automatically adjusts the nominal computer numerically controlled (CNC) trajectory to fixturing and tolerance variations while maintaining the feedrates and force parameters necessary to remove the burr and to form the desired chamfer.

Publications

Refereed

Narayanaswami, R., and D. A. Dornfeld. 1996. "Burr Minimization in Face Milling of Flat Polygonal Parts." *Trans. ASME, J. Eng. Industry* **118** (November): 127–148. New York, NY: ASME Press.

Powell, M. 1996. "Agile Robotic Edge Finishing." Paper presented to the 2nd Annual Robotic Grinding, Deburring, and Finishing Workshop, Cincinnati, OH, 11 June.

Powell, M. 1995. "Agile Robotic Edge-Finishing System Development at Sandia National Laboratories." Paper presented to Autofact '95—Society of Manufacturing Engineers, Chicago, IL, 12–16 November.

Powell, M. 1995. "Agile Robotic Edge-Finishing System Research at Sandia National Laboratories." Paper presented to SME Finishing '95, Cincinnati, OH, 16 May.

Powell, M., and G. Star. 1995. "On the Edge Finishing of Curved Planar Parts." *J. Vibration and Control*, in press. Sage Science Press.

Stein, J., and D. A. Dornfeld. 1995. "An Analysis of the Burrs in Drilling Precision Miniature Holes Using a Fractional Factorial Design." *Trans. ASME, J. Eng. Industry* **2-1** (November): 127–148. New York, NY: ASME Press.

Stein, J., I. Park, and D. A. Dornfeld. 1996. "Influence of Workpiece Exit Angle on Burr Formation in Drilling Intersecting Holes." *Trans. North Amer. Manufact. Res. Inst.* 24: 39–44. Dearborn, MI: Society of Manufacturing Engineering.

Virtual Prototyping

P. L. Dreike, J. A. McCoy

Virtual prototyping (VP) is a computer modeling methodology that enables engineers to develop designs that are verified to be correct and ready to go directly into production, without the time and expense of traditional preproduction hardware prototypes. Many products have aspects that are designed or evaluated by different engineering disciplines. A complete VP methodology needs to couple simulations and simulators from many disciplines. In this project Sandia explored coupling commercial simulators from two disciplines, software and digital hardware.

We built a simulation version of a tool called an in-circuit emulator (ICE). An ICE is a microprocessor that is instrumented for control and monitoring from a workstation. It provides a capability to control and observe execution of software in hardware prototypes. The simulated ICE provides software and hardware developers an opportunity to integrate software on prototype embedded-processor designs in a simulation environment with simultaneous visibility of the software and hardware. Its significance is that it provides an opportunity to develop software and hardware concurrently in a model-based environment, before completion of a hardware prototype. In a typical embedded system project, about 50% of the development time occurs after construction of the first hardware prototype, so there is an opportunity to reduce development time by 2x.

The simulated ICE has four components. The first is a software debugger with a network interface called SourceGate IITM. It provides a graphical user interface (GUI) for a software developer to use to issue commands to a simulator running software. The second is a command translator called Vemulator. The third component is a VHDL (VHSIC Hardware Description Language) simulator called Viewsim and its companion waveform viewer, Viewtrace, from Viewlogic Corp. The fourth component is a VHDL model of an Intel 8051 microcontroller connected to VHDL peripheral models that is executed by Viewsim using Viewtrace to show logic-analyzer–like waveforms of the hardware operation.

We demonstrated a prototype simulated ICE. We (1) reverse-engineered SourceGate II's command language, (2) used Unix interprocess controls to connect SourceGate II to Vemulator, and to connect Vemulator to Viewsim and Viewtrace, (3) wrote a clock-cycle accurate instruction set simulator (ISS) model of an Intel 8051 microcontroller, (4) compared performance of the ISS model of the 8051 with that of a register transfer level (RTL) model of the 8051, (5) and ran software on a demonstration circuit containing the 8051 and two controller area network (CAN) controllers using both 8051 models.

Commercial tools with similar objectives emerged during FY96. We evaluated their methodologies and capabilities. In this process we explored modeling tradeoffs and alternate methods of VP software and hardware.

Publications

Other

Dreike, P. L., and J. A. McCoy. 1997. "Introduction to Co-Simulation of Software and Hardware in Embedded Systems." Paper to be presented to the Embedded Systems Conference East, Boston, MA, 12 March.

Dreike, P. L., and J. A. McCoy. 1996. "Introduction to Co-Simulation of Software and Hardware in Embedded Systems." *Proc. Embedded Syst. Conf.* 3 (San Jose, CA, 16–19 September): 997–1012. Miller Freeman.

Development of an Immersive Environment to Aid in Automatic Mesh Generation

C. Pavlakos

This work explores the use of immersive technologies, such as those used in synthetic virtual environments (i.e., virtual reality [VR]), in enhancing the mesh-generation process for complex 3-D models. The idea is to demonstrate the ability to interact with the mesh-generation process in a highly visual and intuitive manner, allowing a much greater understanding of the mesh as it is being constructed, as well as allowing powerful interactive feedback to the creation process. This work is based on Sandia's CUBIT mesh-generation research, and explores use of capabilities developed for Sandia's Multidimensional User-Oriented Synthetic Environment (MuSE).

We accomplished the following:

(1) Completed the acquisition and setup of a low-end VR desktop workstation.

(2) Implemented a prototype MuSE application for viewing and understanding CUBIT meshes, with a focus on features for the meshing algorithm developer. Features include the ability to visually differentiate between nodes in the mesh according to mesh complexity at each node; the ability to turn on/off mesh edges; the ability to highlight specific elements in the mesh for scrutiny; the ability to highlight all elements associated with a particular node in the mesh; the ability to grab and move nodes in the mesh; and the ability to interact with all of these visual features in a fully stereoscopic environment, supported by the advanced human-computer interface capabilities provided by MuSE. This capability on the desktop would increase productivity by a factor of four or five for looking at meshes.

(3) Migrated the prototype application to the low-end workstation configuration, and initiated an OpenGL port of the application (to be used with the new OpenGL version of MuSE).

(4) Investigated a couple of different mechanisms for integrating MuSE and CUBIT. We completed a design for an initial coupling that would make use of dual communicating processes.

General Application of Rapid 3-D Digitizing and Tool-Path Generation for Complex Shapes

K. S. Kwok

Many machining and finishing operations of machine parts require the ability to digitize a complex surface with high precision. One system demonstrates digitization of a turbine blade surface and automatic creation of five-axis toolpaths that match the surface. However, this system works only for turbine blades with certain dimensions because it is specifically designed to accept the cross-sectional shape of a particular type of turbine blades. Sandia proposes to further develop this technology for general application of 3-D digitizing and tool-path generation for complex shapes. This is extremely difficult to implement using conventional techniques because specifications and boundary conditions of the parts need to be defined precisely at the outset. We propose to apply fuzzy technologies, where appropriate, to solve problems associated with developing technologies applicable to digitization and tool-path generation of complex shapes. Fuzzy techniques, such as fuzzy modeling, fuzzy measure theory, fuzzy mathematics, and fuzzy logic, are suitable tools for solving problems that require high degrees of adaptation. By using fuzzy techniques, uncertainties associated with constraints not yet defined can be addressed in a natural way and solved.

We added a moiré sensor to expedite digitizing an average size part. The structured light system can be used to scan fine features that are undetectable to the moiré sensor. We experimented with different ways to mount both sensors and will make recommendations. When both sensors are mounted simultaneously on the computer numerically controlled (CNC) platform, the two sensors provide a unique platform on which fault-tolerant technology can be developed for advanced manufacturing. We can use the redundancy provided by the two sensors to provide fault tolerance in critical processes or quality-control inspections in Defense Program (DP) manufacturing processes. Adaptive algorithms generally require training and committing mistakes. Combinations of fuzzy logic, genetic algorithms, and neural-net techniques may eliminate some of these. We developed an adaptive algorithm in conjunction with fuzzy techniques that have the potential to decrease or eliminate training and committing mistakes during production.

We completed the following:

(1) Produced an industry-accepted computer-aided design (CAD) description of the simple part using the fuzzified structured light system.

(2) Applied fuzzy mathematics to the algorithm for tool-path generation.

(3) Produced an industry-accepted CAD description of the toolpath for finish-machining of a simple part using the fuzzified algorithm.

(4) Finish-machined a simple part using the fuzzified tool-path generation algorithm and filtering routines for the structured light system.

(5) Applied fuzzy logic through the PC interface to the controller of the CNC machine.

(6) Finish-machined a simple part using the fuzzified controller.

(7) Designed an algorithm of structured light system for scanning acute and complex objects.

(8) Developed criteria on minimum measurements for surface definition.

(9) Measured and digitized surfaces of varying curvature and concavity with dimensions up to 5 inches.

(10) Produced an industry-accepted CAD description of the toolpath for finish-machining of a part with varying curvature and concavity using the fuzzified algorithm.

(11) Finish-machined a part that is complex in shape with dimensions up to 5 inches.

Publications

Refereed

Kwok, K. S., C. S. Loucks, and B. J. Driessen. 1997. "Automatic Tool-Path Generation for Finished Machining." Paper to be presented to the IEEE International Conference on Robotics and Automation, Albuquerque, NM, 20–25 April.

Ultra-Precise Assembly of Micromechanical Components

J. T. Feddema

The main contribution of this work is to develop a visual feedback and robotic control system that improves positioning accuracy and eliminates the manual assembly of microelectromechanical systems (MEMS) components. Sandia proposes to integrate a set of computer-controlled XYZ translation stages (resolution to 0.1 microns) with a commercially available robot and a vision system imaging through a long-distance microscope. Attached to the end of the robot will be a microgripper for grasping parts. The robot will act as the coarse positioning device between two platens containing MEMS parts. The robot will first move the microgripper into the vicinity of the precision stages that have the MEMS parts randomly oriented on their surfaces. The translation stages will then provide the fine motion control needed to position the gripper over the part. The visual servo-based control system and an instrumented gripper will provide real-time feedback to the stages and the robot to achieve accuracies of 0.5 micron. After picking up the part, the robot will move to another location to mate the part in the gripper with another part on the stages.

We built an ultra-precise robotic workcell that includes a 4-degree-of-freedom (DOF) AdeptOne robot; a 4-DOF precision stage; a long-distance microscope with motorized zoom, focus, and aperture; a computer vision system; and three types of microgrippers. Sandia developed the first type of gripper using the LIGA (lithography galvonoforming abforming) process. The second type of gripper was developed at University of California-Berkeley (UCB) using a polysilicon process. Both grippers have been used to pick up and stack several silicon and LIGA test parts with outside dimensions of 100 microns. The Sandia gripper has proven to be much more robust than the second gripper, although not as dexterous.

We demonstrated the ability to perform 4-DOF visual servoing at a 30-Hz rate using binary image processing. We also developed a routine that centers (in x and y) and focuses (in z) a 100-micron

gear under the microscope. We use the image gradient to perform the auto focus by controlling the z position of the stage under the microscope. The visual servo rate with the image gradient is 10 Hz. The repeatability is 1 micron in x and y, and 60 microns in z.

Smart Cutting Tools for Precision Manufacturing

J. M. Redmond, P. S. Barney

The goal of this project is to demonstrate increased metal-removal rate in machining through the integration of smart material actuators with a conventional tool. In many metal-cutting processes, the metal-removal rate is limited by the phenomenon of chatter, a regenerative vibration that is driven by workpiece surface undulations resulting from previous tool vibrations. Because resistance to chatter in the absence of workpiece flexibility is a function of the damping inherent to the tool structure, using feedback control to stabilize the primary modes of vibration should permit substantially higher metal-removal rates. To facilitate the development of a smart materials-based active control system for chatter mitigation, Sandia selected the boring process as the featured machining process of this research. This selection enables project emphasis to be placed on modeling and control of the cutting process without considering the hardware complexities associated with sensing and actuating rotating tools. Piezoelectric actuators incorporated into the bar structure enhance the damping through feedback control. Preliminary damping tests combined with computer simulations of the boring process indicate that greater than a sevenfold increase in metal-removal rate can be readily achieved for some processes.

The first year of this two-year project featured three primary accomplishments: (1) the creation of a computer simulation of the boring process, (2) the development and evaluation of a surrogate tool, and (3) the conceptual design of a prototype smart boring bar.

We developed a simulation of the boring process in the Matlab programming environment assuming a rectangular cutting insert with zero rake angle. We enter process parameters through a graphical user interface (GUI); a tool-workpiece interaction model predicts the cutting forces that drive the tool vibrations. Under certain cutting conditions the workpiece waviness can regenerate, leading to the development of classical chatter. Simulation output includes an estimate of the tool vibration history and the resulting workpiece surface profile.

We used the simulation to evaluate the smart boring bar concept as demonstrated in a surrogate tool test-bed. We mounted four lead zirconate titanate (PZT) stack actuators at ninety-degree intervals around the root of a 2-inch-diameter boring bar. We grouped opposite actuators in bi-morph pairs to provide two-axis control. We input open- and closed-loop system models obtained through benchtop testing to the boring simulation, demonstrating the capability of the proposed smart tool concept to improve bar performance.

Testing and analysis efforts yielded a conceptual design for the prototype boring bar. We will use single as opposed to bi-morph actuator sets since this configuration was shown to provide adequate control authority while minimizing the boring bar's static stiffness loss resulting from actuator integration. We will mount two orthogonal actuators in the normal and tangential directions on the lower and aft sides of the bar relative to the workpiece. At these locations, the mechanical and electrical preloads of the actuators can be used to partially compensate for static tool deflections produced by the cutting forces.

Other project efforts included modal and operational characterization of two machines.

Publications

Other

Barney, P. S., J. M. Redmond, and D. Smith. 1997. "Characteristics of a Self-Sensing Actuator for Active Vibration Control." Paper presented to the 15th International Modal Analysis Conference, Society for Experimental Mechanics, Orlando, FL, 3–7 February.

Redmond, J. M., P. S. Barney, and D. Smith. 1997. "Development of an Active Boring Bar for Chatter Immunity." Paper presented to the 4th Annual Symposium on Smart Structures and Materials, International Society for Optical Engineers, San Diego, CA, 3–6 March.

Solid Variant Geometry Modeling

S. W. Parratt, R. H. Wilson

Solid modeling technology and systems are a core component of Sandia's model-based product realization process. Solid modeling systems represent ideal parts, but they do not account for the unavoidable presence of geometric variations in actual parts. Our research goal is to develop match models, representations, and algorithms for assembly analysis and planning of toleranced product models. We will embed theoretical results in a prototype assembly analysis system through its application interface. This system will process product model assembly and tolerance specifications and construct maximum material part (MMP) models. MMPs are used to determine if the product is an interchangeable assembly.

Current tolerancing standards are not based on any mathematical foundation. Even American National Standards Institute (ANSI) standards are ambiguous and conflicting. Computerized solid modeling has been confined to idealized perfect parts. Tolerancing must be given mathematical rigor so that computer analyses can be based on all variations of a part. We made a theoretical breakthrough in applying MMP models to static assembly analysis. The original graph-based MMP algorithm uses recursive tree-traversal to determine whether a toleranced part has an associated MMP. We found that we can apply a derivative algorithm to a static assembly of parts to determine whether the assembly may be analyzed via an MMP analysis. In the software domain, we found a product that models toleranced parts. Using their software will spare us significant effort. Work is steadily progressing to extend the 1-D MMP concepts to three dimensions.

Rapid Prototyping/Rapid Manufacturing via Freeform Fabrication of Polymer-Matrix Composites

S. G. Kaufman, T. R. Guess

Sandia developed, prototyped, and demonstrated the feasibility of a novel robotic technique for rapid fabrication of composite structures. Its chief innovation is that, unlike all other available fabrication methods, it does not require a mold. Instead, the structure is built patch by patch, using a rapidly reconfigurable forming surface and a robot to position the evolving part. Both of these components are programmable, so only the control software needs to be changed to produce a new shape. Hence, it should be possible to automatically program the system to produce a shape directly from a model of it. It is therefore likely that the method will enable faster, less expensive fabrication of composites.

We demonstrated the soundness of the proposed method of forming composite structures. The structure is built up patch by patch under the control of a robot. We built and tested the patch-forming apparatus and integrated it into a robotic workcell. We fabricated composite structures of thermoplastic resin and continuous fibers (graphite and Kevlar) under automatic control.

Each patch is formed on a small, rapidly reconfigurable forming surface. To form a patch, we configure the mold to the appropriate shape, the robot positions the part relative to the patch mold, and we apply heat and pressure to cure the patch. We successfully formed both commingled and prepreg composites of thermoplastic and continuous fiber material with this apparatus. We found that very low pressures (about 3 psi) suffice to cure the material. Available forming methods require about 100 psi, probably because they do not apply the pressure hydrostatically as we do.

Publications

Refereed

Kaufman, S. G., B. Spletzer, and T. R. Guess. 1997. "Free-Form Fabrication of Polymer-Matrix Composite Structures." *Proc. 1997 IEEE Internat. Conf. on Robotics and Automation* (Albuquerque, NM, April): in press. IEEE Computer Society Press.

Low-Cost Pd-Catalyzed Metallization Technology for Rapid Prototyping of Electronic Substrates/Devices

K. S. Chen, G. D. Peterson, G. L. Cessac

Polymeric-substrate metallization is widely employed in Defense Program (DP)-related and industrial applications, e.g., radar and communication antennas/horns, and electronic interconnects such as flex circuits. This project aims at developing a low-cost, rapid-prototyping metallization process. Conventional metallization technologies are either capital-intensive or involve adhesives or too many wet-processing steps (often with poor adhesion). Metallic patterns such as electronic interconnects are conventionally fabricated

by the subtraction process in which metallized patterns are produced by chemical etching, a process known to be time-consuming, costly, and environmentally unfriendly.

For full-coverage applications we are developing a low-cost, rapid-prototyping process in which no adhesive is used, but an intermediate semimetallic layer is thermally generated. This semimetallic layer contains catalytic palladium clusters and serves as an adhesion anchor between the metal coating and polymeric substrate. Essentially, our process involves catalyzing substrate surface via thermal activation and depositing metal by electroless/electrolytic plating. The main advantage, as compared with the standard electroless/electrolytic plating technology, lies in its ability to reduce the wet-processing steps during surface catalyzation and to create good adhesion. For patterned metallization we are developing an additive process in which metal is deposited only in desired areas by selective substrate catalyzation. With our additive technology, the time-consuming, costly, environmentally unfriendly etching process is completely eliminated.

We developed two palladium-catalyst formulations: a polyamic-acid–based, high-temperature (> 3000° C) activation formulation that is suitable for substrates such as polyimide, and a polyvinyl-butyral–based, low-temperature (< 1800° C) activation formulation that works well on substrates such as epoxy-based polymers. We also developed prototypical full-coverage and additive-patterned metallization processes using polyimide, epoxy-based polymer, and IBM's biopolymer substrates (also called "green" substrate).

We successfully metallized scaled-down models of radar-and-communication antenna and pulsed-power-accelerator electrode, which we manufactured using Sandia's state-of-the-art photolithography equipment and simple electronic interconnect patterns. Using our additive process, we successfully produced metal strips (1/8-inch wide and 2-mil, or 50-microns, thick) for peel-strength measurement without etching. We obtained peel strength as high as 6.5 lbs/in. for copper-on-polyimide samples. We gained fundamental understanding of adhesion mechanisms involved in our metallization process. To help guide process optimization in electrolytic plating, we also developed a general 2-D computer code that can be employed to simulate a variety of substrate geometries. Finally, we filed a disclosure of technical advance.

Publications

Other

Chen, K. S. 1996. "Polymeric Substrate Metallization Research." Paper presented to the 1996 AIMCAL Fall Conference, Atlanta, GA, 22 October.

Chen, K. S., W. P. Morgan, and J. L. Zich. 1996. "An Environmentally Conscious Additive Plating Process for Patterned Metallization on Polymeric Substrates." Paper presented to the 1996 AIChE Annual Conference, Chicago, IL, 14 November.

Hexapod Characterization and Benchmarking

J. M. Baldwin, L. F. Bieg, C. A. Steinhaus, J. S. Korellis, V. De Sapio, T. M. Berg

Sandia examined the use of parallel mechanism technology for defect reduction in fabricating complex Defense Program (DP) components. Our initial focus is on a specific parallel mechanism called the hexapod *that has the flexibility, dexterity, and stiffness to do multiple processes (multimode manufacturing) in a single unit, which should result in a product with fewer defects and increased reliability.*

We assessed hexapod capability to produce DP products while reducing defects created during design and production. Our study reveals that the hexapod can reduce defects significantly without additional cost because of its ability to do multiple operations in a single setup. One of the largest sources of defects in production comes from having to set up components/parts again due to movement between various manufacturing processes. The high dexterity of the hexapod (8 degrees of freedom), coupled with the ability to conduct multiple operations (machining, welding, cleaning, assembly, inspection, etc.) within a single workspace, greatly reduces the number of setups required and thus improves the ability to achieve the tolerances required, thereby decreasing the probability of introducing defects. Preliminary tests on prototype machines support this conclusion and the need to continue development of this technology.

Biomedical Engineering

Predicting 3-D protein structure from amino acid sequences: compare sequences with unknown structure to those with known structure.

The ability to predict the function of proteins from primary sequence data can aid in understanding disease and designing drugs. Predicting 3-D protein structure from amino acid sequences is accomplished by comparing sequences with unknown structure to those with known structure.

New Miniature Gamma-Ray Camera for Improved Tumor Localization

R. B. James

The overall goal of this work was to develop a new miniature gamma-ray camera for use in nuclear medicine. The camera will meet widespread needs of the medical community for an improved means to image radio-pharmaceuticals in the body. In addition, this new instrument, with only slight modifications, should prove very useful in applications requiring the monitoring and verification of special nuclear materials (SNMs). Utilization of the excellent energy resolution of mercuric iodide detectors provides a unique and viable means for producing gamma-ray images with spatial resolution of 1 mm or better, which is a significant improvement over the capability of current instruments. These spatial resolutions are achieved by operating the detector array in the spectrometer mode so that only the unscattered gamma-rays are used to construct the image. The project culminated in the demonstration of the imaging capabilities of the instrument by imaging radioisotopic sources.

The primary focus of this project was testing the detector arrays, evaluating the gamma camera, and evaluating overall system performance. Specifically, we investigated (1) the performance of the HgI_2 detector array, (2) the performance of the readout electronics, (3) the characteristics of the collimator, and (4) the development of software to read out both the array and the energy spectra from each pixel. We also focused attention on adapting this new instrument to imaging and monitoring SNM sources and rigorously measuring its performance in such an application. In particular, we modified the detector array and collimator to allow the imaging of plutonium sources. After completing these tasks, we tested the system by acquiring images of radioisotopic sources.

In addition, we devised a new electronic readout system for the detector arrays based on application-specific integrated circuits (ASICs) developed specifically for this project. The ASIC readout system will allow the size of the entire gamma-ray imaging system to be reduced dramatically and enable the development of much higher-resolution imaging systems as well as gamma cameras that can be demonstrated in the field.

Publications

Refereed

Bao, X. J., T. E. Schlesinger, and R. B. James. 1995. "Electrical Properties of Mercuric Iodide." *Semiconductors for Room-Temperature Nucl. Detector Appl.* **43** (June): 111–128. Edited by R. B. James and T. E. Schlesinger. New York, NY: Academic Press.

Chang, Y. C., and R. B. James. 1997. "Theoretical Studies of Carrier Transport in Mercuric Iodide." *Phys. Rev. B,* accepted. New York, NY: American Physical Society.

James, R. B., J. M. Van Scyoc, T. E. Schlesinger, and T. S. Gilbert. 1995. "Defects and Impurities in Mercuric Iodide Processing." *Defect and Impurity Engineered Semiconductors and Devices* **378** (November): 795–895. Pittsburgh, PA: Materials Research Society.

Lund, J. C., J. M. Van Scyoc, R. B. James, D. S. McGregor, and R. W. Olsen. 1997. "Large-Volume Room-Temperature Gamma-Ray Spectrometers from CdZnTe." *Nucl. Instrum. and Meth. in Phys. Res. (A),* accepted. Amsterdam, Netherlands: North-Holland.

Lund, J. C., R. W. Olsen, J. M. Van Scyoc, and R. B. James. 1996. "The Use of Pulse-Processing Techniques to Improve the Performance of CdZnTe Gamma-Ray Spectrometers." *IEEE Trans. on Nucl. Sci.* **43** (June): 1411–1416. New York, NY: IEEE.

Medlin, D. L., R. B. James, J. M. Van Scyoc, T. S. Gilbert, T. E. Schlesinger, D. Boehme, M. Schieber, and M. Natarajan. 1997. "Reaction of Palladium Thin-Film Contacts Sputter-Deposited onto Mercuric Iodide Crystals." *Nucl. Instrum. and Meth. in Phys. Res. (A),* accepted. Amsterdam, Netherlands: North-Holland.

Schieber, M., R. B. James, J. C. Lund, R. W. Olsen, D. S. McGregor, J. M. Van Scyoc, and E. Bauser. 1996. "Material Properties and Room-Temperature Nuclear Detector Response of Wide-Bandgap Semiconductors." *Nucl. Instrum. and Meth. in Phys. Res. (A)* **A377** (June): 492–498. Amsterdam, Netherlands: North-Holland.

Van Scyoc, J. M., R. B. James, and T. S. Gilbert. 1997. "Electrical Characterization of Impurities in and Contacts on Mercuric Iodide." *Electrically-Based Microstructural Characterization,* accepted. Pittsburgh, PA: Materials Research Society.

Other

James, R. B. 1996. "Fieldable Nuclear Detectors Based on Wide-Bandgap Semiconductors." Paper presented to a Technical Seminar, Lawrence Berkeley National Laboratory, Berkley, CA, 24 April.

James, R. B. 1995. "Miniature Gamma-Ray Imaging Systems Based on Mercuric Iodide Sensors." Paper presented to a Seminar, LETI, Commissariat a L'Energie Atomique, Grenoble, France, 27 June.

James, R. B. 1996. "Quantitative Gamma-Ray Imaging for Medical Applications." Paper presented to a Seminar, University of Arizona, College of Medicine, Tucson, AZ, 1 March.

James, R. B. 1995. "Room-Temperature Radiation Detectors." Paper presented to a Laboratory Colloquium, Laboratorie de Physique et Applications des Semiconducteurs, Strasbourg, France, 30 June.

Designed Supramolecular Assemblies for Biosensors and Photoactive Devices

J. A. Shelnutt, J. Cesarano, A. J. Ricco, D. J. Hobbs

The objective of this project to develop a new class of supramolecular assemblies for applications in biosensors and biodevices. The supramolecular assemblies are based on membranes and Langmuir-Blodgett (LB) films composed of naturally occurring or synthetic lipids that contain electrically and/or photochemically active components. The LB films are deposited onto electrically active materials (metal, semiconductors). The active film components (lipoporphyrins) at the surface function as molecular-recognition sites for sensing proteins and other biomolecules, and the porphyrins and other components incorporated into the films serve as photocatalysts and vectorial electron-transport agents. We use computer-aided molecular design (CAMD) methods to tailor the structure of these film components to optimize their function. Molecular modeling is also used to predict the location, orientation, and motion of these molecular components within the films. The result is a variety of extended, self-assembled molecular structures that can be used for sensing proteins and biochemicals and as other bioelectronic devices.

The project goals for were (1) to complete the synthesis of a new lipoporphyrin that we engineered to allow self-assembly onto gold electrodes, (2) to continue modeling structure and dynamics of films, (3) to fabricate and test photoelectrochemical properties of gold-supported films for recognition of cytochrome c, and (4) to determine selectivity and sensitivity of the protein sensor. Unfortunately, we were unable to complete the synthesis of the new lipoporphyrin receptor element, in spite of the application of several synthetic procedures. The main problem came in the final step in the synthesis, in which the bromine atoms at the ends of the lipid tails attached to the polar molecular-recognition group (tin porphyrin) were to be converted to thiol groups. These thiol groups are the means by which the molecular-recognition elements are covalently self-assembled onto the gold electrodes. We still see no fundamental reason why a suitable lipoporphyrin-thiol cannot be synthesized in the future. In the absence of the lipoporphyrin-thiol, we concentrated instead on further characterizing the existing lipoporphyrin with respect to its interactions with a target guest and its photochemical properties in films. Specifically, we investigated the photoactive lipoporphyrin and other reference porphyrins in a variety of micellar and film environments to determine the mechanisms involved in interaction between the target guest molecule and lipid membranes containing the lipoporphyrin receptor site. We found that several factors influence the rates of vectorial electron transport across the lipid layer, including (1) the interfacial layer between aqueous and organic phases, (2) the positively and negatively charged and neutral lipid membrane surfaces, (3) the polarity and charge of the receptor site on the molecule, and (4) the solubilities of electron donors and acceptors. The electron-transfer rates could be understood in terms of a mechanism involving the electrostatic charge distributions on the target, receptor, and lipid, and the relative solubilities of the electron donor and acceptor components in organic and aqueous phases. This allowed us to determine (1) the optimum conditions for electron-transport to and across the lipid layer of the biosensor device, and (2) the optimum design for the molecular-recognition site for the target protein or herbicide. In further investigating the interaction between cytochrome c and a model porphyrin receptor, we also determined that a chiral receptor molecule will be necessary to obtain high selectivity and sensitivity.

Publications

Refereed

Fan, B., D. L. Fontenot, R. W. Larsen, M. C. Simpson, J. A. Shelnutt, R. Falcon, L. Martinez, S. Niu, S. Zhong, T. Niemczyk, and M. R. Ondrias. 1996. "Synthesis and Physical Characterization of Novel Heme-Based Model Systems for Photoinitiated Electron Transfer I. Complexation of RuProHis Bifunctional Peptide and Micorperoxidase-11." *Inorg. Biochem.*, in press. Washington, DC: American Chemical Society.

Fan, B., M. C. Simpson, J. A. Shelnutt, L. Martinez, R. Falcon, A. J. Pastuszyn, and M. R. Ondrias. 1996. "Synthesis and Physical Characterization of Novel Heme-Based Model Systems for Photoinitiated Electron Transfer II. Direct Ruthenation of Microperoxidase-11." *Inorg. Biochem.*, in press. Washington, DC: American Chemical Society.

Gao, F., H. Qin, M. C. Simpson, J. A. Shelnutt, D. B. Knaff, and M. R. Ondrias. 1996. "Isolation and Characterization of Vibrational Spectra of Individual Heme Active Sites in bc1 Complexes from Rhodobacter Capsulatus." *Biochem.* **34**: 12812–12819. Washington, DC: American Chemical Society.

Jensen, W., E. Unger, G. Karvounis, J. A. Shelnutt, W. Drybrodt, and R. Schweitzer-Stenner. 1993. "Conformational Properties of Nickel(II) Octaethylporphyrin in Solution 1. Resonance Raman Profiles and Temperature Dependence of Structure-Sensitive Raman Lines." *J. Phys. Chem.* **100** (33): 14184–14191. Washington, DC: American Chemical Society.

Medforth, C. J., C. M. Muzzi, K. M. Shea, K. M. Smith, R. J. Abraham, S. Jia, and J. A. Shelnutt. 1996. "NMR Studies of Nonplanar Porphyrins. Part II: Effect of Nonplanar Conformational Distortions on the Porphyrin Ring Current." *J. Chem. Soc., Perkins Trans. II*, in press. Washington, DC: American Chemical Society.

Song, X. Z., M. Miura, X. Xu, K. K. Taylor, S. A. Majumder, J. D. Hobbs, J. Cesarano, and J. A Shelnutt. 1996. "Langmuir-Blodgett Films of Steric Acid Containing Octaaceticacid-meso-tetraphenylporphyrin Tetraeicosanate Octamethylester." *Langmuir* **12** (August): 2019–2027. Washington, DC: American Chemical Society.

Other

Shelnutt, J. A. 1996. "Possible Functional Roles of Nonplanar Conformers of Tetraphyrroles in Proteins." Paper presented to the National Biophysical Society Meeting, Baltimore, MD, 17–24 February.

A New Approach to Protein Function and Structure Prediction

C. A. Phillips

The goal of this project is to assist prediction of protein function and tertiary structure from primary sequence structure. Our approach is mathematical, using multiple sequence alignment and phylogenetic (evolutionary) tree construction. We seek algorithms with provably good performance in both speed and accuracy. We seek to bring mathematically good solutions closer to biologically correct solutions through investigations of cost functions. For instances where the space of near-optimal solutions can be described, we seek improved solutions via random sampling of near-optimal solutions. This year we also sought to apply the new algorithmic techniques we developed for this project to related optimization problems in other areas.

We accomplished the following:

(1) Phylogenetic tree construction: We continued work on a new metric: l-phylogeny. If species are represented as characters (usually representing morphological characters), a l-phylogeny is a tree labeled with (potentially hypothetical) species where each character state evolves at most one time. We previously showed that in the fixed-topology version (when given a hypothesized tree topology), it is provably intractable to find a l-phylogeny for l at least 3. We developed an efficient algorithm to find a 2(l) phylogeny when a l-phylogeny exists, and an (optimal) algorithm to find a 4-phylogeny when a 3-phylogeny exists. This routine can be used as a filter to distinguish otherwise comparable trees generated by standard software.

We applied our phylogenetic-tree construction techniques to phylogenetic problems in another area. We gave complexity analyses of a new problem we defined from an application in computer virus detection/classification. For the case of directed, nontree evolution (from a single archetype), we have only nonapproximability results. We developed two efficient algorithms for the case where we require an evolutionary tree, and an efficient approximation when the history is an undirected graph, with performance bounds that match nonapproximability results we have proved.

(2) Multiple sequence alignment: We investigated the structure of alignment under our new min-error metric. New structural insights led to new heuristics methods, but no provably good algorithm. We proved a number of hardness results.

Publications

Refereed

Bonet, M., C. A. Phillips, S. Yooseph, and T. J. Warnow. 1996. "Constructing Evolutionary Trees in the Presence of Polymorphic Characters." Paper presented to the 28th Annual ACM Symposium on the Theory of Computing, New York, NY, 22–24 May. New York, NY: ACM Press.

Goldberg, L. A., P. W. Goldberg, C. A. Phillips, and G. B. Sorkin. 1996. "Constructing Computer Virus Phylogenies." *Proc. Combinatorial Pattern Matching Conf.* **1075** (Berlin, Germany, 10–12 June): 253–270. Berlin, Germany: Springer-Verlag.

Goldberg, L. A., P. W. Goldberg, C. A. Phillips, E. Sweedyk, and T. J. Warnow. 1996. "Minimizing Phylogenetic Number to Find Good Evolutionary Trees." *Discrete Appl. Math.*, in press. Amsterdam, Netherlands: Elsevier Science.

Phillips, C. A., and T. J. Warnow. 1996. "The Asymmetric Median Tree—A New Model for Building Consensus Trees." Paper presented to the Combinatorial Pattern Matching Conference, Berlin, Germany, 10–12 June. Amsterdam, Netherlands: Elsevier Science.

Improved Treatment of Prostate Neoplastic Disease

W. P. Ballard, L. E. Larsen, J. H. Stofleth, J. D. Weiss, J. M. Arellano

This project is designed to test in vitro *an improved method of treatment for benign prostatic hyperplasia (BPH). The goal is to retain normal anatomy to the greatest extent possible by selective injury to hyperplastic cellular elements. This distinguishes the proposed method from all others in use today as they indiscriminately destroy both normal and diseased tissue. The use of pulsed microwave power is central to the desired differential cellular injury. Theory and results in another target tissue indicate that the controlling factor is absorbed energy/pulse. We designed and tested a novel leaky-wave microwave applicator for clinical use of the method.*

We completed repairs on the klystron transmitter, began execution of the experimental matrix, continued morphometrics with prostate explants, and fabricated and tested a novel transurethral applicator. We continued testing the klystron to 20–25 kV at 100-ms pulsewidth. Design improvements to the floating deck modulator resulted in 35 kW of radio-frequency (RF) power at 19-kV beam voltage and 100-ms pulsewidth. Improvements in the exposure system improved the power coupling into the samples to > 99%.

Analysis of the critical-angle fiber-optic sensor for the 1-D case suggested a detectable change in reflected light at the critical angle for the temperature and pressure effects we expected to have *in situ*.

Because of the problems with tissue delivery, we shifted emphasis to the transurethral applicator and morphometrics. We built and tested six transurethral applicator designs, and tested six leaky wave designs in a tissue-equivalent phantom. We estimated uniformity of heating patterns by scanning infrared radiometry. We achieved good results by optimization of pitch and slot-to-land ratio, and filed a technical advance based on this work.

The morphometric portion of the project expanded the histochemistry to include cytoskeleton (intermediate fibrils), prostate-specific alkaline phosphate, prostate-specific antibody (PSA), blood factor VIII, actin, and trichrome stains in addition to hematoxylin and eosin (H&E). We began to verify the accuracy of feature extraction based on the strategy developed in the first year. The classification step will classify microscope fields into fibroadenoma, fibromuscular, fibromyoadenoma, occult carcinoma, and normal groups on the basis of the features extracted.

Development of Sensory Feedback Systems for Minimally Invasive Surgery Applications

D. R. Foral, A. K. Morimoto, J. L. Novak

Minimally invasive (MI) tools and procedures are being used to reduce trauma to patients compared with that caused by open surgery and consequently to reduce recovery time and hospital stays. The limitations of MI procedures lie within the requirement to use characteristically long, slender tools that are operated at distances of 1–2 feet from the tool tip. These tools are inserted into the body cavity through an orifice or small incision and essentially remotize the surgeon or physician—limiting and distorting the sense of touch, tissue characterization, and visual acuity. Although the benefits to patients justify the means, surgeons continue to weigh benefits against the limitations in feedback during MI procedures along with the associated increase in difficulty and risk.

The goal of this project is to provide feedback systems that will allow physicians and surgeons to regain lost tool/tissue force information, or in the case of blood vessel detection, to augment senses that did not previously exist in order to improve the efficacy and safety of MI procedures performed in laparoscopy, endoscopy, and arthroscopy. We will integrate both the force/torque sensor and the blood vessel detector into existing laparoscopic hardware for experimental use. The force/torque sensor provides feedback on tool/tissue forces of interaction; the blood vessel detector will be used to detect blood vessels larger than 1 mm in diameter. Having these feedback systems integrated into existing MI tools will benefit physicians and surgeons and is a necessary precursor to robotic surgical systems for the future.

We successfully integrated a force/torque sensor into an actual laparoscopic tool. We used this prototype unit to help quantify the range of forces that can be expected and as an input device for the development of the force feedback system. In addition, we fabricated a development tool to use to characterize different tissue types (i.e., stomach, intestine, liver, etc.). We are using the information obtained from these tissue characterization studies to specify the design parameters for a custom force transducer. We purchased hardware for the implementation of a video-based force feedback system and accomplished proof-of-concept testing. We wrote prototype user-interface software and are using input from surgeons to modify the software.

The development of the blood vessel detection system progressed further than expected this year. We fabricated a working prototype unit and used it in an actual surgical environment to obtain pertinent data for further modifications. Initial indications are that the sensor will be able to differentiate between blood vessels and the surrounding tissues.

Personal Status Monitor

J. T. Love, J. B. Boyce, K. Eras, C. J. Helms, G. R. Laguna, S. Warren

The primary goal for this project is to identify and understand the scientific and medical issues associated with development of a personal status monitor (PSM) for monitoring ambulatory patient vital signs—blood pressure, heart rate, respiration, core body temperature, and blood oxygen saturation. Team members isolated the important engineering issues associated with the use of visible and near-infrared (NIR) light sensors for gathering biological information. The goals for FY96 were to identify and resolve the engineering issues for the measurements and techniques to collect the vital signs information with a focus on oximetry and blood pressure techniques. We invested significant effort in (1) design of the associated sensor hardware, (2) optimal detection schemes for optically acquiring these biological data, and (3) appropriate signal processing approaches for minimizing the effects of motion artifacts.

Ambulatory monitoring of vital signs could significantly impact the cost and effectiveness of health care by minimizing duration of patient hospitalization and providing independent living for elderly patients. Automated battlefield monitoring of vital signs could save many lives by (1) reducing the time required to check widely dispersed field personnel, (2) decreasing the risk to field medical personnel through incorporation of a telemetric link, and (3) determining which soldiers should be treated first based on the seriousness of their injuries.

Work in FY96 concentrated on the development of hardware platforms for gathering vital signs information and on signal processing approaches for extracting clean plethysmographic data from noisy photodetector signals. Experiments identified the following locations as promising sensor sites: the

finger, wrist, ear, and temporal branch of the external carotid artery. We placed much effort on the design of hardware amplifiers and circuitry for collection of these biological signals using light sources and appropriate photo-transducers at these physical locations.

Fourier analysis of these plethysmographic data yielded promising results for the extraction of pulse rate in the presence of motion. We implemented this technique on the distress monitor, proving useful for the continuous calculation of pulse rate in situations where the signal is weak or has low temporal stability. However, for reliable calculation of blood oxygen saturation, the processed signals must be more faithful representations of the actual arterial signals. We concluded that a zero-phase, forward-reverse bandpass filter provided adequate filtering over the spectral region of interest (0.5 to 12 Hz) without phase distortion. Using the filtered signals, a weighted-moving-average scheme had the best trade-offs for speed and effectiveness. We implemented this real-time technique in Labview to calculate blood oxygen saturation. We used time-frequency analysis to determine motion spectral characteristics as a function of time. Using this knowledge, we devised a method for motion artifact rejection based on cross-correlation of the reflectance signals from the red and NIR light sources. These cross-correlation data provide Fourier coefficients that are used to reconstruct approximations to the actual arterial signals. We need to do further work on the phase relationships of these harmonics to differentiate between meaningful and artifactual biometric data.

We recommend pursuit of funding to continue development of the PSM effort to support battlefield applications. This sensor platform would support the development of a radar platform currently under development at Sandia.

Development of a One-Step ELISA Using Microencapsulation Immunoreagents

C. C. Henderson, K. Wally, J. S. Schoeniger

Microencapsulation of biological reagents is potentially a useful way of packaging small quantities of immunoreagents for use in robust, fieldable bioassays such as enzyme-linked immunosorbant assays (ELISA), single-use microsensors for biological or chemical reagents, or advanced laboratory analytical systems. For many of these applications, exact amounts of protein or antibody could be delivered to the assay or sensor surface by rupture of the polymeric microcapsules at predetermined times, eliminating the need for a trained technician to add the required reagent manually. In the first year of this project, we demonstrated microencapsulation of protein molecules in aqueous solution using an "in-solution drying" method. We dissolved the biological molecule to be encapsulated in water, which was then dispersed into a benzene solution of dissolved polystyrene by rapid shear mixing. We then dispersed the resulting emulsion into an aqueous colloid suspension to form a water/oil/water double emulsion. Slow evaporation of the benzene formed the desired polymer shell around the internal water droplet containing the protein. This method did produce encapsulated proteins but with a significant amount of debris (broken capsules and polymer film) in addition to mostly nonspherical capsules.

Characterization of the microcapsules and improvements in the process were the major accomplishments of this year's research. To determine the location of the encapsulated protein, e.g., amount in the nucleus, trapped in the walls, or adsorbed on the walls, we encapsulated horse-radish peroxidase (HRP) with a fluorescent label (fluorene isothiocyanate [FITC]) using polystyrene to produce irregularly shaped capsules (ten to several hundred microns in diameter) that were imaged with a fluorescent microscope. The micrographs revealed that the capsules were mostly multinuclear with several smaller capsules combined into one larger capsule. Furthermore, a considerable amount of the fluorescence originated from the walls of the capsules, indicating that a significant amount of the HRP-FITC was trapped in the semipermeable walls of the polystyrene capsules. This characterization showed that process improvements were necessary to produce smaller, rounder, mononuclear capsules with less debris and protein trapped in the walls. Variations in the shear-mixing speed, volume ratios, and emulsification process led to significant improvements in the encapsulation process. This improved method produces smaller (about 1–10 microns) round microcapsules that appear optically to be mononuclear. We expanded the types of polymeric wall materials used to include both hydrophobic (polystyrene) and hydrophilic (polymethylmethacrylate) polymers. We found the stability of the microencapsulated proteins in aqueous solution to be relatively low, with apparent leakage of the protein into the aqueous phase. Further research is necessary to improve the capsule stability to the level necessary for bioassay or sensor use, as well as a complete investigation of the rupture and protein release characteristics. Recent advances reported elsewhere in the literature included the ability to pattern well-defined, sealed reservoirs for biological reagents, which may be a superior option for the inclusion of immunoreagents in a self-developing bioassay. Although this project in microencapsulation of immunoreagents for self-developing ELISA has ended, the capability to microencapsulate reagents is now established at Sandia and may play a future role in advanced sensors, latent catalysts, tamper-indicating devices, or related applications.

Decision Trees and Integrated Features for Computer-Aided Mammographic Screening

W. P. Kegelmeyer, Jr.

Breast cancer is a serious problem with wide impact on mortality and health-care costs. It can be aided by a computer-based visual inspection system that will distinguish between normal mammograms and those that require the closer scrutiny of a radiologist. Sandia developed a biomedical computer-vision system for the detection of the three major cancer signs in screening mammograms by extending the dense feature map (DFM) and probability image methodology to the detection of spiculated lesions, microcalcifications, and masses. This effort involved the continued acquisition and truthing of mammogram data, the investigation and refinement of pertinent image features, and large-scale statistical test simulations. We also refined a "combination of multiple classifiers" approach, useful both for improving classifier performance and for serving as an algorithmic framework to support feature space integration efforts.

We acquired a data base of 114 four-view cases from the Bowman-Gray School of Medicine (BGSM) and distributed half/half across normal and mass-containing cases. This new set of images provided a considerably wider range of both masses and normals than did our prior data base. We developed an algorithm to register those mammograms truthed by a radiologist with the originals, which allowed us to create binary truth images for the 129 images containing lesions.

We placed the combination of multiple classifiers (CMC) method on a firm theoretical footing through further statistical analysis and study of its application to a variety of datasets. As a result, we sharpened CMC performance predictions and were able to show the superior efficacy of this approach, as compared to related and competing methods.

We made a number of improvements in the mass detection algorithm in the areas of preprocessing, edge detection, and Hough accumulator filtering, which helped reduce both inter- and intra-image performance variations. Two areas that brought significant improvement were the design and incorporation of an algorithm for suppressing linear structure such as blood vessels, and incorporation of an edge classification algorithm due to Venkatesh and Rosin.

We applied the mass detection algorithm to the BGSM-Sandia data base and analyzed the algorithm performance at each significant step in the processing.

Mass detection presents three areas of difficulty, as masses vary widely in scale, in brightness and texture contrast with surrounding tissue, and with size. We addressed the scale issue through the use of the Hough transform. We lessened the impact of variations in contrast by preprocessing the images to flatten the contrast over the breast region. Shape continues to be an issue, with our performance to date directly proportional to how round the lesion is, as might be expected, given our use of the circular Hough transform parameterization.

Publications

Refereed

Woods, K., and W. P. Kegelmeyer, Jr. 1996. "Local Accuracy Methods for Combination of Multiple Classifiers." *Proc. IEEE Comp. Soc. Conf. on Comp. Vision and Pattern Recog.* (San Francisco, CA, 16–20 June).

Other

Bowyer, K., W. P. Kegelmeyer, Jr., D. Kopans, and R. Moore. 1996. "The MGH-USF-Sandia Digital Mammography Research Database." Paper presented to the 3rd International Workshop on Digital Mammography, Chicago, Illinois, 9–12 June.

Groshong, B., and W. P. Kegelmeyer, Jr. 1996. "Detecting Circumscribed Lesions Using the Hough Transform." *Proc. 3rd Internat. Workshop on Digital Mammography* **2710**: 59–70.

Groshong, B., and W. P. Kegelmeyer, Jr. 1996. "Evaluation of a Hough Transform Method for Circumscribed Lesion Detection." Paper presented to the 3rd International Workshop on Digital Mammography, Chicago, IL, 9–12 June.

Energy and Environmental Science and Technology

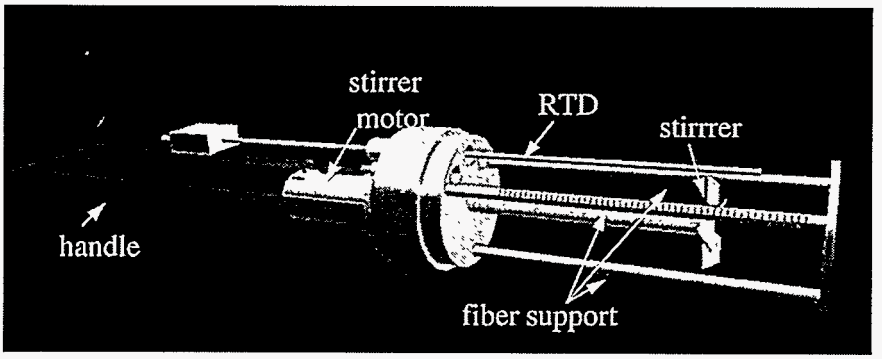

Current methods for determining concentrations of chlorinated hydrocarbons in aqueous matrices are both expensive and time-consuming. A fiber-optic sensor (RTD) based on evanescent-wave spectroscopy was designed that can remain *in situ* for extended periods of time without maintenance or calibration. Also shown is the sensor mount.

Delineating DNAPLs: A Probabilistic Approach for Locating DNAPLs in Subsurface Sediments

R. G. Cox, E. K. Webb

Roughly half of the U.S. Superfund sites, and most DOE contamination sites, have significant dense nonaqueous phase liquid (DNAPL) contamination, threatening groundwater quality. DNAPLs include common bulk industrial solvents such as engine degreasers. Because it is difficult to remediate subsurface DNAPL contamination, it is important to characterize DNAPL plumes accurately. But it also is important to remediate sites as quickly and effectively as possible. These two goals compete and are difficult to balance with ad hoc *methodologies, often resulting in costly delays and greater public health risks.*

We developed a multidisciplinary methodology to predict probable DNAPL subsurface migrations and, using these predictions, to provide the cheapest/fastest characterization strategy (location and stopping rule) to locate DNAPLs. Models include simulation of the subsurface geology, as well as a percolation model to predict migration patterns given a simulated geology. We calibrated these percolation models against laboratory experiments to validate the flow dynamics through saturated heterogeneous soils. We used the mathematical models in a Monte Carlo analysis to provide a probabilistic DNAPL migration pattern. This, in turn, led to a decision tree to estimate which characterization scheme is cheapest and fastest in terms of both characterization and ultimate remediation costs.

We made the following accomplishments in FY96:

(1) We implemented geologic and hydrologic codes on the Environmental Protection Agency (EPA) supercomputers. We developed decision trees based on the resulting Monte Carlo simulations. The methodology resulted in 40% improvement in characterization and remediation cost as compared to a simple heuristic approach.

(2) We completed the laboratory models for 2-D DNAPL transport and compared them against the computational DNAPL percolation models developed during the DNAPL study. The computational models reproduced the salient features seen in the laboratory test cases, and we feel confident the models have achieved world-class performance in predicting DNAPL migration through heterogeneous subsurface features.

(3) We validated the physical models at two DOE field sites—Portsmouth and Paducah. Both have significant DNAPL contamination. We coupled the geologic models with the percolation models to predict DNAPL location. We had already performed site characterization at the two sites, so we were calibrating performance of the geology and hydrology models against actual field measurements. Based on the results of the field tests, we feel confident that DNAPL migration can be reasonably predicted under field conditions.

Publications

Refereed

Borchers, B. S., S. H. Conrad, R. G. Cox, R. J. Glass, Jr., and E. K. Webb. 1995. "A Simulation and Decision Analysis Approach to Locating DNAPLs in Subsurface Sediments." Paper presented to the EPA Conference on Next-Generation Environmental Models Computational Methods (NGEMCOM), Bay City, MI, 7–9 August.

Glass, R. J., Jr., and L. X. Yarrington. 1996. "Simulation of Gravity-Driven Fingering in Porous Media Using a Modified Invasion Percolation Model." *Geoderma*, special issue on fingered flow **70** (2–4): 231–252. Amsterdam, Netherlands: Elsevier Science. SAND95-2283J.

Glass, R. J., Jr., and M. J. Nickoll. 1996. "Physics of Gravity-Driven Fingering of Immiscible Fluids Within Porous Media: An Overview of Current Understanding and Selected Complicating Factors." *Geoderma*, special issue on fingered flow **70** (2–4): 133–163. Amsterdam, Netherlands: Elsevier Science. SAND95-1357J.

Glass, R. J., Jr., S. H. Conrad, and E. K. Webb. 1995. "An Upscaled Buoyant Invasion Percolation Model for Use in Approaches to Delineate Subsurface DNAPL Location." *Proc. AIChE/ASME National Heat Transfer Conf., Special Session on Multiphase Flow and Transport in Environmental Problems* (Portland, OR, 5–9 August): 23–29. SAND95-1007C.

Webb, E. K. 1994. "BCS: A Program to Simulate the Surface Topography of Braided Channel Networks." *Computers and Geosciences*, in review.

Webb, E. K. 1994. "Simulating the Three-Dimensional Distribution of Sediment Units in Braided Stream Deposits." *J. Sedimentary Research B* **64** (2) (12 February): 219–231.

Webb, E. K. 1996. "Simulation of Braided Channel Topology and Topography." *Water Resources Research* **31** (10) (October): 2603–2611. Washington, DC: AGU.

Other

Conrad, S. H., R. J. Glass, Jr., W. Peplinski, L. X. Yarrington, and E. K Webb. 1995. "Nonaqueous Phase Liquid Movement Within Heterogeneous Porous Media: Physical Experiment and Numerical Simulation." Paper presented to the American Geophysical Union Fall Meeting, San Francisco, CA, 11–15 December.

Development of a Portable X-Ray and Gamma-Ray Detector Instrument and Imaging Camera for Use in Radioactive and Hazardous Material Management

R. B. James, D. A. McArthur, A. J. Antolak

The overall goal of this project was to develop prototype x-ray fluorescence (XRF) instruments using mercuric iodide (HgI_2) crystals for environmental monitoring and remediation applications. HgI_2 sensors fabricated at Sandia now have energy resolutions that are much better than gas-filled proportional detectors and scintillator-photomultiplier–based systems, and even approach the performance of laboratory-sized cryogenically cooled silicon detectors. We integrated these HgI_2 sensors with miniaturized electronics, leading to the development of a new portable field instrument for real-time monitoring of contaminant concentrations in soils, paints, and a variety of effluents. The instrument is lightweight, easy to operate, powered by batteries, requires no maintenance for months, and is capable of remote unattended data collection. It can quickly and nonintrusively quantify contaminants ranging from sulfur through uranium. We also built a portable gamma-ray camera that can be used to produce images of radioactive materials sealed in containers or scattered in the environment.

In FY96, we developed a new gamma-ray camera, based on a monolithic HgI_2 detector array, for real-time imaging of radionuclides. The field-portable imaging system provides a powerful tool for monitoring gamma-emitting radionuclides stored in containers or scattered in the environment. The gamma-ray camera is capable of detecting and locating the radiation and determining the particular radioisotopes responsible for the radiation. This work was motivated by the current needs for such an instrument in environmental monitoring and surveillance of nuclear materials and waste, and the lack of suitable room-temperature sensor technology suitable to produce a compact detector array. The technological approach involved coupling each HgI_2 pixel in the detector array with miniaturized hybrid pulse-processing electronics. We used a "pin-hole" collimator to form an image of the gamma-rays on the detector plane. We built a laboratory prototype of the instrument, and an effort is currently under way to miniaturize the system even further using application-specific integrated circuits (ASICs) to reduce the size of the readout electronics. We completed a variety of tests with the gamma-ray camera to determine performance specifications for several radionuclides.

Publications

Refereed

Chang, Y. C., and R. B. James. 1996. "Theoretical Studies of Carrier Transport in Mercuric HgI_2." *Phys. Rev. B* **53** (1 June): 14200–14211. Woodbury, NY: American Institute of Physics.

Chen, K. T., L. Salary, A. Burger, E. Soria, A. Antolak, and R. B. James. 1996. "Chemical Impurity Distribution of Zone-Refined Mercuric Iodide by ICP-AES and TSC." *Nucl. Instru. and Meth. A* **380** (1 October): 53–57. Amsterdam, Netherlands: North-Holland.

Cross, E. S., G. Buffleben, E. Soria, R. B. James, R. Natarajan, and V. Gerrish. 1996. "The Effect of Elemental and Hydrocarbon Impurities on Mercuric Iodide Gamma-Ray Detector Performance." *Nucl. Instru. and Meth. A* **380** (1 October): 23–25. Amsterdam, Netherlands: North-Holland.

Goorsky, M. S., H. Yoon, M. Schieber. R. B. James, D. S. McGregor, and M. Natarajan. 1996. "X-Ray Diffuse Scattering for Evaluation of Wide-Bandgap Semiconductor." *Nucl. Instru. and Meth. A* **380** (1 October): 6–9. Amsterdam, Netherlands: North-Holland.

James, R. B., M. Roth, H. Yao, M. Devries, and M. Goorsky. 1995. "Bulk and Surface Stoichiometry of Vapor-Grown Mercuric Iodide Devices." *J. Crystal Growth* **146** (January): 15–22. Amsterdam, Netherlands: North-Holland.

Medlin, D. L., J. M. Van Scyoc, T. S. Gilbert, T. E. Schlesinger, D. Boehme, M. Schieber, M. Natarajan, and R. B. James. 1996. "Formation of PdHg by Reaction of Palladium Thin-Film Contacts Deposited onto Mercuric Iodide (a-HgI_2) Radiation Detector Crystals." *Nucl. Instru. and Meth. A* **380** (1 October): 241–244. Amsterdam, Netherlands: North-Holland.

Olsen, R. W., R. B. James, A. J. Antolak, and C. Wang. 1994. "Development of High-Resolution Cadmium Zinc Telluride and Mercuric Iodide Detectors for Use in Nonproliferation." *Proc. 35th Annual Mtg. on Instru. for Nucl. Mater. Mgmt.* **23** (June): 565–589. Northbrook, IL: Institute of Nuclear Materials Management.

Schieber, M., J. C. Lund, R. W. Olsen, D. S. McGregor, J. M. Van Scyoc, R. B. James, E. Soria, and E. Bauser. 1996. "Material Properties and Room-Temperature Nuclear Detector Response of Wide-Bandgap Semiconductors." *Nucl. Instru. and Meth. A* **377** (1 August): 492–495. Amsterdam, Netherlands: North-Holland.

Schieber, M., R. B. James, J. C. Lund, D. S. McGregor, T. S. Gilbert, J. M. Van Scyoc, R. W. Olsen, A. E. Pontau, T. E. Schlesinger, and J. Toney. 1996. "State of the Art of Wide-Bandgap Semiconductor Nuclear Radiation Detectors." *Il Nuovo Cimento A*, Series 2 **109A**: 1253–1260. Amsterdam, Netherlands: North-Holland.

Sim, H. K., Y. C. Chang, and R. B. James. 1994. "Phonon Dispersion in Red Mercuric Iodide." *Phys. Rev. B* **49** (15 February): 4559–4564. Woodbury, NY: American Institute of Physics.

Van Scyoc, J. M., R. B. James, A. Burger, E. Soria, C. Perrino, E. Cross, M. Schieber, and M. Natarajan. 1996. "Electrodrift Purification of Mercuric Iodide for Improved Gamma-Ray Detector Performance." *Nucl. Instru. and Meth. A* **380** (1 October): 36–41. Amsterdam, Netherlands: North-Holland.

Van Scyoc, J. M., R. B. James, T. E. Schlesinger, and T. S. Gilbert. 1995. "Defects and Impurities in Mercuric Iodide Processing." *Defect- and Impurity-Engineered Semiconductors and Devices, MRS Symp. Proc.* **378**: 795–801. Pittsburgh, PA: Materials Research Society.

Van Scyoc, J. M., R. B. James, T. E. Schlesinger, T. S. Gilbert, and M. Schieber. 1996. "Characterization of Silver Impurities in Mercuric Iodide and Their Relationship to Gamma-Ray Detector Performance." *J. Crystal Growth* **166** (2 September): 384–389. Amsterdam, Netherlands: North-Holland.

Van Scyoc, J. M., T. E. Schlesinger, H. Yao, R. B. James, M. Natarajan, X. J. Bao, J. S. Iwanczyk, B. E. Patt, and L. van den Berg. 1994. "Process Monitoring for Fabrication of Mercuric Iodide Room-Temperature Radiation Detectors." *Diagnostic Techniques for Semiconductor Materials Processing, MRS Symp. Proc.* **324**: 65–71. Pittsburgh, PA: Materials Research Society.

Van Scyoc, J. M., T. S. Gilbert, R. B. James, and T. E. Schlesinger. 1996. "Electrical Characterization of Impurities in and Contacts on Mercuric Iodide." *Electrically-Based Microstructural Characterization, MRS Symp. Proc.* **411**: 203–208. Pittsburgh, PA: Materials Research Society.

Van Scyoc, J. M., T. S. Gilbert, T. E. Schlesinger, and R. B. James. 1994. "Photoionization Investigation of Defect Traps in Mercuric Iodide Room-Temperature X-Ray Spectrometers." *Gamma-Ray Detector Physics and Applications, SPIE Proc.* **2305** (July): 174–182. Bellingham, WA: SPIE.

Yao, H., L. A. Lim, R. B. James, M. Schieber, and M. Natarajan. 1996. "Surface Aging of HgI_2 Crystals Studied by VASE and AFM." *Nucl. Instru. and Meth. A* **380** (1 October): 26–29. Amsterdam, Netherlands: North-Holland.

Other

Bao, X. J., T. E. Schlesinger, and R. B. James. 1995. "Electrical Properties of Mercuric Iodide." Chapter 4 in *Semiconductors for Room-Temperature Nuclear Detector Applications* **43** (Semiconductors and Semimetals): 111–165. San Diego, CA: Academic Press.

Bao, X. J., T. E. Schlesinger, and R. B. James. 1995. "Optical Properties of Red Mercuric Iodide." Chapter 5 in *Semiconductors for Room-Temperature Nuclear Detector Applications* **43** (Semiconductors and Semimetals): 169–216. San Diego, CA: Academic Press.

Brunett, B. A., D. C. David, T. S. Gilbert, T. E. Schlesinger, J. M. Van Scyoc, and R. B. James. 1995. "Two-Dimensional Photocurrent Mapping of Mercuric Iodide Detectors and Crystals." Paper presented to the 9th International Conference on Room-Temperature Semiconductor X- and Gamma-Ray Detectors, Associated Electronics, and Applications, Grenoble, France, 19 September.

James, R. B. 1996. "Integration of Room-Temperature Radiation Sensors with a Mobile Robot for Characterization of Nuclear Wastes." Presentation to Center 6300, Sandia National Laboratories, Albuquerque, NM, January.

James, R. B. 1995. "Miniature Gamma-Ray Imaging Systems Based on Mercuric Iodide Sensors." Paper presented to the Seminar, LETI, Commissariat a L'Energie Atomique, Grenoble, France, June.

James, R. B. 1995. "New Method for Purifying Detector-Grade Mercuric Iodide Crystals." Paper presented to Sandia Seminar, Livermore, CA, November.

James, R. B. 1996. "Radiation Monitoring of High-Level Storage Waste Tanks." Presentation to staff from DOE/HQ Environmental Monitoring Office, Albuquerque, NM, November.

James, R. B. 1996. "Room-Temperature Nuclear Detectors for Environmental Monitoring." Paper presented to Seminar for Intelligent Systems and Robotics Department, Sandia National Laboratories, Albuquerque, NM, February.

James, R. B. 1995. "Room-Temperature Radiation Detectors." Laboratory Colloquium, Laboratoire de Physique et Applications des Semiconducteurs, Centre National de la Recherche Scientifique, Strasbourg, France, June.

James, R. B., and T. E. Schlesinger. 1995. "Introduction and Overview." Chapter 1 in *Semiconductors for Room-Temperature Nuclear Detector Applications* **43** (Semiconductors and Semimetals): 1–20. San Diego, CA: Academic Press.

James, R. B., M. Schieber, and T. E. Schlesinger. 1995. "Summary and Remaining Issues for Room-Temperature Radiation Spectrometers." Chapter 15 in *Semiconductors for Room-Temperature Nuclear Detector Applications* **43** (Semiconductors and Semimetals): 561–581. San Diego, CA: Academic Press.

Schieber, M., M. Roth, H. Yao, M. DeVries, M. S. Goorsky, and R. B. James. 1994. "Stoichiometry of Vapor-Grown Mercuric Iodide Devices." Paper presented to the International Conference on Crystal Growth and Epitaxy, July.

Van Scyoc, J. M., R. B. James, and T. E. Schlesinger. 1995. "Mobile Impurity-Related Defects in Mercuric Iodide." Paper presented to the American Physical Society March Meeting, San Jose, CA, 22 March.

Yao, H., B. Johs, and R. B. James. 1994. "Optical Anisotropic Dielectric Response of HgI_2." Paper presented to the American Physical Society Meeting, Pittsburgh, PA, March.

Automated Detection and Reporting of Volatile Organic Compounds (VOCs) in Complex Environments

P. J. Hargis, G. C. Frye, A. J. Ricco, S. J. Martin, J. W. Bartholomew, G. C. Tisone, G. C. Osbourn

This project provides a multidisciplinary approach to the problem of automated detection and reporting of volatile organic compounds (VOCs) in complex environments. The project developed and optimized two distinct sensing mechanisms: ultraviolet (UV) fluorescence and surface acoustic-wave (SAW) sensor arrays. Both of these techniques exhibited the ability to detect VOCs in isolation. We developed pattern-recognition (PR) software to handle VOC detection, identification, and quantification in the presence of other complex gas mixtures. The project also investigated software techniques for robust and intelligent monitoring/reporting using multiple sensor inputs.

We expanded the range of materials examined for VOC sensing using SAW arrays to include several custom polymers as well as surface-attached dendrimer films. We also addressed the omnipresent species water and CO_2, which can act as interferants and/or introduce errors in the determination of concentrations of VOCs. We used a CO_2-selective polyimide developed at Sandia and the hydrophilic commercial polymer poly(N-vinylpyrrolidone) to target these two species. We also expanded the range of analytes to include the VOCs kerosene, tributylphosphate (hydraulic fluid), and methyl isobutyl ketone.

We measured UV absorption spectra of the VOCs tributylphosphate and dibutylphosphate to determine the feasibility of UV detection. Both species showed absorption features that can be used for detection in pulsed molecular beam expansions.

We previously carried out optimization studies, using our visually empirical visually empirical region of influence (VERI) PR algorithm, for selecting sensor combinations in an SAW array that best distinguish volatile organics. These computations directly identify which choices of sensors provide the best chemical recognition, so long as the sensor sensitivities do not change with time. We carried out new optimization studies that include model aging effects in the sensor sensitivities. The results allow an improvement in array selection, as they identify SAW arrays that will best maintain the chemical recognition performance in the field. The results compared SAW array sizes from 3 sensors to 13 sensors, and showed that the largest arrays actually exhibit much more rapid performance degradation with sensor aging than intermediate array sizes. The results further emphasize the crucial role of these types of analyses in designing practical array systems for field operation.

We also developed three techniques for quantifying the concentrations of analytes in mixtures that can be used for sensor responses that are nonlinear and nonadditive as a function of mixture component concentrations. The methods directly use training data for the mixture responses to estimate each component concentration and require no particular mathematical form for the mixture responses. We compared these methods against each other for a model set of three-component mixtures, obtained by adding nonlinear experimental sensor responses for the individual mixture components. We found that all give errors that can be made small (less than 1% standard deviation over the entire range of the three-component concentrations) if sufficiently large mixture training data sets are created.

Compact Environmental Sensing Spectroscopy Using Advanced Semiconductor Light-Emitting Diodes and Lasers

I. J. Fritz, A. J. Howard, R. L. Dawson, J. F. Klem, B. R. Stallard, O. Blum

Sandia improved the operation of their broadband light-emitting diodes (LEDs) for environmental sensing in the near-infrared (NIR) by optimizing quantum-well designs to obtain flatter spectral outputs. We developed a novel graded-index separate confinement heterostructure emitter, employing a digital alloy scheme, to operate as a broadband, superluminescent LED at NIR wavelengths. To demonstrate the use of modulation spectroscopy for spectroscopic chemical sensing, we used a commercial distributed feedback laser to detect water in air at a sub-part-per-billion detection limit. We used advanced statistical techniques along with data from a new NIR spectral data base to determine the natural classes found in molecular spectra and the separability of those classes based on spectroscopic measurements in various spectral bands.

We are developing technology to enable field-based detection of environmentally important chemical species, using miniaturized, low-power spectroscopic equipment, for applications such as process and effluent monitoring of volatile organic compounds (VOCs). Sensing is to be based on absorption at 1.3–1.8 mm from overtones of C-H and N-H stretch resonances.

We achieved improved operation of our broadband LED sources. These LEDs are grown by molecular-beam epitaxy using specially developed digital-alloy techniques to obtain the variety of bandgaps and refractive indices needed for effective broadband operation. Our first design employs three quantum wells with different bandgaps, with a broadband output derived from simultaneous

emission from the three wells. The relative intensities of the three emissions depend on the details of the quantum-well structure, especially on the thicknesses of the barrier layers between the wells. We systematically investigated this barrier-width dependence to improve the flatness of the output response and succeeded in obtaining operation with less than 50% output variation over a 420-nm–wavelength range (1500–1920 nm).

By extending our digital-alloy techniques we developed a novel approach to fabricate a device operating as a broadband, superluminescent LED at NIR wavelengths near 1700 nm. This device uses graded-refractive-index layers from lattice-matched digital alloys to enhance carrier capture and optical confinement, along with strained-layer digital alloys for the multi-quantum-well recombination region having the desired optical bandgap. The highly efficient capture of injected carriers leads to strong energy-band filling effects, which results in optical emission from higher-lying quantum-well transitions in addition to the ground-state emission. We obtained strong emission over the 1450–1850-nm-wavelength range.

We applied advanced statistical techniques such as principal component scatter plots, linear discriminant analysis, etc., to explore class separability among alkanes, alcohols, and ketone/aldehydes. The data base for this study was the recently published Buback-Vogele NIR library. We find that there is sufficient class separability in the NIR region to ensure that organic compounds of one class can be determined in the presence of interference from other classes.

The novel solid-state NIR sources we developed have many advantages over incandescent filament sources typically used in spectroscopic systems and have potential applications in customized miniature spectrometers for a variety of environmental-sensing applications.

Publications

Refereed

Stallard, B. R. 1996. "Near-IR Versus Mid-IR, Separability of Three Classes of Organic Compounds." *Appl. Spectroscopy*, in press. Frederick, MD: Society for Applied Spectroscopy.

Stallard, B. R., M. J. Garcia, and S. Kaushik. 1996. "Near-IR Reflectance Spectroscopy for the Determination of Motor Oil Contamination in Sandy Loam." *Appl. Spectroscopy* **50**: 334. Frederick, MD: Society for Applied Spectroscopy.

Wang, L., S. Y. Lin, M. J. Hafich, and I. J. Fritz. 1996. "Time-Resolved Study of Carrier Recombination Dynamics of 1.3–1.8mm Broadband Light-Emitting Diode Structures." *J. Appl. Phys.* **80**: 6965. Argonne, IL: AIP.

The Development of Ion Mobility Spectroscopy to Analyze Explosives at Environmental Restoration Sites

P. J. Rodacy, S. E. Klassen, P. K. Leslie

Literally hundreds of sites within Sandia, DoD, and DOE facilities are contaminated by explosive materials. At parts-per-million (ppm) levels, most of these explosives are very toxic. Currently, an efficient, low-cost method to detect these explosives in the field does not exist, nor can the existing techniques meet proposed detection limits. We propose to develop ion mobility spectroscopy (IMS) as an analytical method to detect explosives in both water and soil samples. IMS can offer a number of benefits, including significantly lower analysis costs, faster turnaround times, and superior sensitivity and selectivity. In addition, no hazardous waste is generated by IMS analyses. The development of IMS technology will result in much better site characterization and improved worker and public protection. Sandia and the DOE will assume a lead role in this area of environmental restoration technology. If this phase of the project is successful, the IMS will be adapted for remote (robotic) monitoring or as an analysis/control system for unattended groundwater remediation.

FY96 accomplishments include the following: (1) demonstrating that IMS can be used to determine the amount of organic explosives present in soil and water samples, (2) examining the effect of controlling the ion chemistry to maximize the selectivity and sensitivity of the IMS, (3) preparing appropriate soil standards, (4) determining the recovery efficiency for explosives/soil interfaces, and (5) writing software that will allow automated identification and quantification of the explosives detected, and (6) performing field demonstrations to show that IMS can be used to quickly, efficiently, and inexpensively screen environmental sites for the presence of explosives. We are currently comparing the IMS results obtained from the field testing to the EPA-approved High-Performance Liquid Chromatographic (HPLC) methods (EPA Method 8330). We compared a limited number of samples to EPA-approved colorimetric methods and immunoassay methods in the laboratory.

Publications

Refereed

Rodacy, P. J., and P. K. Leslie. 1994. "Ion Mobility Spectroscopy (IMS) Detection of Organic Explosives in Soils." Paper presented to the International Symposium on Energetic Materials Technology, Orlando, FL, 21–24 March.

Rodacy, P. J., P. K. Leslie, S. Klassen, and R. Silva. 1995. "Ion Mobility Spectroscopic Techniques for the Detection and Identification of Explosives." Paper presented to the 5th International Symposium on Analysis and Detection of Explosives, Washington, DC, 4–8 December.

Other

Rodacy, P. J., and P. K. Leslie. 1994. "Ion Mobility Spectroscopy (IMS) Detection of Organic Explosives in Soils." Sandia Technical Report, SAND94-0127A.

Development of Inexpensive Metal Macrocyclic Complexes for Direct Oxidation of Methanol in Fuel Cells

N. Doddapaneni

Fuel cells are being considered for electric vehicle and stationary energy-storage applications. Precious metals (platinum and ruthenium) have been exclusively used for both anode and cathode reactions. Due to the instability of these catalysts, the performance of fuel cells declines on long-term operation. Furthermore, these catalysts are easily poisoned by both fuel impurities and the byproducts formed during fuel-cell operation. We initiated a program to develop metal macrocyclic complexes as catalysts for the direct oxidation of methanol and hydrogen in fuel cells. The main objective of this project is to design, synthesize, and evaluate inexpensive and stable metal macrocyclic complexes. To achieve this goal we attached the metal macrocyclic moiety to the carbon substrate. These bound complexes should possess good catalytic activity and exhibit stability on long-term storage and use in the fuel-cell environment.

During FY96 we designed and synthesized several transition and precious metal macrocyclic complexes. We fabricated these carbon/catalyst mixtures into electrodes that we then tested in both half- and full-proton exchange membrane fuel cells (PEMFC). Based on the initial performance for hydrogen oxidation, we selected a platinum-ruthenium phthalocyanine (Pt-RuPc) polymeric catalyst for further in-depth evaluation.

To evaluate both the performance and long-term stability of the catalyst, we built 40 cm^2 hydrogen/oxygen fuel cells containing Pt-RuPc/Vulcan membrane electrode assembly (MEA) and Pt-black cathode MEAs containing various amounts of these catalysts. The anode used for the life test contained 5 mg/cm^2 of Pt-RuPc/Vulcan mix (0.035 mg Pt/cm^2) coated with 20 wt.% of Nafion cast onto Teflonized carbon-fiber paper. The cathode MEAs contained either 2.5 mg/cm^2 of 20% Pt/Vulcan mix (0.5 mg Pt/cm^2) or 2.5 mg Pt-black/cm^2. These were coated with 20 wt.% Nafion cast onto Teflonized carbon-fiber paper.

PEMFC results with Pt-RuPc show very promising catalytic activity for hydrogen oxidation. For example, at a current density of 500 mg/cm^2 the performance of the Pt-RuPc/Vulcan anode MEA was only 75 mV lower than an MEA containing 4 mg/cm^2 Pt-black. However, when compared with an MEA containing 2.5 mg/cm^2 of 20% Pt/Vulcan mix, the PEMFC with our catalyst has a 40-mV higher terminal voltage, 650 mV vs. 610 mV. The PEMFC with our catalyst has undergone nearly 1100 hours of continuous operation without any degradation of fuel-cell performance. The stability studies are still in progress.

Finally, we initiated initial studies of the effect of impurities, such as carbon monoxide, on fuel-cell performance. Preliminary results showed voltage drops of 25 mV, 30 mV, and 325 mV for CO levels of 10 ppm, 20 ppm, and 100 ppm, respectively, in the hydrogen fuel. By way of comparison, Los Alamos National Laboratory (LANL) reported voltage drops of 90 mV and 390 mV at CO levels of 5 ppm and 20 ppm, respectively. The LANL results were obtained using Pt/Vulcan anode having a Pt loading of 0.14 mg/cm^2, which is four times the normal metal loading of the Pt-RuPc/Vulcan anode. We believe that the voltage drop with our catalyst can be further reduced by optimizing the electrodes. In summary, we believe our catalyst can be used in place of the expensive, commonly used Pt catalyst and achieve better overall performance.

Publications

Refereed

Doddapaneni, N., and D. Ingersoll. 1996. "Fuel Cell Development for Transportation: Catalyst Development." Paper presented to the 1996 Fuel Cell Seminar, Orlando, FL, 17–20 November.

Doddapaneni, N., and D. Ingersoll. 1996. "Novel Electrolyte Additives to Enhance Zinc Electrode Cycle Life." *Proc. 188th Electrochem. Soc. Mtg.* **96-4** (Chicago, IL, 8–13 October). Pennington, NJ: Electrochemical Society.

Ortiz, B., S. M. Park, and N. Doddapaneni. 1996. "Electrochemical and Spectroelectrochemical Studies of Cobalt Phthalocyanine Polymers." *J. Electrochem. Soc.* **143** (June): 1800–1805. Pennington, NJ: Electrochemical Society.

Cooperating Robot Arms

R. J. Anderson

The simultaneous control of multiple robots in coordinated and cooperating modes of operation is beyond the scope and expertise of individual robot manufacturers, but is crucial to the success of many proposed DOE and DoD tasks, such as waste storage tank remediation, decommissioning of nuclear facilities, and dismantlement of DoD submarines. This project addresses this need by developing software technologies for controlling advanced cooperating robotics systems through the use of modular controls software and 3-D graphical programming.

Our research plan focuses on two areas: (1) building a modular low-level control system that will allow rapid reconfiguration of control system parameters for multi-arm modes of operation, and (2) building a high-level graphical programming environment with an underlying multirobot task sequencer to simplify programming complex multirobot tasks. We will base the modular control system on Sandia's Sequential Modular Architecture for Robotics and Teleoperation (SMART), a modular, icon-based, distributed control architecture for robots. The high-level task-sequence control will be based on Sandia's Robot Independent Programming Language (RIPL). The research will culminate in two high-profile demonstrations showing cooperative and coordinated modes of operation focused on DOE and DoD needs.

We proved that it is possible to control a complex multirobot system by combining software modules representing the different system components in different fashions. Thus, moving from two-robot behaviors to three-robot behaviors requires the addition of a few interchangeable modules. This is the fundamental theoretical concept that the project is based on and is the key to simplifying the programming of multiple robot systems.

We took this theoretical result to its logical conclusion by developing an icon-based graphical user interface (GUI) showing the underlying SMART modules, which the operator can use to define different modes of multirobot operation. The operator moves icons on the screen representing robots, input devices, kinematics, etc., for all of the robots in the workcells, then validates, configures, and generates code for the run-time system by clicking on the appropriate mouse buttons. We also developed an event-based graphical programming environment that allows us to simultaneously preview and plan motions for all of the robots in the workcell. The RIPL serves as the bridge between the graphical programming environment and the low-level SMART control environment. We extended it to enable multirobot behaviors.

We equipped the robots with some of the necessary tools needed for doing dismantlement operations. We outfitted each of the PUMAs (industrial robots) with cameras, drills, and grippers. The gantry robots have cameras, grippers, a magnet tool, and a jigsaw cutting tool. With these tools we are able to manipulate our truss structure (actually a 2x2 framework with a plywood skin), wire brushes to remove simulated polycarbonate byproduct (PCB) material on the inside of the truss structure, then drill, cut out, and remove the skin from each window of the truss.

We met every stated milestone in the original proposal, but were not able to accomplish the gantry integration work proposed as an additional task for the second year of the project.

Publications

Refereed

Anderson, R. J. 1996. "Autonomous, Teleoperated, and Shared Control of Robot Systems." *Proc. IEEE Internat. Conf. on Robotics and Automation* **3** (Minneapolis, MN, 22–28 April): 2025–2032.

Anderson, R. J. 1996. "Building a Modular Robot Control System Using Passivity and Scattering Theory." *Proc. 1996 IEEE Internat. Conf. on Robotics and Automation* **1** (Minneapolis, MN, 22–28 April): 698–705. New York, NY: IEEE.

Anderson, R. J. 1995. "SMART: A Modular Control Architecture for Telerobotics." *IEEE Robotics & Automation Magazine* **1** (September): 10–18. New York, NY: IEEE.

Anderson, R. J., and K. W. Lilly (Penn. State). 1995. "A Modular Approach to Multi-Robot Control." *Proc. IEEE Internat. Conf. on Decision and Control* (New Orleans, LA, 13–15 December): 1021–1031. New York, NY: IEEE.

Organically Enhanced In Situ Electrokinetic Removal of Uranium from Soils

P. V. Brady, M. D. Siegel, E. R. Lindgren

We calibrated a new in situ *method for electrokinetically removing contaminant metals (uranium) from soils. This process involves the introduction of citrate, a biodegradable tricarboxylate, into contaminated soils, whereupon it is electrokinetically migrated through the soil to a collection electrode. In bench-scale tests, we found that citrate removes > 80% of sorbed uranium. We found similar results with contaminated soils from Hanford. Parallel experiments demonstrated that residual U-citrate complexes left after treatment can be rapidly biodegraded by microorganisms, thereby ensuring that subsequent transport of uranium will be unlikely. The latter is particularly critical for regulatory acceptance.*

We demonstrated at the bench scale that uranium is effectively mobilized by citrate-leaching solutions, and that the aqueous species thus formed move quite rapidly in an electric field. Extraction efficiencies exceeded 90% from a uranium-doped sand and from a uranium-contaminated soil given us by Bechtel-Hanford. For regulatory acceptance of field application of the process for removing uranium with citrate, it is critical that any residual citrate be rendered inert. Otherwise, there would remain a potential "fast-track" for any uranium left behind to follow into the biosphere. We demonstrated that citrate and uranium-citrate compounds are effectively degraded by bacteria indigenous to most soils.

At this point we have proven that *in situ* electrokinetic contaminant removal can be greatly enhanced by use of biodegradable leaches. In a companion project we also scaled up bench-scale tests (without the leach) to demonstrate electrokinetic removal of contaminants in the field. The combination of results suggests that the leach procedure might similarly be applied to good effect in the field. Consequently we are in the process of identifying field sites where we might demonstrate the leach technique. We specifically dealt with Bechtel-Hanford and are in the process of exploring further funding through them.

Publications

Refereed

Booher, W. F. 1996. "Electrokinetic Remediation of Uranium-Contaminated Soils." Ph.D. thesis, University of New Mexico, July.

Oriented Inorganic Thin-Film Channel Structures with Unidirectional Monosize Microscopes

J. Cesarano, J. A. Shelnutt, J. C. Brinker, D. A. Loy, D. Y. Sasaki

The goal of this project is to develop a new generation of inorganic membranes with oriented, unidirectional, monosized porous channels. Such membranes would yield high selectivity along with high flux. Our methodology takes advantage of the two-dimensionality of Langmuir-Blodgett (LB) films, sol-gel synthesis, and fugitive molecular spacers to engineer idealized microporous membranes with pore sizes in the 3- to 20-Å range. The membrane will be amorphous SiO_2, which exhibits good thermal, chemical, and mechanical stability. Success requires uniform placement of organic molecular spacers throughout a thin silica precursor matrix and application of the mixed film to a substrate.

Currently, silica microporous membranes are fabricated using sol-gel techniques. Molecular selectivity of such membranes is good due to precise control of the pore size; however, the porous paths are long and tortuous, resulting in low flux. In contrast, there is a great demand for membranes that exhibit high flux in addition to high selectivity. Such membranes could be worth billions of dollars for gas-separation applications; in particular, separating CO_2, N_2, He, and H_2S from CH_4 for natural-gas processing; O_2/N_2 separation for enhanced combustion; and H_2 from CO/CO_2 for fuel cells.

We are attempting to develop a new generation of inorganic (silica) membranes with oriented, unidirectional monosized porous channels that have high selectivity along with high flux. The methodology is to use two-dimensional LB films combined with sol-gel synthesis and fugitive molecular spacers to engineer idealized microporous membranes with channel sizes in the 3- to 20-Å range. A critical requirement for success of this technique is that amphiphilic silicon-containing molecules must be capable of forming Langmuir monolayers and must be completely miscible with nonreactive spacer molecules. If the silane and organic amphiphiles phase-separate, the resulting channels will be much larger than predicted. We studied two general approaches to meet this objective. In the first approach, we fabricated mixed LB films of commercial silane amphiphiles and organic amphiphiles. After hydrolysis, we removed the organic spacers, leaving behind a membrane with a thickness on the order of 10 Å. The second approach required the synthesis of siloxane amphiphiles that have the ability to form LB films and be subsequently crosslinked. If successful, these molecules could yield films with thicknesses greater than 50 Å after the resultant structure was converted into silica.

Our results demonstrated that miscible mixed monolayers of octadecyltrimethoxysilane (OTMS) and an organic amphiphile could be used to fabricate LB films on silicon substrates. Before and after pyrolysis, we characterized the mixed monolayers by surface acoustic-wave (SAW) devices, ellipsometry, and scanning-force microscopy, and compared them to computer simulation. The LB films applied to silicon were miscible and uniform with a thickness of 23 Å. After pyrolysis, the films with 15% fugitive organic amphiphile resulted in 10-Å-thick layers of textured amorphous silica with what appears to be 4-Å-diameter pores penetrating the layers. This structure resembles the ideal structure that we initially hoped to fabricate. However, we are uncertain of the exact hole size and whether the holes actually penetrate completely through the amorphous silica. We are certain they are less than 20 Å from SAW analysis, but a routine analysis for smaller pores is not available. We are recommending an electrochemical technique that may be used to probe and decorate the porous structure for more complete characterization. Our second approach to build microporous channels, using synthetic siloxane amphiphiles, has not been successful to date. There have been problems purifying the molecules to the extent necessary for LB film fabrication.

Quantitative Analysis of Trace Contaminants in Aqueous Media

D. J. Rakestraw, D. S. Anex

In this project Sandia developed a rapid method for quantitative chemical analysis that is highly sensitive and selective. High sensitivity (ppt) is achieved using laser-induced fluorescence detection, and high selectivity (> 500,000 theoretical plates/meter) is accomplished using electrokinetic chromatography. The combination of these two techniques provides unprecedented chemical analysis capability for neutral chemical species in a compact, low-cost format. We applied the technique to the analysis of polycyclic aromatic hydrocarbons (PAHs) using laboratory standards, Sandia well-water samples, and soil extracts provided by the EPA. The success of this project was instrumental in an increased effort in chemical analysis for both environmental and national security.

The thrust of this project was to test and develop electrokinetic chromatography for the quantitative analysis of trace contaminants in aqueous media. We coupled this separation technique with laser-induced fluorescence to provide high-sensitivity detection.

We made these major technical accomplishments:

(1) We demonstrated gradient electrochromatography. In this technique we generate a solvent gradient under computer control by varying the applied voltage to two solvent reservoirs that feed a packed microcapillary used for electrokinetic chromatography.

(2) We demonstrated a separation of five PAHs in less than 5 seconds using electrokinetic chromatography, and the separation of 16 PAHs in less than 120 seconds. The 5-second separation represents the fastest separation of a mixture of neutral compounds by any liquid-phase chromatography reported to date. The separation of the 16 PAHs is almost an order of magnitude faster than conventional high-performance liquid chromatography (HPLC) methods.

(3) The packed capillaries used in the work for electrokinetic chromatography resulted in the observation of a physical phenomenon that was not previously recognized. We found that

extreme amounts of force can be generated by electroosmotically driven fluids through the packed columns.

The project had the following impact:

(1) It was a major driving force in creating an effort toward developing a "chemistry laboratory-on-a-chip." Electrokinetic chromatography with optically-based detection is a major component of this effort. We also used the results as a building block for the technology to be developed for nuclear nonproliferation (NN).

(2) We are currently using electrokinetic chromatography to study the aging of energetic material.

(3) A collaborative effort among several Sandia groups is now investigating the use of electroosmotically driven fluids for making pumps and valves that will contain no moving parts.

This has been an extremely successful project that initially focused on environmental analysis and has resulted in a number of new technologies that we are now exploiting for a wide range of applications, including environmental analysis.

Publications

Refereed

Dulay, M. T., C. Yan, D. J. Rakestraw, and R. N. Zare. 1996. "Automated Capillary Electrochromatography: Reliability and Reproducibility Studies." *J. Chromatography A* **725**: 361–366. Amsterdam, Netherlands: Elsevier Science.

Yan, C., R. Dadoo, H. Zhao, R. N. Zare, and D. J. Rakestraw. 1995. "Capillary Electrochromatography: Analysis of Polycyclic Aromatic Hydrocarbons." *Analytic. Chem.* **67** (13) (1 July): 2026–2029. Washington, DC: American Chemical Society.

Yan, C., R. Dadoo, R. N. Zare, D. J. Rakestraw, and D. Anex. 1996. "Gradient Elution in Capillary Electrochromatography." *Analytic. Chem.* **68**: 2726–2732. Washington, DC: American Chemical Society.

Replacement of Liquid H_2SO_4 and HF Acids with Solid Acid Catalysts for Paraffin Alkylation Process

N. B. Jackson

This past year the project focused on the testing and optimization of zirconium-titanium phosphate materials, which are novel solid acid catalyst materials. Sandia also studied a sulfated version of the phosphate catalysts. We identified the structure of the more catalytically active materials to be in an NZP (sodium-zirconium phosphate) crystal structure, which is a proton-conducting crystalline-type structure. The phosphate materials have high surface areas (400 m^2/g) and show remarkably small deactivation during isomerization of an olefin even though significant amounts of carbon are depositing on the surface. The sulfated version of these materials deactivates much more quickly than the nonsulfated.

We began to study and understand a novel new set of compounds made from zirconium, titanium, and phosphate ($Zr/Ti/PO_4$). This material is a good solid acid catalyst and shows properties unique to acid catalysts. In particular, $Zr/Ti/PO_4$ is a high-surface-area catalyst (400 m_2/g) that deactivates quite slowly, particularly relative to the amount of carbon that builds up on the surface (and ordinarily poisons other acid catalysts). We systematically studied the effect that synthesis calcination temperatures and $Zr/Ti/PO_4$ ratios had on the catalysts' activity as well as the effect of the addition of sulfate. We found that the most active catalysts were those in the atomic proportions, which caused the formation of an NZP-type crystal structure. The NZP crystal structure is based on the sodium-zirconium phosphate ion-conducting solid-state material. $Zr/Ti/PO_4$ materials that had been calcined at high enough temperatures (500°C) to form the pyrophosphate were not at all active as acid catalysts. The isomerization of 2-methyl-2-pentene, which we used as our model reaction, appears to be catalyzed by the Bronsted acid sites on the catalyst surface. We studied the acid sites using probe molecules such as pyridine.

Publications

Other

Jackson, N. B., S. Thoma, T. M. Nenoff, and S. Kohler. 1996. "Deactivation over Zirconium-Titanium Phosphate Solid Acid Catalysts." Paper presented to the 11th International Congress on Catalysis, Baltimore, MD, 2–4 July.

Jackson, N. B., S. Thoma, T. M. Nenoff, and S. Kohler. 1996. "Isomerization over Zirconium-Titanium Phosphates." Paper presented to the Florida Catalysis Conference, Daytona Beach, FL, 18 April.

Jackson, N. B., S. Thoma, T. M. Nenoff, and S. Kohler. 1995. "Zirconium-Titanium Phosphates as Solid Acid Catalysts." Paper presented to the Chemical Congress Pacific Rim Meeting, Honolulu, HI, 18 December.

Jackson, N. B., T. M. Nenoff, S. Thoma, and S. Kohler. 1996. "Titanium-Zirconium Phosphates as Solid Acid Catalysts." Paper presented to the American Chemical Society Meeting, Orlando, FL, 20 August.

Nenoff, T. M., N. B. Jackson, S. Thoma, and S. Kohler. 1996. "Novel Solid Acids." Paper presented to the American Institute of Chemical Engineers Meeting, New Orleans, LA, 12 February.

Advanced Tomographic Flow Diagnostics for Opaque Multiphase Fluids

T. J. O'Hern, N. B. Jackson, J. R. Torczynski, D. R. Adkins

There are many industrial processes in which the flow of opaque multiphase fluids plays a key role, for example in the petrochemical, chemical, and pharmaceutical industries. Measurements in such processes are very difficult, since optical techniques are generally ineffective and the use of sampling probes often disturbs the multiphase flow. One flow with such characteristics is the Fischer-Tropsch (F-T) process in slurry-phase bubble-column reactors, which promises to improve coal liquefaction efficiencies from 30% to 90%. However, the lack of diagnostics capable of characterizing opaque multiphase flow has hampered acquisition of the data necessary for the design of industrial-scale reactors. We performed an experimental study to develop and characterize new diagnostics for measurements in industrial-scale opaque multiphase flow systems. We developed and evaluated several complementary techniques for spatially resolved void-fraction and bubble-size measurements, including gamma-densitometry tomography (GDT), electrical-impedance tomography (EIT), and x-ray tomography (XRT). We expect these techniques to be applicable to other important multiphase flows, including environmental flows in geological porous media, petroleum extraction and processing, and liquid-metal flows in solar energy applications. We chose the F-T process as the benchmark case for these newly developed diagnostics; we developed and operated a laboratory-scale research reactor system similar to an F-T bubble-column reactor in our labs as an experimental test-bed.

We completed development and application of new tomographic diagnostic techniques (GDT and EIT), as well as differential pressure (DP) measurements to study flow in a research-scale reactor and a larger, industrial-scale reactor. We refined the GDT system to near "turn-key" status, while the EIT system remains more of an application-specific device.

For each fluid system examined (air-water, air-oil, air-water-solid, air-oil-solid), the experimental test matrix included varying gas-feed rates, overall system pressure, and system temperature. In addition, for the three-phase systems we examined the effect of catalyst loading by testing at several different values (e.g., 20% and 40% catalyst loading by mass). GDT and DP data indicate that raising overall system pressure increases void fraction uniformly across the bubble column, while increasing the gas-feed flowrate leads to a more peaked void-fraction distribution, with the column centerline value increasing faster than that near the walls.

We assembled and tested a high-frequency EIT system for capacitive impedance measurements needed for direct EIT application to hydrocarbon systems.

We developed and tested several finite-element method (FEM)-based EIT reconstruction algorithms and compared reconstructions with those of a boundary-element method (BEM)-based EIT reconstruction algorithm. While both techniques gave acceptable results for known zero-conductivity inclusions in the measurement region, the FEM method was able to reconstruct continuous conductivity variations in the field, as expected for a bubble-column flow.

Publications

Refereed

Adkins, D. R., K. A. Shollenberger, T. J. O'Hern, and J. R. Torczynski. 1996. "Pressure Effects on Bubble-Column Flow Characteristics." *Proc. Natl. Heat Transfer Conf.* **9** (Houston, TX, July): 318–325. LaGrange Park, IL: American Nuclear Society.

Jackson, N. B., J. R. Torczynski, K. A. Shollenberger, T. J. O'Hern, and D. R. Adkins. 1996. "Hydrodynamic Characterization of Slurry Bubble-Column Reactors for Fischer-Tropsch Synthesis." *Proc. 13th Ann. Internat. Pittsburgh Coal Conf., Coal-Energy and the Environment* **2**: 1226–1231. Edited by S. H. Chiang. Pittsburgh, PA: University of Pittsburgh Center for Energy Research.

Jackson, N. B., J. R. Torczynski, K. A. Shollenberger, T. J. O'Hern, and D. R. Adkins. 1996. "Sandia Support for PETC Fischer-Tropsch Research: Experimental Characterization of Slurry-Phase Bubble-Column Reactor Hydrodynamics." *Proc. First Joint Power and Fuel Syst. Contractors Conf.: Indirect Liquefaction.* Pittsburgh, PA: Pittsburgh Energy Technology Center.

Shollenberger, K. A., J. R. Torczynski, D. R. Adkins, and T. J. O'Hern. 1995. "Gamma Densitometry Tomographic Measurements of Void-Fraction Spatial Distribution in Bubble Columns." *Frontiers in Industrial Process Tomography* (San Luis Obispo, CA, 29 October–3 November): 329. Edited by D. M. Scott and R. A. Williams. New York, NY: Engineering Foundation.

Shollenberger, K. A., J. R. Torczynski, D. R. Adkins, T. J. O'Hern, and N. B. Jackson. 1997. "Gamma Densitometry Tomography of Gas Holdup Spatial Distribution in Industrial-Scale Bubble Columns." *Chem. Eng. Science*, accepted.

Other

Jackson, N. B., J. R. Torczynski, K. A. Shollenberger, T. J. O'Hern, and D. R. Adkins. 1996. "Hydrodynamic Characterization of Slurry Bubble-Column Reactors for Fischer-Tropsch Synthesis." Paper presented to the 13th Annual International Pittsburgh Coal Conference, Pittsbugh, PA, 3–7 September.

Jackson, N. B., J. R. Torczynski, K. A. Shollenberger, T. J. O'Hern, and D. R. Adkins. 1996. "Sandia Support for PETC Fischer-Tropsch Research: Experimental Characterization of Slurry-Phase Bubble-Column Reactor Hydrodynamics." (Invited) Paper presented to the First Joint Power and Fuel Systems Contractors Conference: Indirect Liquefaction, Pittsburgh Energy Technology Center, Pittsburgh, PA, 9–11 July.

O'Hern, T. J., J. R. Torczynski, K. A. Shollenberger, and S. L. Ceccio. 1995. "Electrical Impedance Tomography for Spatial Measurements of Gas Distribution in Multiphase Flows." *Bull. Amer. Phys. Soc.* **40** (9) (Irvine, CA, 20 November): 2004. New York, NY: American Physical Society.

O'Hern, T. J., J. R. Torczynski, S. L. Ceccio, A. L. Tassin, G. L. Chahine, R. Duraiswami, and K. Sarkar. 1995. "Development of an Electrical Impedance Tomography System for an Air-Water Vertical Bubble Column." *Proc. ASME Forum on Measurement Techniques in Multiphase Flows* **FED-211** (ASME International Mechanical Engineering Conference & Exposition) (San Francisco, CA, 12–17 November): 531–537.

Torczynski, J. R., D. R. Adkins, K. A. Shollenberger, and T. J. O'Hern. 1996. "Application of Gamma-Densitometry Tomography to Determine Phase Spatial Variation in Two-Phase and Three-Phase Flows." *Proc. ASME Fluids Eng. Div. Summer Conf.* **FED-236** (San Diego, CA, 10 July): 503–508.

Torczynski, J. R., K. A. Shollenberger, T. J. O'Hern, and D. R. Adkins. 1996. "Gamma Densitometry Tomographic Measurements of Gas Distribution in a Large-Diameter Bubble Column." Paper presented to the American Physical Society Division of Fluid Dynamics Annual Meeting, Syracuse, NY, 20 November.

Torczynski, J. R., K. A. Shollenberger, T. J. O'Hern, and D. R. Adkins. 1995. "Tomographic Measurements of Volume Fractions in Multiphase Flows." *Bull. Amer. Phys. Soc.* **40** (9) (Irvine, CA, 20 November): 2004. New York, NY: American Physical Society.

Torczynski, J. R., K. A. Shollenberger, T. J. O'Hern, D. R. Adkins, and N. B. Jackson. 1996. "Tomographic Diagnostics for Determining Phase Distribution in Bubble-Column Flow." Paper presented to the 12th Annual Arizona Fluid Mechanics Conference, Tempe, AZ, 1–2 March.

Torczynski, J. R., T. J. O'Hern, K. A. Shollenberger, S. L. Ceccio, and A. L. Tassin. 1996. "Finite Element Method Electrical Impedance Tomography for Phase Distribution Determination in Multiphase Flows: Calculations and Experiments." *Proc. ASME Fluids Eng. Div. Summer Conf.* **FED-236** (San Diego, CA, 10 July): 497–501.

Evanescent Fiber-Optic Sensor for In Situ Monitoring of Chlorinated Organics

D. S. Blair, M. K. Alam, E. V. Thomas

Current methods for determining concentrations of chlorinated hydrocarbons (CHCs) in aqueous matrices are both expensive and time-consuming. An alternative to the technologies presently employed is a fiber-optic chemical sensor based on evanescent-wave spectroscopy. Being both passive and selective, the fiber-optic sensor can remain in situ *for extended periods of time without maintenance or calibration. We built a sensor by coating bare silica core fibers with hydrophobic polymer films. Upon exposure of the coated fibers to aqueous analyte mixtures, CHCs selectively partition into the polymer cladding, and their presence is detected by evanescent-wave spectroscopy in the near-infrared (NIR). The cladding serves to protect the moisture-sensitive silica core and to provide a stationary phase for the CHCs to partition into and preconcentrate, providing an enhanced spectral response. We generated a concentration calibration model for various dilute aqueous CHCs with mixtures containing individual analyte concentrations between 20 and 300 ppm, resulting in a cross-validated root-mean-squared (RMS) error of prediction of less than 30 ppm.*

Based on FY95 accomplishments we determined that poly(dimethyl)siloxane was the optimal cladding material due to its mechanical and chemical stability, high degree of partitioning of CHCs from aqueous solutions, and speed of response. We designed, fabricated, and tested a number of prototype sensors, focusing on devices that would allow deployment of the device for extended periods of time without mechanical failure. We accomplished and tested this using field-portable Fourier transform infrared (FTIR) spectroscopy.

We then used the final sensor design to generate the sensor response to complex aqueous mixtures, containing up to five volatile organic compounds (VOCs) (both chlorinated and aromatic) identified as analytes of concern in the environmental arena. We subsequently modeled the sensor response using the linear chemometric models of partial least squares analysis and principle component regression. With individual analyte concentrations between 50 and 300 ppm, these models could use the sensor response to predict concentrations with a standard error of prediction of less than 12 ppm. However, we determined that using an internal standard—a unique cladding spectral feature—to correct for pathlength changes in the sensor did not significantly improve the sensor precision. Optimal wavelength selection, using a genetic algorithm, for reducing error and for simplifying spectral requirements for the field spectrometer proved to limit the robustness of the resultant prediction model.

Publications

Refereed

Blair, D. S., L. W. Burgess, and A. M. Brodsky. 1995. "Study of Analyte Diffusion into a Fiber-Optic Chemical Sensor by Evanescent-Wave Spectroscopy." *Appl. Spectroscopy* **49** (November): 1636–1645. Austin, TX: Society for Applied Spectroscopy.

Other

Blair, D. S. 1995. "A Sensor to Quantitate Low-Level Concentrations of Organic Compounds in Aqueous Matrices." Paper presented to the International Chemical Congress of Pacific Basin Societies (PACIFICHEM '95), Honolulu, HI, 17–22 December.

Nanoreactors as Novel Catalyst Systems for Waste-Stream Remediation

A. Martino, S. K. Showalter, S. A. Yamanaka, D. A. Loy

The first part of this project involved the study of a fundamental nanocluster system in sol-gel encapsulation chemistry. We encapsulated nanometer-sized gold particles in the micropores of xerogels and aerogels. The synthesis involves the sequential reduction of a gold salt followed by sol-gel processing in an inverse micelle solution. The inverse micelle solution solubilizes the metal salt and provides a microreactor for the nucleation, growth, and stabilization of the nanometer-sized clusters. Hydrolysis and condensation of an added siloxane precursor produces a wet gel embedding the particles. We completed characterization of the particle size and composition and the particle-growth process with transmission-electron microscopy (TEM), electron diffraction, and UV-visible absorption spectrometry. We completed characterization of the gel surface areas with N_2 porosimetry. We discussed material properties determined as a function of the gel precursor, the water-to-gel precursor reaction stoichiometry, and surfactant concentration in terms of the unique solution chemistry occurring in the microheterogeneous inverse micelle solutions. The second part of this project involved the development of a practical catalyst system. We encapsulated palladium nanoclusters in silica monoliths. We studied the materials as hydrogenation catalysts, and related activity to material properties and original synthesis variables.

We encapsulated nanometer-sized Au particles in the micropores of xerogels and aerogels. The synthesis is a sequential reduction of a gold salt and sol-gel processing in an inverse micelle solution. We use the inverse micelle solution to solubilize the metal salt and provide a microreactor for the nucleation, growth, and stabilization of the nanometer-sized clusters. Hydrolysis and condensation of an added siloxane precursor produces a wet-gel embedding the particles. The presence of gel precursors destabilizes the inverse micelle structure, resulting in larger particle sizes compared to typical inverse micelle synthesis techniques. Particle size control is complicated by the gel precursor effect on inverse micelle structure and the production of water and alcohol in the hydrolysis and condensation reactions. Finally, a unique gelation technique is outlined in these microheterogeneous solutions. Gelation occurs across the surfactant interface, increasing the effective H_2O:Si ratio. Gelation occurs even at low H_2O:Si ratios, and condensation rates are high. Sol-gel parameters like the H_2O:Si ratio and the surfactant concentration have unique and sometimes not intuitive effects on the hydrolysis and condensation rates and the resulting material properties. Post-synthesis heat treatment to the materials indicates little to some degree of particle sintering, depending on material support properties. Further thermal and hydrothermal stability tests are needed.

We completed initial catalyst testing on a series of Pd nanocluster-supported SiO_2 materials. No reaction takes place when the support material is added without palladium. When palladium is present, activity strongly depends on the type of support. Catalyst activity is much higher when tetraethylorthosilicate (TEOS) rather than the pre-hydrolyzed TEOS oligomer is used to form the support. As no activity originates from the support, it is likely that a metal-support interaction is responsible for the activity difference. Support surface areas, metal loadings, and post-synthesis heat treatments do not affect catalyst performance. For this rather facile hydrogenation, activity is high in all cases with a non-negligible amount of isomerization occurring. The hydrogenation of hexene has been successful at screening out the TEOS oligomer as a support reagent. More rigorous tests must be developed to screen future samples.

Publications

Refereed

Martino, A., S. A. Yamanaka, J. S. Kawola, and D. A. Loy. 1996. "Encapsulation of Gold Nanoclusters in Silica Materials via an Inverse Micelle/Sol-Gel Synthesis." *Chemistry of Materials*, in press.

Martino, A., S. A. Yamanaka, J. S. Kawola, S. K. Showalter, and D. A. Loy. 1995. "Encapsulation of Gold Clusters in Silica Materials via an Inverse Micelle/Sol-Gel Synthesis." Paper presented to the Materials Research Society Fall Meeting, Boston, MA, 23–27 November.

Yamanaka, S. A., A. Martino, D. A. Loy, J. S. Kawola, and S. K. Showalter. 1995. "Encapsulated Metal Nanocluster Materials Prepared by a Novel Inverse Micelle/Sol-Gel Technique." Paper presented to the 210th American Chemical Society Fall Meeting, Chicago, IL, 20–24 August.

Yamanaka, S. A., A. Martino, D. A. Loy, J. S. Kawola, and S. K. Showalter. 1995. "Encapsulation of Metal Nanoclusters via a Combined Inverse Micelle/Sol-Gel Synthesis." Paper presented to the 7th Annual Joint Meeting of the New Mexico Sections of the Materials Research Society and the American Ceramic Society, Albuquerque, NM, 30 October.

Yamanaka, S. A., A. Martino, D. A. Loy, J. S. Kawola, and S. K. Showalter. 1995. "Encapsulation of Metal Nanoclusters via a Combined Inverse Micelle/Sol-Gel Synthesis." Paper presented to the 47th Pacific Coast Regional Meeting of the American Ceramic Society, Seattle, WA, 1–3 November.

Yamanaka, S. A., A. Martino, D. A. Loy, and J. S. Kawola. 1996. "Non-Polar Processing of Silica Sol-Gel Materials via a Combined Inverse Micelle / Sol-Gel Technique." Paper presented to the Materials Research Society Spring Meeting, San Francisco, CA, 13–18 April.

Reapplication of Energetic Materials as Fuels

L. L. Baxter, D. W. Vehar, J. Lipkin

The purpose of this project is to evaluate the combustion properties of energetic fuels (propellants and explosives) to determine their viability as boiler fuels. To accomplish this, we tested a variety of materials of hazard class 1.1 and 1.3, including polybutadiene solid rocket engine binder with embedded aluminum flake, a double-base propellant consisting of nitrocellulose and nitroguanidine, TNT, and nitroguanidine. We measured the combustion properties and developed a good understanding of the mechanisms of NO_x formation based on fuel structure. In addition, we developed a new index of performance for oxygenated fuels and ranked fuels using this index. We addressed issues such as corrosion due to energetic materials firing that could possibly cause boiler damage.

The purpose of this project is to identify the combustion properties of various forms of energetic material (rocket propellants and explosives) to determine their suitability as co-fired fuels in industrial boilers. This has both the benefits of energy recovery and a much lower environmental impact than the traditional open-burn/open-detonation disposal.

This year we completed combustion tests of polybutadiene rocket binder, a double-base nitroglycerin/nitrocellulose propellant, TNT, and nitroguanidine. These tests show that fuel-bound nitrogen can be easily converted to nitrogen oxides in combustion systems, particularly if they are bound to the energetic material in the form of nitrate (NO_2) groups. The role of aluminum flake, which is embedded in the polybutadiene rocket binder, in formation of thermal NO_x during the high-temperature aluminum combustion has also been identified. This flake and metals in energetic materials in general are a potential source of boiler damage due to their extremely high combustion temperatures. Further research into NO_x-reduction methods shows that a decrease in nitrogen oxides of up to three times can easily be accomplished using staged combustion techniques.

In addition, traditional heating value analysis would predict that energetic fuels would not thermodynamically compare very well with traditional fuels. We showed that this is an artifact of the traditional analysis, which takes no account of the oxidizer chemically bound in the fuels. We extended this analysis and showed that energetic materials are often actually more efficient than their traditional counterparts. This removes a major objection to their use in boilers as fuel.

The key accomplishment of this project has been to prove the viability of energetic materials as boiler fuels. We have come to a good understanding of the NO_x formation mechanisms that come into play with the various forms of energetic fuel and have shown that these fuels are thermodynamically at least as efficient as typical boiler fuels.

Publications

Other

Baxter, L. L., J. Lipkin, J. Ross, and G. Sclippa. 1996. "NO_x Formation During Combustion of Energetic Materials." Paper presented to the 2nd International Conference on Combustion (ICOC '96), Conversion and Environmental Problems of Energetic Materials, Peaceful Utilization of Energetic Materials, St. Petersburg, Russia, 3–6 June.

Baxter, L. L., K. Davis, S. Sinquefield, S. Huey, J. Lipkin, D. Shah, J. Ross, and G. Sclippa. 1995. "Combustion Aspects of the Reapplication of Energetic Materials as Fuels as a Viable Demil Technology." *Proc. 1995 Global Demilitarization Symp. and Exhibit.* **1** (St. Louis, MO, 15–18 May): 17–27.

Baxter, L. L., K. Davis, S. Sinquefield, S. Huey, J. Lipkin, D. Shah, J. Ross, and G. Sclippa. 1995. "Reapplication of Energetic Materials as Fuels." *Proc. of the Joint Conf. of the Amer. Flame Res. Council and the Combined Central States/Western States/ Mexican Natl. Sections of the Combustion Inst.* **1** (San Antonio, TX, 23–26 April): 382–387.

Baxter, L. L., S. Huey, J. Lipkin, D. Shah, J. Ross, and G. Sclippa. 1996. "Boiler Fuel as a Recycling Option for Energetic Materials." Paper presented to the 4th International Symposium on Special Topics in Chemical Propulsion, Stockholm, Sweden, 27–30 May.

Baxter, L. L., S. Huey, J. Lipkin, D. Shah, J. Ross, and G. Sclippa. 1996. "Reapplication of Energetic Materials as Boiler Fuels." Paper presented to the Global Demilitarization Symposium, Sparks, NV, 13–17 May.

Designed Molecular-Recognition Materials for Chiral Sensors, Separations, and Catalytic Materials

T. M. Nenoff, D. J. Hobbs, J. A. Shelnutt, A. J. Ricco, D. Y. Sasaki, S. A. Yamanaka, M. C. Showalter

The goal of this project is to develop materials that are highly sensitive and selective for chiral chemicals and biochemicals (such as nerve agents) to be used as sensors, catalysts, and separation membranes. The work focuses on both organometallic and inorganic (silicate and nonsilicate) materials modified with chirally pure functional groups for the catalysis or separation of enantiomerically pure molecules. Surfactant and quaternary amine templating are being used to synthesize porous frameworks, containing mesopores of 30 to 100 Å. We are using molecular modeling methods to (1) tailor chiral molecular-recognition sites with high affinity and selectivity for specified agents, and to (2) predict the catalytic and separation selectivities of the modified mesoporous materials. The ability to design and synthesize tailored asymmetric molecular-recognition sites for sensor coatings will allow a broader range of chemicals to be sensed with the desired high sensitivity and selectivity. Initial experiments are targeting the selective sensing of small molecule gases and nontoxic model neural compounds. Further efforts will address designing sensors that will greatly extend the variety of resolvable chemical species and form a predictive, model-based method for developing advanced sensors.

Our goal is to develop materials that are highly sensitive and selective for chiral chemicals and biochemicals (e.g., nerve agents) to be used as sensors, catalysts, and separation membranes. To achieve this, we are using a combination of molecular modeling and inorganic/organic syntheses.

Two of the milestones we completed in FY96 are selection of a target molecule for sensing, separation, and/or catalytic conversion, and design of a porphyrin receptor for this target molecule. We chose trans-4-hydroxy-L-proline (THLP, relatively nontoxic) as the molecule for which we will tailor the receptor site. We also achieved the initial design by molecular modeling of the porphyrin receptor molecule: meso-tetrakis(cyclopropyl)porphyrin (TcPrP), nickel, and zinc derivatives as the molecules from which a porphyrin-based chiral receptor site for THLP was constructed. The characterization of the structure of the receptor molecule and receptor-substrate complexes, substrate binding affinities, and receptor-site enantio-selectivity is already well under way. Modeling of potential chiral surface-modifying agents is finished, and only the modeling of the surface-receptor interaction remains to complete this task.

We accomplished the synthesis of a range of pore sizes for silicate/sol-gel materials. We synthesized and characterized four different categories of materials: (1) crystalline mesoporous silicate "frameworks," with predetermined pore-sized materials of 40 Å and 100 Å; (2) amorphous silica sol-gel matrices, pore size of ~ 20 Å; (3) intercalated silica-based 2-D montmorillonite clays, interlayer distances of 15 Å; and (4) crystalline molecular sieves including hexagonal faujasite and AlPO-5 with pore sizes 7–15 Å. We have begun coupling the designed chiral porphyrins to these silicate/sol-gel support materials.

We successfully templated a chiral sugar molecule (D-Glucosamine), a novel zinc-phosphate mesoporous material. Characterization studies indicate ~ 40-Å pores, with some long-range ordering of the zinc and phosphorus atoms. This leads to the possibility of chiral ordering in the inorganic portions of the material, necessary for chiral separations.

Publications

Refereed

Mazzanti, M., J. C. Marchon, M. Shang, W. R. Scheidt, S. L. Jia, and J. A. Shelnutt. 1996. "A Molecular Venus Fly Trap. Induced-Fit Complexation of Pyridine Guests by Flipping of a Zinc (II) Chiroporphyrin Host Triggered by Axial Binding." *Science*, in press. Washington, DC: American Association for the Advancement of Science.

Medforth, C. J., C. M. Muzzi, K. M. Shea, K. M. Smith, R. J. Abraham, S. L. Jia, and J. A. Shelnutt. 1996. "NMR Studies of Nonplanar Porphyrins. Part 1. Axial Ligand Orientations in Highly Nonplanar Porphyrins." *Perkins Trans. II*, in press. London, UK: Chemical Society.

Medforth, C. J., C. M. Muzzi, K. M. Shea, K. M. Smith, R. J. Abraham, S. L. Jia, and J. A. Shelnutt. 1996. "NMR Studies of Nonplanar Porphyrins. Part 2. Effect of Nonplanar Conformation of the Porphyrin Ring Current." *Perkins Trans. II*, in press. London, UK: Chemical Society.

Nenoff, T. M., S. G. Thoma, and P. P. Newcomer. 1997. "Chirally Templated Zinc-Phosphate Phases." Paper to be presented to the Materials Research Society National Spring Meeting, Pittsburgh, PA, 5 May.

Nenoff, T. M., S. G. Thoma, P. P. Newcomer, and R. S. Maxwell. 1996. "A Chirally Templated Mesoporous Zinc Phosphate." *Chemistry of Mater.*, in press. Washington, DC: American Chemical Society.

Senge, M. O., C. J. Medforth, T. P. Forsythe, D. A. Lee, M. M., W. Jentzen, R. K. Pandey, J. A. Shelnutt, and K. M. Smith. 1996. "Comparative Analysis of the Conformation of Symmetrically and Asymmetrically Deca- and Unadeca-Substituted Porphyrins Bearing meso-alkyl or -aryl Groups." *Inorg. Chem.*, in press. Washington, DC: American Chemical Society.

Advanced Information Technologies

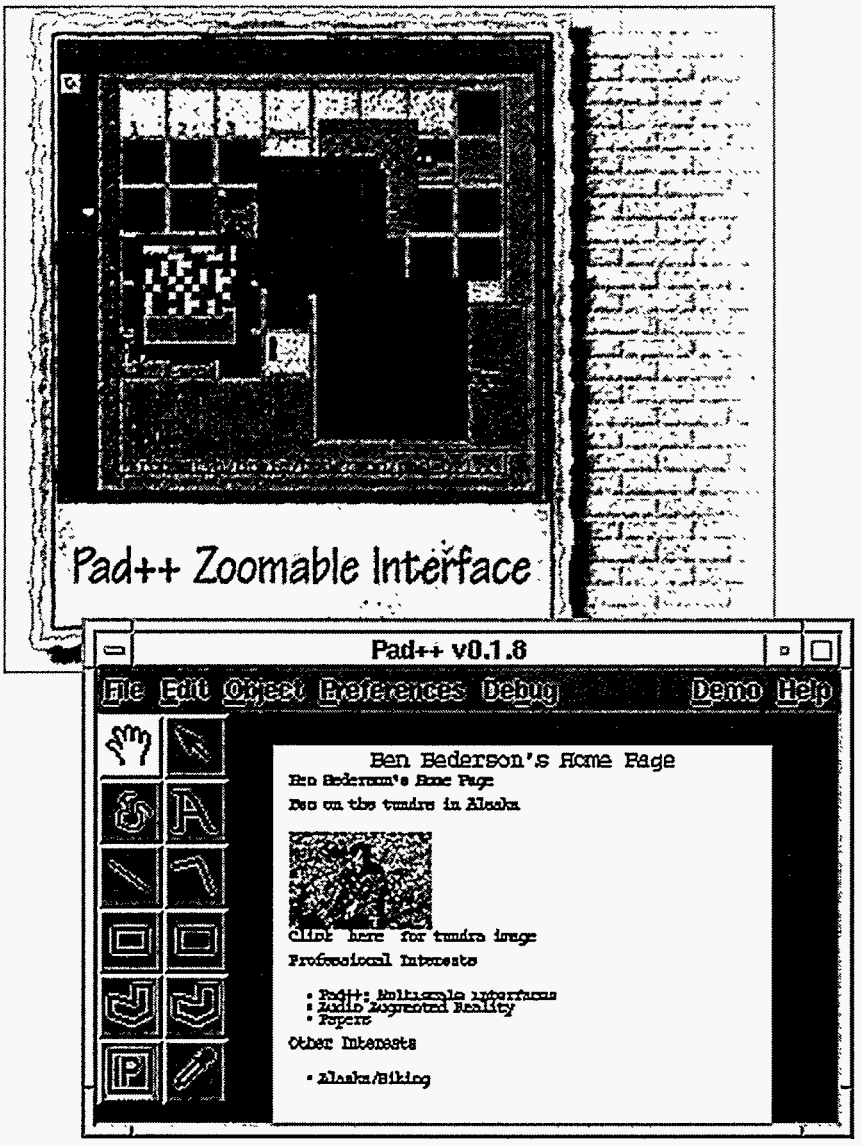

Pad++ explores user interfaces in which zooming is a fundamental part of the user's interaction with the computer (also known as "multiscale interfaces").

Learning Efficient Hypermedia Navigation

P. C. Chen, G. A. Laguna

This project addresses the need for tools that help the user navigate through large hypermedia systems. Hypermedia is an approach to linking and traversing many forms of related computer-based information, such as text, video, audio, and computer graphics, in a nonlinear fashion. In this project Sandia developed new machine-learning algorithms that use the actions of past users of the system to suggest hypermedia paths to the current user. By using learning techniques, the system will be able to adapt to new users throughout the life of the system. To test the algorithms, we implemented a World Wide Web (WWW) server that dynamically creates a path for the user to follow through the hypermedia data base.

We developed new machine-learning algorithms that use the actions of past users of the system to suggest hypermedia paths to the current user. By using learning techniques, the system will be able to adapt to new users throughout the life of the system. Ultimately, the system will use this same learning to physically alter the underlying structure of the hypermedia itself, allowing more efficient data access as well.

To test the algorithm, we implemented a WWW server that dynamically creates a path for a user to follow through the hypermedia data base. The server gathers information about how previous users have navigated the data base and creates a path for each new user accordingly. We tested this software on a moderately large hypermedia data base, consisting of a 90-page brochure containing text, pictures, and references to publications.

The new machine-learning algorithm links keywords to user attributes to create probable initial search paths. More generally, the algorithm can be used for document classification. Given a sequence of examples (a set of document features, e.g., a particular word containment) and an associated action (e.g., read with great interest), the learning algorithm produces a compact rule base composed of patterns (generalized document features) and (recommended) actions.

Publications

Refereed

Chen, P. C. 1995. "Adaptive Path Planning: Algorithm and Analysis." Paper presented to the IEEE International Conference on Robotics and Automation, Nagoya, Japan, 29 May.

Chen, P. C. 1996. "Interactive Task Planning Through Natural Language." Paper presented to the IEEE International Conference on Robotics and Automation, Minneapolis, MN, 27 May.

Design of a Highly Secure Smartcard

C. L. Musselman, K. M. Tolk, T. I. Barger, G. J. Bloom, P. S. Gemmell, L. M. Moore

The goal of this project is to develop an inherently secure, multiple-application smartcard system. Our approach is to integrate a spectrum of Sandia-unique surety technologies to design, prototype, and test a smartcard system that could be commercially relevant and substantially more secure than any other smartcard system in production or under development. Such a system should be useful in a variety of applications, including electronic banking, personal identification, access control, advanced information management, and secure access to information on the National Information Infrastructure (NII). We expect this project will result in a system that satisfies requirements for both the Department of Energy's Defense Programs and the NII.

We accomplished the following in FY96:

(1) Completed conceptual design and initial prototype of optical smartcard authentication technique.

(2) Continued survey, prototype, and testing of low-cost secure volume technologies, including capacitive, piezoelectric, guided acoustic wave, titanium/carbon, and conductive foam.

(3) Concluded adversary analysis of Concept of Operations (CONOPS), which documents system architecture, hardware, and software components, and submitted a report. We concluded that the CONOPS has no obvious flaws; concepts are sound and approach is secure. Method of implementation is critical for later adversarial analysis efforts.

(4) Continued survey, procurement, and testing of smartcard integrated circuit devices.

Publications

Refereed

Frankel, Y., and M. Yung. 1996. "Protective Sharing of Any Function: Trust Distribution via Secure Multi-Coprocessors." *Proc. 1st Internat. Conf. on the Theory and Applic. of Cryptology–PragoCrypt '96* 1 (Prague, Czechoslovakia, 30 September–3 October): 156–168. Prague, Czechoslovakia: CTU Publishing House.

Other

Moore, L. M., G. J. Bloom, P. S. Gemmell, and C. L. Musselman. 1996. "Concept of Operations for a Highly Secure Smart Card System," Sandia Technical Report, SAND96-0109, March.

Enhanced Internet Firewall Design Using Stateful Filters

J. A. Hutchins

Sandia examined a new approach to firewall design using "stateful" routers that allowed the simultaneous examination and manipulation of network packets at multiple levels within the protocol hierarchy. We designed a stateful firewall framework architecture and implemented a prototype base "operating system" using a workstation. We identified applications and developed prototype control entities over the framework architecture to filter these application protocols using the new stateful approach. We performed various tests to evaluate the prototype's and concept's functionality and performance.

To prevent attacks from outside networks, many sites protect their computers by placing them on an internal network and connecting to the outside through a "firewall," a device designed to allow only trusted, well-controlled connections to pass. Most designs today are primitive, using basic packet filtering functions supplied in many of today's routers, or utilizing simple application gateways. The filtering performed in these routers is "stateless" since each decision is based solely upon the information contained in the packet. Application gateways can provide a higher degree of security by allowing the whole data stream to be inspected in context, but at the cost of considerable software development and poor performance.

A new approach became necessary that combines these two technologies. A device that can filter those aspects of a protocol that are well-suited for it at a lower level, and those at a higher level that are not, can benefit by operating at the lowest level currently necessary to accomplish the task. Such a device can switch the level at which it is operating on the fly. This allows the modification of the data stream by a higher-level application for such purposes as adding or strengthening authentication information without impacting the performance once the exchange is completed.

In this year of the project, we completed a prototype system that implemented the lower level of the stateful filter architecture developed during the project's first year, as well as the development of some prototype upper-level systems to handle identified test protocols. While the lower-level system is automatically able to handle general filtering rules like a normal filtering router, the upper-level systems define and enforce the rules for specific protocols. The prototyped protocols include FTP (File Transfer Protocol), Telnet, and HTTP (HyperText Transfer Protocol).

We performed various tests on the prototype and found good controllability and robustness as well as little or no degradation in performance despite the initial test system being a lower-power SunSPARC IPC. While the prototype system provided ethernet-to-ethernet functionality, the good performance characteristics suggest that higher-speed networks such as Fiber Distributed Data Interface (FDDI) should be achievable with newer, higher-speed workstations or customized processors incorporated into router-firewalls.

We noted that while no known commercial product utilized these techniques at the time the project began, many commercial firewall products are beginning to utilize aspects originally proposed for the "stateful router," though today solely for two protocols, User Datagram Protocol (UDP) applications in general (normally with no regard for what application is employing UDP), and FTP to guard against unrequested port requests. For these products, we observe outgoing packets, and if an operation is requested from the inside, we allow the outside entity to perform it (such as to send a file requested via FTP), but block unrequested operations.

Publications

Other

Hutchins, J. A. 1996. "Firewall Design." Paper presented to Lawrence Livermore National Laboratory, Livermore, CA, 17 October.

Network-Based Collaborative Research Environment

D. Callow

A VCE (Virtual Collaborative Environment) is a system for sharing mechatronic technologies (e.g., robots or machine systems and associated software) among a group of participants. The basic VCE approach is analogous to how multi-user computers are shared by many users. In a multi-user computer environment, the computer is brought virtually to the desk of the user by redirecting the computer's data streams (e.g., a terminal is a virtual connection to the operator's console). In a VCE system, machines are brought virtually to the desks of the users through simulated or graphical representations of the machines. Development of a true VCE will enable team-based research in important areas such as advanced manufacturing and environmental clean-up. In addition, the environments developed to support VCE then become the distributed system control environments that enable agile distributed enterprises. VCEs enhance technology transfer since individual organizations can access large, dispersed resources to stimulate their technology environment. Thus, for example, a small developer of software can access the VCE and test new software innovations on actual state-of-the-art equipment located at Sandia.

The main goals for this project in FY96 were to attempt to lower the cost of the VCE developed under this project in FY95, to complete testing of the system, to continue in the technology transfer efforts, and to have outside potential users evaluate the system. We successfully accomplished these goals during FY96. Specifically, FY96 accomplishments include the following:

(1) Solicited evaluations by several potential users of VCE technology by customer site visits, trade-show demonstrations, conference presentations, technical papers, and technical proposals. We published an internal report of these potential user evaluations and developed application models for virtual system evaluation and analysis.

(2) Developed full-scale interface systems for both local and remote operators using low-cost hardware and

software, including interfacing low-cost remote and local systems and interfacing a low-cost remote system with a high-performance local system.

(3) Sponsored an interface workshop at a national robotics conference.

(4) Completed testing of the VCE system.

Deneb Robotics is now offering a VCE environment on their robot simulation software as a result of working with us on the VCE technology.

Publications

Other

Davies, B. R., and R. D. Palmquist. 1996. "System Composer: Technology for Rapid System Integration and Remote Collaboration." Paper presented to the IEEE International Conference on Robotics and Automation, Albuquerque, NM, 22–28 April.

Davies, B. R., F. J. Oppel, and R. D. Palmquist. 1995. "Remotely Accessing and Integrating Mechatronic Resources Over Networks Using Virtual Collaborative Environments (VCE) and the Distributed Collaborative Workbench (DCW)." *Proc. Internat. Robots and Vision Automation Conf.* (Detroit, MI, 8–11 May): 4-27–4-38.

Davies, B. R., M. J. McDonald, and R. W. Harrigan. 1994. "Virtual Collaborative Environments: Programming and Controlling Robotic Devices Remotely." Paper presented to the SPIE Telemanipulator and Telepresence Technologies Conference, Boston, MA, 31 October–2 November.

Harrigan, R. W., M. J. McDonald, and B. R. Davies. 1994. "Remote Use of Distributed Robotics Resources to Enhance Technology Development and Insertion." Paper presented to the ISRAM '94, Maui, HI, 14–17 August.

McDonald, M. J., and L. Ice. 1997. "Rocinante: A Virtual Collaboration Visualizer." Paper to be presented to the ANS 7th Topical Meeting on Robotics and Remote Systems, Augusta, GA, 28–30 April.

McDonald, M. J., D. Small, C. Graves, and D. Cannon. 1997. "Virtual Collaborative Control to Improve Intelligent Robotic System Efficiency and Quality." Paper presented to the IEEE ICRA '97, Albuquerque, NM, 12 February.

Oppel, F. J., and R. D. Palmquist. 1996. "A Systems Configuration Toolkit for Modular Integration of Mechatronic Resources." Paper presented to the 3rd IASTED Conference of Robotics and Manufacturing, Cancun, Mexico, 3 April.

Object-Oriented Parallel Discrete Event Simulation System—An Enabling Foundation for Rapid Development of High-Performance, Large-Scale Simulations

M. M. Johnson, E. J. Friedman-Hill, M. E. Colvin

Traditional discrete-event simulations employ an inherently sequential algorithm and are run on a single computer. However, the demands of many real-world problems exceed the capabilities of sequential simulation systems. Often the capacity of a computer's primary memory limits the size of the models that can be handled, and in some cases parallel execution on multiple processors could significantly reduce the simulation time. Parallel discrete-event simulation is a research topic in academia; no parallel discrete-event system exists that satisfies the software engineering requirements of robustness, portability, and scalability.

We are developing a parallel, distributed, discrete-event simulation system that is robust, portable, and scalable. The system is based on a conservative simulation protocol and maps a message-based model of distributed computing onto an object-oriented programming model. It is portable across heterogeneous computing architectures, including single-processor systems, networks of workstations, and multiprocessor computers with shared or distributed memory. The primary goal of the software system is to provide a simple, sufficient application programming interface (API) that can be used by scientists to quickly model large-scale, complex systems. In the background and without involving the user, the simulation system will be capable of making dynamic use of idle processing power available throughout the enterprise network.

We completed all FY96 milestones in the original proposal. We selected the underlying communication mechanism and finished the design and an implementation of the abstract simulation API on the Silicon Graphics, Inc. (SGI) Irix platform. Through the application of object-oriented design techniques, we were able to encapsulate the simulation infrastructure (messaging and timing mechanisms). We have already made practical use of the simulation API, developing example models using the system.

We structured the system architecture to support two disparate areas of simulation: (1) batch-oriented simulations (BOS), where legacy codes can be bundled with input and run remotely over any number of network available machines, and (2) real-time simulations of enterprise models (EM), supporting object-oriented discrete-event simulation across networks of heterogeneous machines. In support of these models, we developed the Infrastructure for Distributed Enterprise Simulation (IDES). We have begun work to complete the implementation of the simulation API on the Win32 platform. The current hypertext design documentation is located at URL: *http://agatha.ran.sandia.gov/~mmjohns/ides.html.*

Reliability Assessment of Dynamic Communication Networks

G. D. Wyss

This project seeks to develop a quantitative risk-based design and analysis methodology for data networks. Most risk assessments of complex information systems have produced only qualitative results, while previous probabilistic risk assessment approaches to communication networks have been hampered by a combinatorial expansion of the analysis effort as the number of network nodes increases. A quantitative risk-based reliability analysis method would be useful to groups as diverse as Sandia, communication equipment manufacturers, network service providers, and the Federal Communications Commission (FCC).

Our approach was to form an interdisciplinary team with expertise from diverse fields, including information surety, network management, and the probabilistic risk assessment, to incorporate features from all appropriate disciplines. We extended methods developed for analysis of the public telephone network common channel signaling network to remove the limitations peculiar to that specific architecture. We adapted existing software tools to enable their application to this new class of problems. Finally, we demonstrated the resulting methods by analyzing demonstration problems that represent typical installed network architectures.

This project determined that each type of network can be placed into one of two classes based on its physical and logical architecture: hierarchical or nonhierarchical.

We found that the connectivity nonhierarchical networks can be adequately modeled using fault-tree analysis, and developed a "plug-and-play" fault-tree analysis methodology to assist persons who are not risk-analysis experts in analyzing networks. We also found that one can easily extend these connectivity models to consider the availability of network services, as well as classes of network traffic.

We also found that nonhierarchical networks cannot be adequately modeled using fault trees because of the combinatorial expansion that can occur as one considers all paths between nodes in the "everybody can talk to everybody" problem. For this reason, we developed a new, efficient method that searches for cut sets from such networks without the need to construct a fault-tree model. The method obtains orders-of-magnitude-speed increases over traditional search methods because it first searches for cut sets based only on link ("edge") failures, then infers the existence of (but does not construct) the combinations of link and node failures that can cause a lack of network connectivity. A link cut set that contains n links can generate up to 3^n power cut sets based on both link and node failures. Since our method does not have to generate or perform Boolean reduction on these cut sets, it achieves dramatic computational savings over previous methods. This method is the subject of a patent application.

We found that networks in which some parts are hierarchical while others are not can be modeled by combining the results of the two methods we developed using simple mathematical rules. We applied these methods to a variety of typical network architectures to demonstrate the method.

Publications

Refereed

Wyss, G. D., H. K. Schriner, and T. R. Gaylor. 1996. "Probabilistic Logic Modeling of Network Reliability for Hybrid Network Architectures." Paper presented to the 21st Annual IEEE Conference on Local Computer Networks (LCN '96), Minneapolis, MN, 13–16 October.

Other

Wyss, G. D., H. K. Schriner, and T. R. Gaylor. 1996. "Risk and Reliability Assessment for Telecommunications Networks." *Proc. Probabilistic Safety Assessment, Moving Toward Risk-Based Regulation (PSA '96)* 1 (Park City, UT, 30 September–3 October): 167–174. American Nuclear Society.

Wyss, G. D., S. L. Daniel, H. K. Schriner, and T. R. Gaylor. 1996. "Information Systems Vulnerability: A Systems Analysis Perspective." Paper presented to the American Defense Preparedness Association Joint Security Technology Symposium, Williamsburg, VA, 17–20 June.

Agent-Based Remediation of the Mosaic Classification Problem

E. J. Friedman-Hill, R. L. Clay

The term mosaic classification problem *refers to the possibility that a collection of unclassified data could be used to infer classified information. With the increasing use of intranets at Sandia to publish and distribute information, the possibility of such situations occurring is on the rise.*

In this project, we are investigating the feasibility of building software agents that help mitigate this problem by searching for examples of mosaic classified information in the data accessed by one individual on a computer network and notifying appropriate personnel if such examples are found. We are building the agents using recently developed portability technologies, which makes them extremely platform-independent and mobile.

We accomplished the following in FY96:

(1) Designed and implemented JIDL, the first software solution for using the Java programming language with the distributed object architecture CORBA. JIDL was a proof-of-concept project, the announcement of which resulted in technical contacts with DEC, Expersoft, Apple, and other companies.

(2) Designed, implemented, and distributed Jess, the Java Expert System Shell. Jess is a clone of CLIPS, a popular shell written and distributed by NASA. Jess and JIDL interoperate extremely well, allowing distributed rule-based systems to be built easily. Jess has been distributed as free software and has more than 1200 registered users around the world. See *http://herzberg.ca.sandia.gov/jess* for more information, a demo, and to obtain Jess source code.

(3) Implemented a functional English-language parser in Java, which serves as an input module for the developing agents.

(4) Demonstrated distributed operation of the combination of the above three components, during which textual information from Sandia's internal web was browsed, parsed, and rephrased by the agent.

(5) Contributed to the development of Idldoc, a documentation tool for CORBA IDL objects.

Biometric Identity Verification for Remote-User Authentication and Access-Control Applications

A. M. Bouchard, J. W. Bartholomew, R. F. Martinez, J. J. Carlson

The goal of this project is to research and develop a new biometric identity verification system that not only is reliable and user-accepted, but that also addresses the needs of remote access applications. Our approach emphasizes three innovative concepts: (1) the use of an entirely new biometric, the acoustic signature of the individual's ear canal, (2) the fusion of multiple biometric features, and (3) remotely extracting, digitizing, and encoding the biometric data. We envision incorporating all of the required sensors for the multifeature data acquisition into a single compact and affordable device, capable of communicating digitized and encoded data via modem over an ordinary phone line. Our goal is to exceed the performance achieved by the best remote access (speaker verification) systems currently available.

We completed construction of a prototype device to acquire acoustic data from the ear and store the data on a computer. It consists of a speaker and microphone strategically placed relative to the individual's ear. A computer-generated signal, a broadband soundburst, drives the speaker; the response signal detected by the microphone is digitized and stored on the computer for analysis. We acquired extensive data on a small number of individuals. Spectra-like features extracted from the data appear to distinguish individuals effectively.

We purchased microphones and associated software for recording voice waveforms on the computer. We developed several feature-extraction algorithms for the voice. Some are standard speaker-recognition features from the literature, including linear-predictive-coding cepstral coefficients and delta-cepstra. Others are more speculative, including the attack and decay times of certain phonemes.

We investigated several image-based biometrics to select one that appears to be particularly promising from among many possible choices. The image-based biometrics considered were face, face profile, hand-geometry, iris, and fingerprint. From those considered, we implemented the face, face profile, and hand-geometry for further investigation. Based on a comparison of the features acquired from these three different image types, we selected hand-geometry for extensive investigation. We have now established a data base of 1000 hand images acquired for each of 100 individuals.

Development of an Intelligent Geographic Information System

T. E. Drennen, L. A. Malczynski, D. Brown

The goal of this project was the development of a tool that combines Dynamic Simulation Modeling (DSM) and Geographic Information Systems (GIS) software so as to allow geographic visualization of policy options for a wide range of applications. We met our technical milestones for the first year.

Combining DSM and GIS capabilities into a state-of-the-art policy support tool has not yet been attempted. The GIS/DSM project took a novel approach—direct communication between the two tools. This approach allows an effective and efficient use of funding resources to permit full access to the power and flexibility of each tool without the added burden of a shell or custom file translation. A literature review indicates that this is a wished-for but missing "next-generation" technology.

We accomplished the following:

(1) Assessed Windows GIS software. Developed criteria and analysis methodology for comparison of both client/server and component GIS technologies.

(2) Assessed several DSM software products. Selected Powersim for the DSM software.

(3) Conducted literature reviews on technical integration issues.

(4) Reviewed and tested alternative methodologies for linking GIS/DSM.

(5) Developed a generic software script library (referred to as the Generic ArcView Object-Style Scripts Library, or GAVOS) for linking to the ArcView GIS (Sandia Technical Advance Filing SD-5842).

(6) Developed SylvanShadow, a Dynamic Link Library (DLL) for the SylvanMaps/OCX GIS component.

(7) Developed collection of ArcView utility scripts and objects.

(8) Designed a graphical user interface (GUI) and began implementation of design using Visual Basic.

(9) Conducted literature reviews, including discussions with national experts, on potential policy applications, including climate change, energy flows, and nuclear smuggling.

(10) Developed simple policy model (climate change) for prototyping.

Use-Control of "Robustness-Agile" Encryption Devices

T. D. Tarman, B. J. Wood, L. G. Pierson

The current state-of-the-art in asynchronous transfer mode (ATM) network encryption technology is "key-agile" encryption; that is, an encryption device that can maintain an independent encryption context for each virtual circuit that passes through it. Although key-agile encryption saves money and physical space by allowing a single device to serve the encryption needs of a group of users, it can only provide one level of "cryptographic robustness" for the group. ("Cryptographic robustness" refers to the strength of the encryption algorithm and depends on the algorithm and the length of the key.)

The purpose of this project is to develop "robustness-agile" ATM encryption technology and a prototype unit that is capable of associating separate cryptographic robustness levels with different ATM virtual circuits. In addition, we will develop appropriate use-control measures. These measures will allow a site security officer to ensure that users who are not authorized to use the more "robust" algorithms available in the encryptor will not have access to them (and hence, access to data that may exceed the clearance level of the user).

We accomplished the following in FY96:

(1) Completed architecture design. We developed system-level and basic unit-level design descriptions. System-level components include the encryption hardware, public-key certificate server, access control (policy) server, and ATM network components. Unit-level components include encryption modules, ATM cell multiplex/demultiplex, authentication/authorization functions, access control list client, and certificate client.

(2) Completed study of use-control mechanisms and made recommendations. As a result of the architecture study described above, particularly the study of authentication methods, we decided to adopt a single-level authentication engine resident in the robustness agile encryption (RAE). The specific algorithm and level of robustness for authentication will be determined by policy, rather than technically (e.g., via some sort of mapping to the level of encryption robustness). The authentication engine itself will be integrated with the signaling software in the RAE and will be based on the Rierivest Shamir Adleman (RSA) algorithm. We determined that RSA scales better to large networks than the other authentication alternatives.

(3) Developed a mechanism that can quickly switch cryptographic context. (The context information includes algorithm, key, and algorithm robustness.) We will pursue a two-stage mechanism for switching cryptographic contexts. The first stage consists of a fast content addressable memory (CAM) that provides an index to the cryptographic module. The second stage will use the index to address context information in a flat memory. We selected this two-stage approach because it scales well in terms of speed and number of supported algorithms.

(4) Determined the RAE's effect on ATM quality of service. We determined the effects of RAE on ATM quality of service analytically and validated them through simulation. We documented the results of this study and will validate further once the encryption hardware is built.

Publications

Other

Pierson, L. G., and E. L. Witzke. 1996. "The Role of Decimated Sequences in Scaling Encryption Speeds Through Parallelism." *Proc. IEEE 15th Ann. Phoenix Conf. on Comp. and Comm.* **96CH35917** (Phoenix, AZ, 27–29 March): 515–519.

Tarman, T. D. 1996. "Mechanism for Control Plane Authentication." Paper presented to the ATM Forum Technical Committee, Orlando, FL, 9–14 June.

Tarman, T. D. 1995. "Requirements for Signaling Channel Authentication." Paper presented to the ATM Forum Technical Committee, London, UK, 11–15 December.

Tarman, T. D. 1996. "Security Technologies and Protocols for Asynchronous Transfer Mode (ATM) Networks." Paper presented to the 12th Annual Joint Government-Industry Symposium and Exhibition on Security Technology, Williamsburg, VA, 17–19 June. American Defense Preparedness Association.

Virtual Channel Encryption

D. J. Gibson

Modern networked computers typically support multiple simultaneous "virtual" communication channels to different destinations over a single physical connection to a data communication network. This project is the development of a proof-of-concept system that will support the encryption of multiple virtual channels over the single physical connection between the computer and the network, eliminating the need for multiplexing and demultiplexing operations and individual encryption devices for each channel. We are developing both a software module for installation in the user's computer and an external hardware module to perform these functions. Issues being addressed include maintenance of multiple encryption algorithms inside a single encryption device, synchronization of multiple encrypted virtual channels, transmission of routing information through the encryption units, and key handling.

We completed work on the virtual circuit encryption software for operation on a SUN workstation running the Solaris operating system. We demonstrated the operation of this software by running a "telnet" session between two SUN workstations using the virtual encryption software to encrypt the communications channel. We installed a copy of Kerberos, the network security software from the Massachusetts Institute of Technology, on a SUN workstation and examined its principles of operation to perform key distribution and access control functions for the virtual circuit encryption software. We obtained the necessary VME (Versa Module Eurocard) hardware to support the development of a hardware version of the virtual circuit encryption processor, and also installed a copy of the VxWorks development system from Wind River Systems on a SUN workstation to support development of the virtual circuit encryption hardware processor. We did some development work on the hardware processor, but could not complete it by the end of the project.

Data Zooming—A New Physics for Information Navigation

G. S. Davidson

This research project, in collaboration with the University of New Mexico (UNM), used Pad++, a user interface originally developed at Sandia. The objective was to explore the utility of that user interface to large data bases of information such as those found on the World Wide Web (WWW). We developed a web browser based on Pad++ in the first year of this project. We documented the first-year results, including the human factors, in a video and presented them at a Sandia-wide seminar. The second year of this research project focused on applying the results of the first-year research. The work in the second year involved using Pad++ as a basis for tools to manage large complicated web sites. Pad++ is ideally suited to this complex activity. We developed a prototype, which presents Web relationships in 3-D hyperspace, following research from the Geometry Center at the University of Minnesota. We completed various human factors studies, which indicate Pad++ web browsers allow users to comprehend 23% faster than when using Netscape.

Sandia has an exceptionally well-designed, very complex internal website (intranet). As websites like Sandia's grow in complexity and size, better tools are needed to design, develop, and manage them. Because Pad++ is very well suited to navigating large data spaces made up of diverse data, it seemed natural to investigate using Pad++ as a tool for Website design and maintenance.

We added a Sandia staff member on the EVE team (Sandia's internal web) to the project to provide suggestions on what would be useful in a website design and maintenance tool. He provided feedback on the utility of the tool as the prototype was developed.

We began the process by outlining what was involved in designing a website. Some of the tasks involved in this process are to identify needs, define the target audience, write down the objectives of the site, outline the content, and create a rough map of the site.

We identified desirable features for a website design tool based on multiscale user-interface technology. The tool should have an intuitive combination of frame and graphical user interface (GUI)-based authoring. All design tasks should be interrelated, not separate elements. Templates should be provided that would make the tool easier to use.

For existing sites, the tool should automatically create a layout of the site, which could be easily viewed using Pad++. For site maintenance, portal filters could be used to highlight specific file types. An analysis capability should be developed to determine if the site is meeting the original design goals. A weighting scheme should be developed to determine if the target audience is visiting the intended pages at the site.

Other capabilities already supported in the Pad++ substrate used in this prototype are the directory browser and the hyptertext markup language (HTML) browser (including the camera view). Applying other research, such as the concepts in HyperG, also provided a more intuitive method for defining the structure of the site.

Varying amounts of text related to a link can be displayed by using the zoom factor. From far away, the links in a document may appear as lines; as you get closer, additional information is provided, including keywords, titles, and abstract information.

Publications

Refereed

Bederson, B. B., J. D. Hollan, J. Stewart, D. Rogers, A. Druin, and D. Vick. 1996. "A Zooming Web Browser." *Proc. SPIE Multimedia Computing and Networking* **2667** (San Jose, CA, January): 260–271.

Bederson, B. B., J. D. Hollan, J. Stewart, D. Rogers, A. Druin, D. Vick, L. Ring, E. Grose, and C. Forsythe. 1997. "A Zooming Web Browser." Chapter 22 in *Human Factors and Web Development.* Edited by C. Forsythe, J. Ratner, and E. Grose. Lawrence Earlbaum, pub.

Davidson, G. D., and J. F. Mareda. 1996. "Data Zooming—A New Physics for Information Navigation." Sandia Technical Report, SAND96-3003, December.

Advanced Concurrent Engineering Environment

J. N. Jortner, J. A. Friesen

Sandia demonstrated large-scale virtual reality (VR) in a conference room-size environment. Using a high-end visualization server, 3-D modeling and animation software, and leading-edge World Wide Web (WWW) technology, we simulated a collaborative engineering environment where a design team was able to work together, rather than as solely disjointed individual efforts. Work focused on the installation of hardware for visualization and display, and the integration of software tools for design and animation of 3-D parts. Finally, we created an animation of a Sandia part and generated a computer video. This video is now accessible on a Sandia internal web server.

A VR environment provides an engineer the capability to design, assemble, and test a simulated component, subsystem, or system before actual production. In the immersive collaborative environment, a design team is able to work together rather than in disjointed individual efforts. This environment can be used to facilitate interactions between design, manufacturing, and stockpile support personnel while still in the design stage.

The Sandia part chosen for demonstration of the advanced concurrent-engineering (ACE) environment was the MC4438 single stronglink assembly (SSA). This mechanism is one of two independent stronglinks used in the Pit Reuse for Enhanced Safety and Security, Cruise Missile (PRESS/CM) applications. The stronglink is a rugged, mechanical device used to ensure the safety of nuclear weapons in both normal and abnormal environments. In the prototype ACE built for this project, the simulated design team was able to view and manipulate the SSA by using both a solid modeling application (ProEngineer) and an interactive engineering visualization/animation tool (Visfly/Vislab). Additionally, we generated a static VR modeling language (VRML) model of the assembly and a kinematic animation for viewing with a WWW browser.

The results of this project demonstrated the following capabilities:

(1) Achieved immersion of an entire work group into a 3-D scene for a greater sense of reality, while permitting close interaction and communication between team members as they navigated interactively through the simulated component, subsystem, or system.

(2) Quickly generated real-time motion simulations of mechanical assemblies imported as ProEngineer models.

(3) Distributed results to remote locations using web technology.

We performed demonstrations for several groups at Sandia, all of which are very interested in applying this test-bed to their projects. For example, the animation of the SSA was the first time the designers of the assembly were able to demonstrate the motion of the mechanism without having to use a physical model. Based on the feedback from Sandia project managers and engineers, we recommend the following: (1) expand to include links to engineering analysis (kinematics, finite element, test data); (2) continue development of the environment into a larger system; and (3) apply system to other projects that can reap immediate benefits.

Other–Counterproliferation

High-value facilities such as this aircraft hanger are being built deeper underground, making them less vulnerable to current conventional weapons. Enhanced attack options are required to hold these facilities at risk. New computational techniques for the higher-velocity region between strength dominance and hydrodynamic behavior are being developed.

Electromagnetic Induction Tunnel Detection

D. H. Cress, B. C. Brock, L. C. Bartel, R. V. Duncan

Subsurface structure detection is a priority capability for inspection and for surveillance of activities of threatening nations. We directed this work toward developing (1) an improved instrument for detection of electromagnetic (EM) fields induced by subsurface structures, (2) an improved EM model to predict fields induced by an arbitrary 3-D subsurface source, (3) theoretical analysis of a conceptual system for further improvement, and (4) an analysis of the potential EM receiver. We demonstrated the improved system for several stand-off transmitter and receiver offset distances, underground structure geometries, and source depths. Underground source depths ranged from 5 meters to more than 30 meters. Frequency ranges of demonstrated performance ranged from 5 kHz to 100 kHz.

Our accomplishments in FY96 include the following:

(1) Developed an improved instrument for measuring the induced currents in subsurface structures by (a) removing far-field illuminations through use of a gradiometer, (b) achieving very high signal gain through use of coherent signal integration and very narrow noise bandwidth, and (c) by multifrequency agility (five preselectable frequencies).

(2) Developed an improved design for the gradiometer with emphasis on digital design components and coherent integration analysis to define the digital dynamic range requirements.

(3) Demonstrated detection performance at three subsurface structures: U.S. Geological Survey (USGS) Seismological Facility (Kirtland AFB, NM); Cloud Chamber (Nevada Test Site [NTS]); and Yucca Mountain Exploratory Tunnel. Structures varied in depth from 5 meters to more than 30 meters. DOE supported the field tests at NTS under separate funding.

(4) Implemented a 3-D frequency domain EM numerical solution for sensing buried man-made structures in the earth that includes "perfect conductors" in arbitrary geometries.

(5) Analyzed the potential of Superconducting Quantum Interference Device (SQUID) technology for improving the EM response over the frequency range of interest (1 kHz to 500 kHz).

(6) Evaluated a University of Arizona (Department of Mining and Geological Engineering) geophysical system that measures the polarization rotation between the illuminating and received EM fields for detection of subsurface anomalies.

Publications

Refereed

Cress, D. H., and L. C. Bartel. 1996. "Sensing of Gradient Electromagnetic Fields from Subsurface Conducting Targets." Paper presented to IEEE International Geoscience and Remote Sensing Conference, Lincoln, NE, 27–31 May.

Newman, G. A., and D. L. Allumbaugh. 1996. "Three-Dimensional Electromagnetic Modeling of Highly Conductive Man-Made Structures in a Lossy Earth." Paper presented to IEEE International Geoscience and Remote Sensing Conference, Lincoln, NE, 27–31 May.

Sternberg, B. K., and M. M. Poulton. 1996. "Demonstration of the LASI High-Resolution Electromagnetic Sounding System at the Nevada Test Site." Paper presented to IEEE International Geoscience and Remote Sensing conference, Lincoln, NE, 27–31 May.

Other

Allen, C. T. 1995. "Electromagnetic Induction Research Issues: Magnetic Dipole and SQUID Technologies." *Report: University of Kansas Contract No. 95-10* (September). Manhatten, KA: University of Kansas.

Sternberg, B. K., and M. M. Poulton. 1996. "LASI Ellipticity Survey at the Nevada Test Site for Sandia National Laboratories." *Report: University of Arizona Contract No. AS-2042-0144* (29 June). Tucson, AZ: Laboratory for Advanced Subsurface Imaging.

Theater Missile Defense Integrated Simulation

J. I. Crowther, R. M. Allen

Scabbard Threat Generator: *In FY96, we conducted two tests at the Theater Air Command and Control Simulation Facility (TACCSF) of the Scabbard threat generator we developed during FY95. Some incompatibilities surfaced during the first test, which we addressed at our Sandia/CA Distributed Interactive Simulation (DIS) facility. During the second test, we successfully transmitted threat data that we then correctly processed and displayed by other LAN workstations, including a Joint Surveillance and Target Attack Radar System (JSTARS) emulator.*

Sensor Evaluation Model (SENSEM): *We completed development and coding of algorithms that represent transmission of pressure waves from missile launch events to seismic launch-detection sensors. These algorithms include user-defined parallel-layer geology configurations and produce perceived missile launch-point location envelopes. We used these new features in SENSEM to investigate sensitivities of launch-point estimation and missile intercept to sensor performance parameters and operational deployment factors.*

This research produced a unique means to investigate important Theater Missile Defense sensor applications.

Research during FY96 closely followed our proposed plan concerning both the SENSEM model and the distributed Scabbard threat generator, extending progress made during the first year of this project.

Scabbard Threat Generator: We conducted a test of our DIS-compatible Scabbard threat generator at the TACCSF at Kirtland AFB in early FY96. Threat data were successfully passed through the TACCSF gateway across the national DIS network to a workstation at the Theater Battle Arena in the Pentagon. Some incompatibilities surfaced during this experiment connected with the timing of threat updates provided by the Scabbard tape player to the more complex TACCSF local-area network (LAN). Following the experiment, we modified the threat generator at our Sandia/CA DIS LAN to fix the timing problems and acquired an alternate DIS interface software package. We then conducted a follow-on test of the threat generator at the TACCSF in late FY96 and demonstrated successful transmission of our threat data across the LAN. Our threat data were processed and displayed correctly by other LAN workstations, including a Grummann JSTARS emulator.

SENSEM Model: We completed development and coding of methodologies begun in FY95 that represent the transmission of pressure waves from a missile launch event at the earth's surface through parallel layers of geology (with differing sound speeds) to seismic sensor locations also at the earth's surface. We then incorporated these algorithms into the SENSEM model; they now produce perceived missile launch-point locations based on relative times-of-arrival of the seismic wave from the launch event at the various sensor locations. A range of sensor performance capabilities can be represented by means of the sensor line-of-bearing performance data tables in the model. Using these new features in SENSEM, we conducted an investigation of launch-detection sensor sensitivities. Results included launch-detection accuracies and missile-intercept probabilities as a function of numbers of seismic sensors deployed, deployment patterns, and sensor performance parameters.

As a result of the above research, we developed a unique and practical means to investigate, evaluate, and demonstrate important sensor technologies applied to the Theater Missile Defense problem.

Fiber-Optic Biosensors for Biological Warfare Counterproliferation

J. S. Schoeniger, C. E. Hackett, P. H. Paul, D. J. Rakestraw

The goal of this project is to develop technologies for improved detectors for biological warfare (BW) agents. The project focuses on exploring ways in which the interface between engineered biological materials and optical, chemical, and systems engineering can be improved to form a foundation for sensor technologies that are agile (i.e., can be adapted to new threats), sensitive, and scalable to large numbers. The approach taken is to implement fluorescence-based fiber-optic immunosensor designs for Clostridial toxins (e.g., tetanus and botulinum). Questions addressed include:

(1) Can modular fiber-optics, small solid-state lasers, and novel waveguide designs improve sensor performance?

(2) How may recombinant deoxyribonucleic acid (DNA) engineering of biomolecules be used to produce materials for biosensor applications?

(3) What are the most effective bioconjugate chemistry approaches to create the interface between the molecular-recognition event and the sensor response?

This report discusses progress made during the first year of this project toward answering these questions.

Proliferation of BW agents (e.g., biological toxins) is recognized as one of the greatest potential threats to national security. A critical need exists for sensors to detect agents at sub-lethal concentrations. Discrimination of agents from natural background is not possible using traditional chemical sensor technologies, but is a suitable application for biosensors that employ biomolecules as molecular-recognition elements. Using biotechnology, antibodies (Abs) may be designed that bind to a designated molecular target species with great affinity and selectivity. Abs immobilized on a surface may be used as the basis for an assay or sensor system for the target molecule: immobilized on the surface of an optical component, they can form a fluorescence-based optical immunosensor, if the binding of the target molecule can be coupled to a change in the fluorescence of the surface.

Outstanding problems include integration of compact optical sources, optical components, and microfluidic components into an easily manufacturable design; and improving the cost and properties of Abs and Ab bioconjugates.

(1) We optimized procedures for covalent immobilization for Abs on silica surfaces. We found that 20–50% of a theoretical Ab monolayer could be achieved, and measured immobilized Ab dissociation constants on the order of 10^{-7} Molar, demonstrating functional attachment. We made flow-through immunosensors with micromolar sensitivity thresholds.

(2) We found compact near-infrared (NIR) diode lasers combined with suitable NIR fluors (cyanine dyes) to be preferable for fluorescence biosensors. We tested compact diode-pumped YAG (532 nm) lasers with fluors such as BODIPY and rhodamine, but encountered excess background fluorescence from optics and biomolecules. Minimizing discrete optics and utilizing modular fiber-optic components maximized flexibility of system configurations.

(3) We found a novel hollow-fiber multimode waveguide to be capable of exciting and capturing fluorescence on its surface using evanescent-wave coupling. This design can be manufactured inexpensively, and covalent attachment of Abs using organosilane crosslinkers can be accomplished using flow-though techniques.

(4) We were able to produce recombinant Abs to tetanus toxin in a baculovirus expression system. We also used nontoxic recombinant toxin fragments for safe sensor development.

We recommend the following:

(1) Optimize covalent attachment techniques for attachment of monoclonal anticlostridial Abs to optimize sensitivity.

(2) Fabricate second-generation hollow waveguides using ceramic claddings and characterize efficiency of excitation and fluorescence collection.

(3) Continue work on expression of recombinant anticlostridial Abs to increase expression levels, and create materials for regenerable Ab surfaces (e.g., Ab-avidin fusion proteins).

Moving Mass Trim Control for Precision-Strike Warheads

B. R. Sturgis, R. D. Robinett

Precision-guided warheads are critical to improving the effectiveness of nuclear and conventionally armed strike systems. This research project will develop a validated simulation tool for the design and evaluation of moving mass controllers on precision-guided reentry systems. The simulation tool will include a multiple-body dynamics model, an autopilot model, and a guidance system algorithm. Sandia will design, build, and test a prototype moving mass controller, based on the Mk4 reentry body, for the purpose of gathering experimental controller performance data. We will use the data to validate the modeling and simulation process.

We accomplished the following in FY96:

(1) Developed two guidance algorithms for the moving mass controller. We chose one for use in the final simulation tool.

(2) Integrated the general-purpose simulation tool, the autopilot, and the guidance algorithm.

(3) Completed several detailed system simulation studies to assess the overall performance and to refine the moving mass controller design. The moving mass controller hardware was redesigned as a result of some of these simulations.

(4) Completed 90% of the mechanical design of the moving mass controller hardware.

(5) Procured long lead items needed to build the prototype moving mass controller.

Results from simulation studies indicated the need for a moving mass unit that takes up less volume and consumes less power than the original hardware design. The redesigned hardware accomplishes this goal.

System simulations indicate that moving mass controllers are capable of removing inaccuracies introduced by booster pointing errors, ablation effects, etc. Since the moving mass unit is internal to the reentry vehicle, there is no change in the aerodynamic properties of the reentry vehicle. This means that a moving mass retrofit to an existing system may be performed at relatively low cost.

Publications

Refereed

Dohrmann, C. R., G. R. Eisler, and R. D. Robinett. 1996. "Dynamic Programming Approach for Burnout-to-Apogee Guidance of Precision Munitions." *J. Guidance, Control, and Dynamics* **19** (2) (March/April): 340–346. Washington, DC: American Institute of Aeronautics and Astronautics.

Robinett, R. D., B. R. Sturgis, and S. A. Kerr. 1994. "Moving Mass Trim Control for Aerospace Vehicles." *Proc. Amer. Inst. of Aeronautics and Astronautics Missile Sciences Conf.* **19** (5) (Monterey, CA, 7–9 November): 1064–1070. Washington, DC: American Institute of Aeronautics and Astronautics.

Unexplored Penetrator Regime Against Super-Hard Underground Facilities

J. D. Rogers, N. R. Hansen, A. V. Farnsworth, S. W. Hatch

A major national security concern for the U.S. is how to put at risk the increasing number of hardened underground facilities that are being constructed throughout Russia and third-world countries. Both DoD and policy leaders are devoting attention to military options for countering weapons of mass destruction, all of which involve attacks against underground facilities. The primary option against underground facilities is the earth penetrator weapon (EPW).

The technology problem is that the target depth of these proliferating facilities is increasing, requiring higher-velocity penetrator impacts to put them at risk. Only three full-scale penetrator tests have been run from 3000 to 3500 fps, and there is no credible capability or knowledge base above 3500 fps. This proposal addresses the unexplored regime from 3000 fps (where strength behavior dominates) up to 10,000 fps (where the penetration process transitions to a hydrodynamic phenomenon). The research assembles a computational data base on system design, survivability, and weapons effects against a set of representative underground facilities. New computational techniques must be developed to address this unexplored regime between strength-dominated response and hydrodynamic behavior.

We considered a variety of targets, which we characterized by depth and hardness based on the latest intelligence information. We performed weapon effects and target response calculations for conventional and nuclear weapons options against a large set of targets. We included these calculations in the target characterization methodology producing a single measure that provides a useful starting point for weapon concept trade-off studies. Ongoing mission planning studies evaluate the potential merits of delivery concepts. We developed an abrasion model and implemented it in the CTH code. Work on the coupling of the Lagrangian and Eulerian codes has progressed and should be completed by the end of FY96. Test results from subscale penetrators and code predictions led to work on tailored nose hardness. Tests are under way to validate the computational method. Concepts for local hardening and/or softening the penetrator nose to develop a "self-sharpening" penetrator are also under way.

Publications

Refereed

Rogers, J. D., and D. S. Strack. 1996. "Holding Hardened Facilities at Risk." *Defense Intelligence Reference Document* **PC-8010-1-96** (March): iii–DL-2. Washington, DC: Defense Intelligence Agency.

Advanced Transportation

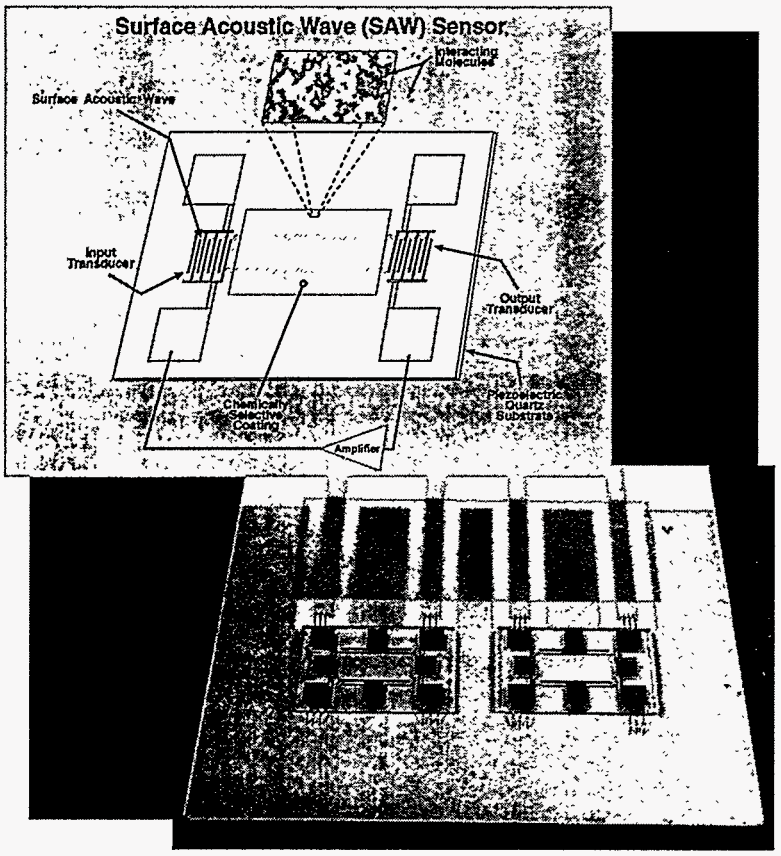

On-line, real-time monitoring of toxic exhaust gases is urgently needed to meet compliance with EPA atmospheric emission regulations for internal combustion engines. Surface acoustic-wave (SAW) devices are wire-bonded onto ceramic substrates *(lower photo)* and tested as gas sensors in high-temperature, simulated, vehicle exhaust environments. A schematic of SAW sensor operations is shown in the upper drawing.

Vehicle Exhaust-Gas Chemical Sensors Using Acoustic-Wave Resonators

R. W. Cernosek, K. O. Wessendorf, R. E. Anderson, G. C. Frye

A need exists for on-line, real-time monitors that continuously analyze the toxic gases—nitrogen oxides (NO_x), carbon monoxide (CO), and hydrocarbon (HC) species—found in vehicle exhaust. Directly measuring gas concentration simplifies documenting compliance to EPA atmospheric emission regulations. Additionally, such a monitoring system can be used in a closed loop for engine control and performance optimization, leading to better fuel efficiency, lower toxic emissions, and generally higher customer satisfaction. In this project we are developing acoustic-wave microsensors consisting of piezoelectric substrates coated with robust thin-film surface layers that have a specific affinity or reactivity to the target gas molecules. Acoustic-wave devices use quartz substrates for operating temperatures below ~ 500°C and $LiNbO_3$ substrates for higher-temperature implementations. Significant thin-film coating development is under way using pure and doped binary metal oxides (TiO_2, SnO_2, ZrO_2, and CuO), periodic mesoporous materials with specific ion binding sites, zeolites with controlled porosity to match the molecular kinetic diameters of target gases, and the noble metal catalytic films. When fully developed, these acoustic-wave sensors promise a unique combination of sensitivity, selectivity, size, and cost.

Acoustic-wave sensors indicate gas molecule concentration by measuring the shift in electrical operating parameters (resonant frequency or damping, propagation phase delay, or power loss) when the chemical species interacts with the sensor coating. Changes in the coating mass, surface temperature, or film conductivity are mechanisms that can produce a measurable response. We fabricated several acoustic sensors to measure the toxic gases found in vehicle exhaust.

Essentially all sensors characterized over the past year use ST-cut quartz crystals operating as 97-MHz SAW delay lines. Quartz has a Curie point of 573° C, and the ST-cut crystals have a frequency-temperature coefficient that is zero near 25° C with a quadratic dependence at higher temperatures. We tested bare and film-coated surface acoustic-wave (SAW) devices up to 450° C in a special thermally controlled test cell that allows temperature to be ramped over a specified range or fixed at any elevated temperature with a stability of < 0.2° C.

Device thin-film coating materials include the noble metal platinum; the undoped binary metal oxides TiO_2, SnO_2, and ZrO_2; and periodic mesoporous silica. We e-beam deposited polycrystalline platinum films ~ 500-nm thick between the SAW transducers and annealed them at 450° C. These devices act as hydrocarbon calorimeters or combustible-gas detectors. They exhibited no measurable response to 1% concentrations of CO and limited response above 400° C to 10% propylene in air. We measured sensitivity to hydrogen gas in air as 4.85×10^{-2} ppm Df/ppm H_2 at 300° C. The hydrogen-oxygen catalytic reaction at the hot platinum surface produces a temperature rise of several degrees. However, hydrogen atom trapping in the film grain boundaries slows gas-sensor reversibility and creates stresses leading to a remanent elastic deformation, even at low (30° C) temperatures.

We deposited the binary metal oxides on SAW substrates using sol-gel techniques. Solutions employed metal precursors with rapidly hydrolizable alkoxide ligands and high water-to-metal ratios. Layers were spin-deposited and then calcined at 500° C or less. Film thicknesses ranged from 50 nm to 350 nm with surface areas of < 5 m^2/g. SAW attenuations were 2 dB to 6 dB at 97 MHz. Although designed to have a specific affinity to the electron-donating species such as CO, NO, and NO_2, these films were too low in surface area to exhibit any measurable sensitivity to 1% concentrations of those gases. One device with a 300-nm ZrO_2 coating was extensively tested with hydrogen gas, exhibiting a response of 2.1×10^{2} ppm Df / ppm H_2 diluted in nitrogen at 420° C (the highest temperature tested). The response appears to be generated by a combination of thermal interactions at the surface and a conductivity increase in the film. Peak response temperatures are greater than 420° C.

Publications

Refereed

Martin, J. E., M. T. Anderson, J. Odinek, and P. P. Newcomer. 1996. "Synthesis of Periodic Mesoporous Thin Films." *Langmuir,* accepted.

Other

Anderson, M. T., and R. W. Cernosek. 1996. "Metal-Oxide Coatings for Piezoelectric Exhaust Gas Sensors." Paper presented to the 3rd International High-Temperature Electronics Conference, Albuquerque, NM, 9–14 June.

Anderson, M. T., J. E. Martin, P. P. Newcomer, and J. Odinek. 1996. "Synthesis of Periodic Mesoporous Thin Films." Paper presented to the Materials Research Society Spring Meeting, San Francisco, CA, 8–12 April.

Cernosek, R. W., M. T. Anderson, and J. R. Bigbie. 1996. "High-Temperature Surface Acoustic-Wave Delay Line Gas Sensors." Paper presented to the Acoustic Wave-Based Sensors Symposium, Fall Electrochemical Society Meeting, San Antonio, TX, 6–11 October.

Fuel-Cell Applications for Novel Metalloporphyrin Catalysts

G. N. Ryba, K. R. Zavadil, N. Doddapaneni, J. A. Shelnutt

The objective for this project was the development of a new class of metalloporphyrin materials as catalysts for use in fuel-cell applications. Fuel-cell efficiency and reliability are controlled largely by the catalytic processes occurring at the cell electrodes. New classes of metalloporphyrin materials, including the dodeca-substituted porphyrins and porphyrins with hydrogen-bonding and ionic groups developed at Sandia, are excellent candidates for use as catalysts at both the fuel electrode (anode) and the air electrode (cathode). Proper design of these materials could provide solutions to many (and potentially all) of present-day catalyst limitations, particularly for the fuel-cell systems that are most appropriate for transportation applications (phosphoric acid fuel cell [PAFC], alkaline fuel cell [AFC], and polymer electrolyte membrane [PEM] fuel cells). Sandia pioneered the use of 3-D computer modeling to design metalloporphyrin materials to have specific physical and chemical properties. This, combined with existing characterization/testing techniques (Raman, x-ray photoelectron spectroscopy [XPS], nuclear magnetic resonance [NMR], and ultraviolet-visible [UV-Vis] spectroscopies, electrochemical voltammetry, fuel-cell testing stations) and access to leading synthesis expertise, is being used to design, synthesize, and test new catalysts with the necessary chemical and physical properties to overcome present catalyst limitations.

In FY96 we took data showing for the first time that our nonplanar, fluorinated porphyrins were better catalysts for the reduction of oxygen than the planar species that have been studied for many years by other workers. In these experiments, at a voltage of 0.30 V vs. Ag/AgCl (which is 0.50 V vs. normal hydrogen electrode [NHE]), we measured a current of 3.58 and 3.17 mA/cm^2 (avg. 3.38 mA/cm^2) for the planar porphyrins cobalt octaethylporphyrin (CoOEP) and cobalt tetraphenylporphyrin (CoTPP), respectively, while for the nonplanar porphyrins, we measured values of 4.97, 4.58, and 4.76 mA/cm^2 (avg 4.77 mA/cm^2) for cobalt dodecaphenylporphyrin (CoDPP), cobalt dodecaphenylporphyrin-F20 (CoF20DPP), and cobalt dodecaphenylporphyrin-F28 (CoF28DPP), respectively. Roughly speaking, the current improved by 30–40% at this voltage. However, these currents, for both the previously known planar porphyrins and new, nonplanar porphyrins, fell by about 30% in 10 minutes, and continued falling during the course of 60-minute experiments. We performed experiments to try to determine the cause of this loss of current. We performed UV-Vis spectroscopy on the electrolyte, but detected no loss of porphyrin from the electrode into the solution. In an effort to stabilize these porphyrins on the surfaces of electrodes, we co-polymerized porphyrins with aniline and pyrrole into films on the electrode surfaces. We made good-quality polymer films with catalytic properties, but they did not adhere to the glassy carbon surfaces used for these experiments.

There appeared to be no trend in either stability or oxygen-reduction activity as a function of fluorination. The fluorines on the periphery of the porphyrin macrocycle withdraw electron density from the cobalt center, but in oxygen-reduction experiments in nonaqueous solvents, there was no shift in the redox potential at which oxygen was reduced. However, very clear shifts in three of the porphyrin redox states were observable. For DPP, F20DPP, and F28DPP, we observed sets of peaks at (-0.57, -0.25, and -0.17), (0.91, 1.49, and 1.55), and (1.11, 1.64, and 1.74) (each, V vs. Ag wire). Thus, the shifts between the first and second sets due to the 20 fluorines were 320, 320, and 530 mV, respectively, and between the second and third sets were 80, 60, and 100 mV, respectively.

Publications

Other

Ryba, G. N., J. D. Hobbs, J. A. Shelnutt, and V. M. Rivera. 1996. "Metalloporphyrin Catalysts for Oxygen Reduction Developed Using Computer-Aided Molecular Design." Invited talks, University of Puerto Rico–Mayaguez and University of Puerto Rico–San Juan, San Juan, PR, 13 February.

High-Density Direct Methanol Fuel Cell

K. Wally

The goal of this research is to investigate the adaptation of Sandia's innovative high-density proton exchange membrane (PEM) fuel-cell design to a direct methanol fuel cell. The design has the potential to achieve a tenfold improvement in power density over state-of-the-art fuel cells. The keys to the design are thin-ply fabrication and lamination techniques adapted from hybrid microcircuit and printed wireboard technologies. At the heart of the design is a PEM electrochemical sandwich employing thin PEM membranes and thin-film electrocatalysts.

We accomplished the following in FY96:

(1) Successfully completed the development of an adhesive laminating process to produce thin-ply high-power-density PEM fuel cells. We achieved these using very thin bipolar separator/diffuser structures fabricated using chemical milling techniques. We employed commercial thin-film adhesives and cut gaskets of these adhesives to shape using a computer-controlled die-cutting process. We needed as many as five custom gasket shapes to laminate the different elements of the unit cell together. The typical thickness for completed unit cells was about 0.040 inch.

(2) Prepared and tested unit cells of three different PEM thicknesses: .002≤, .005≤, and .007≤. In all cases, methanol fuel crossover (i.e., diffusion from the anode to the cathode side) proved the greatest inefficiency in performance. Due to crossover, open-cell voltages were no greater than about 0.5 volts, while voltages dropped to under 0.25 volt at

current densities of 40 mA/cm², and to 0.12 volts at current densities of 80 mA/cm². This performance is about half the best performance reported in the literature for direct methanol fuel cells. However, for us to achieve the higher reported current densities would require a PEM with significantly better cross-over characteristics than the Nafion membranes, and whose development was beyond the scope of this project.

(3) Were unsuccessful in applying thin-film catalytic inks to the surface of the PEM electrodes as has been done successfully for hydrogen fuel cells. The reasons for this failure are twofold. First, the membranes undergo significant swelling (about 38% overall, and more than 25% in each linear direction) when exposed to water/alcohol mixtures. Second, the fine Nafion particles in the catalytic inks also undergo this same swelling. The combination caused delamination of all the thin-film electrodes we attempted.

(4) Produced working fuel cells employing commercial electrode structures of the gas diffusion type, which support the catalyst on porous matrices of carbon and polymer particle sponge supported on a carbon-fiber cloth. However, long-term exposure of these unit cells resulted in the eventual delamination of the electrodes from the Nafion membranes due, again, to the aforesaid swelling. Once delaminated, cell performance was erratic.

Although we successfully demonstrated a thin-ply unit cell structure suitable for achieving the high-power densities we hypothesized, we could not achieve successful long-term cells with Nafion membranes due to both methanol crossover and membrane swelling.

Hydrogen Production for Fuel Cells by Selective Dehydrogenation of Alkanes in Catalytic Membrane Reactors

T. J. Gardner, J. C. Brinker, R. W. Schwartz, A. G. Sault

Hydrogen-powered polymer electrolyte membrane (PEM) fuel cells, fueled by on-board H_2 generation from liquid fuels, represent an important technology for all electric or hybrid electric vehicles. Proposed technologies for on-board H_2 generation (steam reforming or partial oxidation) from liquid fuels generate large amounts of CO and CO_2, which can poison PEM fuel cells. Sandia proposes to develop a catalytic membrane reactor system for the generation of pure H_2 via selective dehydrogenation of liquid fuels. We will achieve separation of hydrogen from hydrocarbons by modifying commercial alumina membrane tubes with size-selective hydrous titanium oxide (HTO)/silica composite membranes. HTO films offer an advantage over other candidate membrane materials, such as titania and silica, in that they can be synthesized to contain high concentrations of sodium ions, which can be ion exchanged with transition-metal ions that are catalytically active for selective dehydrogenation. Thus, by using HTO-modified membranes, we can closely associate a proven catalytic function with the membrane, thereby increasing conversions achievable with only a bulk catalyst inside the membrane tube. This scheme offers a potential method for increasing hydrogen production rates without increasing reactor size, an important consideration for transportation applications or for remote electricity generation for civilian or military applications.

In the first year of our three-year effort, we successfully identified a suitable reaction with high hydrogen production yield, as well as promising catalyst compositions for this reaction. We demonstrated the ability to synthesize an HTO/SiO_2 composite membrane system that performs similarly to TiO_2/SiO_2 membranes in terms of low-temperature gas permeability and selectivity. Also, we performed high-temperature gas-permeance measurements that indicate that excellent separation of propane from hydrogen can be achieved using microporous SiO_2 membranes. This result is important since propane represents a typical reaction product from cracking reactions with higher alkanes, implying that membrane separation of H_2 from the actual product gas is quite feasible. We are also active in establishing ties to potential U.S. Department of Energy (DOE)/Energy Efficiency and Renewable Energy/Office of Transportation Technologies (OTT) and Partnership for a New Generation of Vehicles (PNGV) customers regarding a follow-on program. These agencies are very interested in the catalytic membrane reactor as an advanced concept for vehicle applications, as well as a membrane separation system to purify current H_2-based reformate products to meet H_2 purity requirements for PEM fuel cells.

Hybrid Vehicle Engine Development

P. Van Blarigan

As emissions regulations and fuel economy have become the driving forces behind engine design today, an attractive approach to increasing the fuel efficiency of motor vehicles is the hybrid drive train. In a series-type hybrid drive train, the engine drives only an electrical generator, and the wheels are powered by electric motors. With some type of energy storage, this allows the internal combustion engine to be run at its most efficient operating point.

To take advantage of this type of system, we submitted a Technical Advance to DOE for a variable compression ratio free piston internal combustion electrical generator. A double-ended piston oscillates in a cylinder that is closed on both ends. We placed ports in the cylinder walls, allowing introduction of a fresh fuel/air charge and venting of exhaust gases. Electrical output is generated directly from piston motion by fixing magnets on the piston that move through magnet steel and generate a time-varying flux in fixed coils. Ignition is by compression-heating of a homogeneous fuel/air charge with ignition-timing accomplished by electronically controlling the compression ratio. The goal of this project is to design, build, and test the performance of a prototype engine.

We developed a comprehensive numerical model, including piston dynamics, two-stroke cycle scavenging, chemical kinetics of combustion, and control stability algorithms. The literature search added credibility to the engine concept.

We designed and built a single-stroke combustion experiment to assess the viability of homogeneous charge compression ignition in a high-pressure test cell. Operated remotely, the piston is driven from one end of a closed cylinder to compress the fuel/air charge. The piston is then driven back toward the starting position by the combustion products. By monitoring the piston position, cylinder pressure, and mass of fuel, we can calculate the compression ratio, ignition position, and indicated efficiency. We ran the test with varying compression ratios to determine the effect this has on performance. We achieved indicated efficiency of greater than fifty percent.

The piston motion of our model was experimentally confirmed. Lawrence Livermore National Laboratory is integrating the model into the chemical kinetics code HCT to simulate the steady-state operation and to determine the sensitivity of engine efficiency and emissions to changes in compression ratio, equivalence ratio, scavenging efficiency, inlet temperature, and port sizing. Los Alamos National Laboratory offered to help study the scavenging characteristics of the engine using the three-dimensional KIVA computational fluid dynamics code. During the study of stability issues of the engine, we found that this nonlinear system performed best with a fuzzy logic controller.

Development of Innovative Combustion Processes for a Direct-Injection Diesel Engine

J. E. Dec, D. L. Siebers

The Partnership for a New Generation of Vehicle (PNGV) selected a small-bore, high-speed, direct-injection (DI) diesel engine as being the best candidate for meeting its goal of 80 miles per gallon. Despite the many advantages of these engines, improvements in power density, efficiency, and emissions are essential. Achieving these improvements requires major advances in understanding and controlling the combustion and emissions formation processes. Some promising new techniques are fuel injection-rate modulation, water injection, enhanced swirl combustion chambers, exhaust-gas recirculation, and modified fuels. This project proposes to evaluate these technologies, down-select to the most promising, develop a research engine, and conduct research to determine the viability of the most promising technologies. During FY96, we completed the first two steps with two novel approaches, injection-rate modulation and water injection, selected as the most promising new technologies. The development of the research engine is well under way. In addition, we negotiated a new small-bore diesel research program with industry and DOE support. This new project focuses on more conventional research on small-bore DI diesel combustion and is highly synergistic with this project.

We evaluated several techniques for reducing emissions while maintaining or enhancing the efficiency of high-speed, small-bore, DI diesel engines. The evaluation considered an examination of the literature, discussions with representatives from industry, and recent new insights on diesel combustion developed by the principal investigators of this project. The techniques considered included retarded injection timing, higher injection pressures, optimized in-cylinder flows (e.g., variable swirl), high-pressure, common-rail fuel injectors, fuel additives, exhaust-gas recirculation, water injection (either injected with the fuel or into the intake air), and injection-rate modulation (pulsating the injection rate or splitting the injection event). In "down-selecting" the techniques, we considered both their potential and their current research efforts. We concluded that current efforts on many of the more conventional techniques were adequate, but that meeting PNGV's fuel-economy and emissions goals will also require novel, advanced techniques.

We selected water injection and injection-rate modulation as the two most promising advanced techniques. Water injection could break the soot-NO_x trade-off that often limits diesel combustion strategies. It is well known that water addition can reduce NO_x emissions by lowering the combustion temperatures. However, a new understanding of diesel combustion resulting from our recent research, combined with equilibrium chemistry calculations, indicates that water could also inhibit soot formation if introduced correctly. Empirical evidence indicates that injection-rate modulation also offers the potential for significant emissions reduction; however, the mechanisms are not understood. Further investigations of the effects of water addition and injection-rate modulation on diesel combustion are needed to develop their potential.

As an outgrowth of the new DOE-supported research program and recent decisions made by PNGV regarding the base engine configuration, the development of an engine for this project research is proceeding differently from that originally planned. Extensive discussions with industry made it clear that modifying an existing research engine would not be adequate and that a new optically accessible, high-speed DI diesel engine was required. The engine and head design have been decided on, and the laboratory space is under development with the dynamometer and other equipment already installed.

Conceptual Design and Prototyping for a Next-Generation Geographic Information System

J. Espinoza

This project applied recent developments in object-oriented and spatial data modeling to develop a comprehensive and rigorous spatial data model for transportation systems for Geographic Information Systems for Transportation (GIS-T). Beginning with the list of pathological road segments (which cannot be represented in the current data models), we applied object-oriented methods to include these frequent but difficult-to-handle cases. We also presented several examples of how GIS-T applications will be simplified by a rigorous 3-D object-oriented spatial data model.

We developed a prototype of the Linear Referencing Method (LRM) engine as described by the object model from the GIS–T/ISTEA Pooled Fund Study. The LRM engine is designed to support transportation systems in determining spatial locations using different referencing methods. The concepts behind the LRM engine are fundamental and complement the design of our object-oriented geospatial model. Additional work is needed to fully test the engine and to validate the data models it is based upon.

We prepared several reports describing network pathologies that would be remedied by the introduction of a 3-D data model for GIS-T applications. These transportation application-related pathologies solved by the use of the 3-D mathematical model developed during the project. The 3-D model has yet to be fully tested and validated.

We also found a significant lack of understanding of the importance of improving spatial data. The current thinking by policymakers is that standardizing interfaces and data structures for the current 2-D data is more than adequate. We attempted to show via our participation in the Volpe/Harvard/MIT and Enterprise-LRS projects that this is shortsighted and likely wasteful.

Publications

Refereed

Bespalko, S. J., J. H. Ganter, and M. Van Meter. 1995. "Converging Infrastructures Intelligent Transportation and the National Information Infrastructure." *Proc. Harvard/MIT Joint Conf. on the Information Infrastructure Project* (Boston, MA, 21 July): 209–226. Boston, MA: MIT Press.

Other

Fletcher, D., J. Espinoza, R. D. Mackoy, S. Gordon, B. Spear, and A. Vonderohe. 1996. "The Case for a Unified Linear Reference System." Paper presented to the Enterprise Linear Reference System Workshop, Salt Lake City, UT, 26 July.

Sutton, J. 1996. "Network Pathologies Analysis." Paper presented to the Workshop on Navigable Object Databases, Irvine, CA, 15–16 March.

Sutton, J. 1996. "Transportation Planning Pathologies." Paper presented to the CALTRANS Workshop on Implementing Object Databases, Irvine, CA, 3–4 December.

Vanderveer, J. 1997. "GIS: Reaching the Third Dimension." Paper to be presented to the Conference of the Society of Women Engineers, Albuquerque, NM, 24–28 June.

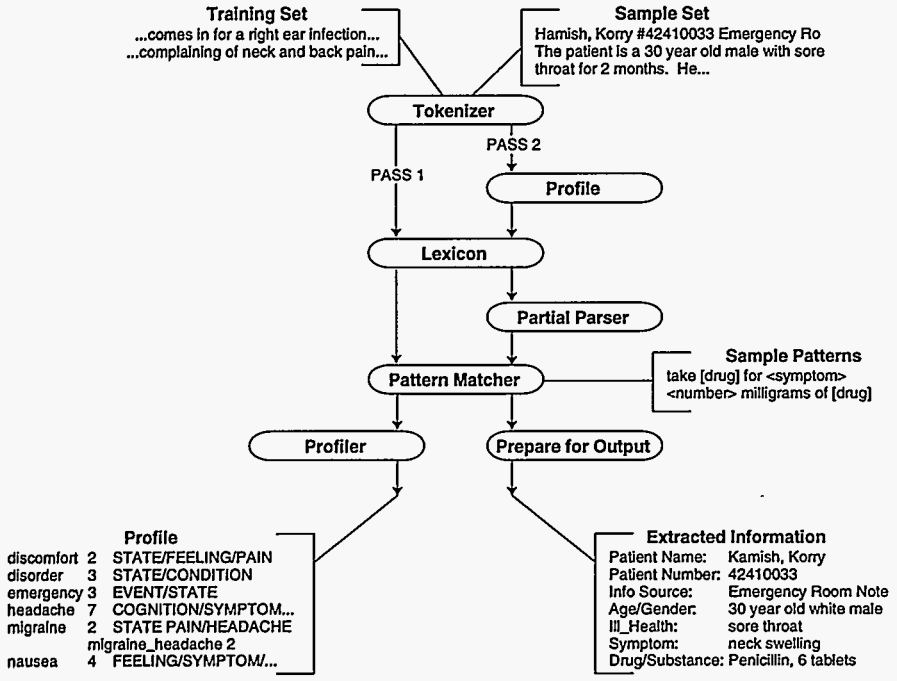

Extracting information from unstructured text has become important due to the large amount of text now electronically available. Domain-independent approaches offer adaptation and learning that will outpace systems with *a priori* knowledge.

Superconductive Gravity Gradiometers for Underground Target Recognition

M. J. Adriaans, R. M. Axline

During FY96, Sandia focused on the fabrication of the major superconducting components for the gradiometer. We completed detailed structural and vibrational analysis of the angular accelerometer component of the gradiometer. The ultimate goal of the project is to develop an instrument with laboratory-like sensitivity that can be flown on an aircraft and can measure the gravity signatures from underground structures. In addition to the superconductive gravity gradiometer (SGG), we initiated work on a hand-held magnetometer system for measuring biomagnetic signals with some additional funding.

We proposed this project to develop a sensor that would take advantage of the fact that all objects have a gravitational field associated with them. *Inside Sandia* quoted the original PI as saying, "You can hide something by painting it the same color as its background, by minimizing its radar reflection or making it throw back random radar pulses, or by sealing it in a lead box. But you can't hide the gravitational field it generates. You can't stealth gravity. Someone might hide fissile material in a concealed lead vault to fool a Geiger counter, but a gravity gradiometer would detect the suspicious presence of that massive vault." The SGG uses superconducting quantum interference devices (SQUIDs) and other superconducting technology to achieve high sensitivity (~ 1 Eotvos) to gravity gradients.

We made several major accomplishments. We completed a detailed design and partial fabrication of the SGG device and performed a detailed structural and vibrational analysis of the angular accelerometer component of the SGG. Additional funding allowed work on an ultra-sensitive, hand-held SQUID device that can measure magnetic signals from the heart. This year, we completed partial design and partial fabrication of the device.

Publications

Other

Canavan, E. R., M. V. Moody, R. V. Duncan, and J. A. Demko. 1995. "Superconducting Gravity Gradiometer for Airborne Survey." *Proc. Amer. Geophys. Union 1995 Fall Mtg.* **76** (46) (San Francisco, CA, 11–15 December): F144.

Bandwidth Utilization Maximization for Scientific Radio-Frequency Communication

V. P. Salazar

Sandia presented a method for more efficiently utilizing the frequency bandwidth allocated for data transmission. Current space and range communication systems use modulation and coding schemes that transmit 0.5 to 1.0 bits per second per Hertz of radio-frequency (RF) bandwidth. The goal of this project is to increase the bandwidth utilization by employing advanced digital communications techniques. This is done with little or no increase in the transmit power, which is usually very limited on airborne systems.

Teaming with New Mexico State University (NMSU), we developed an implementation of trellis-coded modulation (TCM), a coding and modulation scheme pioneered by Ungerboeck, for this application and simulated it on a computer. TCM provides a means for reliably transmitting data while simultaneously increasing bandwidth efficiency. The penalty is increased receiver complexity. In particular, the trellis decoder requires high-speed, application-specific, digital signal processing (DSP) chips. A receiver solution based on the QualComm Viterbi decoder and Graychip DSP receiver chips is presented.

The purpose of this project is to develop a bandwidth-efficient communication system suitable for satellite or range applications. FY95 work focused on requirements definition, research and selection of a modulation scheme, and computer simulations to verify feasibility of the selected scheme. FY96 work focused on the design, development, and implementation of the selected communication system.

The originally proposed system comprised an analog modulator with a digital encoder for the transmitter and an analog demodulator with a digital decoder. The goal was to emulate the proposed system with test equipment and hardware provided by NMSU along with the Sandia-provided encoder and decoder PC boards. Using this equipment, we were to build a test-bed to allow conceptual testing in the laboratory.

The goal of using commercial equipment to emulate the proposed system in a conceptual demonstration did not provide the performance levels suggested by computer simulations. This was due to the non-ideal performance of critical components of the systems. The laboratory testing convinced project team members that we needed a different design approach. Advances in DSP technologies allowed for a redirection in the design to use DSP chips for a digital implementation. As a result of this redirection, we exceeded our original goals when we completed a state-of-the-art prototype design. FY96 accomplishments are as follows:

(1) Designed, implemented, and tested all required logic for encoding and decoding.

(2) Designed, implemented, and tested a quadrature amplitude modulation (QAM) modulator. This modulator design includes the ability to perform signal pre-distortion to correct for system nonlinearities. System nonlinearities were major flaws discovered with the laboratory test-bed.

(3) Designed and implemented a QAM demodulator, a robust design that includes a programmable equalizer, automatic gain control, and automatic frequency control. These additional features were not originally planned at the beginning of phase II.

The development and fabrication of a modern system prototype exceeded original expectations. This prototype awaits an application to complete application-specific tasks such as mechanical packaging, carrier frequencies, etc.

Extraction of Information from Unstructured Data

S. M. Deland, N. H. Irwin

Extracting information from unstructured text has become an important research area in recent years due to the large amount of text now electronically available. Building on the first year's work of identifying important entities, the project's second year focused on implementing techniques used to group words into semantic categories and to output templates containing selective document content. Using word profiles and category clusterings derived during a training run, the time-consuming knowledge-building task can be avoided. Though the output still lacks in completeness when compared to systems with domain-specific knowledge bases, the results do look promising. The two approaches are compatible and could complement each other within the same system. Domain-independent approaches retain appeal because a system that adapts and learns will soon outpace a system with any amount of a priori *knowledge.*

We originally proposed that the verbs in the sentence might provide the glue in an "entity-relationship" type of organization. Verbs did not fill this role in a domain-independent solution because the words had too many meanings, making disambiguation difficult, and the meanings were too general in nature.

We developed a second algorithm in its place. Using the already-identified entities, a clustering analysis of their semantic categories within WordNet, a public domain semantic net, provided an organization for grouping the entities. The selected semantic categories provided both a name for the group and a constraint for selecting fillers.

The testing and development this year focused on the large set of aliased medical patient records made available to us by Scott & White Hospital. In this domain, the clustering analysis selection included categories such as symptom, illness, drug, and body part. The fillers for the categories included entities such as headache, heart attack, aspirin, and chest. We selected the semantic categories during a training run. During the extraction run, we identified entities or fillers in the current text based on inclusion in targeted semantic categories or targeted linguistic patterns in the pattern matcher.

We based the pattern-matcher facilities extraction and semantic assignment on linguistic patterns found in the language. Elements of the patterns include part of speech, semantic category, and exact word match. To date, we have written all the patterns by hand. A nontrivial, but believed obtainable, next step would be to produce the patterns automatically using the instances in the text of the words within the semantic clusters.

We gave a demonstration in which a search on a selected entity or set of entities retrieved appropriate sentences in the original text.

Publications

Other

Irwin, N. H. 1996. "Domain-Independent Information Extraction in Unstructured Text." Internal Sandia Report, SAND96-2337, September.

Irwin, N. H., S. M. DeLand, and S. V. Crowder. 1995. "Extraction of Information from Unstructured Text." Internal Sandia Report, SAND95-2532, November.

Feature-Based Methodology for Sensor Fusion

J. J. Carlson, A. M. Bouchard

Future-generation automated and autonomous systems will rely on multiple sensors together with internal and external information sources to achieve high performance, accuracy, and reliability. The primary objective of this research is the development of a theoretical and practical basis for a robust information, or sensor, fusion methodology. The basic problem is to select multiple sensors/features that provide sufficient information to design and optimize a decision process in terms of uncertainties caused by measurement errors, randomness, ambiguities, and information warfare tactics. The approach is to develop a feature-based fusion methodology for discovering and fusing multiple features to achieve near minimum probability of error decision and control algorithms. The fusion methodology is applied to develop a biometrics-based human identity verification system for security applications. The system obtains its robustness and reliability by fusing many coarse and easily measured features into a minimum probability of error decision algorithm.

This project, concluded in FY96, was very successful. By partnering with New Mexico State University, we made significant technical strides that otherwise would not have been possible. Our research thrusts and accomplishments this year focused on the development of a theoretical and practical basis for a robust

information, or sensor, fusion methodology. Of significant importance was the development of a mathematical framework for feature-based information fusion. The fusion problem is formulated in terms of a statistical hypothesis testing problem. We presented a fusion theorem that ensures that the achievable minimum probability of error for any decision or control problem can not increase by adding more features or sensors. This theorem motivates the application of sensor fusion techniques to real-world problems. We also showed that an *n*-dimensional feature vector can be fused into a single feature without increasing the minimum probability of error. We developed a weighted nearest neighbor (WNN) fusion model to fuse features into a near-minimum probability of error decision algorithm. We developed a method, based on Wavelet Packet Decompositions, to assist in the discovery and extraction of features at different levels of resolution. We developed nonparametric statistical methods to evaluate features in high-dimensional spaces. We developed a genetic algorithm to select and weight features to optimize decision and control algorithms. Finally, we developed a modified K nearest neighbor (KNN) algorithm for one-class classification. We applied the developments made through the course of this research project to a biometrics-based, human identity-verification problem. Through this application, we successfully demonstrated the value of the feature-based methodology for multisensor fusion.

Publications

Other

Bao, Z. 1995. "Locating and Finding Multiple Meaningful Trajectories." Ph.D. dissertation, New Mexico State University, July.

Carlson, J. J., J. B. Jordan, G. M. Flachs, Q. Meng, X. Niu, W. Wang, Z. Bao, and D. Marten. 1995. "High-Confidence Identity Verification Using Multiple, Coarse Features Acquired from the Face, Hand, and Voice." *Proc. Amer. Defense Preparedness Assoc. (ADPA)* 1 (Virginia Beach, VA, 19–22 June): 249–256.

Carlson, J. J., J. B. Jordan, G. M. Flachs, Z. Bao, and C. Hardin. 1996. "Fusion of Multiple, Coarse Features Acquired from the Face, Hand, and Voice for Reliable Human Identity Determination." Paper presented to the SPIE–1996 Conference on Signal Processing, Sensor Fusion, and Target Recognition IV, Orlando, FL, 17–19 April.

Flachs, G. M., J. B. Jordan, J. J. Carlson, C. L. Nelson, and D. R. Scott. 1995. "Feature Space Mapping for Sensor Fusion." *Proc. Multisensor Integration and Fusion for Intelligent Machines and Syst. Mtg.* (November): 283–308. Norwood, NJ: Ablex Publishing Corporation.

Marten, D. G. 1995. "Determining Optimal Phrases for Use in Speaker Verification." Masters thesis, New Mexico State University, June.

Meng, Q. 1996. "Human Biometric Verification and Recognition Based on Feature Fusion and Computer Vision Techniques." Ph.D. dissertation, New Mexico State University, May.

Wang, W., Z. Bao, Q. Meng, G. M. Flachs, and J. B. Jordan. 1995. "Hand Recognition by Wavelet Transform and Neural Networks." Paper presented to the SPIE–1995 Conference on Signal Processing, Sensor Fusion, and Target Recognition IV, Orlando, FL, 17–19 April.

Nonflammable Deterrent Materials

T. A. Ulibarri, S. H. Scott, T. J. Shepodd, P. B. Rand

Silicones (polydimethylsiloxanes [PDMS] polymers) are environmentally safe, nonflammable, weather-resistant, thermally stable, low glass-transition temperature (Tg) materials. Therefore, silicone-based materials meet the nonflammability, lack-of-toxicity, and broad-temperature-range-of-use criteria for deterrent applications, and represent a possible alternative to hydrocarbon-based sticky foams. However, the technology base required to generate siloxane materials with the appropriate properties for deterrent applications did not previously exist. The major goal of this project was to create a series of silicone sticky-foam materials based on modified PDMS networks. Sandia achieved successful demonstration of silicone sticky foams based on both commercial and experimental silicone formulations.

Overall, this project successfully generated relatively low-density silicone foam materials with excellent tack, moderate elongation, and satisfactory modulus for some deterrent applications. We demonstrated one-component silicone sticky foams utilizing commercial platinum-catalyzed silicone materials and a variety of thixotropic agents. We determined that the most effective thixotropes for this application are fibrid systems based on aramid and polyethylene pulp. The fibrids undergo shear thinning, which enhances dispensing and at the same time is not detrimental to foam stability. We evaluated commercial polymer systems from NuSil, Dow-Corning, and GE, with the Nusil systems leading to the best foam materials. We also investigated sol-gel systems based on monomodal, bimodal, and trimodal formulations and found them to generate viable sticky-foam materials for deterrent applications. We established optimal molecular weights and compositions and found experimental resins from GE to be useful additives, providing enhanced tack and strength.

Microholographic Tagging

D. A. Tichenor, W. C. Sweatt, A. K. Ray-Chaudhuri

Sandia patterned phase-only and phase-amplitude microholograms onto Mo/Si multilayer substrates. We printed both types of holograms with a 0.4-micron pitch holographic carrier frequency in ZEP 520 resist using our 10x-I extreme ultraviolet (EUV) imaging system. The holographic image, reconstructed using HeNe light, is in good agreement with computer-simulated image. We characterized the modulating depth and side-wall angle of the printed microholograms using atomic force microscopy (AFM). To obtain higher diffraction efficiency in microtags, we developed a bilayer resist that enables the formation of high-aspect-ratio patterns.

We completed a software interface to input the phase and amplitude values, computed using an Iterative Fourier Transform Algorithm (Gerchberg and Saxton), into an electron-beam mask writer for patterning of holographic EUV masks. We used this capability to pattern both phase-only and phase-amplitude microholograms. Simulated playback of these holograms indicates that including both amplitude and phase information in the hologram increases the image quality over that of phase-only holograms. Phase-only holograms, on the other hand, offer greater diffraction on playback.

The holographic mask for producing the initial microtags comprises an array of 8 x 8 cells representing the phase and amplitude of the far-field diffraction pattern of the letter *E*. The mask uses a 100-nm-thick gold absorber pattern on an EUV-reflective Mo/Si multilayer substrate. We printed EUV images of the holographic pattern with 10x reduction in 1250 angstroms of ZEP 520 resist to produce a microtag having a 0.4-micron pitch holographic carrier frequency and overall dimensions of 80 x 160 microns.

We played back the printed microhologram using HeNe light. The reconstructed image of the letter *E* is in good agreement with computer-simulated image. Not only is the letter *E* clearly reconstructed, but also the details of the speckle pattern in the acquired image closely match that of the simulated image.

We also evaluated the microhologram using AFM. The results indicate that the modulation depth in the resist was only 200 to 300 angstroms of the 1250-angstroms resist thickness. The limited depth may have been due to the aberrations in the 10x-I projection optics, focus error, dose error, or the contrast of the resist. A side-wall angle of 20 degrees, as measured by the AFM, was much lower than the desired value and possibly due to the same factors that reduce modulation depth.

To improve the modulation depth and side-wall angle for higher diffraction efficiency in microtags, we developed a bilayer resist that enables the formation of high-aspect-ratio patterns. We printed grating patterns ranging in pitch from 0.6 microns down to 0.3 microns with aspect ratios exceeding 5:1. These structures can be used directly as the medium for encoding microtags, or they can be used as etch masks for transferring the microtag pattern into the underlying substrate.

Interactive Control of Virtual Actors for Simulation and Training

S. A. Stansfield

This research addresses the use of virtual reality (VR) for situational training, mission planning, and rehearsal. Sandia is specifically concerned with operations for which live exercises are limited due to danger, expense, and logistical complexity. During such live exercises, situations such as terrorist attacks are staged using people to play the parts of terrorists, hostages, etc. Most interesting scenarios involve many participants, only a few of whom are actually being trained. For example, training antiterrorism requires not only the trainees and instructor, but also other people to play bystanders, hostages, and terrorists. In a VR-based training system, we would like to limit the number of live participants to the instructor and the trainee. In addition, we would like to provide a mechanism to allow the instructor to alter the course of the simulation during a training session, rather than have it driven solely by the actions of the participants. This work addresses these issues. We are developing methods for adding simulated humans, called virtual actors, *to VR-based simulations and are developing the techniques that will allow an instructor to alter the behaviors of these virtual actors while the simulation is running.*

This year we developed a counterterrorism simulation with input from the FBI hostage rescue team. The scenario involved a room-clearing operation. In this operation, agents must enter a room where hostages are being held, rescue the hostages, and apprehend or subdue the terrorists.

We built a virtual environment for this operation, including creation of the room, the props, and the virtual people who would be the hostages and terrorists. The user can experience this operation in VR.

We developed behaviors for the virtual hostages and terrorists, including animations. Behaviors were (1) surrender by putting hands up, (2) surrender by falling to floor, (3) shoot at the agent, and (4) die after being shot.

We developed a menu-driven interface to allow (1) the placement of the virtual people anywhere in the room, (2) the assignment of a role to each virtual person (hostage or terrorist), and (3) the assignment of a behavior (listed above) to each virtual person.

This system thus allows one to program any number of different scenarios based upon this rescue operation. The user can then practice these scenarios to become familiar with all the possible things that could happen during the actual operation. The instructor can reprogram the scenario so the user never knows what is going to happen. The user interacts with the virtual people and may shoot them or be shot. The goal is to train agents to make shoot/no-shoot decisions correctly under high-stress situations.

A video illustrating this system is available upon request.

Publications

Refereed

Shawver, D. M. 1997. "Virtual Actors and Avatars in a Flexible User-Determined Scenario Environment." Paper to be presented to the IEEE Virtual Reality Annual International Symposium, Albuquerque, NM, 1–5 March. IEEE Computer Society Press.

Investigation of Spray Techniques for Use in Explosive Scabbling of Concrete

R. A. Benham

Sandia investigated a new method for the scabbling of concrete surfaces using a thin layer of explosive material sprayed onto the surfaces and developed a new explosive mixture that could be applied with commercial spray-painting equipment. The first part of our investigation describes experiments that studied methods for the initiation of the sprayed explosive. We successfully initiated layers 0.014-inch thick using a commercial exploding bridge wire (EBW) detonator and a flying plate detonator, and by pellet impact. The second part of our investigation included a survey of spray methods and tests with two commercial spray systems that we believe could be used for developing a robotic spray system.

This study was successful in all aspects of the project. We accomplished the following:

(1) We developed a new explosive mixture that could be spray-painted with commercial spray equipment. Trial spray tests with an inert explosive simulant verified that spray depositions consistent with scabbling requirements were possible. We used this mixture in the explosives initiation study.

(2) Explosive wedge tests demonstrated that the new explosive mixture could be reliably initiated and that the explosive would sustain a detonation front to the thinnest layers tested (0.014-inch thick).

(3) Explosive strip tests showed that mechanical (shock and impact) stimulus would consistently initiate the thin explosive layer. Contact detonators, detonators with a 0.010-inch-thick flyer plate (with air gaps from 0.15 to 1.00 inch) and pellet impact (0.250-inch-diameter steel ball at 1500 and 600 fps), all caused prompt explosive initiation. Direct electrical stimulus (bare EBW bridgewire and bare SCB) did not initiate the explosive layer.

(4) We surveyed commercial spray-painting systems and purchased and evaluated two systems.

(5) We conducted trial sprays with inert powders (Al_2O_3 or MgO) and binder mix to simulate the explosive mixture. We successfully spray-deposited thin layers of material on a vertical surface with both systems, implying that the explosive mix developed in this study can be used in concrete scabbling.

These studies demonstrated that the concept of using spray-deposited explosive for scabbling of concrete is sound. The demolition and decommissioning of nuclear power plants will be made safer and more efficient using this concept. Future development should be aimed at optimizing the spray deposition, shortening the explosive application time, and optimizing the explosive mix to achieve a higher sprayed-mass density of the explosive layer and, therefore, more efficient scabbling of concrete. The demonstration of concrete scabbling with a simple initiator could be done as the next phase in the evolution of this mechanical process.

Data relating the quantity and quality of the sprayed explosive to amount of concrete to be scabbled needs to be generated or collected from the available literature. The explosive scabbling process should be integrated with robotics.

This technology is believed to be mature enough for further development; a scabbling demonstration on a concrete target should follow.

Publications

Other

Benham, R. A., R. W. Bickes, Jr., M. C. Grubelich, D. E. Wakerbarth, and J. L. Brock. 1996. "LDRD Summary Report Part 1: Initiation Studies of Thin-Film Explosives Used for Scabbling Concrete; Part 2: Investigation of Spray Techniques for Use in Explosive Scabbling of Concrete." Sandia Technical Report, SAND96-2470, November.

Electronics Technologies

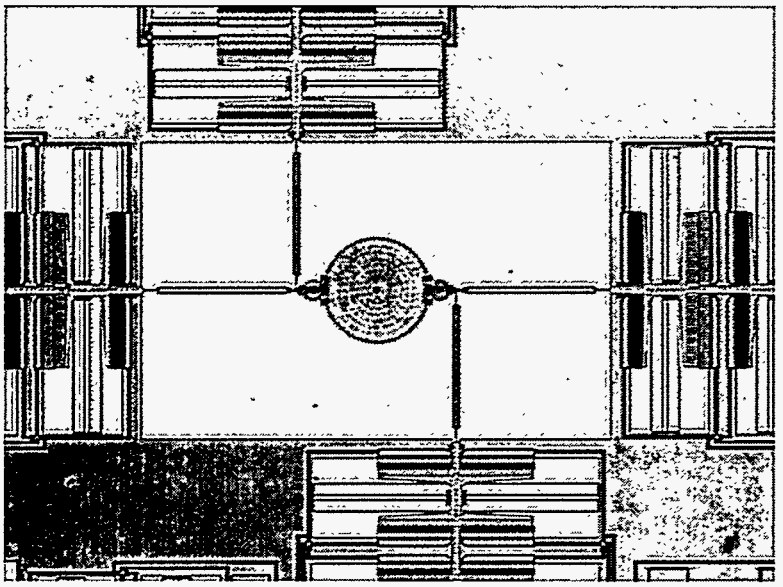

A microminiature inertial guidance system has the potential to spawn new industrial and military applications worldwide. Shown is a microengine-driven microgyroscope in surface-micromachined, monolithic silicon. This is the first step toward realizing an "inertial guidance system on a chip."

Jet Applications of Solder Bumps with Laser Ablation for MCM Packaging

H. C. Peebles, P. A. Sackinger, D. E. Peebles, K. R. Treece

Sandia constructed and demonstrated an on-demand solder-jetting device based on the magnetohydrodynamic effect using 63Sn–37Pb eutectic solder at operating temperatures between 230°C and 280°C. Single droplets 400 μm in diameter were ejected from a 200-μm-diameter orifice with no observable satellites at a velocity of 600 mm/sec using a simple bipolar square-wave current pulse. Emitted droplets were very consistent in size and exhibited a directional reproducibility better than ± 0.1°. The droplet diameters were two times that predicted by theoretical modeling; however, the observed droplet emission velocity was in general agreement with the theoretical predictions.

Multichip module (MCM) technology utilizing solder bump interconnects is necessary for the small circuit volumes and faster processing speeds required in future weapon systems. This two-year project seeks to develop a solder-jetting device for on-demand delivery of small drops of solder and to combine this device with laser ablation for fluxless solder bump formation. We encountered an extended delay in this project during FY96 due to the loss of access to a glove box necessary for jetter operation and testing. We redesigned the jetter and supporting hardware for operation within an 8-inch-diameter glass vacuum chamber. The ability to evacuate and backfill this chamber with ultra–high-purity helium gas provided a sufficient atmosphere for jetter operation. However, we had to drop MCM assembly tasks from the project due to limitations in the available space in the chamber. An evaluation of sealing choices for solder-wetted components in the jetter resulted in the selection of a high-temperature ceramic cement for the formation of joints between alumina, macor, and tantalum parts. We initially encountered problems with crack formation in the cemented joints due to assembly stresses resulting in the leakage of the molten solder. We solved these problems by redesigning several jetter parts and modifying the assembly process to minimize these stresses. We demonstrated on-demand jetter operation using 63Sn–37Pb eutectic solder at operating temperatures between 230° C and 280° C. Single droplets 400 μm in diameter were ejected from a 200-μm-diameter orifice with no observable satellites at a velocity of 600 mm/sec using a simple bipolar square-wave current pulse. Emitted droplets were very consistent in size and exhibited a directional reproducibility better than ± 0.1°. The droplet diameters were two times that predicted by theoretical modeling; however, the observed droplet emission velocity was in general agreement with the theoretical predictions.

Publications

Other

Essien, M., P. A. Sackinger, and H. C. Peebles. 1996. "Computational Modeling of On-Demand Solder Delivery for Fluxless MCM Packaging Applications." Paper presented to the 26th International Symposium on Microelectronics, Minneapolis, MN, 8–10 October.

High-Reliability Plastic Packaging for Microelectronics

J. N. Sweet, J. A. Emerson, D. W. Peterson

In FY96 Sandia focused on developing tools and techniques for analyzing the reliability of plastic integrated circuit (IC) packaging in extreme temperature and humidity environments. With Sandia ATC02.5 and ATC02.6 test die, we verified that the dense triple-track structures are suitable for testing transfer molded parts. However, the unpassivated structures on ATC02.6 showed premature failures associated with particulate-induced damage, particularly at high test voltages. As a result, we cannot recommend their use without further development. Tests of mechanical stress measurement with ATC04 demonstrated the suitability of the test circuits on that die. Temperature and humidity tests with Sandia-developed static random access memories (SRAMs) demonstrated the detection of a fabrication-related failure mode, although not the one we had originally set out to find. Nevertheless, we demonstrated the test concept conclusively. As a result of this research, we developed a conceptual design for a new assembly test chip (ATC) to be used in evaluation of high-reliability plastic IC packaging.

A major FY96 accomplishment was the demonstration that the bondpad resistance structure on the ATC02.6 ATC worked well for non-invasive detection of Au-Al bond degradation and failure in a plastic encapsulated IC. In a high-temperature aging experiment, we correlated the increase in resistance to current flow under a bond to the loss of bond pull and bond shear strength in destructive mechanical tests. As a result, we feel that the bondpad resistance circuit we developed would be well suited for an advanced ATC.

In another accomplishment, we demonstrated the use of temperature and humidity testing to accelerate failures on a Sandia SRAM chip caused by moisture-induced contact resistance increase at Al metal to Si contacts on the IC.

A third accomplishment was the demonstration that the stress measurement circuits on the ATC04 chip worked well for measuring both encapsulation stresses and stresses produced by flip-chip assembly. We also determined some desirable circuit modifications from attempts to measure thermal stresses at high temperature. As a result, we developed a new modified design of the basic stress sensor cell for future ATCs, which would be used for evaluation of high-reliability plastic packaging for DOE weapons applications.

Publications

Other

Sweet, J. N., D. W. Peterson, J. A. Emerson, and S. N. Burchett. 1995. "Experimental Measurements and Finite Element Calculations for Liquid Encapsulated ATC04 Assembly Test Chips." *Proc. ASME Internat. Mechanical Eng. Congr. and Expo.* **EPP-13** (San Francisco, CA, 11–17 December): 61–71.

Sweet, J. N., S. N. Burchett, D. A. Peterson, and J. A. Emerson. 1996. "Finite Element Model Predictions and Measured Die Surface Stresses in Delaminated IC Packages." *Proc. 7th Internat. Congr. on Experimental Mech.* (Nashville, TN, 10–13 June): 88–89. Society for Experimental Mechanics.

Micromachined Inertial Sensors (Accelerometer, Gyroscope)

E. J. Garcia, C. C. Barron, J. L. Wilcoxen

The major goals for this project are to develop, fabricate, and test an accelerometer and a gyroscope in surface micromachining technology. The motivation for this project is the long-term realization of a low-cost (< $500) "inertial guidance system-on-a-chip" with a wide range of military and commercial applications. The work completed in FY96 includes fabrication of an accelerometer with increased proof mass, using the silicon micromolding process, and demonstration of the microengine driving a rotating disk, which will ultimately be used as the sensing mass for the gyroscopic sensor.

We selected a force-feedback teeter-totter design for the accelerometer implementation because this configuration offers the opportunity for high resolution (bias stability), resolution being the most glaring shortcoming of current micromachined accelerometers. We fabricated a version of this design in the previous year. The original intent to use tungsten to increase the accelerometer proof mass was not successful since the deposited tungsten was very highly stressed and resulted in problems with warpage of the silicon structure. More recent techniques developed in the Microelectronics Development Lab (MDL) now appear to permit the use of tungsten. However, a different approach led to success. This technique, known as *silicon micromolding*, permitted the fabrication of thicker structures than possible with standard surface micromachining techniques. The process uses deep reactive ion etching to cut into a silicon substrate to a depth of 10–20 times the thickness of typical surface micromachined structures. In this process, narrow trenches are cut in the silicon substrate, the silicon is oxidized, and polycrystalline silicon is deposited on the oxidized side walls to form a thick structure from a thin chemical vapor deposition (CVD) film of silicon. We then planarize the structure and can fabricate other features such as torsional flexures and electrostatic forcers and sensors. During this project we encountered difficulties with the proof mass sticking to the substrate. This is an ongoing problem in surface micromachining, and several techniques are under development to eliminate the problem.

The major idea for gyroscope development was to use the microengine, which is capable of driving gears or rotors at high speeds, to drive an appropriately designed rotor that can be used to sense angular rate. We designed and fabricated a prototype gyroscopic device that demonstrates the ability of the microengine to rotate a large gyro rotor. In this preliminary design, a rotor is configured to be driven by two microengines. The location of the microengine actuator masses is such that they will not contribute to the inertia torque that will be generated when the base experiences an angular velocity. We also completed an improved design to this configuration. The issue of what would constitute an appropriate bearing is not resolved, but we have completed a scheme for incorporating a gas bearing.

Publications

Refereed

Sniegowski, J. J., and E. J. Garcia. 1996. "Surface Micromachined Gear Trains Driven by an On-Chip Electrostatic Engine." *IEEE Electron. Device Lett.* **17** (July): 366–368. Piscataway, NJ: IEEE Electron Devices Society.

Other

Fleming, J. G., and C. C. Barron. 1995. "Characterization and Application of Deep Si Trench Etching." Paper presented to the SPIE Micromachining and Microfabrication Process Technology II, Austin, TX, 23–24 October.

Fleming, J. G., and C. C. Barron. 1995. "Novel Silicon Fabrication Process for High-Aspect-Ratio Micromachined Parts." *Proc. SPIE Micromachining and Microfabrication Process Technol.* **2639** (Austin, TX, 23–24 October): 185–190.

Ultra–Low-Power Microwave CHFET Integrated Circuit Development

D. F. Dubbert, R. J. Shul, M. E. Sherwin, L. R. Sloan, M. L. Lovejoy, A. G. Baca, V. M. Hietala

Microwave-active devices such as gallium-arsenide metal-semiconductor field-effect transistors (GaAs MESFETs) and silicon bipolar junction transistors (BJTs) typically do not exhibit low-power dissipation characteristics when optimized for high-frequency, low-noise applications. Logic functions implemented with GaAs MESFETs and BJTs also require relatively high operating power. Many high-frequency, wireless, battery-powered applications such as portable global-positioning system (GPS) receivers, miniature tagging and monitoring devices, cellular phones, pagers, and personal status monitors (PSMs) would greatly benefit by the availability of a high-frequency amplification device that requires a low-voltage, low-current, single-ended supply. The activities proposed here are to develop the complementary-heterostructure field-effect transistor (CHFET) as an enabling technology for ultra–low-power microwave devices. Current activity at Sandia in the CHFET development area aimed toward digital integrated circuit (IC) development would be expanded to solve the problem of realizing high-gain, low-noise, low-power, positive-threshold devices for high-frequency and microwave applications. This activity includes the development of device gate lengths down to 0.3 μm, which has yet to be done with CHFET technology.

We made the following accomplishments in FY96:

(1) *2.4 GHz amplifier demonstration.* We designed and fabricated a hybrid narrowband, 2.4-GHz amplifier as a test vehicle for demonstration of the feasibility of utilizing the CHFET technology for RF and microwave, analog applications. The hybrid amplifier was realized using both a

packaged device (centered at 2.12 GHz) and a chip-and-wire technology (centered at 2.4 GHz). The amplifier exhibits a gain of 9.5 dB with only a 1-mW DC power consumption. Temperature tests also reveal that the amplifier, which does not require active biasing, is very temperature stable in terms of both RF gain and voltage standing-wave ratio (VSWR).

(2) *Small gate-length (0.3 μm) CHFET device development.* We achieved performance enhancements of the CHFET devices by shrinking the gate length from 0.8 mm to 0.3 mm for the nJFET and 0.4 mm for the pHFET. We improved intrinsic ft (maximum frequency of oscillation) almost threefold for both devices over the 0.8-mm numbers to near 60 GHz for the nJFET and 11.5 GHz for the pHFET.

(3) *Microwave monolithic integrated circuit (MMIC) fabrication process development.* We added six MMIC passive element process mask steps in a compatible way to the CHFET digital process, which now provides capacitors, transmission lines, airbridges, and inductors. Future MMICs will also include thin-film resistors and via grounds to the wafer backside.

Publications

Refereed

Baca, A. G., *et al.* 1996. "Complementary HFET Devices for Wireless Digital and Microwave Applications." *Proc. 191st Electrochem. Soc. Mtg.* (San Antonio, TX, 6–11 October).

Baca, A. G., *et al.* 1996. "Complementary HFET Technology for Low-Power Mixed-Mode Applications." *Proc. Mater. Res. Soc. (MRS) Spring Mtg.* (San Francisco, CA, 8–12 April).

Application-Specific Tester-on-a-Resident-Chip (TORCH)

D. V. Campbell, E. S. Snyder

In year two of this project, Sandia redesigned the application-specific tester-on-a-resident chip (TORCH) integrated circuit (IC) and applied it to a real, functional design by implementing a quiescent current (I_{DDQ}) test function. The new design also features die-to-die communications more appropriate for multichip modules (MCMs), an improved boundary scan interface, improved timing measurements, and programmable faults for testing I_{DDQ} measurements. We added a method of measuring impedance of an IC pad and simplified or improved analog functions.

A Windows-based hierarchical software control system runs the TORCH chip and collects data. Control of the TORCH test chip is now simple, portable, and inexpensive, involving a laptop computer, commercial off-the-shelf (COTS) personal computer memory card interface adapter (PCMCIA) *cards, and an open software control system that allows complete freedom of design while maintaining IEEE standard 1149.1 boundary scan conventions.*

We completed the design and fabrication of the TORCH-2 device as a test-bed for on-chip I_{DDQ} testing to explore *in situ* mixed-signal testing. Additionally, we advanced the control interface to be highly compatible with commercial test systems.

A new fabrication facility produced the TORCH-2 product, which caused us to retool for the new manufacturer's specifications. We received test samples approximately three months late, constraining those tasks we could complete in FY96. Nevertheless, we were able to test out many functions of TORCH-2.

We verified operation of the improved boundary scan interface, verified I_{DDQ} test circuits, and extensively tested the logarithmic analog-to-digital converter. The simplified analog switch matrix worked, and we made an external pad impedance measurement.

We found design margin problems in a critical timing generation block, compounded by converting our design to the new manufacturing specifications. This rendered some of the mixed signal circuitry inoperative. We have since corrected this problem in design and submitted modifications to our production facility. A follow-on customer (satellite group) is investing in the second production run of TORCH-2.

We now have a better appreciation of the intricacies involved in designing, simulating, and producing complex mixed-signal circuits such as the timing generation block mentioned above. The goals that we set for TORCH-2 were high and covered a wide range of topics. We recommend future IC designs be set to very specific and doable goals. The prime example is TORCH-3, where we will focus only on establishing a method of testing IC reliability *in situ*. We learned much about the limits of our design and simulation capabilities that will positively impact the design of TORCH-3.

We verified the digital circuitry in TORCH-2 to be operational via boundary scan. Measurements showed that the timing circuit is not generating proper clock signals to drive the analog-to-digital converter circuitry correctly, preventing accurate measurements *in situ*. We found circuit loading to be higher than simulations indicated, requiring increased time or drive strength.

As evidence of successes and learning achieved via this project, both hardware and software concepts from the TORCH-2 effort are being applied to the design of a new customer's part. This customer has embraced TORCH-2 test system philosophy and is using our PC-based COTS control system.

Microelectronic Biosensors

K. Wally, J. L. Rodriguez, S. H. Kravitz, J. S. Schoeniger

BioFETs are biologically modified ion-sensitive field-effect transistors (ISFETs). In a bioFET, an enzyme is attached to the gate of the ISFET. The enzyme promotes a biocatalytic reaction involving the target chemical, producing ionic reaction products that are detected by the underlying ISFET, providing information about the presence and concentration of the target chemical. In this first year, Sandia successfully demonstrated the bioFET principle using a Sandia-prepared bioFET based on discrete, commercially available, solid-state pH measurement probes. We obtained representative response curves of a prototype bioFET coated with acetylcholinesterase enzyme. We demonstrated successful covalent attachment of enzymes to the ion-sensitive semiconductor surfaces silicon nitride, tantalum oxide, and silicon dioxide. We successfully demonstrated the attachment of enzyme to layers of silicon dioxide sol-gel. Regarding enzymes, we successfully demonstrated that covalently attached enzymes exhibit significantly better resistance to degradation than the unattached enzyme. We are currently preparing an integrated bioFET that includes both the bioFET and a RefFET, as well as a platinum pseudoreference electrode on a single chip.

Over the past year, our research group made substantial progress in developing the capability to perform this type of sensor development at Sandia. We successfully demonstrated the bioFET principle using a Sandia-prepared bioFET based on discrete, commercially available, solid-state pH measurement probes. We obtained representative response curves of a prototype bioFET coated with acetylcholinesterase enzyme and a second, uncoated ISFET that served as a Reference FET (RefFET).

In the preparation of bioFETs, we made progress in the area of enzyme attachment. We demonstrated successful covalent attachment of enzymes to the ion-sensitive semiconductor surfaces silicon nitride, tantalum oxide, and silicon dioxide. We successfully demonstrated the attachment of enzyme to layers of silicon dioxide sol-gel, and demonstrated that multiple layers (0, 1, 2, 3) of sol-gel result in the covalent attachment of increased amounts of enzyme with increased enzymatic activity (up to 20 times the enzyme activity for a three-layer thickness of sol-gel).

Ordinary microphotolithography techniques are too harsh to use with biocoatings. Nevertheless, certain techniques modified to make them more biochemical-compatible can be adapted to the patterning of bioproteins onto semiconductor substrates. Researchers in our group successfully demonstrated the selective patterning of protein biocoatings. This ability is required to produce arrays of bioFETs on a single chip.

In the area of enzymes, we successfully demonstrated that covalently attached enzymes exhibit significantly better resistance to degradation than the unattached enzyme. Although the covalent attachment produced a sensor with a usable life, we began to investigate cross-linked enzyme crystals (CLECs). CLECs are a modified, highly robust form of enzyme that still exhibits true enzymatic activity despite cross-linking and crystallization. They are currently being developed in the biochemical technology field for continuous reuse in large biochemical reactors. We propose to investigate their use in bioFETs.

We are currently in the process of preparing an integrated bioFET that includes both the bioFET and a RefFET, as well as a platinum pseudoreference electrode on a single chip. We obtained the chip that serves as the basis for this integrated bioFET in limited quantity from a discontinued commercial source. We wirebonded and encapsulated the prototype chip, and it awaits enzyme coating to produce an integrated bioFET for test.

Validation of the MDL ASIC Prototyping Process

J. M. Green, M. Henry

Sandia is in the process of procuring electronic design automation (EDA) tools and physical libraries to establish captive application-specific integrated circuit (ASIC) prototyping service. We executed a pilot ASIC design project that validates that service. Validation addresses such issues as detailed library characterization, design methodology, and tool interoperability evaluation. In addition, this project encompasses all tasks associated with the definition, logic design, functional verification, physical design, performance evaluation, fabrication, and test of the pilot device. Critical byproducts of the project include a documented and proven design methodology, a characterization of the complementary metal-oxide semiconductor 6 (CMOS6) library cells (limited to those used in the MicroController Core [MCC] design), and development of the interfaces between the various EDA tools that comprise the ASIC design environment.

The selection of design tools and libraries, definition of the design process, and implementation were the first steps in developing Sandia's capability to manufacture high-performance, radiation-hardened ICs for space and military applications. We chose the candidate design, an MCC, for its modest complexity and universal application. The MCC design allowed the demonstration of advanced place-and-route tool features such as timing-driven layout and clock tree compilation.

The market for semiconductor components used in noncommercial applications such as Sandia's weapon and space systems has become very small. Commercial ASIC foundries, which allocate most of their capability to high-volume applications, are saturated with business from the personal computer and consumer electronics markets. To entice an ASIC vendor to produce a given component, the prospective customer must guarantee a large annual contract for volume purchases. As a result, it is

becoming difficult to find commercial ASIC foundries that are willing to fabricate ASICs for Sandia's low-volume requirements.

Sandia's requirements for microelectronics continues to be strong, both in the Defense Program (DP) and Work For Others (WFO) applications. However, without a sophisticated, captive service for ASIC prototyping and low-rate production, Sandia will fail to meet its programmatic needs for specialized high-density ICs. System applications include stockpile support for nuclear weapons, reentry vehicles, and satellite payloads. Upon completion of this project, the Microelectronics Development Laboratory (MDL) strategically positions itself to become a source of complex low-volume components for both internal and reimbursable customers.

To enable the capability to manufacture ICs, it was first necessary to have a complete cell library and compatible design-tool infrastructure in place. The targeted technology was 0.6-mm minimum feature size with 5-volt, CMOS-compatible processing.

Sandia's microelectronic processing is compatible with Compass's portable Passport, 0.6-mm library. The compatibility offered the quickest method to produce high-performance silicon since the design and characterization of the silicon could be done concurrently. In effect, this reduced the design/implementation cycle time by not requiring that library development be done prior to the actual commencement of the design cycle.

We installed the design tools and libraries and ordered the masks for manufacture. We received the silicon and accomplished wafer-probe characterization of the ASIC to demonstrate first-pass success.

We proved four wafers, each containing 78 MCC die. We debugged functional vectors within ten days of the delivery of material and confirmed the successful capture of the design's intent. All four wafers yielded 70+%. The highest yield on any wafer was 74%.

High-G Accelerometer for Earth-Penetrator Weapons Applications

B. R. Davies, J. J. Sniegowski, M. A. Polosky, T. R. Christenson, V. I. Bateman

The acceleration environment experienced by sensors and electronics in an earth-penetrator weapon (EPW) can exceed average accelerations of 20,000 Gs with peak transient accelerations in excess of several hundred thousand Gs. Commercially available accelerometers built for these shock levels are both expensive ($1800 each) and prone to failure. The purpose of this project is to develop a micromachined high-G accelerometer capable of measuring accelerations up to 50,000 Gs that will take advantage of the size, power, performance, reliability, and cost advantages inherent to surface micromachined polycrystalline silicon.

This project has progressed to the fabrication of the second prototype sensor, which is being packaged and will soon be tested. Both the second and third prototype sensors will consist of a two-plate capacitor, with one plate stationary with respect to the sensor housing and the second plate suspended by flexible beams that deflect in proportion to the magnitude of the acceleration experienced by the sensor housing.

We designed, fabricated, and tested the first prototype accelerometer. We based this device on an adaptation of a piezoresistive pressure sensor using silicon nitride diaphragm technology developed at Sandia. Once the prototype was tested, we determined that a capacitive plate multilevel polysilicon process would provide better performance. We also conducted a failure analysis study to characterize the failure mechanisms associated with high acceleration sensors.

We also designed and fabricated a second prototype polysilicon high-G accelerometer. This sensor consists of a two-plate capacitor, with one plate stationary with respect to the sensor housing and the second plate suspended by flexible beams that deflect in proportion to the magnitude of the acceleration experienced by the sensor housing. We designed the system with a sensor and reference capacitance, both being equal to approximately 100 femtoFarads (100×10^{-15}), and a sensor sensitivity of 100 attoFarads (100×10^{-18}). We designed the sensor to measure accelerations up to 50,000 Gs with a resolution of 50 Gs. Dominant design trade-offs included balancing large plate deflections sufficient to obtain acceptable signal-to-noise ratios from the capacitive sensors with the high stiffness suspension system necessary to obtain responsive sensor measurements (high natural frequency). Additional design trade-offs included optimizing response by designing a critically damped system being subjugated to processing constraints dictated by silicon dioxide wet-etch rates.

Agile Prototyping of Microelectromechanical Systems (MEMS)

C. C. Barron, C. L. Henderson, K. Current, E. J. Garcia, J. J. Sniegowski, S. M. Rodgers

The goal of this project is to establish an agile prototyping capability for microelectromechanical sensors and actuators based on Sandia's state-of-the-art tri-level polysilicon micromachining process. Development of this capability requires (1) baselining the fabrication process, (2) developing multi-user reticle capability, (3) developing design rules and layout tools for new designers, and (4) developing the infrastructure to make these tools and the necessary training available to designers. This capability will make our micromachining manufacturing process more widely available to Sandia programs and outside customers and thus vastly increase its impact on, and Sandia's visibility within, the microelectromechanical systems (MEMS) community. Sandia is well ahead of schedule in successfully completing the milestones for this project, having already developed a basic set of layout tools and trained over 20 new designers to design structures in the process. We also developed the capability to manufacture multiple customers' designs together on one reticle set, and at the end of FY96 have completed one such multi-user fabrication run.

In the area of baselining the process, we designed and fabricated a diagnostic module for the process that provides parametric test data to allow us to control the process. We also solved a number of outstanding manufacturing issues. In the area of multi-user reticles, we developed a "template" that allows us to drop customer modules into a file that already contains the diagnostic module and other structures necessary for the manufacturing process. The template procedure streamlined the process for generating new masks considerably. We completed fabrication of lots with the first multi-user reticle and are presently in the process of fabricating lots with two more multi-user reticles. In the design tools area, we developed the capability to generate complex mechanical structures in AutoCAD and, at the same time, retain the ability to do design rule checking with standard electronics layout tools. We also developed and gave two very popular short courses to train new users in the MEMS literature, the particulars of our process, and the use of the design tools. In short, this has been a very productive year for this high-performance team, and this project is so far very successful and months ahead of schedule.

Highly Parallel, Low-Power, Photonic Interconnects for Inter-Board Signal Distribution

R. F. Carson, I. A. Erteza, M. L. Lovejoy, D. C. Craft, B. T. Meyer, L. G. Pierson, M. E. Warren, K. L. Lear

As clock speeds and wordwidths increase in digital electronic systems, the problem of signal connection between circuit boards becomes increasingly acute. In many cases, these boards become connector-limited due to the large size of present electrical connector technology. When cross-talk and power consumption issues are included, the problems of interconnecting boards become limiting factors in system performance. Contact force and electrical cross-talk also become issues for large numbers of small-area connections. Recent advances in photonic device technology now enable additional solutions to the problems of high-speed, low-power, massively parallel (MP) interconnection between boards. Highly efficient vertical-cavity surface-emitting lasers (VCSELs) with built-in microlenses can be connected with low-power photoreceivers over free-space, noncontacting channels that directly connect circuit boards. Alternately, the VCSELs and photoreceivers can be configured to connect via small, direct board-level optical fiber, planar waveguide, or rod-lens arrays. In either case, data throughput can be greatly enhanced, while connector footprint, contact force, and cross-talk are reduced. These new photonic device technologies provide the first potentially practical approaches to MP optical interconnects because they use devices that can be mass-produced in arrays and that consume far less electrical power than the devices in traditional optical links.

We identified three application areas and developed basic requirements. These include (1) data links using optical fibers and/or free space for connection between isolated weapon circuit modules; (2) serial optical fiber interconnections for workstation-to-display applications; and (3) parallel free-space board-to-board interconnects for protocol processing applications. We performed initial tests to determine the suitability of present VCSEL and photoreceiver technologies for use in these applications using a breadboard setup, and demonstrated high data fidelity at 100 Mb/s. In response to the requirements established for the above applications, we identified several directions for device-level designs. The parameters associated with these designs include basic lensing and/or fiber requirements and optimal wavelength of operation. For the present board-level and connector-level applications, shorter wavelengths and front-emitting and collecting devices will be used. To this end, we laid out and built a new photoreceiver design and are applying new VCSEL devices.

Publications

Other

Carson, R. F. 1996. "Free-Space Low-Power Optoelectronics for MCMs and Circuit Boards." Paper presented to the Optical Society of America Annual Meeting, Rochester, NY, 20–24 October.

Carson, R. F., M. L. Lovejoy, K. L. Lear, M. E. Warren, P. K. Seigal, D. C. Craft, S. P. Kilcoyne, G. A. Patrizi, and O. Blum. 1996. "Low-Power Approaches for Parallel, Free-Space Photonic Interconnects." *Proc. SPIE Critical Rev. Conf. on Optoelectron. Interconnects and Packaging* **CR62** (San Jose, CA, 19–30 January): 35–63.

Carson, R. F., M. L. Lovejoy, K. L. Lear, M. E. Warren, P. K. Seigal, G. A. Patrizi, S. P. Kilcoyne, and D. C. Craft. 1996. "Low-Power Modular Parallel Photonic Data Links." *Proc. IEEE 46th Electron. Components and Technol. Conf.* (Orlando, FL, 28–31 May): 321–326.

A Planar Silicon Fabrication Process for High-Aspect-Ratio Micromachined Parts

C. C. Barron, W. D. Bonivert, J. J. Sniegowski, J. G. Fleming

Under this continuing project, Sandia is developing a new manufacturing process for high-aspect-ratio micromachined parts that will compete with the much-touted LIGA (lithography galvonoforming abforming) process but, unlike LIGA, (1) can be accomplished in a silicon integrated circuit (IC) fabrication facility and (2) is not limited to fabricating parts out of metal. The process we proposed, which builds on Sandia's existing micromachining expertise, enables us to fabricate 250x to 2000x stiffer microstructures—including much less floppy miniature metal machine parts, much stronger microactuators, and much more sensitive silicon accelerometers—than are obtainable with conventional silicon surface micromachining. The process is also planar and therefore compatible with subsequent integration with complementary metal oxide semiconductor (CMOS) and surface micromachined structures. The capability to integrate thick microstructures with silicon CMOS circuitry on the same chip will make possible revolutionary products in fields of both strategic and commercial importance, including, but not limited to, seismology, inertial guidance, atomic force microscopy (AFM), and remote sensing for vibrational analysis. In short, this technology will revolutionize micromachining by combining the high-aspect ratios heretofore only obtainable with the LIGA process with the inherent manufacturability and integrability of silicon micromachining.

We proposed the following goals for FY96: (1) to integrate the micromolding process with surface-micromachining, (2) to demonstrate integrability with CMOS, and (3) to design and fabricate molded electroplated metal parts. The first goal, by far the most important, was substantially completed. We did indeed demonstrate the fabrication of devices with both micromolded and surface-micromachined components. Under other funding we are continuing to perfect this integrated process, concentrating especially on successful "release" of the structures. Because of ES&H concerns associated with one of the manufacturing process steps required, we were not able to complete the second goal, but are continuing, again under other funding, to pursue CMOS integrability. Finally, we dropped the third goal, originally intended to demonstrate the competitiveness of silicon micromolding with LIGA, because it is less important to our micromechanics customers. Specifically we are focused on inertial guidance and seismic sensors, neither of which requires metal piece parts. Although our record of completing stated goals was mixed, we did advance the state-of-the-art in the area of high-aspect-ratio micromachining through the demonstration of the integration of surface micromachining with micromolding. This advance, when combined with CMOS integration, still promises to revolutionize the silicon sensor market, in particular, inertial guidance sensors and seismic accelerometers. In addition, we also expanded the scope of the micromolding technique by fabricating innovative micromolded devices with applications in optical displays and optical data storage. All of these accomplishments led to technical publications, and several will lead to patent applications in the coming year.

Publications

Other

Barron, C. C., J. G. Fleming, S. Montague, J. J. Sniegowski, and D. L. Hetherington. 1996. "Integrated Mold/Surface-Micromachining Process." Paper presented to the Smart Electronics and MEMS, San Diego, CA, 28–29 February.

Fleming, J. G., and C. C. Barron. 1996. "Characterization and Application of Deep Si Trench Etching." Paper presented to the Micromachining and Microfabrication Process Technology Meeting, Austin, TX, 16–18 October.

Fleming, J. G., and C. C. Barron. 1995. "Novel Silicon Fabrication Process for High-Aspect-Ratio Micromachined Parts." Paper presented to the Micromachining and Microfabrication Process Technology Meeting, Austin, TX, 23–24 October.

Fleming, J. G., C. C. Barron, B. Stallard, and S. Kaushik. 1997. "Fabrication of Large-Area Gratings with Submicron Pitch, Using Mold Micromachining." Paper presented to Optoelectronics '97, San Jose, CA, 13 February.

Mask and PMMA resist holder *(left)* and the cooling unit *(right)*.

Inside of the cooling unit.

An alternative micromachining process, known as LIGA, uses a deep x-ray lithographic. Shown is a precision mask holder used to hold up to a four-inch mask for synchrotron radiation exposure.

Experimental Replication of the Reifenschweiler Effect

R. S. Goeke

This report describes the work conducted at Sandia to fabricate the experimental apparatus and develop the titanium preparation process required to reproduce Reifenschweiler's experiment. The actual experiments involving tritium will be conducted at Los Alamos National Laboratory (LANL).

Reifenschweiler's experiment indicated a 40% decrease in the measured count rate of tritium. If this effect were real, the savings on our tritium stockpile could be as much as $1 billion/year as estimated by DOE. Team members from Sandia, LANL, and the University of New Mexico (UNM) met to critically evaluate Reifenschweiler's results, discussing possible explanations and experimental errors. Out of this meeting came the design requirements for the experimental apparatus. The equipment needed to be capable of repetitive experiments, using ultra-high-vacuum (UHV) technology, passivated stainless-steel components, a residual gas analyzer to monitor O_2 levels and T_2 release, a solid-state x-ray detector, ability to admit a controlled amount of T_2, and a nonhydriding heated stage. The ability to apply an electric field and introduce oxygen or glass also was required since these were potential artifacts of Reifenschweiler's system.

The system consists of two chambers. The first chamber is used for the titanium deposition. The titanium is evaporated from a heated tungsten filament wound with titanium wire. The evaporation, which looks like smoke, is created in an atmosphere of 10 torr of argon. Then 0.5 mg of the soot-like titanium is collected on the bottom of a 1"-square molybdenum substrate using time and power to control the deposition process. After the deposition, the substrate is rotated 180° and transferred to the second chamber using a linear actuator. The substrate is removed from the actuator onto a boralectric heating element. After the sample is isolated in the second chamber, a measured amount of tritium is introduced and quickly absorbed by the titanium preparation. We used only deuterium at Sandia to test this portion of the process. At LANL approximately 1 mCi of tritium will be used. At this point the sample is ready for the heating experiment.

After completion of the apparatus fabrication and titanium soot evaporation process, we transferred the equipment to LANL for conduction of the replication experiments. Results of these experiments are expected by the end of FY97.

Molecular Concentrator

J. E. Parmeter

The purpose of this project is to apply Sandia's trace explosives-detection technology (currently employed in a stationary personnel portal) into a portable system for the trace detection of narcotics. The system that we constructed contains two principal components: (1) a preconcentrator, designed and built at Sandia, that serves to collect and concentrate organic vapors or airborne particulate matter contained in an inlet airflow, and (2) a commercial ion-mobility spectrometer (IMS) that serves as the trace chemical detector. The preconcentrator operates by adsorbing incoming organic materials on a metal screen, while the incoming airflow (from an attached sampling hose) passes on to an exhaust line. Once this collection cycle is completed, the screen is heated to evolve the organic molecules into the gas phase. The resulting vapor-enriched air in the preconcentrator is then pulsed into the IMS, where the target analyte molecules are detected via the presence of atmospheric pressure chemical ionization. We constructed the system to fit on a wheeled cart. We showed the system to function for explosive (RDX) detection in a laboratory environment and will utilize it to "sniff" for narcotics in the near future.

The primary focus of this project was to transfer proven trace chemical detection technology developed at Sandia from a stationary personnel portal designed to detect explosives to a portable system that could be used for field detection of narcotics. The bulk of the effort was thus in the engineering and construction of this portable unit. Significant accomplishments in FY96 included the following:

(1) Designed and constructed a reduced-scale molecular preconcentrator to be utilized in the portable chemical trace detection unit. This preconcentrator is a smaller version of the one developed for use in our explosives personnel portal.

(2) Assembled the integrated portable chemical trace detection system, including preconcentrator, IMS, air blower to provide inlet airflow, personal computer for data acquisition, electrical circuitry, and all ancillary equipment.

(3) Initiated testing of the trace chemical detection system in a laboratory environment. We performed the initial testing with the explosive compound RDX (cyclotrimethylenetrinitramine) and showed that the unit is functional. In the near future (when permits allow it) we will test the system for narcotics detection in the laboratory and will ultimately use it in field tests in Albuquerque schools to "sniff" for drugs.

Investigation of Concepts for Storing and Releasing Energy from Nuclear Isomers

J. F. Cuderman

Nuclear isomers are nuclei that exist in excited, metastable states. Some nuclei have the ability to absorb energy, then store the energy in the form of increased spin (spin isomers) or a distortion of the shape of the nucleus (shape isomers). Energy is released from these excited nuclei (isomers) only in the form of gamma rays or electrons ejected from the atom by the emitted gamma rays. Proposals that nuclear isomers could be developed as sources of high-energy density if the energy stored in the metastable state could be released on demand have recently appeared in the nuclear physics literature. If this could be achieved, the potential exists for bridging the gap between conventional explosives and fission. We proposed to review the literature and evaluate the possibilities for making nuclear isomers and developing techniques for releasing the energy on demand. We received funding for a literature and technology survey, and for analysis and evaluation of production possibilities and energy release options. This summary presents the general results of these studies.

The literature survey revealed many hundreds of references on the subject of nuclear isomers. However, we found that there are only a small number that deal with production of nuclear isomers and stimulated energy release from them. Much of the earlier work dealt with using isomers as the medium in gamma-ray lasers. We identified and evaluated several possible approaches for making nuclear isomers and for effecting energy release from the metastable states. Isomers can be made in nuclear reactors, high-energy accelerators, and photon sources. They might be separated from nuclear reactor waste. One isomer, 180M Ta, occurs in nature. All require extensive processing, separation, and purification after manufacture. All have proven to be extremely difficult to obtain in sufficient quantities to do definitive experiments. Our study identified isomers that could be made in Sandia's reactors, obtained from nuclear waste, or purchased. We suggested that the small amounts of available material might be sufficient to study de-excitation mechanisms using Bose-Einstein condensates. We identified four promising techniques for de-exciting isomers: (1) x-ray–triggered release, (2) stimulated emission, (3) neutron autocatalysis, and (4) the nuclear excitation by electron transition (NEET)/TEEN process. Half a dozen or so experimental and a dozen or more theoretical papers offer evidence that these de-excitation approaches are possible. X-ray–triggered release appears to have been demonstrated experimentally. Stimulated emission was reported to have been successfully initiated in one experiment. Some experimental data exist for neutron autocatalysis and for NEET. Our study evaluated in some detail two of the possible de-excitation approaches—neutron autocatalysis and the NEET/TEEN approach. The results of the neutron catalysis and NEET/TEEN analyses indicate that the neutron catalysis approach is likely to be of limited utility, but that the NEET/TEEN processes have more promise. While we conclude that there are not currently sufficient physics data to undertake a high-energy-density material (HEDM) development program, we recommend that (1) modest amounts of research on nuclear isomers with a goal of developing HEDMs be supported at the four national weapons laboratories, (2) the research at the national labs be coordinated to optimize the use of limited funds, (3) the use of Bose-Einstein condensates be examined further as a possible way to study energy release mechanisms, (4) methods be explored to manufacture sufficient amounts of materials to do definitive experiments (perhaps find nuclear isomers that are relatively easy to make, to do initial physics demonstration experiments), even though they might not be optimum HEDM candidates, and (5) experiments that have been done only once with marginal results be independently verified.

CLERVER, Win95

K. C. Bauer

Sandia examined the feasibility of designing and writing software for the Windows 95 and Windows/NT platform to allow native Windows applications to be "shared" across the network between two or more geographically separated collaborators. This software was intended to provide similar functionality to the Unix X11 system that Sandia developed and licensed to commercial industry. The Unix version of the software is known as the CLERVER (part Client and part Server).

Sandia has already developed and licensed to the commercial industry a product that allows a Unix X11-based application to be shared; this product was greeted with favor by Unix users. There were many questions about the availability of products to provide similar functionality to run native applications on Windows NT or Windows 95. We wanted to investigate the architecture of Windows to find out if it was feasible and, if so, how much effort it would take to design and code a proof-of-concept system to share a limited set of Windows applications.

The primary conclusion of this project is that it is possible to write the software to "share" a native Windows application between two or more machines in a network. There were some significant stumbling blocks along the way. The internal details of Windows 95 are quite complex, and Microsoft was not helpful in answering detailed technical questions on how some of the low-level internals really work. As a result, we spent a good deal of time digging out details on our own that we could not obtain answers to. In the end, we produced a limited prototype system that will allow a simple Windows application to be shared. The performance of the shared application was quite good.

However, we recommend that product development not proceed any further. In the last part of FY96, Microsoft released a Beta version of a product

(Microsoft NetMeeting) onto the market. The purpose of this product is the same as ours: to share Windows applications. The fact that this product was coming was a complete surprise to us and may help explain why Microsoft was not forthcoming with information to our technical questions. It is certainly not in Sandia's best interest to develop software that would compete with software that Microsoft plans to market.

A Tool to Detect External Cracks from Within a Tube

T. W. Caffey

The goal of this project is to see whether or not the electric fields from a magnetic dipole within a metal tube are both uniform and small enough to allow the detection of cracks in the external tube wall.

A magnetic dipole, with its moment along the x-axis of a Cartesian coordinate system, is known to provide an electric field with a component along the z-axis. This Ez-field is zero throughout the entire xz-plane, and has a bi-lobed distribution with maximums along the $\pm y$-axis. If the axis of a metal tube is taken as the z-axis, and if the magnetic dipole is centered in the tube, the total Ez-field should be nearly zero at the walls of the tube due to the large conductivity of the metal. Because of symmetric out-of-phase reflection, the net interior Ez-field should be very small and relatively uniform throughout the interior of the tube. A small electric dipole, oriented along the z-axis and centered within the tube near the magnetic dipole, might be able to detect the effects of cracks on the exterior of the tube if the operating frequency were properly chosen.

We wrote a computer code to predict the Ez-fields from a horizontal magnetic dipole in a tube based on the work of Wait and Hill. The code is written in Microsoft and Fortran and consists of over 5000 noncomment source statements. We found the total Ez-field to be symmetric in the xy-plane, but unfortunately, the field was also relatively large and non-uniform. We concluded that the internal field is too great to permit the detection of scattered fields from a crack in the exterior tube wall.

This code can be used to examine the electromagnetic fields from either magnetic or electric dipoles, of any orientation and combination, within a tube or borehole, and thence to the surrounding medium. The code has possible applications to instrumentation for oil and gas exploration, and to the analysis of data obtained with electromagnetic borehole tools.

Infrastructural Decision Support

P. A. Davis

Sandia produced a design prototype for a water resources management decision support system (DSS). The prototype illustrates the application of technical advances in information processing, display, and communication to reaching and communicating decisions affecting resource management. The prototype illustrates a decision process developed for water resource management in Puerto Rico. This decision process was designed from the results of a Vital Issues Process conducted with representatives of government, academia, and the public in Puerto Rico. The prototype further illustrates integration of on-line communication and remote execution in the context of a World Wide Web (WWW) site.

We developed a prototype interface illustrating the performance of a proposed DSS for water resources in Puerto Rico. We designed the interface and the underlying decision processes on which it was predicated to address concerns of diverse stakeholders in Puerto Rico. Information gathered during a Vital Issues Process conducted with representatives of government, academia, and the public formed the basis of the design.

We implemented the prototype on the WWW to illustrate a proposed approach to decision support and to demonstrate and test the performance of two supporting capabilities: on-line multiparty communication, and execution of compute-intensive processes on remote systems. We demonstrated the completed prototype in Puerto Rico before the final Vital Issues Panel. We also prepared a brief report describing the relationship between the Vital Issues Process and the DSS, outlining the design of the DSS, and describing the design of the prototype.

We successfully implemented the communication and remote execution functions in the prototype. The prototype design process underscored the need to work from a clear and coherent conception of the underlying DSS.

Development of Quiescent Power-Supply Voltage (V_{DDQ}) Testing

E. I. Cole, W. J. Witkowski, C. L. Henderson, J. M. Soden

Sandia examined the feasibility of using quiescent power-supply voltage (V_{DDQ}) testing to analyze integrated circuits (ICs) for defects. We developed the hardware and software necessary for data analysis and determined the sensitivity of the V_{DDQ} analysis method. This report discusses the signal acquisition methodology and compares the data acquisition speed and resolution to existing testing techniques.

Recently, several new failure analysis techniques with great sensitivity for locating IC failures were developed using constant current biasing. These techniques have proven to be very successful to Sandia and the microelectronics industry. We examined the feasibility of a new IC testing methodology that takes advantage of increased sensitivity of constant current biasing employed by the new failure analysis techniques. We call this methodology V_{DDQ} testing.

Our analysis to date has provided several significant findings: (1) V_{DDQ} variations with IC operation can be measured and recorded using standard laboratory equipment, (2) simulated defects have been detected with equivalent sensitivity and an order-of-magnitude faster than existing analysis methods, and (3) the bandwidth response and sensitivity are largely dependent upon the hardware setup used.

We propose that the V_{DDQ} work started under this project be continued to determine if V_{DDQ} could complement or supplement existing testing approaches. The demonstrated high sensitivity and speed of data acquisition are most promising. We are presently pursuing additional funding to further V_{DDQ} analysis.

As stated above, the V_{DDQ} signal was used to detect with high sensitivity and improved system bandwidth. We acquired these data using a production tester in conjunction with external hardware. The V_{DDQ} signals acquired clearly indicate where the defects are activated.

Development of Failure and Yield Enhancement Analysis for Integrated Microelectromechanical Systems

K. A. Peterson, D. H. Cooper, P. Tangyunyong, J. L. Rife

We accomplished our initial goal in development of a first-of-its-kind failure analysis (FA) capability that is of immediate use for both FA and yield enhancement for integrated microelectromechanical systems (IMEMS). We briefly considered current FA problems, including wear and stiction, ambient conditions, stress and strain measurement and control, thermal effects, contamination, and systems analysis. We identified four techniques and used them to address current FA problems. These include infrared (IR) microscopy for thermal effects, scanning-electron microscopy (SEM) for charge effects, acoustic microscopy for stiction, and light-emission (LE) microscopy for wear sites. The first two of these provided new results that enhance localization of the problematic sites in IMEMS performance degradation.

New techniques are needed to perform FA on micromachines and to characterize wear. Microengines exhibiting wear and stiction normally show degrading performance without any physical indication of wear. We identified several areas for study: thermal effects, electrostatic effects, stiction, and the possibility of light emission. We designed and fabricated a controller to permit operation of microengines under ambient and vacuum conditions. We equipped an SEM with electrical feedthroughs for *in situ* examination. We obtained microengine die in 40-pin ceramic dual in-line packages and characterized them with regard to initial behavior.

We observed heating due to operation of the comb structures that drive microengines at possible defective locations, which implies contact of differentially charged structures. Arcing could not be associated with this contact as we did not observe light emission. We observed electrostatic charge imparted to operating microengine elements via an electron beam to interrupt normal operation of these microengines. Electron beam exposure on static structures had no effect. Preliminary acoustic microscopy resolved gear and comb features such as gear tilting and geometrical symmetry, but did not clarify stiction behavior.

The results from SEM images strongly indicate an effect from electrostatic charging. This warrants additional work to see if electrostatic charging can explain degradation of performance that doesn't leave other physical evidence (scratches, debris, etc.). The results from the IR microscopy show hot spots that do not involve the gear or hub. We recommend additional work on technique development as an important step in developing FA capability for MEMS.

We used IR radiation in a study of thermal effects to image microengines that were operating smoothly for comparison to those that were not. The results indicate a small temperature rise in the certain areas of the comb structure of the "choppy" microengines that were not present in those operating smoothly. This suggested arcing or sticking of combs. We saw no temperature difference associated with the rotation of the gear on the hub. We investigated electrostatic effects using an SEM to image microengines that were running. These engines became stuck in the electron beam and stayed stuck following removal from the SEM. Other engines that were imaged for 20 minutes without being run were free following removal from the equipment chamber. An apparatus capable of detecting minute amounts of light did not reveal any light emitted from the comb regions of choppy microengines.

Exploration of Multichip Module (MCM) Test Solutions for Reliability Enhancement

A. W. Righter

Sandia examined the reliability implications of two novel test methods that can be used in multichip module (MCM) applications. We applied the two test methods' stress voltage I_{DDQ} (quiescent current measurement) at the V_{DD} node of an integrated circuit (IC) testing and low-voltage maximum frequency testing, to a large sample size of an I_{DDQ} testable complementary metal-oxide semiconductor (CMOS) IC. We subjected subsets of these ICs, as well as subsets of ICs not exposed to these tests, to a long-term lifetest. We desired to determine the reliability implications of these tests as opposed to a lifetest of a control sample of the ICs not undergoing the tests.

Industry applications of I_{DDQ} testing have noted correlation between high-I_{DDQ} ICs and burn-in failures. Also, low-voltage speed testing of ICs has been reported to detect additional defects that I_{DDQ} testing may not detect. However, the effect on reliability of these ICs and MCMs using these ICs has not been studied. We examined the feasibility of (1) I_{DDQ} testing of an IC at a stress voltage to simulate a quick burn-in–like stress on burn-in reduction and reliability improvement and (2) low-voltage maximum-frequency testing (operating the IC at the lowest supply voltage to sustain correct functional operation and measuring the maximum operating frequency at that voltage) on reliability.

Our analysis to date has provided several significant findings: (1) I_{DDQ} testing at a stress voltage does improve reliability of ICs subjected to a 2000-hour industry standard lifetest in comparison to a control nominal voltage-only sublot, (2) low-voltage maximum-frequency test-only failures do not functionally fail during lifetest, and (3) many of the low-voltage maximum-frequency–only failing ICs healed (became operational at higher frequency at later stages in the lifetest).

We propose that the reliability work started under this project be continued to determine the time that the control and optimized test ICs do eventually fail. No study has yet been completed in industry to determine this. We desire to find these fail-times because it has reliability implications for defense systems using ICs tested this way. The microelectronics industry has expressed interest as well.

Out of 49 low-voltage maximum-frequency–only failing ICs beginning lifetest, none failed functionally during lifetest; however, 10 ICs gradually increased their operating frequency through lifetest, and passed at the last post-lifetest measurement. Six additional ICs had their maximum frequencies increase. None decreased further in maximum frequency from their initial pre-lifetest readings. Comparison of a sublot of 72 nominal (5 V) voltage ICs with 72 8-volt I_{DDQ} stress-tested ICs revealed that one IC from the control lot failed functional after 2000 hours of lifetest, and six had markedly increased I_{DDQ}, indicating defects were impacting the performance. The 8-volt lot had no functional fails, and only two ICs had minor increases in I_{DDQ} after 2000 hours.

Optical Actuation of Micromechanical Components

D. R. Koehler

Electromagnetic (EM) momentum is a fundamental physical concept that has been demonstrated experimentally and incorporated theoretically in various areas of physics. Because the force upon an object impacted by an advancing energy wave is proportional to the wave's "energy content per unit length," EM energy produces a weak impulsive force (inversely proportional to wave velocity = c). Acoustic waves also carry momentum and, because of the smaller wave velocities, are more energetically effective in wave-momentum transfer processes. In spite of the weak character of the EM momentum transfer process, the combination of latter-day, high-energy laser light sources and microminiature mechanical elements suggested the possibility of optical excitation of these structures. Therefore, Sandia undertook a theoretical analysis to determine the viability of imparting actuation energies to micromechanical structures via optical energy. We considered a simple beam element to determine what energy and momentum levels were necessary for stimulation, whether current high-energy sources were adequate for the task, and whether these energies could be imparted without destruction of the structure. Analysis has, in fact, shown that available laser light sources can deliver the requisite optical energy to mechanically actuate the structures. Therefore, this actuation mechanism could be considered viable should device design warrant its application.

One outcome of the present analytical formulation is the prediction of an optopiezic effect wherein EM momentum causes a mechanical stress on a dielectric layer. If this is a valid prediction, such an optically induced, expansional pressure effect could be utilized as an extensional optical-to-mechanical transduction means.

The unique features of this optical actuation concept and its advantages over competing technologies include (1) use of an external light source, no transducers; (2) remote actuation; and (3) simpler construction with smaller element dimensioning possible. The disadvantages are that it (1) requires high powers and (2) requires extremely low optical absorptive characteristics.

Analysis of microminiature beam elements has, however, shown that available laser light sources can deliver the requisite optical energy to mechanically actuate the structures, 24 watts and 14 mJoules for the example chosen. This actuation mechanism can be considered viable should device design warrant its application.

We predicted an optically produced strain effect, that is, an optopiezic effect wherein EM momentum causes a mechanical stress on a dielectric layer, within the present analytical formulation. If this is a valid prediction, it would be theoretically possible, although energetically inefficient, to utilize this optically induced, expansional pressure effect as an extensional optical-to-mechanical transduction means.

Statistical Characterization of MEMS Microengine Devices

N. F. Smith

This report describes the design and construction of a system used to test a statistically significant number of microelectromechanical systems (MEMS) microengine devices. MEMS is a key enabling technology that will form the basis for advanced weapon, intelligence, and commercial components in the 21st century. The report covers the construction of the test fixture and the video microscope positioning system that the operator uses to observe the performance of each MEMS device. It was the first experiment to measure performance data (time to failure) for 40 microengines simultaneously.

The performance characterization of MEMS devices up to this point has been limited to a few individual devices. This method of testing is very inefficient and expensive. We built a system to test these microengines in parallel. Our approach was to apply a stress stimulus to eighty packaged microengines with quartz covers. This minimized the time required to test each device while maximizing the amount of data collected. Each microengine was powered and running. At specified time increments, we scanned the microengines to determine functionality.

The system that we designed consisted of the following: (1) a test fixture capable of stressing up to eighty MEMS devices, all in parallel, (2) a computer-controlled gantry-style XYZ positioner, (3) a video microscope mounted to the positioner, and (4) associated control hardware and software to make the entire system functional.

The test fixture consisted of twenty integrated circuit (IC) sockets. Each socket was electrically isolated from the other sockets on the test fixture and was capable of stimulating four MEMS devices. This electrical isolation allowed each device to fail without affecting the signals applied to the other devices under test.

The gantry positioner holds the test fixture firmly to its mounting surface, which prevents the samples from being dislocated by someone bumping the system. We equipped the gantry with a 365x magnification video microscope. This microscope can be positioned to view any device under test to within 10 microns. Due to variations in the packaging of the devices, the operator must first teach the gantry where each device is located. Once we "mapped" each device, we applied the stress stimulus. The operator only needed to view each device and note whether or not it had failed. The viewing process took about 10 minutes to complete, thus minimizing the time the operator had to spend working on the system. We scanned for failures on an hourly basis.

The success of our initial test determined that the overall technical approach was indeed sound. The gantry positioner was accurate enough for this use. The video system worked appropriately.

We had several findings that will allow us to fine-tune this ongoing experiment. The first was the difficulty experienced by the operator in making the decision for a failed part. When the microengines were operating at 150 K rpm, it was difficult to determine rotation. Second, the magnification of the video microscope was lower than we would have liked. Third, using an operator to view the parts limited the timing increments to regular working hours.

We will add a strobe unit to determine microengine rotation. We should increase the magnification of the video microscope. Removing the operator from the task of scanning the part by using video recognition software would be extremely useful.

Our data from the initial test were very sketchy. We did observe two parts fail during the test, but have not gotten enough data to truly analyze.

Optical State-of-Charge Monitor for Lead-Acid Batteries

J. D. Weiss, B. R. Stallard

This report describes experimental results demonstrating the feasibility of a proposed optical state-of-charge monitor for lead-acid batteries. The operating principle of this device would be changes in the optical absorption of the aqueous sulfuric acid electrolyte with sulfuric acid concentration, which varies considerably during discharge. Absorption measurements concentrated on the vicinity of the absorption peaks of pure water at 1450 nm, 1200 nm, and 975 nm on solutions containing a representative range of sulfuric acid concentration. The results demonstrated a substantial and nearly linear drop in absorption with sulfuric acid concentration and appear explicable by assuming that the drop in absorption is caused simply by the concomitant reduction in the number of water molecules in the optical path.

As an expected contribution to pollution abatement, we are pursuing the development of electric vehicles with all deliberate speed. Since the state-of-charge of a battery in an electric vehicle is equivalent to the volume of gasoline in the tank of a conventional automobile, it is essential that this state be measured continuously and in a non-interfering manner. Electrical methods of determining the charge delivered through a time-integration of the total current are, by nature, interfering and could accumulate inaccuracies if any offsets exist in the measurement system. We demonstrated the feasibility of using an optical method of measuring the state-of-charge of lead-acid batteries, anticipated to be the power source of electric vehicles. Being optical,

this sensor would be electrically non-interfering, and it would provide an instantaneous measure of the charge-state.

The operation of this sensor is based on the fact that as a lead-acid battery discharges, the concentration of sulfuric acid in its electrolyte diminishes, resulting in a drop in specific gravity from about 1.31 to about 1.1 during this process. In addition to this well-known reduction in specific gravity, we speculated that the solution's optical absorption would also change with sulfuric acid concentration. Measurements described below verify this speculation and thus identify an optical means to monitor the state-of-charge of this kind of battery.

Sandia performed these absorption measurements on various solutions ranging in specific gravity from 1.45 to 1.0 over a wavelength region from 909 nm to 1450 nm. We paid particular attention to the absorption peaks of pure water at 975 nm, 1200 nm, and 1450 nm, where it was thought that the presence of sulfate ions would have its greatest effect. The optical pathlength at 1450 nm was 1 mm; at the others, it was 1 cm. A marked absorbence drop did occur at those three wavelengths, with the greatest occurring at 1450 nm, where the absorbence in pure water is greatest. At this wavelength, the absorbence dropped essentially linearly from 1.35 to .31 as the specific gravity increased from 1.0 to 1.45. Furthermore, the shape of the absorbence peaks changed only slightly. These results suggest that the effect can be explained by the reduction in the number of water molecules in the optical path. We proposed two sensor configurations, depending on whether a flooded cell or an absorbed glass mat is used.

Impact of Focused Ion-Beam Microsurgery on Integrated Circuit Reliability

A. N. Campbell, J. L. Rife, J. M. Soden, K. A. Peterson

This project studied the degradation effects of Ga^+ focused-ion beam (FIB) irradiation on n- *and* p-*channel metal-oxide-semiconductor (MOS) transistors. The degradation was characterized by monitoring the change in transistor parameters (threshold voltage [V_{TH}], transconductance, etc.) as a function of ion dose, ion dose rate, and transistor geometry. We explored two possible methods for mitigating the degradation of transistor parameters: (1) electron flood charge neutralization during exposure and (2) thermal annealing following ion beam exposure. We use the results of these experiments to help identify the degradation mechanism.*

FIB systems are used routinely to perform "microsurgery" on integrated circuits (ICs) for IC modification, design verification, and failure analysis applications. FIB microsurgery involves precisely removing and/or reconstructing electrically insulating and conducting regions to perform circuit edits on localized areas of an IC. In the National Security Sector (NSS) programs with small volumes of ICs and critical cost and time schedules, it would be desirable to be able to use FIB-modified ICs for long-term critical applications. However, an important limitation of this approach is that FIB irradiation (30 keV Ga^+) can adversely affect IC performance. Whereas degradation due to electrostatic discharge (ESD) and electrical performance changes arising from physically rewiring the IC are understood, very little work has been done to understand how FIB irradiation degrades transistors or how to prevent it.

We found that transistor degradation occurs for both *n*- and *p*-channel transistors, although the effects are larger for the *n*-channel transistors. The changes in transistor parameters with dose, dose rate, and transistor geometry are consistent with the formation during irradiation of traps (silicon dangling bonds) at the interface between the gate oxide and the silicon substrate. We learned that the use of an electron floodgun to minimize surface-charging and ESD also significantly reduces transistor degradation. Degraded transistors recovered during post-irradiation thermal annealing.

The finding that degradation is minimized by using electron flood charge neutralization indicates that charge neutralization should be used whenever possible in performing FIB modification of ICs. When charge neutralization is not an option, our results show that post-FIB annealing will reduce the degradation.

All of the transistor parameters that we monitored (including V_{TH}, transconductance, and mobility) showed measurable changes as a result of FIB irradiation. For example, the V_{TH} for *n*-channel transistors increased in magnitude from 0.8-V pre-irradiation to 2.6 V after an ion dose of 1 nC/mm^2. The increase in V_{TH} is approximately linear with the total ion dose plotted on a logarithmic scale. The use of an electron floodgun for charge neutralization significantly reduced the shifts in V_{TH} and other measured parameters. Post-irradiation annealing at 150° C for 10 hours eliminated the parameter shifts. We found the change in transistor parameters to be larger for shorter channel devices. These measured parameter shifts are consistent with the activation of an interface trapping mechanism during irradiation.

Extended Cavity Fiber/VCSEL for Photonic Application

K. D. Choquette, C. T. Sullivan

Optical fiber has enabled the information "super highway," providing the means for electronic services and data access to the home and office. In addition, there has been rapid commercial development of Bragg fiber gratings (BFGs), which are written into standard or custom single-mode optical fiber with reflectivity as high as 99%. It is our proposal to integrate a BFG with a vertical-cavity surface-emitting laser (VCSEL) to pursue a potentially low-cost, high-performance laser source for optical fiber applications. The BFG coupled to the VCSEL will enable both wavelength selection and control within a robust and potentially low-cost device configuration.

The VCSEL structures used in this work will either completely lack a monolithic top mirror (i.e., "half" VCSEL), or have a low-reflectivity (high-output) top mirror for current spreading and passivation. Thus, the BFG will effectively serve as the second mirror to form an extended laser cavity. The BFG coupled to the VCSEL will enable wavelength and transverse mode control within a robust and potentially low-cost device configuration. The advantages of this hybrid semiconductor/fiber laser structure are high-power, single-mode output; the gain and the optical cavity are thermally decoupled, allowing external control of the wavelength selection and stability; fiber-based components can be inserted easily for amplitude, frequency, or polarization modulation; and the laser output is automatically coupled to the fiber. Our accomplishments to date include the following:

(1) Designed and fabricated a VCSEL structure containing a monolithic bottom distributed Bragg reflector (DBR) mirror and an active region.

(2) Determined that a modified intracavity contact is required for the "half" VCSEL structure.

(3) Integrated BFG with conventional 980-nm VCSEL.

(4) Observed novel transverse mode evolution with increasing injection current to the fiber/VCSEL combination due to laser feedback.

(5) Demonstrated transverse mode filtering using BFG; obtained single-mode output from 980-nm fiber/VCSEL.

Characterization of Semiconductor Piezoelectricity for Chemical-Sensing and High-Frequency Applications

S. A. Casalnuovo, B. E. Hammons, D. J. Rieger, G. C. Frye

Sandia designed and fabricated surface acoustic-wave (SAW) devices in the piezoelectric compound semiconductors gallium arsenide (GaAs) and aluminum gallium arsenide (AlGaAs) using standard microelectronic fabrication processes. This work represents the first step toward the monolithic integration of acoustic devices with high-frequency microelectronics and optoelectronics for chemical sensing, radar, and telecommunications applications. We report the characteristics of these SAW devices as well as the performance of the first chemical sensor based on a GaAs SAW device. We compare test results to conventional quartz SAW devices.

The piezoelectric properties of compound semiconductors, coupled with the ability to grow or deposit thin films of these materials, make compound semiconductors candidate substrates for integration of high-frequency acoustic devices and microelectronics for chemical sensing, radar, and telecommunications applications. However, relatively little is known about the piezoelectric properties of compound semiconductors in comparison to other piezoelectric materials, and little work has been done to characterize acoustic devices in the semiconducting materials. In this project, we studied acoustic device performance in GaAs and AlGaAs, two materials of particular importance to the compound semiconductor microelectronics industry, as a function of design and fabrication process parameters by fabricating SAW devices using standard microelectronics fabrication techniques. We also fabricated and tested the first GaAs chemical sensor based on an acoustic device.

We succeeded in producing low-loss, low-noise SAW delay lines on GaAs substrates, operating at frequencies of 100 megahertz (MHz) and 200 MHz. These devices match or exceed the loss and noise characteristics of quartz SAW devices, the current standard for chemical-sensing applications. We also produced a GaAs SAW delay line operating at 500 MHz, although this design has not yet been optimized. We demonstrated chemical sensing with GaAs SAW devices, using a 100-MHz delay line as a chemical sensor. This device can detect trichloroethylene, an organic solvent, at a level of five parts per million, comparable to the detectivity of quartz SAW sensors. We also developed a fabrication process for patterning the chemically selective layer on these sensors that may permit the fabrication of arrays of sensors on a single substrate.

Results on AlGaAs layers are not as promising. SAW devices had higher loss and greater noise than the GaAs devices. We believe that this is the result of problems with the AlGaAs epitaxial growth process and can be solved in future fabrication runs.

Future efforts should concentrate on three aspects: (1) the optimization of higher-frequency (500 MHz and higher) SAW devices for improved chemical sensitivity and greater relevance to radar and telecommunications applications; (2) improved AlGaAs epitaxial growth, since AlGaAs is expected to be a superior piezoelectric material compared to GaAs; and (3) the integration of microelectronics with the SAW devices, which should be straightforward, given the results of this work.

Magnetically Excited Flexural Plate Wave Device

K. W. Schubert, G. C. Frye

This report documents the successful demonstration a new type of acoustic wave device, the magnetically excited flexural plate wave (mag-FPW) device. The device structure and operation are briefly described, as well as the fabrication method. Prototype designs include both one-port resonators and two-port delay lines that operate at three different frequencies. We outline unique aspects of the mag-FPW device and contrast the device with similar devices such as piezoelectrically excited FPW devices and related surface acoustic-wave (SAW) devices. We briefly discuss potential advantages arising from these unique aspects. We present representative data that demonstrate damping effects due to ambient pressure and discuss the effects of input power and magnetic field strength.

Acoustic devices have a number of applications, including frequency filtering, oscillator control, signal processing, and sensors. The FPW device is similar to the SAW device in exciting an acoustic wave, but also has some important differences. Since the wave is excited in a thin membrane rather than a thick substrate, two advantages are realized: (1) the FPW wave velocity is much lower, providing a lower operating frequency and simpler associated electronics; and (2) the FPW wave velocity is more sensitive to surface perturbations (e.g., mass accumulation). The latter results in greater sensitivity in chemical sensor applications. The mag-FPW embodies a new means for exciting and detecting acoustic waves in a membrane. These waves are typically excited in FPW devices using interdigital electrode transducers (IDTs) patterned on a piezoelectric membrane. The mag-FPW replaces the IDT with a meander-line transducer (MLT) and eliminates the piezoelectric layer in the membrane. A static in-plane magnetic field is imposed to excite and detect the acoustic waves. The acoustic wave in the membrane is set up due to the alternating Lorentz force on the MLT legs arising from the interaction of the static in-plane magnetic field with the alternating current imposed on the MLT. Elimination of the piezoelectric film simplifies the structure and should make it easier to integrate with standard silicon processing. Furthermore, the transducer coupling strength can be "tuned" by adjusting the externally applied magnetic field.

We designed and fabricated prototype mag-FPW devices using bulk silicon micromachining techniques. The device consists of a silicon nitride membrane suspended within a crystalline silicon frame. We patterned MLTs on the top surface of the silicon-nitride before removing the underlying silicon to free the membrane. We demonstrated delay-line (two-port) and resonator (single-port)–type devices. We used both permanent magnets and a tunable laboratory electromagnet to supply the magnetic field. We developed models to describe the effects of magnetic field strength and ambient pressure on the coupling. The quality-factor (Q) for typical two-port devices increased from about 1000 to 7500 as the pressure was reduced from atmospheric to 100 millitorr. We observed and modeled nonlinear effects due to the magnetic field strength and input power.

Crack Propagation in Energetic Materials

A. M. Renlund, W. W. Tarbell

This project focused on evaluating the usefulness of flash x-ray for imaging cracks in energetic materials (EMs). The temporal evolution of cracks following low-level shocks, such as those that would be encountered in earth penetrator ordnance, or impact of EM is important to predicting their survivability and performance. For these preliminary tests, we chose to image static cracks to see what spacings were detectable and what geometries would optimize the contrast on the x-ray image. We were also interested in the depth of cracks in the material sample. To complete this project in the short period of time allotted, we studied materials we had on hand, including two plastic-bonded explosives (PBX 9404 and PBX 9502) and one propellant (Al/AP/HTPB). We describe here the results of several flash x-ray tests on these samples, with both well-defined spatial cracks and irregular partial cracks.

We used a multihead flash x-ray system to image the EM test specimens (0.5- to 1.5-inch diameter, up to 0.5-inch thick). Initial tests used a .004-inch mylar spacer between two machined pellets. We imaged the test specimens both from the side and from angles (not from the face). The mylar spacers showed up clearly as a lighter band in the x-ray photograph. There appeared to be no appreciable sensitivity to which of the EMs were used in this configuration. We then cleaved or cracked one pellet each of the three EMs and reassembled the sample halves. A hairline crack was visible in each of the two reassembled PBX samples; the propellant sample had a more irregular crack, including some gaps. We imaged each of these rejoined samples using the flash x-ray system. When viewed from the face, each crack was clearly visible. Even when viewed from a 45° angle, the cracks remained well-defined. (The optimal geometry may not be feasible for tests of dynamic crack propagation due to limitations on positioning of the x-ray heads on ports of an explosion or impact chamber.)

We performed other tests using two cracked specimens, stacked so their cracks were perpendicular to each other. X-ray images showed both crack patterns, indicating that a crack that propagates only through part of the depth of a sample can be detected, even though its position within the sample remains unknown. We also looked at the effects of shielding materials typically used in actual explosive testing to protect the equipment from fragment and over-pressure damage. We observed attenuation of overall signal and less contrast, but the crack patterns remained distinctive. These results are promising for future work on monitoring the temporal evolution of cracks formed in impacted and shocked EM. Depending on geometrical constraints, it will be possible to obtain up to five separate x-ray images at different times per impact event. In summary, these tests demonstrated that it will be possible to observe the temporal evolution of significant cracks in impacted or shocked EM specimens using the flash x-ray technique.

Alternative Joining by Diffusion Bonding with a Common Brazing Alloy

L. E. Brown, R. S. Goeke

This report evaluates the feasibility of diffusion bonding ceramic substrates with a 50% gold/50% copper (50/50 alloy) thin film, a common brazing filler metal alloy. We utilized and modified existing processes and materials developed for brazing when necessary to metallize the ceramic tensile button substrates. We tested and analyzed two groups of samples: (1) a test group that was diffusion-bonded with thin-film 50/50 alloy interlayers, and (2) a control group that was brazed with the 50/50 alloy filler metal. We compared the diffusion-bonded samples with the brazed samples in bond strength, hermetic seals, and failure modes.

Diffusion bonding below the melting temperature (Tmp) to as low as 1/2 Tmp of an interlayer material provides an alternative joining method to brazing processes that requires melting of the filler metal used. The approach of diffusion bonding with a thin-film alloy interlayer (Tmp=970°C), 50% gold/50% copper by weight, provides several key advantages: it reduces process temperatures, addresses x-ray exposure concerns, minimizes interlayer materials, and maintains critical geometries. This project identified key process issues that affect hermeticity and bond strength when diffusion bonding ceramic substrates with the thin-film alloy.

Diffusion bonding ceramic tensile button substrates with the alloy proved that the area of intimate contact at the interface has the most significant effect in creating hermetic seals and bond strengths comparable to brazed samples. Four brazed joints were hermetic with an average tensile test strength of 1047 ± 252 lbf, and primary failures occurred within the ceramic substrates. Eight diffusion-bonded samples were nonhermetic and had an average bond strength of 402 ± 171 lbf. Qualitative optical and scanning-electron microscopy (SEM) showed that the lower tensile strength and hermetic seal were directly affected by a reduced area of intimate contact achieved during the diffusion bond at 500°C, vacuum environment, and 15,000 psi. Diffusion-bonded samples primarily failed within the metallization and ceramic substrates where contact was made.

The reduced area of contact results from the ceramic metallization process utilized to improve the adhesion of interlayer materials. The metallization process involves the sintering of metal powder coatings followed by a nickel-plating process. We used a screen-printing process developed for brazing samples to apply a manganese-oxide powder coating. We made the utilized screen for brazing tensile buttons with a larger area. The excess area of the screen caused the application of excess powder coating material at the corners where surface tension effects created material buildup at the edge. This resulted in a trough-like surface, between the inside diameter (ID) and outside diameter (OD), with peaks to valleys as high as 0.7 mils. The surfaces were lapped after the metallization processes to create a flat surface for intimate contact. The trough effect was not sufficiently removed and was carried through the sputter deposition of the alloy thin film. Computer modeling work supports the results by indicating the need for very high stresses to fill large shallow valleys.

This project indicates that a 50/50 alloy typically used in brazing can be successfully diffusion-bonded. To create hermetic joints, we recommend a proper screen design to eliminate large shallow valleys.

Composite Carbon Anodes for Rechargeable Li-Ion Cells

R. A. Guidotti, W. R. Even

Current disordered carbons for rechargeable Li-ion cells that have a high reversible capacity (> 600 mAh/g) for Li intercalation also have an undesirable high irreversible capacity that results during the first intercalation because of co-reduction of solvent. Graphite, on the other hand, has a theoretical capacity of only 372 mAh/g but a much lower irreversible capacity on first intercalation. We investigated the concept of a composite *material that contains a core of a disordered (hard) carbon surrounded by a graphite layer. The graphite coating would reduce the irreversible capacity on first intercalation, while the core carbon would provide the desired high-reversible capacity.*

We examined various vapor-deposition (pyrolysis) techniques with metal substrates to determine if a coherent coating of graphitic carbon could be deposited. This included pyrolysis of appropriate carbonaceous materials in the vapor phase and thermal treatment of the carbon surface using a laser. We evaluated electropolymerization of thin organic films and polymerization by UV initiation. We pyrolyzed and tested these materials in our ambient-temperature Li-ion cells.

Current disordered carbons for rechargeable Li-ion cells that have a high-reversible capacity (> 600 mAh/g) for Li intercalation also have an undesirable high-irreversible capacity that results during the first intercalation because of co-reduction of solvent. Graphite, on the other hand, has a theoretical capacity of only 372 mAh/g but a much lower irreversible capacity on first intercalation. We investigated the concept of a *composite* material that contains a core of a disordered (hard) carbon (e.g., carbons from polymethylacrylonitrile [PMAN]) surrounded by a graphite layer. The graphite coating would reduce the irreversible capacity on first intercalation while the core carbon would provide the desired high-reversible capacity.

We coated stainless-steel discs by vapor-phase pyrolysis at 1,000°C of the following organic materials, using argon as the carrier gas: methane, hexane, benzene, and xylene. The films were thin and not very coherent using methane. We obtained carbon fuzz and whiskers with 30% hexane. We obtained improved results at 21% hexane. Film formation was limited using 10–20% benzene under these conditions. Much better coherent films resulted when we substituted xylene mixtures for benzene.

We deposited a polymer film based on cycloaliphatic epoxides on stainless-steel substrates and pyrolyzed them by heating at 700°C. The overall mass loss was excessive for the precursor used, which made this material unacceptable.

We examined direct coating of a copper substrate using a carbon sputter (vapor) coater for samples for scanning-electron microscopy (SEM). Only a very thin film of carbon was obtained, even after very long sputtering times. This

technique may work, however, with a more robust coater.

We deposited thin polymer films on a metal substrate by electropolymerization. This technique may be a viable one for controlling film thickness. Time and resource constraints did not permit carbonization of this material, however.

We performed several experiments using a laser to anneal the surface of a PMAN carbon in an attempt to increase the order. This sample has not been tested yet. We are currently testing the remaining samples in electrochemical cells but the performance data are not yet available.

We evaluated various techniques for forming carbon films with mixed results. Vapor phase reactions tend to produce more-uniform films, but when applied to low-temperature (e.g., 700°C) carbon powders, they change the structure and reduce the Li-intercalation capacity. Vapor deposition may not be practical when applied to carbon powders. More work is needed in this area to validate the concepts presented in this work.

Silicon-Based Nondestructive Read-Out Memories

W. L. Warren, M. G. Knoll, J. R. Schwank

Many DoD and DOE programs require nonvolatile memories that can store program and critical data without loss of information in the harsh environments associated with satellites and nuclear weapons. What is needed is a low-cost, silicon-compatible, low-power memory that is radiation tolerant and nonvolatile with reasonable write speeds and endurance. Unfortunately no such device exists at this time.

To address this important need, the materials and microelectronics research divisions at Sandia established a team to develop and characterize the fundamental device and materials properties for a new nonvolatile memory developed at Sandia termed a nonvolatile field-effect transistor *(NVFET). This effort addresses the development of novel radiation-hardened, nonvolatile memories using silicon-on-insulator (SOI) and standard metal-oxide silicon technologies that are based on the presence of mobile positively charged protons. In this effort, Sandia coordinated a broad-based program that we hope will lead to cheaper, lower-power, Si-based, nonvolatile memories.*

The Si/SiO_2 system is the cornerstone of modern microelectronic devices. The SOI concept was developed to electrically isolate the active device volume (a thin single-crystal Si layer) from the detrimental influence of the Si substrate. Today, SOI substrate and device processing is a fast-emerging technology with applications such as radiation-hard, low-power, high-temperature, and three-dimensional devices.

In this work, we demonstrated that annealing SOI material, and even more generally $Si/SiO_2/Si$ structures, in hydrogen (deuterium)-containing ambients introduces mobile H^+ (D^+) ions into the buried SiO_2 layer of these structures. Changes in the H^+ (D^+) spatial distribution within the buried SiO_2 layer were directly monitored by capacitance voltage (*C-V*) and current-voltage (*I-V*) measurements. These experiments enable us to directly observe proton drift in SiO_2 thin films. This work shows that the latter phenomenon has great potential in the design of a novel NVFET electronic memory device, an as-yet unrealized application of SOI technology.

We showed that elevated-temperature (> 500°C) anneals in ambients containing hydrogen can generate mobile protons in thermal oxides capped with poly-Si, or in the buried oxides of SOI materials. The protonic transport has potential applications in the design of new nonvolatile electronic and optical memory devices. For instance, an *n*-channel transistor can be changed to "normally on" or "normally off" by applying a positive or negative gate (substrate) bias that will drift the protons to the top Si/SiO_2 or substrate Si/SiO_2 interface, respectively. For a memory device this can be interpreted as writing the device to a bit state "1" or "0," respectively. To read the device, the zero bias drain current I_0 is simply measured (high current then corresponds to logic state "1," low current to "0"). In contrast with the instabilities usually associated with mobile ions in SiO_2, charge retention experiments on this device show that once written to a specific state, the device remains in that state for over 10^4 seconds while heated to 200°C. Furthermore, fatigue experiments performed on these structures show that the device easily endures over 10^4 write-erase cycles without any degradation.

For memory devices, a short write time is desirable. Early on in the project, we found the write time to be about 100 seconds. However, we found that the protons move via space-charge limited current flow. That is, the speed is enhanced by scaling the dielectric thickness; with the device, speed is proportional to d^3, where d is the buried oxide thickness. For devices fabricated using the poly-Si–capped 40-nm thermal oxide substrate, we observed a write time of about 30 ms at room temperature, in good agreement with the d^3 dependence predicted from theory. Write times as fast as 1 ms can be expected for 10-nm thermal oxides. Even more significantly, the latter result demonstrates that these NVFET memory devices do not require SOI substrates, but can be fabricated using thermal oxides capped with a poly-Si layer, a standard procedure in Si-MOS (metal-oxide semiconductor) processing.

Clearly this NVFET device has potential advantages over state-of-the-art, nonvolatile memory technologies such as Flash and electronically erasable programmable read only memory (EEPROM). While its speed, retention, and lifetime performance are certainly competitive with these existing technologies, it is simpler in design, requires fewer processing steps, operates at much lower voltages, and can be built using standard FET processing.

Use of X-Ray Mirrors for Enhanced Thin-Film X-Ray Diffraction

M. O. Eatough, R. G. Tissot, M. A. Rodriguez

We purchased an x-ray mirror to enhance our thin-film x-ray diffraction capability. These mirrors provide a parallel beam and increase the incident beam intensity 4–10 times. X-ray mirrors greatly reduce the divergence of the incident beam. This will allow us to do rocking curves while still maintaining enough divergence to work with films that have fiber texture and a large mosaic spread. The use of the mirrors will enable us to perform x-ray reflectivity analysis and structural refinement of thin-film diffraction data. X-ray reflectivity enables us to determine film thickness (of each layer), surface and interfacial roughness, and density of each layer.

The use of x-ray mirrors to enhance parallel beam optics for thin-film x-ray diffraction is currently the hottest development area of x-ray diffraction. These mirrors make a 4x–10x increase of incident beam intensity. We would be able to markedly increase our capabilities in the area of thin-film x-ray analysis and remain the leader in this field. X-ray mirrors also greatly reduce the divergence of the incident beam. This last advantage will allow us to do rocking curves while still maintaining enough divergence to work with films that have fiber texture and a large mosaic spread. The use of the mirrors would expand development in the areas of x-ray reflectivity analysis and structural refinement of thin-film diffraction data. X-ray reflectivity enables us to determine film thickness (of each layer), surface and interfacial roughness, and density of each layer. We are currently one of only two labs attempting structural refinement using rietveld analysis of thin-film diffraction data.

We made these x-ray mirrors using a similar method developed at Sandia. The mirrors are graded multilayers specifically designed to focus x-rays with wavelengths of about 1.5 Å. We determined that a set of parabolic mirrors could be retrofitted to the incident beam side of the diffractometer. We purchased a set of these mirrors, which we will attach to a state-of-the-art diffraction system.

High-Speed Shutter/Attenuator for Direct Fabrication Technology

D. M. Keicher

Sandia personnel examined the options for developing high-speed laser shutter/attenuator for direct fabrication applications. We considered rotational, accoustooptical, and electrooptical devices. The results of this study suggested that, for laser power up to approximately 400 watts, the most effective device would be the electrooptical device. The electrooptical shuttering/attenuating mechanism would separate the unpolarized laser beam into two polarization components and then recombine the beams after each of the beams was passed through pockels cell. When no voltage was applied to the pockels cell, the full beam power would be transmitted to the beam work location; when a quarter-wave voltage was applied, the beam would be directed away from the work area. The response time of the device is expected to be less than 1 μsec. We are developing a shuttering mechanism for this application.

Many of the direct fabrication technologies utilize lasers as a heat source to fuse materials together. This is also the case for the Laser-Engineered Net Shaping (LENS™) process currently being developed at Sandia. The laser power required to melt and fuse the metal powder materials together is on the order of several hundred watts. At this power level, the typical shuttering device is a solenoid-actuated mechanical shutter. The time response of these devices is on the order of 10 msec, which is insufficient for laser processing. Instead, a response time of less than 1 msec would be adequate. To further complicate this issue, recent experimentation on the LENS™ process showed that there is a linear dependence on the material deposition layer thickness as compared to the volumetric exposure (irradiance/velocity). To control the layer thickness as the motion control system velocity is changing requires that the shuttering mechanism also have the capability to continuously vary the laser power from threshold to full power. We identified a method to both shutter the laser beam and control the laser power in a continuously variable fashion using a pair of electrooptical crystals and polarization separating optical elements. This shutter/attenuating scheme allows the two polarization components of the laser beam to be separated and attenuated individually before the two beams are recombined for use in the laser process. We identified this scheme; performance limitations with the electrooptical crystal suggest that this device should work up to a power range of around 400 watts. This system has been breadboarded and is currently being tested to measure response time, optical losses, and attenuation efficiency.

Direct Fabrication of Aerogel-Supported Metal Nanocluster Catalysts

J. C. Brinker, A. Martino, M. L. Phillips

This project studied the in situ *synthesis of colloidal noble metals in aerogels. These materials combine the high activities of colloidal metal catalysts with the high-surface areas of aerogel substrates with the goal of improving performance of automotive catalysts. We investigated alumina and zirconia aerogels, based on their improved thermal stabilities vs. traditional silica aerogels. We made recipes for synthesizing these aerogels compatible with synthesis of Au and Pt nanoclusters in toluene. In addition, we prepared alumina aerogels with dopants such as Si and Zr to determine their effect on phase and surface-area stability at very high temperatures (1000°–1200°C). Preliminary catalyst testing in collaboration with Engelhard Corporation is in progress.*

Oxidative catalysts with improved activities and/or lower precious metal content are desired for automotive and industrial exhaust cleanup. Nanophase Pt and Au catalysts prepared inside surfactant-generated inverse micelles may be highly active due to their high-surface-volume ratios, but need high-surface-area substrates to realize high activities. We previously incorporated Pt and Au nanoclusters in silica aerogels, but porous silicas lose surface area under the hydrothermal conditions of automotive exhaust gas and melt at temperatures ambient of hotter catalytic processes (1000°–1200° C).

We successfully adapted our process to yield Au and Pt nanoclusters in alumina aerogels, accomplishing this by dissolving an alumina alkoxide complex in toluene, then adding this to a toluene suspension of metal colloids prepared by reducing metal salts trapped in surfactant micelles. We then added a stoichiometric quantity (3 mol H_2O/mol Al) of water; we induced gelation by adding a catalytic amount of hydrochloric acid (HCl). We can then dry the resulting tolugel to a xerogel by removing toluene at ambient pressure, or an aerogel by removing solvent in supercritical CO_2.

We also demonstrated the first synthesis of zirconia aerogels from tolugels and tested the phase stability of alumina aerogels that were doped with Si, Zr, La, and Ba. Doping appears to increase the temperature required to effect the θ-Al_2O_3 α-Al_2O_3 transition, but its effects on surface-area retention have not yet been measured. We are also testing the effects of reducing Au-doped silica xerogels in hydrogen at 600° C on hydrothermal stability; it is possible that under these conditions Si-C bond formation reduces Si-O dangling bonds, improving surface stability.

Engelhard Corporation in Iselin, NJ, is measuring catalytic activity and catalyst stability. These include both silica- and alumina-supported nanophase catalysts, as well as benchmark catalysts prepared by washcoating alumina aerogels with a commercial Pt catalyst coating.

Exploration of Surety Improvements via the Use of Ada in High-Consequence Software Projects

G. J. Dodrill

Sandia conducted this project to determine which computer programming language should be used to provide the safest software to control devices that could endanger human life or the environment in the event that the software failed. The report lists the various computer programming languages in common use at Sandia and compares them on the bases of cost, safety, and availability. The report discusses these attributes and others and contains many references from technical literature and from the World Wide Web (WWW). It summarizes the benefits and liabilities of each of the commonly used languages at Sandia.

Some software will be used in a situation where human life or the environment can be jeopardized by a software failure. This report summarizes a comparison of the languages currently in use at Sandia concerning their ability to prevent unsafe constructs that could lead to arbitrary failures. A small part of the study included an examination of why a particular language was chosen for each project.

We studied and compared the most popular languages in use at Sandia, including C, FORTRAN, C++, BASIC, Cobol, Assembly, and Ada. We found Ada to be the best language at preventing the programmer from writing code that appears to be correct, but actually can produce different results, depending on the compiler used. We also showed Ada to be best at producing the most debugged and polished code per unit of time, potentially indicating a reduced cost for any given project. We cited instances that indicate that a good Ada compiler produces small, efficient executables, so there is little reason to not use Ada for any project, including high-consequence software projects.

We recommend that Ada be used for all applications where there is a high consequence to be paid when the software inadvertently fails.

Measurement of Stress in Large-Area Thin Films

J. A. Ruffner, J. Cesarano, R. W. Schwartz, J. C. Brinker

We investigated the possibility of using a commercially available stress-measurement system in conjunction with a software "stitching" technique to enable stress analysis of large-area thin-film samples. Our approach was to obtain standard 2-D images from the stress-measurement system and write a software program to piece them together into a complete 3-D composite image of the entire thin-film sample regardless of its diameter. This technique required development of methods to manipulate raw data files and to acquire and electronically stitch together constituent images.

Excessive stress in thin films can lead to such serious problems as complete delamination, severe warpage of the substrate, or a significant shift in optical or electronic behavior. Presently, it is difficult to measure stress in large-area thin films using commercially available instruments because of their limited image field sizes (≤ 8" diameter).

Our approach was to obtain standard 2-D images from a stress-measurement system and write a software program to piece them together into a complete 3-D composite image of the entire thin-film sample, regardless of its diameter. We chose the Tencor FLX-2908 Stress-Measurement System for this investigation because of its variable image field size, computer-generated 3-D stress modeling capabilities, and "turn-key" installation.

This investigation required solutions to two technical problems:

(1) How can we manipulate the raw data files?

Data files could be imported into an Excel spreadsheet when delimiter-filtered and stored as a graph file by the Tencor application program. Data concatenation, appending, and manipulation were possible without file corruption by the importation conversion routine.

(2) How can we stitch together partial scans of a large sample to form a composite image?

We used several methods in attempts to generate partial scans of a large sample. Unfortunately, none of these methods resulted in useful constituent images. The manufacturer-supplied computer program requires the substrate to be physically defined by a laser edge-detection routine, regardless of the desired scan size. This requirement disabled analysis of any substrate larger than the physical limitations of the Tencor system. Because we were unable to obtain partial scans of a large wafer, we were unable to implement a stitching technique to form a composite image.

Future work on this project would require the manufacturer's software code to be edited to omit the edge-verification routine. Additionally, the 3-D modeling program should be upgraded to include automated rotational scanning.

Develop Capability to Measure Electrical Conductivity of Molten Slags

J. M. Buckentin, J. W. Braithwaite

Sandia constructed and tested an apparatus for determining electrical conductivities of molten slags by means of electrical impedance spectroscopy. In the electroslag remelting (ESR) process, heat is generated by the application of a current to a resistive oxyfluoride slag. The efficiency of the process is thus related to the electrical conductivity of the slag. The electrical signals generated by the ESR process, which are used in feedback control, are affected by the electrical response of the slag. Conductivity is also a measure of ion mobility, which influences the kinetics of slag/metal reactions and hence the chemistry and quality of the alloy produced. Molten slag properties are difficult to measure due to the high liquidus temperatures and corrosive slag properties. We measured the conductivities of some ESR slags using a two-probe method and, as expected, found conductivities to be dependent upon the frequency of the applied signal. Although ESR furnaces operate at frequencies of 60 Hz, values found in the literature were determined at frequencies above 1000 Hz. We used thermodynamic modeling to predict the formation of complex ions with low expected mobilities. The conductivity cell has added to our understanding of the electrochemical phenomena that affect ESR performance.

In ESR, the slag acts as a resistive medium for the conversion of electrical energy into thermal energy to perform alloy melting. The slag is a site for thermochemical and electrochemical reactions that are affected by ion mobility. In modeling, conductivity is important in determining electromagnetic fields and flow conditions. In this study, we induction-melted slags in graphite crucibles while monitoring temperatures by means of dip thermocouples and an optical pyrometer. We applied a voltage to a two-electrode probe and used an electrochemical impedance device to determine the resistance as a function of frequency. We performed thermochemical modeling to identify possible reactions between slag constituents.

For each slag system tested, we showed the electrical conductivity to be dependent upon the frequency of the AC voltage applied. Values of cell resistance measured at 60 Hz were lower than those measured at 4000 Hz. The use of molybdenum electrodes proved to be unsuitable for these measurements, as

they dissolved in the slag. We subsequently used tungsten electrodes. The measured conductivity of a slag containing equal amounts of calcia, alumina, and calcium fluoride was slightly lower than values reported by other researchers. Addition of calcium fluoride to this slag raised its conductivity, as we expected, due to the ionic nature of calcium fluoride and the mobility of its ions.

Our current setup allows us to accurately record slag temperatures, but it is difficult to control them. Relationships between conductivity and temperature could be developed if our conductivity cell could be placed in a furnace with a feed-back temperature controller. Additionally, we designed a four-probe test cell that will minimize polarization to provide a more accurate means of measuring slag conductivity and to determine the nature of frequency effects.

The frequency dependence of the conductivity observed with the two-probe cell raises important mechanistic questions regarding the factors that govern the signals used to control the ESR process. ESR is essentially a "two-probe" conductivity cell with a 60-Hz voltage applied between the electrode and the molten ingot pool through the slag as a resistive medium. We evaluated literature values of slag conductivity (which are limited in number and contradictory in nature) at frequencies higher than 60 Hz. The conductivity cell represents an important addition to Sandia's Liquid Metal Processing Laboratory.

Ensuring Critical-Event Sequence in High-Consequence Software by Applying Finite Automata Theory

M. C. Kidd

Currently, software engineers use ad hoc *methods to ensure that critical software sequences are maintained. The purpose of this project is to explore and demonstrate the utility of derivatives of finite automata theory to ensuring critical-event sequences in high-consequence software systems.*

Finite automata theory is a well-known, firmly established area within computer science. Finite automata theory has been applied to real-world problems in areas such as compilers, software testing, and protection of shared data resources in concurrent systems. We proposed to create a concept demonstration of the application of finite automata to show its utility in improving surety. We made extensions to existing automata theory to track an event sequence through software execution. This work expanded upon path expressions that are based on regular expression theory and finite automata theory. The target environment for this method is harsh environments where malevolent attacks or hardware failures occur (possibly due to environmental conditions such as lightning strikes).

The deliverable was a concept demonstration of the application of finite automata theory applied to ensuring critical-event sequences in software and contains a graphical user interface (GUI) that is executed on a PC. We used a real Sandia project to represent an application with a software critical-event sequence. We attached code "behind" the GUI to implement the finite automaton module as described in the following paragraphs. The GUI allows the user to see parts of the software "code," a graphical representation of the underlying finite automaton, and system status. The user directs the flow of software and can either follow the expected critical-event sequence or perturb the sequence to see how the system detects such errors and reacts. The user has the choice of using or removing the protection module. The user can also request a "playback" of the most recent event sequence.

The critical-event sequence fault-detection method implemented by the concept demonstration consists of deriving regular expressions from a software model or the software requirements and then embedding (1) check points and (2) update points based on those regular expressions into the target code along with a (3) module that implements the underlying finite automaton. This extra software is added to the target code to verify that the correct event sequence is maintained. The granularity of the regular expression is flexible and should be determined by the software requirements. Examples of appropriate software models are data-flow diagrams, state-transition diagrams, and flowgraphs. All of these models chart out a type of software flow. It is the flow that regular expressions will be used to enforce, whether protecting an actual software path or a software sequence.

Basically, a module "in the background" tracks the critical-event sequence by calls made from the epilogues and prologues of each critical event. This serves to localize or encapsulate the functionality in one module. That module will determine when and how to fail safe if necessary as determined by fault detection. This one function also maintains the history of execution at the critical-event sequence level of granularity. It is therefore easy to access this history after execution.

Investigation of Reducing Photovoltaic Systems Life-Cycle Costs Through System-Reliability Improvement

D. L. King, J. E. Campbell

Sandia investigated a collection of grid-tied, residential photovoltaic energy systems installed for the Environmental Protection Agency (EPA) to gain insights into their reliability. The system-level analysis was primarily aimed at determining attributes such as mean time between failure (MTBF), system downtime, system availability, and life-cycle costs. In addition to characterizing the reliability, work also focused on identifying areas where improvements could be made to increase the reliability, and ultimately lower the costs, of these photovoltaic systems.

Historically, the focus of photovoltaic systems improvements has been directed at getting more electrical efficiency from photovoltaic modules to produce more useful power. In contrast, less attention has been paid to other parts of the system that have contributed to a large percentage of the system downtime. A need has been highlighted for system-level investigations to demonstrate that this environmentally friendly power source can provide the maximum amount of AC power possible.

For this study, the systems of primary interest were residential, grid-tied, photovoltaic systems that provide power in the 2–12-kilowatt range. Recent experience showed that the power conditioning units, which convert the modules' DC power into usable AC power, have been the major contributor to system downtime. Because photovoltaic systems put in service for the EPA in 1993–1994 included maintenance data, we modeled these systems and used the data to quantify reliability characteristics and to determine the kinds of enhancements that we could use to improve system reliability.

The analysis of the EPA systems confirmed that the power conditioning unit is the cause for the majority (60%) of downtime events with a MTBF around 170 days. Eliminating the failures associated with the power conditioning unit would remove many of the opportunities for downtime. Better maintenance strategies can also improve availability by reducing the amount of downtime required to perform repairs from the current average of 9 days. Note that a wide uncertainty exists in the results because of the sparse amount of data available.

Fortunately, the existing records of system maintenance were adequate enough to do a baseline reliability analysis. To realize more benefit from future reliability analyses, we proposed suggestions to photovoltaic system operators to improve the quality of failure reporting. With better data, more accurate reliability measures can be determined and energies can be better directed at the most unreliable components.

Optical High-Voltage Sensor for Advanced Firing Sets

M. J. De Spain, J. D. Weiss, F. M. Dickey

Advanced firing sets are not just smaller and more reliable with enhanced surety when compared with past units, but there is also interest in designs that are modular, adaptable, and easy to maintain with enhanced testing and monitoring features to track parametric performance over the weapon life cycle. Many of these objectives can be realized if critical firing set voltage and current can be remotely sensed and controlled. Since advanced firing sets typically utilize an optical interface, direct optical sensing of voltage and current is desired. Any such sensor must meet a stringent set of parameters. These include passive, nonpowered operation; very high reliability; small size; and environmental robustness (temperature, mechanical, radiation). This project investigated technologies for direct optical sensing of voltage and current that will meet the desired criteria.

We investigated three voltage-sensing technologies: light attenuation through a strain-induced shift in the bandgap of GaAs; electrooptic effect in a bulk crystal; and electrooptic effect in a GaAs photonic integrated circuit (PIC). We identified one technology employing the Faraday effect and studied it for sensing current.

Strain of a GaAs crystal can be induced with voltage by bonding the crystal to a piezoelectric or electrostrictive substrate. Testing of GaAs indicates a strong dependence of the bandgap on strain; however, it also has a significant dependence on temperature. This effect can be compensated by several means. The most straightforward is to reference the output of the strained crystal with the output from a separate unconstrained crystal at the same temperature. This approach can also provide correction for other factors, particularly radiation-induced occlusion. This technology has the potential for developing inexpensive, reliable sensors.

In the electrooptic effect, the change in refraction with applied E-field is measured in a bulk Bismuth Garnet (BGO) crystal sensor by detecting the attenuation of polarized light, and in a PIC using an on-chip, Mach-Zehnder interferometer. For bulk crystal sensors, temperature and other common mode effects can be compensated by splitting the elliptically polarized light into two cross-polarized outputs that can be readily reformulated as a pure sine function of the applied field. In the PIC implementation, common mode effects are automatically compensated by the balanced arms of the Mach-Zehnder interferometer.

The National Institute of Standards (NIST) developed a bulk BGO crystal technology that appears to meet most, if not all, of the requirements for a small (1 mm x 1 mm x 5 mm), robust, high-voltage sensor that is accurate to 1.5% over the temperature range of –54° C to +74° C. If there is an immediate need for a sensor, this would be the technology of choice.

Sandia has the in-house capability of developing a PIC sensor that should meet all the requirements. PIC technology offers tremendous flexibility in features and configuration. Output can be provided as a pure amplitude signal, a pure fringe-count signal, or a combination of fringe-counting and amplitude signal. PIC also enables unique sensor implementations such as a voltage-controlled prism or a voltage-controlled digital "register."

With regard to sensing current, NIST developed a YIG (Yitrium-Iron-Garnet) film sensor that should meet weapon requirements.

Toward Experimental Verification of New Dual-Permeability Conceptual Model in Fracture/Matrix Networks

R. J. Glass, V. C. Tidwell, L. C. Meigs

Dual-permeability models are being used by many current projects across the DOE complex and will likely form the basis of many future calculations where flow and transport in fractured rock are of concern (e.g., environmental contamination, high-level radioactive waste management, and fossil and geothermal energy recovery). However, both lab experiments in unsaturated systems (Yucca Mountain Project [YMP]) and field experiments in saturated fractured rock (Waste Isolation Pilot Project [WIPP]) showed that even the most advanced dual-permeability models are fundamentally incorrect. Of particular concern in these models is the manner in which mass transfer between the fractures and rock matrix is treated. To reconceptualize these critical fracture/matrix interaction submodels, we need data from systematic experiments at the lab-scale. As a step toward this end, we propose to develop and test a meter-scale experimental system for both visualizing and quantifying processes governing the transfer of fluids and solutes between fractures and the host matrix.

We constructed and tested an experimental test system for investigating fracture/matrix interaction. The analog, 2-D fracture network/porous matrix test system comprises a "wall" of fire brick. This design allows maximum flexibility in characteristics of the test system. For example, hydraulic properties of the matrix can be varied by simply changing the brick used; the fracture network can be varied by stacking the brick in different ways and/or by sawing subsets of the brick, while a wide range of boundary and initial conditions can also be prescribed. The 2-D fracture/matrix system measures 1-m wide by 2-m tall by 6-cm thick and is secured in a Unistrut frame. The entire system is encased in a clear Plexiglas box to minimize evaporation.

We also automated the data-acquisition system. Water is added at the top of the test system under a prescribed flowrate while a computer-monitored scale records the mass of fluid supplied to the system as a function of time. Wicks from each of the fractures separating bricks along the bottom row of the test system direct outflow to a series of scales that are likewise computer-monitored. We automated and secured a series of tensiometers at key locations throughout the test system to measure matrix fluid potential. We routinely monitored test cell humidity and temperature. We also constructed a 45-by-35-by-6-cm mock-up fracture network/brick system in which we performed a potassium iodide tracer study to develop procedures for measuring outflow solute concentrations using an ion-specific electrode.

We also attempted imaging of the transient, 2-D fluid flow and solute concentration fields. One approach relied on photography to capture the fluid-flow field as a function of time using the contrast in brick color between the dry and wet state to indicate the position of the wetting front. We later digitized, overlaid, and false-colored the photographs to produce a time-lapsed image of the wetting of the fracture/matrix system. We also employed x-ray absorption imaging to measure the fluid-flow and solute concentration fields. However, because of mechanical difficulties with the x-ray equipment and the large thickness of the brick, we encountered significant difficulties. We tested a number of modifications to the imaging procedure, none of which yielded satisfactory results.

Theoretical Development of a Prototype Assumption-Based Modeling System

P. A. Davis, T. J. Brown

Developing simulation models for complex engineered and natural systems has traditionally been a long-term, labor-intensive undertaking. The effort required for model development creates barriers to the development of customized models and therefore to the practical application of advances in numerical simulation. Environmental regulatory assessments are often based on conservative results from widely used generic simulation codes due to the high cost of code development and verification. This project describes a conceptual approach to practically eliminating this cost through automated development of simulations, and assesses the feasibility of automation by comparing the identified requirements of such a system to the current expert system capabilities.

We prepared a report describing a conceptual approach to automated modeling of physical systems characterized by coupled conservation equations and assessing the feasibility of automated simulation in view of existing software systems. We regarded developing models for physical systems as two separate tasks: (1) formulation of a mathematical model and (2) algorithmic approximation of the mathematical model. Current expert system technology appears applicable to automating the process of mathematical model formulation and evaluation. Many existing software systems address elements of this complex process; however, we identified no system that integrates these elements within a single framework. The practicality of developing a comprehensive integrated system will be determined by the ability to define critical heuristic knowledge in two areas: (1) constraints placed on the structure and elements of the mathematical model by qualitative statements about physical features of the system, and (2) the relationship between structural features and parameter values in the mathematical model and the anticipated performance of numerical approximations. This may place practical barriers on the ultimate scope of the system; however, a useful system can be developed around a core representation scheme for the mathematical model. The scope and functionality of this prototype can be incrementally enlarged by supplementing the inferential knowledge base.

Sensor Fusion for Predictive Maintenance

J. E. Campbell

Sandia examined the potential integration of sensors and software to continuously update a reliability model for real-time failure prediction. Current maintenance strategies for machines are based primarily on reactive or preventive maintenance, which can prove costly for many systems. A predictive maintenance capability based on in situ *data collected by sensors could indicate problems that might develop between scheduled maintenance intervals and result in costly downtime and repairs. Work centered on determining how this sensor fusion is best accomplished and on examining the issues in implementing a predictive maintenance capability for a candidate system.*

For systems in which repairs and excessive downtime are costly, an optimal maintenance strategy is especially desirable. The available strategies can include reactive, preventive, and predictive maintenance. Reactive maintenance fixes problems as they occur and could result in high cost due to lost availability, unplanned repairs or replacement, and possible secondary equipment damage. Preventive maintenance is performed at regular intervals but also may not be optimal because the system may not require maintenance, and the maintenance does not guarantee the elimination of failures.

Predictive maintenance targets failures in the system that cause the highest costs and that can be monitored so that maintenance is performed only when an impending failure is detected. Predictive maintenance is currently being used primarily in power-generation plants to maximize the amount of time between maintenance activities, thus increasing the power output. Using WinR™ reliability software, we propose to extend this capability by linking the sensor output with a reliability model. Thus, the probability of a failure over a future time interval can be continuously updated, and the key failure modes can be monitored.

To investigate the issues involved with fusing sensors to a reliability model for a predictive maintenance capability, we selected a candidate system from among many for a virtual design. To learn and build on work already done, we chose a Sandia-designed viscosity/density sensor that could monitor lubricating oil in a generic piece of rotating equipment. (This could include motors, generators, machine tools, etc.) This sensor was previously used to monitor the engine oil in a Sandia vehicle and showed oil viscosity changing as the oil degraded. An appropriate algorithm could interpret these changes and input this data into the model to update the reliability prediction.

Due to the enormous numbers of sensors and computer interface circuitry, a "plug-and-play" solution is not possible without assembling a library of sensor information so that a dedicated sensor expert is still required to make the sensor data available to a computer. Libraries of available sensors and interpretive algorithms would be the next step to be able to quickly pick sensors for a system based on the physical property to be monitored. With these types of libraries, a repairable system could very easily be outfitted with a predictive maintenance capability.

Modeling of Multicomponent Transport with Microbial Transformation in Subsurface System

Y. Wang

Microbial degradation of organic matter is widely recognized as an important process that controls toxic metal transport and transformation in the subsurface. However, this process has not been fully explored in the existing groundwater transport model, and thus our ability to predict the fate of toxic metals is greatly limited. In this research, we developed a multicomponent reactive transport model capable of dealing with the complex biogeochemical interactions of elements C, O, H, N, S, Mn, Fe, and Ca in groundwater systems. The model fully takes into account the following coupled processes: microbial degradation, redox reactions, mineral dissolution and precipitation, aqueous speciation, advection, and dispersion. We constrained the relevant chemical kinetic and thermodynamic data, based on a broad literature search. We tested the model against published field data. The model can predict water chemistry changes and the distribution of toxic-metal–scavenging mineral phases along a transport pathway and thus provides the key information required for accurately predicting the fate of toxic metals in the subsurface. The model can be used as a tool for contaminant risk assessment and for designing engineering reactive barriers to reduce the contaminant release from landfills and other waste sites.

We successfully completed all planned activities for the project. We (1) identified important biogeochemical reactions that control the chemistry of contaminant plumes, (2) constrained the kinetic and thermodynamic parameters for those reactions, (3) formulated a

kinetic reaction-transport model to simulate subsurface biogeochemical interactions, (4) developed the corresponding computer code (BIORXNTRN) for the model, and (5) conducted numerical simulations with the code, then compared the simulation results with field observations.

We identified about 150 chemical reactions that may affect the chemistry of contaminant plumes and compiled the kinetic/thermodynamic parameters for those reactions. We further identified 28 reactions to be included in the current model. In the model, we use rate expressions to describe the oxidation of organic carbon, the oxidation of secondary reduced species, and the dissolution/precipitation of authigenic minerals. Based on Monod kinetic law, total organic oxidation rate is broken down into different biodegradation pathways. The model is solved by a finite-difference method, and we successfully implemented the corresponding computer code (BIORXNTRN) on a SUN workstation. The code can calculate 1-D distributions of 24 chemical species as a function of time.

We conducted numerical simulations with the code. The code reproduces commonly observed subsurface redox patterns. The simulations showed that, depending on the intensity of biodegradation, the pore-water pH can vary dramatically across the plume front. The simulations also indicated that organic compound biodegradation induces intensive subsurface Mn and Fe redox reactions. Mn(IV) and Fe(III) are reduced in the anaerobic zone, producing Mn^{2+} and Fe^{2+}, which in turn are partly precipitated as carbonate minerals behind the plume front or are re-oxidized, forming oxyhydroxides at the forefront of the plume. Thus, our simulations demonstrate that organic compound biodegradation controls not only the overall groundwater chemistry but also the availability of solid phases capable of scavenging toxic metals. The model developed in this project is able to provide the key information required for accurately predicting the fate of toxic metals in the subsurface.

The success of our preliminary modeling work points out the three important areas that need to be further studied: (1) extend the current model to include more chemical reactions and to higher-dimensional problems; (2) experimentally determine the kinetics of the relevant chemical reactions; and (3) apply the model to actual waste sites, in particular, to DOE mixed-waste sites.

Precision Stage for LIGA Micromachine Fabrication

M. X. Tan, R. P. Nissen

Sandia is conducting process and product research and development on the micromachining process known as LIGA, which uses a deep x-ray lithographic. LIGA is an acronym for German words meaning lithography, electroplating, and molding. It is a technique that requires exposure using synchrotron radiation through a lithographic mask onto polymethylmethracalate (PMMA). The synchrotron exposure of the PMMA causes rupture of the bonds and hence allows the dissolution of the exposed region in a chemical developer. The developed regions in the PMMA form an open pattern that can then be filled with metal from an electroplating process. This technique allows for deep, parallel-walled structures with fine definition. Aspect ratios of patterns are typically between 20:1 and 200:1. In this work, we designed and fabricated an exposure stage for LIGA synchrotron exposure.

Sandia is conducting process and product research and development on the micromachining process known as LIGA, which uses a deep x-ray lithographic. LIGA is a technique that requires exposure using synchrotron radiation through a lithographic mask onto PMMA. The synchrotron exposure of the PMMA causes rupture of the bonds and hence allows the dissolution of the exposed region in a chemical developer. The developed regions in the PMMA form an open pattern that can then be filled with metal from an electroplating process. The high-energy, high-flux, and highly collimated characteristics of synchrotron radiation enable exposure of thick x-ray resists from 100 μm to nearly 100 mm with side-wall slope of less than 1 μm/mm.

To conduct synchrotron exposure on the PMMA, one needs a scanning stage that scans the LIGA mask and PMMA in the x-ray path. A reliable fixture is needed to hold the mask and the PMMA resists sheet parallel to each other, and fit onto the computer-controlled scanner. The fixture needs to provide water-cooling and -heating and helium gas-cooling capability. We designed and fabricated the fixture in FY96.

Affinity Chromatography Supports for Separation and Detection of Biological Toxins

J. S. Schoeniger

The goal of this short-term project was to determine strategies for making capillary affinity chromatography (CAC) materials for the separation and detection of biological toxins, especially those that are of particular significance as potential biological warfare agents (BWAs) or food contaminants. First, we identified a number of significant bacterial and plant toxins and compiled from the literature information on their structures, chemical properties, and mechanisms of action. Second, we surveyed biochemical manufacturers and identified commercial sources of toxins, toxin fragments, and molecular recognition materials such as antibodies or receptors that would bind selectively to each toxin. Finally, we purchased toxin fragments, antibodies, and materials for capillary chromatography and synthesized separation materials.

Affinity chromatography can be used to identify molecules in solution by detecting their binding to an immobilized receptor material referred to as a *stationary phase*. To establish the feasibility of developing sensors for biological toxins based on using CAC, this project addressed two questions: (1) How can we obtain and work safely with toxins that are significant in terms of potential threat, and chemically detectable using CAC sensors? (2) How do we obtain reagents for and synthesize CAC stationary phases?

A survey of biological toxins identified the following criteria to distinguish between toxin classes that can be used evaluate their potential significance and to identify appropriate separation strategies:

(1) Microorganism-produced toxins are of note because of potential mass production (fermentation.)

(2) Toxins are either small molecules or toxic proteins (macromolecules).

(3) Have available knowledge of toxin molecular structure/function and receptor binding.

(4) Obtain knowledge of weaponization or concern by public authorities (e.g., water quality boards).

Applying these criteria to information on toxins available in the literature, we identified the following groups of toxins to be of interest:

(1) *Small-molecule toxins*: aflatoxins (polycyclics), ciguatoxin (polyethers), anatoxins (organophosphate), mycotoxins, microcystins, and saxitoxin.

(2) *Protein toxins*: bacterial toxins (botulinum A-F, tetanus toxin, cholera, pertussis, diphtheria, staph enterotoxin, *E. coli*, heat-labile enterotoxin, latrotoxin), plant toxins (ricin, jequirity toxin)

We reviewed specific molecular properties of these toxins in detail and contacted suppliers to determine availability of both toxin and molecular recognition materials suitable for CAC. We could purchase the following toxins (and antibodies that bind to them): aflatoxin, ricin (purified A and B chains), cholera toxin B subunit, botulinum heavy chain, and tetanus toxin (C fragment). We synthesized a CAC stationary phase by covalent immobilization of anti-aflatoxin antibodies on silica microbeads. We drew the following conclusion:

(1) Development of CAC stationary phases can be safely undertaken for protein toxins with these common features: (a) the toxin has multiple subunits, (b) antibodies are available that bind to specific subunits, (c) the toxin has a specific receptor-binding domain distinct from the toxic domain, and (d) inactivated toxin and separated toxin subunits are available commercially. Sensors can then be developed using nontoxic but structurally equivalent versions of the toxin.

(2) For small-molecule toxins listed above, (a) the toxins and antibodies for the toxins were difficult to obtain from commercial vendors, (b) it is necessary to work with intact, active toxin since distinct subunits with separate functions do not exist. Some small molecule toxins may have properties that enhance their detectability (e.g., aflatoxins are fluorescent).

(3) This short-term project was extremely helpful in laying the groundwork for CAC toxin sensors.

Design and Evaluation of Sampling, Detection, and Control Technology for Field-Portable Capillary-Based Chemical Analysis

D. S. Anex

Capillary-based chemical analysis techniques—including capillary electrochromatography (CEC) and capillary electrophoresis (CE), for example—show great promise for field portability. Although CEC and CE columns generally require high-driving voltage (kilovolts), operating currents are small (microamps), so they are natural candidates for battery-powered operation. This project evaluated some of the key technologies that will be required for a completely battery-powered, field-portable CEC and CE instrument. Essential components include battery-driven ultraviolet (UV) lamps, detectors, and power supplies. Auxiliary components include optics and mounts, the sampling interface, and electronics. These components will eventually comprise a field-deployable instrument for chemical analysis. Target compounds include chemical weapon (CW) and biological weapon (BW) agents, as well as species of environmental and forensic interest.

High-efficiency CEC and CE are chemical analysis techniques for complex chemical samples. They are based on the separation of a liquid sample into its components by using high voltage to drive fluid flows through a capillary column. These techniques provide benefits beyond those of conventional chromatographic techniques that include (1) superior separations, (2) small sample volumes (10 nl), (3) low solvent consumption (~ 100 nl/min) and waste generation, and (4) low-power requirements. Such instrumentation would allow on-site analysis of complex samples that currently require the transfer of samples to a laboratory. The benefits would be substantial, ranging from reduced sample handling to better sample integrity to fast on-site results.

Battery-operated components will be needed to advance current progress in capillary-based analysis into a field-portable instrument. A simple, versatile instrument would consist of (1) a capillary column using a battery-powered voltage supply to drive the fluids, (2) high-voltage relays for switching operations, and (3) an absorption detector based on a battery-powered UV lamp. These components have been investigated. Battery-powered, high-voltage power supplies are commercially available. For example, compact (6 inches by 6 inches by 3 inches) 1-kV to 30-kV power supplies are available that require 24–32-V input. For high-voltage switching applications, small relays (2 inches by 2 inches by 1 inch) are available that can switch up to 10 kV and have low-voltage coils (5–24 V). These relays will be useful for momentary switching related to sample introduction. We tested a battery-operated UV mercury lamp as a detector for CEC and CE. By mounting it on our existing instrument, we found that the intensity was sufficient for detection, but the useful lifetime of the lamp was less than one hour (insufficient for a field-portable instrument) because of the limited capacity of the 9-V alkaline battery. Satisfactory operation using an external 9-V power supply showed that this lamp would be useful with a battery with sufficient capacity to supply 300 mA at 9 V for several hours.

Based on currently available components, a completely battery-powered, field-portable CEC/CE instrument could be designed. Such an instrument would be controlled by a notebook computer and would fit into a small suitcase. Sample introduction would be done manually, but the rest of the operation and data collection would be performed by the computer.

New Applications of Damage Detection and Structural Health-Monitoring Methods

G. H. James, J. E. Hurtado

Two separate reports resulted from this project study. The first discusses the use of transmittance functions (TFs) in identifying structural damage. The TF is a complex ratio between the Fourier transforms of a response and the reference point on a structure and is sensitive to damage. The change in a structure's TFs can be directly linked to the presence of damage and thus is a promising measure of damage detection. In fact, to some degree, the TF is independent of input loading. The report includes a development of the theory of the method and an application to an aluminum panel with rivets.

The second report covers the use of traditional modal methods in monitoring the health of an AT-400A transportation and storage container. This type of container will be kept in storage for many years in a radioactive environment, and thus the structural integrity of the container is an important safety issue. We identified changes in the structural integrity of the container following a series of contrived damage scenarios through traditional modal testing and analysis.

The first report, titled "Detecting Structural Damage Using Transmittance Functions," describes a new non-invasive technique for detecting, locating, and quantifying damage of flexible structures that we used to detect simulated cracks in an aluminum rib-stiffened panel. We investigated a total of five different damage indicator algorithms. Using a small sensor set, we detected damage and correctly located it in most cases. The experiments were repeatable, and this project was a successful first step toward using transmittance functions to detect small damage on a relatively large structure.

The second report is titled "Health Monitoring of the AT-400A Pit Storage and Transportation Container." The AT-400A containment vessel tests consisted of the lower shell, transition flange, backing plates, and inside pit and spring fixture. We positioned accelerometers on the outside containment vessel and at various points on the inside fixture. We used a 1-lb impact hammer to excite the structure, and the accelerometers to sense the structural response. Our objective was to determine if the outside sensors, i.e., sensors on the outside containment vessel only, could detect changes occurring on the inside fixture. The changes to the inside fixture that we investigated included (1) changes to the fixture weight and orientation, and (2) changes to the inside pit spring resulting from the entire structure being dropped a known distance. The damage scenarios mentioned above are clearly revealed by frequency shifts associated with the first few modes of the system. We consistently identified these frequency shifts using modal analysis methods.

Exploration of Methods for Bridging Length and Time Scales

J. B. Aidun, T. G. Trucano

We examined a sampling of current concepts and analytical tools from nonequilibrium statistical physics to evaluate their relevance to the problem of relating the results of numerical simulations of microscopic mechanisms to macroscopic properties and continuum mechanical behavior. Correctly and efficiently relating microscopic process simulations to macroscopic quantities is critical to many efforts to develop modeling- and simulation-based life-cycle engineering (MSBLCE) capabilities at Sandia. This can entail extrapolating over eight orders of magnitude in size and twelve orders in duration from the underlying processes to the macroscopic continuum behavior. Because this cannot be accomplished directly by increasing the size of the simulated system to macroscopic dimensions and increasing the duration of the simulated time interval to those relevant to stockpile issues (i.e., seconds to years), it is necessary to identify potential approaches for making the connection.

The computational tool for much of the engineering analysis performed at Sandia is macroscopic solid mechanics simulations by the finite-element (FE) method. Predictive simulations require, among other things, the use of accurate values for material properties and internal state variables. When these are not or cannot be measured, the alternative is to generate values of needed properties by performing numerical simulations of the underlying microscopic mechanisms or processes. Then the question arises of how to average the results of microscopic process simulations to determine values of a macroscopic quantity.

The problem of scaling can be characterized in terms of the representative volume element (RVE) of the material. For mesh elements larger than the RVE, volume averages ("densities") define macroscopic quantities. For smaller mesh elements, the "densities" depend on the size of the averaging volume. Statistical physics suggests that the correlation length (CL) is the appropriate measure of RVE size and demonstrates that the CL is not constant, though, in some cases, the size-dependence of the "densities" can be determined. Hence, defining an appropriate CL and developing methods for determining its value would help in identifying whether a simple volume average suffices. Additionally, approaches need to be developed for bridging length and time scales when RVE averages are not feasible.

Resolving issues associated with relating microscopic simulation results to macroscopic properties would advance efforts to achieve reliable, predictive MSBLCE capabilities at Sandia. Recent developments in both statistical physics and theoretical mechanics appear to offer fruitful lines of inquiry for developing new concepts and analysis tools to address the problem of scaling between small lengths and short time intervals of microscopic mechanisms and the much larger lengths and longer time intervals of macroscopic constitutive behavior.

Scaling Laws for RoBugs

B. L. Spletzer

We developed scaling laws, particularly those with applications to miniaturized vehicles. We applied first principles of engineering and physics in generic ways to predict how various physical properties and forces change in relation to each other as the scale (or size) of the object in question varies. We reduced these laws to simple numerical results that help provide direction in the non-intuitive realm of very small objects. The simple laws developed this way are easily combined to allow the relative importance of various factors to be examined as a function of scale. We discovered several unexpected relationships, providing insight and direction that would be costly and time-consuming to develop by more conventional means.

Dozens of scaling laws are derived and presented, primarily directed toward the development of small smart machines (SSMs). All scaling laws are presented by examining the dependence of physical forces and properties on the linear scale of an object. This way, the laws become simple integers that are the exponents describing how a property varies with scale. Laws developed this way can be easily combined to examine the relative effects of multiple properties.

Wherever possible, examples in nature and engineering are used to provide intuitive confirmation of the laws defined. Even though the approach used to derive these laws is simplistic and based primarily on first principles, the results are insightful and sometimes surprising. For example, consideration of simple weight and aerodynamic force laws explains why the frequency of wing beats increases with decreasing scale for flying animals. Also, the fact that motors, from large to small scale, employ induction, quasi-static magnetic fields, and electrostatic forces, is discussed and shown to be a consequence of the scaling of electrical effects.

Overall, we designed this collection of scaling laws to provide direction to the research, concentrating on the development of small-scale mechanisms. While not exhaustive, the laws encompass some of the more important aspects of fluid mechanics, electrical effects, and mechanical stresses.

Damage Detection Analysis Using Wavelets and Neural Nets

P. S. Barney, S. E. Klenke, W. N. Sullivan, T. L. Paez

Sandia examined the use of wavelet transforms combined with neural networks for damage detection in the area of rotating equipment. The project began from discussions with the American Association of Railroads (AAR) in which we targeted wayside bearing damage detection as an area of extreme interest. Work focused on the use of temporal filtering, transformation, condensation, and subsequent classification of damage-type data. We created data that simulated damaged and undamaged bearings, and constructed and implemented the various processes to evaluate their potential performance in the area of damage detection and prediction.

This report presents the results of damage detection using wavelet transforms and neural networks. The motiva-

tion for this work originated from a wayside bearing damage-detection project headed by AAR (funded by the Federal Transportation Association [FTA]). We used simulated damage typical of roller element bearings as an input to the proposed damage-detection algorithm. The simulated data included three types of damage (i.e., roller, cone, and race), as well as a no-damage case and a set of blind samples with one or more damages incurred. We used the fault-seeded data sets to train the algorithm while using the blind samples to determine the overall performance. Simulated data sets had a signal-to-noise ratio from 1.0 to 0.10.

The proposed algorithm was a three-step process: (1) raw-data filtering designed to enhance the signal-to-noise ratio, (2) data transformation designed to extenuate differences due to damage and to condense the data, and (3) a neural network classification algorithm to determine if damage is present.

As a performance test of the proposed algorithm, we analyzed a set of blind sample data. Again, the blind sample data included both single-failure types as well as multiple-failure simulations. The performance of the proposed system appeared to be quite good. We saw a 100% detection for one failure type, although we observed a 10% detection for another. The intermediate data quality indicates that additional training of the networks may substantially increase the ability of the network to make accurate predictions.

The work performed in this project indicates that there is good potential for this type of method to accurately predict when there is damage and what type of damage has been incurred (in rotating equipment). If this method can be made effective using real-world data, it does meet an industry need. The industry is also looking for a solution that goes one step further in that the output would include estimated time before catastrophic failure.

As stated earlier, the process developed in this project was a three-stage effort. The first stage of the process utilizes synchronous averaging and match filtering based on the nature of the damage. Each type of damage has a filter that is generated for that particular case. The output of stage one was three blocks of averaged data.

The second stage of the detection algorithm utilized temporal transformation routines designed to retain both spectral information and time information. The transformations used in the work included wavelets (D2 and D6) and a variable-block-size, fast Fourier transform (FFT) method. We then reduced the data from the transformations to a single scalar value using Cepstrum analysis. We performed the second-stage reduction for each damage filter; therefore three scalar values were produced as outputs for each of the three transformation types, bringing the total of outputs to nine scalar values.

The third and final stage utilized the neural network for the decision making as to whether specific damage was incurred for the given input. We exercised two types of networks in this project: the classical probabilistic neural net and the probabilistic. We trained each network using the output of phase-two data for both damaged and undamaged cases. We used various sets of data from the output of phase two as inputs to the different networks for identification of particularly good or bad methods.

A Comparison of System Identification Techniques

R. Rodeman, J. P. Lauffer, P. S. Barney

In structural dynamic system identification, three commonly used techniques are Eigensystem realization algorithm (ERA), Kalman filtering (KF), and canonical variates analysis (CVA). In this study we examined the similarities and differences of these techniques. In addition, we used ERA and CVA on data obtained from an inherently nonlinear magnetic levitation system to obtain state-space models of the system. We determined the accuracy of these results by comparing synthesized frequency response functions (FRFs) with experimental FRFs.

All of the above-mentioned system identification techniques assume that there is an underlying linear state-space model that adequately represents the input-output characteristics of the system. While these techniques are used independently, there is an unknown commonality among them. Our ability to correctly identify a model depends on selecting the most appropriate tool for the particular situation. To make the correct selection, we need to be able to differentiate among the available techniques. We directed this effort at examining the commonality and differences of the three methods.

We used both CVA and ERA in an attempt to identify a state-space model of a machine tool system controlled by magnetic levitation. We judged the quality of the identification by comparing FRFs from the identified state-space models with actual FRFs obtained from the machine tool system. CVA produced superior results. In fact, with ERA, details of the FRFs were almost entirely missed, which was certainly unexpected.

Since CVA is relatively unknown compared to ERA, yet produced superior results, it would be beneficial to further pursue the understanding of this technique. In addition CVA purportedly has application in identification of nonlinear systems. Currently we do not have any general techniques for nonlinear system identification.

Coaxial Extractor Diode Conceptual Design

J. E. Maenchen

This project studied engineering issues and developed a preliminary design for a portable coaxial extraction diode producing a sterilization device. The design calls for a pulsed-power ion-beam accelerator operating at the highest repetition rate (500 Hz), the highest average power (200 kW), and the largest target area (2000 cm²) of any such system yet built at Sandia. In particular, the issues examined and developed were the required insulating magnetic field, power feed, thermal management, target fabrication details, and structural engineering.

A need exists for a portable sterilization device. The work reported took an initial concept, examined the technical issues, and developed a preliminary design. The design uses a high-repetition-rate, high-average-power (200 kW) converter. This device operates at such high average powers due to the much larger magnetically insulated pulsed-power diode current. Such diodes were developed at Sandia for the Inertial Confinement Fusion (ICF) Program over the past decade. The system's parameters are 200 kV, 33 kA per shot (pulselength = 60 ns), 500 shots/s onto a 2000 cm² target coated with a thin-film converter. The design was extensively extrapolated from an existing diode to provide a rep-ratable sterilization system with minimal anode wear.

In the course of this work we identified and addressed the following issues:

(1) *General engineering: size and weight.* The weight of the prototype device will have an assembled weight of 650 lbs with a volume of about 6000 cu in. To be portable, the device will comprise three separate pieces, the heaviest of which is about 400 lbs.

(2) *Voltage feed design.* The recommended option is to use eight 50-W cables feeding an inductive core. This option adds complexity in that the magnetization of the 60-cm² core must be reversed following each shot, but it eliminates the need for plastic or ceramic insulating standoffs, which pose greater safety and lifetime concerns.

(3) *Insulating magnetic-field topology.* Iterations using the magnetic-field design codes ATHETA and DATHETA identified a reasonable magnetic-field topology. We will use two coaxial solenoids, one of which (the outer) operates at steady state, and the other (the inner) is pulsed to provide an induced electric field to position the beam source for conversion.

(4) *Target film fabrication.* The converter will be a thin (10–20 mm) film covering 2000 cm² on the inside of a grounded cylinder. Research into thin-film capabilities at Sandia indicates that such films can be deposited onto the desired geometry.

(5) *Thermal analysis.* The target film will decompose at temperatures greater than several hundred degrees centigrade, which becomes a serious concern when irradiated with ion-beam power of 200 kW for several minutes. We carried out thermal analysis simulations using various cooling coil placements and substrate materials assuming an average power of 100 W/cm². The target surface can be kept below decomposition if cooling coils are placed 3 mm behind the target surface, and the surrounding bulk substrate is copper. The thermal conductivity of alternative substrates such as stainless steel or titanium precluded their use.

(6) *Power components.* We specified and installed electrical and mechanical components for a high rep-rate modulator (used to supply power to the diode) in support of making an existing modulator compatible with the prototype device.

Using the information outlined above and ascertained under this project, a preliminary design now exists for a portable sterilization device.

A Novel Methodology to Determine Dynamic Pressure-Volume States of Transportation Materials

R. J. Dukart

Sandia developed a novel experimental technique to allow a determination of the high-pressure equation-of-state (EOS) of transparent materials. We sandwich the transparent material—a polymethylmethracalate (PMMA) sample—between a tantalum driver and a transparent lithium-fluoride window. We used graded-density impactor materials to introduce a time-dependent loading history into the target. The input loading history (at the tantalum/PMMA interface) and the output loading pulse (at the PMMA/LiF interface) are determined as particle-velocity profiles using two different high-precision velocity interferometers. We performed predesign calculations and experiments successfully. Experiments indicated the following: (1) the observed transparency of PMMA under time-dependent loading, i.e., under continuous compression to ~ 42 GPa, far exceeds the transparency limit of 22 GPa determined under shock compression, and (2) refractive index corrections for PMMA will be necessary to estimate the continuous stress-strain response of PMMA.

Transparent materials such as frozen hydrogen and deuterium are of strategic importance to DOE for inertial confinement fusion (ICF) applications. Unfortunately, the pressure-volume compressive behavior of these materials is not known at extreme compression due to the difficulty in making direct measurements because of its extreme low density and low shock-impedance. In this project we proposed a novel methodology to determine the high-pressure EOS of these materials. In this method, we sandwich the transparent sample between a tantalum driver and a transparent lithium-fluoride interferometer window. Upon pressure loading, the methodology calls for monitoring the driver/sample and sample/window motion simultaneously using two different high-precision velocity interferometers. The technique will, therefore, allow a direct determination of continu-

ous compression states with a limited amount of experimentation. Prior to its intended use for hydrogen and deuterium, we evaluated the methodology in the present study using a low-density surrogate (transparent material) such as PMMA.

We sandwiched the transparent material—PMMA— between a tantalum driver and a transparent lithium-fluoride window and used graded-density impactor materials to introduce a time-dependent loading history into the target. We performed experiments using a powder gun at impact velocities of 0.6 km/s and 2.2 km/s. This is expected to generate a time-dependent stress-loading history in the transparent PMMA sample up to 8 GPa and 41 GPa, respectively. We determined the input loading history (at the tantalum/PMMA interface) and the output loading pulse (at the PMMA/LiF interface) as particle-velocity profiles using two different high-precision velocity interferometers. We performed predesign calculations and experiments successfully. Preliminary analysis of the two experiments indicated the following: (1) intermediate loading rates of ~ 105 s^{-1} and 6 x 105 s^{-1} are achieved through the use of graded-density impactors as the sample is loaded through peak stresses of 8 GPa and 41 GPa, respectively. In each case, these are at least three orders of magnitude lower than the comparable loading rates obtained by shock loading to the same stress; (2) PMMA under time-dependent loading, i.e., under continuous compression, remains transparent at least up to ~ 41 GPa; this far exceeds the transparency limit of ~ 22 GPa under single-shock compression; and (3) refractive index measurements for PMMA will be necessary to accurately estimate the continuous stress-strain response of PMMA.

We demonstrated this revolutionary approach for use with a transparent material such as PMMA. The experiments indicated that the experimental technique can be implemented. This definitely has the potential to allow measurements of extreme compression states for hydrogen and deuterium on guns at least up to 2 Mbars. (Lithium fluoride is transparent at least up to 2 Mbars and hydrogen [static tests] up to 3 Mbars.) If successful, the new methodology will allow the determination of the EOS of hydrogen to extreme pressures. This technique appears to be sufficiently flexible for use on the record-breaking x-ray energy sources of Saturn and those available on the PBFAII-Z and the National Ignition Facility (NIF) facility to pressures over 10 Mbars to 100 Mbars (limited by transparency of materials). Refractive index measurements of these strategic materials will, however, be necessary for a detailed data analysis.

Experiments were successful in that we measured the particle velocity profiles at the tantalum/PMMA and PMMA/LiF interface. However, a detailed data analysis of these profiles is necessary to estimate continuous compression states of PMMA up to 8 GPa and 41 GPa, respectively. A detailed analysis of the experiments should include an uncertainty in the pressure-volume states for PMMA up to 8 GPa and 41 GPa, respectively, resulting from (1) the phase transformation in PMMA due to dissociation and bond breaking of the polymeric chains in excess of 22 GPa, (2) the lack of refractive index measurement in PMMA at stresses above 22 GPa, and (3) uncertainties from experimental input conditions. We highly recommend that such data analysis methods be implemented now because the experimental method appears to be sufficiently flexible for use with pulsed-power technology such as Saturn of PBFAII-Z to investigate strategic (transparent) materials (hydrogen, deuterium) of interest for ICF applications.

Remote Optical Detection of Obscured Objects in Turbid Oceanographic Environments

S. M. Cameron, R. B. Spielman, D. R. Neal

The development of versatile light-based sensors to remotely detect hostile threats at a distance in optically and sonar-limited environments such as coastal seawater is a critical prerequisite for non-acoustic detection of submarines and coastal sea mines. Optical techniques that enhance the visualization of underwater objects obscured by scattering boundaries, thermoclines, and acoustic clutter are important refinements for bathymetry, surveillance, target acquisition, and line-of-sight communication functions. Implementation of range-resolved hydrographic imagery under conditions of pervasive scatter requires active compensation for dispersive effects induced by diffuse scattering and turbulence, which progressively degrade image quality and limit quantitative determination of optical pathlength. We developed a new quasi-ballistic imaging technique.

This work focused on increasing the range and resolution of locating underwater objects using laser bathymetry in highly-scattering environments such as coastal seawater. We examined the feasibility of using an optical parametric amplifying (OPA) gate to enhance return signals from the object over the diffusely scattered background. We systematically studied the operating conditions of the laser sources, amplifying gate, and detector to optimize overall performance. We constructed a test geometry in which we used a multipass cell to obtain long pathlengths in turbid water. With conservative improvements in the detector quantum efficiency and the laser source energy, the detection range could be extended to 20 m for the same conditions. A related experiment confirmed the applicability of this technique to the detection of objects obscured by flames and smoke. In these experiments, we achieved submillimeter spatial image resolution under conditions for which standard methods of thermal imaging and active-infrared (IR) range-gating fail. The unprecedented level of performance demonstrated by the OPA approach exceeded any previous benchmarks in the published literature.

RoBug Conceptual Design and Analysis System

P. C. Bennett

Miniature and microrobotic intelligent systems (RoBugs) are of increasing importance to Sandia and will find use in a host of applications for DOE offices and other federal agencies. In keeping with Sandia's new strategic objectives, we pursued Model and Simulation-Based Life-Cycle Engineering (MSBLCE) through the development of a conceptual design and analysis tool suitable for use on MacIntosh desktop and laptop computers. With this tool, given overall performance requirements for a system of RoBugs, we are able to carry out limited trade studies among the RoBug component technologies and thereby understand the requisite performance of the component technologies. Component technologies of interest include sensing, computing, behaviors, communication, power, and navigation.

RoBugs are of increasing importance to Sandia and will find use in a host of applications for DOE offices as well as other federal agencies. Single, multiple, or heterogeneous systems may be called upon to work together to accomplish some task. Designing the systems requires a careful balance of physical components, capabilities, and behaviors to accomplish a given mission. To facilitate the design process, we developed a RoBug Conceptual Design and Analysis System for Apple MacIntosh computers. Personal computer platforms were desirable due to availability and cost, while MacIntosh was chosen due to its prevalence as a personal platform.

RoBugs can be represented by simple geometric shapes chosen from a graphical user interface (GUI), including a predefined representation of a small-scale Robotic All-Terrain Lunar Exploration Rover (RATLER) robotic vehicle, and rapidly inserted into the simulation field. Obstacles of various shapes can likewise be inserted and defined as goals if desired.

Predefined sensors can be assigned to each RoBug together with sensor parameters from the GUI. Software hooks exist to define and add new sensors to the menu as needed.

Goal-seeking behaviors can be assigned to each RoBug through the GUI. One predefined behavior seeks to evenly deploy an array of bugs along a defensive line. Other potential behaviors include formation movement and point target seeking.

Graphical update rates can be set via GUI slide bar, speeding the simulation or refining step sizes.

Limited predefined behaviors—goal-seeking based upon a proximity sensor, and fundamental array deployment—are currently the only implemented behaviors. We accomplished array deployment by assigning different goals to each RoBug.

Limited predefined sensors—proximity sensors with a predefined range and sensitivity, as well as global positioning system (GPS)—were defined options for each simulated RoBug.

Two-dimensional graphics—graphics packages available for the platform—were practically limited to 2-D displays at the time of the work. Expectations are that within a year, better, faster packages will be available.

The Tcl/TK GUI interface is slow on the target platform, The graphical updates are slow as implemented using the Tcl/TK interface, up to 100 times slower than the power of the processor would allow. While Tcl/TK is useful in cross-platform porting, it is an obstacle for laptop computers when smooth, real-time movement is desired.

Communications to, from, and between RoBugs is not implemented. This limits the amount of cooperative behaviors that can be developed and tested using this tool.

Collision avoidance between bugs and obstacles is not yet implemented.

Prediction of Seismic Rocket Launch Signatures

D. C. Smathers

This report describes the models developed to predict the rocket launch seismic signatures that would occur at 0.1 to 10 km from the launch site at Area 26, Nevada Test Site (NTS). The models support system studies of covert ground-based sensors for tactical launch detection of theater missiles. One model describes how the acoustic and mechanical energy is coupled into the ground. A geologic model describes seismic velocities and densities of strata around the launch point. A third model calculates the propagation of seismic energy using a 2-D finite-difference elastic modeling code. We tuned the models using previously measured rocket launch signatures from White Sands Missile Range, NM, and Sandia's Kauai Test Facility, HI. We used the predictions from the models to set up instrumentation at rocket launches.

Reliably detecting a rocket launch and determining its location using a few seismic unattended ground sensors (UGS) would be a significant new capability for the military. This project developed the models required to establish the bounds for application feasibility of seismic UGS for launch detection. Predicting seismic rocket launch signatures requires a set of interrelated models. The acoustic energy levels and frequency spectrum produced by any rocket motor can be predicted from the total thrust, engine exhaust velocity, effective engine diameter, and Strouhal number using empirical equations developed by the National Aeronautics and Space Administration (NASA). An acoustic coupling model translates the acoustic energy levels at the surface of the ground into seismic source terms for the seismic propagation model. The geologic model uses previous geologic studies to produce descriptions of the strata that underlie the area and seismic velocity and density estimates for each strata. The seismic propagation model uses a first-order system of wave equations for velocities and stresses at each node of the 2-D model space to propagate the wavefield through the seismic velocity model. The calculations

result in not only first arrival information but a complete synthetic seismogram for the duration of the seismic source.

The predictions for the rocket launches at NTS indicate that the most useful measurements can be made at distances to five kilometers using microphones and geophones with a frequency range of 5 to 2000 Hz. In addition, validation of the acoustic-to-seismic-coupling model would benefit from measurement of atmospheric pressure at the base of the rocket launcher with a frequency range of 0.01 to 50 Hz.

Evaluation of Shocked PVDF for Compact, High-Power Electric Pulse

R. J. Kaye, M. U. Anderson, P. W. Cooper

Methods for disabling electronics include high-power radio frequency (RF) and ionizing radiation, and direct application of high-voltage pulses to electrical systems. Battlefield application of these methods could be practical if powered by compact, low-cost, megavolt pulsers. This report evaluates the limits and feasibility of using explosively driven, shock-loaded polyvinylidine fluoride (PVDF) for the development of nanosecond-duration, megavolt, electrical generators capable of providing gigawatt peak power. PVDF is a highly polar, polymer film with well-characterized, strong piezoelectric properties. We present concept geometries that utilize simultaneously initiated shocks in multiple thin PVDF films. We evaluate electrical performance with an equivalent circuit model to determine the sensitivity of system parameters. We identify critical design issues in areas of explosive initiation and shock formation, piezoelectric film response, pulsed-power output, and packaging structure.

Disabling an adversary's electronic systems will be important to maintain battlefield advantage in future conflicts. An alternative to developing very high-power RF generators at long range for asset protection is deployment of numerous, low-cost, compact generators close to the target. Such generators that convert explosive energy to megavolt and gigawatt electrical levels could also drive diodes that produce intense ionizing radiation or be coupled directly to the target's power grid for system disruption. Should the compact generators be capable of scaling to tens of megavolts, a launched generator could irradiate an airborne target with intense radiation to neutralize its payload just prior to destruction by impact or explosive blast. The scope of this work considers whether the development of such generators is feasible with current materials and systems, and what research is needed over a period of 20 years.

Compact, explosively driven, piezoelectric generators for nanosecond-duration, megavolt-level pulsers are feasible. An equivalent circuit analysis that uses self-consistent system parameters shows that a 1.2-m-tall, 22-cm-diameter generator consisting of 160 explosive/film stages in series could drive a 1-MV, 20-ns full-width half-max (FWHM) pulse into a 73-ohm load in a few years. This will require near-term demonstrations of (1) high-current output and high-voltage standoff by relatively large areas of PVDF film, (2) shock uniformity over tens of square centimeters with low-initiation energy meshes and thin explosive sheets, and (3) synchronization of the short output pulses from each stage (10 to 20 nanoseconds) with low jitter.

Development of Periodically Poled Laser Sources for Ultra-Sensitive Analysis

P. E. Powers, S. E. Bisson

This report describes a test of a new concept in quasi-phasematching (QPM). We fabricated periodically poled lithium niobate (PPLN) crystal that has a sloped grating pattern, thereby allowing the potential of continuous tuning over the phase-matched bandwidth of the sloped region. Tunable PPLN crystals generated in the past used only discretely stepped grating patterns. This allowed only discrete tuning between selected wavelength ranges. A continuously tuned infrared (IR) laser source is highly desirable for chemical-sensing applications.

QPM is a newly emerged method of generating light via nonlinear mixing. In all nonlinear mixing processes, phasematching is necessary. Traditionally, this is done via birefringent phasematching, which requires the use of nonlinear crystals that have specific refractive properties. In QPM, crystals are engineered to allow phasematching. The most common method of accomplishing QPM is periodic-poling. Through a photolithographic process, a crystal is fabricated in which the optical axis is periodically inverted. This region of periodically inverted domains is often referred to as a "grating." The periodic modulation of the crystal axis leads to a periodic modulation of the nonlinear properties of the crystal. This, in turn, corrects phase mismatches that occur as nonlinearly interacting waves travel through the crystal. To accomplish this in a particular wavelength range, the size of the grating periods must be carefully controlled. Tuning has been demonstrated by mechanically stepping between different grating regions on a crystal. In this project, we investigated the use of a continuously varying grating pattern, which we refer to as a "fan" grating. This would provide continuous rather than discrete tuning.

We fabricated two crystals having different fanout designs to cover two wavelength ranges. The fanout patterns differed in the slope of the domain walls of the poled regions. We tested the more aggressive (higher-risk) grating in the laboratory in a continuous-wave (CW) optical parametric oscillator (OPO). We found the OPO to oscillate at the expected threshold level of ~ 4 W. We determined the tuning curve of the OPO by manually stepping the crystal through the cavity, thereby inserting different regions of the fan into the pump volume. Using a CW wavemeter, we found it to tune between 2.9 and 3.4 μm. This agreed with the range expected from the fan dimensions.

Based on this experiment, the fan grating approach appears feasible and should be pursued in the design of tunable laser systems for spectral sensing applications.

The OPO performed as expected. As indicated above, the tuning curve met the design specification at the expected threshold and at the expected idler output power of ~ 1 W.

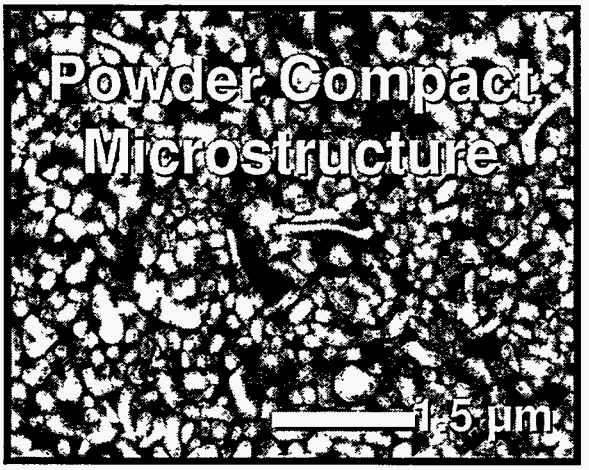

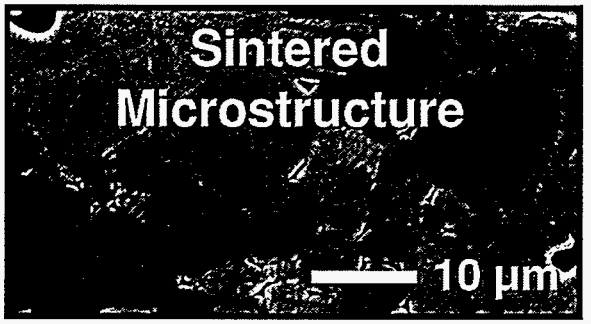

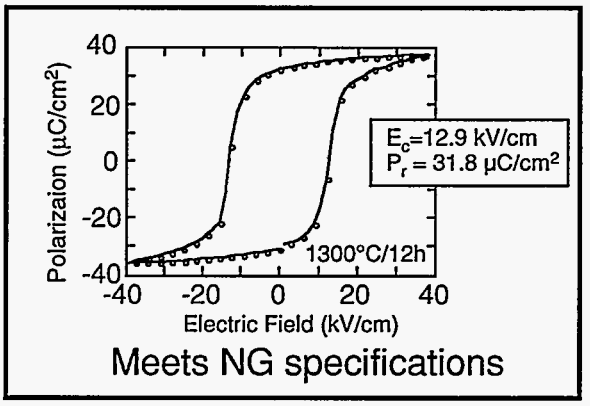

Special ferroelectric materials are an essential ingredient in neutron generators. The new solution synthesis process provides an excellent ability to control the stoichiometry and yields minimum hazardous waste.

Production

Distributed Object and Intelligent Agent Technologies in a Wide-Area Network Test-Bed

C. M. Pancerella

To meet changing DOE needs, it is necessary to recognize that a heterogeneous distributed information system is critical, and that distributed intelligent software components (those combining distributed objects, intelligent agents, and distributed knowledge-base systems) must be integrated in a wide-area distributed system. We propose to integrate these technologies in support of concurrent engineering, team collaboration, and manufacturing across organizational and geographic boundaries. An emerging standard for the deployment of wide-area distributed objects is the Common Object Request Broker Architecture (CORBA). CORBA addresses issues of interoperability in a distributed heterogeneous system; however, it does not define a protocol for knowledge exchange. The Advanced Research Projects Agency (ARPA) knowledge-sharing effort defined an agent communication language. Further, Java is very promising for implementing a portable agent template (for knowledge-sharing concepts) and for integrating with World Wide Web (WWW) and Internet technologies.

We are researching the integration strategies for developing agents that cooperate in a wide-area network (WAN) based on the above technologies. The integration of distributed object and intelligent agent technologies results in reliable, distributed knowledge systems, spanning domain boundaries. The deployment of this in a WAN results in an extended enterprise, spanning both geographic and organizational boundaries.

The Java language, not deployed at the time the project was written, is very promising for implementing a portable agent template (wrapper) and for integrating with both the WWW and CORBA. Hence, we can write an agent template, deployable in either a web browser or as a stand-alone application, that can access distributed objects in a wide-area environment.

We made the following conclusions and accomplishments in FY96:

(1) Continued to investigate research issues of agents and objects.

(2) Completed the development of manufacturing services in CORBA.

(3) Worked with Stanford University's Center for Design Research to develop a Java agent template that can interface to Pro/Engineer and CORBA.

(4) Began developing an interface between a design agent and a manufacturing service agent.

(5) Concluded that the architecture is flexible (easy to add functionality) and scalable (easy to add additional agents).

Publications

Refereed

Pancerella, C. M., and R. A. Whiteside. 1996. "Using CORBA to Integrate Manufacturing Cells to a Virtual Enterprise." Paper presented to the SPIE Plug and Play Software for Agile Manufacturing, Boston, MA, 18–19 November.

Pancerella, C. M., A. J. Hazelton, and H. R. Frost. 1995. "An Autonomous Agent for On-Machine Acceptance of Machined Components." *Proc. Modeling, Simulation, and Control Technol. for Manufact. Mtg.* **2596** (Philadelphia, PA, 25–26 October): 146–159. SPIE.

Whiteside, R. A., C. M. Pancerella, and P. A. Klevgard. 1997. "A CORBA-Based Manufacturing Environment." Paper presented to the Hawaii International Conference on System Sciences, Maui, HI, 7–10 January. IEEE Computer Society.

Carbon Coatings for Improved Sprytron Tube Performance and Reliability

T. A. Friedmann, D. R. Tallant, M. E. Smith, M. P. Siegal

Sandia is developing enhanced carbon coatings for new sprytron tube designs that have simplified the construction, improved the reliability, and reduced the cost of these devices. The sprytron tube relies on a carbon-based coating to fire the device. The coating technology now used, chemical vapor deposition (CVD), produces a form of carbon that is nondirectional in its application and difficult to mask, thus coating the entire piece. This is undesirable in some cases because further processing (laser etching of the coated piece) is required to make a functioning sprytron tube, and this limits the design of sprytron tubes to certain specific geometries. This project studies the use of pulsed-laser deposition of carbon coatings for simplified design fabrication.

We combined two Sandia capabilities in a synergistic manner, namely, understanding of carbon film deposition developed in part under research foundation support, with sprytron tube manufacturing expertise developed under long-term Defense Program (DP) support. This unique combination allowed for improved sprytron tube understanding, leading to enhanced reliability and performance and lower cost.

The first year of this project allowed the development of several new sprytron designs with enhanced properties. For example, several designs show increased lifetime (some were fired over 5000 times without failure), and one operates at a trigger voltage reduced by a factor of ten. The simplified new designs require fewer process steps, leading to reduced production costs. In addition, we developed more compact packages. Combined, these improvements not only help ensure that future DP demands can be met at a much reduced cost, but also open the possibility of new applications and customers.

Laser-Spray Fabrication for Net-Shape Rapid Product Realization

D. M. Keicher, C. L. Atwood, J. E. Smugeresky

The goal of this new project is to demonstrate the feasibility of using the laser spray coating process to fabricate solid metallic components directly from a computer-aided design (CAD) solid model. We demonstrated that this process is indeed feasible and that the localized heating characteristics provided by the laser allow improved material properties to be obtained. In addition, we also demonstrated that minimization of the laser input power allows flexibility in processing and enables precision application of the metallic material for near-net-shape applications.

We demonstrated the feasibility of using the laser-engineered net-shaping (LENS™) process for fabricating geometrically complex shapes in a fully dense metallic structure directly from a CAD solid model. We demonstrated that the localized heating provided by the laser source provides rapid quenching of the deposited material, leading to a fine-grain structure and subsequently a 2–3-times increase in material strength with no loss in ductility. We developed software to allow CAD files to be used to directly fabricate geometrically complex shapes directly from a CAD solid model. We identified the process parameter that will allow us to control the process and implement closed-loop process control. Component accuracy in the deposition plane is =/- 0.002" and =/- 0.015" in the growth direction. We used high-speed photography to observe the deposition process, and the results of this work suggest that LENS™ process is essentially a welding process. The laser creates a molten puddle on the surface of a substrate, and the powder metal particles are then injected into the puddle and subsequently melted. We optimized the laser scanning pattern and identified that the best surface finish is obtained by first depositing the outline of the structure and then raster filling the area contained within the outline. We also performed work to optimize the mechanical components of the LENS™ system to improve process robustness.

Publications

Other

Griffith, M. L., C. L. Atwood, and D. M. Keicher. 1996. "Laser-Engineered Net Shaping (LENS™) for the Fabrication of Three-Dimensional Ceramic Components." Paper presented to the American Ceramic Society Annual Meeting and Exposition, Indianapolis, IN, 14–17 April.

Griffith, M. L., J. E. Smugeresky, J. A. Romero, D. M. Keicher, D. L. Greene, L. D. Harwell, and C. L. Atwood. 1996. "Free-Form Fabrication of Metallic Components Using Laser-Engineered Net Shaping (LENS™)." Paper presented to the Solid Freeform Fabrication Conference, Austin, TX, 12–14 August.

Griffith, M. L., J. E. Smugeresky, J. A. Romero, D. M. Keicher, D. L. Greene, L. D. Harwell, and C. L. Atwood. 1996. "Laser-Engineered Net Shaping (LENS™) for Fabrication of Metallic Components." Paper presented to the 12th Annual Meeting of JOWG-31, Livermore, CA, 13–16 May.

Keicher, D. M., F. P. Jeantette, M. L. Griffith, J. E. Smugeresky, C. L. Atwood, and J. A. Romero. 1996. "Laser-Engineered Net Shaping (LENS™) for Additive Component Processing." Paper presented to the Rapid Product Development Consortium Meeting, National Tooling and Machining Association, Hartford, CT, 18 June.

Keicher, D. M., F. P. Jeantette, M. L. Griffith, J. E. Smugeresky, C. L. Atwood, and J. A. Romero. 1996. "Laser-Engineered Net Shaping (LENS™) for Additive Component Processing." Paper presented to the Rapid Prototyping and Manufacturing Conference, Dearborn, MI, 21 April.

Keicher, D. M., J. A. Romero, L. P. Schanwald, and J. L. Jellison. 1996. "Understanding the Laser-Engineered Net-Shaping (LENS™) System Through Process Characterization." Submitted to the IMOG Joining Group Meeting, Los Alamos, NM, November.

Keicher, D. M., M. L. Griffith, C. L. Atwood, and J. A. Romero. 1996. "Laser Metal Deposition of Alloy 625 for Free Form Fabrication." Paper presented to the 1996 World Congress on Powder Metallurgy & Particulate Materials, Washington, DC, 16–21 June.

Solid-Model Design Simplification

A. L. Ames, A. J. Webb

In developing automatic analysis and manufacturing applications, Sandia faces a curious dilemma: Designers are rewarded for including as much information as possible, while that detail causes automatic geometric reasoning applications to execute very slowly or fail altogether. We are developing software to automatically search through design data and find unnecessary details, automatically suppress that detail (where possible), and suggest simplification approaches (when automatic suppression fails). We are testing the approach by implementing extensions to Pro/Engineer and using simplification tools in a production setting.

With the ability to rapidly simplify models and focus on just the information that is important, we can dramatically improve our ability to use the design information we create. The increasingly small lot sizes and varied product mix we address will demand that we make sharing data among all disciplines more tightly coupled and commonplace, with each discipline viewing only the data they wish to see. This project is developing a fundamental manufacturing technology that is in demand for Defense Program agile strategies for future weapon development and that can be shared with agencies throughout government and industry.

We developed algorithms to search through Pro/Engineer part data and to identify suppressible details based on geometric metrics, such as lengths and areas of edges and faces, nearness of edges and faces to a point in space, and the presence of degeneracies in higher-order surfaces.

We developed software to iterate through a list of features (produced by searching algorithms), determine parent/child relationships between the features, and, if possible, suppress them. We defined an algorithm for automatically rerouting features to mitigate parent/child relationships; implementation of that algorithm awaits enhanced functionality in Pro/Develop. We also investigated approaches, such as dimensioning only to datums, that would reduce the impact of parent/child relationships on suppressability.

We developed a capability for suppressing parts in an assembly based on a variety of geometric metrics. This simplification is easier to perform outside of the context of Pro/Engineer's assembly representation, as assemblies can be easily represented without parent/child relationships.

We investigated application-driven feature suppression. Our approach will allow an outside application to define what geometric elements would be preferable to eliminate, with Pro/Develop software deciding what elements could be deleted. Simplification would then occur by feature suppression and regeneration, as is performed in non-application–driven scenarios.

Process Optimization for Electron-Beam Joining of Ceramic and Glass Components

B. N. Turman, S. E. Gianoulakis, L. Kovacic, J. A. Halbleib, R. S. Chambers, J. S. Glass, R. H. Moore

With a penetration depth into a typical ceramic of 1 cm for a 10-MeV electron beam, this method provides the capability of rapid, transient, brazing operations where temperature control of critical components is essential, or the capability of directing energy into a buried or inaccessible joint. Because of transient heating and the lower heat capacity and melting temperature of braze metals relative to the ceramic materials, a pulsed high-power beam can melt a braze metal without excessive heat input to the ceramic. The purpose of this project is to develop and extend the electron beam joining process to applications related to Mo/Al_2O_3 cermets for neutron tube fabrication, glass seals for flat-panel displays, and structural ceramics. The key issue is the identification of the allowable operating ranges that produce thermal conditions favorable to robust joining and sealing. We conducted a combination of theoretical and experimental studies to determine the proper thermodynamic, beam, and materials parameters, and successfully joined and sealed ceramic and glass tubes with a 10-MeV electron beam.

High-energy electron beam brazing of ceramic components was first modeled numerically. We modeled energy deposition resulting from electron beam irradiation by simulating the coupled electron-photon transport with the Integrated TIGER Series (ITS) code system. We assumed that thermal transport was governed by the thermal diffusion equation with temperature-independent density and thermal conductivity assumed. We assumed specific heat to be constant for all materials except the braze. We assumed that braze specific heat varied, with an increased value between the liquidus and solidus temperatures to account for latent heat effects during melting. We included radiative and conductive thermal boundary conditions. We performed the thermal analysis using the finite-element (FE) code COYOTE II. We performed parametric simulations for a range of beam currents in addition to variations in thermal boundary conditions and apparatus, braze, and part materials to optimize the experimental apparatus and process. We performed a large number of simulations to define the thermal and radiation parameters for the problem and confirmed them by experiment. These simulations and experiments showed that alumina parts with thicknesses up to 0.8 cm are adequately penetrated by a 10-MeV beam. We joined 19 Pyrex glass tubes, 21 ceramic tubes, and more than 35 coupon combinations using a matrix of beam power and exposure time settings to identify successful operating ranges. Most of the alumina tube experiments used Cusil ABA, typically 75-μm thickness, because of its intermediate melting point and Ti content. At 380-W beam power, we were able to join and seal alumina tubes in 300 seconds. The joints showed high strength and excellent hermeticity, approaching or even exceeding the shear strength of alumina. We conducted coupon joining tests using various ceramic substrates and brazes. The substrate materials included Si_3N_4, SiC, Al_2O_3, Mo-Al_2O_3 cermet, and soda lime silicate glass. Brazes included Ticusil, Cusil ABA, Incusil ABA, and Nioro ABA. The first three brazes contain Ti as the active element, and Nioro ABA contains V as the active element that promotes wetting and reaction with the ceramic. We tested Ti as an interlayer between Si_3N_4 and SiC coupons with Ticusil as the braze material. In general, we found that the active brazes provided stronger, more consistent joints and seals. We used schott glass frit for joining glass coupons.

Self-Tuning Process Monitoring System for Process-Based Product Validation

R. G. Hillaire, C. S. Loucks, K. L. Schroder

This work will create a process monitoring system for milling machines that will autonomously correlate the physical characteristics of the product to the forces, torque, vibration, and acoustic emissions generated during a cutting cycle. The resulting force, torque, vibration, acoustic hyperpoints, and correlated physical characteristics will be overlaid on the product geometry model, which can be analyzed and visualized with extendible Virtual Reality Meta Language (VRML) or advanced virtual reality (VR) systems.

We will develop the autonomous correlation by statistically comparing the very detailed inspection records to the process hyperpoint values. Once deployed, the detailed inspection may be significantly reduced or eliminated. The work will deploy a feature-extraction routine, machine-calibration methodology, a stable sensor array, a sensor-calibration routine, a self-tuning sensor-inspection correlation routine, a hyperpoint overlay routine, and an advanced visualization interface.

The technology created in this project will help validate production of war reserve (WR) components by generating a process signature for products, processes, and lot runs. The signatures of all products can be compared across all products made within and across lot runs to determine if the processes that produced the product are consistently providing superior quality. Furthermore, the quality of the process and product will be quantified and visibly apparent.

Simply by monitoring the output from the sensor array displayed on the process monitoring computer screen, the machinist began to develop techniques to homogenize the machining process. Once they saw how the feeds, speeds, and toolpaths they chose were quantified against cutting force, vibration, and acoustic emissions, they began to think about incremental changes to make each cut more uniform. The researchers believe that once the cuts are consistent, the quality of the process can be better quantified and honed. This astounding result developed in the infancy of the project. Once we develop the full package, the results may be beyond initial expectations.

We accomplished the following in FY96:

(1) Installed existing sensor systems on Haas four-axis milling machine. We modified and used a Montronics tool-monitoring system as the process-monitoring system. The system has sensors for Spindle Power, three-axis force, vibration, and acoustic emissions. In addition, we monitored the position of the machine using a four-axis encoder interface card and also monitored the coolant pH with an Omega pH sensor. A PC with a National Instruments Data Acquisition Card reads all sensor signals. The entire system is very modular and is transferable to any machine tool.

(2) Developed a machine-calibration methodology. Machine calibration is critical to ensure that process monitoring will provide consistent indication of product quality across different machining platforms. Before sensor information could be useful, characteristics such as machine accuracy, natural frequencies, and spindle runout needed to be characterized. This information will help identify the sources of phenomenon that the sensors will measure.

(3) Developed a robust sensor-calibration routine. Calibrating the sensors is critical to ensuring that the information obtained is consistent and meaningful. Power is measured directly through current and voltage; therefore, no calibration is needed. We will calibrate the force sensors by applying forces through a previously calibrated portable dynamometer to the process-monitoring dynamometer, and by noting readings and adjusting discrepancies.

Solution Synthesis and Processing of PZT Materials for Neutron Generator Applications

J. A. Voigt, J. S. Glass, K. G. Ewsuk, S. J. Lockwood, B. A. Tuttle, M. T. Anderson, T. W. Scofield, J. D. Keck

Neutron generator power supplies require two unique ferroelectric materials, specifically lead zirconate titanate with a Zr-to-Ti ratio of 95:5 (PZT 95/5) and PZT 95/5 with a partial substitution of tin for zirconia (PSZT). These PZT formulations are unique to neutron generators, and there are no current U.S. suppliers of the material. Based on our past experience in which we successfully developed and transferred to industry chemical preparation processes, we propose to develop an alternate process based on solution chemistry to prepare the PZT powders. We will develop the process such that the concerns of the previously used mixed-oxide process are satisfactorily addressed. We will emphasize the underlying fundamentals of system solution chemistry and how these fundamentals relate to the ceramic material properties that are critical to neutron generator applications.

A complete review of the literature on work related to the chemical synthesis of PZT and related materials revealed several synthesis techniques worthy of further evaluation for application to the PZT 95/5 material system. These processes included the Dosch alkoxide/lead lactate process, the Haertling/Land alkoxide/PbO process, and the British Zr/Pb nitrate process. We investigated the solution chemistry of each of these processes.

Since the British at AWE, Aldermaston, have been working on developing a chem-prep process specifically for PZT 95/5 for some time, we decided that an opportunity exists for possible collaboration. Through a visit to their facility at Aldermaston, we signed a

nondisclosure agreement and obtained details about their process. We prepared several batches of powders using their process. As developed by the British, the aqueous-based process produces an excessive amount of liquid waste, a precipitate that is difficult to filter and requires spray drying, and a cation precursor solution that is unstable with respect to the source of niobium. We modified their process to reduce the problems associated with these issues and are currently evaluating the powders prepared by the modified processes.

Because of potential problems associated with the processes given above, we developed a new PZT 95/5 synthesis process. The route uses Zr, Nb, and Ti alkoxides mixed with a concentrated lead acetate solution as the cation solution. This solution is added to an alcoholic oxalic acid precipitant solution. Unlike previous processes, this method produces an easily filterable precipitate formed from true solutions. Chemical analysis of filtrates indicates that the process removes greater than 99.9% of all of the PZT constituent cations from solution, indicating an excellent ability to control stoichiometry. Finally, we designed the process such that the number of powder-handling steps and the amount of waste generated are minimized. We are currently evaluating the densification behavior of powders prepared by this process.

We will file a patent disclosure for the process as soon as we complete some of the initial electrical and physical characterization data on the ceramic material. We have already demonstrated the versatility of the process by modifying it to prepare lead magnesium niobate/lead titanate, PMN/PT, powders. To date, we have prepared powders with a stoichiometry appropriate for a high-energy-density capacitor DP application and are in the process of preparing a PMN/PT formulation suitable for lightning arrestor connector granules.

Effect of Composition and Processing Conditions on the Reliability of Cermet/Alumina Components

J. J. Stephens, K. G. Ewsuk, S. N. Burchett, J. S. Glass, R. H. Moore, S. L. Monroe

Evidence of cracking in several cermet feedthroughs used in neutron tube subassemblies has raised questions regarding the suitability of cermet components in war reserve (WR) applications. Moreover, cracking is exacerbated in larger, more complex geometries such as the MC4277 tube frame. Preliminary failure and stress analysis indicate that the cracking is most likely associated with the considerable mismatch in thermal expansion between the cermet insert and the ceramic. Additional issues such as the strength of the cermet/alumina interface, and the control of relative sintering kinetics between cermet and alumina in the production of sintered cermet/alumina composite parts, need to be evaluated.

We accomplished the following in FY96:

(1) *Fabricated Mo-31V alloy.* The electrode was vacuum arc-remelted (VAR) three times at the Sandia melting facility. We are currently processing the ingot to permit fabrication of powder via the Plasma Rotating Electrode Process (PREP). Further milling and classification of powder will be needed to realize the powder size required for cermets.

(2) *Performed mechanical alloying of Mo-22V-3Fe alloy powder.* Under contract with UC–Irvine, we produced 100 gms of ternary alloy powder. We are in the process of characterizing this material, prior to trial hot-pressing of bars and cermet evaluation.

(3) *Developed reduced V-content ternary alloy.* We measured the coefficient of thermal expansion (CTE) and hydrogen compatibility of two new ternary alloys that appear promising for use in the cermets: Mo-22V-3Fe and Mo-22V-3Co alloys (composition in wt.%). We showed both alloys to be single-phase body-centered cubic-crystal structure (BCC) alloys and reduced hydrogen uptake relative to the Mo-31V alloy.

(4) *Documented suitable sintering conditions for cermet/alumina composites.* We observed shape distortions in composite parts because the alumina phase tends to shrink more than the cermet phase during sintering. Compaction experiments demonstrated that if the ceramic and cermet phases are prepressed to the same relative density prior to sintering, warpage in composite parts can be avoided. For the cermet/alumina system under consideration, prepressing the 94% alumina at 30 ksi prior to machining and backfilling with the cermet slurry will produce the proper relative density.

(5) *Acquired mechanical properties data for cermets.* As a baseline to compare with mechanical behavior of the new ternary alloy cermet, using ASTM C1161 we completed strength measurements on CND50, 94ND2, and composite cermet/alumina specimens. We developed a three-step process to fabricate composite test bars so that the microstructure at the cermet/alumina interface is truly representative of the manufacturing environment.

Publications

Other

Glass, J. S., S. L. Monroe, R. H. Moore, and G. A. Pressly. 1995. "Percolation Effects on the Structure and Properties of Alumina-Mo Cermets." Paper presented to the American Ceramic Society Basic Science Meeting, New Orleans, LA, 5–8 November.

Stephens, J. S., B. K. Damkroger, S. L. Monroe, and R. H. Moore. 1996. "Thermal Expansion and Solidification Behavior of Mo-V Alloys." Paper presented to the 1996 Annual TMS Meeting, Anaheim, CA, 4–8 February.

A Multilevel Code for Metallurgical Effects in Metal-Forming Processes

P. A. Taylor, D. J. Bammann, D. A. Hughes, S. A. Silling

The goal of this project is to develop a computational capability for simulating metal-forming processes that display phenomenology occurring on two different-length scales. Forging and deep-extrusion processes are examples from this class. Our modeling methodology focused on predicting both (1) the overall flow of workpiece material and (2) the microscale effects that control distribution of mechanical properties throughout the final product. The microscale effects are a result of friction and anisotropic hardening, which tend to occur on a small length scale (relative to typical workpiece dimensions) in a "boundary layer" near the interface between the workpiece and tool/die hardware. The goal of this project is the development and demonstration of a computational methodology for coupling process simulations occurring on two different-length scales in certain metal-working operations. Such computational techniques offer the potential for drastic reductions in time and cost of new metal-forming process development, where current practices rely on empirical, trial-and-error methods.

The technical challenges that must be accomplished for this project to be successful include the following:

(1) Develop a multigrid, Lagrangian/Eulerian, computational simulation methodology that captures the overall flow of the workpiece material in a forging or extrusion operation and the micromechanical effects that occur in a "boundary layer" at the interface between the workpiece and tooling hardware.

(2) Develop a computational scheme that will alleviate the time-step constraints that currently restrict our computer code to simulation time scales that are two to three orders of magnitude smaller that those of typical forging or extrusion operations.

(3) Identify and implement constitutive models into our solid mechanics computer code, describing the thermomechanical processes occurring in a workpiece material whenever it is subjected to a forging or extrusion process.

(4) Gather experimental data that permit the fitting of the constitutive models and validation of the overall computational scheme.

We were successful in completing and demonstrating the usefulness of each of the challenges listed above. We had a difficult time, however, in merging all of these new features into a single computational platform and in validating its use in simulating metal-forming processes. The separate accomplishments of the project were sufficiently encouraging to the extent that we are continuing with the work in FY97 using our own tech-based funds to evaluate the completed computational platform.

Publications

Other

Taylor, P. A. 1996. "CTH Reference Manual: The Bammann-Chiesa-Johnson Viscoplastic/Damage Model." Sandia Technical Report, SAND96-1626, July.

Automated Reasoning About Tools for Assembly

R. H. Wilson

Many important constraints on assembly, servicing, and disassembly come from the need to apply tools of various types, ranging from screw drivers to laser welders to robot grippers and cameras. Sandia proposes to develop a system for automatically reasoning about the geometric and mechanical applicability of tools in mechanical assembly processes. Few programs reason about such tools, and those that do use ad hoc, *special-purpose techniques. We will develop and implement a homogeneous approach to representing and reasoning about mechanical assembly tools that will cover the large majority of common robotic and handtools.*

We accomplished the following in FY96:

(1) Specified tool language for 2-degree-of-freedom (DOF) tools. This includes tools such as screwdrivers that can access a screw from a nonvertical angle, as well as tools such as human inspection and pipe wrenches.

(2) Programmed geometric engine to preprocess 2-DOF tools.

(3) Expanded library to include 30 tools, covering a robotic workcell and service of an industrial assembly. In fact, the current tool library includes 65 tools of various types, and we have modeled but not incorporated an additional 45 tools.

(4) Developed robotic gripper reasoning capability and connected it to the tool assembly planner. The robotic gripper planning system was not in the original proposal and is far more powerful than the tools envisioned there, requiring reasoning about gripped surfaces, finger travel, centers of mass, and gripping force.

(5) Delivered system to two beta sites for testing and evaluation.

(6) Wrote user-friendly interface to tools constraints in assembly planner.

Publications

Refereed

Wilson, R. H. 1997. "Automated Reasoning About Tools for Assembly." *Internat. J. Robotics Res.*, accepted.

Wilson, R. H. 1996. "Automatic Reasoning About Tools for Assembly." Paper presented to the International Conference on Robotics and Automation, Minneapolis, MN, 10 April.

Other

Wilson, R. H. 1996. "Automated Reasoning About Tools for Assembly." Sandia report, SAND95-2423, January.

Analysis-Driven Mechanical Redesign

R. H. Robison, W. R. Witkowski, J. F. Schulze, D. B. Saylors

Sandia advanced the technology of model-based simulation by prototyping an analysis-driven mechanical redesign loop that feeds analysis results through an optimization algorithm into Pro/Engineer to modify the design. This prototype system provides for the addition of nearly any type of analysis that utilizes CAD geometry. This coupling between a part's geometric description and its engineering analysis results benefits Sandia's work in product realization and advanced manufacturing by assisting in reducing production costs and designing higher-quality products. We also extended the field of large-scale design optimization by developing a set of sparse matrix routines that will ultimately yield a new large-scale optimization algorithm. We defined a technical problem referred to as solid model scalability *and proposed a possible solution that could result in robust parametric solid model geometry.*

We accomplished the following in FY96:

(1) Successfully implemented a functioning prototype redesign loop that generates Pro/E geometry, performs some analysis activity, extracts objective function information, and drives a constrained nonlinear optimizer to produce the next set of design parameters. We developed tools for selecting and constraining design parameters. Analysis loop is able to use part tolerances to achieve an optimal design that is not brittle (too close to a constraint).

(2) Conducted research in the area of large-scale optimization problems. In mechanical redesign, there exists a potential for an overwhelmingly large number of design variables, which can easily exceed the ability of current optimization algorithms. We developed a library of sparse matrix routines in C++ to support the development of a large-scale sequential quadratic programming (SQP) algorithm.

(3) Identified the need for topology verification as a first-order verification tool to prevent the optimization from violating design intent. We identified ACIS-based algorithms for comparing topologies and designed a Pro/Develop-based approach for working directly with Pro/Engineer. We identified and investigated the area of solid model scalability; that is, the ability of a given parametric model to robustly survive design modification.

Liaison-Based Assembly Design

A. L. Ames, K. Eras, R. H. Wilson, S. W. Parratt

Liaison-based assembly design extends the current information infrastructure to support design in terms of kinematic relationships between parts, or liaisons. *These liaisons capture information regarding contact, degrees-of-freedom (DOFs) constraints, and containment relationships between parts in an assembly. The project involved defining a useful collection of liaison representations, investigating their properties, and providing for maximum use of the data in downstream applications. We tested our ideas by implementing a prototype system involving extensions to Pro/Engineer and the Archimedes assembly planner. With this improved product model, the design system is better able to capture design intent. When we attempt a product update, increased knowledge availability improves our ability to understand the effect of design changes. Manufacturing and analysis disciplines benefit from having liaison information available, so less time is wasted arguing over incomplete design specifications, and our enterprise is more completely integrated.*

We accomplished the following in FY96:

(1) Extended our collection of liaison representations to include snap fits, press fits, welds, glue joints, and fasteners. We developed a mechanism for specifying limits on DOFs at the request of a potential customer. We defined liaison representations for loads and boundary conditions; implementation is incomplete. We identified requirements and defined representations for "promoting" liaisons, to provide for representation of increasing design and manufacturing information. We investigated the use of liaisons in conceptual design, before part geometries are defined. The use of liaisons to capture conceptual intent is very promising.

(2) Thoroughly investigated the ramifications of editing liaisons within a commercial feature-based solid modeler, Pro/Engineer. We developed functionality for adding, modifying, deleting, and graphically displaying liaison information. We identified limitations in Pro/Engineer that constrained the generality of liaison representations, specifically in the area of constraining the geometric extent of a liaison to a portion of an edge or face. We successfully demonstrated the ability for liaisons to survive regeneration, where the geometric underpinnings of a liaison might not always be available in the model due to parameter changes.

(3) Developed a generic capability for transferring liaison information to analysis and manufacturing applications. We developed a custom capability for exporting liaisons to the DADS (Dynamic Analysis & Design System) package.

(4) Tested the liaison modeling capability on a real design, a pin-in-maze discriminator. Current liaison modeling capability captures all of the kinematic relationships in the assembly.

An Enabling Architecture for Information-Driven Manufacturing

M. J. Griesmeyer

A basic element of agile manufacturing concepts is the development of information-driven manufacturing systems that permit rapid system reconfiguration to produce new and modified products and to support intermittent production of established products. This project focuses on the development of principal components essential to such information-driven manufacturing systems. We completed definition of a prototype production script grammar that allows portable proscription of the production steps required to produce quality products. We also completed definition of a complementary prototype equipment description grammar for expressing equipment capabilities and physical characteristics. It provides for both matching of equipment capabilities to production step requirements and data-driven interactions with the selected equipment to accomplish a step. A Task Sequence Controller (TSC) orchestrates the product production by processing the production scripts and dispatching production steps to selected equipment based upon the equipment descriptions. We integrated the TSC into a simulation system based upon the equipment descriptions to provide for preproduction manufacturing validation using the same supervisory control system as is used to orchestrate the operations of the actual production system equipment.

During FY96 we applied the results of the production script project efforts to supervisory control software for the Agile Manufacturing Prototyping System (AMPS) assembly cell. We demonstrated rapid software reconfiguration in AMPS. We used the experience in AMPS to develop a more fully featured production script grammar and developed a reengineered task sequencer to execute the production scripts with the new grammar. The new task sequence is just coming online. In addition, performance issues required that more of the script processing be done by the subsystems themselves. The fourth-quarter efforts for FY96 focused on testing an approach to do this. At the end of the project we were testing the system for scripts for which the task sequencer ensures only that material is routed to the selected subsystem and the appropriate subscript is available to it. The subsystem is autonomous in the execution of the subscript. The results of this project are providing major foundations for the system integration and virtual manufacturing work under the AMPS umbrella during FY97.

Publications

Other

Griesmeyer, J. M., and F. Oppel. 1996. "Process Subsystem Architecture for Virtual Manufacturing Validation." *Proc. IEEE Conf. on Robotics and Automation* 3 (Minneapolis, MN, 24–26 April): 2371–2376.

Science at the Interfaces: Engineering with Atoms

Cells placed in the laser cavity formed with semiconductor and dielectric mirror surfaces are shown.

The spectra provide unique signatures and can be used to identify cell type, size, and shape.

A new biomedical laser sensor rapidly quantifies size and shape of different kinds of living human cells for early detection of disease.

Nanocavity Effects on Misfit Accommodation in Semiconductors

S. M. Myers, R. L. Dawson, C. J. Barbour, S. R. Lee, J. A. Floro, D. M. Follstaedt

This project explored the use of nanometer-scale interfacial cavities formed by helium (He)-ion implantation to influence dislocation behavior and strain relaxation in heteroepitaxial semiconductor structures. We experimentally demonstrated and theoretically described a strong attractive interaction between cavities and dislocations. In heteroepitaxial SiGe/Si structures, the introduction of cavities greatly enhanced the rate of strain relaxation and increased the equilibrium extent of relaxation with no significant increase in the density of threading dislocations. In InGaAs on GaAs, we developed and applied methods for cavity formation, but did not observe this treatment to enhance relaxation at temperatures up to 400°C.

We mechanistically explored the use of nanometer-scale interfacial cavities to influence dislocation behavior and the resulting strain relaxation in heteroepitaxial semiconductor structures. This is a new approach to the growth of strain-relaxed epitaxial layers with minimized threading defects. A central challenge is the control of dislocations, which accommodate lattice misfit between substrate and overlayer but are detrimental when they thread into the overlayer. Introducing nanocavities into the interfacial region is expected to alter lattice relaxation and dislocation behavior through (1) enhanced dislocation nucleation, (2) strong attractive forces between dislocations and cavities, and (3) reduction of dislocation line energies. The work had two broad objectives: to understand these effects at a mechanistic level, and to manipulate them to maximize relaxation while minimizing dislocation threading. Cavities were formed by He-ion implantation and annealing. We extensively studied SiGe layers on Si with limited examination of InGaAs on GaAs.

(1) After previously demonstrating that cavities strongly accelerate the relaxation of strain in SiGe on Si, we measured this effect as a function of temperature. Additionally, we showed that the asymptotic, equilibrium degree of relaxation is increased by interfacial cavities and explained this as arising from the reduction in misfit-dislocation line energy when the dislocation intersects cavities.

(2) We showed that the above enhancement of relaxation is achieved with essentially no change in the number of residual threading dislocations.

(3) We found that introduction of cavities during growth results in dislocation microstructures and strain relaxation similar to that resulting from post-growth formation.

(4) We developed a predictive theoretical model of cavity-dislocation interactions by treating simple configurations exactly in elastic continuum theory and employing the results to describe more complicated situations.

(5) We developed methods to form cavities in the interfacial region of InGaAs on GaAs and characterized the resulting microstructure and strain state. We did not observe significant enhancement of strain relaxation in the relatively low-temperature range below 400°C.

(6) We experimentally demonstrated and theoretically interpreted the large effects of interfacial nanocavities on dislocation behavior and strain relaxation in semiconductor heterostructures. As a result, enhancement of strain relaxation and strong trapping of dislocations by cavities can now be regarded as tools with which to manipulate dislocation behavior controllably. Moreover, the basic knowledge developed here will facilitate understanding of the interactions of dislocations with open volumes in other systems, such as heteroepitaxial GaN where these effects are of current concern.

Publications

Refereed

Follstaedt, D. M., S. M. Myers, J. A. Floro, and S. R. Lee. 1996. "Interaction of Cavities with Misfit Dislocations in SiGe/Si Heterostructures." *Nucl. Instrum. and Meth. B*, in press. Amsterdam, Netherlands: Elsevier Science B.V.

Follstaedt, D. M., S. M. Myers, and S. R. Lee. 1996. "Cavity-Dislocation Interactions in SiGe and Implications for Heterostructure Relaxation." *Appl. Phys. Lett.* **69** (30 September): 2059–2061. Woodbury, NY: American Institute of Physics.

A New Paradigm for Near Real-Time Downhole Data Acquisition

J. R. Waggoner, D. E. Gallegos, R. J. Franco, H. E. Morris

This report describes the proof-of-concept of a novel telemetry technology called Surface Area Modulation (SAM). SAM has the ability, as demonstrated in this project, to transmit high-data-rate information from a downhole location to the surface in a producing oil well. While the technology is useful to many applications, this project focused on the producing oil-well application because it was deemed to be lower cost and easier to field than other applications. Sandia established the proof-of-concept with field-test results and model studies.

Many deep underground operations have difficulty establishing a two-way data communications link between remote sensors and the surface data-acquisition system. When the downhole environment is too severe to allow a wire to survive, even with appropriate shielding, the downhole data are either approximated from surface measurements, gathered with memory tools that must be sent down the hole and then retrieved, or just neglected. Unfortunately, the last option, neglecting the downhole data, is the most commonly adopted, and leads to a dependence upon unsubstantiated assumptions or costly and untimely information.

In most applications, knowing the downhole data is critical to the success of the operation. This is especially true in the oil and gas, geothermal, and environmental industries. With approximately 10% of the U.S. economy dependent on the oil and gas industry, the efficiency of producing oil and gas is a critical issue. Of the approximately 500,000 producing oil wells in the U.S., about 400,000 use the sucker rod pumping technique, which uses a long string of steel rods to translate the up and down motion at the surface to a downhole piston pump. This pumping system can be optimized only by knowing the rod loading and fluid pressures at the downhole pump. For this reason, the sucker rod pumping application was the primary focus of this project.

The main conclusion is that the SAM telemetry concept has been proven for this application. Two field tests conducted in FY96 demonstrated that the half-duplex data link could be established, that 2400-baud data rate is possible, and that a bandwidth of 64 kHz existed. In addition, the data link can be established with bare steel (uncoated) sucker rods with only minor changes to the tubing string. This suggests the final conclusion that SAM telemetry can be a low-cost technique for high-data-rate, real-time, half-duplex telemetry.

With the proof-of-concept established, there are two specific recommendations that result from this project. First, take this proven application to industry for commercialization, which has already begun. Second, follow this proven application with risky, proof-of-concept studies in other applications with commercial potential.

Publications

Refereed

Waggoner, J. R. 1997. "A New Technology for High-Data-Rate Borehole Telemetry." Paper to be presented at the Southwestern Petroleum Short Course, Lubbock, TX, 1–3 April.

Extending the Applicability of Cluster-Based Pattern Recognition with Efficient Approximation Techniques

R. F. Martinez, J. W. Bartholomew

Sandia designed this project to develop, implement, and evaluate a set of approximation techniques for their visually empirical region of influence (VERI) pattern-recognition (PR) techniques. We designed the approximations to make our PR technique applicable to problems with very large numbers of training points, test points, and measurements per point. The project emphasized approximations that are especially suited to large problems of programmatic interest, e.g., chemical sensing of complex chemical mixtures, image analysis of Landsat and multispectral thermal imaging (MTI), nonproliferation satellite images, and personnel access-control applications, which can have huge numbers of points representing many classes of interest. This project provides the advantages of VERI PR while maintaining practical computation times in workstation and embedded PC environments.

We developed a new PR algorithm using the VERI shape. The algorithm produces PR results superior to standard commercial algorithms, but the time required to run the algorithm limited its use to small training sets (the classification of all the data points in a training set is known) and small test sets (the classification of data points in a test set is unknown). The runtime of the original algorithm A is proportional to the number of points in the test set (Ntest) times the square of the number of points in the training set (Ntrain2), i.e., A ~ (O(Ntest*Ntrain2)). Our goal in this work was to develop new versions of the algorithm using either exact or approximation techniques to produce the final PR results.

During FY96 we successfully developed and refined divide-and-conquer (D&C) approaches to implementing our PR algorithm in K dimensions. The

training set is partitioned in a preprocessing pass (and can then be used indefinitely) into subsets (hyper-rectangles) of the original set. At most, P_T training points exist in each hyper-rectangle, P_T << Ntrain. The partitioned data allow us to search the training set quickly (O(K*log Ntrain)), i.e., find where in the training set a test point occurs.

The quality of the final classification results and the PR algorithm runtime depend on P_T and the metrics used to classify a test point.

With the D&C approach, we demonstrated that a test set can be reliably classified (< 5% error from exact VERI results) in time proportional to O(P_T*Ntest*K*log Ntrain), a significant reduction in the runtime required to run the original VERI algorithm, thus allowing the PR algorithm to operate on much larger data sets than ever before.

Biocavity Laser Microscopy/ Spectroscopy of Cells

P. L. Gourley, B. E. Hammons, T. M. Brennan, M. E. Warren, W. W. Chow

This project investigates novel methods for characterizing biological cells and particles using vertical-cavity surface-emitting laser (VCSEL) technology developed at Sandia. This biological microcavity laser provides high-contrast light images and lasing spectra that serve to rapidly quantify size and shape of living or fixed cells and particles. The method can be integrated onto a chip and has several critical advantages over conventional flow cytometers. Already, we have shown the technique to be useful for probing the human immune system (size and shape of human lymphoctyes), characterizing genetic disorders (sickled red blood cell size and shape) and sizing of small particles (polystyrene and glass microspheres). The technique has potential for high-speed analysis of cells and deoxyribonucleic (DNA) for biomedical analysis, and particulates, liquids, and gases for environmental monitoring.

Microfabricated sensors will create new opportunities for biomedical research and clinical application. Conventional instrumentation is quite bulky and expensive. Microminiature analytical systems incorporating microfabricated sensors will enhance the speed and efficiency of gathering patient vital signs. Microfabricated laser sensors like the biological microcavity laser offer extremely high-speed operation and accuracy. To this end, we examined high-speed scanning operation of the laser. Using pulse-height spectroscopy developed for nuclear instrumentation, we showed that up to 20,000 cells can be analyzed in one second, limited only by the read-out electronics. The intrinsic limit of the laser is several orders of magnitude higher.

We also demonstrated a new mode of laser operation, employing spontaneous emission spectroscopy. The light emitted from the microcavity below the lasing threshold comprises spectral peaks associated with cell optical modes. With broadband spontaneous emission, we can observe many modes simultaneously to uniquely characterize a given cell type. Using this method we were able to distinguish normal cells from cancerous cells. We developed a spectral method of analysis to create cluster plots to accomplish this identification. Finally, we constructed a compact benchtop version of the analysis system incorporating the microfabricated laser for microscopy and spectroscopy. We recommend that future research focus on the integration of microfluidic flow with intracavity spectroscopy to make an ultra-small analytical system.

Publications

Refereed

Gourley, P. L. 1996. "Semiconductor Microlasers: A New Approach to Cell-Structure Analysis." *Nature Medicine* **2**: 942.

Gourley, P. L., A. E. McDonald, and M. F. Gourley. 1996. "Vertical-Cavity Surface-Emitting Laser Scanning Cytometer for High-Speed Analysis of Cells." *Proc. SPIE Photonics West '96 Conf.* **2679** (Paper No. 24) (San Jose, CA, 19–30 January): 131–141.

Gourley, P. L., and M. F. Gourley. 1996. "A Biological Microcavity Laser." *1996 Technical Digest, Proc. 20th Internat. Quantum Electron. Conf.* (Paper No. WD7) (Sydney, Australia, 14–19 July).

Gourley, P. L., and M. F. Gourley. 1997. "Integration of MEMS and Medicine Will Have Pervasive Impact." *OE Reports* **157** (January): 1, 6–7. SPIE.

Gourley, P. L., K. E. Meissner, M. F. Gourley, and J. Lyo. 1995. "A Radically New Approach to Cell Structure Analysis." *Biophoton. Internat.* **2** (July/August): 48–56.

Gourley, P. L., K. E. Meissner, T. M. Brennan, B. E. Hammons, and A. E. McDonald. 1995. "Biological Microcavity Laser for Rapid Probing of Human Cells." *Technical Digest, CLEO '95* (Paper No. CTHS2) (Baltimore, MD, 21–26 May).

Gourley, P. L., M. F. Gourley, T. Bocklage, and M. Luke. 1996. "A Vertical-Cavity Surface-Emitting Laser Cytometer for Analysis of Cells." *Technical Digest, Proc. Conf. on Lasers and Electro-Optics* (Paper No. CTUH3) (Anaheim, CA, 2–7 June).

Meissner, K. E., P. L. Gourley, T. M. Brennan, B. E. Hammons, and A. E. McDonald. 1996. "Intracavity Spectroscopy in Vertical-Cavity Surface-Emitting Lasers for Micro-Optical-Mechanical Systems." *Appl. Phys. Lett.* **69**: 1517.

Meissner, K. E., P. L. Gourley, T. M. Brennan, B. E. Hammons, and M. F. Gourley. 1996. "Intracavity Surface-Emitting Laser Spectroscopy of Dielectric Spheres." *Quantum Electron. Laser Science Digest, Proc. Quantum Electron. and Laser Science Conf.* (Baltimore, MD, 2–7 June): 141.

Sol-Gel Preservation of Mankind's Cultural Heritage in Objects Constructed of Stone

J. C. Brinker, K. L. Nagy, R. T. Cygan, T. M. Alam, R. A. Assink, C. S. Scotto

This project focused on the development of customized treatments for the preservation of carbonate minerals (limestone and marble) against weathering. Sandia's approach is designed to passivate the rock against further chemical and physical degradation and to consolidate the material to impart strength and arrest subsequent granular disintegration. Current work focused in three areas: (1) molecular modeling of ideal passivating systems and their relative affinities for carbonate surfaces, (2) deposition of synthetic target passivants onto calcite materials and subsequent characterization of calcium leaching behavior under conditions that simulate acid rain, and (3) in situ *polymerization of the passivant and consolidating materials to form a stable network that imparts strength, promotes hydrophobicity, and minimizes further leaching. This report discusses results in areas (1) and (2), and preliminary results in area (3). In addition to the critical need for science-based solutions to the wholesale loss of limestone and marble historic buildings and objets d'art to environmental damage, this work has relevance and potential applications where stabilization of mineral surfaces against chemical degradation is required (e.g., chemical migration in hazardous waste storage areas, groundwater protection).*

An ideal stone preservation scheme must address both chemical and physical modes of deterioration. Effective treatments must (1) passivate the weathered mineral surface against further attack, (2) prevent water adsorption, and (3) strengthen or consolidate the surface. The treatment must also be easy to apply, remain ultraviolet (UV)-stable, and preserve the appearance of the stone. Simple alkoxysilanes protect sandstones (silicate rock) with moderate success, but are ineffective on limestones and marble (carbonate rock). Preservation of these minerals requires both a comprehensive understanding of carbonate surface chemistry and an innovative approach to surface protection. Our protection strategy—customized bifunctional passivating agents that act as calcium-coupling molecules and provide attachment sites for *in situ* polymerization of a subsequent consolidant layer—improves resistance to chemical degradation and imparts mechanical strength to stone objects. This report briefly summarizes our results during FY96.

We ranked four general passivant classes with respect to predicted effectiveness using the following metrics: molecular interaction energy, packing density, step-coverage, and configuration of functionalized "tails." Our hypothesis, that multifunctional organosilane chelates effectively attach to calcite surfaces in predictable orientations, was supported by nanoscale and bulk calcium dissolution experiments. The experimental validation of our model identified key structural elements that we used to improve the design of the passivant/consolidant system. Solid-state nuclear magnetic resonance (NMR) experiments revealed conditions under which a tight chemical network between the passivant and consolidant was achieved. In concert with empirical evidence, modeling studies continue to guide the design and synthesis of coatings tailored to meet the requirements of the preservation community.

We synthesized selected passivant derivatives to test the correlation between modeling and dissolution experiments. We observed a general trend in passivant binding to calcite (104): (silylalkyl)aminocarboxylate salts (Class I) > (silylalkyl)phosphonate salts (Class II) > alkoxysilanes > aminoethylaminopropylsilanes (Class III). The di-anion passivant forms exhibited greater binding energies than either the mono-anion or neutral species. Monte Carlo packing simulations suggested surface coverage of approximately 17.5–21 nm^2 per passivant molecule. Surface coverage followed the trend: Class II > Class I > Class III. Confirming limestone and calcite dissolution experiments measured significant decreases in dissolution rates for treated surfaces. Dissolution of calcite passivated with trialkoxy derivatives (class III) was comparable to that observed with commercial consolidants. As expected, addition of a polymerizable inorganic matrix to the passivated surface further reduced the dissolution.

Publications

Refereed

Alam, T. M., R. A. Assink, and D. A. Loy. 1996. "Hydrolysis and Esterification in Organically Modified Alkoxysilanes: A ^{29}Si NMR Investigation of Methyltrimethoxysilane." *Chem. of Mater.* **8** (January): 2366–2372.

Alam, T. M., R. A. Assink, S. Prabakar, and D. A. Loy. 1996. "Identification and Characterization of the Hydrolysis Products in TMOS and MTMS Monomers Using ^{29}NMR and Polarization Transfer Techniques." *Magnetic Resonance in Chem.* **34** (January): 603–609.

Roa, S. M., C. J. Brinker, and T. J. Ross. 1996. "Environmental Microscopy in Stone Conservation." *Scanning* **18** (7) (October): 508–514.

Other

Alam, T. M., and R. A. Assink. 1997. "Solid-State 13C MAS NMR Investigation of EDTA-Metal Complexes." *Magnetic Resonance in Chem.*, accepted.

Alam, T. M., R. A. Assink, and D. A. Loy. 1996. "Investigation of Hydrolysis and Initial Condensation in Organically Modified Sol-Gel Systems: ^{29}Si NMR and the INEPT Sequence." Paper presented to the Spring Meeting of the Materials Research Society, San Francisco, CA, 8–12 April.

Cygan, R. T., K. L. Nagy, C. S. Scotto, and C. J. Brinker. 1996. "Weathering and Stabilization of Monument Materials." Invited abstract presented to the Annual Meeting of the Geological Society of America, Denver, CO, 28–31 October.

Tailorable, Visible, Room-Temperature Light Emission from Si, Ge, and Si-Ge Nanoclusters

J. P. Wilcoxon, E. B. Stechel, G. A. Samara

Although its outstanding properties are the key to modern microelectronics technology, silicon (Si) has a major drawback as a semiconductor: Its indirect bandgap prevents it from emitting light efficiently. The goal of modifying Si to achieve intense, tailorable, visible light emission at room temperature is one of the most important current challenges in materials science. Realization of this goal, which would have an enormous technological impact, requires a practical synthesis approach and understanding of the physics involved. Size-selected nanoclusters represent the best hope for the foreseeable future, but the tried cluster synthesis techniques are inadequate.

Sandia recently developed and patented a novel synthesis method based on using inverse micelles as reaction vessels to produce useful quantities of size-selected clusters from different classes of materials. We propose to use this method to produce the first size-selected Si and germanium (Ge) nanoclusters, to study and understand the size dependence and mechanisms for their expected intense, tailorable, room-temperature photoluminescence, and to assess their technological potential. A unique feature of our synthesis method is the ability to produce mixed or composite clusters.

We met the following objectives in FY96:

(1) *Demonstrated the ability to synthesize Ge clusters and improved that of Si clusters.* Using our patented inverse micelle synthesis process, we successfully synthesized what we believe to be the highest quality, monodisperse, pure Ge nanoclusters ever produced. We separated the clusters from excess surfactant and reaction products by liquid chromatography.

(2) *Studied and understood the properties of Ge clusters.* We investigated the size-dependent properties of Ge nanoclusters using high-pressure liquid chromatography (HPLC). The chromatography elution time for the clusters provides an estimate of their size. We also used high-resolution transmission-electron microscopy (TEM), TEM, and x-ray diffraction to determine the size and crystal structure. We demonstrated size-dependent luminescence from Ge clusters in solution with room-temperature quantum efficiencies of up to 4%. The Ge solution absorbence features, like those of Si nanoclusters, were found to have distinct structure, showing the discrete, molecule-like nature of their electronic band structure.

(3) *Synthesized and processed Si/Ge composite clusters, and studied and understood their optical properties.* We successfully synthesized two types of Si/Ge composite nanoclusters, one with a Si core and a Ge coat and the other with a Ge core and a Si coat. We found the chemical and optical properties of both types to differ significantly even though both had identical atomic-composition ratios of Si:Ge = 1:1. Both types were successfully purified by HPLC and shown to be quite monodisperse and nanocrystalline by high-resolution TEM (HRTEM).

(4) *Studied methods of processing the Si and Ge nanoclusters to allow them to be dispersed in polymeric or glassy matrices, and studied the optical properties.* We successfully transferred both Si and Ge nanoclusters formed in hydrophobic oil solutions to hydrophilic alcoholic solutions of ethylene glycol and methanol. The former forms glasses and low temperature and will allow incorporation into glass matrices.

(5) *Prepared an assessment of technological implications.* The most significant benefit of this research is the development of a solution-based synthetic/processing procedure that makes available for the first time inexpensive, purified, nanosize Si and Ge powders with reasonable light-emitting quantum efficiencies. The main barrier to commercial application involves integrating these quantum dots into modern circuitry. We expect that the long-term development of a molecular approach to chemically tether the dots to surfaces would allow hole and electron injection that might lead to novel optoelectronic devices.

In Situ Determination of Composition and Strain During MBE Using Electron Beams

E. H. Chason, J. L. Reno, J. A. Floro

Molecular beam epitaxial (MBE) growth of semiconductor heterostructures for advanced electronic and optoelectronic devices requires precise control of the surface composition and strain. The goal of this project is to develop in situ *diagnostics to enhance control of these parameters during MBE growth of semiconductor heterostructures. Sandia can measure strain by using a new optical technique for measuring wafer curvature developed in this project. We can determine surface composition by measuring x-ray fluorescence (XRF) induced by surface electron irradiation during growth. We will develop these techniques for use as real-time monitors of growth quality to improve process control during deposition.*

We made the following accomplishments in FY96:

(1) *Strain relaxation.* We fully implemented and utilized the new multibeam laser curvature technique developed under this project for measuring film stress in real time. The sensitivity and stability of this technique are much higher than could be obtained with electron diffraction, so we abandoned the electron beam-based approach. We obtained a radius of curvature sensitivity of 4 km *in situ*, a factor of 6.5 better than last year. For a 100-Å film, this sensitivity is sufficient to resolve strains of 0.00005, which is 20 times greater than our initial goal of 0.001. This technique enabled us to quantitatively determine, for the first time, the amount of strain relief obtained from morphological instabilities (i.e., surface undulations or islands). We used measurements of stress evolution during growth of SiGe alloys on Si substrates to directly measure the process of surface segregation during deposition with monolayer sensitivity. This is an order-of-magnitude better depth resolution than can be obtained by *ex situ* techniques. We also obtained measurements of strain relaxation kinetics and strained-layer elastic constants. We filed a technical advance on this technique and are preparing a patent application. We are negotiating a technology transfer commercialization agreement with an industrial partner and will sign it when the patent application is completed.

(2) *Surface composition.* We implemented the electron beam-induced XRF technique for measuring surface composition on the EPI reactor. Implementation includes the development of data-acquisition software and ultra–high-vacuum compatible detector hardware. We demonstrated the technique during the chemical vapor deposition (CVD) growth of Fe films on Si substrates, in which we measured clear Fe fluorescence signal. Sensitivity was sufficient to observe Fe growth with monolayer resolution. We will begin initial data collection for the growth of compound semiconductors during the next set of growth runs on the EPI reactor.

(3) *Assessment.* We significantly exceeded our goals in the strain relaxation part of this project by developing a new technique that is 20 times more sensitive and robust than the one originally proposed. This new growth-monitoring capability enabled the determination of phenomena such as morphology-induced relaxation and surface segregation that could not be observed previously. For surface composition, we demonstrated the sensitivity of the new detector and the effectiveness of the acquisition software during Fe CVD growth, and will soon begin measurements on compound semiconductors.

Publications

Refereed

Chason, E., and J. A. Floro. 1996. "Measurement of Stress Evolution During Thin-Film Deposition." Paper presented to the Materials Research Society Spring Meeting, San Francisco, CA, 8–12 April.

Floro, J. A., E. Chason, and S. R. Lee. 1996. "Ge Segregation Profiles Determined by Real-Time Surface Stress Measurements During SiGe Molecular Beam Epitaxy." *Appl. Phys. Lett.* **69** (16 December): 3830. Woodbury, NY: AIP.

Floro, J. A., E. Chason, and S. R. Lee. 1996. "Real-Time Measurements of Epi-Layer Strain Using a Simplified Wafer Curvature Technique." *Proc. Mater. Res. Soc. Fall Mtg.* **406** (Boston, MA, 27 November–1 December): 491–496.

In Situ Optical Flux Monitoring for Precise Control of Thin-Film Deposition

K. P. Killeen, R. L. Dawson, J. F. Klem, W. J. Alford, T. D. Raymond

We developed optical techniques for monitoring atomic-beam fluxes for use in molecular beam epitaxy (MBE) machines used to grow semiconductor devices. We developed laser sources based on near-infrared (NIR) diode lasers and frequency doubling to provide atom-specific light for detection of Al, Ga, and In. We demonstrated atomic absorption to yield atomic fluxes with a precision of a few percent. Laser-induced fluorescence has a larger dynamic range than absorption and should prove useful for detection of low-concentration dopants used in many devices.

MBE is a common technique for producing semiconductor devices. The technique uses atomic beams incident on heated substrates to grow materials such as AlGaAs. *In situ* monitors of beam fluxes are desirable for precise control of growth rate and composition. This year we developed a second laser source based on a commercial diode-laser. With these types of sources becoming more readily available, we see diode-laser–based sources for Group III element detection becoming easier and cheaper to implement. Using frequency-doubled NIR sources, we carried out experiments on the Sandia EPI MBE machine used to grow III–V semiconductor devices. These experiments used a Ti:Sapphire laser instead of the diode-laser sources primarily because of convenience and a desire to demonstrate the utility of optical flux monitoring before switching to diode sources. We demonstrated that atomic absorption can be used to precisely measure Group III (Al, Ga, and In) atomic fluxes by comparing the optically measured flux to that measured with Reflection High-Energy Electron Diffraction (RHEED). Results show we can measure the atomic flux to a precision of a few percent. Laser-induced fluorescence shows promise as a monitor of dopant beam fluxes that are much lower than Group III fluxes. Convenient laser sources for the ultraviolet wavelengths required for dopant detection are not currently available and will require further development. Optical flux monitoring promises to become a useful tool for real-time measurement of atomic fluxes.

Understanding and Control of Energy-Transfer Mechanisms in Optical Ceramic

C. J. Barbour, R. K. Brow, S. K. Lyo, D. M. Follstaedt, J. A. Ruffner, J. A. Knapp, M. B. Sinclair, D. R. Jennison, B. G. Potter

Sandia developed a radically new material strategy for rare-earth (RE) hosts. In this approach, we modified the optical performance of the dopant through atomic-level engineering of its local structural environment in a nanocomposite, optical ceramic host material. To this end, we experimentally manipulated and theoretically modeled the local environment of RE ions in multiphase, multicomponent composites produced in thin-film form. A goal of these efforts is to gain greater understanding of RE/host interactions for improved luminescence efficiency and lifetimes. Controlling the optical activity of dopants in this important new class of photonic materials provides a versatile strategy for manufacturing next-generation optical components where electrical components are inadequate or undesirable, e.g., wireless data communication, or integrable optical amplifier and laser elements. We used both direct optical evaluation of the dopant behavior and theoretical structural modeling and simulation to evaluate these novel host materials. We successfully modeled the local atomic structure in the vicinity of RE dopants using a powerful Sandia-developed computational approach (QUEST) based on local-density functional theory. In Al_2O_3, we used this technique to model the difference in tetrahedral vs. octahedral site symmetry on the density of electronic and vibrational states.

The basic goal of this project is to experimentally manipulate and theoretically model the local environment of RE ions (lanthanides) in multiphase or nanocomposite optical-ceramic host materials to understand and improve the luminescence efficiency and lifetimes of this important class of photonic materials. Our efforts resulted in the deposition of multiphase, multicomponent (nanocomposite) RE-doped Al_2O_3, the optical characterization of these materials, and the modeling of these materials using *ab initio* QUEST calculations and molecular dynamics (MD) simulations.

The first goal was to develop electron-cyclotron-resonance (ECR) plasma deposition and pulsed-laser deposition capabilities to make the samples. We synthesized both amorphous and polycrystalline alumina and RE-doped glassy nanocomposite thin films. We evaluated these materials using photoluminescence (PL) and optical absorption to demonstrate the influence of host microstructure on RE-ion optical performance and thereby validate the multiphase host concept. The PL emission lifetimes of Er (l=1.54 mm) increased from ~ 2.5 ms in g-Al_2O_3:Er to ~ 4.9 ms in $Zn_xTe_yO_z$:Er/alumina composites, indicating a change in the vibrational nature of the local structure and a reduction in nonradiative decay rates. Thus, we successfully modified the symmetry and vibrational energy of the dopant site and significantly influenced the Er optical behavior. Contrary to expectations, the PL spectra from amorphous and large-grain Er-doped g-Al_2O_3 were similar to each other, but different from Er-doped sapphire (a-Al_2O_3). The similarity between the amorphous and crystalline g-phase PL spectra may be a result of Er occupying the different Al sites in the spinel structure (octahedral and tetrahedral sites, with a random distribution of vacancies on these sites), whereas the more distinct features from the sapphire PL spectrum arise from Er occupying only the octahedral sites. *Ab initio* calculations determined the lowest-energy configurations (and density of states) of local atomic sites for an RE-ion in octahedral sites of Al_2O_3. These results showed that a Density Functional Theory-Local Density Approximation (DFT-LDA) treatment reproduces the value of the insulating energy gap (E_{gap}) of sapphire with a discrepancy of only 35% relative to experimental values. For comparison, the discrepancies observed for E_{gap} in similar calculations for Si are ~ 50% or more. In addition, we successfully performed MD simulations through collaborations with the University of Florida. This is the first time that MD simulations have been used to predict the crystal field splitting of the Er^{+3} energy levels in g-Al_2O_3.

Molecular-Scale Lubricants for Micromachine Applications

A. R. Burns, S. L. Miller, R. R. Rye, J. J. Sniegowski, J. P. Wilcoxon, T. A. Michalske

The nature of this work is to develop the physics and chemistry base for designing molecular-scale lubricants for the reduction of friction- and stiction-induced failure in silicon micromachines. We acquire this new knowledge by tailoring the molecular properties of lubricants, applying local probes that can directly monitor the response of lubricants in contact conditions, and evaluating the performance of model lubricants on micromachine test structures specifically designed for friction and stiction studies. Model lubricants under investigation are the silane coupling agents that form self-assembling monolayer (SAM) films on native oxide silicon surfaces. With atomic force microscopy (AFM) and interfacial force microscopy (IFM), we will examine the role of chain length, chemical end group, and chain structures on the frictional and adhesive properties of the SAM films. Since micromachine structures are treated with SAMs under identical conditions, we may simultaneously test the model lubricants for friction/stiction under micromachine operation.

We initiated micromachine lubrication by SAMs. We fabricated micromachine test-beds designed specifically for lubrication studies; they are ready for performance evaluation. Encouraging preliminary tests reveal that SAM-coated micromachines have a coefficient of friction that is one-half that of untreated substrates. We formed a micromachine friction measurement device working group to aid in the design of machines that allow precise characterization of molecular-scale friction. Surface characterization of SAMs yielded significant results concerning packing density of the hydrocarbon chains and new insights in the chemistry of silane coupling to silicon surfaces. Macroscopic friction studies of SAM-covered native silicon surfaces revealed an order-of-magnitude reduction in friction (lateral forces) under various normal force loads. We have completed the scanning near-field optical microscope (SNOM). In addition to the capacitance-balanced normal-force sensor, the instrument has independent shear (lateral)-force sensing, which promises to be sensitive to changes in boundary layer lubrication. We identified candidate guest chromophores and are evaluating procedures for incorporation into SAMs.

Ultra-Hard Multilayer Coatings

T. A. Friedmann, P. B. Mirkarimi, D. L. Medlin, D. M. Follstaedt, J. A. Knapp

We are exploring the production of ceramic multilayer structures that are potentially harder than any natural or artificial material. Diamond and cubic boron nitride (cBN) are the two hardest substances known to man. Numerous proven technologies rely on the superior mechanical properties of these materials. The question arises: Is it possible to manufacture a material that is harder than diamond? In theory, the answer is yes. Experiment indicates that properly grown multilayer coatings of two materials are harder than either of the materials making up the individual layers. The increase in hardness is mainly due to the resistance of dislocation flow across the interfaces between phases of different elasticity. This experimental fact leads to the possibility that a new class of ultra-hard materials—harder than diamond—can be made by growing the appropriate multilayer film.

We propose to establish the state-of-the-art in ultra-hard multilayers by synergistically merging Sandia capabilities. This proposed work is a combination of growth, analysis, and theoretical modeling capabilities at Sandia that could possibly lead to a revolutionary jump in both materials understanding and performance—a material harder than diamond.

Our work in FY96 progressed rapidly. We optimized the adherence and hardness of the single-layer cBN, B4C, TiN, DLC, and CNx materials. Significantly, we developed a new cBN deposition process—ion-assisted sputter deposition—that produces cBN films with vastly improved mechanical properties. These cBN films have a columnar grain structure and high hardness (higher than bulk cBN), are smooth, and adhere well to Si substrates. Also, we grew films of TiN and B4C that are as hard as bulk samples. We grew bilayer samples of B4C/cBN using the new ion-assisted sputter process. These bilayer samples are hard, adhere well to the substrate, and have smooth interfaces. We also grew some large period TiN/cBN multilayers (repeating layers of thick cBN on top of thin TiN) that adhere well to Si. We used finite-element modeling (FEM) techniques to extract yield and elastic stresses from nanoindentation curves of these thin films. We calculated the stress/strain field due to a dislocation in a multilayer film coating. This calculation shows that the multilayer structure does not screen significantly the interdislocation interactions, indicating that these interactions cannot be neglected in any realistic model of plastic flow. These calculations will form the basis for an extended theory of dislocation interactions in multilayer structures.

Publications

Refereed

Cardinale, G. F., D. L. Medlin, P. B. Mirkarimi, K. F. McCarty, and D. G. Howitt. 1996. "Orientation-Dependence of Elastic Strain Energy in Hexagonal and Cubic Boron Nitride Layers in Energetically Deposited BN Films." *J. Vac. Sci. Technol.–Rapid Commun.*, accepted. Minneapolis, MN: American Vacuum Society.

McCarty, K. F., D. L. Medlin, P. B. Mirkarimi, and G. F. Cardinale. 1996. "How Nucleation and Growth Mechanisms Control Microstructural Evolution in Cubic Boron Nitride Films." *Proc. Mater. Res. Soc. Mtg.* (Boston, MA, 2–6 December).

McCarty, K. F., P. B. Mirkarimi, D. L. Medlin, D. L. Medlin, T. A. Friedmann, and J. C. Barbour. 1996. "On the Low-Temperature Threshold for Cubic Boron Nitride Formation in Energetic Film Deposition." *Diamond and Related Materials,* accepted. New York, NY: Elsevier Science, Inc.

Medlin, D. L., K. F. McCarty, P. B. Mirkarimi, and G. F. Cardinale. 1996. "Microstructural Development in Cubic Boron Nitride Films." *Proc. Amer. Vac. Soc. Mtg.* (Invited) (Philadelphia, PA, 14–18 October).

Mirkarimi, P. B., K. F. McCarty, D. L. Medlin, N. R. Moody, and D. C. Dibble. 1996. "Synthesis and Mechanical Characterization of Very Hard Cubic BN-Based Films Deposited by Ion-Assisted Sputtering," *Proc. Mater. Res. Soc. Mtg.* (Boston, MA, 2–6 December).

Missert, N. A., T. A. Friedmann, P. P. Newcomer, P. B. Mirkarimi, K. F. McCarty, and D. L. Medlin. 1996. "X-Ray Reflectivity Studies of the Density and Thickness of BN Thin Films." *Proc. Mater. Res. Soc. Mtg.* (Boston, MA, 2–6 December).

Sullivan, J. P., T. A. Friedmann, D. R. Tallant, L. J. Martinez-Miranda, J. Mikkalson, D. J. Rieger, and A. G. Baca. 1996. "Stress Relief in Pulsed-Laser–Deposited Amorphous Tetrahedrally Bonded Diamond-Like Carbon Films." *Appl. Phys. Lett.*, accepted. Woodbury, NY: American Institute of Physics.

Smart Interface Bonding Alloys (SIBA): Tailoring Thin-Film Mechanical Properties

R. Q. Hwang, S. J. Plimpton, N. D. Shinn, N. R. Moody, J. C. Hamilton

Sandia is exploring the use of the newly discovered strain-stabilized 2-D interfacial alloys as smart interface bonding alloys (SIBA). These materials will be used as templates for the heteroepitaxial growth of metallic thin films. SIBA are formed by two metallic components mixing at an interface to relieve strain and prevent dislocations from forming in thin-film growth. The composition of the SIBA is determined locally by the amount of strain and can react "smartly" to areas of the highest strain to relieve dislocations. In this way, SIBA can be used to tailor the structure of thin films.

This project will include growth, characterization, and modeling of films grown using SIBA templates. Characterization will include atomic imaging of the dislocations structure, measurement of the mechanical properties of the film using interfacial force microscopy (IFM), and the nanoindenter. We will use the Paragon parallel processing computer to calculate the structure of the SIBA in order to develop predictive ability of thin-film behavior.

This work will lead to the development of a new class of thin-film materials with SIBA serving as a buffer layer. Such films will have improved mechanical and corrosion resistance, allowing application as protective barriers for weapons applications.

We accomplished the following in the previous year:

(1) Predicted phase diagram for SIBA as a function of composition.

(2) Measured phase diagram for SIBA as a function of composition using scanning-tunneling microscopy (STM).

(3) Developed code to model indentation process. We predicted force vs. displacement curves for indentation of gold and ran simulation for 196,000-atom slab using a workstation.

(4) Measured indentation force vs. displacement curves for Au(111).

(5) Began porting indentation code to Paragon computer.

We made minor changes in direction that slightly altered the milestones for this proposal, largely due to our dramatic success in modeling ambient indentation of films with thiol buffer layers. We presented this modeling at an invited talk at the MRS Spring Meeting and to DOE Office of Basic Energy Sciences (OBES) as part of a successful new-initiative proposal. It also helped to guide program development in the general area of combining continuum and atomistic modeling of materials, two areas in which Sandia excels, but which neither Sandia nor any other laboratory has combined successfully. Thus the research performed to date in this project helped clarify needs and methods for bridging length scales in the computer modeling of materials. To align the experimental and the modeling work as closely as possible and to allow model verification, we made the following minor changes:

(1) Since modeling of 196,000-atom slabs was successful on a fast workstation, we delayed porting indentation code to the Paragon.

(2) Since modeling of ambient indentation with thiol buffer layers was highly successful, we emphasized such indentation experiments in the experimental part of the project. Because modeling of vacuum experiments indicates that bonding of tip to surface will be a major factor, we deferred some of the vacuum indentation work in favor of the thiol-buffered experiments, which allows us to concentrate on nonmechanical properties of SIBA films themselves instead of tip-sample interactions.

We were highly successful in measuring and modeling the initial stages of indentation. The understanding gained will be of tremendous value in the understanding and interpretation of nanoindenter studies of film hardness and cracking resistance. The knowledge gained in modeling these systems also guided project development in the area of combining continuum and atomistic calculations, an important goal for the Sandia Accelerated Strategic Computing Initiative (ASCI) program.

Scanning Probe-Based Processes for Nanometer-Scale Device Fabrication

T. M. Mayer, M. E. Sherwin, A. J. Howard, J. A. Simmons, B. S. Swartzentruber, D. G. Adams

Nanometer-scale electronic device technology requires a novel physics base that includes fabrication processes, characterization techniques, and materials properties allowing reliable performance of devices at this very small-length scale. Our object is to achieve an order-of-magnitude decrease in feature size compared to conventional fabrication technology. We will explore approaches to nanostructure fabrication using scanning probe-based (scanning-tunneling microscopy [STM], atomic-force microscopy [AFM]) processes. We will emphasize limits to performance and fabrication and characterization of electronic effects in nanostructures. For prototype device structures, we will integrate critical nanoscale components with conventional test structures to allow full electrical accessibility. We will explore two approaches to nanostructure fabrication. First, we will investigate molecular layer resists based on simple adsorbed atoms and molecules that can be patterned by electron-induced desorption or reaction. Second, we will develop a more general AFM-based nanolithographic capability, based on anodic oxidation under an AFM tip. In parallel with these fabrication approaches, we will perform low-temperature electrical measurements, and fabricate and characterize selected nanoelectronic devices.

We demonstrated and systematically characterized < 10-nm lithography on Si(001) substrates by STM-based desorption of adsorbed H atoms. We used these nano-patterned surfaces as templates for selective growth of metal (Fe) wires. We investigated limits to lithographic performance using the STM by field-emission simulations. We showed that routine < 10-nm lithography is feasible using low-energy electron exposure, thin atomic or molecular layer resists, and standard STM tips. We completed designs for nano-wire device fabrication and anticipate initial fabrication and measurement runs. We completed design and procurement of a new STM facility for nanostructure fabrication.

Publications

Refereed

Adams, D. P., T. M. Mayer, and B. S. Swartzentruber. 1996. "Nanometer-Scale Lithography on Si(001) Using H as an Atomic Layer Resist." *Proc. 40th Internat. Conf. on Electron., Ion, Photon Beam Technol.* **14** (Atlanta, GA, 1 June): 1642–1649. AVS.

Adams, D. P., T. M. Mayer, and B. S. Swartzentruber. 1996. "Selective Area Growth of Metal Nanostructures." *Proc. of the AVS Natl. Symp.* **68** (Woodbury, NY, 18 October): 2210–2212. Woodbury, NY: American Institute of Physics.

Mayer, T. M., D. P. Adams, and B. M. Marder. 1996. "Field-Emission Characteristics of the Scanning-Tunneling Microscope for Nanolithography." *Proc. 40th Internat. Conf. on Electron., Ion, Photon Beam Technol.* **14** (Atlanta, GA, 31 May): 2438. AVS.

Wide-Bandgap Compound Semiconductors to Enable Novel Semiconductor Devices

M. H. Crawford, R. J. Shul, S. R. Lee, E. D. Jones, E. J. Heller, W. W. Chow

Sandia proposed an interdisciplinary investigation into the growth and physical properties of wide-bandgap compound semiconductors for the purpose of enabling both optoelectronic and microelectronic device development. The AlGaInN material system is widely considered to be essential to the development of a wide array of ultraviolet (UV) and blue optical devices as well as high-temperature microelectronics. A critical limiting factor in the demonstration of advanced III–N–based devices is the lack of an in-depth understanding of the physics and chemistry that govern the unique properties of these materials.

Two major milestones for the first year of this project involved theoretical investigations of the properties of the III–N materials. We determined the following approach at the beginning of the project to calculate the optical properties of the III–N materials. First, we applied a first-principles bandstructure calculation to arrive at a consistent set of bulk material parameters. We could then use this parameter set as input in a Luttinger Hamiltonian calculation for the strained or unstrained quantum-well bandstructure and optical transition matrix elements. We would then feed the results of this calculation into a microscopic laser theory for computing gain spectra. During the first year, we developed the tools necessary for implementing the above approach. We completed bulk bandstructure calculations for the GaN, AlN, InN, and ternary materials. Included in these results was a determination of the bowing parameters for the ternary materials that enables the calculation of the material bandgaps over the entire composition range. As the current heterostructure designs used in III–N LEDs use InGaN and AlGaN alloys, these bowing parameters are very relevant.

Another milestone was to evaluate the effects of post-growth annealing on the optical and electrical properties of the III–N materials. Post-growth annealing is

used to enhance the acceptor activation and significantly improve the conductivity of the doped materials. We therefore performed rapid thermal annealing (RTA) experiments on metalorganic vapor phase epitaxial (MOVPE)-grown GaN films in a variety of gas ambients and evaluated the effect on photoluminescence (PL), surface morphology, and electrical conductivity. We found that RTA annealing of GaN in either Argon (Ar) or nitrogen (N_2) ambient up to 1100°C improves both surface morphology and PL intensity. In addition, the ratio of deep-level emission to band-edge emission is improved for both cases.

We also proposed the study of ion implantation of III–N materials for the first year. One of the major impediments in developing III–N materials for photonic device applications is the difficulty in achieving *p*-type doping. We explored the ion implantation of Ca and Ca + P species to achieve *p*-type conductivity in GaN bulk films. Our experiments revealed that *p*-type conduction was possible by implanting these species and performing a post-implant anneal at temperatures of 1100°C or greater.

Publications

Refereed

Chow, W. W., A. F. Wright, and J. S. Nelson. 1996. "Theoretical Study of Room-Temperature Optical Gain in GaN Strained Quantum Wells." *Appl. Phys. Lett.* **68** (January): 296–299. Woodbury, NY: American Institute of Physics.

Vartuli, C. B., S. J. Pearton, C. R. Abernathy, R. J. Shul, A. J. Howard, S. P. Kilcoyne, J. E. Parmeter, and M. H. Crawford. 1996. "High-Density Plasma Etching of III–V Nitrides." *J. Vac. Sci. Technol.* **A14** (May/June): 1011–1014. Woodbury, NY: American Institute of Physics.

Zolper, J. C., M. H. Crawford, A. J. Howard, J. Ramer, and S. D. Hersee. 1996. "Morphology and Photoluminescence Improvements from High-Temperature Rapid Thermal Annealing of GaN." *Appl. Phys. Lett.* **68** (January): 200–202. Woodbury, NY: American Institute of Physics.

Recognizing Atoms in Atomically Engineered Nanostructures: An Interdisciplinary Approach

A. M. Bouchard, G. C. Osbourn, R. M. Biefeld, M. P. Sears, D. R. Jennison

Scanning-tunneling microscopy (STM) is a powerful tool for both characterizing and manipulating the atomic topographies of surfaces. For chemically uniform model systems, e.g., clean Si surfaces, STM can provide considerable scientific insights. However, STM has typically been unable to provide unambiguous chemical recognition of atomic sites in many technologically relevant but chemically heterogeneous systems. We will develop the theoretical and experimental underpinnings to address the key difficulties with the goal of enabling unambiguous, computer-based identification of atomic sites in multivariate STM imagery, focusing on heterogeneous III–V semiconductor materials and atomically engineered nanostructures.

The project will have several subtasks: (1) We will seek to develop the first "data base" of multivariate STM spectral features (i.e., the analogue of satellite "ground truth" spectra); (2) we will study the effects of different tip states on the STM spectral features and attempt to establish procedures for computationally removing or minimizing variable-tip effects; and (3) we will use pattern recognition (PR) of STM spectral imagery, based on the results of (1) and (2) tasks, to map out the atomic-scale chemical structure of selected cleaved (110) III–V surfaces. We will specifically attempt to understand the alloy ordering and interfacial structure of III–V structures of current programmatic interest for infrared (IR) device applications.

This project is on track, with all expected milestones accomplished and with some progress ahead of schedule. We optimized a III–V sample set design across team requirements. The team established a set of alloy, quantum-well, and superlattice designs in the low-bandgap III–Vs, primarily using InGaAs and InAsSb alloys. We grew the series of samples, InAsSb/InAs multiple quantum wells (MQWs) and InAsSb/InGaAs strained-layer superlattices (SLSs), for evaluation by STM. We adapted pseudopotential codes and QUEST code to treat simulated STM imagery and STM tips, respectively. The QUEST code has had several important modifications to enable the tip calculations, which will set records for transition-metal cluster size. First, the cluster sizes (~ 150–200 transition-metal atoms) would have produced prohibitive amounts of memory requirements for wavefunction storage. A new version of QUEST computes the wavefunctions as needed and does not store them, allowing calculations on fewer nodes. Secondly, the QUEST post-processing code now permits local density of states calculations, essential for the tip studies as input to tunneling current calculations. Third, we constructed tip models, and tests are under way concerning how many atom layers are necessary to obtain proper geometric relaxation at the tip end. We extended the visually empirical region of influence (VERI) bootstrap algorithm for automated use with k-d imagery, and performed analysis of existing Pb-on-Ge dual-bias STM imagery. First parallel computation results on simulated STM imagery and tips are in progress. In addition to the original project plan, we have also begun training to operate our STM to produce multispectral STM images in-house for this project.

Photonic Bandgap Structures as a Gateway to Nano-Photonics

S. Y. Lin, J. F. Klem, B. E. Hammons, J. R. Wendt, G. A. Vawter, V. M. Hietala, E. D. Jones, S. K. Lyo, P. L. Gourley

The goal of this project is to explore the fundamental physics of a new class of photonic materials, photonic bandgap structures (PBG), and to exploit its unique properties for the design and implementation of photonic devices on a nanometer-length scale for the control and confinement of light. The low-loss, highly reflective, and quantum interference nature of a PBG material makes it one of the most promising candidates for realizing an extremely high-Q resonant cavity, > 100,000, for optoelectronic applications and for the exploration of novel photonic physics, such as photonic localization, tunneling, and modification of spontaneous emission rate. Moreover, the photonic bandgap concept affords us with a new opportunity to design and tailor photonic properties in very much the same way we manipulate, or bandgap engineer, electronic properties through modern epitaxy.

We successfully realized several high-performance PBG devices in the millimeter (mm)-wave regime. Among them, the PBG-resonant cavity we constructed has a cavity-Q value of ~ 23,000, the highest reported so far for all two- and three-dimensional PBG structures. We also realized the PBG prism that we proposed. We show that a well-designed PBG prism has many unprecedented unique features that make it ideally suited for system applications such as miniature spectrometer for sensing applications and wavelength division multiplexing for telecommunications. These features are high sensitiveness, ultra compactness, broad bandwidth, and ease of planar integration.

We also established a solid foundation for implementing PBG devices, such as PBG cavities, PBG light-emitting diodes (LEDs), and PBG lasers, in the optical spectral regime. In the case of PBG LED, we optimized our broadband LED sample design and achieved a record-breaking LED spectral bandwidth of ~ 750 nm, from 1150–1900 nm. Such a high-quality LED would enable us to probe a broad range of PBG devices. In our nanofabrication effort, we not only continued taking advantage of Sandia's unique electron-beam/reactive ion-beam etching capability, but also invented a new technique, called *additive lithography*, for sample fabrication. We have filed a U.S. patent on this invention.

Publications

Refereed

Lin, S. Y., H. P. Wei, D. C. Tsui, and J. F. Klem. 1995. "Cyclotron Resonance of 2-D Holes in Strained-Layer GaAs/InGaAs/GaAs Quantum-Well Structures." *Appl. Phys. Lett.* **67** (9 October): 2170–2172. New York, NY: American Institute of Physics.

Lin, S. Y., V. M. Hietala, S. K. Lyo, and A. Zaslavsky. 1996. "Photonic Bandgap Quantum-Well and Quantum Box Structures: A High-Q Resonant Cavity." *Appl. Phys. Lett.* **68** (3 June): 3233–3235. New York, NY: American Institute of Physics.

Lin, S. Y., V. M. Hietala, S. K. Lyo, H. W. P. Koops, P. R. Villeneuve, and J. D. Joannopoulos. 1996. "High-Q Photonic Bandgap Resonant Cavities: From mm-Wave to Optical Regime." *Proc. SPIE Phys. and Simulation of Optoelectron. Devices IV* **2693** (Bellingham, WA, 29 January–2 February): 170–175.

Artificial Atoms

J. A. Simmons, M. E. Sherwin, J. F. Klem, S. K. Lyo

This project involves the fabrication and study of novel semiconductor nanostructures sufficiently small that the electronic energy states are confined in all three dimensions and are thus zero-dimensional. They contain only a handful of electrons and are therefore similar to individual atoms, but artificially made. With sensitive measuring techniques at millikelvin temperatures, the individual electrons can be observed and controlled. We are investigating two types of artificial atoms (AAs): (1) capacitive AAs, quantum dots linked to an electron reservoir by tunnel barriers, and (2) resonant tunneling AAs, quantum antidots around which electrons are magnetically bound. Because at high magnetic fields 2-D electrons must travel in 1-D "edge states" along the boundary of the sample, we are also investigating edge states to determine if they can exhibit self-interference when sufficiently small. This report describes progress made in (1) growing ultra–high-purity GaAs material for AAs, (2) developing low-noise cryogenic measurement circuitry using an in situ *high electron mobility transistor (HEMT), itself at temperatures below 1 K, (3) capacitive measurements of edge states in high magnetic fields, (4) fabrication of gate-defined submicron capacitive AAs fractional quantum Hall effect (FQHE) materials, and (5) measurements of electron focusing around large arrays of antidots in the FQHE regime.*

The project goal is deeper understanding of the basic science of electrons in confined nanostructures, especially at high magnetic fields. The project direction changed somewhat because of a change in personnel, which allowed us to place more emphasis on capacitive techniques, focusing especially on the capacitive detection of edge states in the fractional quantum Hall regime. During FY96 we met the following milestones:

(1) We achieved new Sandia records for ultra–high-purity GaAs material growth, achieving mobilities of 3.6×10^6 cm^2/Vs at densities sufficiently low that the FQHE regime can be reached.

(2) We developed two sensitive measurement circuits for detecting capacitance. The technique uses an *in situ* HEMT located within the cryostat and kept at a temperature of less than 1 K. Because the transistor is cold, it not only acts as a capacitance buffer, but also has exceptionally low noise. We were able to measure capacitance to a resolution of 30 attofarads.

(3) In perhaps our most significant result, we demonstrated by capacitive measurements that edge-state transport breaks down not only at low magnetic fields, as expected, but also for special values of high magnetic fields where each electron is associated with an even number of magnetic flux quanta. At these special values of magnetic field, new particles form called *composite fermions*, which behave like electrons at zero magnetic field. The ability to measure the breakdown is expected to provide

important information on the properties of composite fermions, currently an exciting research topic at the forefront of basic condensed-matter physics.

(4) We also fabricated submicron capacitive AAs using suspended airbridge gates with submicron posts descending from them.

(5) Large arrays of etched quantum antidots exhibited focusing phenomenon both for electrons near zero magnetic field and for composite fermions near special values of magnetic field (even number of flux quanta for each electron). These data, once analysis is complete, should also provide important information on the properties of composite fermions.

Publications

Refereed

Simmons, J. A., M. E. Sherwin, M. V. Weckwerth, N. E. Harff, T. M. Eiles, W. E. Baca, H. Hou, and B. E. Hammons. 1996. "Advanced Fabrication Technologies for Nano-Electronics." *Proc. State-of-the-Art Program on Compound Semiconductors XXIV* **96-2** (Pennington, NJ, 5–10 May): 186–202. Electromechanical Society, Inc.

Simmons, J. A., R. R. Du, M. A. Zudov, H. C. Chui, N. E. Harff, and B. E. Hammons. 1996. "Composite Fermions in 2 x 10^6 cm^2/Vs Mobility AlGaAs/GaAs Heterostructures Grown by MOCVD." *Proc. 23rd Internat. Conf. on the Phys. of Semiconductors* **3** (Berlin, Germany, 21–26 July): 2511–2514. Singapore: World Scientific.

Other

Simmons, J. A., H. C. Chui, N. E. Harff, B. E. Hammons, H. Q. Hou, R. R. Du, and M. A. Zudov. 1996. "MOCVD Growth of GaAs/AlGaAs Heterostructures for Fractional Quantum Hall Effect Studies." *Proc. March Mtg. Amer. Phys. Soc.* **41** (Woodbury, NY, 18–22 March): 77. Woodbury, NY: AIP.

Zudov, M. A., R. R. Du, J. A. Simmons, and H. C. Chui. 1996. "Electron and Composite Fermion Transport in MOCVD-Grown GaAs/AlGaAs Heterostructures." *Proc. March Mtg. Amer. Phys. Soc.* **41** (Woodbury, NY, 18–22 March): 77. Woodbury, NY: AIP.

Modeling and Characterization of Molecular Structures in Self-Assembled and Langmuir-Blodgett Films

J. Cesarano

This project is a collaboration between Sandia and Los Alamos National Laboratory (LANL) to extend characterization techniques and molecular modeling capabilities for self-assembled (SA) and Langmuir-Blodgett (LB) 2-D thin films, with the objective of improving our control of the fabrication of these structures for specific applications, including chemical sensors and templates for growth of other materials. Achieving this requires understanding both the structure throughout the thickness of the films and the in-plane lattice of the amphiphilic molecules. To help meet these objectives we are exploring the use of atomic force microscopy (AFM) and x-ray reflectivity characterization, and molecular modeling of SA and LB films.

SA thin films and LB thin films are emerging technologies for the development of chemical and biochemical sensors, electrooptic films, second harmonic generators (frequency doublers), templates for biomimetic growth, etc. However, the growth of these technologies is dependent on the development of our understanding and control of the molecular arrangement of these films. We started an informal collaboration with LANL to extend characterization techniques and molecular modeling capabilities for these complex 2-D structures.

Work this past year was successful in coupling the techniques of scanning-force microscopy (SFM), x-ray reflectivity, ellipsometry, and Biosym molecular modeling to characterize and understand the structure of SA and LB films, both in-plane and out-of-plane. We fabricated and characterized traditional and nontraditional films, including SA films on lead-zirconate-titanate (PZT) substrates. This has never before been demonstrated and may have utility for electronic memory devices. We demonstrated SFM as a convenient tool to measure the molecular in-plane lattice parameters of simple fatty acids and nontraditional LB films of octadeclytrimethoxysilane (OTMS). We developed an x-ray reflectivity capability and used it for the characterization and modeling of out-of-plane structures for SA and LB films up to 10 layers thick (approximately 250 Å). Molecular modeling provided a predictive capability for the structures for these largely 2-D films.

In summary, we demonstrated modeling and in-plane and out-of-plane characterization for fatty acids and proved them useful for the understanding of biomimetic growth of materials using LB film templates. Similarly, we modeled and characterized nontraditional LB films of OTMS and found that they show promise for use in chemical sensors and/or membranes. We believe this set of tools and methodology concerning the fabrication, characterization, and modeling of SA and LB films will be useful for the development and incorporation of SA and LB films into devices and for the development of future unforeseen applications. We were successful in that the necessary techniques and capabilities are developed and are now being utilized for the further development of thin-film structures at Sandia.

Publications

Refereed

Vaidya, R., R. J. Simonson, J. Cesarano, D. Dimos, and G. P. Lopez. 1996. "Formation and Stability of Self-Assembled Monolayers on Thin Films of Lead Zirconate Titanate (PZT)." *Langmuir* **12** (November): 2830–2836. Columbus, OH: American Chemical Society.

Novel Laser-Based Diagnostics Capability for Chemical Science

D. W. Chandler, P. H. Paul, R. L. Farrow

We are developing high-intensity laser sources with picosecond times resolution in order to perform laser-based diagnostics for both chemical dynamics studies and combustion. In particular, we are building tunable ultraviolet (UV) laser sources with approximately 100-picosecond time resolution, and exploring various schemes for generating the tunable light. The first application of this light was the detection of CO molecules using several ionization schemes. We generated several different wavelengths of light, which corresponded with different ionization pathways in the CO molecule, and used them for detection.

In an effort to increase the sensitivity of resonantly enhanced multiphotonic ionization (REMPI) for product detection in photodissociation experiments, we investigated several techniques for generating short laser pulses in the UV region of the spectrum with high intensity that still maintain the narrow bandwidth (< 0.5 cm^{-1}) necessary for state selection of gas-phase products. We generated 100-picosecond laser pulses at two different wavelengths to probe state-selective REMPI of CO molecules on three different transitions. The first method employed the ~ 5-ns output of a Nd:YAG (yttrium aluminum garnet)-pumped dye laser system operating at 650 nm. The dye laser output was pulse-amplified in a dye cell with the 532-nm output from a 100-ps regeneratively amplified Nd:YAG laser. This pulse of 650-nm light was then summed with the 355 nm from the YAG regenerative amplified system to generate tunable 230-nm light. By changing the wavelength of the dye laser, we also used this same scheme to generate light between 215 and 218 nm. A second method involved using low-intensity tunable output from a nanosecond pulse-length dye laser to seed a single-pass optical parametric amplifier (OPA), which was pumped by the 355-nm, 100-ps output of the YAG regenerative amplified laser. We then further amplified these pulses in a dye cell pumped by the residual 355-nm light from the OPA stage and doubled them in a nonlinear crystal to generate the necessary UV light. We used this light to probe CO through three different 2+1 REMPI transitions at 215.2 nm, 217.5 nm, and 230 nm. Ionization through the E state (215.2 nm) and C state (217.5) had detection limits of 3x106 and 6x105 molecules/quantum state/cm^3, respectively, while ionization through the B electronic state at 230 nm had a detection limit of 2x105 molecules/quantum state/cm^3.

We made progress in adapting an existing synchronously pumped tunable laser to generate high-intensity UV pulses. We measured the spectrum and time profile of the synch-pumped pulses using an optical multichannel analyzer and high-speed detector. Under normal operation we found the spectrum to be too broad for most applications in pump/probe energy transfer (10 cm^{-1} fwhm). However, we found an unusual but stable operating mode that results in a 2.5 cm^{-1} bandwidth and 40–50-ps pulsewidth. These pulses should suffice for numerous experiments, so we are proceeding with the next step of implementing the dye amplifiers. We are currently comparing amplification geometries by investigating gain vs. amplified stimulated emission. After we implement the amplification stages, we will be able to perform preliminary investigations of energy transfer using two-color, four-wave mixing and picosecond laser pulses.

Antipodal Focusing of Shock Energy from Large Asteroid Impacts on Earth

M. B. Boslough

We continued to study the consequences of asteroid impacts on the Earth. We developed methods to simulate and validate models for atmospheric entry and terminal explosion physics. In the current year we (1) further developed a validated atmospheric entry model using Shoemaker–Levy 9 impact observations, (2) applied the new model to Earth impact simulations and analyzed impact threat to Earth assets, focusing on satellites in low-Earth orbit, (3) performed 2-D and 3-D simulations of the 1908 Tunguska explosion in Siberia, providing new insight for understanding that event, (4) developed better quantitative constraints for risk assessment, (5) modified shock physics codes for these applications, (6) simulated interacting plume collapse as a mechanism for formation of enigmatic natural glass in S.E. Asia and Egypt, (7) wrote proposals and white papers to build on our results, (8) organized a scientific conference and edited a proceedings volume, and (9) wrote and presented numerous abstracts, and published papers.

We took advantage of our newly developed and validated atmospheric entry models and methods by applying them to asteroid impacts on Earth. We continued to advance the entry modeling capability by generating synthetic light-emission curves and comparing them to the data from the 1994 Shoemaker–Levy 9 collision. We focused this year's efforts on plume-forming impacts on Earth, and assessed the risk associated with these impacts.

Previous years' conclusions were that (1) impact-generated seismic energy is strongest at the antipode within the asthenosphere, and (2) satellites in low-Earth orbit may be vulnerable to impact-generated plumes. This year's main conclusions are that (1) the fragments of comet Shoemaker–Levy 9 were at least two orders of magnitude less massive (and energetic) than we originally believed, and (2) the Tunguska explosion in Siberia may have been much less energetic than is generally believed. Taken together, these conclusions imply that the consequences of a given impact are much greater than previously acknowledged, and that risk assessment should be revisited.

We recommend that a formal, independent assessment of the impact threat to Earth assets be undertaken. Such a program would combine experiments, observations, theory, and computational modeling to perform cost/benefit analysis of detection and mitigation schemes.

Publications

Refereed

Boslough, M. B., and D. A. Crawford. 1995. "Impact-Generated Atmospheric Plumes: Observations on Jupiter and Implications for Earth." *Shock Compression of Condensed Matter–1995,*

Proc. Amer. Physical Soc. Topical Conf. on Shock Compression of Condensed Matter (Seattle, WA, 13–18 August): 1187–1190. Edited by S. C. Schmidt, *et al.* Amsterdam, Netherlands: North-Holland.

Boslough, M. B., and D. A. Crawford. 1996. "Impact-Generated Atmospheric Plumes: The Threat to Satellites in Low-Earth Orbit." *Proc. Space '96, the 5th Internat. Conf. and Expo. on Eng., Constr., and Operations in Space* (Albuquerque, NM, 1–6 June).

Boslough, M. B., and D. A. Crawford. 1995. "The Shoemaker–Levy 9 Impact Plumes on Jupiter: Implications for Threat to Satellites in Low-Earth Orbit." Paper presented to the Planetary Defense Workshop, Livermore, CA, 22–26 May.

Boslough, M. B., D. A. Crawford, A. C. Robinson, and T. G. Trucano. 1994. "Mass and Penetration Depth of Shoemaker–Levy 9 Fragments from Time-Resolved Photometry." *Geophys. Res. Lett.* **21**: 1555–1558.

Boslough, M. B., D. A. Crawford, A. C. Robinson, and T. G. Trucano. 1994. "Watching for Fireballs on Jupiter." *EOS—Transactions of the American Geophysical Union* **75**: 305–310.

Boslough, M. B., D. A. Crawford, T. G. Trucano, and A. C. Robinson. 1995. "Numerical Modeling of Shoemaker–Levy 9 Impacts as a Framework for Interpreting Observations." *Geophys. Res. Lett.* **22**: 1821–1824.

Boslough, M. B., E. P. Chael, T. G. Trucano, and D. A. Crawford. 1995. "Axial Focusing of Energy from a Hypervelocity Impact on Earth." *Inter. J. Impact Engineering* **17**: 99–108.

Boslough, M. B., E. P. Chael, T. G. Trucano, D. A. Crawford, and D. L. Campbell. 1995. "Axial Focusing of Impact Energy in the Earth's Interior: A Possible Link to Flood Basalts and Hotspots." *Proc. Conf. on New Developments Regarding the KT Event and Other Catastrophes in Earth History* (Houston, TX, 29 January–1 February): 511–550. Edited by G. Ryder. Geological Society of America.

Crawford, D. A. 1996. "Models of Fragment Penetration and Fireball Evolution." *The Collision of Comet Shoemaker–Levy 9 and Jupiter* **9** (Space Telescope Science Institute Symposium Series): 133–156. Edited by K. S. Noll, H. A. Weaver, and P. D. Feldman.

Crawford, D. A., and M. B. Boslough. 1996. "A Model of Meteoroid Atmospheric Entry with Implications for the NEO Hazard and the Impact of Comet Shoemaker–Levy 9." *Proc. Space '96, the 5th Internat. Conf. and Expo. on Eng., Constr., and Operations in Space* (Albuquerque, NM, 1–6 June).

Crawford, D. A., M. B. Boslough, T. G. Trucano, and A. C. Robinson. 1994. "The Impact of Comet Shoemaker–Levy 9 on Jupiter." *Shock Waves* **4**: 47–50.

Crawford, D. A., M. B. Boslough, T. G. Trucano, and A. C. Robinson. 1995. "The Impact of Periodic Comet Shoemaker–Levy 9 on Jupiter." *Inter. J. Impact Engineering* **17**: 253–262.

Other

Boslough, M. B. 1996. "Atmospheric Impact Plumes and the Threat to Satellites in Low-Earth Orbit." Paper presented to SPIE's International Symposium on Optical Science, Engineering, and Instrumentation, Denver, CO, 4–9 August.

Boslough, M. B. 1996. "Atmospheric Plumes from Tunguska-Scale Impacts and the Threat to Satellites in Low-Earth Orbit." Paper presented to the International Workshop Tunguska '96, Bologna, Italy, 14–17 July.

Boslough, M. B., and D. A. Crawford. 1996. "Ballistic Model for Plume Collapse and a Possible Means of Independently Constraining Fragment Size." Paper presented to the International Conference on the SL9–Jupiter Collision, Paris, France, 3–5 July.

Boslough, M. B., and D. A. Crawford. 1996. "Collapse of Interacting Atmospheric Plumes from Bolide Swarms: Evidence in the Geologic Record?" Paper presented to Silica '96: Meeting on Silica Glass and Related Desert Events, Bologna, Italy, 18 July.

Boslough, M. B., and D. A. Crawford. 1996. "Impact-Generated Atmospheric Plumes: The Threat to Satellites in Low-Earth Orbit." Paper presented to the 5th International Conference and Exposition on Engineering, Construction, and Operations in Space, Albuquerque, NM, 1–6 June.

Boslough, M. B., and D. A. Crawford. 1996. "Interacting Atmospheric Plumes from Bolide Swarms." Paper presented to the 27th Lunar and Planetary Science Conference, Houston, TX, 18–22 March.

Crawford, D. A. 1996. "An Analytical Model of Meteoroid Entry into Planetary Atmospheres." Paper presented to the 27th Lunar and Planetary Science Conference, Houston, TX, 18–22 March.

Crawford, D. A., and M. B. Boslough. 1996. "A Model of Meteoroid Atmospheric Entry with Implications for the NEO Hazard and the Impact of Comet Shoemaker–Levy 9." Paper presented to Space '96, 5th International Conference and Exposition on Engineering, Construction, and Operations in Space, Albuquerque, NM, 1–6 June.

Crawford, D. A., and M. B. Boslough. 1996. "Dynamics of the Entry and Early Fireball: Do Light Flux and Plume Height Provide Constraints on Fragment and Mass?" Paper presented to the International Conference on the SL9–Jupiter Collision, Paris, France, 3–5 July.

Crawford, D. A., and M. B. Boslough. 1996. "Models of Radiative Output from Meteoroid Impacts." Paper presented to the 2nd Russian-American Nonproliferation and Arms Control Technologies Workshop, Livermore, CA, 16–20 September.

Crawford, D. A., and M. B. Boslough. 1996. "Using HST Plume Height Data to Place Lower Bounds on Comet Shoemaker–Levy 9 Fragment Mass and Penetration Depth." Paper presented to the 27th Lunar and Planetary Science Conference, Houston, TX, 18–22 March.

UV Spectroscopic Detection and Identification of Pathogens

P. J. Hargis, T. J. Sobering, G. C. Tisone, J. S. Wagner

Sandia analyzed the effectiveness of multivariate analysis algorithms for recognizing ultraviolet (UV) fluorescent signatures of several representative food pathogens. For simple samples, the algorithms showed good preliminary results indicative of the potential for these algorithms to automatically detect food pathogens.

We analyzed fluorescence spectra measured with the UV fluorometer with a "patch" multivariate analysis algorithm that was optimized in two ways. First, a human operator selected patches to both include and exclude scattered light and second-order fluorescence signals. The purpose of this approach was to (1) identify spectral regions containing useful fluorescence information, (2) test the linear concentration assumption used in the multivariate analysis algorithm, and (3) obtain a preliminary assessment of the ability of the "patch" algorithm to identify different bacteria. Second, we used a genetic algorithm to mathematically optimize the "patch" multivariate analysis algorithm for biological detection and identification. Even though this work is still in progress, we have obtained a significant improvement in sensitivity.

We first used the algorithm to analyze an unknown mixture of diluted *E. coli* in phosphate-buffered saline (PBS). We used various concentrations of *E. coli*, PBS, and *S. aureus*, calculated using the multivariate algorithm. The algorithm correctly identified the unknown as *E. coli*.

Next, we used the algorithm to analyze an unknown mixture of diluted *S. aureus* in PBS. The algorithm identified *S. aureus* as the dominant species in the unknown mixture. The algorithm was, however, slightly confused by incorrectly identifying a small concentration of *E. coli* in the unknown. The "trained" algorithm will be much less susceptible to this type of confusion.

Finally, we used the algorithm to analyze an unknown mixture containing 25% *E. coli* and 75% *S. aureus* in PBS. The "untrained" algorithm correctly identified the relative concentrations of *E. coli* and *S. aureus* in the unknown mixture.

We believe these preliminary results demonstrate the potential of multispectral UV fluorescence measurements in conjunction with multivariate analysis to distinguish *E. coli* and *S. aureus*. Measurements on chemical species have already demonstrated that a full analysis of *E. coli* and *S. aureus* fluorescence signatures using a "trained" multivariate analysis algorithm with built-in correlations will significantly improve the discrimination and identification capabilities of the algorithm.

Physico-Chemical Stability of Solid Surfaces

T. A. Michalske, G. Kellogg, D. R. Jennison, P. J. Feibelman

The application of physico-chemical phenomena to either increase machinability of hard materials, improve the wear resistance of cutting surfaces, or enhance sintering of particle compacts can have large economic impact on technologies ranging from materials-forming processes to oil-well drilling. Unfortunately, the broad application of these physico-chemical principles is limited by our ability to predict the optimum conditions for a wide variety of materials surfaces. Predictive models must be built upon understanding of the elementary events involved in surface damage and mobility. We are developing a new approach to examine the fundamental mechanisms controlling physico-chemical surface stability that combines (1) atomic-scale control of surface contact forces and displacements under well-controlled adsorbate conditions using the interfacial force microscope (IFM), (2) atomic-level imaging of surface and near-surface structure and defects using field ion microscopy (FIM) and transmission-electron microscopy (TEM), and (3) first-principles modeling of the effect of surface stress on adsorbate bonding interactions and the subsequent generation of surface damage. This unique combination of approaches will provide new insights into observed physico-chemical phenomena and provide the basis for developing true predictive models that are needed for wide application of these important new approaches to modifying the surface sensitive properties of materials.

Having completed the necessary physical and electronic modifications to the IFM that permit operation in ultra–high-vacuum (UHV), we designed and conducted a series of experiments to explore the role of liquid-metal adsorbates on the mechanical properties of clean metal surfaces and interfaces. In these experiments, we were able, for the first time, to clean the IFM probe tip (W) and the substate surface (Au) and directly measure the mechanical interactions as these metal surfaces were brought together in UHV conditions. In conventional force microscopy, the proximity of the tip is determined by physically contacting the substrate prior to any actual force measurements. Since clean metal surfaces interact so strongly, we had to invent a new method by which data could be obtained on the first approach to the substate. By applying a bias voltage to the tip, we were able to guide it into position for the first measurement using the field-emitted electron intensity. With this new experimental technique developed, we conducted experiments that contrast the mechanical interaction for a clean Au surface against one that has to be covered with monolayers of Hg. Since Hg is a classic embrittling agent for gold, we used these experiments to study the details of the embrittling process. Our results showed, contrary to expectations, that monolayer coverage of Hg actually strengthened the mechanical bond between the clean metals by greater than a factor of six. In addition, these measurements showed for the first time that the liquid metal actually softens the Au substate surface, allowing an adhesive instability as the outermost atomic layer of metal atoms "jumps" across to form the adhesive bond. In the remainder of this year we will complete instrumentation that allows us to measure the atomic-scale contact area as a function of interaction force so that we can directly deduce the chemical influence on the surface mechanical response.

Our university collaborator conducted macroscopic wear studies that complemented these atomic-level mechanical measurements. Using a unique microscrotching apparatus, he demonstrated the effect of liquid embrittling metals on the surface wear of Al. His results show a dramatic softening of the Al surface by Ga (a known embrittling agent for Al). This softening is consistent with our atomic-scale IFM measurements for the Hg/Au system.

Publications

Refereed

Houston, J. E., and T. A. Michalske. 1996. "Near-Plastic Threshold Indentation and the Residual Stress in Thin Films." *Proc. MRS Spring Mtg.* (San Francisco, CA, April), in press.

Jennison, D. R., P. A. Schultz, and M. P. Sears. 1997. "*Ab Initio* Calculations of Adsorbate Hydrogen-Bond Strength: Ammonia on Pt(111)." *Surface Science—Proc. 8th Internat. Conf. on Vibrations on Surfaces* **368** (10 December): 253.

Jennison, D. R., P. A. Schultz, and M. P. Sears. 1997. "*Ab Initio* Calculations of Ru, Pd, and Ag Cluster Structure with 55, 135, and 140 Atoms." *J. Chem Phys.* **106** (February): 1856.

Stumpf, R., and P. J. Feibelman. 1996. "Toward an Understanding of Liquid Metal Embrittlement: Energetics of Ga on Al Surfaces." *Phys Rev. B.* **54** (7) (August): 5145–5150.

Awards/Recognition	Project Number	Project Title
1996 Young Scientist Award, Office of Energy Research: Brian Swartzentruber	3501.270	Adaptive Scanning Probe Microscopies
Gottardi Prize for glass research by a person under 40 years of age: awarded by International Commission on Glass to R. K. Brow in recognition of his development of novel sealing glasses and R&D 100 Award	3501.320	PbO-Free Composites for Low-Temperature Packaging
Environmental Management Science Program Award	3501.460	Synthesis and Modeling of Field-Structured Anisotropic Composites
SAFE, for development of a smart agent-based model of the economy	3503.690	Development of Time-Dependent Monte Carlo Techniques for Massively Paralleled Computers
LEOS Distinguished Lecturer: Kevin Lear	3505.490	High-Speed Modulation of Vertical-Cavity Surface-Emitting Lasers
Finalist: Best Paper at 1996 International Conference on Robotics and Automation	3515.310	Cooperating Robot Arms
R&D 100 Award	3515.050	Radioactive Waste Processing Using Titanate Ion Exchangers
Environmental Management Science Program Award	3515.090	Using a Prehistoric Waste Disposal Site as a Natural Analogue for Validation of Risk Assessment Groundwater Flow and Transport Models
Environmental Management Science Program Award	3515.210	Delineating DNAPLs: A Probabilistic Approach for Locating DNAPLs in Subsurface Sediments
R&D 100 Award	3517.260	Use Control of "Robustness-Agile" Encryption Devices
R&D 100 Award	3517.190	Protocol Extensions for Asynchronous Transfer Mode Security
Amigo Award, Educational Outreach and Special Recognition Award, ARPA Proposal	3521.190	Conceptual Design and Prototyping for a Next-Generation Geographic Information System

Awards/Recognition	Project Number	Project Title
SPIE Milestone Research Paper: Feature Space Mapping for Sensor Fusion	3523.140	Feature-Based Methodology for Sensor Fusion
"Top 5 Technologies of the Year" Award from *Industry Week* for Microengine Driving a Rotating Disk	3526.020	Micromachined Inertial Sensors (Accelerometer, Gyroscope)
R&D 100 Award	3526.050	A Planar Silicon Fabrication Process for High-Aspect-Ratio Micromachined Parts
Sandia National Laboratories' "Award for Excellence" for organizing MEMS Agile Prototyping Short Course: C. C. Barron and B. Davies	3526.120	Agile Prototyping of Microelectromechanical Systems (MEMS)
R&D 100 Award	3536.280	Direct Fabrication of Aerogel-Supported Metal Nanocluster Catalysts
Hypervelocity Impact Society Best Paper Award	3539.190	Antidipodal Focusing of Shock Energy from Large Asteroid Impacts on Earth
1996 Welch Award, the top physics prize: Peter J. Feibelman	3539.430	Physico-Chemical Stability of Solid Surfaces

Project Title	Project #	Performance Statistics (Number of)											Project Qualitative Assessment	
		Refereed Publications	All Other Reports and Publications	Patent Disclosures	Patent Applications	Patents	Copyrights	Students	Post-docs	Permanent Staff Hired*	Awards	New Non-LDRD-Funded Projects	% Milestones Completed	Goals and Hypotheses Status**

* Permanent Staff Hired. Laboratories operate under manpower cap. There are no increases in permanent staff.

** Goals and Hypotheses Status

1 - Goals Met, Hypothesis Proved
2 - Goals Partially Met, Hypothesis Modified
3 - Goals Substantially Modified, Hypothesis Redefined
4 - Goals Not Met, Hypothesis Disproved
5 - Project Terminated

		Performance Statistics (Number of)											Project Qualitative Assessment	
Project Title	Project #	Refereed Publications	All Other Reports and Publications	Patent Disclosures	Patent Applications	Patents	Copyrights	Students	Post-docs	Permanent Staff Hired*	Awards	New Non-LDRD-Funded Projects	% Milestones Completed	Goals and Hypotheses Status**
Adaptive Scanning Probe Microscopies	3501.270	3	5						0.5				90%	1
Engineered Monodisperse Porous Materials	3501.280	4						1	1	4			80%	1
Demonstration of Molecular-Based Transistors	3501.290		2						1				25%	5
Chemical Functionalization of Oligosilanes: Economically Attractive Routes to New Photoresponsive Materials	3501.310		3						1	4			70%	2
PbO-Free Composites for Low-Temperature Packaging	3501.320	1	4	1				2	1		1		80%	2
Atomic-Scale Measurement of Liquid-Metal Wetting and Flow	3501.340							2	1	5		1	50%	2
Synthesis and Processing of High-Strength SiC Foams: A Radically New Approach to Ceramic-Ceramic Composite Materials	3501.350	1	2		1			1					95%	1
Carbon Nanotube Composites	3501.360	2	5						1	3		1	65%	3
Nanocomposite Materials Based on Hydrocarbon-Bridged Siloxanes	3501.370		4						2				90%	2
New Adhesive Systems Based on Functionalized Block Copolymers	3501.380	1	3	1	1				1	3			80%	2
Modeling Electrodeposition for Metal Microdevice Fabrication	3501.390			1									100%	1
Catalytic Membrane Sensors	3501.410								1	8			100%	1
Surface-Micromachined Flexural Plate Wave Device Integrated on Silicon	3501.420							3	2				95%	1
Model Determination and Validation for Reactive Wetting Processes	3501.430	1								4			75%	2
Integrated Thin-Film Structures for IR Imaging	3501.440		3	1					3	6			100%	1
Molecular Imprinting in Aerogels for Remote Sensing of Chemical Weapons and Pesticides	3501.450								1			1	90%	1
Synthesis and Modeling of Field-Structured Anisotropic Composites	3501.460											1	100%	1
System Studies in Materials	3501.470											1	100%	1
Engineered Stationary Phases for Chemical Separations	3501.480							2		1			100%	1
Coordinating Robotic Motion, Sensing, and Control in Plans and Execution	3503.280	2					1	1					80%	3
Parallel Optimization Methods for Agile Manufacturing	3503.310	2	6				1	2	1				100%	1
Self-Repairing Control for Damaged Manipulators	3503.350		2					2					85%	1
Physical Simulation of Nonisothermal Multiphase Flow in Porous Media	3503.370	8	1					2				2	90%	1
Monte Carlo Simulation of Radiation Heat Transfer in Reacting Flows by Massively Parallel Computing	3503.410									2			33%	2
MP System Software Libraries: Making High Performance Practical	3503.420		2						2	1			80%	1
A Massively Parallel 2-D Hybrid Continuum-to-Noncontinuum Fluid Code	3503.430		4				2		1				90%	2
General Techniques for Constrained Motion Planning	3503.440	3								3			100%	1
Automated Meshing: A Critical Link in Realizing Large Massively Parallel Adaptive Finite-Element Analysis	3503.450	1	1							2			75%	2
User-Interface Test-Bed for Technology Packaging	3503.470							1		2			70%	2
Self-Consistent Coupling of Atomistic and Continuum Electrostatics Using Boundary Element Methods	3503.490								1	3			100%	1

		Performance Statistics (Number of)											Project Qualitative Assessment	
Project Title	Project #	Refereed Publications	All Other Reports and Publications	Patent Disclosures	Patent Applications	Patents	Copyrights	Students	Post-docs	Permanent Staff Hired*	Awards	New Non-LDRD-Funded Projects	% Milestones Completed	Goals and Hypotheses Status**
Computation of Chemical Kinetics for Combustion	3503.510	1							2	6			33%	3
Parallel, Object-Oriented Toolkit for Simulation Software	3503.520	1	1				1		2			1	100%	1
Optical Communication for Future High-Performance Computers	3503.550	1							1	2			85%	2
Computer-Designed Molecular Memory and Switching Elements	3503.570	4	12					3	2				100%	1
Gradient-Driven Diffusion of Multi-Atom Molecules Through Macromolecules and Membranes	3503.580		1						1	1			75%	2
Modeling Complex Turbulent Chemically Reacting Flows on Massively Parallel Supercomputers	3503.590								1	1			85%	1
Quantitative Predictability of Computer Simulations of Complex Systems	3503.610												70%	1
Density Functional Theory for Classical Fluids at Complex Interfaces	3503.620	3								2			80%	2
A Massively Parallel Sparse Eigensolver for Structural Dynamics Finite Element	3503.630								0.5				100%	1
Automated Geometric Model Builder Using Range Image Sensor Data	3503.640		1										100%	1
Sensing and Compressing 3-D Models	3503.650							1	1	1			100%	2
Parallel Quantum Chemistry for Material Aging and Synthesis	3503.660	1								5			100%	1
Scalability of Cryptographic Algorithms and Protocols	3503.670												80%	2
Development of Time-Dependent Monte Carlo Techniques for Massively Parallel Computers	3503.690		1					1			1		100%	1
InP-Based Materials for Photonic and Microelectronic Devices	3505.260												70%	2
Tunneling Heterostructure Devices for Millimeter-Wave Applications	3505.280			1			2						50%	2
Microsensors for In-Process Control and Monitoring During Semiconductor Fabrication	3505.290								1				90%	1
Smart Packaging for Photonics	3505.340		1										65%	3
Microfabricated Combustible-Gas Detector	3505.350		1	1				1		4		1	100%	2
Integration of Diffractive Optics and VCSEL Arrays for Optical Interconnects	3505.360		3					1					80%	1
Photonic Integrated Circuits for Millimeter-Wave Generation	3505.380	1	1						1	2			85%	2
Subwavelength Diffractive Optics	3505.390	5						1	1				80%	1
In Situ Spectral Reflectance for Improved Molecular Beam Epitaxy Device Growth	3505.410	3		1			1						80%	2
Novel Low-Permittivity Dielectrics for Si-Based Microelectronics	3505.420	3	8					1		9			88%	1
Double Electron Layer Tunneling Transistor	3505.440	7	1		1			2					90%	1
Development of a Process Simulation Capability for the Formation of Titanium Nitride Diffusion Barriers	3505.450	3	1					1		1		2	90%	1
A Passive, Self-Aligned, Micromachined Device for Alignment of Arrays of Single-Mode Fibers to Binary Optics for Manufacturable Photonic Packaging	3505.460	1	2			1				1			95%	1
Red-to-Blue-Wavelength Photonic Devices	3505.470	1	1						1	7			95%	1
High-Speed Modulation of Vertical-Cavity Surface-Emitting Lasers	3505.490	1	1					1		4	1	1	90%	2
GaAs PIC Development for High-Performance Communications	3505.510	7						3					95%	2

		Performance Statistics (Number of)											Project Qualitative Assessment	
Project Title	Project #	Refereed Publications	All Other Reports and Publications	Patent Disclosures	Patent Applications	Patents	Copyrights	Students	Post-docs	Permanent Staff Hired*	Awards	New Non-LDRD-Funded Projects	% Milestones Completed	Goals and Hypotheses Status**
Wafer Fusion for Integration of Semiconductor Materials and Devices	3505.530							1					95%	2
Achromatic Nonlinear Optics for Sensing and Process Control	3505.540		1						1	3			100%	1
Integrated Separation and Optical Detection for Novel On-Chip Chemical Analysis	3505.550								1				90%	1
Integrated Heterojunction Bipolar Transistor Control Electronics and LED/VCSEL Drivers for High-Density Optical Data Links	3505.560												90%	5
Virtual Reactor for the Semiconductor Manufacturing Plant of the Future	3505.570									8			100%	1
Selective Oxidation Technology and Its Applications Toward Electronic and Optoelectronic Devices	3505.580	2			1								95%	1
Advanced Concepts for High-Power VCSELs and VCSEL Arrays	3505.590	11	1		1								100%	1
Midwave-Infrared (2–6 μm) Emitter-Based Chemical Sensor Systems	3505.610	2		1						4			95%	2
Top-Surface Imaging Resists for Lithography with Strongly Attenuated Radiation	3505.630		1						1			1	90%	1
Supersonic Cluster Jet Source for Debris-Free EUV Production	3505.640		1							3		2	100%	1
EUVL Experiments for the 0.1-Micron Lithography Generation	3505.650											2	100%	1
Optimization of Computationally Challenging Problems in Engineering Sciences	3507.230	2	9						3			4	100%	1
Impact and Thermal-Shock Response of Metal-Cutting Tools for High-Strength, High-Speed Milling Operations	3507.240	2						1					85%	2
Coherent Structures in Compressible Free-Shear-Layer Flows	3507.250		1						1			1	75%	2
Predicting Weld Solidification Cracking Using Continuum Damage Mechanics	3507.260	4											90%	2
Model Reduction Techniques for Nonlinear Systems and Control	3507.270	1								5			75%	2
Numerical and Experimental Investigation of Vortical Flow-Flame Interaction	3507.280								2	4			90%	1
Enhanced Vapor-Phase Diffusion in Porous Media	3507.290		2							3			100%	1
Investigation of Nonequilibrium Microscopic Hydrodynamic Phenomena	3507.310		2					1		5			95%	1
Constitutive Models of Stress-Strain Behavior of Granular Materials	3507.320		1							6			100%	5
Using Higher-Order Gradients to Modeling Localization Phenomena	3507.330								1				100%	1
Characterization of Fluid Transport in Microscale Structures	3507.340												90%	1
Scaling Laws for Strength and Toughness of Solid Materials	3507.350								1	1			100%	4
Temporal and Spatial Resolution of Fluid Flows	3507.360											2	90%	1
Stress Evaluation and Model Validation Using Laser Ultrasonics	3507.370							1	1				100%	1
Ultra–High-Speed Studies of Shock Phenomena in a Miniaturized System	3507.380												75%	1
Synchronization of Multiple Magnetically Switched Modules to Power Linear Induction Adder Accelerators	3509.050		1	1				1		1			100%	1
A Feasibility Study of Space-Charge-Neutralized Ion Induction Linacs	3509.060	1	3							4			50%	3
A 700-kV, Short-Pulse, Repetitive Accelerator for Industrial Applications	3509.070		9										95%	2

Project Title	Project #	Performance Statistics (Number of)											Project Qualitative Assessment	
		Refereed Publications	All Other Reports and Publications	Patent Disclosures	Patent Applications	Patents	Copyrights	Students	Post-docs	Permanent Staff Hired*	Awards	New Non-LDRD-Funded Projects	% Milestones Completed	Goals and Hypotheses Status**
Life-Cycle Costing for Nuclear Weapons Security	3509.080							4					75%	2
High-Power Ion Beam (HPIB) Modification of One- and Two-Layer Metal Surfaces	3509.090								1	4			100%	1
Electromagnetic Impulse Radar for Detection of Underground Structures	3509.110	1	1										100%	1
Advanced 3-D Electromagnetic and Particle-in-Cell Modeling	3509.120									5		1	100%	1
Development of Advanced Shock-Wave Diagnostics for Precision EOS Measurements on PBFA-Z/SATURN at Mbar Pressures	3509.130												100%	1
Intelligent Tools for On-Machine Acceptance of Precision-Machined Components	3513.320							1				1	80%	1
VIEWS—Virtual Interactive Environment Work Space	3513.340	3			1			1		3			100%	1
Intelligent Tool and Process Development for Robotic Edge Finishing	3513.360	7						3					100%	1
Holding Things Fast: Automatic Design of Fixtures and Grasps	3513.370	1	1				1	1		4		1	95%	1
Active Control of a Grinding Machine Using Magnetic Bearings	3513.380												50%	2
Virtual Prototyping	3513.390		2	1						5		1	90%	1
General Application of Rapid 3-D Digitizing and Tool-Path Generation for Complex Shapes	3513.410	1							1	3			99%	1
Development of an Immersive Environment to Aid in Automatic Mesh Generation	3513.420												90%	1
Ultra-Precise Assembly of Micromechanical Components	3513.430												100%	1
Smart Cutting Tools for Precision Manufacturing	3513.440		2	1				1		3			100%	1
Solid Variant Geometry Modeling	3513.450									1			100%	1
Rapid Prototyping/Rapid Manufacturing via Freeform Fabrication of Polymer-Matrix Composites	3513.460	1		1									100%	1
Low-Cost Pd-Catalyzed Metallization Technology for Rapid Prototyping of Electronic Substrates/Devices	3513.470		2	1				2					90%	1
Hexapod Characterization and Benchmarking	3513.480												100%	1
Designed Supramolecular Assemblies for Biosensors and Photoactive Devices	3514.040	6	1					3	2	3			70%	2
Decision Trees and Integrated Features for Computer-Aided Mammographic Screening	3514.070	1	3						1				70%	2
A New Approach to Protein Function and Structure Prediction	3514.080	4						1					70%	2
New Miniature Gamma-Ray Camera for Improved Tumor Localization	3514.090	8	4					5	1			1	95%	1
Improved Treatment of Prostate Neoplastic Disease	3514.110			1	1			1					75%	5
Development of Sensory Feedback Systems for Minimally Invasive Surgery Applications	3514.120							1					100%	1
Personal Status Monitor	3514.130			2					1	1			90%	1
Development of a One-Step ELISA Using Microencapsulation Immunoreagents	3514.140								1				60%	5
Development of a Portable X-Ray and Gamma-Ray Detector Instrument and Imaging Camera for Use in Radioactive and Hazardous Material Management	3515.170	17	14					6	1				100%	1
Automated Detection and Reporting of Volatile Organic Compounds (VOCs) in Complex Environments	3515.190									7			95%	1

		Performance Statistics (Number of)											Project Qualitative Assessment	
Project Title	Project #	Refereed Publications	All Other Reports and Publications	Patent Disclosures	Patent Applications	Patents	Copyrights	Students	Post-docs	Permanent Staff Hired*	Awards	New Non-LDRD-Funded Projects	% Milestones Completed	Goals and Hypotheses Status**
Delineating DNAPLs: A Probabilistic Approach for Locating DNAPLs in Subsurface Sediments	3515.210	7	1					1		4		1	97%	1
Compact Environmental Sensing Spectroscopy Using Advanced Semiconductor Light-Emitting Diodes and Lasers	3515.260	3		1	1			1	1				85%	1
The Development of Ion Mobility Spectroscopy to Analyze Explosives at Environmental Restoration Sites	3515.270	2	1		1			3		4		2	90%	1
Development of Inexpensive Metal Macrocyclic Complexes for Direct Oxidation of Methanol in Fuel Cells	3515.290	3						2	1	2			100%	1
Cooperating Robot Arms	3515.310	4						1		4	1		80%	1
Oriented Inorganic Thin-Film Channel Structures with Unidirectional Monosize Microscopes	3515.320			1				1	1				75%	2
Quantitative Analysis of Trace Contaminants in Aqueous Media	3515.330	3		1	1			1	1	1		4	80%	1
Replacement of Liquid H_2SO_4 and HF Acids with Solid Acid Catalysts for Paraffin Alkylation Process	3515.340		5		1				1	2			100%	1
Organically Enhanced In Situ Electrokinetic Removal of Uranium from Soils	3515.350	1			1			7	2				100%	1
Nanoreactors as Novel Catalyst Systems for Waste-Stream Remediation	3515.360	6		1	1				2			1	100%	1
Advanced Tomographic Flow Diagnostics for Opaque Multiphase Fluids	3515.410	5	9						1			1	95%	2
Evanescent Fiber-Optic Sensor for In Situ Monitoring of Chlorinated Organics	3515.430	1	1										100%	1
Reapplication of Energetic Materials as Fuels	3515.440		5					1	1	3			95%	1
Designed Molecular-Recognition Materials for Chiral Sensors, Separations, and Catalytic Materials	3515.450	6						2	2				100%	1
Learning Efficient Hypermedia Navigation	3517.120	2								2			100%	1
Data Zooming—A New Physics for Information Navigation	3517.150	3						1		2			100%	2
Design of a Highly Secure Smartcard	3517.160	1	1		1					9			90%	1
Enhanced Internet Firewall Design Using Stateful Filters	3517.170		1							0.9			85%	1
Network-Based Collaborative Research Environment	3517.180		7					1		5			100%	1
Reliability Assessment of Dynamic Communication Networks	3517.210	1	2	1				2		5			100%	1
Object-Oriented Parallel Discrete Event Simulation System — An Enabling Foundation for Rapid Development of High-Performance, Large-Scale Simulations	3517.220									1			100%	1
Agent-Based Remediation of the Mosaic Classification Problem	3517.230									1			100%	1
Biometric Identity Verification for Remote-User Authentication and Access-Control Applications	3517.240			1	1					5			100%	1
Development of an Intelligent Geographic Information System	3517.250			2				1					90%	2
Use-Control of "Robustness-Agile" Encryption Devices	3517.260		4										100%	1
Virtual Channel Encryption	3517.270									1			80%	2
Advanced Concurrent Engineering Environment	3517.280												100%	1
Electromagnetic Induction Tunnel Detection	3519.160	3	2		1			1		4		2	80%	2
Fiber-Optic Biosensors for Biological Warfare Counterproliferation	3519.170								2				100%	1
Moving Mass Trim Control for Precision-Strike Warheads	3519.180	2								8		1	99%	1
Theater Missile Defense Integrated Simulation	3519.190											1	90%	1

Project Title	Project #	Performance Statistics (Number of)											Project Qualitative Assessment	
		Refereed Publications	All Other Reports and Publications	Patent Disclosures	Patent Applications	Patents	Copyrights	Students	Post-docs	Permanent Staff Hired*	Awards	New Non-LDRD-Funded Projects	% Milestones Completed	Goals and Hypotheses Status**
Unexplored Penetrator Regime Against Super-Hard Underground Facilities	3519.210	1								6			80%	2
Fuel-Cell Applications for Novel Metalloporphyrin Catalysts	3521.120		1					4					90%	1
Vehicle Exhaust-Gas Chemical Sensors Using Acoustic-Wave Resonators	3521.170	1	3	1				3		3		1	90%	1
High-Density Direct Methanol Fuel Cell	3521.180									2			72%	3
Conceptual Design and Prototyping for a Next-Generation Geographic Information System	3521.190	1	4					2	1	1	2		90%	2
Hydrogen Production for Fuel Cells by Selective Dehydrogenation of Alkanes in Catalytic Membrane Reactors	3521.210							2	2				85%	2
Hybrid Vehicle Engine Development	3521.220												100%	1
Development of Innovative Combustion Processes for a Direct-Injection Diesel Engine	3521.230									2		1	100%	1
Superconductive Gravity Gradiometers for Underground Target Recognition	3523.110		1							6			20%	3
Bandwidth Utilization Maximization for Scientific Radio-Frequency Communication	3523.120							3		3			85%	3
Extraction of Information from Unstructured Data	3523.130		2										90%	1
Feature-Based Methodology for Sensor Fusion	3523.140		7					8	1		1	1	100%	1
Nonflammable Deterrent Materials	3523.150							1				1	90%	2
Microholographic Tagging	3523.160											2	100%	1
Interactive Control of Virtual Actors for Simulation and Training	3523.170	1						3		1			90%	1
Investigation of Spray Techniques for Use in Explosive Scabbling of Concrete	3523.180		1										100%	1
Jet Applications of Solder Bumps with Laser Ablation for MCM Packaging	3526.010		1										50%	2
Micromachined Inertial Sensors (Accelerometer, Gyroscope)	3526.020	1	2					1		4	1		100%	1
High-Reliability Plastic Packaging for Microelectronics	3526.030		2					4		4		2	80%	2
Ultra–Low-Power Microwave CHFET Integrated Circuit Development	3526.040	2											80%	1
A Planar Silicon Fabrication Process for High-Aspect-Ratio Micromachined Parts	3526.050		4							2			50%	2
Application-Specific Tester-on-a-Resident-Chip (TORCH)	3526.070						1	1		3		1	85%	2
Microelectronic Biosensors	3526.080								1	2		3	80%	2
Validation of the MDL ASIC Prototyping Process	3526.090												85%	1
High-G Accelerometer for Earth-Penetrator Weapons Applications	3526.110												100%	2
Agile Prototyping of Microelectromechanical Systems (MEMS)	3526.120									2	1		100%	1
Highly Parallel, Low-Power, Photonic Interconnects for Inter-Board Signal Distribution	3526.130		3										70%	2
Experimental Replication of the Reifenschweiler Effect	3536.010												100%	
Molecular Concentrator	3536.020							1		2			100%	
Investigation of Concepts for Storing and Releasing Energy from Nuclear Isomers	3536.030												100%	
CLERVER, Win95	3536.040												100%	
A Tool to Detect External Cracks from Within a Tube	3536.050												100%	

		Performance Statistics (Number of)											Project Qualitative Assessment	
Project Title	Project #	Refereed Publications	All Other Reports and Publications	Patent Disclosures	Patent Applications	Patents	Copyrights	Students	Post-docs	Permanent Staff Hired*	Awards	New Non-LDRD-Funded Projects	% Milestones Completed	Goals and Hypotheses Status**
Infrastructural Decision Support	3536.060												100%	
Development of Quiescent Power-Supply Voltage (V_{DDQ}) Testing	3536.110												100%	
Development of Failure and Yield Enhancement Analysis for Integrated Microlectromechanical Systems	3536.120												100%	
Exploration of Multichip Module (MCM) Test Solutions for Reliability Enhancement	3536.130												100%	
Optical Actuation of Micromechanical Components	3536.140												100%	
Statistical Characterization of MEMS Microengine Devices	3536.150												100%	
Optical State-of-Charge Monitor for Lead-Acid Batteries	3536.160												100%	
Impact of Focused Ion-Beam Microsurgery on Integrated Circuit Reliability	3536.170												100%	
Extended Cavity Fiber/VCSEL for Photonic Application	3536.180												100%	
Characterization of Semiconductor Piezoelectricity for Chemical-Sensing and High-Frequency Applications	3536.190												100%	
Magnetically Excited Flexural Plate Wave Device	3536.210												100%	
Alternative Joining by Diffusion Bonding with a Common Brazing Alloy	3536.220												100%	
Crack Propagation in Energetic Materials	3536.230												100%	
Composite Carbon Anodes for Rechargeable Li-Ion Cells	3536.240												100%	
Silicon-Based Nondestructive Read-Out Memories	3536.250												100%	
Use of X-Ray Mirrors for Enhanced Thin-Film X-Ray Diffraction	3536.260												100%	
High-Speed Shutter/Attenuator for Direct Fabrication Technology	3536.270												100%	
Direct Fabrication of Aerogel-Supported Metal Nanocluster Catalysts	3536.280												100%	
Measurement of Stress in Large-Area Thin Films	3536.290												100%	
Develop Capability to Measure Electrical Conductivity of Molten Slags	3536.310												100%	
Exploration of Surety Improvements via the Use of Ada in High-Consequence Software Projects	3536.320												100%	
Ensuring Critical-Event Sequence in High-Consequence Software by Applying Finite Automata Theory	3536.330												100%	
Optical High-Voltage Sensor for Advanced Firing Sets	3536.340												100%	
Toward Experimental Verification of New Dual-Permeability Conceptual Model in Fracture/Matrix Networks	3536.350												100%	
Investigation of Reducing Photovoltaic Systems Life-Cycle Costs Through System-Reliability Improvement	3536.360												100%	
Theoretical Development of a Prototype Assumption-Based Modeling System	3536.370												100%	
Sensor Fusion for Predictive Maintenance	3536.380												100%	
Modeling of Multicomponent Transport with Microbial Transformation in Subsurface System	3536.390												100%	
Precision Stage for LIGA Micromachine Fabrication	3536.410												100%	
Development of Periodically Poled Laser Sources for Ultra-Sensitive Analysis	3536.420												100%	

Project Title	Project #	Performance Statistics (Number of)											Project Qualitative Assessment	
		Refereed Publications	All Other Reports and Publications	Patent Disclosures	Patent Applications	Patents	Copyrights	Students	Post-docs	Permanent Staff Hired*	Awards	New Non-LDRD-Funded Projects	% Milestones Completed	Goals and Hypotheses Status**
Affinity Chromatography Supports for Separation and Detection of Biological Toxins	3536.430												100%	
Design and Evaluation of Sampling, Detection, and Control Technology for Field-Portable Capillary-Based Chemical Analysis	3536.440												100%	
Exploration of Methods for Bridging Length and Time Scales	3536.450												100%	
Scaling Laws for RoBugs	3536.460												100%	
New Applications of Damage Detection and Structural Health-Monitoring Methods	3536.470												100%	
Damage Detection Analysis Using Wavelets and Neural Nets	3536.480												100%	
A Comparison of System Identification Techniques	3536.490												100%	
Coaxial Extractor Diode Conceptual Design	3536.510												100%	
A Novel Methodology to Determine Dynamic Pressure-Volume States of Transportation Materials	3536.520												100%	
Remote Optical Detection of Obscured Objects in Turbid Oceanographic Environments	3536.530												100%	
RoBug Conceptual Design and Analysis System	3536.540												100%	
Prediction of Seismic Rocket Launch Signatures	3536.550												100%	
Evaluation of Shocked PVDF for Compact, High-Power Electric Pulse	3536.560												100%	
Distributed Object and Intelligent Agent Technologies in a Wide-Area Network Test-Bed	3538.010	3						1		1			85%	3
Laser-Spray Fabrication for Net-Shape Rapid Product Realization	3538.020		7					2					100%	1
Solid-Model Design Simplification	3538.030									3		1	100%	1
Process Optimization for Electron-Beam Joining of Ceramic and Glass Components	3538.040								0.2	1			100%	1
Self-Tuning Process Monitoring System for Process-Based Product Validation	3538.050									4			100%	1
Solution Synthesis and Processing of PZT Materials for Neutron Generator Applications	3538.060											3	100%	1
Effect of Composition and Processing Conditions on the Reliability of Cermet/Alumina Components	3538.070		2	1						2		1	75%	1
Carbon Coatings for Improved Sprytron Tube Performance and Reliability	3538.080									5			100%	1
A Multilevel Code for Metallurgical Effects in Metal-Forming Processes	3538.090		1					1					85%	1
Automated Reasoning About Tools for Assembly	3538.110	2	1							3			95%	1
Analysis-Driven Mechanical Redesign	3538.120									3			100%	1
Liaison-Based Assembly Design	3538.130							1		4		1	100%	1
An Enabling Architecture for Information-Driven Manufacturing	3538.140		1					2		5		1	60%	2
Nanocavity Effects on Misfit Accommodation in Semiconductors	3539.160	2								5			80%	2
Extending the Applicability of Cluster-Based Pattern Recognition with Efficient Approximation Techniques	3539.170												100%	1
Antipodal Focusing of Shock Energy from Large Asteroid Impacts on Earth	3539.190	12	11							3	1	1	90%	2
Biocavity Laser Microscopy/Spectroscopy of Cells	3539.220	9											100%	1

Project Title	Project #	Performance Statistics (Number of)											Project Qualitative Assessment	
		Refereed Publications	All Other Reports and Publications	Patent Disclosures	Patent Applications	Patents	Copyrights	Students	Post-docs	Permanent Staff Hired*	Awards	New Non-LDRD-Funded Projects	% Milestones Completed	Goals and Hypotheses Status**
Sol-Gel Preservation of Mankind's Cultural Heritage in Objects Constructed of Stone	3539.250	3	3					2	2	5			95%	1
Tailorable, Visible, Room-Temperature Light Emission from Si, Ge, and Si-Ge Nanoclusters	3539.270			1	1				1	3			100%	1
A New Paradigm for Near Real-Time Downhole Data Acquisition	3539.280	1		2	1					4			100%	1
In Situ Determination of Composition and Strain During MBE Using Electron Beams	3539.320	3		1									95%	2
In Situ Optical Flux Monitoring for Precise Control of Thin-Film Deposition	3539.330									7		1	40%	2
Understanding and Control of Energy-Transfer Mechanisms in Optical Ceramic	3539.340								2				83%	2
Molecular-Scale Lubricants for Micromachine Applications	3539.350									6			100%	1
Ultra-Hard Multilayer Coatings	3539.360	7								8			90%	2
Smart Interface Bonding Alloys (SIBA): Tailoring Thin-Film Mechanical Properties	3539.370												90%	3
Scanning Probe-Based Processes for Nanometer-Scale Device Fabrication	3539.380	3							1				85%	1
Wide-Bandgap Compound Semiconductors to Enable Novel Semiconductor Devices	3539.390	3								8			90%	2
Recognizing Atoms in Atomically Engineered Nanostructures: An Interdisciplinary Approach	3539.410												100%	1
Photonic Bandgap Structures as a Gateway to Nano-Photonics	3539.420	3			2					11			100%	1
Physico-Chemical Stability of Solid Surfaces	3539.430	4							2				90%	2
Artificial Atoms	3539.440	2	2						1				70%	2
Modeling and Characterization of Molecular Structures in Self-Assembled and Langmuir-Blodgett Films	3539.450	1						2					66%	2
UV Spectroscopic Detection and Identification of Pathogens	3539.460							1	1				100%	3
Novel Laser-Based Diagnostics Capability for Chemical Science	3539.470												100%	
Performance Statistics Summary		265	243	30	20	1	10	141	87	381	10	63		

Pg #	Title	Case Number	Science of Complex Systems	Modeling & Simulation of Complex Systems	High-Performance Computing	Nuclear Weapons Predictive Capability (Classified)	Safety Assessments & Engineering	Use Control & Security	Nonproliferation & Security	Dynamic Testing in Severe Environments	High-Energy-Density Materials	Laser Technology	Pulsed Power and Accelerators	Microelectronics and Photonics	Nuclear Materials	Engineered Materials	Flexible Manufacturing	Environmentally Conscious Manufacturing	Intelligent Machines and Robotics	Other
7	Adaptive Scanning Probe Microscopies	3501270000												●		●				
8	Engineered Monodisperse Porous Materials	3501280000									●					●				●
8	Demonstration of Molecular-Based Transistors	3501290000	●	●	●			●	●					●		●	●	●	●	
9	Chemical Functionalization of Oligosilanes: Economically Attractive Routes to New Photoresponsive Materials	3501310000						●	●							●				
10	PbO-Free Composites for Low-Temperature Packaging	3501320000	●											●		●		●		
10	Atomic-Scale Measurement of Liquid-Metal Wetting and Flow	3501340000								●				●		●		●		
11	Synthesis and Processing of High-Strength SiC Foams: A Radically New Approach to Ceramic-Ceramic Composite Materials	3501350000														●	●	●		
12	Carbon Nanotube Composites	3501360000														●				●
12	Nanocomposite Materials Based on Hydrocarbon-Bridged Siloxanes	3501370000	●	●				●	●	●				●		●	●	●		
13	New Adhesive Systems Based on Functionalized Block Copolymers	3501380000												●		●				
14	Modeling Electrodeposition for Metal Microdevice Fabrication	3501390000		●										●		●				
14	Catalytic Membrane Sensors	3501410000							●							●				

Pg #	Title	Case Number	Science of Complex Systems	Modeling & Simulation of Complex Systems	High-Performance Computing	Nuclear Weapons Predictive Capability (Classified)	Safety Assessments & Engineering	Use Control & Security	Nonproliferation & Security	Dynamic Testing in Severe Environments	High-Energy-Density Materials	Laser Technology	Pulsed Power and Accelerators	Microelectronics and Photonics	Nuclear Materials	Engineered Materials	Flexible Manufacturing	Environmentally Conscious Manufacturing	Intelligent Machines and Robotics	Other
14	Surface-Micromachined Flexural Plate Wave Device Integrated on Silicon	3501420000							•		•			•						
15	Model Determination and Validation for Reactive Wetting Processes	3501430000												•						
16	Integrated Thin-Film Structures for IR Imaging	3501440000							•					•						
16	Molecular Imprinting in Aerogels for Remote Sensing of Chemical Weapons and Pesticides	3501450000		•			•	•	•					•			•	•		
17	Synthesis and Modeling of Field-Structured Anisotropic Composites	3501460000														•				
18	System Studies in Materials	3501470000														•				
18	Engineered Stationary Phases for Chemical Separations	3501480000																		
21	Coordinating Robotic Motion, Sensing, and Control in Plans and Execution	3503280000			•												•		•	
22	Parallel Optimization Methods for Agile Manufacturing	3503310000		•	•									•		•	•			
21	Self-Repairing Control for Damaged Manipulators	3503350000	•	•	•		•							•			•	•	•	
22	Physical Simulation of Nonisothermal Multiphase Flow in Porous Media	3503370000	•	•	•		•													
24	Monte Carlo Simulation of Radiation Heat Transfer in Reacting Flows by Massively Parallel Computing	3503410000	•	•	•		•			•				•			•	•		

Pg #	Title	Case Number	Science of Complex Systems	Modeling & Simulation of Complex Systems	High-Performance Computing	Nuclear Weapons Predictive Capability (Classified)	Safety Assessments & Engineering	Use Control & Security	Nonproliferation & Security	Dynamic Testing in Severe Environments	High-Energy-Density Materials	Laser Technology	Pulsed Power and Accelerators	Microelectronics and Photonics	Nuclear Materials	Engineered Materials	Flexible Manufacturing	Environmentally Conscious Manufacturing	Intelligent Machines and Robotics	Other
24	MP System Software Libraries: Making High Performance Practical	3503420000	●	●	●		●									●			●	
25	A Massively Parallel 2-D Hybrid Continuum-to-Noncontinuum Fluid Code	3503430000		●	●									●						
26	General Techniques for Constrained Motion Planning	3503440000		●	●												●		●	
26	Automated Meshing: A Critical Link in Realizing Large Massively Parallel Adaptive Finite-Element Analysis	3503450000		●	●		●										●		●	●
27	User-Interface Test-Bed for Technology Packaging	3503470000		●																
28	Self-Consistent Coupling of Atomistic and Continuum Electrostatics Using Boundary Element Methods	3503490000		●	●						●			●		●				
28	Computation of Chemical Kinetics for Combustion	3503510000		●														●		
28	Parallel, Object-Oriented Toolkit for Simulation Software	3503520000		●	●															
29	Optical Communication for Future High-Performance Computers	3503550000			●															
30	Computer-Designed Molecular Memory and Switching Elements	3503570000	●	●										●		●				
31	Gradient-Driven Diffusion of Multi-Atom Molecules Through Macromolecules and Membranes	3503580000		●	●											●		●		
32	Modeling Complex Turbulent Chemically Reacting Flows on Massively Parallel Supercomputers	3503590000	●	●	●		●							●		●	●	●		

Pg #	Title	Case Number	Science of Complex Systems	Modeling & Simulation of Complex Systems	High-Performance Computing	Nuclear Weapons Predictive Capability (Classified)	Safety Assessments & Engineering	Use Control & Security	Nonproliferation & Security	Dynamic Testing in Severe Environments	High-Energy-Density Materials	Laser Technology	Pulsed Power and Accelerators	Microelectronics and Photonics	Nuclear Materials	Engineered Materials	Flexible Manufacturing	Environmentally Conscious Manufacturing	Intelligent Machines and Robotics	Other
32	Quantitative Predictability of Computer Simulations of Complex Systems	3503610000	●	●	●	●														
32	Density Functional Theory for Classical Fluids at Complex Interfaces	3503620000	●	●	●											●	●			
33	A Massively Parallel Sparse Eigensolver for Structural Dynamics Finite Element	3503630000		●	●	●			●	●										
34	Automated Geometric Model Builder Using Range Image Sensor Data	3503640000			●				●								●		●	
34	Sensing and Compressing 3-D Models	3503650000	●	●	●				●										●	
27	Parallel Quantum Chemistry for Material Aging and Synthesis	3503660000		●	●						●				●	●				
35	Scalability of Cryptographic Algorithms and Protocols	3503670000			●			●	●											
35	Development of Time-Dependent Monte Carlo Techniques for Massively Parallel Computers	3503690000	●	●	●															
39	InP-Based Materials for Photonic and Microelectronic Devices	3505260000			●							●		●				●		
39	Tunneling Heterostructure Devices for Millimeter-Wave Applications	3505280000										●		●						
40	Microsensors for In-Process Control and Monitoring During Semiconductor Fabrication	3505290000					●		●					●			●		●	
40	Smart Packaging for Photonics	3505340000			●			●				●		●			●			

Pg #	Title	Case Number	Science of Complex Systems	Modeling & Simulation of Complex Systems	High-Performance Computing	Nuclear Weapons Predictive Capability (Classified)	Safety Assessments & Engineering	Use Control & Security	Nonproliferation & Security	Dynamic Testing in Severe Environments	High-Energy-Density Materials	Laser Technology	Pulsed Power and Accelerators	Microelectronics and Photonics	Nuclear Materials	Engineered Materials	Flexible Manufacturing	Environmentally Conscious Manufacturing	Intelligent Machines and Robotics	Other
41	Microfabricated Combustible-Gas Detector	3505350000		●			●	●						●				●		
42	Integration of Diffractive Optics and VCSEL Arrays for Optical Interconnects	3505360000			●			●	●			●		●			●		●	
44	Photonic Integrated Circuits for Millimeter-Wave Generation	3505380000										●								
43	Subwavelength Diffractive Optics	3505390000			●			●	●			●		●			●	●		
41	In Situ Spectral Reflectance for Improved Molecular Beam Epitaxy Device Growth	3505410000		●				●		●		●		●		●	●	●		
44	Novel Low-Permitivity Dielectrics for Si-Based Microelectronics	3505420000												●		●				
46	Double Electron Layer Tunneling Transistor	3505440000							●					●						
47	Development of a Process Simulation Capability for the Formation of Titanium Nitride Diffusion Barriers	3505450000		●										●		●	●			
48	A Passive, Self-Aligned, Micromachined Device for Alignment of Arrays of Single-Mode Fibers to Binary Optics for Manufacturable Photonic Packaging	3505460000												●			●			
49	Red-to-Blue-Wavelength Photonic Devices	3505470000	●	●					●			●								
50	High-Speed Modulation of Vertical-Cavity Surface-Emitting Lasers	3505490000						●	●			●		●			●	●	●	
51	GaAs PIC Development for High-Performance Communications	3505510000			●		●	●						●						

Pg #	Title	Case Number	Science of Complex Systems	Modeling & Simulation of Complex Systems	High-Performance Computing	Nuclear Weapons Predictive Capability (Classified)	Safety Assessments & Engineering	Use Control & Security	Nonproliferation & Security	Dynamic Testing in Severe Environments	High-Energy-Density Materials	Laser Technology	Pulsed Power and Accelerators	Microelectronics and Photonics	Nuclear Materials	Engineered Materials	Flexible Manufacturing	Environmentally Conscious Manufacturing	Intelligent Machines and Robotics	Other
42	Wafer Fusion for Integration of Semiconductor Materials and Devices	3505530000			●			●	●			●		●			●	●	●	
52	Achromatic Nonlinear Optics for Sensing and Process Control	3505540000							●			●								
52	Integrated Separation and Optical Detection for Novel On-Chip Chemical Analysis	3505550000							●			●		●						
53	Integrated Heterojunction Bipolar Transistor Control Electronics and LED/VCSEL Drivers for High-Density Optical Data Links	3505560000																		
54	Virtual Reactor for the Semiconductor Manufacturing Plant of the Future	3505570000	●	●										●			●			
54	Selective Oxidation Technology and Its Applications Toward Electronic and Optoelectronic Devices	3505580000			●			●	●			●		●			●	●	●	
56	Advanced Concepts for High-Power VCSELs and VCSEL Arrays	3505590000			●			●	●			●		●			●	●	●	
57	Midwave-Infrared (2–6 μm) Emitter-Based Chemical Sensor Systems	3505610000			●			●	●			●		●			●	●	●	
55	Top-Surface Imaging Resists for Lithography with Strongly Attenuated Radiation	3505630000										●		●						●
57	Supersonic Cluster Jet Source for Debris-Free EUV Production	3505640000										●		●						●
58	EUVL Experiments for the 0.1-Micron Lithography Generation	3505650000										●		●						●
62	Optimization of Computationally Challenging Problems in Engineering Sciences	3507230000		●	●	●	●							●			●		●	

Pg #	Title	Case Number	Science of Complex Systems	Modeling & Simulation of Complex Systems	High-Performance Computing	Nuclear Weapons Predictive Capability (Classified)	Safety Assessments & Engineering	Use Control & Security	Nonproliferation & Security	Dynamic Testing in Severe Environments	High-Energy-Density Materials	Laser Technology	Pulsed Power and Accelerators	Microelectronics and Photonics	Nuclear Materials	Engineered Materials	Flexible Manufacturing	Environmentally Conscious Manufacturing	Intelligent Machines and Robotics	Other
61	Impact and Thermal-Shock Response of Metal-Cutting Tools for High-Strength, High-Speed Milling Operations	3507240000	●	●											●	●	●	●		
61	Coherent Structures in Compressible Free-Shear-Layer Flows	3507250000	●	●		●			●			●		●		●				
63	Predicting Weld Solidification Cracking Using Continuum Damage Mechanics	3507260000	●	●								●					●	●		
64	Model Reduction Techniques for Nonlinear Systems and Control	3507270000		●	●	●	●		●					●		●	●		●	
64	Numerical and Experimental Investigation of Vortical Flow-Flame Interaction	3507280000		●	●															
65	Enhanced Vapor-Phase Diffusion in Porous Media	3507290000	●	●																
66	Investigation of Nonequilibrium Microscopic Hydrodynamic Phenomena	3507310000		●	●									●						
66	Constitutive Models of Stress-Strain Behavior of Granular Materials	3507320000		●			●									●				
67	Using Higher-Order Gradients to Modeling Localization Phenomena	3507330000		●			●								●	●	●			
68	Characterization of Fluid Transport in Microscale Structures	3507340000							●										●	
68	Scaling Laws for Strength and Toughness of Solid Materials	3507350000	●	●		●	●			●						●	●			
68	Temporal and Spatial Resolution of Fluid Flows	3507360000	●	●	●		●													

Pg #	Title	Case Number	Science of Complex Systems	Modeling & Simulation of Complex Systems	High-Performance Computing	Nuclear Weapons Predictive Capability (Classified)	Safety Assessments & Engineering	Use Control & Security	Nonproliferation & Security	Dynamic Testing in Severe Environments	High-Energy-Density Materials	Laser Technology	Pulsed Power and Accelerators	Microelectronics and Photonics	Nuclear Materials	Engineered Materials	Flexible Manufacturing	Environmentally Conscious Manufacturing	Intelligent Machines and Robotics	Other
69	Stress Evaluation and Model Validation Using Laser Ultrasonics	3507370000	●	●			●	●	●	●				●	●		●		●	
69	Ultra-High-Speed Studies of Shock Phenomena in a Miniaturized System	3507380000	●	●						●	●					●				
73	Synchronization of Multiple Magnetically Switched Modules to Power Linear Induction Adder Accelerators	3509050000	●	●									●			●				
75	A Feasibility Study of Space-Charge-Neutralized Ion Induction Linacs	3509060000											●	●		●		●		●
76	A 700-kV, Short-Pulse, Repetitive Accelerator for Industrial Applications	3509070000					●		●			●	●	●		●				
74	Life-Cycle Costing for Nuclear Weapons Security	3509080000	●	●				●												
74	High-Power Ion Beam (HPIB) Modification of One- and Two-Layer Metal Surfaces	3509090000		●							●		●			●	●	●		
73	Electromagnetic Impulse Radar for Detection of Underground Structures	3509110000							●			●	●	●						
76	Advanced 3-D Electromagnetic and Particle-in-Cell Modeling	3509120000	●	●	●	●					●		●	●			●			
77	Development of Advanced Shock-Wave Diagnostics for Precision EOS Measurements on PBFA-Z/SATURN at Mbar Pressures	3509130000		●	●					●	●		●							
81	Intelligent Tools for On-Machine Acceptance of Precision-Machined Components	3513320000															●		●	
81	VIEWS—Virtual Interactive Environment Work Space	3513340000		●	●	●											●			

Pg #	Title	Case Number	Science of Complex Systems	Modeling & Simulation of Complex Systems	High-Performance Computing	Nuclear Weapons Predictive Capability (Classified)	Safety Assessments & Engineering	Use Control & Security	Nonproliferation & Security	Dynamic Testing in Severe Environments	High-Energy-Density Materials	Laser Technology	Pulsed Power and Accelerators	Microelectronics and Photonics	Nuclear Materials	Engineered Materials	Flexible Manufacturing	Environmentally Conscious Manufacturing	Intelligent Machines and Robotics	Other
82	Intelligent Tool and Process Development for Robotic Edge Finishing	351336000	●	●													●	●	●	
82	Holding Things Fast: Automatic Design of Fixtures and Grasps	351337000		●	●												●		●	
81	Active Control of a Grinding Machine Using Magnetic Bearings	351338000	●	●													●		●	
83	Virtual Prototyping	351339000		●		●		●	●					●			●			
84	General Application of Rapid 3-D Digitizing and Tool-Path Generation for Complex Shapes	351341000		●													●		●	
83	Development of an Immersive Environment to Aid in Automatic Mesh Generation	351342000		●	●	●	●									●	●			
84	Ultra-Precise Assembly of Micromechanical Components	351343000												●			●		●	
85	Smart Cutting Tools for Precision Manufacturing	351344000	●	●					●					●			●		●	
86	Solid Variant Geometry Modeling	351345000															●		●	
86	Rapid Prototyping/Rapid Manufacturing via Freeform Fabrication of Polymer-Matrix Composites	351346000														●	●		●	
86	Low-Cost Pd-Catalyzed Metallization Technology for Rapid Prototyping of Electronic Substrates/Devices	351347000		●									●	●			●	●		
87	Hexapod Characterization and Benchmarking	351348000																		

Pg #	Title	Case Number	Science of Complex Systems	Modeling & Simulation of Complex Systems	High-Performance Computing	Nuclear Weapons Predictive Capability (Classified)	Safety Assessments & Engineering	Use Control & Security	Nonproliferation & Security	Dynamic Testing in Severe Environments	High-Energy-Density Materials	Laser Technology	Pulsed Power and Accelerators	Microelectronics and Photonics	Nuclear Materials	Engineered Materials	Flexible Manufacturing	Environmentally Conscious Manufacturing	Intelligent Machines and Robotics	Other
92	Designed Supramolecular Assemblies for Biosensors and Photoactive Devices	3514040000	●	●	●				●							●				
96	Decision Trees and Integrated Features for Computer-Aided Mammographic Screening	3514070000			●														●	●
93	A New Approach to Protein Function and Structure Prediction	3514080000		●	●															
91	New Miniature Gamma-Ray Camera for Improved Tumor Localization	3514090000	●			●		●	●					●	●		●		●	
93	Improved Treatment of Prostate Neoplastic Disease	3514110000											●	●		●				●
94	Development of Sensory Feedback Systems for Minimally Invasive Surgery Applications	3514120000																		
94	Personal Status Monitor	3514130000		●				●						●		●	●	●		
95	Development of a One-Step ELISA Using Microencapsulation Immunoreagents	3514140000							●							●				
100	Development of a Portable X-Ray and Gamma-Ray Detector Instrument and Imaging Camera for Use in Radioactive and Hazardous Material Management	3515170000							●	●				●	●	●		●		
102	Automated Detection and Reporting of Volatile Organic Compounds (VOCs) in Complex Environments	3515190000							●			●		●						
99	Delineating DNAPLs: A Probabilistic Approach for Locating DNAPLs in Subsurface Sediments	3515210000	●	●	●		●													

Pg #	Title	Case Number	Science of Complex Systems	Modeling & Simulation of Complex Systems	High-Performance Computing	Nuclear Weapons Predictive Capability (Classified)	Safety Assessments & Engineering	Use Control & Security	Nonproliferation & Security	Dynamic Testing in Severe Environments	High-Energy-Density Materials	Laser Technology	Pulsed Power and Accelerators	Microelectronics and Photonics	Nuclear Materials	Engineered Materials	Flexible Manufacturing	Environmentally Conscious Manufacturing	Intelligent Machines and Robotics	Other
102	Compact Environmental Sensing Spectroscopy Using Advanced Semiconductor Light-Emitting Diodes and Lasers	3515260000						●	●			●		●				●	●	
103	The Development of Ion Mobility Spectroscopy to Analyze Explosives at Environmental Restoration Sites	3515270000					●											●	●	
104	Development of Inexpensive Metal Macrocyclic Complexes for Direct Oxidation of Methanol in Fuel Cells	3515290000									●		●			●		●		
104	Cooperating Robot Arms	3515310000	●	●	●												●		●	
106	Oriented Inorganic Thin-Film Channel Structures with Unidirectional Monosize Microscopes	3515320000	●													●		●		
106	Quantitative Analysis of Trace Contaminants in Aqueous Media	3515330000	●				●					●						●		
107	Replacement of Liquid H_2SO_4 and HF Acids with Solid Acid Catalysts for Paraffin Alkylation Process	3515340000	●													●		●		
105	Organically Enhanced In Situ Electrokinetic Removal of Uranium from Soils	3515350000	●	●																
110	Nanoreactors as Novel Catalyst Systems for Waste-Stream Remediation	3515360000									●									
108	Advanced Tomographic Flow Diagnostics for Opaque Multiphase Fluids	3515410000	●	●			●											●		●
109	Evanescent Fiber-Optic Sensor for In Situ Monitoring of Chlorinated Organics	3515430000												●				●		
111	Reapplication of Energetic Materials as Fuels	3515440000	●	●							●									●

Pg #	Title	Case Number	Science of Complex Systems	Modeling & Simulation of Complex Systems	High-Performance Computing	Nuclear Weapons Predictive Capability (Classified)	Safety Assessments & Engineering	Use Control & Security	Nonproliferation & Security	Dynamic Testing in Severe Environments	High-Energy-Density Materials	Laser Technology	Pulsed Power and Accelerators	Microelectronics and Photonics	Nuclear Materials	Engineered Materials	Flexible Manufacturing	Environmentally Conscious Manufacturing	Intelligent Machines and Robotics	Other
112	Designed Molecular-Recognition Materials for Chiral Sensors, Separations, and Catalytic Materials	3515450000														●				
115	Learning Efficient Hypermedia Navigation	3517120000							●										●	
121	Data Zooming—A New Physics for Information Navigation	3517150000		●													●		●	
115	Design of a Highly Secure Smartcard	3517160000						●	●							●				●
116	Enhanced Internet Firewall Design Using Stateful Filters	3517170000																		●
116	Network-Based Collaborative Research Environment	3517180000	●	●	●												●	●	●	
118	Reliability Assessment of Dynamic Communication Networks	3517210000	●	●																
117	Object-Oriented Parallel Discrete Event Simulation System—An Enabling Foundation for Rapid Development of High-Performance, Large-Scale Simulations	3517220000	●	●	●				●						●				●	
118	Agent-Based Remediation of the Mosaic Classification Problem	3517230000	●		●			●											●	
119	Biometric Identity Verification for Remote-User Authentication and Access-Control Applications	3517240000						●												
119	Development of an Intelligent Geographic Information System	3517250000		●					●											
120	Use-Control of "Robustness-Agile" Encryption Devices	3517260000			●			●									●			

Pg #	Title	Case Number	Science of Complex Systems	Modeling & Simulation of Complex Systems	High-Performance Computing	Nuclear Weapons Predictive Capability (Classified)	Safety Assessments & Engineering	Use Control & Security	Nonproliferation & Security	Dynamic Testing in Severe Environments	High-Energy-Density Materials	Laser Technology	Pulsed Power and Accelerators	Microelectronics and Photonics	Nuclear Materials	Engineered Materials	Flexible Manufacturing	Environmentally Conscious Manufacturing	Intelligent Machines and Robotics	Other
120	Virtual Channel Encryption	3517270000						●	●											●
122	Advanced Concurrent Engineering Environment	3517280000																		
125	Electromagnetic Induction Tunnel Detection	3519160000	●	●					●					●		●				●
126	Fiber-Optic Biosensors for Biological Warfare Counterproliferation	3519170000							●			●		●		●				●
127	Moving Mass Trim Control for Precision-Strike Warheads	3519180000		●	●				●	●										
126	Theater Missile Defense Integrated Simulation	3519190000		●																
128	Unexplored Penetrator Regime Against Super-Hard Underground Facilities	3519210000		●		●										●				
132	Fuel-Cell Applications for Novel Metalloporphyrin Catalysts	3521120000														●				●
131	Vehicle Exhaust-Gas Chemical Sensors Using Acoustic-Wave Resonators	3521170000								●				●		●		●		
132	High-Density Direct Methanol Fuel Cell	3521180000																		●
135	Conceptual Design and Prototyping for a Next-Generation Geographic Information System	3521190000		●					●								●		●	●
133	Hydrogen Production for Fuel Cells by Selective Dehydrogenation of Alkanes in Catalytic Membrane Reactors	3521210000														●				

Pg #	Title	Case Number	Science of Complex Systems	Modeling & Simulation of Complex Systems	High-Performance Computing	Nuclear Weapons Predictive Capability (Classified)	Safety Assessments & Engineering	Use Control & Security	Nonproliferation & Security	Dynamic Testing in Severe Environments	High-Energy-Density Materials	Laser Technology	Pulsed Power and Accelerators	Microelectronics and Photonics	Nuclear Materials	Engineered Materials	Flexible Manufacturing	Environmentally Conscious Manufacturing	Intelligent Machines and Robotics	Other
134	Hybrid Vehicle Engine Development	3521220000	●																	
134	Development of Innovative Combustion Processes for a Direct-Injection Diesel Engine	3521230000																		●
139	Superconductive Gravity Gradiometers for Underground Target Recognition	3523110000						●	●											
139	Bandwidth Utilization Maximization for Scientific Radio-Frequency Communication	3523120000							●	●									●	
140	Extraction of Information from Unstructured Data	3523130000							●											
140	Feature-Based Methodology for Sensor Fusion	3523140000						●	●										●	
141	Nonflammable Deterrent Materials	3523150000	●					●	●							●				
142	Microholographic Tagging	3523160000						●	●			●		●					●	
142	Interactive Control of Virtual Actors for Simulation and Training	3523170000		●					●										●	
143	Investigation of Spray Techniques for Use in Explosive Scabbling of Concrete	3523180000																		
147	Jet Applications of Solder Bumps with Laser Ablation for MCM Packaging	3526010000										●		●		●	●	●	●	
148	Micromachined Inertial Sensors (Accelerometer, Gyroscope)	3526020000						●		●				●		●			●	
147	High-Reliability Plastic Packaging for Microelectronics	3526030000			●			●						●		●				

Pg #	Title	Case Number	Science of Complex Systems	Modeling & Simulation of Complex Systems	High-Performance Computing	Nuclear Weapons Predictive Capability (Classified)	Safety Assessments & Engineering	Use Control & Security	Nonproliferation & Security	Dynamic Testing in Severe Environments	High-Energy-Density Materials	Laser Technology	Pulsed Power and Accelerators	Microelectronics and Photonics	Nuclear Materials	Engineered Materials	Flexible Manufacturing	Environmentally Conscious Manufacturing	Intelligent Machines and Robotics	Other
148	Ultra-Low-Power Microwave CHFET Integrated Circuit Development	3526040000							●					●						
153	A Planar Silicon Fabrication Process for High-Aspect-Ratio Micromachined Parts	3526050000							●					●		●				
149	Application-Specific Tester-on-a-Resident-Chip (TORCH)	3526070000					●			●				●					●	●
150	Microelectronic Biosensors	3526080000							●					●						
150	Validation of the MDL ASIC Prototyping Process	3526090000						●	●					●						
151	High-G Accelerometer for Earth-Penetrator Weapons Applications	3526110000								●				●						
152	Agile Prototyping of Microelectromechanical Systems (MEMS)	3526120000		●				●	●	●				●		●	●		●	
152	Highly Parallel, Low-Power, Photonic Interconnects for Inter-Board Signal Distribution	3526130000			●				●			●		●						
157	Experimental Replication of the Reifenschweiler Effect	3536010000																		
157	Molecular Concentrator	3536020000																		
158	Investigation of Concepts for Storing and Releasing Energy from Nuclear Isomers	3536030000																		
158	CLERVER, Win95	3536040000																		
159	A Tool to Detect External Cracks from Within a Tube	3536050000																		

Pg #	Title	Case Number	Science of Complex Systems	Modeling & Simulation of Complex Systems	High-Performance Computing	Nuclear Weapons Predictive Capability (Classified)	Safety Assessments & Engineering	Use Control & Security	Nonproliferation & Security	Dynamic Testing in Severe Environments	High-Energy-Density Materials	Laser Technology	Pulsed Power and Accelerators	Microelectronics and Photonics	Nuclear Materials	Engineered Materials	Flexible Manufacturing	Environmentally Conscious Manufacturing	Intelligent Machines and Robotics	Other
159	Infrastructural Decision Support	3536060000																		
160	Development of Quiescent Power-Supply Voltage (V_{DDQ}) Testing	3536110000																		
160	Development of Failure and Yield Enhancement Analysis for Integrated Microelectromechanical Systems	3536120000																		
161	Exploration of Multichip Module (MCM) Test Solutions for Reliability Enhancement	3536130000																		
161	Optical Actuation of Micromechanical Components	3536140000																		
162	Statistical Characterization of MEMS Microengine Devices	3536150000																		
162	Optical State-of-Charge Monitor for Lead-Acid Batteries	3536160000																		
163	Impact of Focused Ion-Beam Microsurgery on Integrated Circuit Reliability	3536170000																		
164	Extended Cavity Fiber/VCSEL for Photonic Application	3536180000																		
164	Characterization of Semiconductor Piezoelectricity for Chemical-Sensing and High-Frequency Applications	3536190000																		
165	Magnetically Excited Flexural Plate Wave Device	3536210000																		
166	Alternative Joining by Diffusion Bonding with a Common Brazing Alloy	3536220000																		

Pg #	Title	Case Number	Science of Complex Systems	Modeling & Simulation of Complex Systems	High-Performance Computing	Nuclear Weapons Predictive Capability (Classified)	Safety Assessments & Engineering	Use Control & Security	Nonproliferation & Security	Dynamic Testing in Severe Environments	High-Energy-Density Materials	Laser Technology	Pulsed Power and Accelerators	Microelectronics and Photonics	Nuclear Materials	Engineered Materials	Flexible Manufacturing	Environmentally Conscious Manufacturing	Intelligent Machines and Robotics	Other
165	Crack Propagation in Energetic Materials	3536230000																		
166	Composite Carbon Anodes for Rechargeable Li-Ion Cells	3536240000																		
167	Silicon-Based Nondestructive Read-Out Memories	3536250000																		
168	Use of X-Ray Mirrors for Enhanced Thin-Film X-Ray Diffraction	3536260000																		
168	High-Speed Shutter/Attenuator for Direct Fabrication Technology	3536270000																		
169	Direct Fabrication of Aerogel-Supported Metal Nanocluster Catalysts	3536280000																		
170	Measurement of Stress in Large-Area Thin Films	3536290000																		
170	Develop Capability to Measure Electrical Conductivity of Molten Slags	3536310000																		
169	Exploration of Surety Improvements via the Use of Ada in High-Consequence Software Projects	3536320000																		
171	Ensuring Critical-Event Sequence in High-Consequence Software by Applying Finite Automata Theory	3536330000																		
172	Optical High-Voltage Sensor for Advanced Firing Sets	3536340000																		
173	Toward Experimental Verification of New Dual-Permeability Conceptual Model in Fracture/Matrix Networks	3536350000																		

Pg #	Title	Case Number	Science of Complex Systems	Modeling & Simulation of Complex Systems	High-Performance Computing	Nuclear Weapons Predictive Capability (Classified)	Safety Assessments & Engineering	Use Control & Security	Nonproliferation & Security	Dynamic Testing in Severe Environments	High-Energy-Density Materials	Laser Technology	Pulsed Power and Accelerators	Microelectronics and Photonics	Nuclear Materials	Engineered Materials	Flexible Manufacturing	Environmentally Conscious Manufacturing	Intelligent Machines and Robotics	Other
172	Investigation of Reducing Photovoltaic Systems Life-Cycle Costs Through System-Reliability Improvement	3536360000																		
173	Theoretical Development of a Prototype Assumption-Based Modeling System	3536370000																		
174	Sensor Fusion for Predictive Maintenance	3536380000																		
174	Modeling of Multicomponent Transport with Microbial Transformation in Subsurface System	3536390000																		
175	Precision Stage for LIGA Micromachine Fabrication	3536410000																		
183	Development of Periodically Poled Laser Sources for Ultra-Sensitive Analysis	3536420000																		
176	Affinity Chromatography Supports for Separation and Detection of Biological Toxins	3536430000																		
176	Design and Evaluation of Sampling, Detection, and Control Technology for Field-Portable Capillary-Based Chemical Analysis	3536440000																		
178	Exploration of Methods for Bridging Length and Time Scales	3536450000																		
178	Scaling Laws for RoBugs	3536460000																		
177	New Applications of Damage Detection and Structural Health-Monitoring Methods	3536470000																		
178	Damage Detection Analysis Using Wavelets and Neural Nets	3536480000																		

Pg #	Title	Case Number	Science of Complex Systems	Modeling & Simulation of Complex Systems	High-Performance Computing	Nuclear Weapons Predictive Capability (Classified)	Safety Assessments & Engineering	Use Control & Security	Nonproliferation & Security	Dynamic Testing in Severe Environments	High-Energy-Density Materials	Laser Technology	Pulsed Power and Accelerators	Microelectronics and Photonics	Nuclear Materials	Engineered Materials	Flexible Manufacturing	Environmentally Conscious Manufacturing	Intelligent Machines and Robotics	Other
179	A Comparison of System Identification Techniques	3536490000																		
180	Coaxial Extractor Diode Conceptual Design	3536510000																		
180	A Novel Methodology to Determine Dynamic Pressure-Volume States of Transportation Materials	3536520000																		
181	Remote Optical Detection of Obscured Objects in Turbid Oceanographic Environments	3536530000																		
182	RoBug Conceptual Design and Analysis System	3536540000																		
182	Prediction of Seismic Rocket Launch Signatures	3536550000																		
183	Evaluation of Shocked PVDF for Compact, High-Power Electric Pulse	3536560000																		
187	Distributed Object and Intelligent Agent Technologies in a Wide-Area Network Test-Bed	3538010000															●			●
188	Laser-Spray Fabrication for Net-Shape Rapid Product Realization	3538020000	●	●								●				●	●	●	●	
188	Solid-Model Design Simplification	3538030000		●	●														●	
189	Process Optimization for Electron-Beam Joining of Ceramic and Glass Components	3538040000		●									●			●	●	●		●
190	Self-Tuning Process Monitoring System for Process-Based Product Validation	3538050000															●		●	

Pg #	Title	Case Number	Science of Complex Systems	Modeling & Simulation of Complex Systems	High-Performance Computing	Nuclear Weapons Predictive Capability (Classified)	Safety Assessments & Engineering	Use Control & Security	Nonproliferation & Security	Dynamic Testing in Severe Environments	High-Energy-Density Materials	Laser Technology	Pulsed Power and Accelerators	Microelectronics and Photonics	Nuclear Materials	Engineered Materials	Flexible Manufacturing	Environmentally Conscious Manufacturing	Intelligent Machines and Robotics	Other
190	Solution Synthesis and Processing of PZT Materials for Neutron Generator Applications	3538060000												●		●		●		
191	Effect of Composition and Processing Conditions on the Reliability of Cermet/Alumina Components	3538070000														●				
187	Carbon Coatings for Improved Sprytron Tube Performance and Reliability	3538080000		●							●					●	●			
192	A Multilevel Code for Metallurgical Effects in Metal-Forming Processes	3538090000		●	●	●										●	●			
192	Automated Reasoning About Tools for Assembly	3538110000		●	●												●		●	
193	Analysis-Driven Mechanical Redesign	3538120000			●												●		●	●
193	Liaison-Based Assembly Design	3538130000															●		●	●
194	An Enabling Architecture for Information-Driven Manufacturing	3538140000															●		●	
197	Nanocavity Effects on Misfit Accommodation in Semiconductors	3539160000																		
198	Extending the Applicability of Cluster-Based Pattern Recognition with Efficient Approximation Techniques	3539170000																		
210	Antipodal Focusing of Shock Energy from Large Asteroid Impacts on Earth	3539190000																		
199	Biocavity Laser Microscopy/Spectroscopy of Cells	3539220000																		
200	Sol-Gel Preservation of Mankind's Cultural Heritage in Objects Constructed of Stone	3539250000	●	●												●				

Pg #	Title	Case Number	Science of Complex Systems	Modeling & Simulation of Complex Systems	High-Performance Computing	Nuclear Weapons Predictive Capability (Classified)	Safety Assessments & Engineering	Use Control & Security	Nonproliferation & Security	Dynamic Testing in Severe Environments	High-Energy-Density Materials	Laser Technology	Pulsed Power and Accelerators	Microelectronics and Photonics	Nuclear Materials	Engineered Materials	Flexible Manufacturing	Environmentally Conscious Manufacturing	Intelligent Machines and Robotics	Other
201	Tailorable, Visible, Room-Temperature Light Emission from Si, Ge, and Si-Ge Nanoclusters	3539270000	●											●						
198	A New Paradigm for Near Real-Time Downhole Data Acquisition	3539280000							●	●										
202	In Situ Determination of Composition and Strain During MBE Using Electron Beams	3539320000							●			●		●				●		
202	In Situ Optical Flux Monitoring for Precise Control of Thin-Film Deposition	3539330000		●				●		●		●				●	●			
203	Understanding and Control of Energy-Transfer Mechanisms in Optical Ceramic	3539340000						●				●		●						
204	Molecular-Scale Lubricants for Micromachine Applications	3539350000														●				
204	Ultra-Hard Multilayer Coatings	3539360000		●								●				●				
205	Smart Interface Bonding Alloys (SIBA): Tailoring Thin-Film Mechanical Properties	3539370000	●	●	●		●									●				●
206	Scanning Probe-Based Processes for Nanometer-Scale Device Fabrication	3539380000												●		●				
206	Wide-Bandgap Compound Semiconductors to Enable Novel Semiconductor Devices	3539390000	●	●					●			●		●						
207	Recognizing Atoms in Atomically Engineered Nanostructures: An Interdisciplinary Approach	3539410000												●		●				
208	Photonic Bandgap Structures as a Gateway to Nano-Photonics	3539420000			●			●	●			●		●			●	●	●	
212	Physico-Chemical Stability of Solid Surfaces	3539430000			●	●	●							●		●				

Pg #	Title	Case Number				
208	Artificial Atoms	3539440000	●			Science of Complex Systems
209	Modeling and Characterization of Molecular Structures in Self-Assembled and Langmuir-Blodgett Films	3539450000		●		Modeling & Simulation of Complex Systems
212	UV Spectroscopic Detection and Identification of Pathogens	3539460000				High-Performance Computing
210	Novel Laser-Based Diagnostics Capability for Chemical Science	3539470000				Nuclear Weapons Predictive Capability (Classified)
						Safety Assessments & Engineering
						Use Control & Security
					●	Nonproliferation & Security
						Dynamic Testing in Severe Environments
						High-Energy-Density Materials
					●	Laser Technology
						Pulsed Power and Accelerators
			●	●	●	Microelectronics and Photonics
						Nuclear Materials
			●		●	Engineered Materials
			●			Flexible Manufacturing
			●			Environmentally Conscious Manufacturing
						Intelligent Machines and Robotics
						Other

Pg #	Title	Case Number	Waste Management	Energy Efficiency	Renewable Energy	ES & H	Environmental Restoration	Fossil Energy	Radioactive Waste Management	Economic Impact	Energy Research	Intelligence & National Security	Nuclear Energy	Science Education and Technical Information	Defense Programs	Department of Defense (DoD)	Other Federal Agencies*	Other (Industry, Consortia)**	Other Federal Agencies* Other (Industry, Consortia)**
7	Adaptive Scanning Probe Microscopies	3501270000		●						●	●				●				
8	Engineered Monodisperse Porous Materials	3501280000		●														●	
8	Demonstration of Molecular-Based Transistors	3501290000		●						●	●	●		●	●	●			
9	Chemical Functionalization of Oligosilanes: Economically Attractive Routes to New Photoresponsive Materials	3501310000								●	●				●				
10	PbO-Free Composites for Low-Temperature Packaging	3501320000	●			●	●			●	●			●	●	●		●	
10	Atomic-Scale Measurement of Liquid-Metal Wetting and Flow	3501340000	●	●							●				●				
11	Synthesis and Processing of High-Strength SiC Foams: A Radically New Approach to Ceramic-Ceramic Composite Materials	3501350000		●						●					●		●		
12	Carbon Nanotube Composites	3501360000		●						●				●	●	●	●	●	
12	Nanocomposite Materials Based on Hydrocarbon-Bridged Siloxanes	3501370000		●		●		●		●		●		●	●	●			
13	New Adhesive Systems Based on Functionalized Block Copolymers	3501380000								●				●	●	●			
14	Modeling Electrodeposition for Metal Microdevice Fabrication	3501390000		●								●		●	●		●		*NASA
14	Catalytic Membrane Sensors	3501410000													●	●		●	**Automobile Sensors
14	Surface-Micromachined Flexural Plate Wave Device Integrated on Silicon	3501420000	●			●	●					●		●	●				
15	Model Determination and Validation for Reactive Wetting Processes	3501430000													●	●			

Pg #	Title	Case Number	Waste Management	Energy Efficiency	Renewable Energy	ES & H	Environmental Restoration	Fossil Energy	Radioactive Waste Management	Economic Impact	Energy Research	Intelligence & National Security	Nuclear Energy	Science Education and Technical Information	Defense Programs	Department of Defense (DoD)	Other Federal Agencies*	Other (Industry, Consortia)**	Other Federal Agencies* Other (Industry, Consortia)**
16	Integrated Thin-Film Structures for IR Imaging	3501440000								●					●	●			
16	Molecular Imprinting in Aerogels for Remote Sensing of Chemical Weapons and Pesticides	3501450000	●			●	●			●		●			●	●			
17	Synthesis and Modeling of Field-Structured Anisotropic Composites	3501460000													●	●			
18	System Studies in Materials	3501470000										●			●				
18	Engineered Stationary Phases for Chemical Separations	3501480000																	
21	Coordinating Robotic Motion, Sensing, and Control in Plans and Execution	3503280000													●	●			
22	Parallel Optimization Methods for Agile Manufacturing	3503310000		◐						◐	◐			◐	◐				
21	Self-Repairing Control for Damaged Manipulators	3503350000	●				●		●	●					●	●	●	●	
22	Physical Simulation of Nonisothermal Multiphase Flow in Porous Media	3503370000	●			●	●		●	●					●	●		●	
24	Monte Carlo Simulation of Radiation Heat Transfer in Reacting Flows by Massively Parallel Computing	3503410000		●	●			●			●				●			●	
24	MP System Software Libraries: Making High Performance Practical	3503420000	●							●		●		●	●	●			
25	A Massively Parallel 2-D Hybrid Continuum-to-Noncontinuum Fluid Code	3503430000								●		●			●		●	●	
26	General Techniques for Constrained Motion Planning	3503440000	●			●	●		●						●	●			

Pg #	Title	Case Number	Waste Management	Energy Efficiency	Renewable Energy	ES & H	Environmental Restoration	Fossil Energy	Radioactive Waste Management	Economic Impact	Energy Research	Intelligence & National Security	Nuclear Energy	Science Education and Technical Information	Defense Programs	Department of Defense (DoD)	Other Federal Agencies*	Other (Industry, Consortia)**	Other Federal Agencies* Other (Industry, Consortia)**
26	Automated Meshing: A Critical Link in Realizing Large Massively Parallel Adaptive Finite-Element Analysis	3503450000												●	●	●		●	
27	User-Interface Test-Bed for Technology Packaging	3503470000								●				●	●				
28	Self-Consistent Coupling of Atomistic and Continuum Electrostatics Using Boundary Element Methods	3503490000		●			●				●				●	●			
28	Computation of Chemical Kinetics for Combustion	3503510000		●				●			●				●				
28	Parallel, Object-Oriented Toolkit for Simulation Software	3503520000	●					●			●				●				
29	Optical Communication for Future High-Performance Computers	3503550000								●					●				
30	Computer-Designed Molecular Memory and Switching Elements	3503570000								●	●				●				
31	Gradient-Driven Diffusion of Multi-Atom Molecules Through Macromolecules and Membranes	3503580000		●	●		●	●	●	●	●				●	●			
32	Modeling Complex Turbulent Chemically Reacting Flows on Massively Parallel Supercomputers	3503590000	●	●		●		●		●	●				●				
32	Quantitative Predictability of Computer Simulations of Complex Systems	3503610000	●				●			●	●		●		●	●			
32	Density Functional Theory for Classical Fluids at Complex Interfaces	3503620000				●					●					●			
33	A Massively Parallel Sparse Eigensolver for Structural Dynamics Finite Element	3503630000								●					●	●			

Pg #	Title	Case Number	Waste Management	Energy Efficiency	Renewable Energy	ES & H	Environmental Restoration	Fossil Energy	Radioactive Waste Management	Economic Impact	Energy Research	Intelligence & National Security	Nuclear Energy	Science Education and Technical Information	Defense Programs	Department of Defense (DoD)	Other Federal Agencies*	Other (Industry, Consortia)**	Other Federal Agencies* Other (Industry, Consortia)**
34	Automated Geometric Model Builder Using Range Image Sensor Data	3503640000	●	●	●	●	●	●	●	●	●	●		●					
34	Sensing and Compressing 3-D Models	3503650000	●				●					●			●	●			
27	Parallel Quantum Chemistry for Material Aging and Synthesis	3503660000										●			●				
35	Scalability of Cryptographic Algorithms and Protocols	3503670000								●		●			●	●			
35	Development of Time-Dependent Monte Carlo Techniques for Massively Parallel Computers	3503690000	●	●	●		●	●	●	●	●		●		●	●		●	
39	InP-Based Materials for Photonic and Microelectronic Devices	3505260000	●							●	●				●	●		●	
39	Tunneling Heterostructure Devices for Millimeter-Wave Applications	3505280000								●					●	●			
40	Microsensors for In-Process Control and Monitoring During Semiconductor Fabrication	3505290000		●			●	●				●			●			●	
40	Smart Packaging for Photonics	3505340000					●			●	●	●		●	●	●			
41	Microfabricated Combustible-Gas Detector	3505350000		●			●	●		●	●				●	●		●	
42	Integration of Diffractive Optics and VCSEL Arrays for Optical Interconnects	3505360000								●		●			●	●			
44	Photonic Integrated Circuits for Millimeter-Wave Generation	3505380000								●					●	●			
43	Subwavelength Diffractive Optics	3505390000										●		●	●	●		●	**Optoelectronics

Pg #	Title	Case Number	Waste Management	Energy Efficiency	Renewable Energy	ES & H	Environmental Restoration	Fossil Energy	Radioactive Waste Management	Economic Impact	Energy Research	Intelligence & National Security	Nuclear Energy	Science Education and Technical Information	Defense Programs	Department of Defense (DoD)	Other Federal Agencies*	Other (Industry, Consortia)**	Other Federal Agencies* Other (Industry, Consortia)**
41	In Situ Spectral Reflectance for Improved Molecular Beam Epitaxy Device Growth	3505410000	●	●	●					●	●				●	●			
44	Novel Low-Permittivity Dielectrics for Si-Based Microelectronics	3505420000													●	●			
46	Double Electron Layer Tunneling Transistor	3505440000								●	●	●			●				
47	Development of a Process Simulation Capability for the Formation of Titanium Nitride Diffusion Barriers	3505450000		●											●	●	●	●	
48	A Passive, Self-Aligned, Micromachined Device for Alignment of Arrays of Single-Mode Fibers to Binary Optics for Manufacturable Photonic Packaging	3505460000								●					●	●			
49	Red-to-Blue-Wavelength Photonic Devices	3505470000										●			●	●		●	**Optoelectronics
50	High-Speed Modulation of Vertical-Cavity Surface-Emitting Lasers	3505490000								●		●			●	●		●	**Optoelectronics
51	GaAs PIC Development for High-Performance Communications	3505510000										●			●	●		●	*ARPA **Communication, Sensing and Control Industries
42	Wafer Fusion for Integration of Semiconductor Materials and Devices	3505530000								●		●			●	●		●	**Optoelectronics
52	Achromatic Nonlinear Optics for Sensing and Process Control	3505540000									●	●			●				
52	Integrated Separation and Optical Detection for Novel On-Chip Chemical Analysis	3505550000					●					●			●	●			
53	Integrated Heterojunction Bipolar Transistor Control Electronics and LED/VCSEL Drivers for High-Density Optical Data Links	3505560000																	

Pg #	Title	Case Number	Waste Management	Energy Efficiency	Renewable Energy	ES & H	Environmental Restoration	Fossil Energy	Radioactive Waste Management	Economic Impact	Energy Research	Intelligence & National Security	Nuclear Energy	Science Education and Technical Information	Defense Programs	Department of Defense (DoD)	Other Federal Agencies*	Other (Industry, Consortia)**	Other Federal Agencies* Other (Industry, Consortia)**
54	Virtual Reactor for the Semiconductor Manufacturing Plant of the Future	3505570000		●										●	●	●	●	●	**Microelectronics and Photonics
54	Selective Oxidation Technology and Its Applications Toward Electronic and Optoelectronic Devices	3505580000								●		●			●	●		●	**Optoelectronics
56	Advanced Concepts for High-Power VCSELs and VCSEL Arrays	3505590000								●		●			●	●		●	**Optoelectronics
57	Midwave-Infrared (2–6 μm) Emitter-Based Chemical Sensor Systems	3505610000								●		●			●	●		●	**Optoelectronics
55	Top-Surface Imaging Resists for Lithography with Strongly Attenuated Radiation	3505630000																	
57	Supersonic Cluster Jet Source for Debris-Free EUV Production	3505640000																	
58	EUVL Experiments for the 0.1-Micron Lithography Generation	3505650000																	
62	Optimization of Computationally Challenging Problems in Engineering Sciences	3507230000								●					●	●		●	**Goodyear & Sematech, CRADAs, CRMPC consortium
61	Impact and Thermal-Shock Response of Metal-Cutting Tools for High-Strength, High-Speed Milling Operations	3507240000	●						●						●	●			
61	Coherent Structures in Compressible Free-Shear-Layer Flows	3507250000		●				●		●	●	●			●	●	●	●	
63	Predicting Weld Solidification Cracking Using Continuum Damage Mechanics	3507260000	●						●	●	●		●	●	●	●	●	●	
64	Model Reduction Techniques for Nonlinear Systems and Control	3507270000	●				●			●			●		●	●	●	●	
64	Numerical and Experimental Investigation of Vortical Flow-Flame Interaction	3507280000		●				●			●				●				

Pg #	Title	Case Number	Waste Management	Energy Efficiency	Renewable Energy	ES & H	Environmental Restoration	Fossil Energy	Radioactive Waste Management	Economic Impact	Energy Research	Intelligence & National Security	Nuclear Energy	Science Education and Technical Information	Defense Programs	Department of Defense (DoD)	Other Federal Agencies*	Other (Industry, Consortia)**	Other Federal Agencies* Other (Industry, Consortia)**
65	Enhanced Vapor-Phase Diffusion in Porous Media	3507290000	●				●		●		●								
66	Investigation of Nonequilibrium Microscopic Hydrodynamic Phenomena	3507310000		●							●	●			●	●			
66	Constitutive Models of Stress-Strain Behavior of Granular Materials	3507320000									●		●	●	●				
67	Using Higher-Order Gradients to Modeling Localization Phenomena	3507330000								●		●			●	●			**NCMS, USCAR, Aluminum, Steel Suppliers
68	Characterization of Fluid Transport in Microscale Structures	3507340000					●					●			●				
68	Scaling Laws for Strength and Toughness of Solid Materials	3507350000	●	●				●	●	●	●				●	●	●	●	
68	Temporal and Spatial Resolution of Fluid Flows	3507360000				●			●	●		●			●	●	●	●	*DOT, FFA, DOT, MMS, DOA, (USSS) **Insurance
69	Stress Evaluation and Model Validation Using Laser Ultrasonics	3507370000		●							●	●	●	●	●	●	●	●	*NRC, Transportation, Commerce, ect. **Auto, glass, steel, energy, etc.
69	Ultra–High-Speed Studies of Shock Phenomena in a Miniaturized System	3507380000																	
73	Synchronization of Multiple Magnetically Switched Modules to Power Linear Induction Adder Accelerators	3509050000	●			●				●	●				●			●	
75	A Feasibility Study of Space-Charge-Neutralized Ion Induction Linacs	3509060000							●	●	●		●						
76	A 700-kV, Short-Pulse, Repetitive Accelerator for Industrial Applications	3509070000	●						●		●				●				
74	Life-Cycle Costing for Nuclear Weapons Security	3509080000										●			●	●	●		

Pg #	Title	Case Number	Waste Management	Energy Efficiency	Renewable Energy	ES & H	Environmental Restoration	Fossil Energy	Radioactive Waste Management	Economic Impact	Energy Research	Intelligence & National Security	Nuclear Energy	Science Education and Technical Information	Defense Programs	Department of Defense (DoD)	Other Federal Agencies*	Other (Industry, Consortia)**	Other Federal Agencies* Other (Industry, Consortia)**
74	High-Power Ion Beam (HPIB) Modification of One- and Two-Layer Metal Surfaces	3509090000								●		●			●	●			
73	Electromagnetic Impulse Radar for Detection of Underground Structures	3509110000					●					●			●	●			
76	Advanced 3-D Electromagnetic and Particle-in-Cell Modeling	3509120000			●						●				●	●		●	**Microelectronics, Microwave devices
77	Development of Advanced Shock-Wave Diagnostics for Precision EOS Measurements on PBFA-Z/SATURN at Mbar Pressures	3509130000										●				●			
81	Intelligent Tools for On-Machine Acceptance of Precision-Machined Components	3513320000								●					●	●	●		
81	VIEWS—Virtual Interactive Environment Work Space	3513340000									●				●				
82	Intelligent Tool and Process Development for Robotic Edge Finishing	3513360000				●				●					●		●	●	
82	Holding Things Fast: Automatic Design of Fixtures and Grasps	3513370000	●												●		●	●	
81	Active Control of a Grinding Machine Using Magnetic Bearings	3513380000								●	●				●			●	
83	Virtual Prototyping	3513390000		●			●			●				●	●	●	●		
84	General Application of Rapid 3-D Digitizing and Tool-Path Generation for Complex Shapes	3513410000								●					●	●			
83	Development of an Immersive Environment to Aid in Automatic Mesh Generation	3513420000									●	●			●	●		●	**Meshing Consortia
84	Ultra-Precise Assembly of Micromechanical Components	3513430000										●	●		●	●			

Pg #	Title	Case Number	Waste Management	Energy Efficiency	Renewable Energy	ES & H	Environmental Restoration	Fossil Energy	Radioactive Waste Management	Economic Impact	Energy Research	Intelligence & National Security	Nuclear Energy	Science Education and Technical Information	Defense Programs	Department of Defense (DoD)	Other Federal Agencies*	Other (Industry, Consortia)**	Other Federal Agencies* Other (Industry, Consortia)**
85	Smart Cutting Tools for Precision Manufacturing	3513440000	●				●					●			●	●		●	**Machine Tool Industry
86	Solid Variant Geometry Modeling	3513450000													●	●			
86	Rapid Prototyping/Rapid Manufacturing via Freeform Fabrication of Polymer-Matrix Composites	3513460000													●	●			
86	Low-Cost Pd-Catalyzed Metallization Technology for Rapid Prototyping of Electronic Substrates/Devices	3513470000								●					●	●		●	**Industry
87	Hexapod Characterization and Benchmarking	3513480000																	
92	Designed Supramolecular Assemblies for Biosensors and Photoactive Devices	3514040000												●					
96	Decision Trees and Integrated Features for Computer-Aided Mammographic Screening	3514070000								●									
93	A New Approach to Protein Function and Structure Prediction	3514080000									●						●		
91	New Miniature Gamma-Ray Camera for Improved Tumor Localization	3514090000	●			●	●		●	●		●	●		●	●	●	●	
93	Improved Treatment of Prostate Neoplastic Disease	3514110000								●					●		●	●	
94	Development of Sensory Feedback Systems for Minimally Invasive Surgery Applications	3514120000													●				
94	Personal Status Monitor	3514130000								●		●			●	●	●	●	
95	Development of a One-Step ELISA Using Microencapsulation Immunoreagents	3514140000				●	●								●				

Pg #	Title	Case Number	Waste Management	Energy Efficiency	Renewable Energy	ES & H	Environmental Restoration	Fossil Energy	Radioactive Waste Management	Economic Impact	Energy Research	Intelligence & National Security	Nuclear Energy	Science Education and Technical Information	Defense Programs	Department of Defense (DoD)	Other Federal Agencies*	Other (Industry, Consortia)**	Other Federal Agencies* Other (Industry, Consortia)**
100	Development of a Portable X-Ray and Gamma-Ray Detector Instrument and Imaging Camera for Use in Radioactive and Hazardous Material Management	3515170000	●			●	●		●			●	●		●	●	●	●	
102	Automated Detection and Reporting of Volatile Organic Compounds (VOCs) in Complex Environments	3515190000					●			●					●				
99	Delineating DNAPLs: A Probabilistic Approach for Locating DNAPLs in Subsurface Sediments	3515210000	●			●	●			●	●						●		
102	Compact Environmental Sensing Spectroscopy Using Advanced Semiconductor Light-Emitting Diodes and Lasers	3515260000	●	●			●		●			●			●	●			
103	The Development of Ion Mobility Spectroscopy to Analyze Explosives at Environmental Restoration Sites	3515270000	●			●	●			●					●	●	●		
104	Development of Inexpensive Metal Macrocyclic Complexes for Direct Oxidation of Methanol in Fuel Cells	3515290000	●	●	●	●	●	●		●	●				●	●			
104	Cooperating Robot Arms	3515310000	●				●		●	●		●			●	●	●		
106	Oriented Inorganic Thin-Film Channel Structures with Unidirectional Monosize Microscopes	3515320000	●	●		●	●	●	●		●				●			●	
106	Quantitative Analysis of Trace Contaminants in Aqueous Media	3515330000	●			●	●	●	●						●		●		
107	Replacement of Liquid H_2SO_4 and HF Acids with Solid Acid Catalysts for Paraffin Alkylation Process	3515340000		●		●		●		●					●			●	
105	Organically Enhanced In Situ Electrokinetic Removal of Uranium from Soils	3515350000	●			●	●								●				
110	Nanoreactors as Novel Catalyst Systems for Waste-Stream Remediation	3515360000	●	●				●			●						●	●	

Pg #	Title	Case Number	Waste Management	Energy Efficiency	Renewable Energy	ES & H	Environmental Restoration	Fossil Energy	Radioactive Waste Management	Economic Impact	Energy Research	Intelligence & National Security	Nuclear Energy	Science Education and Technical Information	Defense Programs	Department of Defense (DoD)	Other Federal Agencies*	Other (Industry, Consortia)**	Other Federal Agencies* Other (Industry, Consortia)**
108	Advanced Tomographic Flow Diagnostics for Opaque Multiphase Fluids	3515410000	●	●	●			●			●							●	
109	Evanescent Fiber-Optic Sensor for In Situ Monitoring of Chlorinated Organics	3515430000	●			●	●								●		●		
111	Reapplication of Energetic Materials as Fuels	3515440000	●	●	●			●							●	●	●	●	
112	Designed Molecular-Recognition Materials for Chiral Sensors, Separations, and Catalytic Materials	3515450000	●	●		●				●		●							
115	Learning Efficient Hypermedia Navigation	3517120000												●	●				
121	Data Zooming—A New Physics for Information Navigation	3517150000								●				●					
115	Design of a Highly Secure Smartcard	3517160000	●			●			●	●		●			●	●	●	●	*Dept of Treasury, Dept of Commerce, Dept of Ag, HHS, VA, **National Financial Infrastructure Components
116	Enhanced Internet Firewall Design Using Stateful Filters	3517170000										●		●	●	●		●	
116	Network-Based Collaborative Research Environment	3517180000	●	●		●	●		●	●		●		●	●	●	●	●	
118	Reliability Assessment of Dynamic Communication Networks	3517210000								●					●		●	●	
117	Object-Oriented Parallel Discrete Event Simulation System—An Enabling Foundation for Rapid Development of High-Performance, Large-Scale Simulations	3517220000								●	●	●	●	●	●	●			
118	Agent-Based Remediation of the Mosaic Classification Problem	3517230000								●		●		●	●				

Pg #	Title	Case Number	Waste Management	Energy Efficiency	Renewable Energy	ES & H	Environmental Restoration	Fossil Energy	Radioactive Waste Management	Economic Impact	Energy Research	Intelligence & National Security	Nuclear Energy	Science Education and Technical Information	Defense Programs	Department of Defense (DoD)	Other Federal Agencies*	Other (Industry, Consortia)**	Other Federal Agencies* Other (Industry, Consortia)**
119	Biometric Identity Verification for Remote-User Authentication and Access-Control Applications	3517240000										●			●	●			*DOE, State **Industry, Academic, International
119	Development of an Intelligent Geographic Information System	3517250000		●	●					●	●	●					●	●	*DOT,DOTreas. **ATM Forum, FORE Systems
120	Use-Control of "Robustness-Agile" Encryption Devices	3517260000										●			●	●	●	●	
120	Virtual Channel Encryption	3517270000										●		●	●	●	●	●	
122	Advanced Concurrent Engineering Environment	3517280000																	
125	Electromagnetic Induction Tunnel Detection	3519160000	●				●	●			●	●				●			
126	Fiber-Optic Biosensors for Biological Warfare Counterproliferation	3519170000	●				●				●	●			●	●			
127	Moving Mass Trim Control for Precision-Strike Warheads	3519180000										●			●	●			
126	Theater Missile Defense Integrated Simulation	3519190000										●			●	●			
128	Unexplored Penetrator Regime Against Super-Hard Underground Facilities	3519210000													●	●			
132	Fuel-Cell Applications for Novel Metalloporphyrin Catalysts	3521120000		●	●			●								●		●	
131	Vehicle Exhaust-Gas Chemical Sensors Using Acoustic-Wave Resonators	3521170000	●	●						●					●	●		●	*DOT, EPA **USCAR, Industry
132	High-Density Direct Methanol Fuel Cell	3521180000		●	●					●	●								
135	Conceptual Design and Prototyping for a Next-Generation Geographic Information System	3521190000	●	●			●			●		●			●	●	●	●	

Pg #	Title	Case Number	Waste Management	Energy Efficiency	Renewable Energy	ES & H	Environmental Restoration	Fossil Energy	Radioactive Waste Management	Economic Impact	Energy Research	Intelligence & National Security	Nuclear Energy	Science Education and Technical Information	Defense Programs	Department of Defense (DoD)	Other Federal Agencies*	Other (Industry, Consortia)**	Other Federal Agencies* Other (Industry, Consortia)**
133	Hydrogen Production for Fuel Cells by Selective Dehydrogenation of Alkanes in Catalytic Membrane Reactors	3521210000		●				●			●				●	●			
134	Hybrid Vehicle Engine Development	3521220000		●	●										●				
134	Development of Innovative Combustion Processes for a Direct-Injection Diesel Engine	3521230000		●							●								
139	Superconductive Gravity Gradiometers for Underground Target Recognition	3523110000	●								●	●		●			●	●	*NASA ** Petrolium & Mineral exploration
139	Bandwidth Utilization Maximization for Scientific Radio-Frequency Communication	3523120000										●			●	●	●		
140	Extraction of Information from Unstructured Data	3523130000										●		●	●				
140	Feature-Based Methodology for Sensor Fusion	3523140000										●		●	●	●			
141	Nonflammable Deterrent Materials	3523150000										●		●	●	●			
142	Microholographic Tagging	3523160000										●			●				
142	Interactive Control of Virtual Actors for Simulation and Training	3523170000					●		●			●		●	●				
143	Investigation of Spray Techniques for Use in Explosive Scabbling of Concrete	3523180000																	
147	Jet Applications of Solder Bumps with Laser Ablation for MCM Packaging	3526010000		●		●	●								●	●		●	
148	Micromachined Inertial Sensors (Accelerometer, Gyroscope)	3526020000								●		●			●	●			

Pg #	Title	Case Number	Waste Management	Energy Efficiency	Renewable Energy	ES & H	Environmental Restoration	Fossil Energy	Radioactive Waste Management	Economic Impact	Energy Research	Intelligence & National Security	Nuclear Energy	Science Education and Technical Information	Defense Programs	Department of Defense (DoD)	Other Federal Agencies*	Other (Industry, Consortia)**	Other Federal Agencies* Other (Industry, Consortia)**
147	High-Reliability Plastic Packaging for Microelectronics	3526030000										●			●	●		●	
148	Ultra-Low-Power Microwave CHFET Integrated Circuit Development	3526040000	●						●			●	●		●	●			
153	A Planar Silicon Fabrication Process for High-Aspect-Ratio Micromachined Parts	3526050000										●			●	●	●	●	
149	Application-Specific Tester-on-a-Resident-Chip (TORCH)	3526070000								●					●			●	**Electronics/Microelectronics
150	Microelectronic Biosensors	3526080000				●						●			●				
150	Validation of the MDL ASIC Prototyping Process	3526090000										●			●	●			
151	High-G Accelerometer for Earth-Penetrator Weapons Applications	3526110000													●	●		●	**Auto Airbag Actuator
152	Agile Prototyping of Microelectromechanical Systems (MEMS)	3526120000										●		●	●	●			
152	Highly Parallel, Low-Power, Photonic Interconnects for Inter-Board Signal Distribution	3526130000								●		●				●		●	**OIDA (Optoelectronic Industry Development Association) - Consortium
157	Experimental Replication of the Reifenschweiler Effect	3536010000																	
157	Molecular Concentrator	3536020000																	
158	Investigation of Concepts for Storing and Releasing Energy from Nuclear Isomers	3536030000																	
158	CLERVER, Win95	3536040000																	

Pg #	Title	Case Number		Waste Management	Energy Efficiency	Renewable Energy	ES & H	Environmental Restoration	Fossil Energy	Radioactive Waste Management	Economic Impact	Energy Research	Intelligence & National Security	Nuclear Energy	Science Education and Technical Information	Defense Programs	Department of Defense (DoD)	Other Federal Agencies*	Other (Industry, Consortia)**	Other Federal Agencies* Other (Industry, Consortia)**
159	A Tool to Detect External Cracks from Within a Tube	3536050000																		
159	Infrastructural Decision Support	3536060000																		
160	Development of Quiescent Power-Supply Voltage (V_{DDQ}) Testing	3536110000																		
160	Development of Failure and Yield Enhancement Analysis for Integrated Microelectromechanical Systems	3536120000																		
161	Exploration of Multichip Module (MCM) Test Solutions for Reliability Enhancement	3536130000																		
161	Optical Actuation of Micromechanical Components	3536140000																		
162	Statistical Characterization of MEMS Microengine Devices	3536150000																		
162	Optical State-of-Charge Monitor for Lead-Acid Batteries	3536160000																		
163	Impact of Focused Ion-Beam Microsurgery on Integrated Circuit Reliability	3536170000																		
164	Extended Cavity Fiber/VCSEL for Photonic Application	3536180000																		
164	Characterization of Semiconductor Piezoelectricity for Chemical-Sensing and High-Frequency Applications	3536190000																		
165	Magnetically Excited Flexural Plate Wave Device	3536210000																		
166	Alternative Joining by Diffusion Bonding with a Common Brazing Alloy	3536220000																		

Pg #	Title	Case Number	Other Federal Agencies* Other (Industry, Consortia)**	Other (Industry, Consortia)**	Other Federal Agencies*	Department of Defense (DoD)	Defense Programs	Science Education and Technical Information	Nuclear Energy	Intelligence & National Security	Energy Research	Economic Impact	Radioactive Waste Management	Fossil Energy	Environmental Restoration	ES & H	Renewable Energy	Energy Efficiency	Waste Management
165	Crack Propagation in Energetic Materials	3536230000																	
166	Composite Carbon Anodes for Rechargeable Li-Ion Cells	3536240000																	
167	Silicon-Based Nondestructive Read-Out Memories	3536250000																	
168	Use of X-Ray Mirrors for Enhanced Thin-Film X-Ray Diffraction	3536260000																	
168	High-Speed Shutter/Attenuator for Direct Fabrication Technology	3536270000																	
169	Direct Fabrication of Aerogel-Supported Metal Nanocluster Catalysts	3536280000																	
170	Measurement of Stress in Large-Area Thin Films	3536290000																	
170	Develop Capability to Measure Electrical Conductivity of Molten Slags	3536310000																	
169	Exploration of Surety Improvements via the Use of Ada in High-Consequence Software Projects	3536320000																	
171	Ensuring Critical-Event Sequence in High-Consequence Software by Applying Finite Automata Theory	3536330000																	
172	Optical High-Voltage Sensor for Advanced Firing Sets	3536340000																	
173	Toward Experimental Verification of New Dual-Permeability Conceptual Model in Fracture/Matrix Networks	3536350000																	
172	Investigation of Reducing Photovoltaic Systems Life-Cycle Costs Through System-Reliability Improvement	3536360000																	

Pg #	Title	Case Number	Other Federal Agencies* Other (Industry, Consortia)**	Waste Management	Energy Efficiency	Renewable Energy	ES & H	Environmental Restoration	Fossil Energy	Radioactive Waste Management	Economic Impact	Energy Research	Intelligence & National Security	Nuclear Energy	Science Education and Technical Information	Defense Programs	Department of Defense (DoD)	Other Federal Agencies*	Other (Industry, Consortia)**
173	Theoretical Development of a Prototype Assumption-Based Modeling System	3536370000																	
174	Sensor Fusion for Predictive Maintenance	3536380000																	
174	Modeling of Multicomponent Transport with Microbial Transformation in Subsurface System	3536390000																	
175	Precision Stage for LIGA Micromachine Fabrication	3536410000																	
183	Development of Periodically Poled Laser Sources for Ultra-Sensitive Analysis	3536420000																	
176	Affinity Chromatography Supports for Separation and Detection of Biological Toxins	3536430000																	
176	Design and Evaluation of Sampling, Detection, and Control Technology for Field-Portable Capillary-Based Chemical Analysis	3536440000																	
178	Exploration of Methods for Bridging Length and Time Scales	3536450000																	
178	Scaling Laws for RoBugs	3536460000																	
177	New Applications of Damage Detection and Structural Health-Monitoring Methods	3536470000																	
178	Damage Detection Analysis Using Wavelets and Neural Nets	3536480000																	
179	A Comparison of System Identification Techniques	3536490000																	
180	Coaxial Extractor Diode Conceptual Design	3536510000																	
180	A Novel Methodology to Determine Dynamic Pressure-Volume States of Transportation Materials	3536520000																	

Pg #	Title	Case Number	Waste Management	Energy Efficiency	Renewable Energy	ES & H	Environmental Restoration	Fossil Energy	Radioactive Waste Management	Economic Impact	Energy Research	Intelligence & National Security	Nuclear Energy	Science Education and Technical Information	Defense Programs	Department of Defense (DoD)	Other Federal Agencies*	Other (Industry, Consortia)**	Other Federal Agencies* Other (Industry, Consortia)**
181	Remote Optical Detection of Obscured Objects in Turbid Oceanographic Environments	3536530000																	
182	RoBug Conceptual Design and Analysis System	3536540000																	
182	Prediction of Seismic Rocket Launch Signatures	3536550000																	
183	Evaluation of Shocked PVDF for Compact, High-Power Electric Pulse	3536560000																	
187	Distributed Object and Intelligent Agent Technologies in a Wide-Area Network Test-Bed	3538010000													●	●		●	**Academia
188	Laser-Spray Fabrication for Net-Shape Rapid Product Realization	3538020000													●			●	
188	Solid-Model Design Simplification	3538030000												●	●	●		●	**Goodyear, CRADA
189	Process Optimization for Electron-Beam Joining of Ceramic and Glass Components	3538040000		●											●	●		●	**Structural Ceramics
190	Self-Tuning Process Monitoring System for Process-Based Product Validation	3538050000																	
190	Solution Synthesis and Processing of PZT Materials for Neutron Generator Applications	3538060000													●	●			
191	Effect of Composition and Processing Conditions on the Reliability of Cermet/Alumina Components	3538070000								●		●			●	●		●	*DOL **AACC MCI, Inc (A subdivisionof the Association of American Ceramic Component Manufacturers
187	Carbon Coatings for Improved Sprytron Tube Performance and Reliability	3538080000												●	●	●			

Pg #	Title	Case Number	Waste Management	Energy Efficiency	Renewable Energy	ES & H	Environmental Restoration	Fossil Energy	Radioactive Waste Management	Economic Impact	Energy Research	Intelligence & National Security	Nuclear Energy	Science Education and Technical Information	Defense Programs	Department of Defense (DoD)	Other Federal Agencies*	Other (Industry, Consortia)**	Other Federal Agencies* Other (Industry, Consortia)**
192	A Multilevel Code for Metallurgical Effects in Metal-Forming Processes	3538090000								●					●				
192	Automated Reasoning About Tools for Assembly	3538110000								●					●		●	●	
193	Analysis-Driven Mechanical Redesign	3538120000												●	●	●	●	●	
193	Liaison-Based Assembly Design	3538130000												●	●	●	●	●	
194	An Enabling Architecture for Information-Driven Manufacturing	3538140000	●	●						●					●				
197	Nanocavity Effects on Misfit Accommodation in Semiconductors	3539160000												●	●				
198	Extending the Applicability of Cluster-Based Pattern Recognition with Efficient Approximation Techniques	3539170000													●				
210	Antipodal Focusing of Shock Energy from Large Asteroid Impacts on Earth	3539190000																	
199	Biocavity Laser Microscopy/Spectroscopy of Cells	3539220000																	
200	Sol-Gel Preservation of Mankind's Cultural Heritage in Objects Constructed of Stone	3539250000	●				●	●	●	●	●			●			●	●	*Department of Commerce **Metropolitan Museum of Art (NYC), Getty Conservation Institute (LA)
201	Tailorable, Visible, Room-Temperature Light Emission from Si, Ge, and Si-Ge Nanoclusters	3539270000																●	
198	A New Paradigm for Near Real-Time Downhole Data Acquisition	3539280000			●		●	●			●						●		
202	In Situ Determination of Composition and Strain During MBE Using Electron Beams	3539320000	●				●					●				●			

Pg #	Title	Case Number	Waste Management	Energy Efficiency	Renewable Energy	ES & H	Environmental Restoration	Fossil Energy	Radioactive Waste Management	Economic Impact	Energy Research	Intelligence & National Security	Nuclear Energy	Science Education and Technical Information	Defense Programs	Department of Defense (DoD)	Other Federal Agencies*	Other (Industry, Consortia)**	Other Federal Agencies* Other (Industry, Consortia)**
202	In Situ Optical Flux Monitoring for Precise Control of Thin-Film Deposition	3539330000	●	●	●					●	●				●	●			
203	Understanding and Control of Energy-Transfer Mechanisms in Optical Ceramic	3539340000					●				●	●			●	●			
204	Molecular-Scale Lubricants for Micromachine Applications	3539350000													●	●			
204	Ultra-Hard Multilayer Coatings	3539360000												●	●				
205	Smart Interface Bonding Alloys (SIBA): Tailoring Thin-Film Mechanical Properties	3539370000	●	●						●	●				●				
206	Scanning Probe-Based Processes for Nanometer-Scale Device Fabrication	3539380000									●				●				
206	Wide-Bandgap Compound Semiconductors to Enable Novel Semiconductor Devices	3539390000										●			●				
207	Recognizing Atoms in Atomically Engineered Nanostructures: An Interdisciplinary Approach	3539410000													●	●			
208	Photonic Bandgap Structures as a Gateway to Nano-Photonics	3539420000								●		●			●	●		●	**Optoelectronics
212	Physico-Chemical Stability of Solid Surfaces	3539430000									●				●				
208	Artificial Atoms	3539440000									●				●				
209	Modeling and Characterization of Molecular Structures in Self-Assembled and Langmuir-Blodgett Films	3539450000	●	●			●				●								
212	UV Spectroscopic Detection and Identification of Pathogens	3539460000	●				●					●			●	●			
210	Novel Laser-Based Diagnostics Capability for Chemical Science	3539470000																	

Pg #	Title	Case Number	Aeronautics	Applied Molecular Biology	Ceramics	Composites	Computer Simulation & Modeling	Data Storage and Peripherals	Electronics and Photonics	Energy	Flexible Computer-Integrated Manufacturing	High-Definition Imaging and Displays	High-Performance Computing and Networking	High-Performance Metals and Alloys	Intelligent Processing Equipment	Material Synthesis & Processing	Medical Technology	Micro- and Nano-Fabrication	Microelectronics and Optoelectronics	Photonic Materials	Pollution Min., Remediation, and Waste Mgmt.	Sensors & Signal Processing	Software	Surface Transportation Technologies	Systems Management Technologies	Defense-Related (mostly or purely)	Dual-Use (defense and non-defense-related)	Non-Defense-Related (mostly or purely)
7	Adaptive Scanning Probe Microscopies	3501270000			●	●			●	●						●		●	●								●	
8	Engineered Monodisperse Porous Materials	3501280000				●											●					●						●
8	Demonstration of Molecular-Based Transistors	3501290000	●						●			●	●			●	●	●	●	●							●	
9	Chemical Functionalization of Oligosilanes: Economically Attractive Routes to New Photoresponsive Materials	3501310000										●															●	
10	PbO-Free Composites for Low-Temperature Packaging	3501320000			●	●			●							●			●			●					●	
10	Atomic-Scale Measurement of Liquid-Metal Wetting and Flow	3501340000																									●	
11	Synthesis and Processing of High-Strength SiC Foams: A Radically New Approach to Ceramic-Ceramic Composite Materials	3501350000			●	●				●						●		●						●			●	
12	Carbon Nanotube Composites	3501360000				●				●						●		●									●	
12	Nanocomposite Materials Based on Hydrocarbon-Bridged Siloxanes	3501370000	●		●	●			●							●		●	●					●			●	
13	New Adhesive Systems Based on Functionalized Block Copolymers	3501380000				●			●							●			●								●	
14	Modeling Electrodeposition for Metal Microdevice Fabrication	3501390000							●					●		●		●	●			●					●	

Pg #	Title	Case Number	Aeronautics	Applied Molecular Biology	Ceramics	Composites	Computer Simulation & Modeling	Data Storage and Peripherals	Electronics and Photonics	Energy	Flexible Computer-Integrated Manufacturing	High-Definition Imaging and Displays	High-Performance Computing and Networking	High-Performance Metals and Alloys	Intelligent Processing Equipment	Material Synthesis & Processing	Medical Technology	Micro- and Nano-Fabrication	Microelectronics and Optoelectronics	Photonic Materials	Pollution Min., Remediation, and Waste Mgmt.	Sensors & Signal Processing	Software	Surface Transportation Technologies	Systems Management Technologies	Defense-Related (mostly or purely)	Dual-Use (defense and non-defense-related)	Non-Defense-Related (mostly or purely)
14	Catalytic Membrane Sensors	3501410000														●					●	●					●	
14	Surface-Micromachined Flexural Plate Wave Device Integrated on Silicon	3501420000			●				●							●		●	●		●	●					●	
15	Model Determination and Validation for Reactive Wetting Processes	3501430000	●		●	●	●		●							●			●									
16	Integrated Thin-Film Structures for IR Imaging	3501440000			●				●			●				●			●			●					●	
16	Molecular Imprinting in Aerogels for Remote Sensing of Chemical Weapons and Pesticides	3501450000		●		●			●							●	●	●	●		●	●					●	
17	Synthesis and Modeling of Field-Structured Anisotropic Composites	3501460000				●	●									●		●									●	
18	System Studies in Materials	3501470000																								●		
18	Engineered Stationary Phases for Chemical Separations	3501480000																									●	
21	Coordinating Robotic Motion, Sensing, and Control in Plans and Execution	3503280000									●			●	●								●					
22	Parallel Optimization Methods for Agile Manufacturing	3503310000	●				●		●	●	●		●	●	●			●	●				●				●	
21	Self-Repairing Control for Damaged Manipulators	3503350000				●	●				●		●	●	●	●	●		●			●	●	●			●	

Pg #	Title	Case Number	Aeronautics	Applied Molecular Biology	Ceramics	Composites	Computer Simulation & Modeling	Data Storage and Peripherals	Electronics and Photonics	Energy	Flexible Computer-Integrated Manufacturing	High-Definition Imaging and Displays	High-Performance Computing and Networking	High-Performance Metals and Alloys	Intelligent Processing Equipment	Material Synthesis & Processing	Medical Technology	Micro- and Nano-Fabrication	Microelectronics and Optoelectronics	Photonic Materials	Pollution Min., Remediation, and Waste Mgmt.	Sensors & Signal Processing	Software	Surface Transportation Technologies	Systems Management Technologies	Defense-Related (mostly or purely)	Dual-Use (defense and non-defense-related)	Non-Defense-Related (mostly or purely)
22	Physical Simulation of Nonisothermal Multiphase Flow in Porous Media	3503370000					●						●								●		●				●	
24	Monte Carlo Simulation of Radiation Heat Transfer in Reacting Flows by Massively Parallel Computing	3503410000	●				●		●	●			●		●	●			●								●	
24	MP System Software Libraries: Making High Performance Practical	3503420000	●				●						●										●	●			●	
25	A Massively Parallel 2-D Hybrid Continuum-to-Noncontinuum Fluid Code	3503430000	●				●			●			●			●												
26	General Techniques for Constrained Motion Planning	3503440000					●				●				●												●	
26	Automated Meshing: A Critical Link in Realizing Large Massively Parallel Adaptive Finite-Element Analysis	3503450000	●				●				●		●		●								●				●	
27	User-Interface Test-Bed for Technology Packaging	3503470000					●																●				●	
28	Self-Consistent Coupling of Atomistic and Continuum Electrostatics Using Boundary Element Methods	3503490000		●	●		●			●			●			●			●		●					●	
28	Computation of Chemical Kinetics for Combustion	3503510000					●			●			●														●	
28	Parallel, Object-Oriented Toolkit for Simulation Software	3503520000		●			●						●										●				●	

Pg #	Title	Case Number	Aeronautics	Applied Molecular Biology	Ceramics	Composites	Computer Simulation & Modeling	Data Storage and Peripherals	Electronics and Photonics	Energy	Flexible Computer-Integrated Manufacturing	High-Definition Imaging and Displays	High-Performance Computing and Networking	High-Performance Metals and Alloys	Intelligent Processing Equipment	Material Synthesis & Processing	Medical Technology	Micro- and Nano-Fabrication	Microelectronics and Optoelectronics	Photonic Materials	Pollution Min., Remediation, and Waste Mgmt.	Sensors & Signal Processing	Software	Surface Transportation Technologies	Systems Management Technologies	Defense-Related (mostly or purely)	Dual-Use (defense and non-defense-related)	Non-Defense-Related (mostly or purely)
29	Optical Communication for Future High-Performance Computers	3503550000		●			●						●														●	
30	Computer-Designed Molecular Memory and Switching Elements	3503570000		●			●	●	●				●			●		●	●	●							●	
31	Gradient-Driven Diffusion of Multi-Atom Molecules Through Macromolecules and Membranes	3503580000		●			●			●			●	●		●	●				●	●	●	●			●	
32	Modeling Complex Turbulent Chemically Reacting Flows on Massively Parallel Supercomputers	3503590000	●				●			●	●		●		●						●						●	
32	Quantitative Predictability of Computer Simulations of Complex Systems	3503610000	●	●			●				●		◐	◐	◐	◐		◐					◐					
32	Density Functional Theory for Classical Fluids at Complex Interfaces	3503620000		●	●		●			●	●					●	●				●	●	●					
33	A Massively Parallel Sparse Eigensolver for Structural Dynamics Finite Element	3503630000	●				●																	●			●	
34	Automated Geometric Model Builder Using Range Image Sensor Data	3503640000	●						●		●		●				●				●	●	●	●	●		●	
34	Sensing and Compressing 3-D Models	3503650000					●										●				●	●	●				●	
27	Parallel Quantum Chemistry for Material Aging and Synthesis	3503660000					●									●											●	
35	Scalability of Cryptographic Algorithms and Protocols	3503670000					●	●					●										●				●	

Pg #	Title	Case Number	Aeronautics	Applied Molecular Biology	Ceramics	Composites	Computer Simulation & Modeling	Data Storage and Peripherals	Electronics and Photonics	Energy	Flexible Computer-Integrated Manufacturing	High-Definition Imaging and Displays	High-Performance Computing and Networking	High-Performance Metals and Alloys	Intelligent Processing Equipment	Material Synthesis & Processing	Medical Technology	Micro- and Nano-Fabrication	Microelectronics and Optoelectronics	Photonic Materials	Pollution Min., Remediation, and Waste Mgmt.	Sensors & Signal Processing	Software	Surface Transportation Technologies	Systems Management Technologies	Defense-Related (mostly or purely)	Dual-Use (defense and non-defense-related)	Non-Defense-Related (mostly or purely)
35	Development of Time-Dependent Monte Carlo Techniques for Massively Parallel Computers	3503690000					●			●	●		●								●		●				●	
39	InP-Based Materials for Photonic and Microelectronic Devices	3505260000							●				●			●	●	●	●	●	●	●						
39	Tunneling Heterostructure Devices for Millimeter-Wave Applications	3505280000	●						●				●						●								●	
40	Microsensors for In-Process Control and Monitoring During Semiconductor Fabrication	3505290000						●	●	●					●	●		●	●			●					●	
40	Smart Packaging for Photonics	3505340000	●						●		●					●		●	●	●							●	
41	Microfabricated Combustible-Gas Detector	3505350000								●					●			●	●		●	●					●	
42	Integration of Diffractive Optics and VCSEL Arrays for Optical Interconnects	3505360000						●	●				●						●								●	
44	Photonic Integrated Circuits for Millimeter-Wave Generation	3505380000	●						●				●						●								●	
43	Subwavelength Diffractive Optics	3505390000							●		●	●	●		●			●	●			●					●	
41	In Situ Spectral Reflectance for Improved Molecular Beam Epitaxy Device Growth	3505410000						●	●		●	●	●		●	●			●	●	●	●					●	
44	Novel Low-Permittivity Dielectrics for Si-Based Microelectronics	3505420000											●						●								●	

Pg #	Title	Case Number	Aeronautics	Applied Molecular Biology	Ceramics	Composites	Computer Simulation & Modeling	Data Storage and Peripherals	Electronics and Photonics	Energy	Flexible Computer-Integrated Manufacturing	High-Definition Imaging and Displays	High-Performance Computing and Networking	High-Performance Metals and Alloys	Intelligent Processing Equipment	Material Synthesis & Processing	Medical Technology	Micro- and Nano-Fabrication	Microelectronics and Optoelectronics	Photonic Materials	Pollution Min., Remediation, and Waste Mgmt.	Sensors & Signal Processing	Software	Surface Transportation Technologies	Systems Management Technologies	Defense-Related (mostly or purely)	Dual-Use (defense and non-defense-related)	Non-Defense-Related (mostly or purely)
46	Double Electron Layer Tunneling Transistor	3505440000							●									●	●								●	
47	Development of a Process Simulation Capability for the Formation of Titanium Nitride Diffusion Barriers	3505450000			●		●		●	●						●			●								●	
48	A Passive, Self-Aligned, Micromachined Device for Alignment of Arrays of Single-Mode Fibers to Binary Optics for Manufacturable Photonic Packaging	3505460000	●						●				●						●									
49	Red-to-Blue-Wavelength Photonic Devices	3505470000									●	●				●			●									
50	High-Speed Modulation of Vertical-Cavity Surface-Emitting Lasers	3505490000							●		●	●			●			●	●	●		●					●	
51	GaAs PIC Development for High-Performance Communications	3505510000					●		●				●			●		●	●	●		●					●	
42	Wafer Fusion for Integration of Semiconductor Materials and Devices	3505530000							●		●	●	●					●	●	●		●					●	
52	Achromatic Nonlinear Optics for Sensing and Process Control	3505540000								●									●								●	
52	Integrated Separation and Optical Detection for Novel On-Chip Chemical Analysis	3505550000		●					●						●		●		●		●	●					●	
53	Integrated Heterojunction Bipolar Transistor Control Electronics and LED/VCSEL Drivers for High-Density Optical Data Links	3505560000																									●	

Pg #	Title	Case Number	Aeronautics	Applied Molecular Biology	Ceramics	Composites	Computer Simulation & Modeling	Data Storage and Peripherals	Electronics and Photonics	Energy	Flexible Computer-Integrated Manufacturing	High-Definition Imaging and Displays	High-Performance Computing and Networking	High-Performance Metals and Alloys	Intelligent Processing Equipment	Material Synthesis & Processing	Medical Technology	Micro- and Nano-Fabrication	Microelectronics and Optoelectronics	Photonic Materials	Pollution Min., Remediation, and Waste Mgmt.	Sensors & Signal Processing	Software	Surface Transportation Technologies	Systems Management Technologies	Defense-Related (mostly or purely)	Dual-Use (defense and non-defense-related)	Non-Defense-Related (mostly or purely)
54	Virtual Reactor for the Semiconductor Manufacturing Plant of the Future	3505570000					●		●	●	●					●		●	●	●							●	
54	Selective Oxidation Technology and Its Applications Toward Electronic and Optoelectronic Devices	3505580000							●			●	●		●			●	●	●		●					●	
56	Advanced Concepts for High-Power VCSELs and VCSEL Arrays	3505590000							●		●	●	●		●			●	●	●		●					●	
57	Midwave-Infrared (2–6 μm) Emitter-Based Chemical Sensor Systems	3505610000							●		●	●	●		●			●	●	●		●					●	
55	Top-Surface Imaging Resists for Lithography with Strongly Attenuated Radiation	3505630000																									●	
57	Supersonic Cluster Jet Source for Debris-Free EUV Production	3505640000																									●	
58	EUVL Experiments for the 0.1-Micron Lithography Generation	3505650000																									●	
62	Optimization of Computationally Challenging Problems in Engineering Sciences	3507230000					●		●				●						●			●					●	
61	Impact and Thermal-Shock Response of Metal-Cutting Tools for High-Strength, High-Speed Milling Operations	3507240000					●				●			●							●					●	
61	Coherent Structures in Compressible Free-Shear-Layer Flows	3507250000	●				●			●					●	●					●						●	
63	Predicting Weld Solidification Cracking Using Continuum Damage Mechanics	3507260000	●				●			●	●			●	●	●								●			●	

Pg #	Title	Case Number	Aeronautics	Applied Molecular Biology	Ceramics	Composites	Computer Simulation & Modeling	Data Storage and Peripherals	Electronics and Photonics	Energy	Flexible Computer-Integrated Manufacturing	High-Definition Imaging and Displays	High-Performance Computing and Networking	High-Performance Metals and Alloys	Intelligent Processing Equipment	Material Synthesis & Processing	Medical Technology	Micro- and Nano-Fabrication	Microelectronics and Optoelectronics	Photonic Materials	Pollution Mtn., Remediation, and Waste Mgmt.	Sensors & Signal Processing	Software	Surface Transportation Technologies	Systems Management Technologies	Defense-Related (mostly or purely)	Dual-Use (defense and non-defense-related)	Non-Defense-Related (mostly or purely)
64	Model Reduction Techniques for Nonlinear Systems and Control	3507270000	●				●				●	●	●				●		●				●				●	
64	Numerical and Experimental Investigation of Vortical Flow-Flame Interaction	3507280000					●			●											●						●	
65	Enhanced Vapor-Phase Diffusion in Porous Media	3507290000					●			●											●	●						●
66	Investigation of Nonequilibrium Microscopic Hydrodynamic Phenomena	3507310000	●				●			●			●			●		●	●								●	
66	Constitutive Models of Stress-Strain Behavior of Granular Materials	3507320000			●		●							●													●	
67	Using Higher-Order Gradients to Modeling Localization Phenomena	3507330000					●							●		●		●									●	
68	Characterization of Fluid Transport in Microscale Structures	3507340000																●			●	●					●	
68	Scaling Laws for Strength and Toughness of Solid Materials	3507350000			●	●	●			●			●	●				●			●		●				●	
68	Temporal and Spatial Resolution of Fluid Flows	3507360000																			●						●	
69	Stress Evaluation and Model Validation Using Laser Ultrasonics	3507370000	●		●	●	●			●	●			●	●	●			●			●		●			●	
69	Ultra–High-Speed Studies of Shock Phenomena in a Miniaturized System	3507380000																									●	

Pg #	Title	Case Number	Aeronautics	Applied Molecular Biology	Ceramics	Composites	Computer Simulation & Modeling	Data Storage and Peripherals	Electronics and Photonics	Energy	Flexible Computer-Integrated Manufacturing	High-Definition Imaging and Displays	High-Performance Computing and Networking	High-Performance Metals and Alloys	Intelligent Processing Equipment	Material Synthesis & Processing	Medical Technology	Micro- and Nano-Fabrication	Microelectronics and Optoelectronics	Photonic Materials	Pollution Min., Remediation, and Waste Mgmt.	Sensors & Signal Processing	Software	Surface Transportation Technologies	Systems Management Technologies	Defense-Related (mostly or purely)	Dual-Use (defense and non-defense-related)	Non-Defense-Related (mostly or purely)
73	Synchronization of Multiple Magnetically Switched Modules to Power Linear Induction Adder Accelerators	3509050000	●		●	●			●	●				●		●	●				●	●					●	
75	A Feasibility Study of Space-Charge-Neutralized Ion Induction Linacs	3509060000								●				●		●										●		
76	A 700-kV, Short-Pulse, Repetitive Accelerator for Industrial Applications	3509070000			●	●			●					●		●	●		●		●	●						
74	Life-Cycle Costing for Nuclear Weapons Security	3509080000																							●			
74	High-Power Ion Beam (HPIB) Modification of One- and Two-Layer Metal Surfaces	3509090000			●		●				●			●		●											●	
73	Electromagnetic Impulse Radar for Detection of Underground Structures	3509110000							●										●		●						●	
76	Advanced 3-D Electromagnetic and Particle-in-Cell Modeling	3509120000					●	●	●	●						●			●		●						●	
77	Development of Advanced Shock-Wave Diagnostics for Precision EOS Measurements on PBFA-Z/SATURN at Mbar Pressures	3509130000																									●	
82	Intelligent Tools for On-Machine Acceptance of Precision-Machined Components	3513320000									●				●	●						●	●			●		
81	VIEWS—Virtual Interactive Environment Work Space	3513340000					●				●		●										●				●	
82	Intelligent Tool and Process Development for Robotic Edge Finishing	3513360000					●				●		●	●	●							●	●				●	

Pg #	Title	Case Number	Aeronautics	Applied Molecular Biology	Ceramics	Composites	Computer Simulation & Modeling	Data Storage and Peripherals	Electronics and Photonics	Energy	Flexible Computer-Integrated Manufacturing	High-Definition Imaging and Displays	High-Performance Computing and Networking	High-Performance Metals and Alloys	Intelligent Processing Equipment	Material Synthesis & Processing	Medical Technology	Micro- and Nano-Fabrication	Microelectronics and Optoelectronics	Photonic Materials	Pollution Min., Remediation, and Waste Mgmt.	Sensors & Signal Processing	Software	Surface Transportation Technologies	Systems Management Technologies	Defense-Related (mostly or purely)	Dual-Use (defense and non-defense-related)	Non-Defense-Related (mostly or purely)
82	Holding Things Fast: Automatic Design of Fixtures and Grasps	3513370000					●				●				●							●					●	
81	Active Control of a Grinding Machine Using Magnetic Bearings	3513380000									●				●	●						●						
83	Virtual Prototyping	3513390000					●		●		●								●				●					
84	General Application of Rapid 3-D Digitizing and Tool-Path Generation for Complex Shapes	3513410000					●				●				●						●	●						
83	Development of an Immersive Environment to Aid in Automatic Mesh Generation	3513420000					●						●										●					
84	Ultra-Precise Assembly of Micromechanical Components	3513430000							●		●							●	●									
85	Smart Cutting Tools for Precision Manufacturing	3513440000	●		●	●	●									●	●	●								●	●	
86	Solid Variant Geometry Modeling	3513450000									●																●	
86	Rapid Prototyping/Rapid Manufacturing via Freeform Fabrication of Polymer-Matrix Composites	3513460000				●					●				●	●											●	
86	Low-Cost Pd-Catalyzed Metallization Technology for Rapid Prototyping of Electronic Substrates/Devices	3513470000					●		●		●					●			●		●						●	
87	Hexapod Characterization and Benchmarking	3513480000																									●	

Pg #	Title	Case Number	Aeronautics	Applied Molecular Biology	Ceramics	Composites	Computer Simulation & Modeling	Data Storage and Peripherals	Electronics and Photonics	Energy	Flexible Computer-Integrated Manufacturing	High-Definition Imaging and Displays	High-Performance Computing and Networking	High-Performance Metals and Alloys	Intelligent Processing Equipment	Material Synthesis & Processing	Medical Technology	Micro- and Nano-Fabrication	Microelectronics and Optoelectronics	Photonic Materials	Pollution Min., Remediation, and Waste Mgmt.	Sensors & Signal Processing	Software	Surface Transportation Technologies	Systems Management Technologies	Defense-Related (mostly or purely)	Dual-Use (defense and non-defense-related)	Non-Defense-Related (mostly or purely)
92	Designed Supramolecular Assemblies for Biosensors and Photoactive Devices	3514040000		●			●	●	●				●			●	●					●						●
96	Decision Trees and Integrated Features for Computer-Aided Mammographic Screening	3514070000															●					●						●
93	A New Approach to Protein Function and Structure Prediction	3514080000		●													●											●
91	New Miniature Gamma-Ray Camera for Improved Tumor Localization	3514090000							●		●	●					●		●	●	●		●		●		●	
93	Improved Treatment of Prostate Neoplastic Disease	3514110000				●			●								●			●								
94	Development of Sensory Feedback Systems for Minimally Invasive Surgery Applications	3514120000									●															●	●	
94	Personal Status Monitor	3514130000				●			●						●		●	●	●	●		●					●	
95	Development of a One-Step ELISA Using Microencapsulation Immunoreagents	3514140000		●		●										●	●						●				●	
100	Development of a Portable X-Ray and Gamma-Ray Detector Instrument and Imaging Camera for Use in Radioactive and Hazardous Material Management	3515170000							●			●				●	●		●	●	●	●					●	
102	Automated Detection and Reporting of Volatile Organic Compounds (VOCs) in Complex Environments	3515190000											●		●						●		●				●	
99	Delineating DNAPLs: A Probabilistic Approach for Locating DNAPLs in Subsurface Sediments	3515210000					●						●										●					●

Pg #	Title	Case Number	Aeronautics	Applied Molecular Biology	Ceramics	Composites	Computer Simulation & Modeling	Data Storage and Peripherals	Electronics and Photonics	Energy	Flexible Computer-Integrated Manufacturing	High-Definition Imaging and Displays	High-Performance Computing and Networking	High-Performance Metals and Alloys	Intelligent Processing Equipment	Material Synthesis & Processing	Medical Technology	Micro- and Nano-Fabrication	Microelectronics and Optoelectronics	Photonic Materials	Pollution Min., Remediation, and Waste Mgmt.	Sensors & Signal Processing	Software	Surface Transportation Technologies	Systems Management Technologies	Defense-Related (mostly or purely)	Dual-Use (defense and non-defense-related)	Non-Defense-Related (mostly or purely)
102	Compact Environmental Sensing Spectroscopy Using Advanced Semiconductor Light-Emitting Diodes and Lasers	3515260000							●	●					●				●								●	
103	The Development of Ion Mobility Spectroscopy to Analyze Explosives at Environmental Restoration Sites	3515270000																			●						●	
104	Development of Inexpensive Metal Macrocyclic Complexes for Direct Oxidation of Methanol in Fuel Cells	3515290000								●						●	●				●	●		●				
104	Cooperating Robot Arms	3515310000					●	●			●		●		●		●					●	●					
106	Oriented Inorganic Thin-Film Channel Structures with Unidirectional Monosize Microscopes	3515320000		●	●	●			●	●						●	●	●				●				●		●
106	Quantitative Analysis of Trace Contaminants in Aqueous Media	3515330000								●						●					●					●		
107	Replacement of Liquid H_2SO_4 and HF Acids with Solid Acid Catalysts for Paraffin Alkylation Process	3515340000								●						●										●		
105	Organically Enhanced In Situ Electrokinetic Removal of Uranium from Soils	3515350000																			●					●	●	
110	Nanoreactors as Novel Catalyst Systems for Waste-Stream Remediation	3515360000																										●
108	Advanced Tomographic Flow Diagnostics for Opaque Multiphase Fluids	3515410000				●				●						●	●				●							●

Pg #	Title	Case Number	Aeronautics	Applied Molecular Biology	Ceramics	Composites	Computer Simulation & Modeling	Data Storage and Peripherals	Electronics and Photonics	Energy	Flexible Computer-Integrated Manufacturing	High-Definition Imaging and Displays	High-Performance Computing and Networking	High-Performance Metals and Alloys	Intelligent Processing Equipment	Material Synthesis & Processing	Medical Technology	Micro- and Nano-Fabrication	Microelectronics and Optoelectronics	Photonic Materials	Pollution Min., Remediation, and Waste Mgmt.	Sensors & Signal Processing	Software	Surface Transportation Technologies	Systems Management Technologies	Defense-Related (mostly or purely)	Dual-Use (defense and non-defense-related)	Non-Defense-Related (mostly or purely)
109	Evanescent Fiber-Optic Sensor for In Situ Monitoring of Chlorinated Organics	3515430000							●										●	●	●	●					●	
111	Reapplication of Energetic Materials as Fuels	3515440000								●											●						●	
112	Designed Molecular-Recognition Materials for Chiral Sensors, Separations, and Catalytic Materials	3515450000								●						●	●					●					●	
115	Learning Efficient Hypermedia Navigation	3517120000											●				●						●				●	
121	Data Zooming—A New Physics for Information Navigation	3517150000					●				●		●										●					
115	Design of a Highly Secure Smartcard	3517160000				●											●						●				●	
116	Enhanced Internet Firewall Design Using Stateful Filters	3517170000											●														●	
116	Network-Based Collaborative Research Environment	3517180000	●	●	●	●	●	●	●	●	●	●	●	●	◐	●	●	●	●	●	●	●	●		●		●	
118	Reliability Assessment of Dynamic Communication Networks	3517210000					●						●												●		●	
117	Object-Oriented Parallel Discrete Event Simulation System—An Enabling Foundation for Rapid Development of High-Performance, Large-Scale Simulations	3517220000		◐			◐				◐		◐		◐								◐				◐	
118	Agent-Based Remediation of the Mosaic Classification Problem	3517230000					●	●			●		●		●								●				●	

Pg #	Title	Case Number	Aeronautics	Applied Molecular Biology	Ceramics	Composites	Computer Simulation & Modeling	Data Storage and Peripherals	Electronics and Photonics	Energy	Flexible Computer-Integrated Manufacturing	High-Definition Imaging and Displays	High-Performance Computing and Networking	High-Performance Metals and Alloys	Intelligent Processing Equipment	Material Synthesis & Processing	Medical Technology	Micro- and Nano-Fabrication	Microelectronics and Optoelectronics	Photonic Materials	Pollution Min., Remediation, and Waste Mgmt.	Sensors & Signal Processing	Software	Surface Transportation Technologies	Systems Management Technologies	Defense-Related (mostly or purely)	Dual-Use (defense and non-defense-related)	Non-Defense-Related (mostly or purely)
119	Biometric Identity Verification for Remote-User Authentication and Access-Control Applications	3517240000																				●	●				●	
119	Development of an Intelligent Geographic Information System	3517250000					●																					●
120	Use-Control of "Robustness-Agile" Encryption Devices	3517260000											●														●	
120	Virtual Channel Encryption	3517270000						●					●		●		●										●	
122	Advanced Concurrent Engineering Environment	3517280000																									●	
125	Electromagnetic Induction Tunnel Detection	3519160000								●									●		●	●					●	
126	Fiber-Optic Biosensors for Biological Warfare Counterproliferation	3519170000		●					●							●	●	●	●	●	●	●					●	
127	Moving Mass Trim Control for Precision-Strike Warheads	3519180000	●										●										●			●		
126	Theater Missile Defense Integrated Simulation	3519190000					●															●				●		
128	Unexplored Penetrator Regime Against Super-Hard Underground Facilities	3519210000					●							●												●		
132	Fuel-Cell Applications for Novel Metalloporphyrin Catalysts	3521120000								●											●			●			●	

Pg #	Title	Case Number	Aeronautics	Applied Molecular Biology	Ceramics	Composites	Computer Simulation & Modeling	Data Storage and Peripherals	Electronics and Photonics	Energy	Flexible Computer-Integrated Manufacturing	High-Definition Imaging and Displays	High-Performance Computing and Networking	High-Performance Metals and Alloys	Intelligent Processing Equipment	Material Synthesis & Processing	Medical Technology	Micro- and Nano-Fabrication	Microelectronics and Optoelectronics	Photonic Materials	Pollution Min., Remediation, and Waste Mgmt.	Sensors & Signal Processing	Software	Surface Transportation Technologies	Systems Management Technologies	Defense-Related (mostly or purely)	Dual-Use (defense and non-defense-related)	Non-Defense-Related (mostly or purely)
131	Vehicle Exhaust-Gas Chemical Sensors Using Acoustic-Wave Resonators	352117000			●				●						●	●			●		●	●		●			●	
132	High-Density Direct Methanol Fuel Cell	352118000								●											●			●			●	
135	Conceptual Design and Prototyping for a Next-Generation Geographic Information System	352119000					●	●		●					●						●	●		●			●	
133	Hydrogen Production for Fuel Cells by Selective Dehydrogenation of Alkanes in Catalytic Membrane Reactors	352121000			●					●						●		●										
134	Hybrid Vehicle Engine Development	352122000								●											●						●	
134	Development of Innovative Combustion Processes for a Direct-Injection Diesel Engine	352123000								●																		●
139	Superconductive Gravity Gradiometers for Underground Target Recognition	352311000								●																	●	
139	Bandwidth Utilization Maximization for Scientific Radio-Frequency Communication	352312000	●							●														●			●	
140	Extraction of Information from Unstructured Data	352313000																					●				●	
140	Feature-Based Methodology for Sensor Fusion	352314000	●									●			●		●					●		●		●	
141	Nonflammable Deterrent Materials	352315000														●											●	

Pg #	Title	Case Number	Aeronautics	Applied Molecular Biology	Ceramics	Composites	Computer Simulation & Modeling	Data Storage and Peripherals	Electronics and Photonics	Energy	Flexible Computer-Integrated Manufacturing	High-Definition Imaging and Displays	High-Performance Computing and Networking	High-Performance Metals and Alloys	Intelligent Processing Equipment	Material Synthesis & Processing	Medical Technology	Micro- and Nano-Fabrication	Microelectronics and Optoelectronics	Photonic Materials	Pollution Min., Remediation, and Waste Mgmt.	Sensors & Signal Processing	Software	Surface Transportation Technologies	Systems Management Technologies	Defense-Related (mostly or purely)	Dual-Use (defense and non-defense-related)	Non-Defense-Related (mostly or purely)
142	Microholographic Tagging	3523160000						●	●						●			●	●			●					●	
142	Interactive Control of Virtual Actors for Simulation and Training	3523170000					●					●	●										●				●	
143	Investigation of Spray Techniques for Use in Explosive Scabbling of Concrete	3523180000																									●	
147	Jet Applications of Solder Bumps with Laser Ablation for MCM Packaging	3526010000							●		●					●		●	●	●							●	
148	Micromachined Inertial Sensors (Accelerometer, Gyroscope)	3526020000																●	●			●					●	
147	High-Reliability Plastic Packaging for Microelectronics	3526030000							●				●			●			●								●	
148	Ultra–Low-Power Microwave CHFET Integrated Circuit Development	3526040000							●										●								●	
153	A Planar Silicon Fabrication Process for High-Aspect-Ratio Micromachined Parts	3526050000	●						●										●			●		●			●	
149	Application-Specific Tester-on-a-Resident-Chip (TORCH)	3526070000	●					●	●										●								●	
150	Microelectronic Biosensors	3526080000							●													●					●	
150	Validation of the MDL ASIC Prototyping Process	3526090000																	●							●		

Pg #	Title	Case Number	Aeronautics	Applied Molecular Biology	Ceramics	Composites	Computer Simulation & Modeling	Data Storage and Peripherals	Electronics and Photonics	Energy	Flexible Computer-Integrated Manufacturing	High-Definition Imaging and Displays	High-Performance Computing and Networking	High-Performance Metals and Alloys	Intelligent Processing Equipment	Material Synthesis & Processing	Medical Technology	Micro- and Nano-Fabrication	Microelectronics and Optoelectronics	Photonic Materials	Pollution Mtn., Remediation, and Waste Mgmt.	Sensors & Signal Processing	Software	Surface Transportation Technologies	Systems Management Technologies	Defense-Related (mostly or purely)	Dual-Use (defense and non-defense-related)	Non-Defense-Related (mostly or purely)
151	High-G Accelerometer for Earth-Penetrator Weapons Applications	3526110000																●	●			●		●			●	
152	Agile Prototyping of Microelectromechanical Systems (MEMS)	3526120000	●						●		●	●					●	●	●			●					●	
152	Highly Parallel, Low-Power, Photonic Interconnects for Inter-Board Signal Distribution	3526130000						●	●				●						●								●	
157	Experimental Replication of the Reifenschweiler Effect	3536010000																								●		
157	Molecular Concentrator	3536020000																									●	
158	Investigation of Concepts for Storing and Releasing Energy from Nuclear Isomers	3536030000																							●			
158	CLERVER, Win95	3536040000																									●	
159	A Tool to Detect External Cracks from Within a Tube	3536050000																									●	
159	Infrastructural Decision Support	3536060000																									●	
160	Development of Quiescent Power-Supply Voltage (V_{DDQ}) Testing	3536110000																									●	
160	Development of Failure and Yield Enhancement Analysis for Integrated Microelectromechanical Systems	3536120000																									●	

Pg #	Title	Case Number	Aeronautics	Applied Molecular Biology	Ceramics	Composites	Computer Simulation & Modeling	Data Storage and Peripherals	Electronics and Photonics	Energy	Flexible Computer-Integrated Manufacturing	High-Definition Imaging and Displays	High-Performance Computing and Networking	High-Performance Metals and Alloys	Intelligent Processing Equipment	Material Synthesis & Processing	Medical Technology	Micro- and Nano-Fabrication	Microelectronics and Optoelectronics	Photonic Materials	Pollution Min., Remediation, and Waste Mgmt.	Sensors & Signal Processing	Software	Surface Transportation Technologies	Systems Management Technologies	Defense-Related (mostly or purely)	Dual-Use (defense and non-defense-related)	Non-Defense-Related (mostly or purely)
161	Exploration of Multichip Module (MCM) Test-Solutions for Reliability Enhancement	3536130000																									●	
161	Optical Actuation of Micromechanical Components	3536140000																									●	
162	Statistical Characterization of MEMS Microengine Devices	3536150000																									●	
162	Optical State-of-Charge Monitor for Lead-Acid Batteries	3536160000																									●	
163	Impact of Focused Ion-Beam Microsurgery on Integrated Circuit Reliability	3536170000																									●	
164	Extended Cavity Fiber/VCSEL for Photonic Application	3536180000																									●	
164	Characterization of Semiconductor Piezoelectricity for Chemical-Sensing and High-Frequency Applications	3536190000																									●	
165	Magnetically Excited Flexural Plate Wave Device	3536210000																									●	
166	Alternative Joining by Diffusion Bonding with a Common Brazing Alloy	3536220000																									●	
165	Crack Propagation in Energetic Materials	3536230000																									●	
166	Composite Carbon Anodes for Rechargeable Li-Ion Cells	3536240000																									●	

Pg #	Title	Case Number	Aeronautics	Applied Molecular Biology	Ceramics	Composites	Computer Simulation & Modeling	Data Storage and Peripherals	Electronics and Photonics	Energy	Flexible Computer-Integrated Manufacturing	High-Definition Imaging and Displays	High-Performance Computing and Networking	High-Performance Metals and Alloys	Intelligent Processing Equipment	Material Synthesis & Processing	Medical Technology	Micro- and Nano-Fabrication	Microelectronics and Optoelectronics	Photonic Materials	Pollution Mtn., Remediation, and Waste Mgmt.	Sensors & Signal Processing	Software	Surface Transportation Technologies	Systems Management Technologies	Defense-Related (mostly or purely)	Dual-Use (defense and non-defense-related)	Non-Defense-Related (mostly or purely)
167	Silicon-Based Nondestructive Read-Out Memories	3536250000																									●	
168	Use of X-Ray Mirrors for Enhanced Thin-Film X-Ray Diffraction	3536260000																									●	
168	High-Speed Shutter/Attenuator for Direct Fabrication Technology	3536270000																									●	
169	Direct Fabrication of Aerogel-Supported Metal Nanocluster Catalysts	3536280000																									●	
170	Measurement of Stress in Large-Area Thin Films	3536290000																									●	
170	Develop Capability to Measure Electrical Conductivity of Molten Slags	3536310000																									●	
169	Exploration of Surety Improvements via the Use of Ada in High-Consequence Software Projects	3536320000																									●	
171	Ensuring Critical-Event Sequence in High-Consequence Software by Applying Finite Automata Theory	3536330000																									●	
172	Optical High-Voltage Sensor for Advanced Firing Sets	3536340000																								●		
173	Toward Experimental Verification of New Dual-Permeability Conceptual Model in Fracture/Matrix Networks	3536350000																									●	
172	Investigation of Reducing Photovoltaic Systems Life-Cycle Costs Through System-Reliability Improvement	3536360000																									●	

Pg #	Title	Case Number	Aeronautics	Applied Molecular Biology	Ceramics	Composites	Computer Simulation & Modeling	Data Storage and Peripherals	Electronics and Photonics	Energy	Flexible Computer-Integrated Manufacturing	High-Definition Imaging and Displays	High-Performance Computing and Networking	High-Performance Metals and Alloys	Intelligent Processing Equipment	Material Synthesis & Processing	Medical Technology	Micro- and Nano-Fabrication	Microelectronics and Optoelectronics	Photonic Materials	Pollution Min., Remediation, and Waste Mgmt.	Sensors & Signal Processing	Software	Surface Transportation Technologies	Systems Management Technologies	Defense-Related (mostly or purely)	Dual-Use (defense and non-defense-related)	Non-Defense-Related (mostly or purely)
173	Theoretical Development of a Prototype Assumption-Based Modeling System	3536370000																									●	
174	Sensor Fusion for Predictive Maintenance	3536380000																									●	
174	Modeling of Multicomponent Transport with Microbial Transformation in Subsurface System	3536390000																									●	
175	Precision Stage for LIGA Micromachine Fabrication	3536410000																									●	
183	Development of Periodically Poled Laser Sources for Ultra-Sensitive Analysis	3536420000																									●	
176	Affinity Chromatography Supports for Separation and Detection of Biological Toxins	3536430000																									●	
176	Design and Evaluation of Sampling, Detection, and Control Technology for Field-Portable Capillary-Based Chemical Analysis	3536440000																									●	
178	Exploration of Methods for Bridging Length and Time Scales	3536450000																									●	
178	Scaling Laws for RoBugs	3536460000																									●	
177	New Applications of Damage Detection and Structural Health-Monitoring Methods	3536470000																									●	
178	Damage Detection Analysis Using Wavelets and Neural Nets	3536480000																									●	

Pg #	Title	Case Number	Aeronautics	Applied Molecular Biology	Ceramics	Composites	Computer Simulation & Modeling	Data Storage and Peripherals	Electronics and Photonics	Energy	Flexible Computer-Integrated Manufacturing	High-Definition Imaging and Displays	High-Performance Computing and Networking	High-Performance Metals and Alloys	Intelligent Processing Equipment	Material Synthesis & Processing	Medical Technology	Micro- and Nano-Fabrication	Microelectronics and Optoelectronics	Photonic Materials	Pollution Min., Remediation, and Waste Mgmt.	Sensors & Signal Processing	Software	Surface Transportation Technologies	Systems Management Technologies	Defense-Related (mostly or purely)	Dual-Use (defense and non-defense-related)	Non-Defense-Related (mostly or purely)
179	A Comparison of System Identification Techniques	3536490000																									●	
180	Coaxial Extractor Diode Conceptual Design	3536510000																									●	
180	A Novel Methodology to Determine Dynamic Pressure-Volume States of Transportation Materials	3536520000																									●	
181	Remote Optical Detection of Obscured Objects in Turbid Oceanographic Environments	3536530000																									●	
182	RoBug Conceptual Design and Analysis System	3536540000																									●	
182	Prediction of Seismic Rocket Launch Signatures	3536550000																									●	
183	Evaluation of Shocked PVDF for Compact, High-Power Electric Pulse	3536560000																									●	
187	Distributed Object and Intelligent Agent Technologies in a Wide-Area Network Test-Bed	3538010000									●												●				●	
188	Laser-Spray Fabrication for Net-Shape Rapid Product Realization	3538020000																									●	
188	Solid-Model Design Simplification	3538030000					●																				●	
189	Process Optimization for Electron-Beam Joining of Ceramic and Glass Components	3538040000		●	●	●	●		●		●					●			●								●	

Pg #	Title	Case Number	Aeronautics	Applied Molecular Biology	Ceramics	Composites	Computer Simulation & Modeling	Data Storage and Peripherals	Electronics and Photonics	Energy	Flexible Computer-Integrated Manufacturing	High-Definition Imaging and Displays	High-Performance Computing and Networking	High-Performance Metals and Alloys	Intelligent Processing Equipment	Material Synthesis & Processing	Medical Technology	Micro- and Nano-Fabrication	Microelectronics and Optoelectronics	Photonic Materials	Pollution Min., Remediation, and Waste Mgmt.	Sensors & Signal Processing	Software	Surface Transportation Technologies	Systems Management Technologies	Defense-Related (mostly or purely)	Dual-Use (defense and non-defense-related)	Non-Defense-Related (mostly or purely)
190	Self-Tuning Process Monitoring System for Process-Based Product Validation	3538050000									●				●							●					●	
190	Solution Synthesis and Processing of PZT Materials for Neutron Generator Applications	3538060000			●	●			●							●			●							●		
191	Effect of Composition and Processing Conditions on the Reliability of Cermet/Alumina Components	3538070000	●		●	●	●							●		●										●		
187	Carbon Coatings for Improved Sprytron Tube Performance and Reliability	3538080000										●				●			●									
192	A Multilevel Code for Metallurgical Effects in Metal-Forming Processes	3538090000					◐				◐		◐														●	
192	Automated Reasoning About Tools for Assembly	3538110000									●												●				●	
193	Analysis-Driven Mechanical Redesign	3538120000	●				●				●				●								●				●	
193	Liaison-Based Assembly Design	3538130000	●				●				●				●								●				●	
194	An Enabling Architecture for Information-Driven Manufacturing	3538140000													●								●		●		●	
197	Nanocavity Effects on Misfit Accommodation in Semiconductors	3539160000																									●	
198	Extending the Applicability of Cluster-Based Pattern Recognition with Efficient Approximation Techniques	3539170000																									●	

Pg #	Title	Case Number	Aeronautics	Applied Molecular Biology	Ceramics	Composites	Computer Simulation & Modeling	Data Storage and Peripherals	Electronics and Photonics	Energy	Flexible Computer-Integrated Manufacturing	High-Definition Imaging and Displays	High-Performance Computing and Networking	High-Performance Metals and Alloys	Intelligent Processing Equipment	Material Synthesis & Processing	Medical Technology	Micro- and Nano-Fabrication	Microelectronics and Optoelectronics	Photonic Materials	Pollution Min., Remediation, and Waste Mgmt.	Sensors & Signal Processing	Software	Surface Transportation Technologies	Systems Management Technologies	Defense-Related (mostly or purely)	Dual-Use (defense and non-defense-related)	Non-Defense-Related (mostly or purely)
210	Antipodal Focusing of Shock Energy from Large Asteroid Impacts on Earth	3539190000																										●
199	Biocavity Laser Microscopy/Spectroscopy of Cells	3539220000																										●
200	Sol-Gel Preservation of Mankind's Cultural Heritage in Objects Constructed of Stone	3539250000			●	●	●			●						●		●			●							●
201	Tailorable, Visible, Room-Temperature Light Emission from Si, Ge, and Si-Ge Nanoclusters	3539270000															●		●	●								●
198	A New Paradigm for Near Real-Time Downhole Data Acquisition	3539280000								●																		●
202	In Situ Determination of Composition and Strain During MBE Using Electron Beams	3539320000							●							●			●							●		
202	In Situ Optical Flux Monitoring for Precise Control of Thin-Film Deposition	3539330000						●	●		●	●	●		●	●			●	●	●	●				●		
203	Understanding and Control of Energy-Transfer Mechanisms in Optical Ceramic	3539340000			●	●	●		●			●				●		●	●	●		●				●		
204	Molecular-Scale Lubricants for Micromachine Applications	3539350000							●							●		●				●					●	
204	Ultra-Hard Multilayer Coatings	3539360000			●	●	●					●				●						●					●	
205	Smart Interface Bonding Alloys (SIBA): Tailoring Thin-Film Mechanical Properties	3539370000					●	●		●				●					●		●						●	

Pg #	Title	Case Number	Scanning Probe-Based Processes for Nanometer-Scale Device Fabrication	Wide-Bandgap Compound Semiconductors to Enable Novel Semiconductor Devices	Recognizing Atoms in Atomically Engineered Nanostructures: An Interdisciplinary Approach	Photonic Bandgap Structures as a Gateway to Nano-Photonics	Physico-Chemical Stability of Solid Surfaces	Artificial Atoms	Modeling and Characterization of Molecular Structures in Self-Assembled and Langmuir-Blodgett Films	UV Spectroscopic Detection and Identification of Pathogens	Novel Laser-Based Diagnostics Capability for Chemical Science
	Aeronautics										
	Applied Molecular Biology						●		●	●	
	Ceramics								●		
	Composites								●		
	Computer Simulation & Modeling								●		
	Data Storage and Peripherals										
	Electronics and Photonics				●	●	●	●		●	
	Energy						●		●		
	Flexible Computer-Integrated Manufacturing			●		●					
	High-Definition Imaging and Displays			●	●	●	●				
	High-Performance Computing and Networking					●					
	High-Performance Metals and Alloys						●				
	Intelligent Processing Equipment					●					
	Material Synthesis & Processing		●	●	●				●		
	Medical Technology									●	
	Micro- and Nano-Fabrication		●	●	●	●		●	●		
	Microelectronics and Optoelectronics		●	●		●		●	●		
	Photonic Materials			●	●	●	●	●			
	Pollution Min., Remediation, and Waste Mgmt.									●	
	Sensors & Signal Processing			●	●	●	●	●	●	●	
	Software			●			●				
	Surface Transportation Technologies										
	Systems Management Technologies										
	Defense-Related (mostly or purely)										
	Dual-Use (defense and non-defense-related)		●	●	●	●	●	●		●	●
	Non-Defense-Related (mostly or purely)								●		
206	Scanning Probe-Based Processes for Nanometer-Scale Device Fabrication	3539380000									
206	Wide-Bandgap Compound Semiconductors to Enable Novel Semiconductor Devices	3539390000									
207	Recognizing Atoms in Atomically Engineered Nanostructures: An Interdisciplinary Approach	3539410000									
208	Photonic Bandgap Structures as a Gateway to Nano-Photonics	3539420000									
212	Physico-Chemical Stability of Solid Surfaces	3539430000									
208	Artificial Atoms	3539440000									
209	Modeling and Characterization of Molecular Structures in Self-Assembled and Langmuir-Blodgett Films	3539450000									
212	UV Spectroscopic Detection and Identification of Pathogens	3539460000									
210	Novel Laser-Based Diagnostics Capability for Chemical Science	3539470000									